David Jou José Casas-Vázquez Manuel Criado-Sancho

Thermodynamics of Fluids Under Flow

Second Edition



Thermodynamics of Fluids Under Flow

David Jou • José Casas-Vázquez Manuel Criado-Sancho

Thermodynamics of Fluids Under Flow

Second Edition



Prof. Dr. David Jou Grup de Fisica Estadistica, Departament de Fisica Universitat Autonoma de Barcelona 08193 Bellaterra Catalonia, Spain david.jou@uab.es

Prof. Dr. José Casas-Vázquez Grup de Fisica Estadistica, Departament de Fisica Universitat Autonoma de Barcelona 08193 Bellaterra Catalonia, Spain jose.casas@uab.es Prof. Manuel Criado-Sancho Facultad de Ciencias UNED 28040 Madrid Spain mcriado@ccia.uned.es

ISBN 978-94-007-0198-4 e-ISBN 978-94-007-0199-1 DOI 10.1007/978-94-007-0199-1 Springer Dordrecht Heidelberg London New York

© Springer Science+Business Media B.V. 2011

No part of this work may be reproduced, stored in a retrieval system, or transmitted in any form or by any means, electronic, mechanical, photocopying, microfilming, recording or otherwise, without written permission from the Publisher, with the exception of any material supplied specifically for the purpose of being entered and executed on a computer system, for exclusive use by the purchaser of the work.

Cover design: eStudio Calamar S.L.

Printed on acid-free paper

Springer is part of Springer Science+Business Media (www.springer.com).

Preface

The thermodynamics of flowing fluids is an active and very challenging topic in modern non-equilibrium thermodynamics and statistical mechanics. After ten years of publication of the first edition of this book, we felt that a fully renewed, updated and enlarged edition was necessary to cover some of the progress made in these fields. A book on the thermodynamics of flowing fluids was published in 1994 by A. N. Beris and S. J. Edwards, Thermodynamics of Flowing Fluids with Internal Microstructure, Oxford University Press, New York, 1994: it was based on the Poisson bracket formalism and focused on fluids with internal microstructure. The books by D. J. Evans and G. P. Morriss, Statistical Mechanics of Nonequilibrium Liquids (Australian National University E Press, 2007), A. Onuki, Phase Transition Dynamics (Cambridge University Press, 2002) and V. Garzó and A. Santos, Kinetic theory of gases in shear flow (Kluwer, Dordrecht, 2003) have also been useful and important contributions to a global vision of this field, the first with more emphasis on molecular dynamical simulations, the second one with special attention on critical phenomena, and the third one from the perspective of the kinetic theory of gases. The central perspective of the present book is, instead, on non-equilibrium thermodynamics beyond local equilibrium. The more macroscopic and phenomenological character of this approach allows to deal with a wider range of systems, going from ideal gases and phonon hydrodynamics to polymer solutions and melts, and to laminar and turbulent superfluids.

The interest of the thermodynamics of flowing fluids is both theoretical and practical. From the theoretical point of view, the influence of the flow on the thermodynamic potentials requires the formulation of thermodynamic theories beyond the local-equilibrium hypothesis; this is a field with many open challenges, which fosters an active dialogue between macroscopic and microscopic theories, the latter based either on the kinetic theory of gases, or on molecular dynamical simulations of fluids. Furthermore, it also requires an open discussion between thermodynamics and hydrodynamics, because some of the observed phenomena may have a purely thermodynamic origin (due to the modification of some equations of state) or a purely hydrodynamic origin, but in general there will be an interplay of both thermodynamics beyond the local-equilibrium regime, and its relationship with microscopic theories and with hydrodynamic theories currently represents an important frontier

vi Preface

of research. In our book by G. Lebon, D. Jou and J. Casas-Vázquez, *Understanding Non-equilibrium Thermodynamics*. *Foundations, Applications, Frontiers* (Springer, Berlin, 2008) we have discussed and examined in detail several different avenues towards the formulation of such thermodynamics beyond local equilibrium.

From the practical point of view, many situations of technological interest are present in flowing systems. Indeed, the modification of the thermodynamic equations of state for the chemical potential imply modifications in the phase diagram of substances in non-equilibrium steady states, or on the conditions of chemical equilibrium and stability. The ability to control the thermodynamic state of the system is essential in technology and also in fundamental science. For instance, much study has been devoted to flow-induced changes in the phase diagram of polymer solutions or in shear-induced flow of macromolecules. The practical importance of the problems arising under flow is easily understood. Most industrial processes take place in flowing fluids (pumping, extruding, injecting, molding, mixing...), in which the polymer macromolecules undergo different shear and elongational stresses, depending on the position. Thus, a flow-induced change of phase could take place in some positions and not in others, affecting both rheological and structural properties of the flow. The materials formed in these processes may be very sensitive to the extent of the phase transitions occurring in the fluids previous to solidification.

Other related fields of interest are the thermodynamically induced polymer degradation under flow, which may be important in viscous drag reduction, or in flows of polymer solutions through packed porous beds, as in membrane permeation or flow of oil through soil and rocks. Also, in biological experiments shear-induced precipitation and degradation of proteins has been observed, and new separation techniques have been devised on the effects of the interaction between viscous pressure and diffusion. Microfluidics and nanofluidics have experienced a strong development in the last ten years, opening new and surprising applications of flowing fluids at a minuscule scale. In particular, phonon hydrodynamics provides a useful phenomenological basis to analyze heat transport from the diffusive to the ballistic regimes, with application to nanosystems and nanowires, thin layers, tubular layers, porous superlattices and so on.

From a more fundamental point of view, some of the main experiments in nuclear and particle physics refer to the transition from nuclear hadronic to a quark-gluon plasma. This is pursued through very energetic ultrarelativistic collisions of heavy nuclei. The total duration of such collisions is of the order of five to ten times the mean time between successive collisions amongst nucleons in the nuclei. Therefore, the nuclei are rather far from local equilibrium during the collision and it is problematic to what extent an analysis based on the local-equilibrium equations of state for nuclear matter and for quark-gluon plasma and normal hydrodynamics may be sufficient to provide a reliable description of the transition. Efforts towards using more general non-equilibrium thermodynamic and hydrodynamic theories are a challenge in this field. Another topic where the flow has a deep influence on the fluids is in turbulent superfluids, where a tangle of quantized vortex filaments appears for sufficiently high values of the heat flow or of the relative

Preface vii

velocity between normal and superfluid components. This vortex tangle contributes to the internal friction of the fluid, and it is by itself an interesting phase of matter, constituted of vortex loops and filaments. Finally, at a more abstract level, understanding the meaning and the mutual relationships between several definitions of temperature and entropy finds in flowing fluids an interesting benchmark where explicit illustrations are possible.

From a thermodynamic perspective, the already mentioned book by Beris and Edwards was based on Hamiltonian formalisms, as Poisson brackets, which has achieved a more general and elegant formulation in the so-called GENERICS, which has been presented in detail by H. C. Öttinger in the book *Beyond Equilibrium Thermodynamics* (Wiley, New York, 2005). Here, instead, we adopt extended irreversible thermodynamics as our general framework, and we try to emphasise both the general thermodynamic structure underlying fluids without internal structure (namely, ideal gases, phonons, real gases, simple fluids) as well as fluids with internal structure (namely, polymer solutions and blends, and turbulent superfluids). In this way, this volume may be seen as a complement of our monograph D. Jou, G. Lebon and J. Casas-Vázquez, *Extended Irreversible Thermodynamics* (fourth edition, Springer, Berlin, 2010), dealing with a variety of problems that were not included in that volume for the lack of space.

A decisive step in the thermodynamic understanding of flowing fluids is to formulate a free energy depending explicitly on the characteristics of the flow. This important problem in non-equilibrium thermodynamics has not yet received as much attention as it deserves. It must be noted that several authors have preferred to follow another method, to analyse the phase separation or phase homogenization under shear from a dynamical point of view, i.e. by writing dynamical equations for the behaviour of concentration and velocity fluctuations and analysing the stability of the corresponding set of equations. Of course, the dynamical procedure has a wider range of potentialities than the pure thermodynamic analysis: the latter may be able to set the spinodal line limiting the regions of stability, but it certainly cannot give a detailed view of the processes of segregation of both phases, or about the changes in viscosity observed during the segregation. However, the existence of both methods is not contradictory, e.g., the dynamical method may describe the instability through the change of sign of an effective diffusion coefficient, but this change of sign is produced at the spinodal line, and this fact is related, in many situations, to the vanishing of the first derivative of an effective chemical potential with respect to the composition. Furthermore, the dynamical analysis cannot avoid the use of equations of state of the flowing fluid; therefore, to find and analyse equations of state in non-equilibrium conditions is always of interest. Thus, although there is a common ground for thermodynamical and dynamical analyses, both methods have their own advantages and disadvantages, so that it would be unwise to dismiss a priori either of them.

Here, we give a brief description of the contents of the book, and point to the changes made with respect to the first edition. In Chap. 1, we provide the general basis from a macroscopic point of view, or more precisely from the perspective of extended irreversible thermodynamics, and we compare it with other macroscopic

viii Preface

theories, as rational thermodynamics, theories with internal variables, and Hamiltonian theories. Chapters 2 and 3—the much enlarged outcomes of the Chap. 2 of the first edition—deal with ideal gases: in Chap. 2 we use information theory to describe the steady state of flowing ideal gases under Couette flow, and we explore in depth how several definitions of temperature behave in the presence of a non-vanishing viscous pressure, and how they relate to each other. Of course, in the absence of the viscous pressure all of them tend to the same value, identical to the local-equilibrium temperature. In Chap. 3 we remind the basic concepts of the kinetic theory description of flowing ideal gases, and we discuss with some detail the application of thermodynamic ideas to the flow of phonons in the so-called phonon hydrodynamics, with special emphasis on the application of this formalism to heat transfer in nanosystems. This requires taking into detailed consideration the boundary conditions for the slip heat flow along the walls of the system. This topic was not considered in the second edition.

Chapter 4 is devoted to non-ideal gases, with a comparison with some results of molecular dynamical simulations, and with an application to some thermodynamic and hydrodynamic aspects of relativistic ion collisions. Chapter 5 discusses the microscopic description of polymer solutions, as kinetic theory of dilute solutions, reptation model for concentrated solutions, and double-reptation model for polymer blends, to which much attention is devoted in further chapters. Chapter 6 analyzes the influence of a shear flow on the phase diagram of polymer solutions. and shear-induced phase transitions; the first edition was limited to dilute solutions whereas the present one incorporates also concentrated solutions and polymers blends. Chapter 7 considers dynamical effects, the role of hydrodynamically enhanced fluctuations, and provides an understanding of the range of application of the thermodynamic formalism. Chapters 8 and 9 enlarge the contents of Chap. 7 of the first edition. Chapter 8 deals with the couplings of viscous pressure and diffusion; in particular, much attention is devoted to shear-induced diffusion and its applications to macromolecular separation in cone-and-plate and in tube configurations. Chapter 9 is also devoted to diffusion in the presence of a velocity gradient, with special attention to Taylor dispersion and its applications, and to anomalous diffusion, both in a system at rest as in a fluid with a velocity gradient. Chapter 10 deals with chemical reactions under flow, both for ideal gases and polymer solutions; the latter case is applied to the analysis of polymer degradation due to the flow. Chapter 11 discusses the thermodynamics of flowing superfluids, not only in the well-known laminar regime, but also in the more intriguing and challenging turbulent regime, with quantized vortices. Appendix A is devoted to a survey of experimental information on the relevant material functions used for the evaluation of the non-equilibrium chemical potential in the examples considered in the book, and Appendix B briefly describes the results on the influence of a shear flow on the isotropic-nematic transition in liquid crystals. Appendices C–E contain other useful information related to mathematical results.

We acknowledge fruitful discussions on a variety of these topics with Profs. G. Lebon (Université de Liège, Belgium), M. S. Mongiovì (Università di Palermo, Italy), R. Luzzi (Universidade de Campinas, Brazil), M. Grmela (École Polytechnique

Preface ix

de Montréal, Canada), L. F. del Castillo (Universidad Nacional Autónoma de México, México), Y. Katayama (Nihon University, Koriyama, Japan), W. Muschik (Technische Universität Berlin, Germany), H. C. Öttinger (ETH Zurich, Switzerland), V. A. Cimmelli (Università della Basilicata, Potenza, Italy), J. Camacho and V. Méndez (Universitat Autònoma de Barcelona) and J. Fort (Universitat de Girona), and with Drs F. X. Alvarez (Universitat Autònoma de Barcelona), A. Sellitto (Università della Basilicata, Potenza, Italy), and M. Sciacca (Università di Palermo, Italy). Dr V. Ortega-Cejas (Universitat Autònoma de Barcelona) has been very helpful in providing technical help for the final version of the manuscript.

This work has received the support of the Dirección General de Investigación Científica y Técnica of the Spanish Ministry of Education and Science, under grants PB90-0676, PB94-0718, FIS2006-12296-C02-01, Ministry of Science and Technology (grants BFM 2000-0351-C03-01, BFM-2003-06033), Ministry of Science and Innovation (grant FIS2009-13370-C02-01), of European Union in the framework of the Program of Human Capital and Mobility (grant ERB-CHR XCT 920 007) and of the Direcció General de Recerca of the Generalitat of Catalonia (grants 1997 SGR 00387, 1999 SGR 00095, 2001 SGR 00186, 2005 SGR 0087, 2009 SGR 164). M. Criado-Sancho acknowledges the support of the Universidad Nacional de Educación a Distancia (UNED, Madrid, Spain).

July 2010 Bellaterra, Barcelona David Jou, José Casas-Vázquez and Manuel Criado-Sancho

Contents

1	Non	-equilil	brium Thermodynamics and Rheology			
	1.1		rt Review of Rheological Concepts			
		1.1.1	Basic Rheological Quantities			
		1.1.2	Basic Rheological Models			
	1.2	Exten	ded Irreversible Thermodynamics			
		1.2.1	Viscous Pressure			
		1.2.2	Viscous Pressure and Diffusion Flux			
	1.3	Rational Extended Thermodynamics				
	1.4	Theories with Internal Variables				
	1.5	5 Hamiltonian Formulations				
		1.5.1	Microscopic Level: Distribution Function			
			as an Internal Variable			
		1.5.2	Mesoscopic Level: Configuration Tensor			
			as an Internal Variable			
2		Non-equilibrium Temperature and Entropy in Flowing Ideal				
		Gases: Maximum-Entropy Approach				
	2.1	Review of Some Basic Concepts				
	2.2	Information Theory: General Formalism				
	2.3		nation Analysis of an Ideal Gas Under Viscous Pressure			
		2.3.1	Non-equilibrium Entropy and Chemical Potential:			
			General Formalism			
		2.3.2	Analysis of Plane Couette Flow: Pure Shear Effects			
		2.3.3				
	2.4		quilibrium Temperatures in Flowing Gases and Mixtures			
	2.5	Partiti	on Function for a Flowing Relativistic Ideal Gas			
3	Kinetic Theory of Flowing Gases and Phonons. Phonon					
		ydrodynamics and Heat Transport in Nanosystems				
	3.1					
		3.1.1	H Theorem			
		3.1.2	Non-equilibrium Distribution Function			

xii Contents

	3.2	Grad's Approach 6 Comparison with Exact Results 6					
	3.3	Comparison with Exact Results					
	3.4	Kinetic Theory of Phonons and Phonon Hydrodynamics					
	3.5	Poiseuille Phonon Flow and Heat Transport in Nanosystems 6					
	3.6	Boundary Conditions and Effective Thermal Conductivity					
		in Smooth and Rough Nanowires					
		3.6.1 Heat Transfer in Thin Smooth Nanowires					
		3.6.2 Heat Transfer in Thin Rough Nanowires					
	3.7	Thermal Conductivity of Porous Silicon					
4	Non	Non-ideal Fluids and Nuclear Collisions					
	4.1	Modified Equations of State and Shift of Critical Point					
		4.1.1 Van der Waals Fluids					
		4.1.2 Regular Binary Solutions					
		4.1.3 Experimental Results					
	4.2	Kinetic Theory of Dilute Non-ideal Gases					
	4.3	Comparison with Computer Simulations					
	4.4	Nuclear Collisions					
		4.4.1 Internal Collective Flows and Information Theory					
		4.4.2 Generalised Gibbs Equation					
		4.4.3 Causal Dissipative Hydrodynamics					
5	Dok	vmeric Solutions and Blends					
3	5.1	Kinetic Theory of Dilute Polymeric Solutions					
	3.1						
		5					
	5.2	1 6					
	5.2	Derivation of the Steady-State Compliance 11 Maximum-Entropy Approach 11					
	5.3	1,5 1,1					
	5.4	Entangled Solutions. Reptation Model 11					
	5.5	Polymer Blends. Double Reptation Model					
6		-equilibrium Chemical Potential and Shear-Induced					
	Effe	ects in Polymer Solutions and Blends					
	6.1	Survey of Experimental Results					
	6.2	Equilibrium Chemical Potential and Stability Analysis					
	6.3	Non-equilibrium Chemical Potential and Stability Analysis					
		6.3.1 The Choice of Non-equilibrium Variables:					
		Viscous Pressure or Configuration Tensor					
		6.3.2 Stability Analysis					
		6.3.3 Two-Fluids Model					
	6.4	Phase Diagram of Polymer Solutions Under Shear Flow					
		6.4.1 Dilute and Semidilute Polymer Solutions					
		6.4.2 Entangled Solutions 13					
	6.5	A Practical Illustration: Flow Effects in Polymer Extraction					
		from a Porous Matrix					

Contents xiii

	6.6		Induced Effects in Polymer Blends: Two-Fluid Approach
			xtended Approach
		6.6.1	Two-Fluid Approach
		6.6.2	Extended Approach
	6.7	Non-N	Newtonian Effects in Phase Separation
	6.8	Other	Approaches: Flexibility and Droplet Approaches
		6.8.1	The Flexibility Approach
		6.8.2	The Droplet Approach
7	Con	nnarico	on of Thermodynamical and Dynamical Approaches
′	7.1		mical Derivation and Generalization of Thermodynamical
	7.1	-	ity Criteria
		7.1.1	Situations Without Coupling Between Diffusion
		7.1.1	
		712	and Shear
	7.2	7.1.2	Situations with Coupling Between Diffusion and Shear
	7.2		ure Factor
		7.2.1	Generalized Ginzburg–Landau Potential
		7.0.0	in Flowing Systems
	5 2	7.2.2	Dynamical Contributions to the Chemical Potential
	7.3		ation of the Structure Factor
		7.3.1	Evolution Equations
		7.3.2	Equations of State
		7.3.3	Flow Contribution to the Structure Factor
8	She	ar-Indu	nced Migration and Flow Chromatography
	8.1		-Induced Migration of Polymers
		8.1.1	The Simplest Model for Shear-Induced Migration
		8.1.2	Non-equilibrium Chemical Potential and Effective
			Diffusion Coefficient
	8.2	Shear-	-Induced Concentration Banding and Macromolecular
			ation in Cone-and-Plate Flows
	8.3		-Induced Migration and Molecular Separation in Tubes
	0.5	Silvai	induced in granton and motorcalar department in Tuese
9			persion and Anomalous Diffusion
	9.1		nian Motion in Shear Flow
	9.2		r Dispersion and Microfluidics
	9.3		r Dispersion for Short and Intermediate Times
		9.3.1	Evolution Equation for the Flow of Matter
		9.3.2	Evolution of Effective Diffusion Coefficient:
			From Reversible to Irreversible Behaviours
		9.3.3	Entropy and Entropy Flux: From Exhaustive Information
			to the Relevant Information
	9.4	Anom	alous Diffusion and Non-equilibrium Thermodynamics
			Classical Irreversible Thermodynamics and Diffusion

xiv Contents

		9.4.2	Non-conventional Statistical Mechanics	1			
		9.4.3	Generalized Thermodynamics and				
			Anomalous Diffusion	2			
	9.5	Anoma	alous Diffusion in Flowing Systems	2			
	9.6		Dispersion and Anomalous Diffusion	2			
	9.7		ion on Fractals	2			
10	Cher	nical Re	eactions and Polymer Degradation Under Flow	2			
	10.1	Therm	odynamic Formulation	2			
	10.2	Shear-	Induced Polymer Degradation: Kinetic Analysis	2			
	10.3	Shear-	Induced Polymer Degradation:				
		Therm	odynamic Analysis	2			
	10.4	Kinetic	Theory of Chemical Reactions	2			
	10.5	Recurr	ence Method for Probability Weight Distribution				
		Under	Viscous Pressure	2			
11	Non-	eauilibr	ium Thermodynamics of Laminar				
			nt Superfluids	2			
	11.1		ial Concepts and Phenomena of Superfluids	2			
	11.2		vo-Fluid Model and Second Sound	2			
			Evolution Equations and Wave Propagation	2			
		11.2.2	Thermodynamics of Superfluid Helium	2			
	11.3		stended One-Fluid Model of Liquid Helium II	2			
	11.4		zed Vortices in Rotation and Counterflow	2			
		11.4.1	Macroscopic Description of Vortex Friction	2			
		11.4.2	Rotating Frame	2			
		11.4.3	Counterflow Turbulence	2			
	11.5						
			ntized Vortices	2			
		11.5.1	Rotating Cylinders	2			
		11.5.2	Second Sound and Counterflow Turbulence	2			
	11.6		ion Equation for the Vortex Line Density	2			
	11.0	11.6.1	Transition from the Laminar to the Turbulent Regime				
		11.6.2	Simultaneous Rotation and Counterflow	2			
		11.6.3	Non-equilibrium Thermodynamics of Vortex Tangles	2			
	11.7		dynamics of Turbulent Superfluids	2			
	••			_			
Ap	•		perimental Data on Polymer Solutions	2			
	A.1		yrene in Dioctyl-Phthalate (PS/DOP)	2			
	A.2		yrene in Transdecalin (PS/TD)	2			
	A.3	Polysty	yrene Dissolved in Oligomeric Polystyrene	2			
Ap	pendix	B Lic	quid Crystals	2			
	B.1	Equilib	orium Thermodynamics and the Isotropic-Nematic				
			Transition	2			

Contents xv

	B.1.1 Phase Transition Induced by Temperature Changes	264			
	B.1.2 Phase Transition Induced by Density Changes	265			
B.2	Dynamic Equations in the Presence of a Flow	266			
B.3	Thermodynamic Formulation	269			
B.4	Maximum-Entropy Approach	270			
Appendix	C Summary of Vector and Tensor Notation	273			
C.1	Symmetric and Antisymmetric Tensors	273			
C.2	Decomposition of a Tensor	273			
C.3	Scalar (or Dot) and Tensorial (Inner) Products	274			
C.4	(Inner) Tensorial Product (Also Named Dyadic Product)	274			
C.5	Cross Multiplication Between Two Vectors and Between				
	a Tensor and a Vector	275			
C.6	Differentiation	275			
C.7	Tensor Invariants	276			
Appendix	D Useful Integrals in the Kinetic Theory of Gases	277			
Appendix	E Some Physical Constants	279			
References					
Index		297			

Chapter 1 Non-equilibrium Thermodynamics and Rheology

Local-equilibrium thermodynamics assumes that the equations of state retain the same form out of equilibrium as in equilibrium, but with a local meaning (Prigogine 1961; De Groot and Mazur 1962; Gyarmati 1970). According to this point of view, there is not strictly any especial thermodynamic features characteristic of flowing fluids, since the flow does not change the equations of state, though it may modify the transport equations. This approach is insufficient to deal with systems with internal degrees of freedom, in which case the flow may influence the thermodynamic equations of state through its action on such internal variables. In such occasions (Meixner 1949, 1954; Verhas 1997; Lhuillier and Ouibrahim 1980; Maugin and Drouot 1983; Maugin and Muschik 1994a, b, Maugin 1999) one includes in the set of thermodynamic variables some internal variables describing the relevant details of the microstructure of the system, such as, for instance, the polymeric configuration.

In the 1960s was proposed the so-called rational thermodynamics (Truesdell 1971, 1984), which assumes that the entropy and the (absolute) temperature are primitive quantities, not restricted to situations near local-equilibrium. Instead of a local-equilibrium assumption, it was assumed that the entropy, or the free energy, could depend on the history of the strain, or of the rate of strain, or of the temperature gradient, thus allowing for an explicit influence of the flow on the thermodynamic analysis through the history of these non-equilibrium variables. The theory developed a powerful and elegant formalism to obtain thermodynamic restrictions on the memory functions relating viscous stress to the history of the strain. However, the analysis was centred on the constitutive equations, but it paid little attention to the consequences of the generalised entropy on the non-equilibrium equations of state.

At the end of the 1960s, a new approach, called extended irreversible thermodynamics (EIT) (Jou et al. 1988, 1992, 1996, 1998, 1999, 2010; Müller and Ruggeri 1998; Sieniutycz and Salamon 1992; Eu 1992, 1998, 2002; Wilmanski 1998; Nettleton and Sobolev 1995a, b, 1996), was proposed and it was much developed during the 1980s and 1990s. (For a wide bibliography on this topic see http://telemaco. uab.es or Nettleton and Sobolev 1995a, b, 1996; Jou et al. 1988, 1992, 1998, 1999, 2010). This theory assumes that the entropy depends, besides the classical variables, on the dissipative fluxes, such as the viscous pressure tensor, the heat flux or the

1

diffusion flux. Its motivation is to make the relaxational transport equations for the heat flux (Maxwell–Cattaneo equation) or the viscous pressure tensor (Maxwell viscoelastic fluids) compatible with the positiveness of the entropy production, which is not satisfied, in general, when such generalised transport equations are combined with the local-equilibrium entropy. The direct influence of the viscous pressure tensor and other fluxes on the thermodynamic potentials clearly opens a way towards a thermodynamics under flow.

Once the expression of the entropy is known, there is no difficulty in deriving the corresponding equations of state, which are directly obtained as the first derivatives of the entropy with respect to the basic variables. Thus, EIT links the generalised transport equations with generalised equations of state which contain non-equilibrium contributions. A natural question concerns the physical meaning of these equations of state which, of course, depend on the fluxes and therefore differ from their analogous local-equilibrium expressions. Recall that in classical thermodynamics, the first derivatives of the entropy with respect to the internal energy, the volume and the number of moles are related to the absolute temperature, the pressure, and the chemical potential, respectively. At this point, it may be asked whether the derivatives of the generalised entropy introduced in EIT still enable one to define an absolute non-equilibrium temperature as well as a non-equilibrium pressure and a non-equilibrium chemical potential. This is a very subtle question which has, however, received partial answers in recent years, after that some specific thought experiments were proposed (Casas-Vázquez and Jou 1994) a real experiment was interpreted (Luzzi et al. 1997) and non-equilibrium molecular dynamics simulations were carried out (Baranyai 2000a, b; Daivis 2008). Here, we will mainly concentrate our attention on the equation of state for the chemical potential at a given temperature and pressure; this will play a central role in Chaps. 6–10.

In this chapter, we provide a short introduction to the basic rheological concepts. Furthermore, we present EIT, both as an extension of the classical theory and of the rational thermodynamics, and we compare it with two alternative thermodynamic theories: the internal variable approach and the Hamiltonian formalisms. We have not aimed to be exhaustive, but only to provide the necessary basis to work out the consequences of the non-equilibrium equations of state; therefore, we have omitted a comparison with other valuable theories, such as the matrix model of irreversible processes (Jongschaap 1990), or variational approaches (Sieniutycz 1994). Sections 1.3 and 1.5 correspond to a slightly more advanced and specialised level: they may be skipped in a first reading, but will be stimulating to the researcher interested in going beyond the linear approximation presented in Sects. 1.2 and 1.4.

1.1 A Short Review of Rheological Concepts

Since we are dealing with flowing fluids, it is not surprising that in our analysis we will often find rheological quantities, rheology being the science of flow. Here, we provide a short review of some basic rheological concepts and of the most

widely used rheological models. The knowledge of these is necessary since we will often relate rheology and thermodynamics. It must be emphasized that we have attempted to focus our attention on the concepts necessary for the purposes of the present monograph, rather than to provide an extensive account of the wide topic of rheology.

1.1.1 Basic Rheological Quantities

A central quantity in fluid mechanics and rheology is the viscous pressure tensor \mathbf{P}^{ν} , which describes the forces between neighbouring fluid elements moving at different speeds. The knowledge of these forces is necessary to describe the evolution of the flow. The relation between the viscous pressure tensor and the velocity gradient, the tensor describing the local features of the flow, plays an essential role in rheology. The coefficients relating these tensors depend on the fluid being considered and are the basic quantities of interest in rheology. The main coefficients are defined by considering the simplest flow exhibiting a velocity gradient, namely, the plane Couette flow, i.e. the flow between two plane parallel layers moving at different speeds.

The main rheological quantities of interest in steady flows are the shear viscosity and the first and second normal stress coefficients $\eta(\dot{\gamma})$, $\Psi_1(\dot{\gamma})$ and $\Psi_2(\dot{\gamma})$, respectively, which are defined as

$$P_{12}^{\nu} = -\eta(\dot{\gamma})\dot{\gamma},\tag{1.1a}$$

$$P_{11}^{\nu} - P_{22}^{\nu} = -\Psi_1(\dot{\gamma})\dot{\gamma}^2, \tag{1.1b}$$

$$P_{22}^{\nu} - P_{33}^{\nu} = -\Psi_2(\dot{\gamma})\dot{\gamma}^2, \tag{1.1c}$$

where P_{ij}^{ν} , with i, j = 1, 2, 3 indicate components of the viscous pressure tensor \mathbf{P}^{ν} and $\dot{\gamma}$ the shear rate in a planar Couette flow, i.e. $\dot{\gamma} = \partial v_x/\partial v_y$. We will often take as component x or 1 the component along the velocity, y or 2 the component along the velocity gradient, and z or 3 the component orthogonal to the two previous ones. In the so-called Newtonian fluids, the normal stress coefficients vanish. Recall that \mathbf{P}^{ν} is related to the total pressure tensor \mathbf{P} as $\mathbf{P} = p\mathbf{U} + \mathbf{P}^{\nu}$, with p the equilibrium pressure and \mathbf{U} the unit tensor.

In non-steady situations some memory effects, such as those described in viscoelastic models, appear. The rheological properties thus depend on the frequency of the perturbation: for instance, viscoelastic liquids are materials which behave as Newtonian liquids under low frequency perturbations (low in comparison with the inverse of a characteristic relaxation time), and as elastic solids at high frequencies. The shear linear viscoelastic effects are usually summarized in terms of a complex viscosity $\eta^*(\omega)$, or, alternatively, in terms of two other complex functions: a complex stress–strain modulus $G^*(\omega)$; or a complex compliance $J^*(\omega)$. Assuming the simplest oscillatory behaviour for the shear strain γ and the shear stress P_{12}^{ν}

$$\gamma = \gamma^0 \cos \omega t, \quad P_{12}^{\nu} = P_{12}^{\nu 0} \cos \omega t,$$
 (1.2)

with γ^0 and $P_{12}^{\nu 0}$ the amplitudes of the respective oscillations, the coefficients $\eta^*(\omega)$, $G^*(\omega)$ and $J^*(\omega)$ are defined as (Ferry 1980; Coleman et al. 1966; Tanner 1988; Bird et al. 1987a)

$$P_{12}^{\nu 0} = -\eta^*(\omega)\dot{\gamma}^0, \tag{1.3a}$$

$$P_{12}^{\nu 0} = -G^*(\omega)\gamma^0, \tag{1.3b}$$

$$\gamma^0 = -J^*(\omega)P_{12}^{\nu 0},\tag{1.3c}$$

where γ^0 and $\dot{\gamma}^0$ are the amplitudes of the oscillatory shear strain and shear rate, respectively. These three functions are closely related to each other, stemming from their definition, by means of

$$\eta^*(\omega) = (i\omega)^{-1} G^*(\omega), \quad J^*(\omega) = 1/G^*(\omega),$$
 (1.4)

where i is the imaginary unit.

The three mentioned quantities are often split in their real and imaginary parts as

$$J^*(\omega) = J' - iJ'', \quad G^*(\omega) = G' + iG'', \quad \eta^*(\omega) = \eta' - i\eta''.$$
 (1.5)

Complex quantities are used here to account both for the response in phase with the perturbation (real part) as the response 90° out of phase (imaginary part). Note that $J'(\omega)$ is the strain in phase with stress divided by the stress, so that it is a measure of the energy stored and recovered per cycle, while $J''(\omega)$ is the strain 90° out of phase with the stress divided by the stress, and it is a measure of the energy lost into heat per cycle. It is not then surprising that the compliance will play an important role in the connection between thermodynamics and rheology.

1.1.2 Basic Rheological Models

In the study of polymeric systems it is assumed that the viscous pressure tensor depends not only on the velocity gradient but also on its own time rate of change by means of a relaxational term, which will account for the different behaviours observed at low and high frequency. Such a relaxational contribution is usually written in terms of a frame-indifferent time derivative (Ferry 1980; Coleman et al.

1966; Tanner 1988; Bird et al. 1987a), as the co-rotational derivative or the upper convected derivative, rather than in terms of the material time derivative. We will discuss here these different time derivatives, leading to different rheological models.

1.1.2.1 Linear Viscoelastic Models

In the simplest Maxwell model, the viscous pressure tensor is described by the constitutive equation

$$\frac{\mathrm{d}\mathbf{P}^{\nu}}{\mathrm{d}t} = -\frac{1}{\tau}\mathbf{P}^{\nu} - 2\frac{\eta}{\tau}\mathbf{V},\tag{1.6}$$

with **V** the symmetric part of the velocity gradient, whose components are given by $V_{ij} = (1/2)[(\partial v_j/\partial x_i) + (\partial v_i/\partial x_j)]$, and where η is the shear viscosity and τ the relaxation time. Maxwell's model captures the essential idea of viscoelastic models: the response to slow perturbations is that characteristic of a viscous fluid, namely $\mathbf{P}^v = -2\eta\mathbf{V}$, whereas for fast perturbations, with characteristic time t of the order of τ or less, it behaves as an elastic solid with \mathbf{P}^v standing for the elastic pressure, $\mathbf{P}^v = -2G(\nabla X)^s$, X being the deformation vector field, and $\mathbf{G} = \eta/\tau$ being related to the elastic Young modulus of the material.

However, the material time derivative used in (1.6) is not very satisfactory, neither from a theoretical viewpoint, since it is not invariant under rigid rotations, nor on the practical predictions, and it must be substituted by some frame-indifferent derivatives which are invariant under rigid motions of the system. The simplest example of such derivatives is the co-rotational time derivative

$$\frac{\mathrm{D}\mathbf{P}^{\nu}}{\mathrm{D}t} = \frac{\mathrm{d}\mathbf{P}^{\nu}}{\mathrm{d}t} + \mathbf{W} \cdot \mathbf{P}^{\nu} - \mathbf{P}^{\nu} \cdot \mathbf{W},\tag{1.7}$$

where **W** is the antisymmetric part of the velocity gradient, whose components are given by $W_{ij} = (1/2)[(\partial v/\partial x_i) - (\partial v/\partial x_j)]$. This derivative describes the rate of change of **P**^v as seen in a local reference system which rotates with the fluid. Other widely used frame-indifferent time derivatives are the upper or contravariant convected time derivative, namely

$$D^{\uparrow} \mathbf{P}^{\nu} = \frac{\mathrm{d} \mathbf{P}^{\nu}}{\mathrm{d} t} - \left[(\nabla \mathbf{v})^{T} \cdot \mathbf{P}^{\nu} + \mathbf{P}^{\nu} \cdot (\nabla \mathbf{v}) \right], \tag{1.8a}$$

or the lower or covariant convected time derivative

$$D_{\downarrow} \mathbf{P}^{\nu} = \frac{\mathrm{d} \mathbf{P}^{\nu}}{\mathrm{d}t} + (\nabla \nu) \cdot \mathbf{P}^{\nu} + \mathbf{P}^{\nu} \cdot (\nabla \nu)^{T}, \tag{1.8b}$$

where superscript T indicates transposition.

If one uses (1.8a) instead of the material time derivative, one has the upperconvected Maxwell model (Ferry 1980; Coleman et al. 1966; Tanner 1988; Bird et al. 1987a) for which the evolution equation for the viscous pressure tensor \mathbf{P}^{ν} has the form

$$\frac{\mathrm{d}\mathbf{P}^{\nu}}{\mathrm{d}t} - (\nabla \mathbf{v})^{T} \cdot \mathbf{P}^{\nu} - \mathbf{P}^{\nu} \cdot (\nabla \mathbf{v}) = -\frac{1}{\tau} \mathbf{P}^{\nu} - 2\frac{\eta}{\tau} \mathbf{V}. \tag{1.9}$$

If, instead of (1.8a), the time derivative (1.8b) is used, one has the so-called lower-convected Maxwell model.

The fluid will be considered as incompressible from here on. This implies that $\nabla \cdot \mathbf{v} = 0$ and since $\nabla \cdot \mathbf{v}$ is the trace of the $\nabla \mathbf{v}$ tensor one could think that this will mean that the trace of the viscous pressure tensor will also vanish, i.e. $\text{Tr} \mathbf{P}^{\nu} = 0$. However, though it is true that the linear contribution to $\text{Tr} \mathbf{P}^{\nu}$, which is proportional to $\nabla \cdot \mathbf{v}$, will be zero, second-order non-linear contributions may appear, giving a non-vanishing trace of \mathbf{P}^{ν} .

For further discussions it will be convenient to have explicit expressions for \mathbf{P}^{ν} in some steady flows. In a purely shear flow corresponding to $\nu = (\nu_x(y), 0, 0)$, the velocity gradient tensor, is

$$\nabla v = \begin{pmatrix} 0 & 0 & 0 \\ \dot{v} & 0 & 0 \\ 0 & 0 & 0 \end{pmatrix},\tag{1.10}$$

where $\dot{\gamma}$ is the shear rate. Introduction of (1.10) into (1.7) yields, in the steady situation, for the co-rotational Maxwell model

$$\mathbf{P}^{\nu} = \begin{pmatrix} -\tau \eta \dot{\gamma}^2 (1 + \tau^2 \dot{\gamma}^2)^{-1} & -\eta \dot{\gamma} (1 + \tau^2 \dot{\gamma}^2)^{-1} & 0 \\ -\eta \dot{\gamma} (1 + \tau^2 \dot{\gamma}^2)^{-1} & \tau \eta \dot{\gamma}^2 (1 + \tau^2 \dot{\gamma}^2)^{-1} & 0 \\ 0 & 0 & 0 \end{pmatrix}, \quad (1.11)$$

and therefore the steady-state viscometric functions are

$$P_{12}^{\nu} = -\eta \dot{\gamma} (1 + \tau^2 \dot{\gamma}^2)^{-1}, \tag{1.12a}$$

$$P_{11}^{\nu} - P_{22}^{\nu} = -2\tau \eta \dot{\gamma}^2 (1 + \tau^2 \dot{\gamma}^2)^{-1}, \tag{1.12b}$$

$$P_{22}^{\nu} - P_{33}^{\nu} = \tau \eta \dot{\gamma}^2 (1 + \tau^2 \dot{\gamma}^2)^{-1}. \tag{1.12c}$$

For the upper-convected Maxwell model (1.9), one has

$$\mathbf{P}^{\nu} = \begin{pmatrix} -2\tau \eta \dot{\gamma}^2 & -\eta \dot{\gamma} & 0 \\ -\eta \dot{\gamma} & 0 & 0 \\ 0 & 0 & 0 \end{pmatrix}. \tag{1.13}$$

The corresponding steady-state viscometric functions are thus

$$P_{12}^{\nu} = -\eta \dot{\gamma}, \quad P_{11}^{\nu} - P_{22}^{\nu} = -2\tau \eta \dot{\gamma}^2, \quad P_{22}^{\nu} - P_{33}^{\nu} = 0,$$
 (1.14)

so that the second normal stress is zero and the first normal stress coefficient Ψ_1 is

$$\Psi_1(\dot{\gamma}) = 2\tau \eta. \tag{1.15}$$

For the lower-convected Maxwell model, the viscous pressure tensor in the steady state is given by

$$\mathbf{P}^{\nu} = \begin{pmatrix} 2\tau \eta \dot{\gamma}^2 - \eta \dot{\gamma} & 0 \\ -\eta \dot{\gamma} & 0 & 0 \\ 0 & 0 & 0 \end{pmatrix}. \tag{1.16}$$

and therefore, the viscometric coefficients are given by

$$P_{12}^{\nu} = -\eta \dot{\gamma}, \quad P_{11}^{\nu} - P_{22}^{\nu} = 2\tau \eta \dot{\gamma}^2, \quad P_{22}^{\nu} - P_{33}^{\nu} = 0.$$
 (1.17)

It turns out that the upper-convected model agrees rather satisfactorily with a wide range of experimental results, while the predictions (1.17) of the lower-convected model or (1.12) of the co-rotational model are at variance with experiments.

Another flow of much viscometric and practical interest is the planar extensional flow, in which the velocity field has two components $\mathbf{v} = (v_x(x), v_y(y), 0)$, such that its gradient takes the form

$$\nabla v = \begin{pmatrix} \dot{\varepsilon} & 0 & 0 \\ 0 & -\dot{\varepsilon} & 0 \\ 0 & 0 & 0 \end{pmatrix}, \tag{1.18}$$

with $\dot{\varepsilon}(=\partial v_x/\partial x=-\partial v_y/\partial y)$ the extensional rate. In the steady state, (1.6) yields

$$\mathbf{P}^{\nu} = \begin{pmatrix} -2\eta \dot{\varepsilon} (1 - 2\tau \dot{\varepsilon})^{-1} & 0 & 0\\ 0 & 2\eta \dot{\varepsilon} (1 + 2\tau \dot{\varepsilon})^{-1} & 0\\ 0 & 0 & 0 \end{pmatrix}. \tag{1.19}$$

The expressions of P^{ν} for the other viscoelastic models may easily be obtained.

In the previous Maxwell models we have considered only one relaxation time. In many cases, one must consider that \mathbf{P}^{ν} is the sum of several (or many) independent contributions, i.e. $\mathbf{P}^{\nu} = \sum_{j} \mathbf{P}^{\nu}_{j}$ with each \mathbf{P}^{ν}_{j} obeying a linear evolution equation such as (1.6) or (1.9), characterized by its own viscosity η_{i} and relaxation time τ_{i} . These independent contributions arise from the different internal degrees of freedom of the macromolecule, as will be explained in detail in Chap. 5. These models are known as generalised Maxwell models.

It is often useful, in linear models for viscoelasticity, to write the viscous pressure tensor in terms of a memory function as

$$\mathbf{P}^{\nu} = -\int_{-\infty}^{t} G(t - t') \dot{\gamma}(t') \mathrm{d}t'$$
 (1.20)

where the memory function G(t-t') is known as the relaxation modulus, and $\dot{\gamma}$ as the rate-of-strain tensor, which is twice **V**. The Fourier transform of G(t-t') is the complex strain-stress modulus $G^*(\omega)$ defined in (1.3). In a generalised Maxwell model, one has for G(t-t')

$$G(t - t') = \sum_{j} (\eta_j / \tau_j) \exp[-(t - t') / \tau_j], \tag{1.21}$$

with η_i and τ_i the different viscosities and relaxation times corresponding to the different degrees of freedom of the macromolecules (see Chap. 5). If one has only one relaxation time, this expression is the one corresponding to the simple Maxwell model (1.6). Note that for t = t' one has $G(0) = \eta/\tau$ and therefore, according to (1.4b) the compliance is $J(0) = \tau/\eta$. The value J(0) is usually called the steady-state compliance, and it will appear in the generalised Gibbs Eq. (1.31).

In a small-amplitude oscillatory motion, integration of (1.20) and the use of the definitions (1.3–1.5) of η^* and G^* yields

$$\eta'(\omega) = \sum_{j} \eta_{j} [1 + (\tau_{j}\omega)^{2}]^{-1}, \quad \eta''(\omega) = \sum_{j} \eta_{j} \tau_{j} \omega [1 + (\tau_{j}\omega)^{2}]^{-1},$$
 (1.22)

or

$$G'(\omega) = \sum_{j} \eta_{j} \tau_{j} \omega^{2} \left[1 + (\tau_{j} \omega)^{2} \right]^{-1}, \quad G''(\omega) = \sum_{j} \eta_{j} \omega \left[1 + (\tau_{j} \omega)^{2} \right]^{-1},$$
(1.23)

where η_i and τ_i now correspond to the *i*th degree of freedom.

1.1.2.2 Non-linear Viscoelastic Models

In the models defined by (1.6) or (1.9), the viscometric coefficients do not depend on the shear rate. However, there are many phenomena which show that, in general, the viscometric functions depend in a complicated way on the shear rate and which require non-linear constitutive equations for their description. For instance, many fluids exhibit a decrease in viscosity with increasing shear rate, an effect known as "shear thinning" (or pseudoplasticity). A few fluids (usually concentrated suspensions of very small particles) exhibit the opposite behaviour, namely, an increase of viscosity with shear rate, which is known as "shear thickening" (or dilatancy).

Still another non-linear effect is viscoplasticity, which is shown by fluids (such as paints and pastes) which do not flow unless they are acted on by a shear higher than a threshold value.

A well known and rather general non-linear model is the so-called eight-constants Oldroyd model (Ferry 1980; Coleman et al. 1966; Tanner 1988; Bird et al. 1987a), defined by the following constitutive equation

$$\mathbf{P}^{\nu} + \lambda_{1} \mathbf{P}^{\nu}_{(1)} + \frac{1}{2} \lambda_{3} (\mathbf{V} \cdot \mathbf{P}^{\nu} + \mathbf{P}^{\nu} \cdot \mathbf{V}) + \frac{1}{2} \lambda_{5} (\operatorname{Tr} \mathbf{P}^{\nu}) \mathbf{V} + \frac{1}{2} \lambda_{6} (\mathbf{P}^{\nu} : \mathbf{V}) \mathbf{U}$$

$$= -\eta_{0} \left[\mathbf{V} + \lambda_{2} \mathbf{V}_{(1)} + \lambda_{4} \mathbf{V} \cdot \mathbf{V} + \frac{1}{2} \lambda_{7} \mathbf{V} : \mathbf{V} \mathbf{U} \right]$$
(1.24)

where **U** is the unit tensor and $V_{(1)}$ is the convected time derivative of **V**, the symmetric part of the velocity gradient, and $P_{(1)}^{\nu}$ is the convected time derivative of P^{ν} . For a steady shear flow, its explicit form is

$$\mathbf{V}_{(1)} = \begin{pmatrix} 0 & 1 & 0 \\ 1 & 0 & 0 \\ 0 & 0 & 0 \end{pmatrix} \frac{d\dot{\gamma}}{dt} - 2 \begin{pmatrix} 1 & 0 & 0 \\ 0 & 0 & 0 \\ 0 & 0 & 0 \end{pmatrix} \dot{\gamma}^2. \tag{1.25}$$

It follows from (1.24) and (1.25), after a cumbersome but straightforward calculation, that in steady-state shear flow the viscometric functions are

$$\frac{\eta}{\eta_0} = \frac{1 + \sigma_2 \dot{\gamma}^2}{1 + \sigma_1 \dot{\gamma}^2},\tag{1.26}$$

with $\sigma_i = \lambda_i(\lambda_3 + \lambda_5) + \lambda_{i+2}(\lambda_1 - \lambda_3 - \lambda_5) + \lambda_{i+5}(\lambda_1 - \lambda_3 - \frac{3}{5}\lambda_5)$, and

$$\frac{\psi_1}{2\eta_0\lambda_1} = \frac{\eta(\dot{\gamma})}{\eta_0} - \frac{\lambda_2}{\lambda_1},\tag{1.27}$$

$$\frac{\psi_2}{\eta_0 \lambda_1} = -\frac{\psi_1}{2\eta_0 \lambda_1} + \frac{\lambda_1 - \lambda_3}{\lambda_1} \frac{\eta}{\eta_0} - \frac{\lambda_2 - \lambda_4}{\lambda_1}.$$
 (1.28)

The 8-constants Oldroyd model is very general, and we recover from it several especially interesting and widely used models. Indeed, the linear model (1.9) is obtained from (1.24) when $\lambda_2 = \cdots = \lambda_7 = 0$. Furthermore, other well known non-linear models which are special cases of (1.24) are:

- the second-order Rivlin–Ericksen fluid ($\lambda_1 = \lambda_3 = \lambda_5 = \lambda_6 = \lambda_7 = 0$), for which the viscometric functions are $\eta = \eta_0$, $\Psi_1 = -2\eta_0\lambda_2$, $\Psi_2 = \eta_0\lambda_4$;
- the co-rotational Jeffreys model, for which $\lambda_3 = \lambda_1$, $\lambda_4 = \lambda_2$, $\lambda_5 = \lambda_6 = \lambda_7 = 0$, for which the viscometric functions are $\eta(\dot{\gamma})$, $\psi_1(\dot{\gamma})$ and $\Psi_2 = -\frac{1}{2}\Psi_1$;
- the convected Jeffreys model ($\lambda_3 = \lambda_4 = \lambda_5 = \lambda_6 = \lambda_7 = 0$), and, therefore, the viscometric functions are $\eta = \eta_0$, $\Psi_1 = 2\eta_0(\lambda_1 \lambda_2)$ and $\Psi_2 = 0$.

In fact, the Oldroyd model is not truly universal, because the variation in viscosity predicted by (1.26) is too low to describe some real materials, in which the viscosity changes a hundred-fold in a finite range of shear rate. In (1.24), the coefficients λ_i are assumed not to depend on the shear rate. In more general situations, they could be functions of the scalar invariants of the velocity gradient. In some situations described below we will mention some of these non-linear models, but, in general, our analysis will be restricted to linear situations.

1.2 Extended Irreversible Thermodynamics

After having reviewed the most usual constitutive equations for viscoelastic fluids, we start the analysis of the thermodynamic aspects. First of all, we recall the basic ideas of the classical formulation of irreversible thermodynamics (Prigogine 1961; De Groot and Mazur 1962; Gyarmati 1970), which is based on the local equilibrium hypothesis. It states that, despite the inhomogeneous nature of the system, i.e. the values of its physical quantities differ from place to place, the fundamental thermodynamic relations are still valid locally. In particular, the Gibbs equation expressing the differential form of the entropy in terms of its classical variables (internal energy, volume and number of moles of the chemical components of the system) is locally valid.

By combining the Gibbs equation and the evolution equations for mass, momentum and energy, one obtains an expression for the evolution equation for the entropy, with explicit forms for the entropy flux and the entropy production in terms of the fluxes (heat flux, diffusion flux, viscous pressure tensor, reaction rates) and of the conjugated thermodynamic forces, which are expressed as functions of the gradients of temperature, chemical potential, velocity, and of the chemical affinities of the reactions.

Finally, one relates the fluxes to the forces by means of constitutive equations which are required to obey the positive character of the entropy production. In the simplest but most usual versions, one assumes linear constitutive equations in which the fluxes are linear combinations of the thermodynamic forces. In this case it may be shown that the matrix of the transport coefficients relating the fluxes to the forces must obey the reciprocity relations established by Onsager and Casimir.

In this book, we want to focus our attention on the characteristic new aspects that the flow implies on the thermodynamics. As has been said, the classical theory retains the classical Gibbs equation, and therefore the thermodynamic relations are not changed by the presence of a flow. Therefore, instead of presenting all the details of the classical theories, we will directly write the main ideas and concepts of extended irreversible thermodynamics (EIT), which will be the basis of the analyses in this monograph, and we will explain how they reduce to the corresponding local-equilibrium expressions.

EIT, which has been widely discussed in the companion volume (Jou et al. 2010), assumes that the entropy may depend, in addition to the classical variables, on the

dissipative fluxes. In Sect. 1.2.1, we discuss a one-component fluid, in which we neglect thermal conduction and consider that the only non-equilibrium quantity in the space of independent thermodynamic variables is the viscous pressure tensor (Jou et al. 2010; Lebon et al. 1986, 1988). In Sect. 1.2.2, we consider a two-component mixture and incorporate the effects of the diffusion flux, which will play an important role in Chaps. 7–10.

1.2.1 Viscous Pressure

According to EIT, the generalised Gibbs equation for a simple unicomponent fluid in the presence of a non-vanishing viscous pressure tensor is, up to the second order in \mathbf{P}^{ν}

$$ds = T^{-1}du + T^{-1}pdv - \frac{\tau v}{2\eta T}\mathbf{P}^{v} : d\mathbf{P}^{v},$$
(1.29)

with u and v the specific internal energy and the specific volume, T and p the absolute temperature and the thermodynamic pressure, η the shear viscosity and τ the relaxation time of \mathbf{P}^v as defined in (1.6) or (1.9). To avoid unnecessary formal complications we use as a variable the whole tensor \mathbf{P}^v , instead of splitting it into the trace and the corresponding traceless part. In Sect. 1.2.2, a derivation of (1.29) will be presented. The first two terms on the right-hand side on (1.29) correspond to the classical Gibbs equation, whereas the third term is characteristic of EIT. It is related to the non-vanishing character of the relaxation time τ . When τ tends to zero, both the relaxational terms in the constitutive Eqs. (1.6) and (1.9) and the non-equilibrium contribution to the entropy in (1.29) tend to zero, in such a way that the constitutive equations tend to the usual Newton–Stokes law for the viscous pressure tensor and (1.29) reduces to the classical Gibbs equation. Thus, we stress that the presence of relaxational terms in the constitutive Eqs. (1.6) or (1.9) implies the presence of a non-equilibrium contribution to the Gibbs Eq. (1.29).

In general one could take, instead of a single relaxation time, several relaxation times and one could assume that \mathbf{P}^{ν} is the sum of several different contributions \mathbf{P}_{i}^{ν} , each of them with its own relaxation time τ_{i} and its own viscosity η_{i} , as in the generalised Maxwell models introduced in (1.21). In this case, one would have instead of (1.29)

$$ds = T^{-1}du + T^{-1}pdv - \sum_{i} (\tau_{i}v/2\eta_{i}T) \mathbf{P}_{i}^{v} : d\mathbf{P}_{i}^{v}.$$
(1.30)

The total viscosity η is $\eta = \sum_{i} \eta_{i}$. Consequently, τ in (1.29) may be considered as an averaged relaxation time, defined as $\tau = (\sum_{i} \tau_{i} \eta_{i})(\sum_{i} \eta_{i})^{-1}$. Note that in terms of the steady-state compliance introduced after (1.21) $(J = \tau/\eta)$, one may write the generalised Gibbs Eq. (1.29) as

$$ds = T^{-1}du + T^{-1}pdv - \frac{vJ}{2T}\mathbf{P}^{v} : d\mathbf{P}^{v},$$
 (1.31)

which, after integration, becomes

$$s(u, v, \mathbf{P}^{v}) = s_{eq}(u, v) - \frac{vJ}{4T}\mathbf{P}^{v} : \mathbf{P}^{v},$$
(1.32)

where subscript eq stands for the equilibrium value.

For shear flow, the generalised entropy (1.32) reduces to

$$s\left(u, v, P_{12}^{v}\right) = s_{\text{eq}}(u, v) - \frac{vJ}{4T} \left[2\left(P_{12}^{v}\right)^{2} + 2\left(P_{12}^{v}\right)^{4} \right],\tag{1.33}$$

if one takes into account that for the model described by (1.13) $P_{11}^{\nu} = -2J(P_{12}^{\nu})^2$. Notice that P_{12}^{ν} is of the order of $\dot{\gamma}$, and for low values of $\dot{\gamma}$ we may neglect the contribution of P_{12}^{ν} of order higher than two and write

$$s(u, v, P_{12}^{v}) = s_{eq}(u, v) - \frac{vJ}{2T} (P_{12}^{v})^{2}.$$
 (1.34)

Instead of the internal energy it is usual to take as an independent variable the temperature, because it is more accessible to direct measurement. The thermodynamic potential which has as variables temperature and volume is the Helmholtz free energy f, defined as

$$f = u - Ts, (1.35a)$$

where we are using values per unit mass. In view of its interest we comment also on the corresponding non-equilibrium contributions of a viscous pressure tensor. We are interested in the contribution Δf of the flow to the free energy, for which we write, at constant T,

$$\Delta f = \Delta u - T \Delta s, \tag{1.35b}$$

with

$$\Delta f = f - f_{eq}, \quad \Delta u = u - u_{eq}, \quad \Delta s = s(u, v, \mathbf{P}^v) - s_{eq}(u_{eq}, v).$$
 (1.35c)

Note that for fixed temperature, the internal energy under flow u is in general not equal to the internal energy at equilibrium, because the flow may stretch or deform the molecules thus storing internal energy in them.

In order to evaluate the entropic contribution to the free energy, as given in (1.36), we expand $s_{eq}(u, v)$ around the equilibrium value $s_{eq}(u_{eq}, v)$ as

$$s_{\rm eq}(u,v) = s_{\rm eq}(u_{\rm eq},v) + \left(\frac{\partial s_{\rm eq}}{\partial u}\right)_{u=u_{\rm eq}} (u-u_{\rm eq}) + \cdots$$
 (1.36a)

which when inserted in (1.35b) leads to

$$\Delta f = u - u_{\text{eq}} - T \left[s_{\text{eq}}(u, v) - (vJ/2T) (P_{12}^{v})^{2} - s_{\text{eq}}(u_{\text{eq}}, v) \right] = \frac{1}{2} vJ (P_{12}^{v})^{2},$$
(1.36b)

when use of (1.34) and (1.36a) is made.

In a more general situation, when one is not restricted to second order in shear rate, one assumes that the energy contribution, proportional to $(P_{12}^{\nu})^2$, is much higher than the entropic one. We will comment on this point later from a microscopic point of view. One should thus have

$$\Delta f = \Delta u = vJ(P_{12}^v)^2.$$
 (1.37)

This is consistent with the meaning of $J(P_{12}^{\nu})^2$ as stored energy. An expression slightly more general than (1.29) has been derived by Daivis (2008) using the shear rate $\dot{\gamma}$ instead of the viscous pressure as independent variable. His derivation is based on the analysis of the work stored in a viscoelastic fluid when it is brought from the equilibrium state to a shearing steady state. This author writes the generalized Helmholtz free energy as

$$df = -sdT - pdv + \zeta d\dot{\gamma}, \qquad (1.38)$$

with ζ the corresponding conjugate parameter to $\dot{\gamma}$, from which it is obtained the Maxwell relation

$$\left(\frac{\partial \zeta}{\partial \nu}\right)_{T,\dot{\gamma}} = -\left(\frac{\partial p}{\partial \dot{\gamma}}\right)_{T,\nu} = \frac{\partial^2 f}{\partial \nu \partial \dot{\gamma}}.$$
 (1.39)

He carried out non-equilibrium molecular dynamics simulations of a simple shearing fluid, but these Maxwell relations were not verified. Daivis saw as a possible source of disagreement the sensibility of these quantities with temperature, and the fact that out of equilibrium one may define several different temperatures. Indeed, he used for T the kinetic temperature instead of the thermodynamic non-equilibrium temperature depending on $\dot{\gamma}$, which should be used for the sake of internal consistence. Analyses of Maxwell relations stemming from non-equilibrium potentials seem worth to be pursued.

In our formalism, and in the steady state, (1.29) could be rewritten as

$$dS = T^{-1}dU + T^{-1}pdV + T^{-1}\tau V : d(VP^{\nu}),$$
 (1.40a)

where we have written $\mathbf{P}^{\nu} = -2\eta \mathbf{V}$ and the symbol of entropy, energy and volume as capital letters in order to stress that (1.29) is not restricted to values per unit mass s, u and v, but for total volume V, entropy S and internal energy U. Thus, $\mathbf{T}^{-1}\tau\mathbf{V}$ may be considered as the intensive variable conjugate to the extensive quantity $V\mathbf{P}^{\nu}$ whose preferable use as variable rather than \mathbf{P}^{ν} will be commented in Chaps. 2 and 6. Consequently, we may go from the extensive variable $V\mathbf{P}^{\nu}$ to the intensive variable $\tau\mathbf{V}$ through a Legendre transform. In particular, we may rewrite (1.40a) in terms of U as

$$dU = TdS - pdV - \tau \mathbf{V} : d(V\mathbf{P}^{\nu}), \tag{1.40b}$$

and write the corresponding Legendre transforms for $F_1(T, V, V\mathbf{P}^v)$ or $F_2(T, V, \tau \mathbf{V})$ as

$$dF_1 = -SdT - pdV - \tau \mathbf{V} : d(V\mathbf{P}^{\nu}), \tag{1.41a}$$

and

$$dF_2 = -SdT - pdV + V\mathbf{P}^{\nu} : d(\tau \mathbf{V}). \tag{1.41b}$$

The latter expression would be the generalization of Daivis expression (1.38). These Legendre transforms show that it is possible to go from the viscous pressure tensor to the velocity gradient as independent variables. Analogously, in Chap. 5 it will be considered another Legendre transform going from the viscous pressure tensor to the macromolecular configuration tensor, which will be introduced in Chap. 4. However, these Legendre transforms may be carried out in steady states, where \mathbf{P}^{ν} and \mathbf{V} are univocally related, but in general they are not expected to be valid in fast varying states, where \mathbf{P}^{ν} and \mathbf{V} behave in a completely independent way.

Note that an analogous analysis could be carried out for the Gibbs free energy, which has as basic variables the temperature and pressure instead of temperature and volume, and which plays a central role in physico-chemical thermodynamics, in the analysis of phenomena at constant temperature and constant pressure.

1.2.2 Viscous Pressure and Diffusion Flux

In this subsection we consider a binary mixture and introduce the diffusion flux as a further independent variable, because it will play an important role in several of the phenomena studied in this monograph (Nettleton 1988; Jou et al. 1991, 2010; Goldstein and García-Colín 1993, 1994; Pérez-Guerrero and García-Colín 1991; Pérez-Guerrero 1997; Nettleton 1993, 1996a, b). Furthermore, we carry out a detailed justification of the generalised form of the entropy, which was presented in (1.29) without derivation. Our aim is to analyse the couplings between the diffusion flux and the viscous pressure tensor. For the sake of simplicity, the latter will be considered here as a single independent variable with a single relaxation time instead of the addition of several independent contributions, each with its own relaxation time. The extension to the latter situation is straightforward but cumbersome. We will use the coupled evolution equations for the diffusion flux J and P^{ν} in Chaps. 6–8.

Instead of (1.29), we write now the extended Gibbs equation in the form

$$ds = T^{-1}du + T^{-1}pdv - T^{-1}\tilde{\mu}dc_1 - v\alpha_1 \mathbf{J} \cdot d\mathbf{J} - v\alpha_2 \mathbf{P}^{v} : d\mathbf{P}^{v}, \quad (1.42)$$

with c_1 the concentration (mass fraction) of the solute, $\tilde{\mu} \equiv \mu_1 - \mu_2$ the difference between the specific chemical potentials of the solute and the solvent, and α_1 and α_2 coefficients whose form will be identified below. We neglect here the effects of the bulk viscous pressure, for the sake of simplicity. Note the third and fourth terms on

the right-hand side of (1.41), related to changes in composition and to the diffusion flux, which were absent from (1.29).

We assume for the entropy flux the expression

$$\boldsymbol{J}^{s} = T^{-1}\boldsymbol{q} - T^{-1}\tilde{\boldsymbol{\mu}}\boldsymbol{J} + \beta \mathbf{P}^{v} \cdot \boldsymbol{J}. \tag{1.43}$$

The first two terms are classical; the latter one is characteristic of EIT, and it is of second order in the fluxes: β is a phenomenological coefficient characterizing the coupling of \mathbf{P}^{ν} and J.

The energy and the mass balance equations are, respectively,

$$\rho \dot{u} = -\nabla \cdot \mathbf{q} - p(\nabla \cdot \mathbf{v}) - \mathbf{P}^{\mathbf{v}} : \mathbf{V}, \tag{1.44}$$

$$\rho \dot{c} = -\nabla \cdot \boldsymbol{J}.\tag{1.45}$$

Combination of (1.42), (1.44) and (1.45) yields for the time derivative of the entropy

$$\rho \dot{\mathbf{s}} = -T^{-1} \nabla \cdot \mathbf{q} + T^{-1} \tilde{\mu} \nabla \cdot \mathbf{J} - T^{1} \mathbf{P}^{\nu} : \mathbf{V} - \alpha_{1} \mathbf{J} \cdot \dot{\mathbf{J}} - \alpha_{2} \mathbf{P}^{\nu} : \dot{\mathbf{P}}^{\nu}. \quad (1.46)$$

It is convenient to rewrite the two first terms of the right-hand side of (1.46) as

$$T^{-1}\nabla \cdot \boldsymbol{q} = \nabla \cdot (T^{-1}\boldsymbol{q}) - \boldsymbol{q} \cdot \nabla T^{-1}, \tag{1.47}$$

$$T^{-1}\tilde{\mu}\nabla\cdot\boldsymbol{J} = \nabla\cdot(T^{-1}\tilde{\mu}\boldsymbol{J}) - \boldsymbol{J}\cdot\nabla(T^{-1}\tilde{\mu}). \tag{1.48}$$

Then, taking into account (1.43), one obtains for the entropy production

$$\sigma = \mathbf{q} \cdot \nabla T^{-1} + \mathbf{J} \cdot [-\nabla (T^{-1}\tilde{\mu}) - \alpha_1 \dot{\mathbf{J}} + \nabla \cdot (\beta \mathbf{P}^{\nu})] + \mathbf{P}^{\nu} : (-T^{-1}\mathbf{V} - \alpha_2 \dot{\mathbf{P}}^{\nu} + \beta \nabla \mathbf{J}),$$
(1.49)

where use has been made of the general form of the balance equation of entropy

$$\rho \dot{s} + \nabla \cdot \boldsymbol{J}^{S} = \sigma. \tag{1.50}$$

From now on, we consider an isothermal situation and neglect the heat flux. This does not mean, of course, that thermal effects are not important, but that we will focus our analysis on situations in which they are negligible, only for the sake of simplicity. Under this simplification, the simplest evolution equations for J and P^{ν} compatible with the positive character of (1.49) are

$$-\nabla (T^{-1}\tilde{\mu}) - \alpha_1 \dot{\boldsymbol{J}} + \nabla \cdot (\beta \mathbf{P}^{\nu}) = \beta_1 \boldsymbol{J}, \tag{1.51}$$

$$-T^{-1}\mathbf{V} - \alpha_2 \dot{\mathbf{P}}^{\nu} + \beta (\nabla \mathbf{J})^s = \beta_2 \mathbf{P}^{\nu}, \tag{1.52}$$

where $(\nabla J)^s$ stands for the symmetric part of ∇J . The positive phenomenological coefficients β_1 and β_2 may be identified in physical terms by comparing (1.51) and (1.52) in the isothermal steady state and without couplings with the well known Navier–Stokes and Fick's equations, namely

$$\mathbf{P}^{\nu} = -2\eta \mathbf{V}, \quad \mathbf{J} = -\tilde{D}\nabla \tilde{\mu}, \tag{1.53}$$

where \tilde{D} is a coefficient related to the usual diffusion coefficient D by means of $D = \tilde{D}(\partial \tilde{\mu}/\partial c_1)$. Such comparison yields $\beta_1 = (\tilde{D}T)^{-1}$, $\beta_2 = (2\eta T)^{-1}$. Furthermore, one may identify the respective relaxation times of J and P^v as $\tau_1 = \alpha_1/\beta_1 = \alpha_1(\tilde{D}T)$, $\tau_2 = \alpha_2/\beta_2 = \alpha_2(2\eta T)$. This allows one to identify in physical terms the coefficients α_1 and α_2 appearing in the extended Gibbs Eq. (1.42) and yields for it the explicit form

$$ds = T^{-1}du + T^{-1}pdv - T^{-1}\tilde{\mu}dc_1 - \frac{v\tau_1}{\tilde{D}T}\boldsymbol{J} \cdot d\boldsymbol{J} - \frac{v\tau_2}{2\eta T}\mathbf{P}^{v} : d\mathbf{P}^{v}.$$
(1.54)

Note that the latter term has the form given in the last term of (1.29), which appears now explicitly justified, as well as its deep and direct relation with the relaxational terms in the constitutive Eq. (1.51).

It is also worthwhile to note that in the absence of viscous pressure and in a steady state, where $J = -D\nabla c_1$, (1.54) may be integrated to give

$$s = s_{eq}(u, v, c_1) - l^2 \nabla c_1 \cdot \nabla c_1, \tag{1.55}$$

with l a correlation length defined by $l = v\tilde{D}\tau_1/T$. The contribution of the density gradients to the entropy, or to the free energy, is usually known as a Ginzburg–Landau contribution, and will be discussed in Chap. 7.

The evolution equations for J and P^{ν} may be rewritten as

$$\tau_1 \dot{\boldsymbol{J}} = -(\boldsymbol{J} + D\nabla c_1) + \beta \tilde{D} T \nabla \cdot \mathbf{P}^{\nu}$$
 (1.56)

and

$$\tau_2(\mathbf{P}^{\nu})^{\cdot} = -(\mathbf{P}^{\nu} + 2\eta \mathbf{V}) + 2\beta T \eta (\nabla \mathbf{J})^s. \tag{1.57}$$

Equations (1.56) and (1.57) clearly exhibit the couplings between diffusion and viscous stresses. For instance, in diffusion of small molecules in a polymer matrix, these couplings are due to the swelling due to the solvent, which produces a relative motion between neighbouring polymer chains, whose mutual friction may cause a viscous stress.

The material time derivatives of J and P^{ν} in (1.56) and (1.57) should be replaced, in general, by frame-invariant time derivatives, as mentioned in Sect. 1.1. Their form for tensors has already been discussed in (1.7–1.8). The corresponding form for the frame-indifferent derivative of J is

$$\frac{\mathrm{D}\boldsymbol{J}}{\mathrm{D}t} = \boldsymbol{\dot{J}} + \mathbf{W} \cdot \boldsymbol{J}. \tag{1.58}$$

which corresponds to the rate of change of J in a local system rotating with the system. Relaxational effects of the diffusion flux are relevant, for instance, in the propagation of fast solidification fronts (Galenko 2007; Lecoq et al. 2009).

1.3 Rational Extended Thermodynamics

EIT can be seen not only as an extension of the classical irreversible thermodynamics, but it may also be formulated along the line of thought of rational thermodynamics (RT), which will be called rational extended thermodynamics (RET). The formalism of RT, whose main objective is to provide a method for deriving constitutive equations, was essentially developed by Coleman, Truesdell and Noll in the 1960s (Truesdell 1971, 1984) and offers an approach whose rationale is drastically different from the classical irreversible thermodynamics. It is interesting to consider EIT from both perspectives of classical and rational irreversible thermodynamics because it provides, in some aspects, a common ground for comparison in spite of the unrelated appearance in their original formulations.

Among the basic hypotheses underlying the earliest versions of RT we can outline: (i) absolute temperature and entropy are considered primitive concepts, whose validity is not restricted to near-equilibrium situations; (ii) it is assumed that systems have memory, i.e. their behaviour at a given instant of time is determined not only by the values of the variables at the present time, but also by their past history, or, in other versions, by additional variables whose evolution is dictated by complementary constitutive equations; (iii) the second law of thermodynamics, which serves fundamentally as a restriction on the form of the constitutive equations, is expressed in mathematical terms by means of the Clausius–Duhem inequality. To obtain restrictions on the memory functionals requires a rather elaborate mathematical theory in functional analysis and is therefore very attractive from the point of view of applied mathematics. Besides these ideas, RT used some auxiliary "principles", such as those of equipresence (all variables are assumed to be present, in principle, in all equations, and some of them may be eliminated by using, for instance, the restrictions of the second law), fading memory (the memory is assumed to be more intense for recent conditions than for old conditions imposed on the system) and frame-indifference (constitutive equations are assumed to be invariant under Euclidean transformations). A comparison of rational thermodynamics with extended irreversible thermodynamics in the linear domain may be found, for instance, in (Silhavy 1997). Let us finally note that although RT considers an entropy which is more general than the local-equilibrium one, since it may depend on non-equilibrium variables, such as, for instance, the gradients of temperature and velocity, the equations of state obtained as derivatives of the entropy are usually not explored in detail, with some exceptions (Silhavy 1997). In contrast, one of the objectives of EIT is precisely the full exploration of such equations of state.

Some aspects of RT (for a description of whose evolution the reader is referred to (Silhavy 1997)) were reformulated at the beginning of the 1970s. One especially

interesting reformulation, due to Shi-Liu, is based on the use of Lagrange multipliers to take into account the restrictions of the balance equations on the admissible processes to be considered, instead of using some artificial source terms in the energy and momentum balance equations, as was done in the Coleman and Truesdell formulation. This method is widely used, for instance, by Müller and Ruggeri (1998) in their formulation of extended thermodynamics. Here, we will use the version of RT based on Lagrange multipliers as a working method to present an alternative analysis of the restrictions of the second law on the evolution equations for the fluxes.

To illustrate our approach, we consider a viscous heat-conducting fluid in motion. The space of the variables, denoted V, is formed by the union of the space of the classical variables C (the density $\rho = v^{-1}$, the specific internal energy u, the velocity v) and the space of the fluxes \mathcal{F} (here the heat flux q, and the viscous pressure \mathbf{P}^v), which imply fourteen independent variables (two scalars, ρ and u, three components of v, and three of q and six components of the symmetric tensor \mathbf{P}^v). The evolution of the classical variables is governed by the balance equations of mass and energy

$$\rho \dot{\mathbf{v}} = \nabla \cdot \mathbf{v},\tag{1.59}$$

$$\rho \dot{u} = -\nabla \cdot \mathbf{q} - \mathbf{P}^{v} : \mathbf{V} - p\mathbf{U} : \mathbf{V}. \tag{1.60}$$

Concerning the extra variables q and P^{ν} , we suppose that they obey evolution equations of the general form

$$\rho \dot{q} = -\nabla \cdot \mathbf{Q} + \sigma^q, \tag{1.61}$$

$$\rho \dot{\mathbf{P}}^{\nu} = -\nabla \cdot \mathbf{J}^{\nu} + \boldsymbol{\sigma}^{\nu}. \tag{1.62}$$

Q is a tensor of rank two representing the flux of the heat flux, and σ^q is a vector corresponding to the supply of heat flux, \mathbf{J}^v is a third-rank tensor designating the flux of the viscous pressure tensor, and σ^v its source term. At this stage of the analysis these quantities are not determined and must be specified by means of constitutive relations in terms of the whole set of variables \mathcal{V} . This implies that s and J^s are given by constitutive relations of the form $s = s(\mathcal{V})$, $J^s = J^s(\mathcal{V})$.

The evolution Eqs. (1.61–1.62) and the constitutive relations are not arbitrary. They have to comply with the constraints of Euclidean invariance (criterion of objectivity or frame indifference), positiveness of the rate of entropy production, and convexity of entropy.

To satisfy the second law of thermodynamics, it is assumed that there exists a regular and continuous function s, called entropy, which obeys a balance law given by

$$\rho \dot{s} + \nabla \cdot \boldsymbol{J}^s = \sigma^s > 0, \tag{1.63}$$

where J^s is the entropy flux and σ^s the non-negative rate of entropy production. As in rational thermodynamics, the non-negative property of σ^s is used to place restrictions on the constitutive equations. The rate of entropy production is calculated by performing the operations indicated on the left-hand side of (1.63).

At this point, let us emphasize some of the main differences between EIT and rational thermodynamics. Whereas in the latter theory the quantities q, and P^{ν} are given by constitutive relations, in EIT they are counted among the set of independent variables. Furthermore, the second law is not in the form of the Clausius—Duhem inequality, as the entropy flux is not imposed a priori to be given by the ratio of the heat flux and the temperature, but may contain extra terms. Finally, the entropy is assumed to depend on the fluxes.

To take into account the restrictions placed by the second law (1.62), on the constitutive equations, we follow the method of Lagrange multipliers. According to this technique, we include in (1.63) the constraints introduced by the mass and the energy balances and by the evolution equations of \mathbf{q} and \mathbf{P}^{ν} via the Lagrange multipliers Λ_0 , Λ'_0 , Λ_1 , and Λ_2 , all depending on u, v, \mathbf{q} , and \mathbf{P}^{ν} ; then the inequality (1.62) will take the form

$$\rho \dot{s} + \nabla \cdot J^{s} - \Lambda_{0}(\rho \dot{u} + \nabla \cdot q + \mathbf{P}^{v} : \mathbf{V} + p\mathbf{U} : \mathbf{V}) - \Lambda'_{0}(\rho \dot{v} - \nabla \cdot v) - \mathbf{\Lambda}_{1} \cdot (\rho \dot{q} + \nabla \cdot \mathbf{Q} + -\sigma^{q}) - \Lambda_{2} : (\rho \dot{\mathbf{P}}^{v} + \nabla J^{v} - \sigma^{v}) \ge 0,$$

$$(1.64)$$

s and J^s are, at this stage of the analysis, unknown functions of u, v, q, and P^v . By differentiating s and J^s with respect to u, v, q, and P^v , and rearranging the various terms one obtains from (1.64)

$$\left(\frac{\partial s}{\partial u} - \Lambda_{0}\right) \rho \dot{u} + \left(\frac{\partial s}{\partial v} - \Lambda'_{0}\right) \rho \dot{v} + \left(\frac{\partial s}{\partial q} - \Lambda_{1}\right) \cdot \rho \dot{q} + \left(\frac{\partial s}{\partial \mathbf{P}^{v}} - \Lambda_{2}\right) : \rho \dot{\mathbf{P}}^{v}
+ \frac{\partial \boldsymbol{J}^{s}}{\partial u} \cdot \nabla u + \frac{\partial \boldsymbol{J}^{s}}{\partial v} \cdot \nabla v + \frac{\partial \boldsymbol{J}^{s}}{\partial q} : \nabla q + \frac{\partial \boldsymbol{J}^{s}}{\partial \mathbf{P}^{v}} : \nabla \mathbf{P}^{v}
- \Lambda_{0} \nabla \cdot \boldsymbol{q} - \Lambda_{0} \mathbf{P}^{v} : \mathbf{V} - \Lambda_{0} \rho \mathbf{U} : \mathbf{V} + \Lambda'_{0} \nabla \cdot \boldsymbol{v} - \Lambda_{1} \cdot (\nabla \cdot \mathbf{Q}) + \Lambda_{1} \cdot \sigma^{q}
- \Lambda_{2} : (\nabla \cdot \mathbf{J}^{v}) + \Lambda_{2} : \sigma^{v} \geq 0.$$
(1.65)

Since the derivatives \dot{u} , \dot{v} , \dot{q} , and $\dot{\mathbf{p}}^{v}$ are arbitrary, a first requirement for the positiveness of (1.64) is that

$$\frac{\partial s}{\partial u} = \Lambda_0 = T^{-1}, \quad \frac{\partial s}{\partial v} = \Lambda'_0 = pT^{-1}, \tag{1.66}$$

$$\frac{\partial s}{\partial \boldsymbol{a}} = \Lambda_1, \quad \frac{\partial s}{\partial \mathbf{P}^{\nu}} = \Lambda_2, \tag{1.67}$$

where we have identified Λ_0 with T^{-1} and Λ_0' with pT^{-1} according to the classical interpretation of derivatives (1.66).

Omitting now second and higher-order terms in the fluxes, the most general expressions of \mathbf{Q} , $\mathbf{\sigma}^q$, \mathbf{J}^v , and $\mathbf{\sigma}^v$ are simply

$$\mathbf{Q} = a_1(u, v)\mathbf{U} + a_2(u, v)\mathbf{P}^v, \quad \mathbf{\sigma}^q = -a_3(u, v)q,$$
 (1.68)

$$\mathbf{J}^{\nu} = b_1(u, \nu)q\mathbf{U} + b_2(u, \nu)\nu\mathbf{U}, \quad \sigma^{\nu} = -b_3(u, \nu)\mathbf{P}^{\nu}, \tag{1.69}$$

with $a_i(u, v)$ and $b_i(u, v)$ undetermined functions of u and v. Calculating the divergence of \mathbf{Q} and of \mathbf{J}^v , without including non-linear terms, and substituting into the last three lines of (1.65) (recall that the first line was eliminated according to (1.66) and (1.67)), one has

$$\left(\frac{\partial J^{s}}{\partial u} - \frac{\partial a_{1}}{\partial u}\mathbf{\Lambda}_{1}\right) \cdot \nabla u + \left(\frac{\partial J^{s}}{\partial v} - \frac{\partial a_{1}}{\partial v}\mathbf{\Lambda}_{1}\right) \cdot \nabla v + \left(\frac{\partial J^{s}}{\partial q} - b_{1}\mathbf{\Lambda}_{2} - \Lambda_{0}\mathbf{U}\right) : \nabla q$$

$$\left(\frac{\partial J^{s}}{\partial \mathbf{P}^{v}} - a_{2}\mathbf{\Lambda}_{1}\mathbf{U}\right) : \nabla \mathbf{P}^{v} - \Lambda_{0}\mathbf{P}^{v} : \mathbf{V} - b_{2}\mathbf{\Lambda}_{2} : \mathbf{V} - a_{3}\mathbf{\Lambda}_{1} \cdot q - b_{3}\mathbf{\Lambda}_{2} : \mathbf{P}^{v} \ge 0,$$
(1.70)

after use is made of the relation $\Lambda_0^{'}=p\Lambda_0$, obtained from (1.66), and of the identity $\nabla\cdot \nu\equiv \mathbf{U}:\mathbf{V}$. As the gradients of independent variables are arbitrary, the coefficients of these quantities in (1.70) must vanish to preserve the inequality. This leads to

$$\frac{\partial \boldsymbol{J}^s}{\partial u} - \frac{\partial a_1}{\partial u} \boldsymbol{\Lambda}_1, \quad \frac{\partial \boldsymbol{J}^s}{\partial v} - \frac{\partial a_1}{\partial v} \boldsymbol{\Lambda}_1, \tag{1.71a}$$

$$\frac{\partial \boldsymbol{J}^{s}}{\partial \boldsymbol{q}} = b_{1} \boldsymbol{\Lambda}_{2} + \Lambda_{0} \mathbf{U}, \quad \frac{\partial \boldsymbol{J}^{s}}{\partial \mathbf{P}^{v}} = a_{2} \boldsymbol{\Lambda}_{1} \mathbf{U}, \tag{1.71b}$$

which suggest for J^s the expression, which is also confirmed by kinetic theory of gases (Jou et al. 2010, Chap. 3),

$$\boldsymbol{J}^{s} = \beta_{1}\boldsymbol{q} + \beta_{2}\mathbf{P}^{v} \cdot \boldsymbol{q}, \tag{1.72}$$

where the coefficients β_i depend a priori on u and v. Comparing now (1.71b) and the derivatives of J^s with respect to q and P^v obtained from (1.72) one has

$$\Lambda_0 = \beta_1, \quad \Lambda_1 = (\beta_2/b_2)\boldsymbol{q}, \quad \Lambda_2 = (\beta_2/b_1)\mathbf{P}^{\nu}. \tag{1.73}$$

Note that the value of β_1 allows us to interpret (1.72) as a classical term (the first one) plus an extended contribution. Also, it is worth pointing out that comparing (1.71a) and the derivatives with respect to u and v obtained from (1.72), it can be demonstrated that β_2 is constant. The remaining terms of (1.70) will be analysed below.

In the linear approximation, the evolution equation of q given by (1.61) can be written as

$$\rho \dot{\boldsymbol{q}} = -\frac{\partial a_1}{\partial u} \nabla u - \frac{\partial a_1}{\partial v} \nabla v - a_2 \nabla \cdot \mathbf{P}^v - a_3 \boldsymbol{q}, \qquad (1.74)$$

when (1.67) is taken into account. For the sake of convenience, (1.74) may be rewritten as

$$\tau_1 \dot{\boldsymbol{q}} = -\boldsymbol{q} - \kappa \nabla u - \delta \nabla v + \alpha \nabla \cdot \mathbf{P}^v, \tag{1.75}$$

where the coefficients are identified as follows

$$\tau_1 = \rho_2/a_3, \quad \kappa = (a_3)^{-1} (\partial a_1/\partial u), \quad \delta = (a_3)^{-1} (\partial a_1/\partial v), \quad \alpha = -a_2/a_3.$$
 (1.76)

Equation (1.75) contains the thermal and viscous contributions to the time evolution of \mathbf{q} . For $\tau_1 = \alpha = 0$ one recovers the Fourier law with $\kappa = \lambda(\partial T/\partial u)$ and $\delta = \lambda(\partial T/\partial v)$, λ being the thermal conductivity. Another result derived from (1.75) when viscous effects are neglected ($\alpha = 0$) is the well-known Maxwell–Cattaneo equation $\tau_1 \dot{\mathbf{q}} + \mathbf{q} = -\lambda \nabla T$.

Similarly, the evolution equation for \mathbf{P}^{ν} is obtained from (1.62) and (1.69). Thus, in the linear approximation, we have

$$\rho \mathbf{P}^{\nu} = -b_1 \nabla \mathbf{q} - b_2 \mathbf{V} - b_3 \mathbf{P}^{\nu}, \tag{1.77}$$

and putting

$$\tau_2 = \rho/b_3, \ 2\eta = b_2/b_3, \ \gamma = -(b_1/b_3),$$
 (1.78)

vields

$$\tau_2 \dot{\mathbf{P}}^{\nu} = -\mathbf{P}^{\nu} - 2\eta \mathbf{V} + \gamma \nabla \mathbf{q}. \tag{1.79}$$

We finally derive the generalised Gibbs equation. To do this, we write the differential of $s = s(u, v, q, \mathbf{P}^v)$ in the form

$$ds = \Lambda_0 du + \Lambda'_0 dv + \mathbf{\Lambda}_1 \cdot dq + \mathbf{\Lambda}_2 : d\mathbf{P}^{\nu}$$

= $T^{-1} du + pT^{-1} dv + \frac{\beta_2}{b_2} q \cdot dq + \frac{\beta_2}{b_1} \mathbf{P}^{\nu} : d\mathbf{P}^{\nu}$, (1.80)

when (1.66) and (1.67) are used. To identify β_2/b_2 we proceed as follows: from the first of relations (1.71a) and the second of (1.73) one has

$$\frac{\partial \mathbf{J}^s}{\partial u} = \frac{\beta_2}{b_2} \frac{\partial a_1}{\partial u} \mathbf{q} \tag{1.81}$$

and taking into account the first equality of (1.73), the derivative of (1.72) with respect to u only up to first order in the fluxes gives

$$\frac{\partial \mathbf{J}^s}{\partial u} = \frac{\partial \Lambda_0}{\partial u} \mathbf{q}. \tag{1.82}$$

Equating now both expressions and using $(\partial a_1/\partial u) = \rho \lambda \tau_1^{-1}(\partial T/\partial u)$ according to (1.76) the equality of the respective first terms leads to

$$\frac{\beta_2}{b_2} = -\frac{\tau_1 \nu}{\lambda T^2}.\tag{1.83}$$

The identification of β_2/b_1 is made in a similar way. The four last terms of (1.70) can be written as

$$-(\Lambda_0 \mathbf{P}^{\nu} + b_2 \Lambda_2) : \mathbf{V} - a_3 \Lambda_1 \cdot q - b_3 \Lambda_2 : \mathbf{P}^{\nu} \ge 0$$
 (1.84)

and preservation of inequality requires that the terms in parentheses vanish, i.e.

$$\mathbf{\Lambda}_2 = -\frac{\Lambda_0}{b_2} \mathbf{P}^{\nu} = \frac{\beta_2}{b_1} \mathbf{P}^{\nu},\tag{1.85}$$

where we have used the third of relations (1.73). From (1.85) and $b_2 = (2\eta\rho/\tau_2)$ derived from (1.78) and $\Lambda_0 = T^{-1}$ according to (1.66), one arrives at

$$\frac{\beta_2}{b_1} = -\frac{\tau_2 \nu}{2nT}.\tag{1.86}$$

Note that the last two terms of (1.84) adopt the quadratic form

$$(\lambda T^2)^{-1} \mathbf{q} \cdot \mathbf{q} + (2\eta T)^{-1} \mathbf{P}^{\nu} : \mathbf{P}^{\nu} \ge 0, \tag{1.87}$$

which imposes the positiveness of transport coefficients λ and η . Summarizing this derivation, the Gibbs equation finally has the form (Jou et al. 2010)

$$ds = T^{-1}du + pT^{-1}dv - \frac{\tau_1 v}{\lambda T^2} \boldsymbol{q} \cdot d\boldsymbol{q} - \frac{\tau_2 v}{2\eta T^2} \boldsymbol{P}^v : d\boldsymbol{P}^v.$$
 (1.88)

If the heat flux may be neglected, (1.88) reduces to (1.29). We have seen here that the main results of Sect. 1.2 with respect to the entropy, the entropy flux and the evolution equations for the fluxes in EIT are confirmed in RET in the linear approximation. The techniques in RET could be useful for obtaining some more detailed information than in the usual presentations of EIT in the non-linear regime.

1.4 Theories with Internal Variables

Another interesting and useful perspective to deal with more general situations than those found in the local-equilibrium theory are theories with internal variables (Meixner 1949, 1954; Verhas 1997; Lhuillier and Ouibrahim 1980; Maugin and Drouot 1983; Maugin and Muschik 1994a, b; Maugin 1999; Manero et al. 2007). These theories introduce additional variables which allow a more detailed description of the system and enlarge the domain of application of thermodynamics; they have been successfully applied in such fields as rheology and in dielectric and magnetic relaxation (Ciancio et al. 1990; Ciancio and Verhas 1991). These theories may provide a link between the apparently very dissimilar formulations of rational thermodynamics and of classical irreversible thermodynamics, by defining an accompanying equilibrium state that is different from the local-equilibrium state, which turns out to be the adiabatic projection of the accompanying equilibrium state on the manifold of equilibrium states in the space of classical variables (Kestin 1990, 1993; Muschik 1990, 1993).

These theories have several connections with EIT, since they introduce more variables and more equations. On the other hand, they differ from it since EIT uses the macroscopic fluxes as variables, whereas the internal variables are either unidentified (when they have as the only purpose to provide more general equations for the classical variables rather than being themselves the subject of direct measurement), or motivated by a microscopic modelling of the systems.

Indeed, when working with polymer solutions the macromolecular configuration of the polymers is incorporated as a supplementary variable into the entropy or the free energy. One usually takes as a description of the configuration the so-called configuration tensor ${\bf C}$

$$\mathbf{C} = \langle \mathbf{Q} \, \mathbf{Q} \rangle = \int \psi(\mathbf{Q}) \, \mathbf{Q} \, \mathbf{Q} \, \mathbf{d} \, \mathbf{Q}, \tag{1.89}$$

with ψ the configurational distribution function. More elaborate thermodynamic functions including as variables the whole distribution function have also been considered. Here, \mathbf{Q} is the end-to-end vector of the macromolecules. Other descriptions are possible in terms of $\langle \mathbf{Q}_i \mathbf{Q}_i \rangle$, with \mathbf{Q}_i the vector from bead i to bead i+1, or the vector related with the ith normal mode in a Rouse–Zimm description.

As will be seen in the next section, the configuration tensors are directly related to the viscous pressure tensor. Indeed, for the contribution of the *i*th normal mode to the viscous pressure tensor one has (Bird et al. 1987b)

$$\mathbf{P}_{i}^{v} = -nH\left\langle \mathbf{Q}_{i} \mathbf{Q}_{i} \right\rangle + nk_{\mathrm{B}}T\mathbf{U},\tag{1.90}$$

n being the number of molecules per unit volume, H an elastic constant characterizing the intramolecular interactions, and $k_{\rm B}$ the Boltzmann constant. Thus, introduction of \mathbf{P}_i^{ν} or of $\langle \mathbf{Q}_i \mathbf{Q}_i \rangle$ as independent variables into the free energy is essentially equivalent, in the case of dilute polymer solutions (this is not so in the case of ideal gases, where there are no internal degrees of freedom). The use of \mathbf{P}_i^{ν} or of $\langle \mathbf{Q}_i \mathbf{Q}_i \rangle$

as variables has, in both cases, some characteristic advantages. For the analysis of non-equilibrium steady states, \mathbf{P}_i^{ν} is directly related to the observables. For a microscopic understanding of the macromolecular processes taking place and for the analysis of light-scattering experiments the use of $\langle \mathbf{Q}_i \mathbf{Q}_i \rangle$ is more suitable. The dynamical equations for the configuration tensor thus provide evolution equations for the viscous pressure tensor.

To give an explicit illustration, assume that one includes C as an independent variable of the theory. The corresponding Gibbs equation would then be

$$ds = T^{-1}du + pT^{-1}dv - \alpha T^{-1}\mathbf{C} : d\mathbf{C}.$$
 (1.91)

As a consequence, the time derivative of the entropy takes the form

$$\rho \dot{s} = T^{-1} \rho \dot{u} + p T^{-1} \rho \dot{v} - \rho \alpha T^{-1} \mathbf{C} : \dot{\mathbf{C}}. \tag{1.92}$$

Taking into account the mass and energy balance equations, (1.92) may be cast in the form

$$\rho \dot{\mathbf{s}} + \nabla \cdot (T^{-1}\mathbf{q}) = \mathbf{q} \cdot \nabla T^{-1} - T^{-1}\mathbf{P}^{\mathbf{v}} : (\nabla \mathbf{v})^{s} - \rho \alpha T^{-1}\mathbf{C} : \dot{\mathbf{C}}. \tag{1.93}$$

We recognize $T^{-1}q$ as the entropy flux and the term on the right-hand side as the entropy production. The simplest constitutive equations satisfying the positiveness of the entropy production are

$$q = L\nabla T^{-1},\tag{1.94}$$

$$\mathbf{P}^{\nu} = -L_{00}T^{-1}(\nabla \mathbf{v})^{s} - L_{01}T^{-1}\rho\alpha\mathbf{C}, \tag{1.95}$$

$$\dot{\mathbf{C}} = -L_{10}T^{-1}(\nabla \mathbf{v})^s - L_{11}T^{-1}\rho\alpha\mathbf{C},\tag{1.96}$$

with the matrix of the transport coefficients L_{ij} being definite positive, and with $L_{10} = -L_{01}$ due to Onsager-Casimir reciprocity relations, due to the different parity of $(\nabla v)^s$ and \mathbb{C} with respect to time-reversal symmetry.

Equation (1.94) yields the usual Fourier law provided one identifies $L = \lambda T^2$. Equation (1.95) relates the viscous pressure tensor to the internal variable ${\bf C}$ and (1.96) describes the evolution of the internal variable. If one does not need to measure ${\bf C}$ but only ${\bf P}^{\nu}$ and $(\nabla {\bf v})^s$, one may eliminate ${\bf C}$ by combining (1.95) and (1.96) to obtain an evolution equation for ${\bf P}^{\nu}$. In the simplest linear situation (i.e. assuming that $L_{00}T^{-1}$, $L_{10}T^{-1}$, $L_{01}T^{-1}\rho\alpha$ and $L_{11}T^{-1}\rho\alpha$ are constant) one may differentiate (1.95) and, combining it with (1.96) one obtains an evolution equation of the so-called Jeffreys (or double-lag) form

$$\tau \frac{\mathrm{d}\mathbf{P}^{\nu}}{\mathrm{d}t} + \mathbf{P}^{\nu} = -2\eta \left[(\nabla \nu)^{s} + \tau_{2} \frac{\mathrm{d}(\nabla \nu)^{s}}{\mathrm{d}t} \right],\tag{1.97}$$

with the relaxation time τ given by

$$\tau = (L_{11}T^{-1}\rho\alpha)^{-1},\tag{1.98a}$$

the shear viscosity η expressed as

$$2\eta = -\frac{L_{01}L_{10} - L_{00}L_{11}}{L_{11}T},\tag{1.98b}$$

and the time τ_2 given by

$$\tau_2 = \frac{L_{00}}{2\eta L_{11}\rho\alpha} = \tau \frac{L_{00}T^{-1}}{2\eta}.$$
 (1.98c)

We recover Maxwell's equation when $L_{00}=0$ (this is indeed the case when (1.90) is satisfied). In this case we have $\tau_2=0$ and $2\eta=-(L_{01}L_{10}/L_{11}T)=L_{01}^2/(L_{11}/T)$. Furthermore, ${\bf C}$ and ${\bf P}^{\nu}$ are directly related as ${\bf C}=-(L_{01}T^{-1}\rho\alpha)^{-1}{\bf P}^{\nu}$. This may be introduced into the Gibbs Eq. (1.91) and yields, in the linear situation we are considering,

$$ds = T^{-1}du + pT^{-1}dv - \frac{\alpha T^{-1}}{(L_{01}\rho\alpha T^{-1})^2} \mathbf{P}^{\nu} : d\mathbf{P}^{\nu},$$
(1.99)

which in view of the above identifications of τ and η , may be rewritten as

$$ds = T^{-1}du + pT^{-1}dv - \frac{\tau}{2\eta\rho T}\mathbf{P}^{\nu} : d\mathbf{P}^{\nu}, \tag{1.100}$$

which is precisely the Gibbs Eq. (1.29) of EIT.

This short development shows that when the conformation tensor is directly related to the viscous pressure tensor (Bird et al. 1987b) it is possible, in principle, to directly compare both theories in the linear approach. The choice of variables will depend on the experimental measurements: if one controls the shear pressure, its choice as an independent variable, as in EIT, is more convenient, whereas if a more microscopic understanding is needed, the conformation tensor will be more useful. In other situations, the relation between \mathbf{C} and \mathbf{P}^{ν} is non-linear, in such a way that several \mathbf{C} may yield the same \mathbf{P}^{ν} , i.e. \mathbf{P}^{ν} is more macroscopic than \mathbf{C} . In such situations, the theories with internal variables would be more detailed than EIT, as expected of a theory using some microscopic information.

Other differences between the two approaches are the following: (a) in the theories of internal variables it is usual to propose purely relaxational equations for these variables. In contrast, in EIT one assumes that the fluxes are field variables which satisfy their own balance equations, where a flux of the flux may be present in a natural way; (b) theories with internal variables usually associate such additional variables with some structure of underlying molecules, as in the mentioned example of macromole-

cules. However, in EIT one uses as variables \mathbf{P}^{v} , \mathbf{q} and other fluxes despite the particles composing the fluid being monatomic and without internal degrees of freedom. From this point of view, EIT aims to build a macroscopic formalism which is able to deal with a wide variety of systems, whereas the theories with internal variables refer usually to a given kind of system, for which the internal variable is explicitly identified.

1.5 Hamiltonian Formulations

Hamiltonian formulations express in an elegant way a feature which is common to many different levels of description, namely, the Hamiltonian structure of the reversible part of evolution equations. This is found in the microscopic level of description (mechanics of the particles composing the system), the level of kinetic theory (based on a distribution function rather than on precise values for the mechanical variables of each microscopic particle), and macroscopic descriptions (such as, for instance, hydrodynamics or equilibrium thermodynamics). Therefore, it is logical to ask that mesoscopic intermediate descriptions should also have this structure. This compatibility condition among different levels is especially useful in the non-linear domain, where the thermodynamic inequalities do not provide useful restrictions (Beris and Edwards 1994; Grmela and Öttinger 1997; Öttinger and Grmela 1997; Dressler et al. 1999; Öttinger 2005).

Here, we will follow the so-called GENERIC (General Equation for the Non-equilibrium Reversible—Irreversible coupling) formulation by Grmela and Öttinger (Grmela and Öttinger 1997; Öttinger and Grmela 1997; Öttinger 2005). These authors propose that the time evolution equations of the physical systems may be written as

$$\frac{\mathrm{d}x}{\mathrm{d}t} = \mathbf{L} \cdot \frac{\delta E}{\delta x} + \mathbf{M} \cdot \frac{\delta S}{\delta x},\tag{1.101}$$

where \boldsymbol{x} represents a set of independent variables required for the complete description of the non-equilibrium system (namely, hydrodynamical fields and additional structural variables), E and S are the total energy and entropy of the system expressed in terms of \boldsymbol{x} , and \boldsymbol{L} and \boldsymbol{M} are linear operators, whose essential features will be specified below. The dot indicates the multiplication of a vector by a matrix and $\delta/\delta\boldsymbol{x}$ usually implies functional rather than partial derivatives. The first term in the right-hand side of (1.101) is purely Hamiltonian and expresses the reversible contribution to the time evolution equations of \boldsymbol{x} generated by the energy E and the entropy S, whereas the second term is Riemannian and corresponds to the irreversible contributions.

Equation (1.101) is supplemented by the following degeneracy requirements

$$\mathbf{L} \cdot \frac{\delta S}{\delta \mathbf{x}} = 0, \tag{1.102a}$$

$$\mathbf{M} \cdot \frac{\delta E}{\delta \mathbf{x}} = 0. \tag{1.102b}$$

The first requirement expresses the reversible contribution of L to the dynamics and requires that the functional form of the entropy must be such that it is unaffected

by the operator **L** generating the reversible dynamics. The second one expresses the conservation of the total energy by the contribution of the dynamics. Note that these degeneracy requirements express very essential and general physical aspects.

Furthermore, one defines the following brackets

$$\{A, B\} = \left\langle \frac{\delta A}{\delta x}, \mathbf{L} \cdot \frac{\delta B}{\delta x} \right\rangle \tag{1.103}$$

$$[A, B] = \left\langle \frac{\delta A}{\delta x}, \mathbf{M} \cdot \frac{\delta B}{\delta x} \right\rangle \tag{1.104}$$

where $\langle \; , \; \rangle$ denotes the scalar product. The bracket $\{ \; , \; \}$ extends the usual Poisson brackets of classical mechanics, whereas the $[\; , \;]$ brackets are intended to describe the dissipative behaviour.

In terms of these brackets, (1.101) and the chain rule yield the following form for the evolution equation of an arbitrary function A

$$\frac{dA}{dt} = \{A, E\} + [A, S]. \tag{1.105}$$

Further conditions for L and M may be stated as the following general properties of the Poisson brackets:

$${A, B} = -{B, A}$$
 (antisymmetry) (1.106a)

$${A, {B, C}} + {B, {C, A}} + {C, {A, B}} = 0$$
 (Jacobi identity) (1.106b)

from which it follows that the matrix L is antisymmetric, and restrict the possible forms of the connection mechanisms for the structural variables, and

$$[A, B] = [B, A], \quad [A, A] \ge 0,$$
 (1.107)

which requires that **M** is symmetric and definite positive. This non-negativeness property guarantees that $dS/dt \ge 0$ and therefore, together with the degeneracy requirement (1.102a), it expresses a form of the second law.

This form of writing the evolution equations in terms of two generators E and S and two matrices L and M aims to capture the most essential features of the dynamics of the systems, in an analogous way to the fundamental thermodynamic potentials capturing all the thermodynamic information into a single potential. The main innovation of GENERIC with respect to previous bracket formalisms is the use of two different generators, E and S, instead of a single generator: this gives more flexibility in the choice of variables. The matrix L is determined by the behaviour of the variables x under space transformations, whereas the dynamical material information enters in the friction matrix M. The symmetry requirements on L are usual in classical mechanics and guarantee the consistency of L with the structure

of the equivalent Poisson bracket, whereas the symmetry of \mathbf{M} is directly related to Onsager's reciprocity relations.

The previous formalism may be applied to many physical situations (such as, for instance, polymer solutions, emulsions and blends, polymer melts, etc). Here, we will apply it to polymeric fluids as an illustration. As will be seen, it yields, amongst other results, non-equilibrium expressions for the entropy S, which are related to the dynamics in a very well specified form through the GENERIC formalism. In fact, entropy appears there as a primary concept, and its form is only verified a posteriori, after the success of the evolution Eq. (1.105) has been verified. We follow here the presentation by Öttinger and Grmela (Grmela and Öttinger 1997; Öttinger and Grmela 1997; Öttinger 2005), specified to a dumbbell solution. We will use two different levels of description.

1.5.1 Microscopic Level: Distribution Function as an Internal Variable

Assume a dumbbell model of a dilute polymer solution and take as essential variables x the mass density $\rho(r)$ of the solution, the momentum density u(r) of the solution, the internal energy of the solvent $\varepsilon(r)$ and the configurational distribution function $\Psi(r, Q)$, where Q is the dumbbell configuration vector (or, in a more general situation, the end-to-end vector of a macromolecule). For dilute polymer solutions, the polymer contributes essentially to stress and internal energy, whereas its contribution to mass and momentum is negligible. We will use these simplifications here, for the sake of simplicity.

The total energy density is obtained by adding the kinetic energy and the solvent and polymer potential energy in the form

$$E = \int \left[\frac{1}{2} \rho(\mathbf{r}) u(\mathbf{r})^2 + \varepsilon(\mathbf{r}) + \int V(\mathbf{Q}) \psi(\mathbf{r}, \mathbf{Q}) d\mathbf{Q} \right] d\mathbf{r}, \quad (1.108)$$

where $V(\mathbf{Q})$ is the interaction potential between the beads of the dumbbell. In fact, since the interaction may be of energetic origin or of entropic origin, they also take into account an entropic potential $V^{(s)}(\mathbf{r}, \mathbf{Q})$, and they write the entropy in the form

$$S = \int \left\{ s(\rho, \varepsilon) - \int \psi(\mathbf{r}, \mathbf{Q}) [T^{-1}V^{(s)}(\mathbf{r}, \mathbf{Q}) + k_{\mathrm{B}} \ln \psi(\mathbf{r}, \mathbf{Q})] d\mathbf{Q} \right\} d\mathbf{r},$$
(1.109)

where $s(\rho, \varepsilon)$ is the solvent entropy and the $\psi \ln \psi$ term is associated with the entropy of the dumbbells, whereas the entropic potential $V^{(s)}(r, \mathbf{Q})$ takes account of the entropic effects on the finer level of polymer segments which have been eliminated in coarse-graining from the macromolecule level to the dumbbell level. Öttinger and Grmela (1997) also write the explicit form for the operators \mathbf{L} and \mathbf{M} , and ex-

press the evolution equation for ψ , but we will not repeat it here because it is rather lengthy. It turns out that the usual equations for the polymer dynamics may indeed be written in the form proposed in GENERIC formalism.

1.5.2 Mesoscopic Level: Configuration Tensor as an Internal Variable

The GENERIC formalism is not exclusive of the microscopic level. On the contrary, one of its appeals is precisely that the GENERIC structure of the equations is found at several levels of description. In particular, for the sake of comparison with the previous results in EIT, Grmela and Öttinger (1997) take as an independent variable, instead of the whole conformational distribution function ψ , the configuration tensor defined as

$$\mathbf{C}(\mathbf{r}) = \int \mathbf{Q} \mathbf{Q} \psi(\mathbf{r}, \mathbf{Q}) d\mathbf{Q}, \qquad (1.110)$$

which is more macroscopic than $\psi(r, \mathbf{Q})$ and has less information than the full $\psi(r, \mathbf{Q})$. They assume that all the dumbbell contribution is of entropic origin, so that they take V=0 in (1.108) and suppose a quadratic form for $V^{(s)}$ (r, \mathbf{Q}) in (1.109), corresponding to a configurational distribution of the Gaussian type. Then, they obtain that $S=S_s+S_p$, with S_s the solvent entropy and S_p the polymer entropy, the latter being given by

$$S_{\rm p} = \frac{1}{2} n_{\rm p} k_{\rm B} \int \left\{ \text{Tr} \left[\mathbf{U} - \alpha \mathbf{C}(\mathbf{r}) \right] + \ln \left[\det \alpha \mathbf{C}(\mathbf{r}) \right] \right\} d\mathbf{r}, \tag{1.111}$$

where the constant α is chosen such that $\mathbf{C}(r) = \mathbf{U}$ at equilibrium. This expression is obtained by integrating over \mathbf{Q} in the entropy given by (1.109) and neglecting the additive constants. Note that

$$\frac{\delta S}{\delta \mathbf{C}} = \frac{1}{2} n_{\rm p} k_{\rm B} \left[\mathbf{C}^{-1}(\mathbf{r}) - \alpha \mathbf{U} \right]. \tag{1.112}$$

The Hamiltonian theory imposes the requirement that the pressure tensor in L space should be chosen in such a way that the gradient of the entropy lies in the null-space of L. A possible choice for the pressure tensor P is then

$$\mathbf{P} = T \left(2\mathbf{C} \cdot \frac{\delta S_{\mathrm{p}}}{\delta \mathbf{C}} + S_{\mathrm{p}} \mathbf{U} \right), \tag{1.113}$$

where a divergence-free term may be added to $\mathbf{P}T^{-1}$. From (1.112) and (1.113) and neglecting the isotropic contributions one obtains

$$\mathbf{P} = n_{\rm p} k_{\rm B} T \left(\mathbf{U} - \alpha \mathbf{C} \right). \tag{1.114}$$

The second-order approximation to the entropy (1.111) would yield instead of the usual form (1.114) the modified form

$$\mathbf{P} = n_{\rm p} k_{\rm B} T \alpha \mathbf{C} \cdot (\mathbf{U} - \alpha \mathbf{C}), \tag{1.115}$$

which is not supported by the microscopic theory and which only coincides with (1.114) for small values of \mathbb{C} . To avoid this, Grmela and Öttinger propose that the non-equilibrium entropy in terms of the viscous pressure should take the form (1.114), which may be written in terms of \mathbb{P} as

$$S_{\rm p} = \frac{1}{2} n_{\rm p} k_{\rm B} \int \left\{ \text{Tr}[\mathbf{P}/n_{\rm p} k_{\rm B} T] + \ln \det[\mathbf{U} - \mathbf{P}/(n_{\rm p} k_{\rm B} T)] \right\} d\mathbf{r}.$$
 (1.116)

This expression generalises the quadratic expression of EIT. In Chap. 5 (see (5.24)) we will also obtain a form analogous to (1.116) in the kinetic theory of polymers.

To describe the dynamics of the system, one needs the expressions for the matrices **L** and **M** which appear in (1.101). These are given by (Grmela and Öttinger 1997; Öttinger 2005)

$$\mathbf{L} = \begin{pmatrix} 0 & \nabla \rho & 0 & 0 \\ \nabla \rho & [\nabla \mathbf{v} + \mathbf{v} \nabla]^T & \varepsilon \nabla + \nabla p + \nabla \cdot \mathbf{P} & \mathbf{C} \cdot \nabla - \mathbf{U} \nabla \cdot \mathbf{C} \\ 0 & \nabla \varepsilon + p \nabla + \mathbf{P} \cdot \nabla & 0 & 0 \\ 0 & \nabla \mathbf{C} - \mathbf{U} \mathbf{C} \cdot \nabla & 0 & 0 \end{pmatrix},$$
(1.117)

where $(\mathbf{C} \cdot \nabla - \overline{\mathbf{U} \nabla \cdot \mathbf{C}})_{ikl} \equiv \nabla_l C_{ik} - U_{kl} (\mathbf{C} \cdot \nabla)_i$, and

$$\mathbf{M} = \begin{pmatrix} 0 & 0 & 0 & 0 & 0 \\ 0 & -(\nabla \eta_s T \nabla + \mathbf{U} \cdot \nabla \cdot \eta_s T \nabla)^T & \nabla \cdot \eta_s T \dot{\gamma} & 0 \\ 0 & -\eta_s T \dot{\gamma} \cdot \nabla & \frac{1}{2} \eta_s T \dot{\gamma} : \dot{\gamma} - \nabla \cdot \lambda T^2 \nabla & 0 \\ 0 & 0 & 0 & \frac{2}{npk_B c\tau} \mathbf{C} \end{pmatrix}.$$

$$(1.118)$$

With these expressions for L and M, and of the potentials E and S, one recovers the balance equations for mass, momentum and energy and the convected Maxwell equation for the viscous pressure tensor.

Thus, the GENERIC formalism constitutes an independent way to assert the consistency between a generalised entropy and the corresponding evolution equations of the system, and it suggests how to generalize the entropy of EIT in the non-linear regime, where terms beyond the second order in the viscous pressure tensor are needed. Instead of a direct formulation of time-evolution equations for the internal variables, GENERIC formalism advocates for their modelling in terms of these

four building blocks, which emphasize their connection with thermodynamics. The special strengths of this formalism are: (i) its application up to the level of the microscopic distribution function, thus allowing for the modelling of kinetic equations; (ii) the restrictions imposed by the Jacobi identity; (iii) the ability to identify, through the form of **L**, the microscopic expression for the pressure tensor. Reviews of modelling of polymer solutions in non-isothermal conditions are provided in (Dressler et al. 1999; Öttinger 2005).

It must finally be mentioned that other formalisms based on a single generator model and Poisson brackets have been used to describe the generalised transport Eqs. (1.56) and (1.57) for the diffusion flux and the viscous pressure tensor, by Beris and Edwards (Beris and Edwards 1994). Another interesting approach is the so-called Matrix Model for thermodynamically driven systems developed by Jongschaap (Jongschaap 1990; Jongschaap et al. 1994) and whose relation to GENERIC model has been explored in (Edwards et al. 1997). The reader is referred to the original literature for these more advanced topics, which depart from the aims of this book, which is more focused on the relations between non-equilibrium thermodynamical equations of state and rheological equations, rather than on rheological equations themselves.

Chapter 2

Non-equilibrium Temperature and Entropy in Flowing Ideal Gases: Maximum-Entropy Approach

The aim of this chapter and of the three subsequent ones is to provide a microscopic basis for the macroscopic thermodynamic description of flowing systems that has been presented in Chap. 1. Indeed, a close interaction between macroscopic and microscopic approaches is necessary and convenient. On the one hand, it gives explicit expressions for the quantities appearing in the macroscopic description and allows understanding the peculiar characteristics of the several different systems. On the other hand, the macroscopic approach outlines some common features which should be shared by very different physical systems. Usually, the microscopic analysis of non-equilibrium systems is focused on the calculation of transport coefficients; here, we pay particular attention to the non-equilibrium contributions to the entropy and the free energy.

The systems we have chosen for this analysis are ideal gases, phonons, real gases, and polymer solutions. Although from the microscopic point of view their study is rather different, we will underline their common aspects concerning the non-equilibrium contributions to the entropy and to the evolution equation for the viscous pressure tensor.

We explore the thermodynamics of ideal gases in shear flows from two different microscopic points of view: information theory and kinetic theory. It will be seen that the entropy exhibits an influence on the viscous pressure tensor or on the velocity gradient, thus leading to a modification with respect to the local equilibrium entropy, as postulated from a macroscopic point of view in Chap. 1. The expressions in this chapter allow us to go beyond the second order in contributions of the viscous pressure tensor to the non-equilibrium entropy, temperature and chemical potential.

Some of the expressions studied here are useful to discuss in detail several definitions of temperature out of equilibrium, and their respective relations as well as their connection with different physical variables. This is a fundamental topic in non-equilibrium statistical physics beyond the local-equilibrium approximation, and therefore we pay to it a detailed attention.

2.1 Review of Some Basic Concepts

The basic quantity in the microscopic description of ideal monatomic gases is the velocity distribution function f(r, c, t), which accounts for the number of particles between r and r + dr with velocity between c and c + dc at time t. The classical hydrodynamic description is based on the first five moments of the velocity distribution function, namely, the mass density ρ , the mean velocity v, and the internal energy u per unit mass, which are, respectively, defined in terms of the distribution function as

$$\rho(\mathbf{r},t) = \int mf(\mathbf{r},\mathbf{c},t)d\mathbf{c}, \qquad (2.1)$$

$$\rho(\mathbf{r},t)\mathbf{v}(\mathbf{r},t) = \int m\mathbf{c} f(\mathbf{r},\mathbf{c},t) d\mathbf{c}, \qquad (2.2)$$

$$\rho(\mathbf{r},t)u(\mathbf{r},t) = \int \frac{1}{2}m\mathbf{C} \cdot \mathbf{C} f(\mathbf{r},\mathbf{c},t) d\mathbf{c}, \qquad (2.3)$$

where C = c - v is the relative velocity of the molecules with respect to the mean motion of the gas and m the mass of the particles. As is well known, these quantities are related to general conservation laws of mass, momentum and energy. Their respective evolution equations are

$$\rho \dot{\mathbf{v}} = \nabla \cdot \mathbf{v},\tag{2.4}$$

$$\rho \dot{\mathbf{v}} = -\nabla \cdot \mathbf{P} + \rho \mathbf{F},\tag{2.5}$$

$$\rho \dot{u} = -\nabla \cdot \mathbf{q} - \mathbf{P} : \nabla \mathbf{v}. \tag{2.6}$$

Here, v is the reciprocal of the mass density ρ , i.e. the specific volume, **P** the pressure tensor and q the heat flux, which are given in microscopic terms by

$$\mathbf{P} = \int m\mathbf{C}\mathbf{C}f \,\mathrm{d}\mathbf{c},\tag{2.7}$$

$$q = \int \frac{1}{2} mC^2 C f \, \mathrm{d}c. \tag{2.8}$$

Since, at equilibrium, f is an isotropic function of C, the pressure tensor reduces in equilibrium to P = pU, with U the identity tensor and p the equilibrium pressure, given by

$$p = \frac{1}{3} \int mC^2 f \,\mathrm{d}\boldsymbol{c}.\tag{2.9}$$

Thus, for ideal gases $\text{Tr} \mathbf{P}^v = \text{Tr} \mathbf{P} - 3p = 0$. It is found from the definition (2.3) of the internal energy that $p = \frac{2}{3}\rho u$. The macroscopic thermal equation of state for ideal gases, $p = nk_{\rm B}T$, leads to define the absolute equilibrium temperature as:

$$p = \frac{2}{3}\rho u = nk_{\rm B}T,\tag{2.10}$$

with n the number of particles per unit volume and $k_{\rm B}$ the Boltzmann constant. Note that (2.10) is a mathematical definition which is very appealing and useful from a microscopic perspective and in computer simulations, because kinetic energy has a clear physical meaning and it is easy to evaluate in molecular dynamics calculations. However, this definition does not bear direct relation to the measurement of temperature in non-equilibrium situations. Thus, the simplicity of the definition (2.10) should not mask the fact that the understanding of temperature in non-equilibrium situations is still a conceptual challenge, as we will underline in Sect. 2.4.

The main challenge in the microscopic description of non-equilibrium situations is to find the non-equilibrium distribution function f. Here, we will obtain it from information theory to explore in a simple way entropy and temperature in non-equilibrium situations.

2.2 Information Theory: General Formalism

The success of the Gibbsian ensemble method in equilibrium statistical mechanics has fostered the search for an extension for it in non-equilibrium situations. Of course, the latter situations are much more complicated than the equilibrium situations; indeed, it is required to determine not only the equations of state (which are often taken to be those of local-equilibrium) but also the temporal and spatial dependence of measurable properties, to calculate transport coefficients and to describe dissipation.

Several methods have been devised with this aim. One of the most appealing is a non-equilibrium statistical operator method based on the maximum entropy approach (Grandy 1987; Levine and Tribus 1979; Zubarev et al. 1997; Luzzi and Vasconcellos 1990; Luzzi et al. 2001, 2002). Another is more inspired by a canonical extension of the moment method in the kinetic theory of gases (Eu 1998, 2002). We will begin this analysis by using the first method.

The maximum entropy method consists in the maximization, in the context of information theory, of Gibbs statistical entropy, subjected to constraints on the average values of a given set of variables. This principle states that the probability distribution function should be taken to maximize the average missing information of the system, subjected to the constraints corresponding to the available information. In this way, the amount of spurious information attributed to the system is minimized. On several occasions, this method has been criticized as being unduly subjective. In our view, this is not a justified criticism. Indeed, the method will give sound physical results only when the choice of variables on which we focus our attention

coincides with the truly relevant variables in the context of the experiments we want to describe, but not when we arbitrarily fix the choice of the variables. Thus, one of the open problems in this field is the choice of which variables are needed to describe the system. In equilibrium these are the conserved variables, which are microscopic constants of motion, but in non-equilibrium the problem is much more complicated, because it involves, in principle, a host of non-conserved variables.

Here, we will focus our attention on non-equilibrium steady states, which are the most natural and simplest non-equilibrium generalization of equilibrium states. The essential difference between them is the presence of non-vanishing fluxes of energy, mass, momentum and charge in non-equilibrium systems. Note, also, that the assumption of maximum entropy in steady states is not in contradiction with the principle that entropy is maximum at equilibrium, since both statements refer to different sets of constraints. The maximum entropy corresponding to a steady state is always less than (or at most equal to) the entropy corresponding to the equilibrium state with the same internal energy, volume and number of particles as the steady state. Indeed, the latter one is submitted to a wider set of constraints than the equilibrium state, because the fluxes, or other relevant non-equilibrium variables, must be also specified. Each restriction reduces the number of accessible microstates and, therefore, it lowers also the value of entropy.

To be specific, let us present the essential ideas of the method for a system of N particles characterized by their positions and momenta, $\mu' = \{r_1, p_1, \ldots, r_N, p_N\}$. Assume that we know the local mean values $\langle A_i \rangle$ of a set of extensive observables $A_i(\mu')$. The aim is to obtain the probability density $f_N(\mu')$ which maximizes the information in the system compatible with the measured quantities. In other words, one calculates the probability density which maximizes the global entropy S defined by

$$S = -k_{\rm B}(h^{3N}N!)^{-1} \int f_N(\mu') \ln f_N(\mu') d\Gamma_N, \qquad (2.11)$$

and subject to the constraints expressing the known values of the controlled variables, namely

$$(h^{3N}N!)^{-1} \int f_N(\mu') \mathbf{A}_i(\mu') d\Gamma_N = \langle \mathbf{A}_i \rangle. \tag{2.12}$$

Here, $d\Gamma_N = d\mathbf{r}_1 d\mathbf{p}_1 \dots d\mathbf{r}_N d\mathbf{p}_N$ is the volume element in the phase space, and h and k_B are, respectively, the Planck and Boltzmann constants.

To achieve the maximization of S subject to constraints (2.12), one has to maximize the quantity

$$-k_{\rm B} \int \left[f_N \ln f_N + f_N \lambda_0 + f_N \sum_i \lambda_i(r) \cdot A_i(\mu') \right] d\Gamma_N, \qquad (2.13)$$

where the $\lambda_i(\mathbf{r})$ are the Lagrange multipliers corresponding to the quantities $A_i(\mathbf{r})$. The dot between λ_i and A_i indicates a scalar product. In equilibrium these quantities are the internal energy and the particle density. Out of equilibrium, additional

restrictions must be imposed. In extended irreversible thermodynamics, these further restrictions are the fluxes across the system. For instance, a simple non-equilibrium situation would consist of a closed system with internal energy U subjected to a viscous pressure tensor \mathbf{P}^{ν} ; in this case, the constraints are U and \mathbf{P}^{ν} . Finally, λ_0 is the Lagrange multiplier accounting for normalization. In what follows, subscript i starts with i=1.

Expression (2.13) is an extremum under the condition that f_N satisfies

$$\frac{\partial}{\partial f_N} \left[f_N \ln f_N + f_N \lambda_0 + f_N \sum_i \lambda_i(\mathbf{r}) \cdot \mathbf{A}_i(\mu') \right] = 0. \tag{2.14}$$

This yields a generalised canonical distribution of the form

$$f_N = Z^{-1} \exp\left[-\sum_i \lambda_i(\mathbf{r}) \cdot \mathbf{A}_i(\mu')\right], \qquad (2.15)$$

where Z, related to λ_0 by $\ln Z = 1 + \lambda_0$, is a generalised partition function that follows from the normalization condition for f_N , namely

$$Z = (h^{3N}N!)^{-1} \int \exp\left[-\sum_{i} \lambda_{i}(\mathbf{r}) \cdot \mathbf{A}_{i}(\mu')\right] d\Gamma_{N}.$$
 (2.16)

The explicit expressions of the Lagrange multipliers in terms of the average values of the basic variables are derived from constraints (2.12). In view of the form (2.16) of the partition function, the constraints may be written in the compact form

$$-\frac{\partial \ln Z}{\partial \lambda_i} = \langle A_i \rangle, \tag{2.17}$$

as follows from definition (2.16) of Z and relations (2.12). These are the equations of state corresponding to this description.

Introduction of the distribution density (2.13) in the definition (2.11) for the entropy yields

$$S(\mathbf{r}) = k_{\rm B} \left[\ln Z + \sum_{i} \lambda_{i} \cdot \langle A_{i} \rangle \right]. \tag{2.18}$$

The differential of S obtained from (2.18) is

$$dS = k_{\rm B} \left[d \ln Z + \sum_{i} \langle A_i \rangle \cdot d\lambda_i + \sum_{i} \lambda_i \cdot d\langle A_i \rangle \right] = k_{\rm B} \sum_{i} \lambda_i \cdot d\langle A_i \rangle. \quad (2.19)$$

The second equality in (2.19) follows from relation (2.17), which cancels the contributions from d ln Z with those coming from $\sum \langle A_i \rangle \cdot d\lambda_i$.

Comparison of (2.19) with the macroscopic Gibbs equation yields a general interpretation for the Lagrange multipliers in physical terms. For instance, in an

equilibrium system with a given average value of the internal energy, (2.15) reduces to

$$f = Z^{-1} \exp \left[-\sum_{i} \lambda_1 \mathcal{H} \right], \tag{2.20}$$

with ${\cal H}$ the Hamiltonian of the system. The corresponding differential form (2.19) is then

$$dS = k_{\rm B} \lambda_1 dU, \qquad (2.21)$$

which, when compared with the macroscopic Gibbs equation $dS = T^{-1}dU$ yields $\lambda_1 = (k_{\rm B}T)^{-1}$, with T the absolute temperature, and (2.20) is simply the well known canonical distribution function. If one imposes as a further restriction the average value of the particle number, (2.15) takes the form

$$f = Z^{-1} \exp[-\lambda_1 \mathcal{H} - \lambda_2 \mathcal{N}], \tag{2.22}$$

with N the particle-number operator. Equating the differential of the entropy in terms of the Lagrange multipliers with the macroscopic Gibbs equation one obtains

$$dS = k_{\rm B} \lambda_1 dU + k_{\rm B} \lambda_2 dN = T^{-1} dU - \mu T^{-1} dN, \qquad (2.23)$$

which corroborates the previous result for λ_1 and yields $\lambda_2 = -\mu(k_{\rm B}T)^{-1}$ with μ the chemical potential. With these identifications, (2.22) is the macrocanonical probability distribution function.

Out of equilibrium, when new non-equilibrium variables are included in the description, the physical meaning of the Lagrange multipliers is, in general, unknown, because of the lack of a Gibbs equation in such situations. Extended irreversible thermodynamics gives a generalised Gibbs equation which allows such a physical interpretation of the Lagrange multipliers conjugated to the fluxes, as will be emphasized below.

In some cases it is important to have information on the fluctuations of the basic variables with respect to their average values. The expression for the second moments of the fluctuations of the observables $A_i(\mu')$ around their average values is straightforwardly derived in terms of Z by differentiation of (2.16) and is given by

$$\left\langle \left(\mathbf{A}_{i}(\mu') - \langle \mathbf{A}_{i} \rangle \right) \left(\mathbf{A}_{j}(\mu') - \langle \mathbf{A}_{j} \rangle \right) \right\rangle = \frac{\partial^{2} \ln Z}{\partial \lambda_{i} \partial \lambda_{j}}.$$
 (2.24)

It must be emphasized that the generalised canonical distribution function (2.11) is not the exact distribution function which would be obtained from first principles (for instance, starting from the Liouville equation). Indeed, it does not satisfy the Liouville equation, it only gives the correct averages and the fluctuations of the basic variables considered in the description, but not for the other variables, and it does not describe the dissipation in the steady state. However, it is the basis of

the thermodynamics in the space of the chosen variables, in the approach known as informational statistical thermodynamics, which also deals with the transport equations, for whose analysis more information than that given in (2.16) is needed (Luzzi and Vasconcellos 1990; Luzzi et al. 2001, 2002).

2.3 Information Analysis of an Ideal Gas Under Viscous Pressure

Now, we apply these general ideas to a flowing ideal gas of N particles in a volume V under the restrictions on the internal energy U and the viscous pressure tensor \mathbf{P}^{v} (Bidar et al. 1996; Jou and Criado-Sancho 2001). Of course, the quality of the results in the description of actual experiments will depend on how the choice of these variables faithfully grasps the essential physical features of the system. It has been shown in Chap. 1 that this choice is satisfactory for viscoelastic fluids, which cover a wide and rich phenomenology on which we focus our attention.

Since the particles are independent, we will resort to the one-particle distribution function f. To obtain the generalised canonical distribution function f, we maximize the entropy

$$S = -k_{\rm B}V \int f \ln f \, \mathrm{d}C \tag{2.25}$$

under the constraints (2.1), (2.3) and (2.7)

$$\int f \, d\mathbf{C} = \frac{N}{V} = n, \quad \int m\mathbf{C}\mathbf{C} f \, d\mathbf{C} = \mathbf{P}, \quad \int \frac{1}{2} m\mathbf{C}^2 f \, d\mathbf{C} = \frac{U}{V} = \rho u, \quad (2.26)$$

C being the relative velocity of the particles with respect to the mean (barycentric) velocity of the system and n the particle number density. Note that Eqs. (2.26) yield the result

$$U = \frac{1}{2} \text{Tr} V \mathbf{P}. \tag{2.27}$$

Note that the presence of a viscous pressure implies dissipation, in such a way that to keep constant internal energy the dissipated heat should be removed. This removal may be carried out locally, as in the molecular dynamics algorithms that will be examined in Chap. 4, or –more realistically– by means of a heat flow across the system; we do not include the heat flux in the constraints, for the sake of simplicity.

In order to take into account the restrictions associated with tensor **P** we consider two options. The first one imposes Lagrange multipliers related to the internal energy and the component P_{12}^{ν} of **P** (Bidar et al. 1996) which is expected to be satisfactory enough when normal viscous pressure is small and P_{12}^{ν} is the dominant viscous term, as in plane Couette or Poiseuille flows. As a second alternative (Jou and Criado-Sancho 2001) it is considered that measurable quantities are the energy

and all the components of **P**, especially those from which the so-called shear flow material functions are defined as

$$P_{12}^{\nu} = -\eta(\dot{\gamma})\dot{\gamma},$$

$$N_{1} = P_{11}^{\nu} - P_{22}^{\nu} = -\Psi_{1}(\dot{\gamma})\dot{\gamma}^{2},$$

$$N_{2} = P_{22}^{\nu} - P_{33}^{\nu} = -\Psi_{2}(\dot{\gamma})\dot{\gamma}^{2},$$
(2.28)

where $\Psi_1(\dot{\gamma})$ and $\Psi_2(\dot{\gamma})$ are the first and second normal stress coefficients, respectively, and $\eta(\dot{\gamma})$ the shear-rate dependent viscosity, and N_1 and N_2 are the viscous normal pressures, introduced in Sect. 1.1.

The distribution function (2.15) under these constraints can be written as

$$f = z^{-1} \exp \left\{ -\frac{1}{2} \left[\sum_{i} (\beta + 2\lambda_{ii}) mC_i^2 + \sum_{i} \sum_{j(>i)} 2\lambda_{ij} mC_i C_j \right] \right\}, \quad (2.29)$$

or in the more compact form

$$f = z^{-1} \exp\left[-\frac{1}{2}\mathbf{M}:mCC\right], \qquad (2.30)$$

with **M** the symmetric tensor given by

$$\mathbf{M} = \begin{pmatrix} \beta + 2\lambda_{11} & \lambda_{12} & \lambda_{13} \\ \lambda_{12} & \beta + 2\lambda_{22} & \lambda_{23} \\ \lambda_{13} & \lambda_{23} & \beta + 2\lambda_{33} \end{pmatrix}. \tag{2.31}$$

When U and P_{12}^{ν} are taken as the unique independent variables, the only non-vanishing Lagrange coefficients will be β and λ_{12} .

In the case that the average values of U, P_{12}^{ν} , $P_{11}^{\nu} - P_{22}^{\nu}$ and $P_{22}^{\nu} - P_{33}^{\nu}$ are imposed as constraints, the expression (2.30) remains valid with \mathbf{M} given by

$$\mathbf{M} = \begin{pmatrix} \beta + 2\lambda_1 & \lambda_{12} & 0 \\ \lambda_{12} & \beta - 2\lambda_1 + 2\lambda_2 & 0 \\ 0 & 0 & \beta - 2\lambda_2 \end{pmatrix}, \tag{2.32}$$

where the parameters β , λ_{12} , λ_1 and λ_2 are the Lagrange multipliers conjugated to the internal energy, the shear viscous pressure P_{12}^{ν} , and the first and second normal pressures N_1 and N_2 respectively.

The matrix M (2.31) can be expressed in the form

$$\mathbf{M} = \beta \mathbf{U} + \lambda \tag{2.33}$$

with U the unity matrix. Note that (2.32) could also be written as $\mathbf{M} = (k_{\rm B}T)^{-1}\mathbf{U} + \lambda'$, with the component of λ' defined accordingly.

The partition function related to the normalization of f is given by

$$z = V \int \exp\left[-\frac{1}{2}m\mathbf{M}: CC\right] dC, \qquad (2.34)$$

which after integration turns out to be

$$z = \frac{(2\pi)^{3/2} V}{m^{3/2} N |\mathbf{M}|^{1/2}},$$
(2.35)

with $|\mathbf{M}|$ the determinant of the matrix \mathbf{M} . A similar result has been obtained by Farhat and Eu (1998), who also included normal-pressure effects in a non-equilibrium ensemble method proposed by Eu (1998). However, our aims are different from those of these authors, because we are interested in obtaining explicit expressions for the entropy, temperature and chemical potential, and in identifying explicitly the Lagrange multipliers conjugated to the non-equilibrium variables N_1 , N_2 and P_{12}^{ν} .

The first aim is the interpretation of the tensor λ in terms of \mathbf{P}^{ν} . To achieve this goal, note that from the Gaussian character of (2.30), which implies $\langle \mathbf{CC} \rangle = m^{-1}\mathbf{M}^{-1}$, one has

$$\mathbf{P} = n \langle mCC \rangle = n\mathbf{M}^{-1}. \tag{2.36}$$

We will write the tensor **P** as

$$\mathbf{P} = n\beta^{-1}\mathbf{U} + \mathbf{P}^{\nu},\tag{2.37}$$

with \mathbf{P}^{ν} the viscous pressure tensor. In fact, it is usually assumed that $\mathbf{P} = nk_{\rm B}T\mathbf{U} + \mathbf{P}^{\nu}$ rather than (2.37) because $\beta \neq (k_{\rm B}T)^{-1}$ is usually ignored in literature. However, the splitting (2.37) is mathematically more convenient and natural in the present context (Camacho and Jou 1995; Criado-Sancho et al. 1994, 1998). Using (2.36) and (2.37) it immediately follows that

$$\mathbf{M} = \beta \left[\mathbf{U} + \sum_{i=1}^{\infty} \left(-\beta n^{-1} \mathbf{P}^{\nu} \right)^{i} \right], \tag{2.38}$$

where the series expansion for $(1 + x)^{-1}$ has been used.

From the latter result, the Lagrange multipliers λ_{12} , λ_1 and λ_2 may be written in terms of β , n and \mathbf{P}^v . Comparing (2.38) and (2.33) it follows that

$$\lambda = \beta \sum_{i=1}^{\infty} \left(-\beta n^{-1} \mathbf{P}^{\nu} \right)^{i}. \tag{2.39}$$

This expression gives the Lagrange multipliers in terms of the viscous pressure in any order in P^{ν} .

A physical interpretation of the Lagrange multipliers can be given from the comparison between expression (2.19), rewritten as

$$dS = k_{\rm B}\beta dU + k_{\rm B} \sum_{i} \lambda_{i} \cdot \langle dA_{i} \rangle, \qquad (2.40)$$

and the non-equilibrium entropy (1.29) in the presence of a shear viscous pressure. If we are only dealing with the Lagrange multipliers β and λ_{12} the Gibbs Eq. (1.29) takes the form

$$dS = \theta^{-1}dU - \frac{\tau P_{12}^{\nu}}{\eta T}d(VP_{12}^{\nu}), \qquad (2.41)$$

with θ a generalised non-equilibrium temperature, τ the relaxation time associated to P_{12}^{ν} and η the coefficient of shear viscosity. Comparison of (2.40) and (2.41) leads to

$$\beta = \frac{1}{k_{\rm B}\theta}, \quad \lambda_{12} = -\frac{\tau P_{12}^{\nu}}{\eta k_{\rm B}T} = \frac{\tau \dot{\gamma}}{k_{\rm B}T},$$
 (2.42)

with $\dot{\gamma}$ the shear rate. Note that (2.41) is valid for small values of P_{12}^{ν} , i.e. the identification proposed here is strictly valid only in this limit. In Sect. 2.3 we will discuss in detail the differences between T and θ or other possible definitions of temperature.

When we use (2.42) and only the first term of the expansion (2.39) is taken into account one has

$$\lambda \approx -\beta^2 n^{-1} \mathbf{P}^{\nu} = -\frac{1}{n k_{\rm B}^2 \theta^2} \mathbf{P}^{\nu}, \tag{2.43}$$

Note that near equilibrium it is known from kinetic theory that the viscosity coefficient $\eta = nk_{\rm B}T\tau$, with τ the collision time and therefore (2.43) may be extrapolated from equilibrium yielding

$$\lambda \approx -\frac{\tau}{k_{\rm B}\theta n} \mathbf{P}^{\nu}. \tag{2.44}$$

in agreement with the second equality in (2.42). This is the expression for λ in the usual formulation of EIT, when only quadratic terms in \mathbf{P}^{ν} are included in the non-equilibrium entropy. The present analysis shows how to incorporate terms at any order in \mathbf{P}^{ν} in a more general non-equilibrium entropy.

2.3.1 Non-equilibrium Entropy and Chemical Potential: General Formalism

The fundamental assumption underlying information theory establishes that in a physical situation described in terms of a complete set of macroscopic restrictions, the entropy takes its maximum value consistent with such restrictions. This does

not imply any subjectivity or arbitrariness in the choice of the restrictions: the description of the system will lead to satisfactory results only when the choice of the restrictions corresponds to the suitable information required to describe the actual physical state of the system. From the Eqs. (2.25), (2.30) and (2.36), the entropy may be written explicitly as

$$\frac{S}{Vk_{\rm B}} = n \ln z + \frac{1}{2}\mathbf{M} : \mathbf{P}. \tag{2.45}$$

In order to stress the role played by the viscous pressure tensor on the non-equilibrium entropy, an alternative expression to (2.45) in terms of \mathbf{P}^{v} can be derived using the Eqs. (2.35-2.37) and the relation

$$\frac{1}{2}\mathbf{M} \cdot \mathbf{P} = \beta \frac{U}{V} + \frac{n}{2} \text{Tr} \left[\mathbf{U} - \beta n^{-1} \mathbf{P} \right]. \tag{2.46}$$

From (2.45) and (2.46) we obtain for the entropy (2.42) the explicit form

$$\frac{S}{Nk_{\rm B}} = \frac{3}{2} \left[\ln \left(\frac{2\pi}{m} \right) - 1 \right] + \ln \left(\frac{V}{N} \right) + \beta \frac{U}{N} - \frac{3}{2} \ln \beta
+ \frac{1}{2} \left[\ln \left| \mathbf{U} + \beta n^{-1} \mathbf{P}^{\nu} \right| - \operatorname{Tr} \left(\beta n^{-1} \mathbf{P}^{\nu} \right) \right].$$
(2.47)

One equivalent but more compact expression for the entropy can be written by using (2.35) and (2.36) together with (2.45)

$$\frac{S}{Nk_{\rm B}} = \frac{3}{2} \left[\ln \left(\frac{2\pi}{m} \right) + 1 \right] + \ln \left(\frac{V}{N} \right) - \frac{1}{2} \ln |\mathbf{M}|. \tag{2.48}$$

When a N-particle distribution function f_N is introduced instead of the one-particle distribution f previously considered, and when we deal with a general system whose energy and extensive observables are given by $\{U, A_i\}$ and their conjugated Lagrange multipliers are $\{\beta, \lambda_i\}$, the distribution function that fulfils the requirements of maximum entropy has the form

$$f_N = Z_N^{-1} \exp\left[-\beta U - \sum_i \lambda_i \cdot A_i\right], \qquad (2.49)$$

where Z_N is the N-particles partition function.

According to (2.18), the expression for the total entropy is given by

$$S = k_{\rm B}\beta U + k_{\rm B} \sum_{i} \lambda_{i} \cdot A_{i} + k_{\rm B} \ln Z_{N}. \tag{2.50}$$

where A_i refer to observables different from U.

Expression (2.50) may be compared with the macroscopic Gibbs equation

$$S = \frac{1}{\theta}U + \frac{\pi}{\theta}V - \frac{1}{\theta}\mu N - \frac{1}{\theta}\sum_{i}X_{i} \cdot A_{i}, \qquad (2.51)$$

with π the generalized pressure defined by $\pi/\theta = (\partial S/\partial V)_{U,V\mathbf{P}^{\nu}}$, whose physical meaning has been examined in (Domínguez and Jou 1995), μ the chemical potential and $X_i \equiv -k_{\rm B}\theta\lambda_i$.

By comparing (2.50) and (2.51) it follows that

$$\frac{\mu}{\theta} - \frac{\pi}{\theta} \frac{V}{N} = -\frac{k_{\rm B}}{N} \ln Z_N,\tag{2.52}$$

which generalizes the equilibrium relation

$$\frac{\mu_{\rm eq}}{T} - \frac{p}{T} \frac{V}{N} = -\frac{k_{\rm B}}{N} \ln (Z_N)_{\rm eq}.$$
 (2.53)

It turns out from (2.47) or (2.48) that

$$\frac{\pi}{\theta} = \left(\frac{\partial S}{\partial V}\right)_{U, V \mathbf{P}^{v}} = nk_{\mathbf{B}} = \frac{p}{T}.$$
 (2.54)

Thus, in spite of the fact that T and p are changed, respectively, to θ and π , the relation between T and p, namely $p/T = nk_{\rm B}$ is the same as that between θ and π , since $\pi/\theta = nk_{\rm B}$. This result was also found independently (Farhat and Eu 1998). Combining (2.54) with (2.52) one has for the chemical potential

$$\frac{\mu}{\theta} - \frac{\mu_{\text{eq}}}{T} = -\frac{k_{\text{B}}}{N} \ln \frac{Z_N}{(Z_N)_{\text{eq}}}.$$
 (2.55)

Taking into account that $Z_N = z^N/N!$ together with the explicit expression (2.35) for z, (2.55) is rewritten as

$$\frac{\mu}{\theta} - \frac{\mu_{\text{eq}}}{T} = \frac{1}{2} k_{\text{B}} \ln \frac{|\mathbf{M}|}{|\mathbf{M}|_{\text{eq}}}.$$
 (2.56)

Since $|\mathbf{M}|$ depends on the whole pressure tensor [cf. Eq. (2.36)], the chemical potential depends also on all the components of the pressure tensor. The chemical potential (2.56) may be useful to describe some shear-induced effects (for instance, modification of the chemical composition of a mixture of gases under shear, or shift of the spinodal consolution line), which will be analysed in Chaps. 6–10.

2.3.2 Analysis of Plane Couette Flow: Pure Shear Effects

In this section we will obtain explicit expressions for the non-equilibrium entropy (2.48) in terms of U, P_{12} , $P_{11} - P_{22} \equiv N_1$ and $P_{22} - P_{33} \equiv N_2$. First of all we note that expression (2.48) may be written as

$$\frac{S - S_{\text{eq}}}{Nk_{\text{B}}} = -\frac{1}{2} \ln \frac{|\mathbf{M}|}{|\mathbf{M}|_{\text{eq}}} = -\frac{1}{2} \ln \left[|\mathbf{M}| (k_{\text{B}}T)^{3} \right]$$
 (2.57)

where we have used $\mathbf{M}_{eq} = (k_{\rm B}T)^{-1}\mathbf{U}$ so that $|\mathbf{M}|_{eq} = (k_{\rm B}T)^{-3}$.

For a system submitted to a fixed shear viscous pressure P_{12}^{ν} , where normal effects are negligible, corresponding to a plane Couette flow with only β and λ_{12} as non-vanishing Lagrange multipliers, and taking into account (2.32) with $\lambda_1 = \lambda_2 = 0$, the determinant $|\mathbf{M}|$ adopts the form

$$|\mathbf{M}| = \beta^3 - \beta \lambda_{12}^2. \tag{2.58}$$

On the other hand, from Eqs. (2.17) and (2.35) it immediately follows that

$$\langle A_i \rangle = \frac{1}{2} \frac{\partial \ln |\mathbf{M}|}{\partial \lambda_i},\tag{2.59}$$

and Eqs. (2.40), (2.41), (2.58) and (2.59) let us write

$$\frac{U}{V} = \frac{1}{2} \frac{\partial \ln |\mathbf{M}|}{\partial \beta} = \frac{3\beta^2 - \lambda_{12}^2}{2(\beta^3 - \beta \lambda_{12}^2)}, \qquad P_{12}^{\nu} = \frac{1}{2} \frac{\partial \ln |\mathbf{M}|}{\partial \lambda_{12}} = -\frac{\lambda_{12}}{\beta^2 - \lambda_{12}^2}. \quad (2.60)$$

Note that near equilibrium, i.e. when $\lambda_{12} \to 0$, Eqs. (2.60) tend to $U/V = 3/(2\beta)$ and $\lambda_{12} = -\beta^2 P_{12}^{\nu}$, respectively. Thus, when $P_{12}^{\nu} = 0$ one recovers from (2.29) the standard Maxwell–Boltzmann distribution function. From (2.60) we obtain β and λ_{12} in terms of u and P_{12}^{ν} as

$$\beta = \frac{1 - y}{2[R^2 + (1 - y)]} \frac{N}{U}, \qquad \lambda_{12} = \frac{3R^2 + 2(1 - y)}{2R[R^2 + (1 - y)]} \frac{N}{U}, \tag{2.61}$$

where the following auxiliary functions have been introduced

$$R = VP_{12}^{\nu}/U, \qquad y = (1 + 3R^2)^{1/2},$$
 (2.62)

which let us write

$$|\mathbf{M}| = \frac{1}{4} \frac{(y-1)^3}{R^2 [R^2 - (y-1)]^2} \left(\frac{N}{U}\right)^3.$$
 (2.63)

It easy to show that $\lim_{R\to 0} |\mathbf{M}| = \beta^3 = (k_{\rm B}T)^{-3}$ as expected.

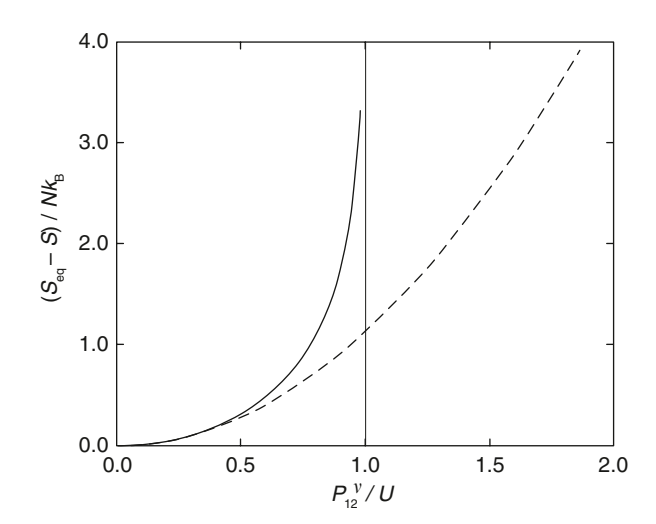
By using (2.57) together with (2.63) and recalling that $k_BT = \frac{2}{3}(U/N)$ the expression for the entropy can be written as

$$\frac{S_{\text{eq}} - S}{Nk_{\text{B}}} = -\frac{1}{2} \ln \frac{27R^2[R^2 - (y - 1)]^2}{2(y - 1)^3},$$
(2.64)

where $S_{\rm eq}$ stands for the equilibrium value of the entropy.

The latter equation, a main result in this section, gives an explicit expression for a non-equilibrium entropy dependent on the shear stress, and which is not limited to second-order non-equilibrium contributions, thus providing a generalization of

Fig. 2.1 Non-equilibrium contribution to the entropy as a function of the ratio VP_{12}^{ν}/U . The solid line corresponds to (2.64) whereas the dashed line corresponds to its second-order approximation in VP_{12}^{ν}/U . (Bidar et al. (1997))



previous results on thermodynamics of fluids systems under shear viscous stress, restricted to second order in P_{12}^{ν} . In Fig. 2.1, is plotted the entropy (2.64) and its second-order approximation in the viscous pressure.

It has been seen in (2.61) that although the present formalism yields the equation of state for τ/η , it does not give any information on τ . Indeed, we have already mentioned that the generalised canonical distribution function (2.13) only gives the thermodynamic quantities (entropy, equations of state) in the space of the selected variables, but not the dynamics nor the dissipation. Thus, τ must be obtained from a kinetic equation, whose formulation requires the full detail of the non-equilibrium statistical operator method (Zubarev et al. 1997; Luzzi and Vasconcellos 1990; Galvao et al. 1995; Luzzi et al. 2002). This is rather complicated, and we will not deal with it in this monograph, which concentrates on the thermodynamic aspects. Here, we will tentatively assume that τ does not depend on $\dot{\gamma}$ in order to explore the consequences of identification (2.61). When (2.61) is combined with (2.60), it yields for the dependence of the shear viscosity $\eta(\dot{\gamma})$ on the shear rate $\dot{\gamma}$

$$\eta(\dot{\gamma}) \equiv \frac{P_{12}^{\nu}}{\dot{\gamma}} = -\frac{3}{2}\eta_0 \frac{R^2 [R^2 + (1-y)]}{R^2 + (2/3)(1-y)}.$$
 (2.65)

Equation (2.65) describes a considerable reduction of the shear viscosity with increasing $\dot{\gamma}$, a phenomenon (shear thinning) which is experimentally well known. For low values of R, this expression tends to η_0 (the shear viscosity in the linear regime), whereas it tends to 0 when R tends to 1. Therefore, the viscous pressure varies in the range $0 < P_{12}^{\nu} < u$ when $\dot{\gamma}$ changes from 0 to ∞ . This limit may be understood from the kinetic interpretation of the pressure. Indeed, in kinetic theory one has $P_{12}^{\nu} = \langle mC_1C_2 \rangle$. Due to the inequality $C_1C_2 < \frac{1}{2}(C_1^2 + C_2^2)$ and $\rho u = \frac{1}{2}m(C_1^2 + C_2^2 + C_3^2)$, it follows that P_{12}^{ν} must be less than or equal to the energy density.

Taking into account that the partition function for the *N*-particle system is $Z_N = z^N/N!$, the characteristic function $F(\beta, V, N, \lambda_{ij})$ which generalizes the usual free energy to the present non-equilibrium situation is

$$F = -\beta^{-1} \ln Z_N = -3B \left\{ F_{\text{eq}} - Nk_{\text{B}}T \ln \left[\left(\frac{27}{2} \right)^{1/2} B(B+1)^{1/2} \right] \right\}, \quad (2.66)$$

where B is the auxiliary function $B = R^2(y-1)^{-1} - 1$, with R and y given by (2.62).

Finally, we may also use the generalised partition function (2.35) to study the fluctuations around non-equilibrium steady states. The second moments of the fluctuations of u and P_{12}^{v} in a steady state with $|\mathbf{M}|$ given by (2.58) and (2.61) may be directly obtained from the well known relationships (2.24), which yield in this case

$$\langle \delta u \delta u \rangle = \frac{\partial^2 \ln z}{\partial \beta^2} = \frac{u^2}{2} \left[3(B+1)^2 + (1-y)^2 \right], \tag{2.67a}$$

$$\langle \delta P_{12}^{\nu} \delta P_{12}^{\nu} \rangle = \frac{\partial^2 \ln z}{\partial \lambda_{12}^2} = u^2 [R^2 + (B+1)^2],$$
 (2.67b)

$$\langle \delta u \delta P_{12}^{\nu} \rangle = \frac{\partial^2 \ln z}{\partial \beta \partial \lambda_{12}} = u^2 R(3 + y + 4B).$$
 (2.67c)

These expressions may be of interest, for instance, in connection with the fluctuation-dissipation theorem in non-equilibrium steady states.

2.3.3 Plane Couette Flow: Shear and Normal Effects

In order to obtain explicit results when, instead of only the β and λ_{12} Lagrange multipliers we consider those conjugated to U, P_{12}^{ν} , $P_{11}^{\nu} - P_{22}^{\nu} \equiv N_1$ and $P_{22}^{\nu} - P_{33}^{\nu} \equiv N_2$, (Jou and Criado-Sancho 2001) we write $|\mathbf{M}|$ as a function of the four later variables, but restricting our attention to the case $N_2 = 0$, which is a good approximation to the experimental observations.

Using the identity $k_{\rm B}T=\frac{2}{3}(U/N)$, the expression (2.57) may be written as

$$\frac{S - S_{\text{eq}}}{Nk_{\text{B}}} = -\frac{1}{2} \ln \left\{ \left(\frac{2}{3} \frac{U}{N} \right)^{3} \left[\det \left(\frac{V}{N} \mathbf{P} \right) \right]^{-1} \right\}, \tag{2.68}$$

and due to the form of the pressure tensor given by (2.26), one finds immediately

$$\det\left(\frac{V}{N}\mathbf{P}\right) = m^{3}\langle C_{3}^{2}\rangle\left[\langle C_{1}^{2}\rangle\langle C_{2}^{2}\rangle - \langle C_{1}C_{2}\rangle^{2}\right].$$
 (2.69)

In equilibrium, $\langle C_1 C_2 \rangle = 0$ and

$$\langle C_1^2 \rangle_{\text{eq}} = \langle C_2^2 \rangle_{\text{eq}} = \langle C_3^2 \rangle_{\text{eq}} = \frac{k_{\text{B}}T}{m} = \frac{2}{3}\frac{U}{N},$$
 (2.70)

and therefore the term inside the logarithm in (2.68) reduces to 1 and one has $S=S_{\rm eq}$, as it should be. Out of equilibrium, $m\langle C_1C_2\rangle=P_{12}^{\nu}$ and the condition $N_2=0$ implies $\langle C_2^2\rangle=\langle C_3^2\rangle$.

The entropy (2.68) may be finally written in terms of P_{12}^{ν} and N_1 as

$$\frac{S - S_{\text{eq}}}{Nk_{\text{B}}} = \frac{1}{2} \ln \left[\frac{1}{4} \left(2 - \frac{V N_1}{U} \right)^2 \left(1 + \frac{V N_1}{U} \right) - \frac{9}{8} \left(2 - \frac{V N_1}{U} \right) \left(\frac{V P_{12}^{\nu}}{U} \right)^2 \right]$$
(2.71)

which is the explicit expression we were looking for, and which is plotted in Fig. 2.2 as a function of VP_{12}^{ν}/U for different values of VN_1/U .

As concerning to the non-equilibrium chemical potential (2.56) we have

$$\frac{\mu}{k_{\rm B}\theta} - \frac{\mu_{\rm eq}}{k_{\rm B}T} = -\frac{1}{2} \ln \left[\frac{1}{4} \left(2 - \frac{VN_{\rm l}}{U} \right)^2 \left(1 + \frac{VN_{\rm l}}{U} \right) - \frac{9}{8} \left(2 - \frac{VN_{\rm l}}{U} \right) \left(\frac{VP_{\rm 12}^{\nu}}{U} \right)^2 \right]. \tag{2.72}$$

Note that (2.71) and (2.72) are mutually consistent. Indeed, recall that by definition

$$\frac{\mu_{\text{eq}}}{T} = -\left(\frac{\partial S_{\text{eq}}}{\partial N}\right)_{U,V}, \qquad \frac{\mu}{\theta} = -\left(\frac{\partial S}{\partial N}\right)_{U,V,VP_{12}^{\nu},VN_{1},VN_{2}}.$$
 (2.73)

Since the right hand side of (2.71) will remain constant during the differentiation with respect to N at the conditions specified by the subscripts attached to the parentheses in (2.73), relation (2.72) follows directly from (2.71) and (2.73). This simple relation between non-equilibrium entropy and chemical potential is a consequence of the fact that in an ideal gas both U and VP are simply additive, namely

$$U = \frac{1}{2} \sum_{\gamma=1}^{N} mC_{\gamma}^{2}, \qquad VP_{ij} = \sum_{\gamma=1}^{N} m(C_{i}C_{j})_{\gamma}.$$
 (2.74)

The presence of interactions amongst the particles, as in real gases, would make more complicated the relation between both non-equilibrium corrections.

Figure 2.2 shows a divergence of $(S-S_{\rm eq})/Nk_{\rm B}$ at a value of VP_{12}^{ν}/U which depends on the value of VN_1/U . In Fig. 2.3 the isentropic curves are plotted, corresponding the dashed one to divergence of $(S-S_{\rm eq})/Nk_{\rm B}$. This divergence indicates in fact a limit of the admissible values for the ratio VP_{12}^{ν}/U , which must be lower than 1.

Fig. 2.2 Non-equilibrium contribution of the viscous pressure to the entropy as a function of VP_{12}^{ν}/U for several values of VN_1/U . (Jou and Criado-Sancho 2001)

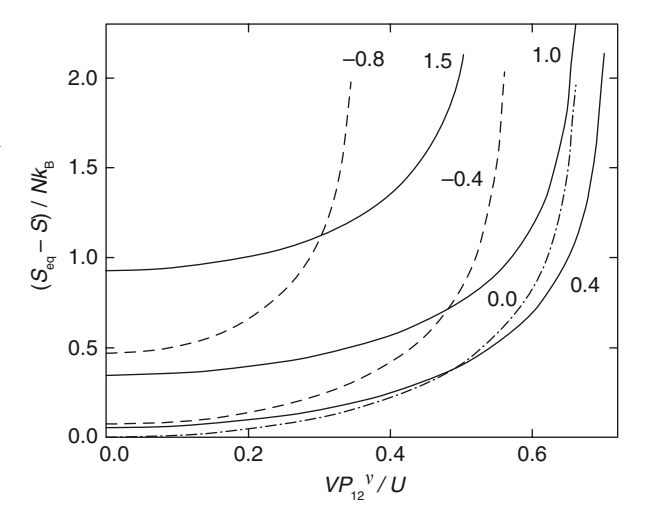
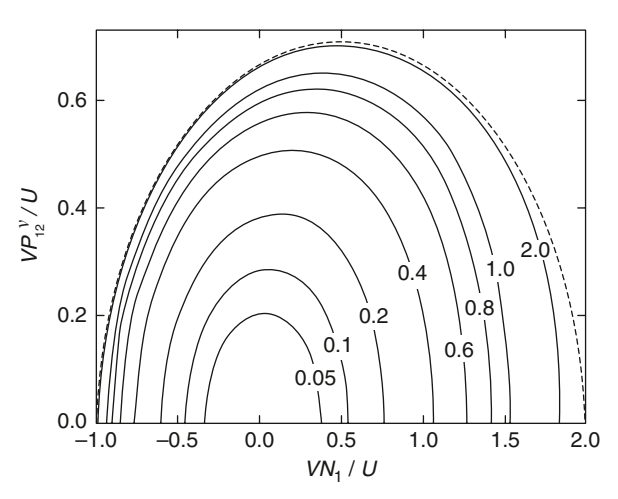


Fig. 2.3 Isentropic curves in the plane VP_{12}^{ν}/U , VN_1/U . The values of $(S-S_{\rm eq})^{\nu}/Nk_{\rm B}$ are given in the corresponding *line*. The *dashed curve* corresponds to the divergence of the entropy. (Jou and Criado-Sancho 2001)



It is not yet clear whether this divergence of the entropy corresponds to an actual instability of the system or to a failure of the classical statistics in the regime where only a few microstates are available; for instance, Boltzmann statistics predicts an infinite entropy (with minus sign) when T tends to zero, but for low T a quantum statistics must be used which yields a vanishing entropy. At this moment, it is still premature to focus the attention on this extreme situation.

In summary, we have explored the influence of non-equilibrium variables (shear viscous pressure, and normal pressures) in the entropy and chemical potential of a dilute gas. In this way, we provide a microscopic basis for these quantities beyond the local equilibrium regime and we generalize extended irreversible thermodynamics beyond the second order in these non-equilibrium parameters.

These results could be used, for instance, to explore the influence of a flow on the composition of a gas mixture in chemical equilibrium but under a velocity gradient

or a viscous pressure, i.e. in a system whose chemical composition is equilibrated but which, nevertheless, is out of hydrodynamical equilibrium as will be done in Chap. 9.

2.4 Non-equilibrium Temperatures in Flowing Gases and Mixtures

The exploration of temperature out of equilibrium is a relevant topic in statistical physics and thermodynamics beyond the local equilibrium approximation (Casas-Vázquez and Jou 2003). In principle, there are several ways to define effective temperatures out of equilibrium by extrapolating several equilibrium relations to non-equilibrium steady states. Since there is not energy equipartition, the temperatures corresponding to different degrees of freedom will be in principle different from each other, and different definitions will lead to different values of temperature out of equilibrium. In the equilibrium limit, all these values tend to the same value, characterizing the equilibrium temperature.

We may take advantage of the results of Sect. 2.2 to illustrate explicitly that different definitions of temperature lead to different values for it, but that these values may be related to each other if a sufficiently detailed knowledge of the system is available. First, we compute from (2.30) and (2.32) the kinetic temperatures associated to the three spatial directions (namely, direction 1, along the flow, direction 2, corresponding to the velocity gradient, and direction 3, perpendicular to the two previous directions) of a flowing ideal gas in a plane Couette flow. The results are

$$\left\langle \frac{1}{2}mc_1^2 \right\rangle = \left\langle \frac{1}{2}mc_2^2 \right\rangle = \frac{1}{2}\frac{\beta}{\beta^2 - \lambda_{12}^2} \equiv \frac{1}{2}k_BT_1 > \frac{1}{2}k_BT$$
 (2.75)

and

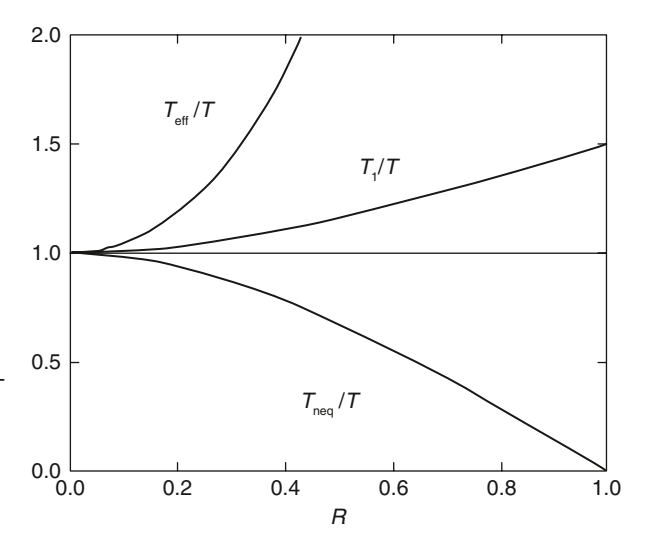
$$\left(\frac{1}{2}mc_3^2\right) = \frac{1}{2\beta} = \frac{1}{2}k_{\rm B}\theta < \frac{1}{2}k_BT,$$
 (2.76)

where $\theta = (k_{\rm B}\beta)^{-1}$. The local-equilibrium temperature *T* has been defined in terms of the total kinetic energy, as in (2.10). Then

$$\left\langle \frac{1}{2}m(c_1^2 + c_2^2 + c_3^2) \right\rangle = \frac{3}{2}k_{\rm B}T. \tag{2.77}$$

Notice that, as it may be checked from (2.75) and (2.76), equipartition of energy in the three spatial directions is broken. The average kinetic energy in the direction perpendicular to the velocity and to the velocity gradient is less than in the other two directions; this is also found in non-equilibrium molecular dynamics for simple fluids with interacting molecules, although in that case the temperature along the

Fig. 2.4 Several temperatures are shown at a given value of U as a function of $R = VP_{12}^{\nu}/U$. The temperatures shown are: local equilibrium temperature T, thermodynamic non-equilibrium temperature T_{neq} (equal to the kinetic temperature along the z axis), the kinetic temperature in the 1 and 2 directions, $T_1 (= T_2)$ and the fluctuation-dissipation effective temperature T_{eff} (Criado-Sancho et al. 2006)



first and the second axes are not exactly equal (Baranyai 2000a, b). Furthermore, it is seen that the kinetic temperature corresponding to direction perpendicular to velocity and to velocity gradient coincides with the non-equilibrium thermodynamic temperature θ , analogously to the situation when a heat flux is present in the system (Camacho and Jou 1995). A third temperature is the thermodynamic one, defined from the non-equilibrium Gibbs Eq. (2.41). It has been evaluated explicitly in terms of U/V and P_{12}^{ν} in (2.61).

In Fig. 2.4, it is seen that θ , denoted as $T_{\rm neq}$ (and therefore the kinetic temperature in the z direction) is reduced for increasing values of viscous pressure, whereas the kinetic temperatures (2.75) in the other two directions increase with viscous pressure (Criado-Sancho et al. 2006).

Still another effective non-equilibrium temperature $T_{\rm eff}$ may be defined from the fluctuation-dissipation theorem (Barrat and Berthier 2000; Berthier and Barrat 2002; Crisanti and Ritort 2003) relating response function and correlation function, as for instance the viscosity and the correlation function of the fluctuations of the shear viscous pressure. Under the assumption of an exponential relaxation for the viscous pressure fluctuations, this effective temperature $T_{\rm eff}$ is defined as

$$\frac{\eta}{\tau} \equiv \frac{1}{k_{\rm B} T_{\rm eff}} \left\langle \delta P_{12}^{\nu}(0) \delta P_{12}^{\nu}(0) \right\rangle. \tag{2.78}$$

In equilibrium, $T_{\rm eff} = T$ and (2.78) is the well-known Green–Kubo relation between shear viscosity and viscous pressure fluctuations when the decay of the latter is exponential with relaxation time τ . In fact, in the general definition of temperature from the fluctuation-dissipation theorem the whole time-dependent response function and correlation function are used, whereas in (2.78) the time integral of both functions are used instead. This may be safely done when the dynamics of the

observable is purely exponential. In the situation we are considering, we find from (2.61) and (2.67b)

$$T_{\text{eff}} = \frac{3\left\{ [R^2/(y-1)]^2 \right\} \left[R^2 + \frac{2}{3}(1-y) \right]}{2R^2(y-1-R^2)} T.$$
 (2.79)

It is seen that $T_{\rm eff} \geq T \geq \theta$ and that both $T_{\rm eff}$ and θ tend to the local-equilibrium temperature T when the viscous pressure tends to zero. However, their asymptotic limit far from equilibrium is very different, as $\theta \to 0$ and $T_{\rm eff} \to \infty$.

It may be noted that $\theta = 1/k_{\rm B}\beta < T$, and that it does not coincide with the local-equilibrium temperature except at equilibrium (Casas-Vázquez and Jou 1994; Camacho and Jou 1995; Jou et al. 1988, 1999a, b, 2010). In fact, the meaning of temperature in presence of a flow is being a subject of recent interest in molecular dynamical simulations (Evans and Morriss 1990; Baranyai and Evans 1991; Todd and Evans 1995, 1997).

It is expected that energy equipartition will be also broken in mixtures. In fact, kinetic theory of mixtures clearly shows that this is so (Garzó and Santos 2003). However, the extent and the conditions of the breaking depend on the model system: for instance, using the full Boltzmann equation or the linearized relaxation-time collision operator yields slightly different results. We have extended our previous analysis of one-component gas to binary mixtures (Criado-Sancho et al. 2008), using the velocity distribution function (2.29) with different values of mass, velocity, and Lagrange multipliers for each species of gases (namely a and b). A breaking of equipartition between different chemical species and different spatial directions is obtained when the entropy is maximized under a fixed energy, number of particles, and shear viscous pressure.

One would may alternatively use the velocity gradient as the non-equilibrium constraint, which would correspond to a slightly different physical situation. The Lagrange multipliers for each species are given by (2.60) and can be determined in terms of U/N and VP_{12}^{ν}/N , from which follows similar equations as (2.75) and (2.76) particularized for the respective species a and b.

We will consider that the total internal energy of the mixture $U=U_a+U_b$ is fixed, and concerning the non-equilibrium constraint on the viscous pressure, two especially relevant situations will be considered: (a) the total shear viscous pressure is fixed; (b) the shear rate is fixed; this will imply, up to the first order in $\dot{\gamma}$, that $P_{12,i}^{\nu}=-n_ik_{\rm B}Tv_i^{-1}\dot{\gamma}$ (where index i refers to species i and v_i the collision frequency of species i).

a. Fixed total viscous pressure. If the total energy and the total shear viscous pressure are fixed, the conditions on the Lagrange multipliers maximizing the total entropy are $\beta_a = \beta_b$, $\lambda_{12,a} = \lambda_{12,b}$ and the energy per particle is the same for both species. By using the definition of the local equilibrium temperature, which in this case is the kinetic temperature, namely $U_i/N_i \equiv \frac{3}{2}k_BT_i$, it follows that both species will share the same kinetic temperature, and also the same "thermodynamic temperature" defined from the reciprocal of β . Equipartition is broken, not at level of the species, but at the level of spatial directions, as in the one-component gas.

b. Fixed velocity gradient. This case is called uniform shear flow, and it has been much studied in kinetic theory (Garzó and Santos 2003). The shear rate $\dot{\gamma}$ is imposed to be equal for both species. Assuming, as before, that the total energy is fixed it follows that, $\beta_a = \beta_b$. The $\lambda_{12,i}$ will be different for each gas and they may be expressed in terms of the collision frecuencies v_a and v_b of the species, which depend on the molar fractions. In this case β , and the corresponding nonequilibrium temperature $T_{\rm neq} = (k_{\rm B}\beta)^{-1}$, is equal for both species but their kinetic temperatures are different implying that equipartition is lost at the level of chemical species, and not only at the level of spatial directions.

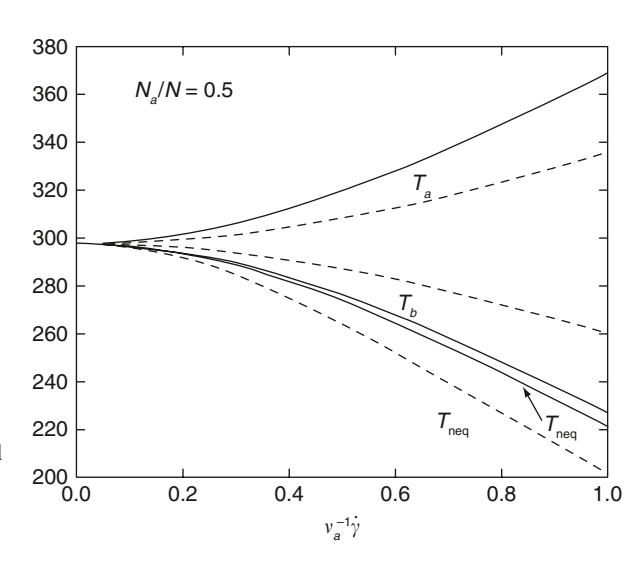
Introducing the variables $w_i \equiv n_i/n$ and $\varepsilon_{ba} \equiv v_b^{-1}/v_a^{-1}$, the additivity of the energy lets us to write $T = w_a T_a + (1 - w_a) T_b$, and we find from the conditions on $\lambda_{12,i}$ the following connection between T_a and T_b

$$\frac{T_a}{T_b} = 1 + \frac{2}{3} (1 - \varepsilon_{ba}^2) (\nu_a^{-1} \dot{\gamma})^2 = 1 + \frac{4}{3} \nu^{-1} (\nu_a^{-1} - \nu_b^{-1}) \dot{\gamma}^2.$$
 (2.79)

In Fig. 2.5 are plotted T_a , T_b and $T_{\rm neq} = T_a \Big[1 + \frac{2}{3} \big(\nu_a^{-1} \dot{\gamma} \big)^2 \Big]^{-1}$. It is seen than the higher the discrepancy in the collision frequencies ν_a and ν_b , i.e. for values of ε_{ba} farther from 1, the differences between the kinetic temperatures of both chemical species are higher and, of course, they increase with increasing $\dot{\gamma}$.

In summary, the results of the present simple analysis are the following ones: (1) Under a non-vanishing viscous pressure, equipartition is broken with respect to the different spatial directions, both for a one-component gas and for each species in the mixture. (2) If the total viscous pressure is imposed on the mixture, both the thermodynamic temperature and the local-equilibrium absolute temperature are the same for both species. In this case, equipartition is broken with respect to different

Fig. 2.5 The kinetic temperatures T_a and T_b of the components a and b and the non-equilibrium temperature $T_{\rm neq} = T_a \Big[1 + \frac{2}{3} (\nu_a^{-1} \dot{\gamma})^2 \Big]^{-1}$ are plotted in terms of $\nu_a^{-1} \dot{\gamma}$ for $N_a = N_b = 0.5N$ for two different values of ε_{ba} , namely 0.25 (solid lines) and 0.75 (dashed lines) and for T = 298 K. (Criado-Sancho et al. 2008)



spatial directions, but not with respect to different chemical species. (3) If homogeneous shear rate is imposed on both kinds of particles, and the total internal energy is fixed, the thermodynamic temperature is the same for both species, but the local-equilibrium absolute temperature is different, and equipartition is broken for the species.

These results show some of the subtleties of temperature in non-equilibrium steady states. For instance, it is surprising that, under some conditions, equipartition may be broken with respect to different spatial directions but not with respect to different chemical species. It is also surprising that the thermodynamic temperature obtained from differentiation of the entropy may be equal, in some circumstances, for both species, although their local-equilibrium absolute temperatures are different.

2.5 Partition Function for a Flowing Relativistic Ideal Gas

In this last section we write for completeness the partition function corresponding to a relativistic ideal gas under a shear viscous pressure P_{12}^{ν} , which complements the information given in Sect. 2.2 concerning the flowing non-relativistic ideal gas. This analysis may be useful for discussions of relativistic nuclear collisions, or of supernovae explosions. The average values of the energy and of the pressure tensor are given, respectively, by

$$\int f(p)pcd\mathbf{p} = u, \quad \int f(p)\frac{1}{2}(\mathbf{p}c + c\mathbf{p})d\mathbf{p} = \mathbf{P}, \quad (2.80)$$

p being the magnitude of the momentum p of the particle and c the speed of light. When these conditions, which are analogous to the conditions (2.22) for non-relativistic ideal gases, are considered, we have instead of (2.23), the following momentum distribution function

$$f(p) = z^{-1} \exp \left[-\beta pc - \sum_{i} \sum_{j>i} \lambda_{ij} \frac{1}{2} (p_i c_j + p_j c_i) \right], \qquad (2.81)$$

with z the one-particle partition function.

After integration over p, the partition function in the presence of a shear viscous pressure turns out to be

$$z = \frac{8\pi V}{(c\beta h)^3} \frac{1}{3} \frac{2[1 + 3(\lambda_{12}/\beta)] + [1 - (\lambda_{12}/\beta)^2]^3}{[1 - (\lambda_{12}/\beta)]^3},$$
 (2.82)

where h is Planck's constant and λ_{12} the Lagrange multiplier related to P_{12}^{ν} . This partition function reduces to the equilibrium partition function of the relativistic gas in the limit of small λ_{12} and $\beta = (k_{\rm R}T)^{-1}$, namely

$$z = 8\pi V \left(\frac{k_{\rm B}T}{ch}\right)^3 \tag{2.83}$$

and it diverges when λ_{12} tends to β . Thus, it shares the same features as (2.32), where these are the two extreme behaviours found. To compute explicitly the Lagrange multipliers, one should use the conditions for the average values of the energy and of the viscous pressure, but taking into account the microscopic expressions for the energy and the pressure of the relativistic gas, by using (2.17) for the average values in terms of the derivatives of the partition function with respect to Lagrange multipliers.

Chapter 3 Kinetic Theory of Flowing Gases and Phonons. Phonon Hydrodynamics and Heat Transport in Nanosystems

In this chapter we focus our attention on the kinetic theory description of dilute gases in shear flow, which provide a different view than that of information theory, explored in the previous chapter. In kinetic theory, the distribution function is found as the solution of a kinetic equation describing the effects of the collisions amongst the particles, which will lead, in the long run, to steady non-equilibrium state under the influence of steady boundary conditions. The kinetic theory of flowing gases is a very rich topic, which has been presented in depth by Garzó and Santos in their well-known book published in 2003, to which the reader interested in the details and advanced developments is referred to. Here, in Sects. 3.1–3.3, we provide a short overview of the essential concepts in this field, which are necessary for the completeness of the presentation. In particular, the theory shows that transport equations, entropy and entropy flux may take more general forms than those of the classical theory.

In Sects. 3.4–3.5 we apply the ideas of the kinetic theory of gases to the kinetic theory of phonons. In particular, the Grad's moment expansion may be used to derive an evolution equation for the heat flux, in which nonlocal effects and memory effects analogous to those considered in Sect. 1.6, appear in a natural way. Here, we apply this formalism to the phonon flow in some nanosystems, which is seen to provide a fruitful approach to the description of heat transport in nanowires and thin layers and in porous materials. This analysis complements Chap. 10 of the fourth edition of the companion book *Extended Irreversible Thermodynamics* (Jou et al. 2010), devoted to heat transport in micro- and nanosystems, and allows one to have a wider view of applications of the topics of fluids under flow. Furthermore, this section pays a special attention to the boundary conditions, referring to a slip heat flow tangential to the walls, which is also important in the analysis of microfluidic problems.

3.1 Kinetic Theory: Basic Concepts

The most usual description of dilute gases in non-equilibrium situations is provided by the kinetic theory. The evolution of the one-particle distribution function $f(\mathbf{r}, \mathbf{c}, t)$ is described by the well known Boltzmann equation, which takes into account

the effects of binary collisions between particles, and neglects collisions involving more than two particles, a quite plausible hypothesis in dilute gases (Grad 1958; Chapman and Cowling 1970). The equilibrium solution of this equation is the well known Maxwell–Boltzmann distribution function, which is a particular example of the canonical distribution function (2.20). The expression for f in non-equilibrium steady states is obtained by solving the Boltzmann equation with suitable boundary conditions. This is not a simple problem, because of the mathematical complexities of this non-linear integrodifferential equation.

The Boltzmann equation has the form

$$\frac{\partial f}{\partial t} + \mathbf{c} \cdot \frac{\partial f}{\partial \mathbf{r}} + \frac{\mathbf{F}}{m} \cdot \frac{\partial f}{\partial \mathbf{c}} = \int d\mathbf{c} \int d\Omega \, |\mathbf{c} - \tilde{\mathbf{c}}| \sigma(\mathbf{c} - \tilde{\mathbf{c}}, \theta) [f'\tilde{f}' - f\tilde{f}]. \tag{3.1}$$

Here, f, \tilde{f} , f', and \tilde{f}' stand for f(r, c, t), $f(r, \tilde{c}, t)$, f(r, c', t), and $f(r, \tilde{c}'t)$ respectively; m is the mass of the particles and F the external force acting on the particles; $\sigma(c-\tilde{c},\theta)$ is the differential cross-section of the collisions between the particles, one of them with initial velocity c and the other with initial velocity \tilde{c} , to give as final velocities after collision c' and \tilde{c}' ; θ is the angle between c and c'; $d\Omega$ is the differential solid angle around θ .

3.1.1 H Theorem

Although the Boltzmann equation is very difficult to solve, several general consequences can be drawn from it even without solving it explicitly, such as, for instance, the form of the balance equations for mass, momentum and energy, as well as the so-called H theorem. We focus our interest on the latter, because of its relation with the topics we are discussing in this monograph. One defines η as follows:

$$\rho(\mathbf{r},t)\eta(\mathbf{r},t) = \int f(\mathbf{r},\mathbf{c},t)\ln f(\mathbf{r},\mathbf{c},t)d\mathbf{c}.$$
 (3.2)

The evolution equation for this quantity may be derived by multiplying the Boltzmann equation (3.1) term-by-term by $\ln f$ and integrating over c. In this way, one obtains

$$\frac{\partial(\rho\eta)}{\partial t} + \nabla \cdot (\boldsymbol{J}^{\eta} + \rho\eta\boldsymbol{v}) = \sigma^{\eta}, \tag{3.3}$$

with the flux J^{η} defined as

$$J^{\eta} = \int C f \ln f \, \mathrm{d}c. \tag{3.4}$$

The production term σ^{η} , defined as

$$\sigma^{\eta} = \int J(f) \ln f \, \mathrm{d}c \tag{3.5}$$

can be written, taking into account well-known symmetry properties of J(f) (Grad 1958; Chapman and Cowling 1970), as

$$\sigma^{\eta} = \frac{1}{4} \int d\mathbf{c} \int d\tilde{\mathbf{c}} \int d\Omega |\mathbf{c} - \tilde{\mathbf{c}}| \, \sigma[f'\tilde{f}' - f\tilde{f}] [\ln f + \ln \tilde{f} - \ln f' - \ln \tilde{f}']$$

$$= \frac{1}{4} \int d\mathbf{c} \int d\tilde{\mathbf{c}} \int d\Omega |\mathbf{c} - \tilde{\mathbf{c}}| \, \sigma[f'\tilde{f}' - f\tilde{f}] \ln [f\tilde{f}/f'\tilde{f}']. \tag{3.6}$$

Inspecting the product of the quantities $[f'\tilde{f}' - f\tilde{f}]$ and $\ln[f\tilde{f}/f'\tilde{f}']$ one sees immediately that $\sigma^{\eta} \leq 0$. This equality holds only for $f'\tilde{f}' = f\tilde{f}$, i.e. for J(f) = 0, which corresponds to equilibrium situations.

The equilibrium distribution function is obtained by realizing that, since $f_{\rm eq}\tilde{f}_{\rm eq}=f_{\rm eq}'\tilde{f}_{\rm eq}'$, then $\ln f_{\rm eq}$ is a collisional invariant and can therefore be expressed as a linear combination of m, mc, and $\frac{1}{2}mc^2$. The result is the Maxwell–Boltzmann distribution function

$$f_{\rm eq} = n \left(\frac{m}{2\pi k_{\rm B}T}\right)^{3/2} \exp\left[-\frac{mC^2}{2k_{\rm B}T}\right].$$
 (3.7)

The *H* theorem, stating the negative character of σ^{η} , suggests that the entropy *s* per unit mass and the entropy flux may be defined in terms of the distribution function respectively as $s = -k_{\rm B}\eta$, i.e.

$$\rho s = -k_{\rm B} \int f \ln f d\boldsymbol{c},\tag{3.8}$$

$$J^{s} = -k_{\rm B} \int C f \ln f dc. \tag{3.9}$$

Indeed, when the equilibrium distribution function (3.7) is introduced into (3.8) the result coincides with the equilibrium entropy of ideal gases, except for additive constants. Out of equilibrium, the classical entropy is not defined. However, it may be asked whether the relation (3.8) may be used as a definition of a thermodynamic entropy out of equilibrium. This is not always strictly possible, because the thermodynamic entropy should be a function of a (small) number of well identified macroscopic variables, whereas out of equilibrium f could have a very complicated form. Despite this, in situations where the non-equilibrium function f depends on r and t parametrically through a (small) number of macroscopic variables, (3.8) may indeed provide a generalization of the entropy to non-equilibrium situations. However, it is important to make the distinction between the H theorem, which refers to the evolution of a microscopic quantity, and the second law, which deals with the increase of a macroscopic quantity. On the other hand, the H theorem is valid for distribution functions which satisfy the Boltzmann equation exactly, whereas the macroscopic non-equilibrium entropy is usually built from an approximated distribution function, in such a way that the connection between its increase and the Htheorem is far from trivial. The reader interested in this topic is referred to (Eu 1992; Woods 1993; Ichiyanagi 1997; Garzó and Santos 2003; Gorban and Karlin 2005).

3.1.2 Non-equilibrium Distribution Function

Out of equilibrium, the distribution function may be expanded as

$$f = f_{eq} \left[1 + \phi^{(1)} + \phi^{(2)} + \cdots \right],$$
 (3.10)

where $\phi^{(1)}$, $\phi^{(2)}$, ... are expressed in terms of a small parameter, for instance the ratio of the relaxation time to the macroscopic time, the ratio of the mean free path to a characteristic length of the macroscopic inhomogeneities, the higher-order moments of the velocity distribution function, etc. The function $f_{\rm eq}$ is the equilibrium distribution function either in global or local equilibrium (in the first case, ρ , ν , and T would not depend on position or time, and in the second case they would depend on these variables).

The quantities $\rho = nm$, v, and T are determined from the first five moments of the distribution function. This imposes on $\phi^{(i)}$ the closure conditions

$$\int f_{eq}\phi^{(i)}d\mathbf{c} = 0, \int f_{eq}\phi^{(i)}\mathbf{C}\,d\mathbf{c} = 0, \tag{3.11a}$$

$$\int f_{eq} \phi^{(i)} C^2 d\mathbf{c} = 0 \quad (i = 1, 2, ...)$$
(3.11b)

and when (3.10) are introduced into (3.8) and (3.9), one obtains up to second order

$$\rho s = \rho s_{\text{eq}} - \frac{1}{2} k_{\text{B}} \int f_{\text{eq}} \phi^{(1)2} dc$$
 (3.12a)

and

$$\mathbf{J}^{s} = \mathbf{q} T^{-1} - \frac{1}{2} k_{\rm B} \int f_{\rm eq} \phi^{(1)2} \mathbf{C} \, d\mathbf{c}.$$
 (3.12b)

Owing to restrictions (3.11), $\phi^{(2)}$ does not contribute to the entropy up to the second order of approximation. Furthermore, it follows from the third of conditions (3.11) that the bulk viscous pressure for an ideal monatomic gas vanishes identically. The first terms on the right-hand side of (3.12a) and (3.12b) are the classical ones; the second are related to the non-classical corrections on which we shall focus our attention in the next section.

As it has been already noted, in contrast to the exact solutions of the Boltzmann equation, approximate solutions do not necessarily satisfy the *H*-theorem beyond the linear approximation. This same problem arises in macroscopic theories when non-linear truncated approximations of the constitutive equations are used. The requirement of a positive entropy production may provide a criterion on the range of validity of a given approximation, both in microscopic and in macroscopic theories. The positive entropy production requirement may also be useful to model the non-linear terms in such a way that entropy production is always positive.

3.2 Grad's Approach 61

3.2 Grad's Approach

Two important models, the Chapman–Enskog and Grad ones, have been proposed to solve the Boltzmann equation in non-equilibrium situations. In the first one (Chapman and Cowling 1970), f is expressed in terms of the first five moments n, v, and T and their gradients. Then, $\phi^{(1)}$ is proportional to ∇v and ∇T , while $\phi^{(2)}$ includes terms in $\nabla \nabla v$, $\nabla \nabla T$ and so on. In Grad's approach (Grad 1958), f is developed in terms of its moments with respect to the molecular velocity. Note that, in view of definitions (2.7–2.8), \mathbf{P} and \mathbf{q} are directly related to the moments of the velocity distribution function (the scalar viscous pressure p^v vanishes in an ideal gas). Therefore, the mean values of \mathbf{q} and of \mathbf{P}^v are considered in Grad's theory as independent variables, so that Grad's theory is very close to the macroscopic developments of EIT in the use of the same independent variables.

In Grad's approach, the non-equilibrium distribution function $f(\mathbf{r}, \mathbf{c}, t)$ is replaced by the infinite set of variables $\rho = mn(\mathbf{r}, t)$, $\mathbf{v}(\mathbf{r}, t)$, $T(\mathbf{r}, t)$, $T(\mathbf{r}, t)$, where \mathbf{a}_n stand for the successive higher-order moments of the distribution function. These moments are chosen in such a way that they are mutually orthogonal, and they are given by Hermite polynomials. In the thirteen-moment approximation, the development is limited to all the second-order moments and to some of the third-order moments, those related to the heat flux. In this approximation, the distribution function is written as

$$f = f_{\text{eq}}[1 + \mathbf{A} \cdot \mathbf{C} + \mathbf{B}^{v} : \overset{0}{\mathbf{C}} \mathbf{C} + (\mathbf{C} \cdot \mathbf{C})(\mathbf{C} \cdot \mathbf{D})]. \tag{3.13}$$

The coefficients $A(\mathbf{r}, t)$, $\mathbf{B}^{\nu}(\mathbf{r}, t)$ and $\mathbf{D}(\mathbf{r}, t)$ are determined by introducing (3.13) into (2.1), (2.2), (2.3), (2.7) and (2.8). Such equations allow us to identify \mathbf{A} , \mathbf{B}^{ν} , and \mathbf{D} in terms of the heat flux \mathbf{q} and the viscous pressure tensor \mathbf{P}^{ν} :

$$A = -\frac{m}{pk_{\rm B}T}q, \quad {\bf B}^0 = \frac{m}{2pk_{\rm B}T}{\bf P}^0, \quad D = \frac{m^2}{5pk_{\rm B}^2T^2}q.$$
 (3.14)

As a consequence, f may be written explicitly as

$$f = f_{\text{eq}} \left[1 + \frac{m}{2pk_{\text{B}}T} \stackrel{0}{\mathbf{C}} \mathbf{C} : \stackrel{0}{\mathbf{P}}^{\nu} + \frac{2m}{5pk_{\text{B}}^{2}T^{2}} \left(\frac{1}{2}mC^{2} - \frac{5}{2}k_{\text{B}}T \right) \mathbf{C} \cdot \mathbf{q} \right]. \quad (3.15)$$

After substitution of (3.15) into (3.12), the expressions for the entropy and entropy flux turn out to be

$$\rho s = \rho s_{\text{eq}} - \frac{1}{4pT} \stackrel{0}{\mathbf{P}}^{\nu} : \stackrel{0}{\mathbf{P}}^{\nu} - \frac{m}{5pk_{\text{B}}T^2} \mathbf{q} \cdot \mathbf{q}, \qquad (3.16)$$

$$\boldsymbol{J}^{s} = \frac{1}{T}\boldsymbol{q} - \frac{2}{5pT} \overset{0}{\mathbf{P}^{v}} \cdot \boldsymbol{q}. \tag{3.17}$$

These results confirm the plausibility of the hypotheses of EIT stating that the entropy may depend on the dissipative fluxes and that the entropy flux contains extra contributions besides $T^{-1}q$.

The evolution equations for the fluxes can be obtained by inserting (3.15) into Boltzmann equation. In the thirteen-moment approximation one is led to (Grad 1958)

$$\frac{\mathrm{d} \mathbf{P}^{\nu}}{\mathrm{d}t} = -\frac{4}{3} (\stackrel{0}{\nabla} \mathbf{q})^{s} - 2p \stackrel{0}{\mathbf{V}} - \rho \gamma \stackrel{0}{\mathbf{P}}^{\nu} - \stackrel{0}{\mathbf{P}}^{\nu} \cdot (\nabla \nu) - (\nabla \nu) \cdot (\stackrel{0}{\mathbf{P}}^{\nu})^{T}
- \stackrel{0}{\mathbf{P}}^{\nu} (\nabla \cdot \mathbf{v}) + \frac{2}{3} [\stackrel{0}{\mathbf{P}}^{\nu} : (\nabla \nu)] \mathbf{U},$$
(3.18a)

and, for the heat flux,

$$\frac{\mathrm{d}\boldsymbol{q}}{\mathrm{d}t} = -\frac{k_{\mathrm{B}}T}{m}\nabla\cdot\mathbf{P}^{v} - \frac{5}{2}\frac{pk_{\mathrm{B}}}{m}\nabla T - \frac{2}{3}\rho\gamma\boldsymbol{q} - \frac{7}{5}\boldsymbol{q}\cdot(\nabla\boldsymbol{v}) - \frac{2}{5}\boldsymbol{q}\cdot(\nabla\boldsymbol{v})^{T}
- \frac{7}{5}\boldsymbol{q}(\nabla\cdot\boldsymbol{v}) - \frac{7}{2}\frac{k_{\mathrm{B}}T}{m}\mathbf{P}^{v}\cdot\nabla T + \rho^{-1}\mathbf{P}^{v}\cdot(\nabla\cdot\mathbf{P}^{v}).$$
(3.18b)

The coefficient γ is given in terms of the collision integrals by

$$\gamma = \frac{2}{5}\sqrt{2\pi} \int_0^\infty x^6 e^{-x^2/2} \left[\int_0^\infty m^{-1} \sigma\left(\theta, x\sqrt{2k_BT/m}\right) \sin^2\theta \cos^2\theta d\theta \right] dx \quad (3.19)$$

and is shown to be a positive quantity, which has the meaning of a collision rate (Grad 1958).

We focus our attention on the linear terms of (3.18) and therefore omit non-linear terms, such as $\mathbf{P}^{\nu} \cdot \nabla T$, because when we take perturbations around equilibrium, both \mathbf{P}^{ν} and ∇T can be considered as small perturbations. In the linear approximation, (3.18a, b) may be directly compared with the linear evolution equations for \mathbf{P}^{ν} and \mathbf{q} derived from the macroscopic theory, namely

$$\tau_2 \dot{\mathbf{P}}^{\nu} + \mathbf{P}^{\nu} = -2\eta \mathbf{V} - 2\eta T \beta (\nabla \mathbf{q})^s$$
 (3.20a)

$$\tau_1 \dot{\boldsymbol{q}} + \boldsymbol{q} = -\lambda \nabla T - 2\lambda T^2 \beta (\nabla \cdot \mathbf{P}^{\nu})$$
(3.20b)

One is then led to the identifications

$$\tau_1 = \frac{3}{2\rho\gamma}, \quad \lambda = \frac{5pk_B}{2m}, \quad -\lambda T^2\beta = \frac{k_BT}{m}\tau_1$$
(3.21a)

$$\tau_2 = \frac{1}{\rho \gamma}, \quad \eta = p \tau_2, \quad -2\eta T \beta = \frac{4}{5} \tau_2.$$
(3.21b)

Furthermore, one obtains for the coefficient in the extra term of the entropy flux $\beta = -2(5pT)^{-1}$. Note also that the relaxation times of \mathbf{q} and \mathbf{p}^{ν} are not equal but $\tau_1 = \frac{3}{2}\tau_2$.

Now, if q = 0 and in the linear flow regime, (3.15) yields

$$f = f_{\text{eq}} \left(1 + \frac{m}{pk_{\text{B}}T} C_1 C_2 \mathbf{P}_{12}^{\nu} \right). \tag{3.22}$$

Since $\mathbf{P}_{12}^{v} = -\eta \dot{\gamma}$, with $\dot{\gamma}$ the shear rate, one may write (3.22) as

$$f = f_{\text{eq}} \left(1 - \tau \dot{\gamma} \frac{m}{k_{\text{B}} T} C_1 C_2 \right). \tag{3.23}$$

The isotropic Maxwellian distribution is then distorted into an ellipsoid in velocity space, with the main axes rotated in the $\pm 45^{\circ}$ direction relative to the direction of the flow. The degree of distortion is determined by the dimensionless product $\tau \dot{\gamma}$. For higher $\tau \dot{\gamma}$ (Loose and Hess 1987, 1991) obtain

$$f = f_{eq} \left[1 - \tau \dot{\gamma} \frac{m}{k_{\rm B}T} \left(1 - \frac{4}{3} \tau^2 \dot{\gamma}^2 + \cdots \right) C_1 C_2 - \tau \dot{\gamma} \frac{m}{k_{\rm B}T} \sqrt{\frac{4}{7}} \left(\frac{m}{2k_{\rm B}T} C^2 - \frac{7}{2} \right) C_1 C_2 \right].$$
 (3.24)

Thus, there appear additional moments and a further dependence on the shear rate leading to further distortion in the C_1C_2 plane which causes shear-thinning, i.e. a reduction of the shear viscosity with increasing shear rate. The corresponding analysis needs then to go beyond the simple Grad approach.

3.3 Comparison with Exact Results

The analysis of dilute gases under shear has received special interest in kinetic theory and in molecular dynamics as a relatively simple situation with many different physical consequences (for a wide bibliography see Garzó and Santos 2003). An exact result for the evolution equations of the viscous pressure tensor was obtained for Maxwell molecules by Ikenberry and Truesdell (Ikenberry and Truesdell 1956). Many analyses with simplified models for the collisions term, such as, for instance, the relaxational BGK (Bhatnagar–Gross–Krook), model have been performed.

Brey and Santos (Brey and Santos 1992; Garzó and Santos 2003) provide a velocity distribution of a dilute gas far from equilibrium for the BGK kinetic equation in uniform shear flow (characterized by a linear profile of the *x*-component of the local velocity along the *y* axis, a constant density and constant temperature: this has the advantage that the only non-zero gradient is $\partial u_x/\partial y = \dot{\gamma}$) for arbitrary shear rates. If we denote $\dot{\gamma}_{ij} = \partial v_i/\partial x_j$, the Boltzmann equation in the BGK approximation is written as

$$\frac{\partial f}{\partial t} + \dot{\gamma}_{ij} c_j \frac{\partial f}{\partial c_i} = -\frac{f - f_0}{\tau}.$$
 (3.25)

Multiplying this equation by mc_ic_j and integrating, one finds for the pressure tensor the following evolution equation

$$\frac{\partial P_{ij}}{\partial t} + (\dot{\gamma}_{ik} P_{jk} + \dot{\gamma}_{jk} P_{ik}) = -\frac{1}{\tau} (P_{ij} - p\delta_{ij}). \tag{3.26}$$

For Maxwell molecules, this has an exact solution which shows non-linear features. For instance, the shear viscosity turns out to be a function of the shear rate

$$\eta = \frac{2}{(\dot{\gamma}\tau)^2} \eta_0 \sinh^2 \left\{ \frac{1}{6} \cosh^{-1} \left[1 + 9(\dot{\gamma}\tau)^2 \right] \right\},\tag{3.27}$$

with $\eta_0 = p\tau$. Non-linear effects are also found in the first normal stress coefficient, whereas the second normal stress coefficient is identically zero (Eu 1998).

Since the equation for P_{ij} has been found without the need to obtain the explicit form of the velocity distribution function, it is not surprising to learn that the behaviour of P_{ij} is rather insensitive to the details of the distribution function. For instance, it has been shown (Brey and Santos 1992; Garzó and Santos 2003) that a Chapman–Enskog expansion is only convergent for $\dot{\gamma}\tau < \sqrt{2}/3$, and that for higher values the distribution function shows highly non-linear features, such as, for instance, a divergence for vanishing velocity for $\dot{\gamma}\tau > \sqrt{6}$. These features are not visible in the behaviour of the second moments, and higher-order moments are necessary to account for them.

Brey and Santos (1992); Santos and Garzó (1995); Garzó and Santos (2003) have studied the fourth and the sixth moments in the BGK relaxation model and also from the exact solution of the Boltzmann equation. Montanero and Santos (Montanero and Santos 1996) have obtained the entropy up to the sixth order in the shear rate $\dot{\gamma}$. If one assumes that

$$f = f_{eq}(1 + \phi_1 + \phi_2 + \phi_3 + \phi_4 + \phi_5),$$
 (3.28)

where f_i are corrections of order i in $\tau \dot{\gamma}$, the entropy may be expanded as

$$S = k_{\rm B} \sum_{n} S^{(n)} (\tau \dot{\gamma})^{n}. \tag{3.29}$$

The odd terms vanish by symmetry considerations, whereas the results for the coefficients of the even terms are

$$S^{(2)} = -\frac{1}{2} \langle \phi_1 | \phi_1 \rangle,$$
 (3.30a)

$$S^{(4)} = -\frac{1}{12} \langle \phi_1 | \phi_1^3 \rangle + \frac{1}{2} \langle \phi_2 | \phi_1^2 - \phi_2 \rangle - \langle \phi_3 | \phi_1 \rangle, \tag{3.30b}$$

$$S^{(6)} = -\frac{1}{30} \langle \phi_1 | \phi_1^5 \rangle + \frac{1}{12} \langle \phi_2 | 3\phi_1^4 - 6\phi_1 \phi_2 + 2\phi_2^2 \rangle$$
$$-\frac{1}{6} \langle \phi_3 | 2\phi_1^3 - 6\phi_1 \phi_2 + 3\phi_3 \rangle + \frac{1}{2} \langle \phi_4 | \phi_1^2 - 2\phi_2 \rangle - \langle \phi_5 | \phi_1 \rangle, \quad (3.30c)$$

where

$$\langle \phi_i | \phi_j \rangle = \int f_{eq} \phi_i \phi_j d\mathbf{c}. \tag{3.31}$$

Montanero and Santos (Montanero and Santos 1996) have obtained $\phi_1, \phi_2, ..., \phi_6$ for the exact solution of the Boltzmann equation, for the relaxation time approximation and for the maximum-entropy approach. Their results for the consecutive contributions to the entropy in (3.29) are

Theory	$S^{(2)}$	$S^{(4)}$	S ⁽⁶⁾
Boltzmann	-0.5000	0.5842	-1.3650
Relaxation time	-0.5000	0.2500	-0.0926
MaxEnt	-0.5000	0.7500	-1.7593

It is interesting to note that the values for $S^{(2)}$ coincide in the three cases. This feature points out an interesting robustness of the second-order non-equilibrium contribution to the entropy.

In contrast, the corresponding coefficients of the higher-order contributions obtained by the different methods differ from each other. This seems to point out a feature which was already noted by Meixner in the 1960s, namely, the non-uniqueness of the entropy in non-equilibrium states. In particular, it is noticed that the maximum entropy expression yields the maximum value for $S^{(4)}$ and the minimum value for $S^{(6)}$, as could be expected. In some sense, if different methods yield different expressions for the non-equilibrium entropy, it is tempting to take the maximum entropy as giving an unequivocally defined expression for the entropy, rather than relying on fine details very sensitive to the mathematical model used to simplify the details of the collision term, or on the different mathematical expansions used to solve the corresponding kinetic equation.

In summary, it is seen that one may compute the non-equilibrium contributions to the entropy at several orders of approximation. This computation requires much more effort in the kinetic theory of gases than in the maximum-entropy approach. However, the possibility of computing non-equilibrium corrections must not lead us to forget the conceptual problems we have mentioned at several points of this chapter, namely, the relations between the microscopic definition of the entropy and its macroscopic expression, the positive character of the entropy production, and the meaning of the temperature.

3.4 Kinetic Theory of Phonons and Phonon Hydrodynamics

In the previous sections we have dealt with ideal gases, but kinetic theory may be applied to many other kinds of systems, as for instance a photon gas colliding with charged particles, or a phonon gas colliding with phonons, impurities or defects in

dielectric solids. Both of them are situations analogous to the ideal gas, but applied to non-conserved quasiparticles. From the thermodynamic point of view, the essential difference between conserved or non-conserved constituents is that in the first case the chemical potential is different from zero, whereas in the second case it is equal to zero. Here, we will refer to some results related to phonons and to their application in heat transfer in nanosystems, which are one of the main topics in transport theory nowadays (Tzou 1997; Cahill 2003; Chen 2005; Zhang 2007; Lebon et al. 2008).

In dielectric crystals, heat is transported by lattice vibrations, which in a quantized formalism are described by means of phonon quasiparticles. The kinetic description of phonons is analogous to that of ideal gases with a few relevant changes. The phonons are characterized by their wavevector \mathbf{k} and their frequency ω , which are respectively related to momentum \mathbf{p} and energy \mathbf{e} as $\mathbf{p} = \hbar \mathbf{k}$ and $\mathbf{e} = \hbar \omega$. The function $\omega(\mathbf{k})$ relating ω and \mathbf{k} is the so-called dispersion relation, which follows from the equations of motion of the atoms of the lattice. Wave packets, and the corresponding phonons, move with the group velocity $\mathbf{v} = \partial \omega / \partial \mathbf{k}$. The function $\omega(\mathbf{k})$ is an anisotropic function of \mathbf{k} , reflecting the differences between longitudinal and transverse waves, and it is usually hard to obtain.

The corresponding Boltzmann–Peierls equation describing the evolution of the momentum distribution function $f(\mathbf{r}, \mathbf{k}, t)$ is (Dreyer and Struchtrup 1993)

$$\frac{\partial f}{\partial t} + \frac{\partial \omega}{\partial k} \cdot \nabla f = S(f) \tag{3.32}$$

where S(f) is the collision term analogous to the collision term on the right-hand side of (3.1), and it includes interactions amongst phonons themselves, with impurity, with defects, and with the boundaries of the crystal.

The energy $e(\mathbf{r}, t)$, and the energy flux $q(\mathbf{r}, t)$, identical to the heat flux because of the absence of convective motion, are given by

$$e(\mathbf{r},t) = \int \hbar\omega(\mathbf{k}) f(\mathbf{k}) d\mathbf{k}$$
 (3.33a)

$$q(\mathbf{r},t) = \int \hbar \omega \frac{\partial \omega}{\partial \mathbf{k}} f(\mathbf{k}) d\mathbf{k}.$$
 (3.33b)

These equations are the analogous to (2.3) and (2.8) for ideal gases. Solutions to (3.32) may be obtained, for instance, by means of a moment expansion analogous to that of Grad's approach. The equilibrium solution for phonons is the Einstein–Planck distribution

$$f_{\rm eq}(k) \sim \frac{1}{\exp\left[\hbar\omega(k)/k_{\rm B}T\right] - 1}.$$
 (3.34)

In the relaxation-time approximation, the collision term S(f) in (3.32) is expressed as

$$S(f) = -\frac{1}{\tau_{\rm R}}(f - f_{\rm eq}) - \frac{1}{\tau_{\rm N}}(f - f_{\rm eq}) - \frac{1}{\tau_{\rm imp}}(f - f_{\rm eq}) - \dots$$
 (3.35)

where τ_R and τ_N are the collision times corresponding to resistive (or umklapp) phonon collisions (momentum non-conserving collisions), and normal phonon collisions (momentum-conserving collisions), and τ_{imp} refers to collisions of phonons against impurities. Other terms related to collisions with defects or with the walls could also be added.

From now on we will consider the linear approximation to the dispersion relation in which $\omega(k) = ck$, and we will expand the solution up to the second-order moment $\mathbf{Q}^{(2)}$. In this way, we will use (Dreyer and Struchtrup 1993; Dreyer et al. 2004; Struchtrup 2005)

$$e(r,t) = c\hbar \int kf(r, \mathbf{k}, t)d\mathbf{k}, \qquad (3.36a)$$

$$\mathbf{q}(r,t) = c^2 \hbar \int \mathbf{k} f(r, \mathbf{k}, t) d\mathbf{k}, \qquad (3.36b)$$

$$\mathbf{Q}(r,t) = c^2 \hbar \int k \mathbf{k} f(r, \mathbf{k}, t) d\mathbf{k}, \qquad (3.36c)$$

and we focus on the evolution of these quantities, one could go to higher-order moments, as $\mathbf{Q}^{(3)}$,

$$\mathbf{Q}^{(3)}(r,t) = c^3 \hbar \int kkk f(r,k,t) dk, \qquad (3.37)$$

and higher-order moments. More convenient definitions for higher-order moments, in view to their orthonormal character—requiring that the different moments are orthogonal to each other—may be found in Dreyer and Struchtrup (1993) and Müller and Ruggeri (1997).

Note that in kinetic theory of ideal gases one could make an analogous approach but by taking for the heat flux q, the flux of the heat flux $\mathbf{Q}^{(2)}$ and the higher order flux $\mathbf{Q}^{(3)}$ the expressions

$$q = \int \frac{1}{2} mC^2 C f(c) dC, \qquad (3.38a)$$

$$\mathbf{Q}^{(2)} = \int \frac{1}{2} mC^2 CC f(\mathbf{c}) dC, \qquad (3.38b)$$

$$\mathbf{Q}^{(3)} = \int \frac{1}{2} mC^2 CCC f(\mathbf{c}) dC. \tag{3.38c}$$

In general terms, the evolution equations for q and $\mathbf{Q}^{(2)}$ in a linear approximation can be written as

$$\tau_1 \dot{\boldsymbol{q}} + \boldsymbol{q} = -\lambda \nabla T - \nabla \cdot \mathbf{Q}^{(2)}, \tag{3.39a}$$

$$\tau_2 \dot{\mathbf{Q}}^{(2)} + \mathbf{Q}^{(2)} = -\lambda_2(\nabla \mathbf{q}) - \nabla \cdot \mathbf{Q}^{(3)}. \tag{3.39b}$$

Here, λ is the thermal conductivity, τ_1 and τ_2 the relaxation times of \boldsymbol{q} and $\mathbf{Q}^{(2)}$, λ_2 a transport coefficient linking $\mathbf{Q}^{(2)}$ and $\nabla \boldsymbol{q}$ and whose physical meaning will be explored below. This procedure could be followed to higher-order tensors, which in a linear approximation leads to a full hierarchy of equations involving couplings only between tensors of order n-1, n, n+1, and has the general form

$$\tau_n \dot{\mathbf{Q}}^{(n)} + \mathbf{Q}^{(n)} = -\lambda_n (\nabla \mathbf{Q}^{(n-1)}) - \nabla \cdot \mathbf{Q}^{n+1}, \tag{3.39c}$$

which will be commented later on.

If it is assumed that $\tau_2 \ll \tau_1$ and that $\mathbf{Q}^{(3)}$ may be neglected, Eq. (3.39b) becomes $\mathbf{Q}^{(2)} = -\lambda_2(\nabla q)$. Introduction of this expression into (3.39a) and assuming λ_2 constant for simplicity, one finally gets

$$\tau_1 \dot{\boldsymbol{q}} + \boldsymbol{q} = -\lambda \nabla T + \ell^2 (\nabla^2 \boldsymbol{q} + 2\nabla \nabla \cdot \boldsymbol{q}). \tag{3.40a}$$

where ℓ may be identified as the phonon mean-free path, and $\lambda_2 = \ell^2$. This is known as the Guyer–Krumhansl equation, because these authors derived it for the first time from the Boltzmann equation for phonons. In particular, they found (Guyer and Krumhansl, 1966a, b)

$$\frac{\partial \boldsymbol{q}}{\partial t} + \frac{1}{\tau_R} \boldsymbol{q} = -\frac{1}{3} \rho c_v c_0^2 \nabla T + \frac{1}{5} c_0^2 \tau_N \left(\nabla^2 \boldsymbol{q} + 2 \nabla \nabla \cdot \boldsymbol{q} \right), \quad (3.40b)$$

with τ_R and τ_N the characteristic times of resistive and non-resistive phonon collisions, c_0 is the phonon speed, and c_v the specific heat per unit volume. Here, we have denoted $\lambda_2 = \ell^2$, where ℓ may be identified with the mean free path. The splitting of $\nabla \cdot \mathbf{Q}^{(2)}$ in $\nabla^2 \mathbf{q}$ and $2\nabla \nabla \cdot \mathbf{q}$ follows from the non-diagonal part of $\mathbf{Q}^{(2)}$ and from the trace of $\mathbf{Q}^{(2)}$ respectively.

The entropy and entropy flux consistent with equation (3.40a) have been studied in detail by Jou and Casas-Vázquez (1990); Dreyer and Struchtrup (1993); Tzou (1996); Cimmelli (2007, 2009); Jou et al. (2010); those corresponding to the hierarchy (3.39c) are discussed in Jou et al. (2010). Here if suffices to mention that the entropy and entropy flux related to (3.39c) are

$$S(U, q^*, ..., Q^{(n)}...) = S_{eq}(U) - \sum_{i} \frac{\tau_i}{\lambda_i T^2} Q^{(i)} \otimes Q^{(i)},$$
 (3.41a)

and

$$J^{s} = \frac{1}{T}q + \sum_{i} \beta_{i} Q^{(i+1)} \otimes Q^{(i)}, \qquad (3.41b)$$

where \otimes stands for the total contraction of indices, and β_i are coefficients proportional to λ_{i+1} . With these expressions, the hierarchy (3.39c) is compatible with the second law of thermodynamics, formulated as the definite positiveness of the production of the generalizated entropy (3.41a). In contrast, neither (3.40a, b) nor the hierarchy (3.39c) are compatible with the local-equilibrium formulation of non-equilibrium thermodynamics, since they lead in some occasions to a negative entropy production when entropy is given by the local-equilibrium form (Jou et al. 2010).

3.5 Poiseuille Phonon Flow and Heat Transport in Nanosystems

Now, we will show the application of equation (3.40a) to the description of heat transport in some nanosystems, as nanowires and thin layers. For the sake of simplicity, we will restrict ourselves to situations in which the radius R of the nanowire or the thickness h of the layers is comparable or smaller to the mean free path ℓ . In this case, one has that $q \ll \ell^2 \nabla^2 q$ because $\ell^2 \nabla^2 q$ is of the order of $(\ell^2 / R^2)q$. Furthermore, in the steady state, where $\dot{q} = 0$ and $\nabla \cdot q = 0$, (3.40a) reduces to

$$\nabla^2 q = \frac{\lambda}{\ell^2} \nabla T. \tag{3.42a}$$

This equation is analogous to the Navier-Stokes equation for Poiseuille flow of viscous fluids in rectilinear ducts, which is

$$\nabla^2 \mathbf{v} = \frac{1}{\eta} \nabla p,\tag{3.42b}$$

where v is the velocity, η the shear viscosity and p the pressure. Thus, q, ∇T and ℓ^2/λ play a role analogous to v, ∇p and η with this analogy, Eq. (3.40a) is analogous to the so-called Stokes–Brinkman equation of hydrodynamics in resistive—or porous—media.

If one considers a nanowire of radius *R*, with a longitudinal heat flow along it and assumes non-slip heat flow on the boundaries, one obtains for the heat profile a parabolic form, analogous to the well-known parabolic Poiseuille profile of viscous fluid velocity,

$$q(r) = \frac{\lambda \Delta T}{4\ell^2 L} (R^2 - r^2), \tag{3.43}$$

	T = 300 K	T = 150 K	T = 100 K	T = 80 K	T = 50 K	
λ (W/m K)	148	409	884	1340	2680	_
ℓ (nm)	40	181	557	1432	6681	

Table 3.1 Bulk thermal conductivity λ and mean free path of phonons ℓ in silicon at several temperatures

with L being the length of the nanowire and $\nabla T \approx \Delta T/L$, with ΔT the difference of temperatures between the two longitudinal ends of the system. Integrating this velocity profile across the transversal surface one has for the total longitudinal heat flow $q_{\text{(tot)}}$

$$q_{\text{(tot)}} = \int_0^R 2\pi r q(r) dr = \frac{\pi R^4 \lambda}{8\ell^2} \frac{\Delta T}{L}.$$
 (3.44)

From here it is usual to define an effective thermal conductivity for the nanowire as

$$\lambda_{\text{eff}} \equiv \frac{q_{\text{(tot)}}}{\pi R^2} \frac{L}{\Delta T} = \frac{\lambda}{8} \frac{R^2}{\ell^2} = \frac{\lambda}{8} \frac{1}{(Kn)^2},$$
(3.45)

where Kn is the Knudsen number, $Kn \equiv \ell / R$.

It is seen that the effective conductivity depends on the radius R and that it tends to zero when R tends to zero. Thus, the effective thermal conductivity of nanowires depends on the size of the system, and is smaller than the thermal conductivity λ for the bulk material. This is indeed observed in nanomaterials and very relevant for applications.

For the sake of illustration and for further use, we give in Table 3.1 the values of λ and ℓ for Si at several temperatures. In particular, the value of ℓ indicates the range of sizes below which classical heat transport Fourier law cannot be applied.

Though expression (3.45) gives a reduction of thermal conductivity its predictions are much smaller than those observed. For instance, at 100 K, the bulk thermal conductivity for Si is $\lambda = 884$ W m⁻¹ K⁻¹ and $\ell = 557$ nm; thus, (3.45) indicates that for R = 115 nm or R = 56 nm $\lambda_{\rm eff}$ should be 4.7 and 1.1 W m⁻¹ K⁻¹ respectively, whereas the observed $\lambda_{\rm eff}$ is, respectively, 45 and 24 W m⁻¹ K⁻¹ as seen in Table 3.2. Furthermore, $\lambda_{\rm eff}$ is experimentally seen to tend to zero as R/ℓ rather than as $(R/\ell)^2$. Thus, something is lacking in this description. The drawback of this description comes from the assumption of the non-slip condition on the boundary. This will be incorporated in the next section.

3.6 Boundary Conditions and Effective Thermal Conductivity in Smooth and Rough Nanowires

In the Poiseuille flow of rarefied gases, there is a boundary slip flow tangential to the wall, in a thin layer, called Knudsen layer, whose thickness is of the order of the mean free path. This surface flow is lacking in liquids and dense gases, where the non-slip condition is imposed, requiring that the relative velocity of the fluid on the wall is zero (i.e. the fluid has the same velocity as the wall). In the kinetic theory, this problem is especially outstanding in rarefied gases, where the mean free path may be relevant. The slip velocity on the surface layer is usually given by the so-called Maxwell condition (Roldughin 1996; Cercignani 2000; Sharipov 2004; Struchtrup 2005)

$$v_{\text{wall}} = C\ell \left(\frac{\partial v_{\text{b}}}{\partial r}\right)_{r=R},\tag{3.46}$$

with v_b the solution of the Navier-Stokes equation (3.42a, b) in the bulk of the fluid. The parameter C depends on the properties of the wall as C = (1+p)/(1-p), with p the specular parameter of the surface, $0 \le p \le 1$, which describes the relative probability that a particle hitting the surface undergoes a specular collision, namely, a purely elastic collision leaving the surface with the same reflexion angle as the incidence angle. Thus, 1-p describes the probability of diffuse collisions, in which the particle exchanges energy with the surface and leaves the surface in a random direction and with a random energy whose probability distribution function is the Maxwellian one, corresponding to the temperature of the wall.

3.6.1 Heat Transfer in Thin Smooth Nanowires

Alvarez et al. (2009) have used an analogous condition to (3.46) but applied to phonon hydrodynamics. Thus, they have used

$$q_{\rm w} = C\ell \left(\frac{\partial q_{\rm b}}{\partial r}\right)_{r-R},\tag{3.47}$$

with $q_{\rm b}$ the heat profile solution of (3.42a). Note that $q_{\rm w}$, as well as $v_{\rm wall}$ in (3.46), describes a flow in a layer of thickness of the order of ℓ parallel to the wall. Since we are dealing here with Knudsen numbers higher than 1, i.e. with $R < \ell$, this layer will in fact deeply influence the whole volume of the system. This relevance of the wall flow is one of the characteristic features of the hydrodynamics of dilute systems in narrow channels (Tabeling 2005; Bruus 2007) or in dilute gases (Cercignani 2000).

Combining condition (3.46) with the solution (3.43) one finds for the heat profile

$$q(r) = \frac{\lambda \Delta T}{4\ell^2 L} (R^2 - r^2 + 2C\ell R). \tag{3.48}$$

By introducing this profile in (3.44), and using the definition (3.45) for the effective thermal conductivity one gets

$$\lambda_{\text{eff}} = \frac{\lambda}{8} \frac{R^2}{\ell^2} \left(1 + 4C \frac{\ell}{R} \right). \tag{3.49}$$

	T = 150	K	T = 100	K	T = 80 k		T = 50 F	ζ.
R (nm)	$\lambda_{\rm effexp}$	$\lambda_{\rm effth}$	$\lambda_{\rm eff\ exp}$	$\lambda_{\rm effth}$	$\lambda_{\rm eff exp}$	$\lambda_{\rm effth}$	$\lambda_{\rm effexp}$	λ_{effth}
115	46	68	45	45	40	40	19	19
56	28	28	23	21	21	19	11	9
37	17	17	14	14	11	13	6	6

Table 3.2 Experimental and theoretical values of the effective thermal conductivity of Si wires of three different radii at different temperatures. (Li et al. 2003)

For small values of R, this leads to a linear behaviour of λ_{eff} with respect to R namely

$$\lambda_{\text{eff}} = \frac{\lambda C}{2} \frac{R}{\ell}.$$
 (3.50)

This linear dependence is indeed observed in experiments, in contrast to the quadratic behaviour predicted by (3.45). Thus, the introduction of the wall slip flow is essential in phonon hydrodynamics applied to nanowires. In Table 3.2 are shown the experimental values of the effective thermal conductivity, and the theoretical results obtained from (3.49) by choosing the value of C to fit the thermal conductivity for a given radius. Comparing with Table 3.1 it is seen the drastic reduction in thermal conductivity between one and two orders of magnitude less than that of bulk silicon.

3.6.2 Heat Transfer in Thin Rough Nanowires

In the previous subsection we have assumed a nanowire with smooth wall, namely, such that the roughness of the walls is much smaller than the dominant phonon wavelength. Nanowires with rough walls have also been made and studied, and it has been seen that their effective thermal conductivity is much smaller than that of smooth nanowires as shown in Table 3.3 (Hochbaum et al. 2008). This reduction is attributed to phonon backscattering against the roughness of the wall. Thus, after these collisions, phonons bounce back and reduce the heat flow.

Sellito et al. (2010a, b) have proposed to use, instead of (3.47), the second-order boundary condition

$$q_{\rm w} = C\ell \left(\frac{\partial q_{\rm b}}{\partial r}\right)_{r=R} - \alpha \ell^2 \left(\frac{\partial^2 q_{\rm b}}{\partial r^2}\right)_{r=R},\tag{3.51}$$

in such a way that the coefficient α is assumed to be related to phonon backscattering and C to specular and diffuse collisions as in (3.47). Including terms up to second order in ℓ in the boundary conditions seems justified, as it is consistent with the fact that we have also taken into account second-order terms in ℓ from the bulk equation (3.40a) for the heat flux. Furthermore, it is also a well-known proposal

R (nm)	T = 150	K	T = 100	K	T = 80 k		T = 50 K	(
	$\lambda_{\rm eff\ exp}$	$\lambda_{\rm effth}$	$\lambda_{\rm effexp}$	$\lambda_{\rm effth}$	$\lambda_{\rm effexp}$	$\lambda_{\rm effth}$	$\lambda_{\rm eff exp}$	$\lambda_{ m effth}$
115	7.8	15.1	5.7	6.9	4.9	6.5	2.5	2.3
97	5.3	5.4	3.8	2.4	3.2	3.1	1.7	0.8

Table 3.3 Experimental and theoretical values of the effective thermal conductivity in Si nanowires with rough walls ($\Delta = 3 \text{ nm}$, L' = 6 nm) at different temperatures. (Hochbaum et al. 2008)

for rarefied gases (Cercignani 2000; Lockerby et al. 2004). The effective thermal conductivity may be obtained, by finding the heat profile, introducing it into (3.38) and applying definition (3.45), and it is

$$\lambda_{\text{eff}} = \frac{\lambda R^2}{8\ell^2} \left(1 + 4C \frac{\ell}{R} - 4\alpha \frac{\ell^2}{R^2} \right), \tag{3.52}$$

for R/ℓ higher than the critical value making $\lambda_{\text{eff}} = 0$, and $\lambda_{\text{eff}} = 0$ for smaller values of R/ℓ . In this way, sufficiently rough nanowires could exhibit, in principle, a transition to an insulating behaviour for small enough values of Knudsen number (Sellitto et al. 2010a; Moore et al. 2008). It is worth to note that the heat flux profile corresponding to this situation has a region near the surface with negative value of q, i.e. with q going from cold to hot regions. The integrated heat flux across the surface satisfies of course the usual statement of the second law, i.e. it flows from hot to cold regions. The negative value of q sufficiently near the wall illustrates that the restriction of the positiveness of the production of local-equilibrium entropy, given by $q \cdot \text{grad } T^{-1}$, is not obeyed everywhere; in contrast, the production of the extended entropy (3.41a) is positive everywhere, because it does not depend only on q, but also of $\mathbf{Q}^{(2)}$ and higher-order fluxes. Up to second order and in the steady situation, $\mathbf{Q}^{(2)}$ is proportional to ∇q , and contributes to the entropy production in the external region where the local-equilibrium entropy production $\boldsymbol{q} \cdot \nabla T^{-1}$ is negative (Sellitto et al. 2010a). Thus, the use of the generalized entropy (3.41a) is conceptually advantageous with respect to the local-equilibrium entropy in this situation.

If Δ is the characteristic height of the roughness peaks and L the average separation between them, Sellitto et al. (2010b) have suggested that

$$C = C'(T)\left(1 - \frac{\Delta}{L}\right),\tag{3.53a}$$

$$\alpha = \alpha'(T) \frac{\Delta}{L}.$$
 (3.53b)

In this way, when the roughness scale Δ is very small, α tends to zero and backscattering disappears.

Phonon hydrodynamics plus boundary conditions have been shown to provide a satisfactory description of heat transport in nanowires, and also in thin layers, of radius comparable or smaller than the mean free path ℓ as it may be seen in Tables 3.2 and 3.3. This provides a phenomenological description, much simpler

than usual descriptions based on the Boltzmann equation for phonons. The connection between both approaches is being carried out through microscopic analyses of the phenomenological coefficients τ , ℓ , C and α appearing in this formalism and the microscopic features of phonon collisions against phonons, impurities, and defects (determining τ and ℓ), and with the walls (determining C and α). Going to higher-order approaches to kinetic theory and using them as a basis for phenomenological equations derived from extended irreversible themodynamics is thus a fruitful procedure.

3.7 Thermal Conductivity of Porous Silicon

We end this study on phonon hydrodynamics applied to nanosystems with a further application to the thermal conductivity of porous Si, where the pores will be considered as small insulating spheres of radius *a* (Alvarez et al. 2010). In this case, the system as a whole is not nanometric, but its internal structure is, and this requires the use of the generalized transport equation (3.40a) instead of the Fourier's law. Porous silicon has a much lower thermal conductivity than bulk silicon (Drost et al. 1995; Gesele et al. 1997; Benedetto et al. 1997; Lysenko et al. 1988, 2000; Song and Chen 2004; Lee et al. 2007). Reducing heat conductivity without reducing electrical conductivity is a required feature for thermoelectric energy conversion, one of the most outstanding aims of material sciences nowadays. Thus, describing this reduction of heat transfer is a relevant topic.

Usually, the effective thermal conductivity of a porous medium is referred to the bulk thermal conductivity of the medium through a function of the porosity φ . Such porosity is the ratio of the volume of the pores—namely $\frac{4}{3}\pi a^3 N$, with N the number of pores—to the total volume of the material. For instance, it is assumed that

$$\lambda_{\text{porous}}(\varphi) = f(\varphi)\lambda_{\text{bulk}}.$$
 (3.54)

The function $f(\varphi)$, for which $0 \le f(\varphi) \le 1$, describes a reduction of the thermal conductivity of the porous medium with respect to the bulk system. Several theories have been proposed for $f(\varphi)$ (Gesele et al. 1997; Benedetto et al. 1977). On the other side, the effective thermal conductivity of a material in which there is an array of spheres of a different material is a classical topic when the size of the spheres and their separation is much longer than the mean-free path, but it is a topic of current interest nowadays when the mean-free path is comparable to the size of the spheres or to their separation.

The phonon hydrodynamic model leads us to consider the pores not only as a reduction of the effective volume, but also as a source of resistance to the phonons. We will take for this resistance the expression analogous to the well-known Stokes law for the resistance to the motion of a sphere in a viscous flow. As we have said, the velocity must be substituted by the heat flux, and the viscosity by ℓ^2/λ_{bulk} . However, for small spheres, of the order or less than the mean free path ℓ , the Stokes

law must be changed. On the basis of experimental observations, Millikan (1922) proposed

$$F = \frac{6\pi \eta a}{1 + A\left(\frac{\ell}{a}\right)\frac{\ell}{a}}L,\tag{3.55}$$

with $A(\ell/a)$ a function which changes from A=0.700 for $\ell/a\ll 1$ to A=1.164 for $\ell/a\gg 1$. This expression reduces to Stokes law for $\ell\ll a$ and it describes the transition to the so-called free molecular regime for $\ell\gg a$.

Since there are many spheres, instead of a single sphere, the flow perturbation of the one modifies the forces on the others. In the case of a random distribution of spheres, the force is given by

$$F = 6\pi \eta a \left(1 + \frac{3}{\sqrt{2}} \sqrt{\varphi} \right) v. \tag{3.56}$$

The hydrodynamic resistance force per unit area leads to an enhancement of the resistance to the flow reflected in an increase of the pressure gradient necessary to sustain the flow. Analogously, in phonon hydrodynamics, this would lead to an increment of the temperature gradient necessary to sustain the heat flow or, in other words, this implies a source of additional thermal resistance. Then

$$\frac{1}{\lambda_{\text{porous}}} = \frac{1}{f(\varphi)\lambda_{\text{bulk}}} + \text{porous thermal resistance}. \tag{3.57}$$

The porous thermal resistance obtained by translating the hydrodynamic results (3.55–3.56) to the phonon hydrodynamics is

porous thermal resistance =
$$\frac{9}{2} \frac{\varphi(\ell/a)^2 \left(1 + \frac{3}{\sqrt{2}} \sqrt{\varphi}\right)}{\lambda_{\text{bulk}} \left[1 + A(\ell/a)\right]}.$$
 (3.58)

Thus, one finally gets (Alvarez et al. 2010)

$$\lambda_{\text{porous}} = \frac{\lambda_{\text{bulk}}}{\frac{1}{f(\varphi)} + \frac{9}{2} \frac{\varphi(\ell/a)^2}{1 + A(\ell/a)} \left(1 + \frac{3}{\sqrt{2}} \sqrt{\varphi}\right)}.$$
 (3.59)

This result indicates that for $\ell \ll a$, one recovers that the thermal conductivity of the porous medium is a function of only the porosity. However, for ℓ/a comparable or higher to 1, the radius of the pores has also an influence in the thermal conductivity. In Table 3.4 we illustrate this dependence and compare it with experimental results. We have taken $f(\varphi) = (1 - \varphi)^3$ as in Gesele et al. (1997), for the sake of closer comparison.

In summary, in Sects. 3.4–3.7 we have shown that the formalism of phonon hydrodynamics seems to provide an efficient way to describe in phenomenological,

2010), $\lambda = 140$ W III	K , $\epsilon = 40$ mm			
Porosity (%)	Radius (nm)	$\lambda_{eff}(Wm^{-1}K^{-1})$	Eq. (3.59)	Standard
40	1.5	1.2	2.1	32
40	100	31.2	29.6	32
50	10	3.9	5.9	18.5
60	10	2.5	4.0	9.5
71	2	0.14	0.16	0.18

Table 3.4 Experimental values of thermal conductivity of porous Si at 300 K for differents porosities and pore radii 1, 4, 2, and theoretical results from (3.59), with $f(\varphi) = (1 - \varphi)^3$. (Alvarez et al. 2010), $\lambda = 148 \text{ Wm}^{-1} \text{ K}^{-1}$, $\ell = 40 \text{ nm}$

simple terms some relevant features of heat transport in nanosystems, either when the size of the system itself is small or when the system contains a nanosize internal structure. Furthermore, Navier-Stokes equation or Stokes-Brinkman equation have been the subject of much mathematical research in many different geometries. Thus, the analysis provided here could be applied without much additional effort to the analysis of the effective thermal conductivity in tubular nanowires, concentric nanowires, thin layers perforated through different arrays (square, triangular, random) of cylindrical pores, porous materials having the structure of a superlattice of pores, and other kinds of structures arising often in current nanotechnology. In all these situations, the slip boundary conditions must be carefully considered, instead of the classical non-slip conditions. Such boundary conditions are currently studied in microfluidics. In this way, phonon hydrodynamics provides an interesting bridge between usual microfluidics and heat transport in nanosystems.

As a final comment, it could be argued that (3.40a) is only a truncation of a general hierarchy (3.39c), and that for Knudsen numbers higher than 1, higher-order terms should be incorporated. Indeed, in Alvarez and Jou (2007, 2008), the full hierarchy (3.39c) has been considered. It leads to a continued-fraction expansion of the thermal conductivity of a system of size L and mean-free path ℓ , having the form

$$\lambda_{\text{eff}}(\ell/L) = \frac{\lambda_0}{1 + \frac{a_1(\ell^2/L^2)}{1 + \frac{a_2(\ell^2/L^2)}{1 + \dots}}}.$$
(3.60)

If it is assumed that all coefficients a_i are equal, in particular $a_i = 4\pi^2$, the asymptotic expression yields for the effective thermal conductivity

$$\lambda_{\text{eff}}(L) = \frac{\lambda}{2\pi^2} \frac{\ell^2}{L^2} \left[\sqrt{1 + 4\left(\frac{\pi\ell}{L}\right)^2} - 1 \right]. \tag{3.61}$$

In equations (3.60) and (3.61) L is an effective length given by $L^{-2} = L_x^{-2} + L_y^{-2} + L_z^{-2}$, with L_x , L_y and L_z being the sizes of the system in the different directions. Thus,

for a thin layer parallel to the plane yz, i.e. with long L_y and L_z . L_z will be simply the thickness L_x . Instead, for a nanowire with its axis along the x direction, L_x is long and $L_y = L_y = R$; this implies that the effective size L in (3.61) will be $L = R/\sqrt{2}$; for tubular nanowires with the axis along the x direction, L_x is long and $L_y = \pi(R_1 + R_2)$ and $L_z = R_1 - R_2$, with R_1 and R_2 being the external and the internal radius. When these prescriptions for the effective size are used, the results for the effective thermal conductivity of nanowires, thin layers, and tubular nanowires in terms of the Knudsen number referred to the effective size fall into a same curve, providing in this way an interesting unification of the results for these different geometries. However, the results of such an approach are examined in detail in the companion volume Extended Irreversible Thermodynamics (Jou et al. 2010) and will not be repeated here.

In Sects. 3.5–3.7, we have taken the truncation (3.40a) as a phenomenological efficient way to describe heat transport. This has a practical interest, because more rigorous and detailed methods starting from the Boltzmann equation, or from molecular dynamics simulations, require very long times of computation. Thus, the analysis of phonon hydrodynamics could provide an approximate and fast method to carry out order-of-magnitude estimations of the thermal conductivity of nanodevices. Once found the kind of devices whose thermal properties seem most suitable, their detailed properties and structure may be analyzed with further depth by starting from a microscopic basis. Trying to study all the situations from the microscopic basis, instead, would be too long and inefficient.

Chapter 4 Non-ideal Fluids and Nuclear Collisions

This chapter deals with the microscopic basis for the non-equilibrium thermodynamics of non-ideal fluids. This topic deserves special attention for several reasons: the contributions of the interaction potential to the pressure tensor may be, in some circumstances, more important than the purely kinetic contributions analysed in ideal gases; furthermore, this interaction allows for phase transitions, which may be affected by the non-equilibrium conditions, thus providing experimental possibilities besides those found in ideal gases.

We first explore the non-equilibrium modifications of the equations of state, compare the non-equilibrium contributions of the ideal gas, studied in Chap. 2, with the non-ideal contributions due to the interaction potential amongst the particles, and describe how these non-equilibrium contributions to the equations of state could shift the critical point of van der Waals gases and of regular binary solutions in the presence of a shear flow. Afterwards, we compare the macroscopic formalism with the results of kinetic theory of real gases, up to second order in the density, and with computer non-equilibrium dynamical simulations carried out for fluids of soft spheres, which also yield non-equilibrium contributions to the equations of state.

Finally, we illustrate some consequences of these ideas in the study of high-energy collisions of nuclei, which are carried out in conditions very far from equilibrium and which could offer an interesting area for the use of generalised thermodynamic analyses. The present results are still very preliminary, and the aim of this section is to stimulate attention on the challenging thermodynamic aspects of this interesting and very active topic of research. Indeed, one of the main aims of this research is to achieve the transition between nuclear matter and quark-gluon plasma. Therefore, the non-equilibrium induced shifts in phase transitions studied in this book could also be useful in this field.

4.1 Modified Equations of State and Shift of Critical Point

The modification of the equations of state in the presence of a non-vanishing viscous pressure tensor may lead to changes in the phase diagram of systems. In Chap. 6, we will study in detail such changes for binary polymer solutions, where the relaxation times are long and the non-classical effects are readily evident in experiments. Here, we outline this influence in two different critical points of non-ideal fluids, namely those of a van der Waals gas and of a binary regular solution. Both examples are seen here as simple theoretical illustrations, but the first may be of interest for comparison with non-equilibrium molecular simulations, while the second has been observed in actual experimental situations.

4.1.1 Van der Waals Fluids

First we recall that the conditions defining the gas-liquid critical point in a single-component fluid are (Callen 1960; Kondepudi and Prigogine 1998)

$$\left(\frac{\partial p}{\partial \nu}\right)_{T,N} = 0, \quad \left(\frac{\partial^2 p}{\partial \nu^2}\right)_{T,N} = 0.$$
 (4.1)

The first equality in (4.1) defines the spinodal line, which sets the limit of stability of the one-phase system. The second relation, which is the condition of an extremum of the spinodal line, specifies the critical point. As an explicit equation of state and for the sake of illustration, we take here the van der Waals equation, which is the simplest one leading to gas-liquid phase transition and to a critical point. The van der Waals gas is defined by the well known equation of state

$$\left(p + \frac{a}{v^2}\right)(v - b) = RT. \tag{4.2}$$

Here R is the constant of ideal gases, and a and b are the usual parameters of the van der Waals equation, which depend on the gas being studied and which incorporate in an averaged and phenomenological way the effects of the attractive and the repulsive part of the intermolecular interaction, respectively. Introduction of (4.2) into (4.1) yields two equations for the volume and the pressure of the critical point which give $v_c = 3b$, $p_c = a/27b^2$ and, correspondingly, $T_c = 8a/27bR$. This well known result is derived in detail in all introductory textbooks on thermodynamics.

Let us now consider how this may be changed by the presence of a non-vanishing viscous pressure tensor. We have seen in (2.54) that, up to the second order in the viscous pressure, the pressure of an ideal gas is changed as

$$p = (\theta/T)p_{\rm eq},\tag{4.3}$$

where we denote here the actual pressure by p and the local-equilibrium pressure by $p_{\rm eq}$ and where θ is defined, according to (2.50) and (2.51) as

$$\theta^{-1} = \left(\frac{\partial s}{\partial u}\right)_{v, \mathbf{P}^{v}} = \frac{\partial s_{\text{eq}}}{\partial u} - \frac{\partial}{\partial u} \left(\frac{\tau v}{4\eta T}\right) \mathbf{P}^{v} : \mathbf{P}^{v}. \tag{4.4}$$

Since $\eta = p\tau$ and $du = c_v dT$, with c_v the specific heat at constant volume, (4.4) vields

$$\theta^{-1} = T^{-1} \left(1 + \frac{\tau}{2\eta c_{\nu} T} \mathbf{P}^{\nu} : \mathbf{P}^{\nu} \right). \tag{4.5}$$

Therefore, up to the second order in P^{ν} (4.3) yields

$$p = (\theta/T)p_{\text{eq}} \cong p_{\text{eq}} - \frac{1}{3}\tau\eta^{-1}\mathbf{P}^{\nu}:\mathbf{P}^{\nu}, \tag{4.6}$$

where we have used that $p_{\rm eq} = nk_{\rm B}T$ and $c_{\rm v} = \frac{3}{2}nk_{\rm B}$. Now, if one considers a non-ideal gas under a shear viscous pressure, one should take into account, besides the usual van der Waals correction $p = p_{id} - av^{-2}$ to the pressure p_{id} of ideal gases due to attractive interactions amongst molecules, the nonequilibrium corrections expressed in (4.6). Thus, we are directly led to the following generalised van der Waals equation (Jou and Pérez-García 1983; Grmela 1987)

$$\left(p + \frac{a}{v^2} + \frac{2}{3}p\tau^2\dot{\gamma}^2\right)(v - b) = RT,\tag{4.7}$$

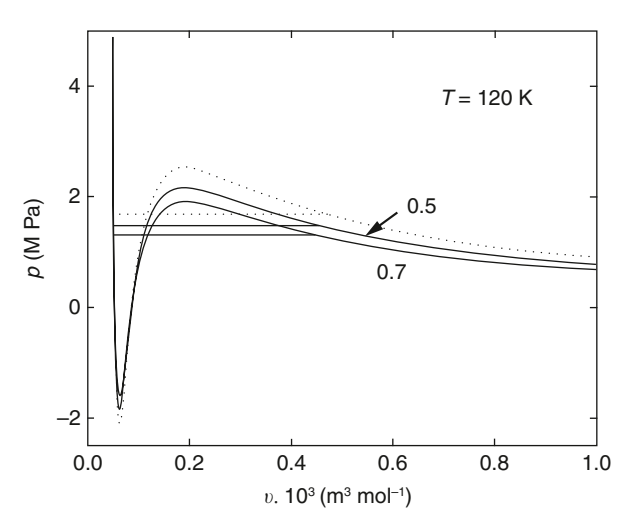
where we have considered a plane Couette flow with shear rate $\dot{\gamma}$, so that \mathbf{P}^{ν} : $\mathbf{P}^{\nu} = 2\eta^2 \dot{\gamma}^2$ and we have taken $\eta = p\tau$, as it is usual in the kinetic theory. The isotherms corresponding to this equation under different values of $\dot{\gamma}$ are shown in Fig. 4.1. From a microscopic perspective, the additional shear-dependent contribution comes essentially from a distortion of the velocity distribution function and the pair correlation function due to the flow. This will be commented more explicitly in Eq. (4.25). These second-order corrections are expected to be valid for relatively small values of $\tau \dot{\gamma}$, less than unit; otherwise, higher-order corrections should also be considered in (4.7).

To apply conditions (4.1) to (4.7), we take into account that for ideal gases $\eta = p\tau = nk_B T\tau$, and thus $\tau = \eta(nk_B T)^{-1}$. Given that the specific volume is $v = (nm)^{-1}$, and η does not depend on ν , the term $\tau\eta\dot{\gamma}^2$ is linear in ν and may be written as $(\eta^2 m/k_B T)v\dot{y}^2$. Thus, when we apply conditions (4.1) to (4.7) we obtain

$$-\frac{RT}{(v-b)^2} + \frac{2a}{v^3} - \frac{2}{3}\frac{\tau\eta\dot{\gamma}^2}{v} = 0,$$
 (4.8a)

$$\frac{2RT}{(v-b)^3} - \frac{6a}{v^4} = 0. {(4.8b)}$$

Fig. 4.1 Isotherms of the equation of state (4.7) under different values of the dimensionless shear rate $\tau \dot{\gamma}$. The horizontal lines correspond to the typical Maxwell construction for the coexistence of liquid and vapour. The dotted line corresponds to a quiescent situation. The data correspond to Ar at 120 K



Since the correction (4.6) is valid up to order $\dot{\gamma}^2$, we solve these equations perturbatively up to order $\dot{\gamma}^2$, i.e. we assume that $v_c(\dot{\gamma}) = v_c + \delta v_c$, $p_c(\dot{\gamma}) = p_c + \delta p_c$ $T_c(\dot{\gamma}) = T_c + \delta T_c$ and linearize the resulting equations with respect to the second-order corrections δv_c , δp_c , and δT_c . We finally obtain

$$v_{\rm c}(\dot{\gamma}) = v_{\rm c} - 0.023 \frac{v_{\rm c}^2}{RT_{\rm c}} \tau \eta \dot{\gamma}^2,$$
 (4.9a)

$$p_{\rm c}(\dot{\gamma}) = p_{\rm c} - 0.667\tau \eta \dot{\gamma}^2,$$
 (4.9b)

$$T_{\rm c}(\dot{\gamma}) = T_{\rm c} - 0.012 \frac{v_{\rm c}}{R} \tau \eta \dot{\gamma}^2,$$
 (4.9c)

where v_c , p_c , and T_c are the respective critical values in equilibrium. We note the negative shift in the critical temperature and the critical pressure. Analogously, the influence of the shear could slightly modify the vapour–liquid as well as solid–liquid coexistence lines, thus inducing some changes in the freezing and boiling temperatures. For instance, in the presence of a shear flow, the freezing of water is expected to occur at a lower temperature than in quiescent water. Furthermore, from (4.7) it will follow that the vapour pressure characterizing the vapour-liquid coexistence in the presence of a small shear will be of the order of $p_{\rm vap} = p_{\rm vap,eq}[1-(2/3)\tau^2\dot{\gamma}^2]$. This would imply an increase of the boiling temperature in the presence of a shear. The reduction of the vapour pressure is illustrated in Fig. 4.1, where the horizontal segments indicate the vapour pressure. The dotted line corresponds to the quiescent situation $(\tau \dot{\gamma} = 0)$, and the other two lines show the reduction of $p_{\rm vap}$ as $\tau \dot{\gamma}$ increases.

4.1.2 Regular Binary Solutions

Binary solutions may be found as a one-phase system, where both components are well-mixed homogeneously over all the system, and as two-phase systems, where the system splits into two phases, one of them richer in one of the components and the other one richer in the second component. The stability conditions are now related to the derivatives of the chemical potential with respect to the concentrations. If we call the number of moles of the two components N_0 and N_1 , and their respective chemical potentials $\mu_i(i=0,1)$, the stability conditions require that the matrix of the second derivatives of the Gibbs free energy G (Callen 1960; Kondepudi and Prigogine 1998), i.e.

$$\begin{pmatrix}
\frac{\partial \mu_0}{\partial N_0} & \frac{\partial \mu_0}{\partial N_1} \\
\frac{\partial \mu_1}{\partial N_0} & \frac{\partial \mu_1}{\partial N_1}
\end{pmatrix}$$
(4.10)

is definite positive, accordingly to the minimal character of G in equilibrium at fixed pressure and temperature. In matrix (4.10) we have taken into account that the chemical potentials are the first derivatives of free energy G, namely, $\mu_i = (\partial G/\partial N_i)_{T,p,N_{j\neq i}}$. The line defined by the condition $(\partial \mu_1/\partial N_1)_{T,p,N_0} = 0$ is the so-called spinodal line, and sets the limit of stability of the one-phase region in the T versus N_0 (or N_1) diagram. The maximum of this line is the critical point, which is thus defined by the two conditions

$$\left(\frac{\partial \mu_1}{\partial N_1}\right)_{T,p,N_0} = 0, \quad \left(\frac{\partial^2 \mu_1}{\partial N_1^2}\right)_{T,p,N_0} = 0, \tag{4.11}$$

which are analogous to the conditions (4.1) specifying the critical point of the gasliquid transition.

As an illustration, we will apply these conditions to the so-called regular binary solutions, defined by the following equation

$$G(T, p, N_0, N_1) = N_0 \mu_0^{(0)}(T, p) + RT N_0 \ln x_0$$

+ $N_1 \mu_1^{(0)}(T, p) + RT N_1 \ln x_1 + \lambda(p) N x_0 x_1,$ (4.12)

where x_i are the molar fractions, namely $x_i \equiv N_i/N$ with $N = N_0 + N_1$ the total number of moles, $\mu_i^{(0)}$ the chemical potential of the corresponding pure substance, and $\lambda(p)$ a parameter depending on p and related to the difference in interaction energy between similar and dissimilar molecules, which is zero for ideal solutions. The chemical potential for component 1 (an analogous expression is valid for component 0) as obtained from (4.12) is

$$\mu_1 = \left(\frac{\partial G}{\partial N_1}\right)_{T,p,N_0} = \mu_1^{(0)}(T,p) + RT \ln x_1 + \lambda x_0^2, \tag{4.13}$$

where it has been used that $(\partial x_1/\partial N_1)_{N_0} = x_0/N$ and $(\partial x_0/\partial N_1)_{N_0} = -x_0/N$. Introduction of (4.13) into (4.11) yields for the spinodal line

$$\left(\frac{\partial \mu_1}{\partial N_1}\right)_{T,p,N_0} = \frac{RTx_0}{N_1} - 2\lambda \frac{x_0^2}{N} = 0,\tag{4.14}$$

which gives in the temperature-composition diagram the relation

$$T = \frac{2\lambda}{R}(1 - x_1)x_1. \tag{4.15}$$

To obtain the critical point we must again differentiate expression (4.14) with respect to N_1 , i.e. we must obtain the maximum of curve (4.15). Since this curve reaches the maximum for $x_{1c} = \frac{1}{2}$, the critical temperature is given by the corresponding value

$$T_{\rm c} = \frac{2\lambda}{R} \left(\frac{1}{2}\right)^2 = \frac{\lambda}{2R}.\tag{4.16}$$

For $x_1 = \frac{1}{2}$ and $T < T_c$ the solution is not homogeneous and splits in two phases. If a non-equilibrium contribution $\Delta G_{\rm f}$ due to the flow is added to (4.12), this would imply a change in the chemical potential. Therefore, (4.14) for the spinodal line would be changed to

$$\left(\frac{\partial \mu_1}{\partial N_1}\right)_{T,p,N_0} = \frac{RTx_0}{N_1} - 2\lambda \frac{x_0^2}{N} + \left(\frac{\partial^2 \Delta G_f}{\partial N_1^2}\right) = 0,$$

i.e.

$$T = \frac{2\lambda}{R}(1 - x_1)x_1 - \frac{x_1}{1 - x_1} \left(\frac{\partial^2 \Delta G_f}{\partial N_1^2}\right) = 0.$$
 (4.17)

The second equation defining the critical point would also be changed, thus yielding a shift in the critical point. The explicit form of this shift depends on the form of $\Delta G_{\rm f}(T,p,N_0,N_1,\dot{\gamma})$, and is negative if $\partial^2 \Delta G_{\rm f}/\partial N_1^2 > 0$. In Chap. 6 we will work out in detail the analogous problem of phase separation in polymer solutions, which is easily observed and has practical interest.

4.1.3 Experimental Results

These results on the shift of the critical temperature may be partially compared with those obtained by Onuki (1980a, b), Onuki et al. (1981) by using renormalization-group techniques, which are beyond the aim of the present monograph. In the case

when the fluid is under shear stress, they obtain for the shear-induced shift of critical temperature

$$T_{\rm c}(\dot{\gamma}) = T_{\rm c} - 0.0832\varepsilon (k_{\rm c}\xi_0)^{1/\nu}.$$
 (4.18)

Here $\varepsilon=4-d$, d being the dimensionality of the system; ξ_0 is a length related to the correlation length of the system by $\xi=\xi_0[(T/T_c)-1]^{-\nu}$, with ν the critical exponent which describes the divergence of ξ when T approaches the critical temperature. The critical wave number k_c is determined by equating the decay rate Γ_k of the order parameter (in this case, the difference of composition of both phases) to the shear rate $\dot{\gamma}$. The decay rate is given in the dynamic scaling theory by $\Gamma_k=k^z\Omega(k\xi)$, where z is a critical exponent. In the situation analysed by Onuki et al. (1981), and for $k\xi>1$, z=3, and $\Omega(k\xi)=k_BT/16\eta$, so that their result (4.18) may be rewritten for d=3 as

$$T_{c}(\dot{\gamma}) = T_{c} - 0.0832T_{c} \left(\frac{16\eta\xi_{0}^{3}}{k_{B}T_{c}}\right)^{\frac{1}{z\nu}} \dot{\gamma}^{\frac{1}{z\nu}}.$$
(4.19)

For an aniline-cyclohexane mixture in three dimensions (z = 3, $v \approx 0.63$), this expression takes the form

$$T_{\rm c}(\dot{\gamma}) = T_{\rm c} - 1.32 \times 10^{-4} \dot{\gamma}^{0.53}.$$
 (4.20)

This is in good agreement with the experimental results of Beysens and Gbadamassi (1979) and Beysens et al. (1979). Note that in EIT one would have a shift proportional to the square of the shear rate; but this exponent does not coincide with 0.53. This is not very surprising since our theory, as well as the classical van der Waals equation, is a "mean field" phenomenological theory with an analytical development. In the case of van der Waals interactions, the mean field is related to the interactions among molecules, while in our case the mean field is related to the non-equilibrium distortion of the pair-correlation function. Thus, a more detailed analysis of these situations would require using renormalization-group ideas, which have not yet been considered in the context of extended thermodynamics.

4.2 Kinetic Theory of Dilute Non-ideal Gases

The treatment of non-ideal gases is obviously more complex than that of ideal gases which we have outlined in Chap. 2, owing to intermolecular interactions which contribute both to the viscous pressure tensor and to the heat flux. Thus, the one-particle distribution function is no longer sufficient for an accurate description of the system, but the two-particle distribution function, accounting for the spatial correlations amongst the particles due to the interaction, is also needed and plays, in fact, a central role.

For simplicity, we deal here only with the influence of the viscous effects on the pressure and the extended entropy, as the influence of a heat flux is considerably more involved. First, we note that in the kinetic theory of non-ideal gases, the pressure tensor is split into a kinetic and a potential part

$$\mathbf{P} = \mathbf{P}_{k} + \mathbf{P}_{n},\tag{4.21}$$

given respectively by the usual kinetic expression (2.7), which we repeat here for the sake of completeness,

$$\mathbf{P}_{k} = \int mCC f_{1} dc \tag{4.22}$$

and

$$\mathbf{P}_{p} = -\frac{1}{2}n^{2} \int \phi'(R)R^{-1}\mathbf{R}\mathbf{R}g(R)d\mathbf{R}.$$
 (4.23)

Note that the kinetic part \mathbf{P}_k is expressed in terms of the one-particle distribution function $f_1(\mathbf{r}, \mathbf{c})$, m is the mass of the particles, and \mathbf{C} their peculiar velocities with respect to the barycentric velocity, and \mathbf{c} their velocity in the laboratory frame of reference. In the potential part \mathbf{P}_p , $\mathbf{R} = \mathbf{r}_1 - \mathbf{r}_2$ is the relative position of molecule 1 with respect to molecule 2, n the particle number density, $\phi(R)$ the molecular interaction potential, with a prime indicating the spatial derivative with respect to R, and g(R) is the pair correlation function defined in terms of the two-particle correlation function $f_2(\mathbf{r}_1, \mathbf{c}_1, \mathbf{r}_2, \mathbf{c}_2)$ as

$$n^2 g(R) = \int f_2(\mathbf{r}_1, \mathbf{c}_1, \mathbf{r}_2, \mathbf{c}_2) d\mathbf{c}_1 d\mathbf{c}_2.$$
 (4.24)

The pair-correlation function g(R) describes how the number density of molecules changes with the distance with respect to one given molecule. Defining the thermodynamic equilibrium pressure as one-third of the trace of **P** at equilibrium, it follows from (4.21-4.23) that

$$p = nk_{\rm B}T - \frac{1}{6}n^2 \int \phi'(R)g_{\rm eq}(R)R\mathrm{d}\mathbf{R},\tag{4.25}$$

with $g_{\rm eq}(R)$ the equilibrium pair correlation function. The first term is the pressure of ideal gases and the second provides the contribution of the intermolecular forces. In dense gases, the second term becomes especially important. If the interaction potential is attractive ($\phi(R) < 0$), its contribution to (4.25) is negative, i.e. the attraction between molecules reduces the pressure they exert on the walls of the system. In the presence of a shear flow, the pair correlation function becomes distorted, and it depends on the shear rate (in fact, it depends not only on R but also on $R \cdot (\nabla v) \cdot R$). This will modify the pressure as it was commented in Sect. 4.1.1.

Since the relaxation times of the one-particle distribution f_1 and of the pair-correlation function g do not necessarily coincide, one should not regard \mathbf{P}^{ν} as a single physical quantity, as was done in Chaps. 2 and 3 for ideal gases, but rather as the sum of two independent quantities, \mathbf{P}_k^{ν} and \mathbf{P}_p^{ν} , each with its own evolution equation. In Chap. 5 it will be seen that for polymer solutions the viscous pressure tensor is usually the superposition of several (or many) independent contributions corresponding to the different normal modes of the macromolecules.

The thermodynamic phenomenological description of the non-ideal gas may be summarized as follows. The entropy has to take into account the independent contributions of the kinetic and the potential part of the viscous pressure, and also the independent character of the bulk viscous pressure (namely, one-third of the trace of the viscous pressure tensor). The natural extension of (1.32) is

$$\rho s = \rho s_{\text{eq}} - \frac{\tau_{\text{k}}}{4\eta_{\text{k}}T} \mathbf{P}_{\text{k}}^{\nu} : \mathbf{P}_{\text{k}}^{\nu} - \frac{\tau_{\text{p}}}{4\eta_{\text{p}}T} \mathbf{P}_{\text{p}}^{\nu} : \mathbf{P}_{\text{p}}^{\nu} - \frac{\tau_{0}}{2\zeta T} p_{\text{p}}^{\nu} p_{\text{p}}^{\nu}.$$
(4.26)

We have only considered the potential bulk viscous pressure since its kinetic part p_k^{ν} vanishes identically, as a consequence of (3.11b).

The relaxation times and viscosities appearing in (4.26) are defined through the evolution equations for their respective fluxes:

$$\frac{\mathrm{d}}{\mathrm{d}t} \mathbf{P}_{k}^{\nu} = -\frac{1}{\tau_{k}} (\mathbf{P}_{k}^{\nu} + 2\eta_{k} \mathbf{V}^{0}), \tag{4.27a}$$

$$\frac{d}{dt} \mathbf{P}_{p}^{\nu} = -\frac{1}{\tau_{p}} (\mathbf{P}_{p}^{\nu} + 2\eta_{p} \mathbf{V}), \tag{4.27b}$$

$$\frac{\mathrm{d}}{\mathrm{d}t}p_{\mathrm{p}}^{\nu} = -\frac{1}{\tau_{0}}(p_{\mathrm{p}}^{\nu} + \zeta \nabla \cdot \mathbf{v}). \tag{4.27c}$$

This is the simplest generalization of the linearized scheme proposed for ideal monatomic gases in Chap. 3.

One may explore the consistency of the thermodynamic scheme (4.26, 4.27) from a microscopic point of view. For this purpose, we need an expression for the entropy in terms of f_1 and f_2 , which is (Jou et al. 2010)

$$\rho s = -k_{\rm B} \int f_1(1) \ln f_1(1) d\Gamma_1 - \frac{1}{2} k_{\rm B} \int f_2(1,2) \ln \frac{f_2(1,2)}{f_1(1) f_1(2)} d\Gamma_{12}, \quad (4.28)$$

where $d\Gamma_1 = d\mathbf{r}_1 d\mathbf{c}_1$ and $d\Gamma_{12} = d\mathbf{r}_1 d\mathbf{c}_1 d\mathbf{r}_2 d\mathbf{c}_2$. The first term is the Boltzmann entropy introduced in (3.8) for the ideal gas, and the second term accounts for the ordering effect of the interparticle correlations.

An explicit form for the entropy in terms of f_1 and g can be obtained by assuming that $f_2(1, 2) = f_1(1)f_1(2)g(1, 2)$. This result is exact at equilibrium and valid up to

the first order in the shear rate for a wide class of interaction potentials. Within this approximation and setting $f_1 = f$ one has

$$\rho s = -k_{\rm B} \int f \ln f \, \mathrm{d}\boldsymbol{c} - \frac{1}{2} n^2 k_{\rm B} \int g \ln g \, \mathrm{d}\boldsymbol{R}. \tag{4.29}$$

By analogy with Boltzmann equation, the evolution equations for f and g can be written as

$$\frac{\partial f}{\partial t} + \mathbf{c} \cdot \frac{\partial f}{\partial \mathbf{r}} = J_{\mathbf{k}}(f), \tag{4.30a}$$

$$\frac{\partial g}{\partial t} + \mathbf{R} \cdot (\nabla \mathbf{v}) \cdot \nabla_{\mathbf{R}} g = J_{\mathbf{p}}(f), \tag{4.30b}$$

where ∇_R stands for the gradient with respect to the relative position R between two molecules. It is not necessary, for our purposes, to know the specific form of operators J_k and J_p on the right-hand sides of (4.30). The only result we need is that at equilibrium $J_k(f_{eq}) = 0$ and $J_p(g_{eq}) = 0$, with f_{eq} and g_{eq} given by

$$f_{\rm eq} \approx \exp\left[-\frac{mC^2}{2k_{\rm B}T}\right], \quad g_{\rm eq} \approx \exp\left[-\frac{w(R)}{k_{\rm B}T}\right].$$
 (4.31)

The last expression defines an effective potential w(R) which coincides with the interaction potential $\phi(R)$ only up to a first-order approximation in the density.

Now, by analogy with the analysis of ideal gases in Sect. 3.2, one expands the non-equilibrium distribution functions f and g in terms of the moments of \mathbf{C} and \mathbf{R} , respectively:

$$f = f_{\text{eq}}[1 + CC : \mathbf{A}^{0}(r, t)], \tag{4.32}$$

$$g = g_{eq}[1 + \mathbf{R}\mathbf{R} : \mathbf{B}(\mathbf{r}, t) + R^2 b(\mathbf{r}, t)].$$
(4.33)

Here $\overset{0}{\mathbf{A}}$ and $\overset{0}{\mathbf{B}}$ are traceless symmetric tensors and b is a scalar, which may be related to $\overset{0}{\mathbf{P}_{\mathbf{k}}^{\nu}}$, $\overset{0}{\mathbf{P}_{\mathbf{p}}^{\nu}}$, and $P_{\mathbf{p}}^{\nu}$ by introducing (4.32, 4.33) into (4.22, 4.23). Note that because of conditions (2.3) the expansion of f is limited to the traceless term \boldsymbol{CC} . It is found that

$$\mathbf{P}_{c}^{v} = \frac{2}{15} m \langle C^{4} \rangle \mathbf{A}, \tag{4.34a}$$

$${\stackrel{0}{\mathbf{P}}}_{\mathbf{p}}^{\nu} = -\frac{1}{15}n^2 \langle \phi'(R)R^3 \rangle {\stackrel{0}{\mathbf{B}}}, \tag{4.34b}$$

$$p_{\rm p}^{\nu} = -\frac{1}{6}n^2 \langle \phi'(R)R^3 \rangle b, \qquad (4.34c)$$

with $\langle \cdots \rangle$ the corresponding equilibrium average.

Furthermore, one can derive an expression for the entropy by substituting (4.32) and (4.33) into (4.29). Letting $f = f_{\rm eq}[1 + \psi_{\rm k}]$ and $g = g_{\rm eq}[1 + \psi_{\rm p}]$, one obtains up to second order

$$\rho s = \rho s_{\text{eq}} - \frac{1}{2} k_{\text{B}} \int f_{\text{eq}} \psi_{k}^{2} d\mathbf{c} - \frac{1}{4} k_{\text{B}} n^{2} \int g_{\text{eq}} \psi_{p}^{2} d\mathbf{R}.$$
 (4.35)

Relations (4.34) then allow us to express the entropy in terms of the dissipative fluxes:

$$\rho s = \rho s_{\text{eq}} - \frac{\alpha_{\text{kk}}}{2T} \mathbf{P}_{\text{k}}^{v} : \mathbf{P}_{\text{k}}^{v} - \frac{\alpha_{\text{pp}}}{2T} \mathbf{P}_{\text{p}}^{v} : \mathbf{P}_{\text{p}}^{v} - \frac{\alpha_{0}}{2T} (p_{\text{p}}^{v})^{2}, \tag{4.36}$$

with

$$\alpha_{\rm kk} = \frac{15k_{\rm B}T}{2m^2} \frac{1}{\langle C^4 \rangle},\tag{4.37a}$$

$$\alpha_{\rm pp} = \frac{15k_{\rm B}T}{n^2} \frac{\langle R^4 \rangle}{\langle \phi'(R)R^3 \rangle^2},\tag{4.37b}$$

$$\alpha_0 = \frac{18k_{\rm B}T}{n^2} \frac{\langle R^4 \rangle}{\langle \phi'(R)R^3 \rangle^2}.$$
 (4.37c)

Expression (4.36) confirms that the entropy depends on \mathbf{P}_{k}^{v} , \mathbf{P}_{p}^{v} , and p_{p}^{v} , but it does not yet give the explicit form of the coefficients used in (4.26). To achieve this identification, we must study the relation between the coefficients α_{kk} , α_{pp} , and α_{0} and their microscopic analogues are derived from the evolution equations for the fluxes. After introducing (4.32, 4.33) into (4.30), and multiplying the resulting equations term by term by \mathbf{CC} , \mathbf{RR} , and \mathbf{R}^{2} , respectively, one is led, after integration with respect to \mathbf{C} and \mathbf{R} , respectively, to

$$\frac{2}{15}\langle C^4 \rangle \frac{\partial \mathbf{A}}{\partial t} + \frac{2m}{15k_B T} \langle C^4 \rangle \mathbf{V} = -\frac{1}{\tau_k} \mathbf{V} + NL, \tag{4.38a}$$

$$\frac{2}{15} \langle R^4 \rangle \frac{\partial \mathbf{B}^0}{\partial t} - \frac{2}{15k_{\rm B}T} \langle w'(R)R^3 \rangle \mathbf{V}^0 = -\frac{1}{\tau_{\rm p}} \mathbf{B}^0 + \text{NL}, \tag{4.38b}$$

$$\langle R^4 \rangle \frac{\partial b}{\partial t} - \frac{1}{3k_{\rm B}T} \langle w'(R)R^3 \rangle \nabla \cdot \mathbf{v} = -\frac{1}{\tau_0} b + \text{NL}.$$
 (4.38c)

Here, NL stands for non-linear terms, while the relaxation times τ_k , τ_p , and τ_0 are related to the collision operators J_k and J_p of (4.30) by

$$-\frac{1}{\tau_{k}} = \langle C_{1}C_{2}J_{k}(C_{1}C_{2})\rangle, \quad -\frac{1}{\tau_{p}} = \langle R_{1}R_{2}J_{p}(R_{1}R_{2})\rangle, \quad -\frac{1}{\tau_{0}} = \langle R^{2}J_{p}(R^{2})\rangle.$$
(4.39)

Here we do not require the explicit expressions for the relaxation times. In the more general case, the relaxation times form a fourth-rank tensor; however, here for simplicity we consider only the particular case for which they reduce to scalar quantities. Because of (4.34a–c), expressions (4.38a–c) truly represent the evolution equations for the fluxes. The ratios $\tau/(2\eta)$ may be obtained directly from the ratio of the coefficients of the terms $d\mathbf{P}^{\nu}/dt$ and the corresponding terms in \mathbf{V} , as immediately seen by inspection of (4.31). Taking into account (4.39), it is found that

$$\frac{\tau_{\mathbf{k}}}{2n_{\mathbf{k}}} = \frac{15k_{\mathbf{B}}T}{m^2} \frac{1}{\langle C^4 \rangle},\tag{4.40a}$$

$$\frac{\tau_{\rm p}}{2\eta_{\rm p}} = \frac{15k_{\rm B}T}{n^2} \frac{\langle R^4 \rangle}{\langle \phi' R^3 \rangle \langle w' R^3 \rangle},\tag{4.40b}$$

$$\frac{\tau_0}{\zeta} = \frac{18k_{\rm B}T}{n^2} \frac{\langle R^4 \rangle}{\langle \phi' R^3 \rangle \langle w' R^3 \rangle}.$$
 (4.40c)

Comparison of (4.40a) with (4.37a) shows that the thermodynamic prediction $\alpha_{kk} = \tau_k/(2\eta_k)$ is satisfied. However, comparison of (4.40b, c) with (4.37b, c) is neither so direct nor general: the thermodynamic prediction is only correct at first order in the density. This is so because the generalised potential w(R) defined in (4.31b) and the interaction potential $\phi(R)$ are identical only at this order of approximation. Up to this order, $w' = \phi'$ and (4.40b, c) coincide with (4.37b, c) respectively, and thereby the thermodynamic identifications $\alpha_{pp} = \tau_p/(2\eta_p)$ and $\alpha_0 = \tau_0/\zeta$ are justified. The restriction of the latter identifications to first order in the density is not

an important drawback, since α_{pp} and α_0 , of order n^{-2} , are multiplied by $\mathbf{P}_p^v: \mathbf{P}_p^v$ and $(P_p^v)^2$, which, because of (4.23), are of order n^4 . The products $\alpha_{pp}: \mathbf{P}_p^v: \mathbf{P}_p^v: \mathbf{P}_p^v$ and $\alpha_0(P_p^v)^2$ in the entropy (4.36) are thus of order n^2 , so that the differences between α_{pp} and $\tau_p/(2\eta_p)$ and α_0 and τ_0/ζ are of order n^3 in the expression of entropy. Such terms cannot be included in the present study because the definition (4.29) of entropy is valid up to order n^2 only. To incorporate terms of order n^3 one should have included f_3 , the three-particle distribution function, in (4.28). This is beyond the aims of the present book.

4.3 Comparison with Computer Simulations

Computer simulations may be very useful to analyse in some specific situations the consistence of general thermodynamical proposals and they have, in fact, fostered much progress in the domain of the statistical mechanics in non-linear regimes

(Evans and Morriss 1990, 2007). The main aims have been to obtain the transport coefficients of fluids in the non-linear domain, i.e. including the effect of a non-vanishing shear rate, and to analyse non-linear extensions of the fluctuation-dissipation theorems relating the transport coefficients and the time correlation function of the fluctuations of the corresponding fluxes. However, this approach may also be of special interest when one tries to formulate a non-equilibrium thermodynamics beyond the local-equilibrium approximation, by postulating, for instance, an entropy or a free energy dependent on the fluxes or on the gradients acting on the system.

However, up to now, these thermodynamic analyses, which have been successfully compared with several microscopic theories such as the kinetic theory of gases or the maximum-entropy formalism, as has been shown in Chaps. 2 and 3, have not yet benefited from a detailed comparison with computer results for the free energy under flow. Such results are available, for instance, from the work by Evans (1981), Evans and Hanley (1981), Evans and Morriss (1990) and of Daivis (2008), who have studied extensively and in great detail many aspects of the non-equilibrium thermodynamics of a system of particles under a shear flow, when a constant shear rate $\dot{\gamma}$ is acting on the system and when a steady state is maintained through a suitable thermostating procedure which removes the dissipated heat in order to keep the temperature constant (Nosé 1984; Hoover 1985).

In this approach, the microscopic equations describing the motion of the molecules under the action of a velocity gradient ∇v are written as (Evans and Morriss 1990, 2007)

$$\dot{\mathbf{r}}_i = \frac{\mathbf{p}_i}{m} + (\nabla \mathbf{v})^T \cdot \mathbf{r}_i, \tag{4.41a}$$

$$\dot{\boldsymbol{p}}_i = \boldsymbol{F}_i - (\nabla \boldsymbol{v})^T \cdot \boldsymbol{p}_i - \alpha \boldsymbol{p}_i, \tag{4.41b}$$

where \mathbf{F} is the external force acting on the molecule i and $\alpha \mathbf{p}_i$ is a Gaussian thermostat which removes energy from the system so as to keep the total kinetic energy fixed. This is achieved by imposing on (4.41b) the condition $\sum_i \mathbf{p}_i \cdot \dot{\mathbf{p}}_i = 0$ which implies

$$\alpha = \frac{\sum_{i=1}^{N} \left[\mathbf{F}_{i} \cdot \mathbf{p}_{i} - (\nabla \mathbf{v})^{T} \mathbf{p}_{i} \cdot \mathbf{p}_{i} \right]}{\sum_{i=1}^{N} \mathbf{p}_{i} \cdot \mathbf{p}_{i}}.$$
(4.42)

This is, in fact, not completely realistic, as it implies that heat is removed at the same point where dissipation is produced, whereas in real situations heat flux is eliminated across the boundaries of the system. Furthermore, this Gaussian thermostat produces sharply defined kinetic energy and only potential energy is distributed canonically. A better choice is the so-called Nosé–Hoover thermostat, which provides results according to the canonical ensemble for equilibrium systems, not only for the potential energy but also for the kinetic. Note that the numerator in (4.42) may be interpreted as the dissipated power, and therefore it may also be written as $-VP^{\nu}$:(∇v). Since the rate of viscous heating is quadratic in the shear rate, the

results of both thermostats are obviously equal in the linear regime; in fact, Evans has shown that even in the non-linear regime, the non-linear response functions obtained by using both thermostats are identical under some conditions. The influence of different thermostats on the results in the non-linear regime is a topic of discussion.

Equations (4.41) are known in the literature as SLLOD equations (Evans and Morriss 1990), in contrast with the so-called DOLLS equations, which were used for the first time to modelize the microscopic equations of motion of the particles, and in which such equations were obtained from an effective Hamiltonian (DOLLS Hamiltonian) given by

$$\mathcal{H} = \mathcal{H}_0 + \sum_i \mathbf{r}_i \, \mathbf{p}_i : (\nabla \mathbf{v})^T, \tag{4.43}$$

with \mathcal{H}_0 the Hamiltonian of the system in the absence of the macroscopic flow. The SLLOD equations (which are not derivable from a Hamiltonian) and the DOLLS equations yield the same dissipation and the same linear behaviour, but the latter algorithm leads to incorrect results which are quadratic in the shear rate, which show up first in the normal stress differences. The main aim of these simulations is to obtain the transport coefficients of the gas, with a precision which is superior to that obtainable by the usual Green–Kubo techniques.

Although most practitioners of simulations do not pay attention to the thermodynamic potentials, and directly identify the temperature as the kinetic temperature of the translational degrees of freedom, Hanley and Evans (1982), Evans (1989), Baranyai and Evans (1989) and Evans and Morriss (1990) have devoted considerable effort to the analysis of entropy, temperature and pressure out of equilibrium. In particular, for a system of soft discs interacting through a potential of the form $\phi(r) = \varepsilon(\sigma/r)^{12}$, truncated at $r = 1.5\sigma$, they calculated the entropy for an isoenergetic planar Couette flow at densities low enough that the configurational contribution to the entropy is negligible as compared with the kinetic contribution. The increased mean free paths in this low-density regime require very long runs to achieve accuracy comparable to that for dense fluids. Table 4.1 shows some of Evans and Morriss' results and shows the difference between the kinetic (local-equilibrium) temperature T and the (non-equilibrium) thermodynamic temperature θ defined as the derivative of the energy with respect to the entropy. Furthermore, they calculated the non-equilibrium pressure, defined as $\pi = -(\partial U/\partial V)_{\dot{\nu}}$, and compared it

Table 4.1 Kinetic and thermodynamic temperatures T and θ at energy u = 2.134 for different ρ and $\dot{\gamma}$. All the quantities are expressed in units of the parameters of the molecular potential ε , σ , and $k_{\rm p}$ (Evans and Morriss 1990, 2007)

ρ	γ	T	θ
0.100	0.5	2.171	2.048
0.100	1.0	2.169	1.963
0.075	0.5	2.190	2.088
0.075	1.0	2.188	1.902

$\dot{\gamma}$	p	π
0.0	0.244	0.215
0.5	0.245	0.145
1.0	0.247	0.085

Table 4.2 Local-equilibrium and non-equilibrium pressure p and π at energy u = 2.134 and density $\rho = 0.100$ for different values of $\dot{\gamma}$. (Evans and Morriss 1990, 2007)

with the kinetic pressure p obtained from the trace of the pressure tensor. Some of their results for p and π (expressed in terms of $\varepsilon \sigma^{-3}$) are reproduced in Table 4.2.

These results show clearly that there are significative differences between the values of θ and T and between those of π and p in presence of shear rates. Evans and Morriss (1990) have noticed that the numerical data for thermodynamic pressure π agree with the minimum eigenvalue of the pressure tensor. If instead of working in a dilute regime one includes also the configurational contribution to the entropy (the second term in (4.29)), the modifications of the potential contribution to the pressure may be understood in terms of a flow-induced distortion of the pair-correlation function g(R) which would then modify the pressure according to the relation (4.25); an analogous modification would be found for the interaction contribution to the internal energy in the caloric equation of state.

Another interesting feature of the computer results (Todd and Evans 1999; Baranyai et al. 1992) is the observation of an isothermal shear-induced heat flow between regions which have the same kinetic temperature. This shows the difficulties associated with the formulation of a "zeroth principle" of thermodynamics out of equilibrium. Indeed, the most natural formulation of such a zeroth law would be to postulate that two steady-state systems have the same thermodynamic temperature when under steady-state conditions heat does not flow from one system to the other (see also Casas-Vázquez and Jou 1994; Domínguez and Jou 1995 for a detailed discussion). However, the results mentioned point out clearly that this condition is not met with the kinetic temperature defined by (2.10). This is one of the reasons we warned the reader in Sect. 2.1 not to ignore the conceptual complexities related to the definition of temperature, and which are often hidden by the simplicity of relation (2.10) which, however, has little to do with the measured temperature in non-equilibrium steady states.

Another approach to thermodynamics from the perspective of molecular dynamics simulations is that of Daivis (2008), who has explored whether the Maxwell relations following from the equality of second-order crossed derivatives of a non-equilibrium thermodynamic potential are or not confirmed from microscopic simulations. For instance, he assumed

$$dF = -SdT - pdV + \zeta_1 d\dot{\gamma}, \qquad (4.44a)$$

with $\zeta_1 = \psi_{10}/2$, ψ_{10} being the first normal stress coefficient. From here it follows the Maxwell relation

$$-\left(\frac{\partial p}{\partial \dot{\gamma}}\right)_{V,T} = \left(\frac{\partial \zeta_1}{\partial V}\right)_{\dot{\gamma},T}.$$
 (4.44b)

Since, in principle, p and ζ_1 can be obtained from molecular dynamics, Daivis checked (4.44b) and showed that it was not satisfied, thus casting doubts on the internal consistency of the non-equilibrium free-energy (4.44a). However, he carried out his simulations not at constant non-equilibrium temperature, but at constant kinetic temperature. This makes a difference which should be explored in future works. In any way, exploration of Maxwell relations like (4.44b) seems to provide an interesting way of checking the consistency of thermodynamic approaches.

Another of the conclusions of Evans (1981, 1989) was that one may define a generalised Helmholtz free energy depending not only on T, V and N but also on the shear rate $\dot{\gamma}$. It was found that the dependence of such a free energy with the shear rate could be written as

$$F(T, V, N, \dot{\gamma}) = F_{eq}(T, V, N) - A(T, V, N) \dot{\gamma}^{3/2}$$
(4.45a)

at an intermediate range of the shear rate $\dot{\gamma}$ i.e. in the range near $\dot{\gamma} \approx \tau^{-1}$, with τ the characteristic collision time, which is also the characteristic relaxation time of the viscous pressure. Furthermore, for very high values of $\dot{\gamma}$ they found a behaviour of the form $\Delta S \approx -\tau \dot{\gamma}$ for the entropy (Evans and Morriss 1990).

Most of the analyses of EIT are restricted to second-order in the fluxes, and in this order of approximation, one finds non-equilibrium corrections to the free energy which are quadratic in the shear rate, and have the explicit form

$$F(T, V, N, \dot{\gamma}) = F_{eq}(T, V, N) + \frac{1}{2}\tau \eta V \dot{\gamma}^{2}. \tag{4.45b}$$

Comparison of (4.45a) and (4.45b) shows a different exponent of $\dot{\gamma}$ in both expressions. This disagreement has been one of the main reasons for the lack of contact between both approaches up to now, because (4.45b) is valid at low values of $\dot{\gamma}$. Indeed, at low $\dot{\gamma}$ Daivis (2008) has seen that molecular dynamics also leads to a quadratic behaviour.

One possibility to understand this difference in the exponents at low $\dot{\gamma}$ and high $\dot{\gamma}$ is an analysis based on a specific microscopic model for a liquid, which introduces the volume fraction of locally dilated spherical regions as an internal state variable, and which at high values of the shear rate exhibits a bifurcation leading to a $\dot{\gamma}^{3/2}$ behaviour (Nettleton 1987). Another more abstract and generic framework to reconcile these different behaviours (Bidar 1997) is to generalise the expressions of EIT to the non-linear regime valid for high values of the fluxes. One could use for this purpose the information theoretical analysis presented in Sect. 2.3 which indicates that the viscosity decreases with increasing $\dot{\gamma}$, in such a way that the viscous pressure tends to a finite saturation value equal to the energy density ρu in the limit of very high $\dot{\gamma}$ ($\dot{\gamma} \gg \tau^{-1}$). The behaviour found in information theory (see (2.65) for the shear viscosity) may be roughly modelled as

$$P_{xy}^{\nu} = -\eta(\dot{\gamma})C = -\eta_0 \left[1 + \left(\frac{2}{3} \tau \dot{\gamma} \right)^n \right]^{-1/n} \dot{\gamma}, \tag{4.46}$$

where η_0 is the value of the shear viscosity in the low shear-rate limit, and n is a fitting parameter.

4.4 Nuclear Collisions 95

Now, we introduce this expression for $\eta(\dot{\nu})$ into (4.45b) and find

$$F(T, V, N, \dot{\gamma}) = F_{\text{eq}}(T, V, N) + \frac{1}{2}\tau V \eta_0 \left[1 + \left(\frac{2}{3}\tau \dot{\gamma} \right)^n \right]^{-1/n} \dot{\gamma}^2.$$
 (4.47)

This expression yields the limiting behaviour (4.45b) for low $\dot{\gamma}$, whereas for high $\dot{\gamma}$ it yields a behaviour of the form

$$F(T, V, N, \dot{\gamma}) = F_{eq}(T, V, N) + \frac{1}{2}V\rho u\tau \dot{\gamma}.$$
 (4.48)

This kind of linear behaviour at high shear rates is also observed in molecular dynamics experiments by Evans and Morriss (1990). Thus, the dependence of the free energy in terms of a dimensionless shear rate $\dot{\gamma}' = \tau \dot{\gamma}$ changes from $(\dot{\gamma}')^2$ at low $\dot{\gamma}'$ to $\dot{\gamma}'$ at high $\dot{\gamma}'$ Therefore, there will be a regime of intermediate values of $\dot{\gamma}'$ for which the behaviour of $F - F_{\rm eq}$ could be fitted by $(\dot{\gamma}')^{3/2}$, in accordance with the trends shown in computer simulations. Furthermore, according to expression (4.48) and to the relation $S = -(\partial F/\partial T)_{V,N}$ one obtains that the non-equilibrium entropy shares this same kind of limiting dependence with the dimensionless shear rate.

Thus, if one takes into account the non-linear behaviour of the viscosity, the results of the non-linear extended thermodynamics may become compatible with those of non-equilibrium molecular dynamics in a regime of intermediate and high values for the shear rate. In fact, these limiting behaviours do not depend essentially on the explicit form of $\eta(\dot{\gamma})$, provided that it yields the expected behaviour of a saturation value of the viscous pressure at high $\dot{\gamma}$, and a linear relation between P_{xy}^{ν} and $\dot{\gamma}$ at the low- $\dot{\gamma}$ regime.

4.4 Nuclear Collisions

We end this chapter with a short look at the non-equilibrium effects for nuclear matter in the description of nuclear collisions, which is another situation where relaxation effects are important, because of the very short duration of nuclear collisions. The duration of the collisions between nuclei is only one order of magnitude longer than the mean collision time between nucleons inside the nuclei. Therefore, it is logical to assess the importance of non-equilibrium corrections and, at higher energies, their role on the shift of the transition line. The non-equilibrium equations of state of EIT provide a simplified framework for studying such problems.

4.4.1 Internal Collective Flows and Information Theory

At moderate energies, one of the topics is up to what point multi-fragmentation processes following from nuclear collisions may be described by local-equilibrium thermodynamics and hydrodynamics. The presence of strong collective flows

inside the nuclei may modify the usual thermodynamic expressions. Gulminelli (2004) and Gulminelli and Chomaz (2004) have used information theory to derive a thermodynamics for systems in the presence of a collective flow, introducing information on such a flow by means of suitable Lagrange multipliers, as it has been illustrated in Sect. 2.3. However, instead of the viscous pressure, or second moments of the particle velocity, they take as variables the memory of the initial momentum of the collision along the beam axis (usually known in this field as "transparency"), or radial flow effects. They take for the probability distribution function of an event the expression

$$P \sim \exp\left[-\beta E - \alpha \sum_{i}^{z} \varepsilon_{i} p_{iz}\right], \tag{4.49}$$

where p_z is the momentum along the beam axis with $\varepsilon_i = -1$ for the particles initially belonging to the target, $\varepsilon_i = +1$ for those belonging to the projectile, and α a Lagrange multiplier. In this way, α describes the internal collective longitudinal flow, and thus they are able to introduce several degrees of "transparency", related to the quadrupolar deformation in the momentum space, namely $\left(\langle p_x^2 \rangle - \langle p_z^2 \rangle\right)/3\langle p_z^2 \rangle$, with $\langle \cdots \rangle$ being averages. They show that different degrees of transparency lead to very different fragment size distribution, thus exhibiting the strong influence of non-equilibium variables. Besides the longitudinal collective motion a radial collective motion could also be introduced in a similar manner.

4.4.2 Generalised Gibbs Equation

At yet higher energies, one of the main questions is related to the transition from nuclear matter to quark–gluon plasma (Schukraft 1993; Mornas and Omik 1995; Pratt 2008; Pratt and Vredevoogd 2008). This would provide an understanding of the inverse transition which took place in the early stages of the universe (at times of the order of 10^{-12} s), when the quarks in the primitive quark–gluon plasma condensated in groups of three quarks (the so-called baryons, among which protons and neutrons), and in groups of two quarks (the so-called mesons). The condition on such groups was that the total color charge (the charge related to the strong interactions between quarks) was white, i.e. "neutral".

Another relevant topic in the thermodynamics of nuclear collisions concerns the definition and measurement of temperature (Casas-Vázquez and Jou 2003). Different measurements may be related, for instance, to the relative probability of fragments of different mass and energy in nucleus fragmentation, or to the relative emission of pions, or to other kinds of observables. The strong anisotropy of the collisions makes that the disordered kinetic energy in the several directions may be considerably different, in analogy with what has been discussed in ideal gases in Couette flow in Sect. 2.4. The question of temperature is still under active discussion underlying any hydrodynamic and thermodynamics analysis of this topic.

4.4 Nuclear Collisions 97

To write explicitly the non-equilibrium contributions to the Gibbs equation, we need expressions for the transport coefficients and the relaxation times for nuclear matter. They may be derived, for instance, from the kinetic theory by expanding the quantum version of the Boltzmann equation (the so-called Uhlenbeck–Uehling equation), in a way analogous to that of Chapman–Enskog, i.e. by expressing the non-equilibrium correction to the distribution function in terms of the temperature and the velocity gradients. In this way, Danielewicz (1984) has obtained for the shear viscosity η and the thermal conductivity λ

$$\eta = \frac{1700}{(k_{\rm B}T)^2} \left(\frac{n}{n_0}\right)^2 + \frac{22}{1 + 10^{-3}(k_{\rm B}T)^2} \left(\frac{n}{n_0}\right)^{0.7} + \frac{5.8(k_{\rm B}T)^{1/2}}{1 + 160(k_{\rm B}T)^{-2}}, \quad (4.50a)$$

$$\lambda = \frac{0.15}{k_{\rm B}T} \left(\frac{n}{n_0}\right)^{1.4} + \frac{0.02}{1 + 10^{-6}(k_{\rm B}T)^4/7} \left(\frac{n}{n_0}\right)^{0.4} + \frac{0.225(k_{\rm B}T)^{1/2}}{1 + 160(k_{\rm B}T)^{-2}}, \quad (4.50b)$$

where $k_{\rm B}T$ is expressed in MeV, η in MeV/fm²c, λ in c/fm², the nucleon number n in fm⁻³ and where $n_0 = 0.145$ fm⁻³ (here, fm stands for fermi, with 1 fm = 10^{-15} m and c is the speed of light).

The relaxation times for the viscous pressure tensor \mathbf{P}^{ν} and the heat flux \mathbf{q} in terms of the density and the temperature are given, respectively, by (Danielewicz 1984)

$$\tau_2 = \frac{850}{(k_{\rm B}T)^2} \left(\frac{n}{n_0}\right)^{1/3} \left(1 + 0.04k_{\rm B}T\frac{n_0}{n}\right) + \frac{38(k_{\rm B}T)^{-1/2}}{1 + 160(k_{\rm B}T)^{-2}} \left(\frac{n_0}{n}\right), \quad (4.51a)$$

$$\tau_1 = \frac{310}{(k_{\rm B}T)^2} \left(\frac{n}{n_0}\right)^{0.4} \left(1 + 0.1k_{\rm B}T\frac{n_0}{n}\right) + \frac{57(k_{\rm B}T)^{-1/2}}{1 + 160(k_{\rm B}T)^{-2}} \left(\frac{n_0}{n}\right), \quad (4.51b)$$

where τ_i is expressed in fm/c. The last terms in the right-hand side correspond to binary collisions amongst nucleons, whereas the first terms describe collisions of nucleons with the surface of the nuclei. For increasing T, the first term decreases more strongly than the second one. This means that binary collisions are more frequent at higher temperatures, whereas at lower ones, a ballistic regime of the nucleons inside the nucleus becomes dominant, in which the most frequent collisions are produced against the boundaries of the nucleus. The characteristic crossover temperature between these two regimes is of the order of $k_{\rm B}T = 6$ MeV, according to (4.51).

The generalised non-equilibrium entropy up to the second-order contributions in the fluxes is given by the expression

$$s(u, v, \boldsymbol{q}, \mathbf{P}^{v}) = s_{\text{eq}}(u, v) - \frac{\tau_{1}}{2\lambda\rho T^{2}}\boldsymbol{q} \cdot \boldsymbol{q} - \frac{\tau_{2}}{4\eta\rho T}\mathbf{P}^{v} : \mathbf{P}^{v}. \tag{4.52}$$

This is (1.32) plus the contribution of the heat flux. Combination of (4.50–4.51) with (4.52) yields an explicit expression for the non-equilibrium entropy. To avoid

the rather cumbersome general expression, we particularize the results for high temperature, which is the regime of interest in high-energy collisions. In this case, (4.52) takes the form

$$s = s_{\text{eq}} - \frac{1.26 \times 10^3}{mT^3} \frac{n_0}{n} \boldsymbol{q} \cdot \boldsymbol{q} - \frac{1.64}{mT^2} \frac{n_0}{n^2} \mathbf{P}^{\nu} : \mathbf{P}^{\nu}. \tag{4.53a}$$

For a system submitted only to a viscous pressure P_{12}^{ν} , (4.53a) may be written as

$$s = s_{\text{eq}} - \frac{3.28}{mT^2} \frac{n_0}{n^2} (P_{12}^{\nu})^2, \tag{4.53b}$$

where we have taken into account that in a pure shear flow \mathbf{P}^{v} : $\mathbf{P}^{v} = 2P_{12}^{v}P_{12}^{v}$, and where the terms in q^{2} have been neglected.

The caloric equation of state for the temperature, i.e. $\theta^{-1} = (\partial s/\partial u)_{v,q,P_{12}^v}$ may be calculated explicitly by using du = cdT, with c the specific heat per unit mass, which in the high-temperature limit considered here is c = 3/(2m) (recall that we set the Boltzmann constant $k_{\rm B}$ equal to unit). The final expression for θ is (Bidar and Jou 1998)

$$\frac{1}{\theta} = \frac{1}{T} \left[1 + 4.36 \frac{n_0}{n^2 T^2} (P_{12}^{\nu})^2 \right]. \tag{4.54}$$

We may assess the relative importance of these corrections for the collision Au + Au analysed by Fai and Danielewicz (1996). From the results of simulations for the collision Au + Au at 400 MeV/nucleon, one has the following values for the parameters involved: $\dot{\gamma}$ (shear rate) $\approx 0.07 c \text{fm}^{-1}$, $\rho \approx 0.30 \text{ fm}^{-3}$, $T \approx 44 \text{ MeV}$. The shear viscosity at these values of ρ and T is $\eta \approx 55 \text{ MeV/fm}^2 c$. It turns out that under these conditions $\theta^{-1} \approx 1.065 T^{-1}$, so that the relative non-equilibrium contribution to the temperature is of the order of 6.5%.

It is also interesting to compute the non-equilibrium corrections to the pressure from the definition

$$\frac{\pi}{\theta} = \left(\frac{\partial s}{\partial \nu}\right)_{\mu,\nu} P_{\nu}^{\nu}. \tag{4.55}$$

Note that the quantity to be held constant during the differentiation is vP_{12}^{ν} rather than P_{12}^{ν} itself, because of the non-extensive property of P_{12}^{ν} . Expression (4.55) yields $\pi/\theta = p/T$. Therefore, from (4.54) and (4.55) we finally obtain [see also (4.3)]

$$\pi = \frac{\theta}{T}p = p\left[1 + 4.36 \frac{n_0}{n^2 T^2} (P_{12}^{\nu})^2\right]^{-1}.$$
 (4.56)

We may now explore some observable physical consequences of (4.56). To do this we study one of the most relevant parameters in the equations of state for nuclear matter, which is the so-called isothermal nuclear-matter compressibility. It is defined in nuclear physics as

$$K = 9 \left(\frac{\partial p}{\partial \rho} \right)_T. \tag{4.57}$$

4.4 Nuclear Collisions 99

The experimental results for this coefficient exhibit a wide dispersion, even for the same nucleus. Indeed, typical values of *K* range from 165 MeV to 220 MeV according to the kind of experiments in which they have been obtained: some of these experiments are rather close to equilibrium (such as giant-monopole resonance) whereas others are obtained from nuclear collisions far from equilibrium.

To estimate the relative importance of non-equilibrium corrections in the evaluation of K observed in nuclear collisions, Fai and Danielewicz (1996) have proposed using in K the non-equilibrium pressure π instead of the local-equilibrium pressure. If this is done, combination of (4.56) with (4.57) yields

$$K = K_{\text{eq}} + \frac{5.89}{mn^2 T} (P_{12}^{\nu})^2. \tag{4.58}$$

Using the numerical values for the reaction Au + Au given below (4.54) and taking into account $P_{12}^{\nu} = \eta \dot{\gamma}$, one finds from (4.58) that $K - K_{\rm eq} \approx 20$ MeV. Thus, this correction is not negligible and may account at least for a substantial part of the dispersion in the observed values of K.

To explore the shift in the transition line from nuclear matter to quark–gluon plasma, one would need to compute the non-equilibrium contributions to the chemical potential of both phases and to equate the respective chemical potentials, both of which would depend on \mathbf{P}^{ν} . This would lead us too far into technical details. The main concepts related to the possible shift of a coexistence line will be explored in great detail in Chaps. 5 and 6 for polymer solutions, where the observations are more direct and detailed.

4.4.3 Causal Dissipative Hydrodynamics

A proper account of nuclear collisions requires to incorporate relativistic effects. In Sect. 3.4.1 we have introduced the formalism in a non-relativistic framework. In the companion book *Extended Irreversible Thermodynamics* (Jou et al. 2010), the relativistic version of EIT is presented in detail. Here, we will outline a short summary of a closely related approach, the causal dissipative hydrodynamics, developed by Koide et al. (2007a, b), Koide and Kodama (2008), Denicol et al. (2007a, b, c, 2008, 2009) and Kodama et al. (2007), which have paid special attention to some of the problems arising in relativistic hydrodynamics of nuclear collisions.

The collective motion of the matter produced in heavy-ion collisions is generally described in the ideal fluid approach, and the results are amazingly satisfactory. However, viscosity is expected to play a role. The relativistic hydrodynamic formulation is written as the conservation of the energy-momentum tensor $T^{\mu\nu}$

$$\partial_{\nu}T^{\mu\nu} = 0, \tag{4.59}$$

where indices μ , ν may take the values 0, 1, 2, 3. The first one refers to temporal coordinate and the other three ones to the spatial coordinates. The energy-momentum tensor is given by

$$T^{\mu\nu} = (\varepsilon + p + p^{\nu})u^{\mu}u^{\nu} - (p + p^{\nu})g^{\mu\nu} + P^{\mu\nu}, \tag{4.60}$$

where ε , p, p^{ν} and u^{μ} are, respectively, the energy density, pressure, bulk viscous pressure and the four-velocity, which is defined as $u^{\mu} = (\gamma, \gamma v)$, v being the usual three-space velocity and γ the Lorentz factor, $P^{\mu\nu}$ is the relativistic viscous pressure tensor and $g^{\mu\nu}$ is the metric tensor.

To close the system (4.59–4.60) equations of state for p in terms of ε is needed, and transport equations or constitutive equations for p^{ν} and $P^{\mu\nu}$, which in the causal dissipative approach are taken as

$$\tau_0 \frac{\mathrm{d}P^{\nu}}{\mathrm{d}t} + P^{\nu} = -(\zeta + \tau_R p^{\nu}) \partial_{\mu} u^{\mu}, \tag{4.61a}$$

and

$$\tau_2 \frac{\mathrm{d}P^{\mu\nu}}{\mathrm{d}t} + P^{\mu\nu} = -2\eta \partial_\mu u_\nu, \tag{4.61b}$$

where τ_0 and τ_2 are the relaxation times, and ζ and η the bulk and shear viscosity and τ is the proper time. These equations generalize to the relativistic domain the relaxational Maxwell–Cattaneo Eqs. (4.27). We neglect in (4.60) the contribution of the heat flux for the sake of simplicity. The non-linear term in $\tau_R p^{\nu}$ shown in the right-hand side of (4.61a) was obtained by Koide et al. (2007a) and reduces the effects of the bulk viscosity, because in the expansion p^{ν} is negative. In contrast to the Navier–Newton–Stokes equations for viscous behaviour, corresponding to vanishing relaxation times, Eqs. (4.61a, b) lead to finite speed of propagation and, therefore, to causal behaviour. The bulk viscosity may be modelled in terms of the energy density ε or the entropy density s. In particular, Denicol et al. (2009) take $\zeta = as$ and $\tau_R = b\zeta(\varepsilon + p)^{-1}$, with a and b numerical constants. According to their analysis the non-linear term reduces the effects of viscosity and thus it could explain why the description of the collision in terms of ideal hydrodynamics works satisfactorily, although it is expected that viscosity should be relevant. Furthermore, this term stabilizes numerical calculations in ultrarelativistic initial conditions.

Let us finally note that Olson and Hiscock (1989) have studied the restrictions placed by the stability conditions derived from EIT on the possible forms of the equations of state of nuclear matter. In the classical approach, it is required that the sound speed is less than the speed of light and this provides a first restriction on such equations but EIT brings additional limitations by requiring that the speeds of heat and viscous waves are lower than the speed of light. Note that though we have used here a non-relativistic formulation of EIT, a more detailed analysis of high-energy collisions would certainly require a covariant formulation, which may be found, for instance, in (Jou et al. 2010) and (Pavón 1992; Gariel and Le Denmat 1994) and the references therein.

Chapter 5 Polymeric Solutions and Blends

In the presence of velocity gradients, different parts of a macromolecule are submitted to different viscous forces. This produces deformation forces and orientational torques, and the macromolecules become stretched, oriented and displaced with respect to the quiescent situation, what modifies the internal energy stored in the macromolecules and their entropy and, as a consequence, the free energy of the whole system, to a much larger extent than in simple gases and liquids.

In this chapter, we study polymer solutions and blends to obtain explicitly the non-equilibrium contributions to the thermodynamic potentials. These expressions will be used in the following chapters, to analyse flow-induced effects. Since the relaxation times in polymers are much longer than in fluids of small molecules, the non-equilibrium modifications of the equations of state are easier to observe and have much more practical interest. The processing and moulding of polymers take place under flowing conditions and this gives to the corresponding analysis a practical perspective. Furthermore, the blending of polymers is a usual way of producing new materials which combine the properties of the individual constituents to optimize the properties of the joint product. This is the practical reason that thermodynamics and rheology of polymer blends receive much attention.

The essential concepts have already been discussed in detail in the two previous chapters for ideal and real gases. Since the flow contribution to the equation of state is related to the steady-state compliance, according to (1.32), we will focus our attention on this quantity. First, we will stress some simple descriptions of dilute polymer solutions, the freely jointed chain and the Rouse–Zimm approach to bead–spring models. In Appendix B (Sect. B.4) we will deal with rigid dumbbell models to illustrate the basic features of the influence of a shear flow on the isotropic-to-nematic transition in liquid crystals.

The analysis of concentrated solutions and melts, where several macromolecular chains become entangled, requires more sophisticated theoretical models, such as the reptation model, some of whose aspects are discussed in Sect. 5.4. Finally, we present some results for polymer blends in the context of the double-reptation model.

5.1 Kinetic Theory of Dilute Polymeric Solutions

The most usual microscopic models of dilute polymer solutions describe the polymer chain as a system of beads, representing the monomers, linked either by rigid but freely rotating joins or by elastic springs mimicking the bounds between successive monomers. The whole chain is immersed in a Newtonian fluid, which represents the solvent. The interaction between the viscous solvent and the beads is assumed to be described by Stokes' law, and the internal energy of the chain is related to the elastic energy of the chain's configuration. The aim is to understand the flow properties of systems containing polymer molecules as a function of their length, their flexibility and their geometrical configuration. These simple models have been extensively used as the basis to obtain an insight into many rheological and thermodynamical properties of the systems (see, for instance, the well known monographs by Bird et al. 1987b; Doi and Edwards 1986; Doi 1996). This description is not valid for concentrated solutions, as the molecules are no longer independent but start to overlap and to entangle with each other, and other models, such as the reptation model, are needed. Here, as in the two preceding chapters we will focus our attention on the thermodynamic aspects, rather than on the more well known rheological problems.

5.1.1 Freely Jointed Chain

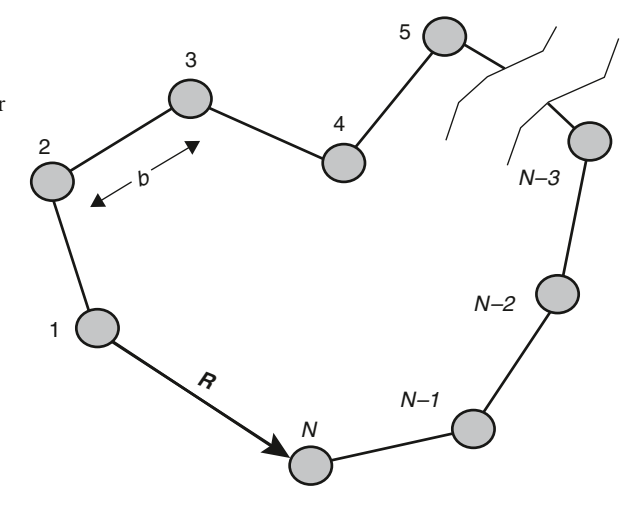
The first attempts to take into account the effects of the flow into the free energy of dilute polymer solutions, namely, the macroscopic consequences of stretching and orienting the macromolecules in the flowing system, were undertaken at the beginning of the 1970s (Marrucci 1972; Janeschitz-Kriegl 1969; Sun and Denn 1972; Sarti and Marrucci 1973; Booij 1984). One of the main results was that the excess free energy per unit volume related to the flow is

$$\Delta f = -\frac{1}{2} \text{Tr} \mathbf{P}^{\nu}, \tag{5.1}$$

where the symbols have the same meaning as in the preceding chapters. Although apparently this form is very different from that involving $(P_{12}^{\nu})^2$ which was given in (1.34) for plane Couette flows, it must be recalled, as was seen in (1.13–1.14), that in this class of flow $\text{Tr}\mathbf{P}^{\nu}$ is proportional to $(P_{12}^{\nu})^2$ for upper-convected Maxwell fluids, which is the rheological model usually adopted in this monograph. In fact, in (5.24) it will be shown an expression for Δf more general than (5.1) and which agrees with the extended entropy for all classes of flows.

The simplest way to show (5.1) is to assume a freely jointed chain of N statistically independent segments of length b. Since one supposes that the orientations of the successive segments \mathbf{r}_i are mutually independent, the average value of the end-to-end vector of the chain, $R = \sum_{i=1}^{N} \mathbf{r}_i$, is given by the well known result

Fig. 5.1 The freely jointed model for the macromolecular chain. The *rigid segments* may rotate freely around their connection points



$$\langle \mathbf{R}^2 \rangle = \left\langle \left(\sum_{i=1}^N \mathbf{r}_i \right)^2 \right\rangle = \sum_{i=1}^N \mathbf{r}_i^2 + \sum_{i \neq j}^N \langle \mathbf{r}_i \cdot \mathbf{r}_j \rangle = Nb^2, \tag{5.2}$$

where $\langle \mathbf{r}_i \cdot \mathbf{r}_j \rangle = 0$ because of statistical independence of different segments, and $\langle \mathbf{r}_i^2 \rangle = b^2$.

The simplest mathematical model to describe the chain is to consider the polymer as a random walk of steps with equal length b but random orientation. In the Gaussian approximation which uses the results of this random-walk model (see Fig. 5.1), the conformational distribution function $\psi(R)$ giving the probability that the end-to-end vector is comprised between R and R + dR is given by the classical result

$$\psi(R) = \left(\frac{3}{2\pi N b^2}\right)^{3/2} \exp\left(-\frac{3}{2N b^2} R^2\right). \tag{5.3}$$

This result is the analogous of diffusion theory with N playing a role analogous to time and with a diffusion coefficient given by $D = \frac{1}{6}b^2$. In fact, this model is excessively simplistic since it allows the chain to loop back onto itself, but this is actually impossible because each segment occupies its own finite volume. To take into account this excluded-volume effect one must use a self-avoiding random walk for the description of the chain. In this case (5.2) and (5.3) are modified (Doi 1996); in particular, it turns out that $\langle R^2 \rangle$ is proportional to $N^{6/5}b^2$ instead of (5.2), i.e. the exponent of N is slightly higher than 1, thus yielding a longer end-to-end distance than the simple Gaussian approximation. Other non-ideal effects which must be taken into account are due to the nature of the interaction between the chain and the solvent. For instance, if the chain is hydrophobic, it will tend to be folded on itself if water is used as the solvent whereas a hydrophilic chain will tend to extend to increase its contact with water as much as possible. Here we will only use the simplest descriptions to understand the physical basis of the phenomena we are considering.

In order to obtain the Helmholtz free energy f of a chain with a given end-to-end vector \mathbf{R} we recall that the canonical equilibrium distribution function $\psi(\mathbf{R})$ is expressed in terms of the free energy as

$$\psi(\mathbf{R}) \propto \exp\left(-f/k_{\rm B}T\right).$$
 (5.4)

Thus, by inverting (5.4) and using (5.3), the free energy of the chain can be written as

$$f = \text{const} + \frac{3k_{\rm B}T}{2Nh^2}R^2. {(5.5)}$$

One may obtain from (5.5) an expression for the force F which should be applied to the ends of the chain to modify R. Indeed, we recall that $-(\partial f/\partial R)_T = F$ (this relation is analogous to the classical expression $-(\partial f/\partial V)_T = p$ in the bulk). By differentiating (5.5) one obtains $-(\partial f/\partial R)_T = (3k_BT/Nb^2)R$. This shows that the force F is proportional to R according to Hooke's law for linear elasticity and therefore indicates that the freely jointed chain has an elastic constant given by

$$k' = \frac{3k_{\rm B}T}{Nb^2}. (5.6)$$

Note that the origin of this elastic constant is purely entropic. Indeed, it is a consequence of the fact that the more stretched configurations have less possible microstates, and therefore stretching the molecule implies a decrease in the entropy of the chain, which requires some work to be done on it. The linear dependence of the elastic constant on temperature is typical of entropic effects. Note, furthermore, that longer chains have lower elastic constant. Systems with entropic elasticity differ from those with energetic elasticity in the fact that the former ones contract when heated, whereas the latter ones expand.

Since there are n independent macromolecular chains per unit volume of the solution, the free energy of the solution per unit volume will be

$$f(T,n) = \text{const} + \frac{3nk_{\text{B}}T}{2Nh^2} \langle R^2 \rangle. \tag{5.7}$$

In order to relate (5.7) with the viscous pressure tensor, we recall that the contribution of the polymer to the viscous pressure tensor for a solution of n Hookean dumbbells, i.e. elastic dumbbells whose spring satisfies the classical Hooke's law, per unit volume is given by the Kramers expression (1.90) (Doi and Edwards 1986; Bird et al. 1987b)

$$\mathbf{P}^{v} = -nk' \langle \mathbf{R} \mathbf{R} \rangle + nk_{\rm B}T\mathbf{U}, \tag{5.8}$$

with k' the elastic constant of the dumbbells and **U** the unit tensor. The tensor $\langle RR \rangle$ describes the average configuration of the chains. Although the freely jointed chain is not in fact a dumbbell, it behaves grossly as an elastic dumbbell with the elastic constant determined in (5.6), and therefore, expression (5.8) may be

used to obtain its contribution to the viscous pressure. In equilibrium, the tensor $\langle RR \rangle$ becomes simply the diagonal $\frac{1}{3}\langle R^2 \rangle \mathbf{U}$ and, according to the equipartition law, $\frac{1}{2}k'\langle R^2 \rangle = \frac{3}{2}k_BT$. As a consequence, expression (5.8) for \mathbf{P}^{ν} will vanish in equilibrium, as expected.

The flow will distort and stretch the chains and this will change the value of $\langle RR \rangle$ and of $\langle R^2 \rangle$ with respect to its equilibrium value in a quiescent state. Its contribution to the free energy Δf may be written, according to (5.7) as

$$\Delta f = \frac{1}{2} n k' \langle R^2 \rangle - \frac{1}{2} n k' \langle R^2 \rangle_{\text{eq}}.$$
 (5.9)

Indeed, we see that, in the absence of the flow, $\langle R^2 \rangle = \langle R^2 \rangle_{eq}$ and therefore $\Delta f = 0$. On the other hand, since $\text{Tr} \mathbf{P}^{\nu} = 0$ in equilibrium, (5.8) can be rewritten as

$$\mathbf{P}^{\nu} = -nk' \langle \mathbf{R} \mathbf{R} \rangle + \frac{1}{3} nk' \langle R^2 \rangle_{\text{eq}} \mathbf{U}, \tag{5.10}$$

and therefore one will have

$$Tr\mathbf{P}^{\nu} = -nk'\langle R^2 \rangle + nk'\langle R^2 \rangle_{eq}. \tag{5.11}$$

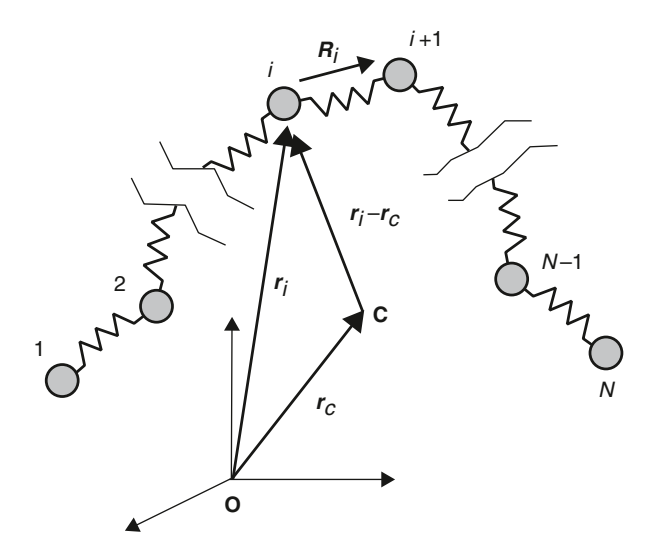
Comparison of (5.9) and (5.11) yields (5.1). In fact, (5.9) is interesting in its own right, as it gives a microscopic understanding of the change in the free energy due to the flow in terms of the chain deformation.

The derivation presented here states clearly its own limitations: (1) the modifications of *f* are of entropic origin; no change in the internal energy of the chain with the flow is considered; (2) the solution must be very dilute so that the chains do not interact; (3) the hydrodynamic interactions between the different parts of the macromolecule are neglected; (4) the internal friction of the molecule is neglected; (5) a linear relationship between elastic forces and end-to-end vectors is assumed, but it breaks down when the macromolecules are much extended. In spite of these limitations, the derivation is very simple and illustrates in a concise way the need to take into account the flow contribution to the free energy.

5.1.2 The Bead-and-Spring Rouse-Zimm Model

A more detailed and realistic description of the macromolecule and a more complete derivation of the non-equilibrium contribution to the free energy may be obtained if one considers that the joins between successive beads are not rigid rods but elastic springs. This allows one to take into account the change in the internal energy of the chains due to the elongation or compression of the springs. Rouse in 1953 (Rouse 1953; see also Doi and Edwards 1986; Bird et al. 1987b) used a Langevin equation to describe the motion of each bead, by taking into account the elastic force, the viscous friction, and a stochastic force due to the random interaction with the molecules of the solvent. This allowed him to obtain, in a rather direct way, a

Fig. 5.2 The bead–spring model for macromolecular chains. *C* is the centre of mass of the macromolecule



description of viscoelasticity, with microscopic expressions for the relaxation times and the viscosities corresponding to the different normal modes of the chain. His analysis was generalised by Zimm (Zimm 1956; Doi and Edwards 1986; Bird et al. 1987b), who included in an averaged way the effects of the hydrodynamic interactions between the different parts of the macromolecule, which had been neglected in Rouse's analysis. Here, we will derive the expression for the flow contribution to the free energy, which now has two parts: an entropic one, due to the changes in the orientation of the molecule under the flow, and an energetic one, due to the stretching of the springs.

To do this, let $\psi(R_1, R_2, ..., R_{N-1})$ denote the configurational distribution function giving the probability that the bead-to-bead vectors R_i going from the *i*th bead to the (i+1)th bead are comprised between the values R_i and $R_i + dR_i$, respectively (see Fig. 5.2). In fact, rather than with these vectors, which are coordinated among themselves through the condition that the end of one vector must coincide with the beginning of the next one, when analysing the energy and the dynamics of these chains it is more convenient to work in terms of the normal modes of the chain, which will be denoted as $Q_1, ..., Q_{N-1}$, which automatically solve the mentioned coordination of motions. Thus, from now on we call ψ the configurational distribution function expressed in terms of these new variables, which are a linear combination of the former ones through the expression reported below in Eq. (5.20).

5.1.2.1 Free Energy

According to Boltzmann's definition of entropy, the configurational contribution of the chains to the entropy per unit volume is

$$s = -nk_{\rm B} \int \psi \ln \psi d\boldsymbol{Q}_1...d\boldsymbol{Q}_{N-1}. \tag{5.12}$$

It has been assumed that the contribution of the velocity of the center of mass is purely the equilibrium one and is not affected by the flow. Although this is not exact, it turns out that the configurational contribution to the entropy is much more affected by the flow than the kinetic one, and therefore this approximation is quite realistic.

The internal energy of the macromolecules is given by the elastic potential energy of the springs, and therefore it may be written as

$$u = -n \int \psi \sum_{i} \frac{1}{2} H Q_{i}^{2} d \mathbf{Q}_{1} ... d \mathbf{Q}_{N-1}$$

$$= -nk_{B}T \int \psi \ln \psi_{0} d \mathbf{Q}_{1} ... d \mathbf{Q}_{N-1}, \qquad (5.13)$$

where H is the Hookean spring constant. To write the second equality, we have taken into account that the equilibrium distribution function ψ_0 has the canonical form

$$\psi_0 = \prod_i \psi_i(Q_i)$$

$$= (H/2\pi k_{\rm B}T)^{3(N-1)/2} \exp\left[-(H/2k_{\rm B}T)(Q_1^2 + \dots + Q_{N-1}^2)\right], \quad (5.14)$$

where advantage has been taken of the fact that the different normal modes are independent of each other, in such a way that the total distribution function factorizes into a product of the respective distribution functions $\psi_i(\mathbf{Q}_i)$ of the *i*th normal mode. According to the canonical distribution function, the argument of the exponential in (5.14) is the energy of the chain, divided by $k_B T$. Therefore, (5.13) is indeed the energy, except for an additive function coming from the logarithm of the normalization factor in (5.14), which will not be important because we are interested in the excess Helmholtz free energy due to the flow rather than in the whole value of the free energy.

By using (5.12) and (5.13), the Helmholtz free energy per unit volume may be expressed as

$$f = u - Ts = -nk_{\rm B}T \int \psi (\ln \psi_0 - \ln \psi) \, \mathrm{d} \, \mathbf{Q}_1 ... \mathrm{d} \, \mathbf{Q}_{N-1}, \qquad (5.15)$$

or, in a more compact form,

$$f = nk_{\rm B}T \int \psi \ln (\psi/\psi_0) \, \mathrm{d} \, \mathbf{Q}_1 ... \mathrm{d} \, \mathbf{Q}_{N-1}. \tag{5.16}$$

Now, to obtain the flow contribution to the free energy one needs to know the form of ψ in the presence of the flow. This may be achieved by solving a kinetic equation describing the evolution of ψ or, in a different approach, by maximizing the entropy under the restrictions on the average value of the viscous pressure tensor, as was done in Sects. 2.2 and 2.3 for ideal gases. We defer an illustration of this latter approach to Sect. 5.3, and use here the kinetic approach.

Under non-equilibrium conditions, the configurational distribution function must fulfil the continuity equation in the configurational space, namely

$$\frac{\partial \psi}{\partial t} = -\sum_{i} \frac{\partial (\psi \, \dot{\mathbf{R}}_{i})}{\partial \mathbf{R}_{i}},\tag{5.17}$$

where the $\dot{\mathbf{R}}_i$ are obtained by a force balance over the beads (Bird et al. 1987b) which reads as

$$\zeta \left[\dot{\mathbf{R}}_i - (\nabla v) \cdot \mathbf{R}_i \right] = -k_{\rm B} T \sum_i A_{ij} \frac{\partial (\psi/\psi_0)}{\partial \mathbf{R}_j}. \tag{5.18}$$

The term on the left-hand side describes the friction of the fluid on the bead; it is proportional to the friction coefficient ζ of the beads and to the relative velocity of the bead with respect to the fluid, the former being $\dot{\mathbf{R}}_i$ and the latter $(\nabla v) \cdot \mathbf{R}_i$. On the right-hand side, the elastic forces are expressed through the function ψ_0 , as already commented below (5.14), whereas ψ gives the contribution of the random force due to the microscopic impacts of the solvent molecules and the beads. Finally, the matrix \mathbf{A} (which is constant and diagonal in the Rouse model) may include the effects of the hydrodynamic interactions amongst the beads through non-diagonal terms in the pre-averaged Zimm treatment. We will not specify the details concerning this point, which are studied in depth in (Bird et al. 1987b; Doi and Edwards 1986).

In terms of the configurational distribution functions of the different normal modes, (5.17–5.18) may be written as

$$\frac{\partial \psi_i}{\partial t} = \frac{\partial}{\partial \mathbf{Q}_i} \cdot \left[\psi_i(\nabla \mathbf{v}) \cdot \mathbf{Q}_i - \frac{H}{\zeta} \lambda_i \psi_i \mathbf{Q}_i - \frac{k_{\rm B} T}{\zeta} \lambda_i \frac{\partial \psi_i}{\partial \mathbf{Q}_i} \right], \tag{5.19}$$

with $\psi_i(\mathbf{Q}_i)$ the distribution function of the normal mode \mathbf{Q}_i . The normal modes are related to the bead-to-bead vectors \mathbf{R}_i through

$$\mathbf{R}_i = \sum_j \mathbf{\Omega}_{ij} \cdot \mathbf{Q}_j, \tag{5.20}$$

where the orthogonal matrix Ω diagonalizes the matrix \mathbf{A} in (5.18). The corresponding diagonal elements of $\Omega \cdot \mathbf{A} \cdot \Omega^T$ are the λ_i , i.e. the eigenvalues of the matrix \mathbf{A} , to each of which corresponds a relaxation time given by $\tau_i = \zeta/(2H\lambda_i)$.

It is usual to try an approximate Gaussian solution to solve (5.19), of the form

$$\frac{\psi_i}{\psi_{i0}} = \left(\frac{H}{k_{\rm B}T}\right)^{-3/2} \left[\det\langle \boldsymbol{Q}_i \, \boldsymbol{Q}_i \rangle\right]^{-1/2}
\times \exp\left[\left(\frac{H}{2k_{\rm B}T}\right) \left(\boldsymbol{Q}_i \, \boldsymbol{Q}_i - \frac{1}{2} \, \boldsymbol{Q}_i \langle \boldsymbol{Q}_i \, \boldsymbol{Q}_j \rangle^{-1} \mathbf{Q}_j\right)\right], \tag{5.21}$$

with ψ_{i0} the *i*th normal mode distribution function at equilibrium. In equilibrium, the matrix $\langle \mathbf{Q}_i \mathbf{Q}_j \rangle$ is diagonal and (5.21) reduces to (5.14). Out of equilibrium, depends on the matrix describing the flow, but some general results for the free energy may be obtained without need of such explicit knowledge.

When the distribution function (5.21) is introduced into the expression (5.16) for the free energy one has,

$$f = \frac{1}{2} n k_{\rm B} T \left\{ \sum_{i} \text{Tr}[(H/k_{\rm B}T) \langle \boldsymbol{Q}_{i} \boldsymbol{Q}_{i} \rangle - \mathbf{U}] - \sum_{i} \ln \left[\det (H/k_{\rm B}T) \langle \boldsymbol{Q}_{i} \boldsymbol{Q}_{i} \rangle \right] \right\}.$$
(5.22)

It is possible to write this equation by outlining in a more explicit way the non-equilibrium contribution. To do this, one may write $\langle \mathbf{Q}_i \mathbf{Q}_j \rangle$ in terms of the viscous pressure tensor. Indeed, each normal mode contributes to the viscous pressure, and one may write, instead of (5.8), the Kramers expression for \mathbf{P}_i^{ν} as

$$\mathbf{P}_{i}^{v} = -nH\langle \mathbf{Q}_{i} \mathbf{Q}_{i} \rangle + nk_{\mathrm{B}}T\mathbf{U}. \tag{5.23}$$

Therefore, (5.22) may be written in terms of \mathbf{P}_{i}^{v} as

$$\Delta f = -\frac{1}{2}nk_{\rm B}T\left\{\sum_{i}\operatorname{Tr}(\mathbf{P}_{i}^{\nu})' + \sum_{i}\ln\left[\det\left(\mathbf{U} - (\mathbf{P}_{i}^{\nu})'\right]\right\},\tag{5.24}$$

with $(\mathbf{P}_i^{\nu})' = (nk_BT)^{-1}\mathbf{P}_i^{\nu}$. Note that (5.24) is analogous to the expression (2.47) for ideal gases except for a change of sign in front of \mathbf{P}^{ν} , which is due to the minus sign in (5.8) in contrast to the positive sign in (2.47). Expression (5.24) generalises (5.1) in two aspects: it takes into account the role of the different normal modes and it includes the contribution of the internal energy to the free energy in the second term of the right-hand side. Thus, the microscopic basis for the non-equilibrium free energy is now clear (Lebon et al. 1988; Pérez-García et al. 1989).

Now, we may work out (5.24) for some special flows. First of all, for shear flows, we may introduce the expression (1.13) in (5.24) and we obtain

$$\Delta f = \frac{1}{2} n k_{\rm B} T \left\{ 2\tau \eta \dot{\gamma}^2 - n k_{\rm B} T \ln \left[1 + 2\tau \eta \dot{\gamma}^2 / (n k_{\rm B} T) - \eta^2 \dot{\gamma}^2 / (n k_{\rm B} T)^2 \right] \right\}. \tag{5.25}$$

For small values of $\dot{\gamma}$ one may develop the logarithm in (5.25) and one finds

$$\Delta f = \frac{1}{2} \frac{\eta^2 \dot{\gamma}^2}{nk_B T} = \frac{1}{2} \frac{\tau}{\eta} (P_{12}^{\nu})^2 = \frac{1}{2} J (P_{12}^{\nu})^2, \tag{5.26}$$

in which we have used the relationships $\tau = \eta(nk_{\rm B}T)^{-1}$ and $J = \tau/\eta$, which will be justified below. Note that (5.26) has precisely the form (1.41) predicted by extended irreversible thermodynamics for low values of P_{12}^{ν} if we bear in mind that in (1.41) the Helmholtz free energy is expressed in units of energy/volume.

For high values of $\dot{\gamma}$, the terms in $2\tau\eta\dot{\gamma}^2$ are more important than the terms in the logarithm, so that (5.25) reduces to

$$\Delta f = \tau \eta \dot{\gamma}^2 = J(P_{12}^{\nu})^2, \tag{5.27}$$

which is the expression following from (5.1) and (1.13).

For planar extensional flows, we may introduce the viscous pressure tensor (1.19) into the free energy (5.24), and we arrive at

$$\Delta f = -\frac{1}{2}nk_{\rm B}T\left\{-\left(\frac{P_{11}^{\nu}}{nk_{\rm B}T} + \frac{P_{22}^{\nu}}{nk_{\rm B}T}\right) - \ln\left[1 - \frac{P_{11}^{\nu}}{nk_{\rm B}T} - \frac{P_{22}^{\nu}}{nk_{\rm B}T} + \frac{P_{11}^{\nu}P_{22}^{\nu}}{(nk_{\rm B}T)^2}\right]\right\}.$$
(5.28)

By developing $\ln(1+x) \approx x - \frac{1}{2}x^2$ one has, up to second order in P_{11}^{ν} ,

$$\Delta f = -\frac{1}{4} (nk_{\rm B}T)^{-1} \left[(P_{11}^{\nu})^2 + (P_{22}^{\nu})^2 \right] = \frac{1}{4} J \left[(P_{11}^{\nu})^2 + (P_{22}^{\nu})^2 \right], \quad (5.29)$$

in agreement with the EIT expression (1.43) for low values of P_{11}^{ν} and P_{22}^{ν} .

This confirmation of EIT at low values of $\dot{\gamma}$ has also been obtained without need of the general expression (5.21) but by writing the second-order solution of (5.19) for ψ . In a steady state, (5.19) reduces to

$$\frac{1}{\psi_i} \frac{\partial \psi_i}{\partial \boldsymbol{Q}_i} = -\frac{H}{k_{\rm B}T} \boldsymbol{Q}_i + \frac{\zeta}{\lambda_i k_{\rm B}T} (\nabla \nu) \cdot \boldsymbol{Q}_i. \tag{5.30}$$

(Note that the subscript *i* refers to the *i*th normal mode, i.e. i = 1, 2, ..., N, whereas j and k refer to the Cartesian components of \mathbf{Q}_{i} , i.e. j, k = 1, 2, 3). For $\nabla \mathbf{v} = 0$, the second term of the right-hand side vanishes and the solution of (5.30) is the equilibrium expression (5.14). Out of equilibrium, Eq. (5.30) is integrable when $\nabla \mathbf{v}$ is symmetric. Its solution is then

$$\psi_i \cong \exp\left[-\frac{H}{k_{\rm B}T} \mathbf{Q}_i \cdot \mathbf{Q}_i + \frac{\zeta}{2\lambda_i k_{\rm B}T} (\nabla v) : \mathbf{Q}_i \mathbf{Q}_i\right]. \tag{5.31}$$

Taking into account the form (5.14) for the equilibrium distribution function ψ_{i0} , and expanding the exponential in powers of the velocity gradient, one may write (5.31) up to the first order as

$$\psi_i = \psi_{i0} \left[1 + \frac{\zeta}{4\lambda_i k_B T} (\nabla \nu)^s : \mathbf{Q}_i \mathbf{Q}_i \right]. \tag{5.32}$$

When this expression is introduced into (5.16), one obtains (5.25) for the flow contribution to the free energy.

When the flow is rotational, as in shear flow, (5.30) cannot be integrated, because it does not satisfy the equality of the second-order crossed derivatives. Indeed, it follows from (5.28) that $\frac{\partial^2 \psi}{\partial Q_k} \frac{\partial Q_j}{\partial Q_j} = \delta_k v_j$ and $\frac{\partial^2 \psi}{\partial Q_j} \frac{\partial Q_k}{\partial Q_k} = \delta_j v_k$, in such a way that these crossed derivatives are equal only if the velocity gradient tensor is symmetric. In fact, it is intuitive to understand that in a rotational flow the molecules do not achieve a stationary distribution function, since they rotate due to the flow. This rotation is described by the non-symmetric part of the velocity gradient. In this situation, expression (5.32) is not an exact solution, but only a time average over the rotation. When this molecular rotation is not macroscopically relevant, it is logical that it should not appear in the macroscopic entropy. Otherwise, the kinetic rotational contribution to the internal energy should be taken into account.

5.1.2.2 Evolution Equation for the Viscous Pressure

Here we are interested in relating the non-equilibrium entropy to the evolution equation for the viscous pressure tensor. Indeed, it has been seen in (1.53) and (1.55) that the non-equilibrium contribution of the viscous pressure to the entropy is intimately related to the relaxation effects in the evolution equation for \mathbf{P}^{ν} . Therefore it is convenient, for the sake of completeness, to derive from microscopic grounds the latter equation. It should take into account the contributions of the different normal modes, as expressed by (5.23), and to each normal mode will correspond a relaxation time τ_i and a viscosity η_i . To obtain them, one may combine the expression (5.23) for \mathbf{P}_i^{ν} with the evolution equation for the configurational distribution function ψ_i , given by (5.19). One obtains in this way, in the linear approximation,

$$\tau_i \frac{\partial \mathbf{P}_i^{\nu}}{\partial t} + \mathbf{P}_i^{\nu} = -2\eta_i (\nabla \nu)^s, \tag{5.33}$$

with the relaxation time τ_i given by $\zeta(2H\lambda_i)^{-1}$ with λ_i the eigenvalues of the matrix **A** defined in (5.20) and $\eta_i = nk_{\rm B}T\tau_i$. Indeed, multiplying (5.19) by \boldsymbol{Q}_i and integrating over \boldsymbol{Q}_i one has

$$\frac{\partial}{\partial t} \langle \mathbf{Q}_i \mathbf{Q}_i \rangle = \int \mathbf{Q}_i \mathbf{Q}_i \frac{\partial}{\partial \mathbf{Q}_i} \cdot \left[\psi_i (\nabla v) \cdot \mathbf{Q}_i - \frac{H \lambda_i}{\zeta} \psi_i \mathbf{Q}_i - \frac{k_B T}{\zeta} \lambda_i \frac{\partial \psi_i}{\partial \mathbf{Q}_i} \right] d\mathbf{Q}_i.$$
(5.34)

Taking into account that $\psi_i(\mathbf{Q}_i)$ and its first and second-order derivatives decay very rapidly with \mathbf{Q}_i , (5.34) becomes, up to the first order in the velocity gradient,

$$\frac{\partial}{\partial t} \langle \boldsymbol{Q}_i \, \boldsymbol{Q}_i \rangle = -\frac{k_{\rm B} T}{H} \nabla v - \frac{2H \lambda_i}{\zeta} \langle \boldsymbol{Q}_i \, \boldsymbol{Q}_i \rangle. \tag{5.35}$$

When the Kramers expression (5.23) for \mathbf{P}_{i}^{v} is taken into account, one is led to (5.33) and the noted identifications of the viscosity and relaxation time.

The explicit values of the relaxation times depend on the model being used in the analysis. For the Rouse model, the relaxation time of the *j*th mode turns out to be (Bird et al. 1987b)

$$\tau_j = \frac{\zeta/(2H)}{4\sin^2(j\pi/2N)}.$$
 (5.36)

In the limit of large N and small j (i.e. for the largest time constants), (5.36) may be written as

$$\tau_j \approx \frac{\zeta / (2H)}{4(j\pi / 2N)^2}.$$
 (5.37a)

It is usual to write H as $H = 3k_BT/b^2$, with b the root mean square length of the strings, by taking into account the relation (5.6) (with N = 1) for the elastic constant of a chain. In terms of these variables, (5.37a) becomes

$$\tau_j \approx \frac{\zeta b^2 N^2}{6\pi^2 k_{\rm B} T j^2} \equiv \tau_{1,R} \frac{1}{j^2}.$$
(5.37b)

Since the relaxation times decay very rapidly with increasing j, it follows that the longer relaxation times (j = 1, 2, 3) account for practically all viscosity; thus, although the number N of normal modes may be very large, in practice only a very small number of them account for the observed viscosity. For the Zimm model, the relaxation times are given by (Bird et al. 1987b)

$$\tau_j = \frac{1}{\sqrt{3}\pi^{1/4}} \frac{\eta_s (Nb^2)^{3/2}}{k_B T j^{3/2}} \equiv \tau_{1,Z} \frac{1}{j^{3/2}},$$
 (5.38)

with η_s the viscosity of the solvent. Note that the relaxation times depend on temperature in several ways: they are inversely proportional to T, in a explicit way, and implicitly, they are also affected by the temperature dependence of the solvent viscosity and of the mean-square separation b^2 of the ends of the segments.

From (5.37) and (5.38) one may obtain the scaling laws which express the dependence of the relaxation times with the mass M of the polymer (or with the number of monomers N) and which are widely used in the study of polymer physics. In the Rouse model and recalling that the number N of monomers is proportional to the polymer mass M, one has from (5.37) that $\tau \cong M^2$ whereas in the Zimm model (5.38) yields $\tau \cong M^{3/2}$. Furthermore, since $\eta_i = nk_B T \tau_i$ and $n = c/(MN_A)$ with c the polymer concentration expressed in terms of mass per unit volume and N_A the Avogadro number, one has $\eta \cong cRT\tau/M$, and thus the scaling laws for the viscosity are, respectively, $\eta \cong cM$ (Rouse) and $\eta \cong cM^{1/2}$ (Zimm). Finally, the steady-state compliance $J = \tau/\eta$ follows the scaling laws $J \cong c^{-1}M$ both for Rouse and for Zimm models. A comparison with experimental data shows (Bird et al. 1987a; Holmes et al. 1966, 1968) that Zimm's theory may be used for low concentrations,

whereas when the concentration increases the system tends to the behaviour predicted by Rouse. Therefore, there is a smooth shift from the Zimm model to the Rouse model with increasing polymer concentration, always in the dilute regime.

5.2 Derivation of the Steady-State Compliance

As has been seen in (1.31) and (1.32), the steady-state compliance J plays a central role in the non-equilibrium contributions to the free energy. Since we will need to know in detail its dependence on the concentration in latter applications, we analyse this coefficient in the framework of the Rouse–Zimm model. For a system with only a single relaxation time one would have $J = \tau/\eta$. However, when there are several normal modes and therefore several different non-equilibrium contributions to the free energy, the effective steady-state compliance J to be used in the thermodynamic analysis is defined from the form of the free energy (1.32) as

$$f = f_{eq} + \sum_{i} \frac{1}{4} (\tau_i / \eta_i) \mathbf{P}_i^{\nu} : \mathbf{P}_i^{\nu} \equiv f_{eq} + \frac{1}{4} J \mathbf{P}^{\nu} : \mathbf{P}^{\nu},$$
 (5.39)

where \mathbf{P}^{ν} is the total viscous pressure of the solution, given by $\mathbf{P}^{\nu} = \sum_{i} \mathbf{P}_{i}^{\nu}$, where the contribution of the solvent is also taken into account. After writing $\mathbf{P}_{i}^{\nu} = -2\eta_{i}(\nabla \nu)^{s}$ and expressing the non-equilibrium contribution in both sides of (5.39) in terms of the velocity gradient, yields

$$J = \left(\sum_{i=1}^{N-1} \tau_i \eta_i\right) \left(\sum_{i=0}^{N-1} \eta_i\right)^{-2},\tag{5.40}$$

where the sum in the denominator must include the solvent viscosity η_s (corresponding to i=0) besides the viscosities related to the different normal modes of the polymer. However, it does not appear in the numerator because we are assuming a purely Newtonian solvent, with vanishing relaxation time, i.e. $\tau_0=0$. Since $\eta_i=nk_{\rm B}T\tau_i$, (5.40) may be rewritten as

$$J = \frac{cRT}{M\eta^2} \sum_{i=1}^{N-1} \tau_j^2.$$
 (5.41)

where we have written n (number of molecules of polymer per unit volume of solution) in terms of the polymer mass per unit volume c taking into account that $c = nM_2N_A$ with M_2 the polymer molecular mass. The total contribution η_p of the polymer to the viscosity is $\eta_p = nk_BT \sum_i \tau_i$. Furthermore, $\eta = \eta_s + \eta_p$, and then (5.41) may be re-written as

$$J = \frac{CM}{ck_{\rm B}T} \left(1 - \frac{\eta_{\rm s}}{\eta}\right)^2,\tag{5.42}$$

where C is a constant. Since $\tau_i = \tau_1 i^{-\alpha}$, with $\alpha = 2$ in Rouse model (5.37) and $\alpha = 3/2$ in Zimm model (5.38), C is given by

$$C = \sum_{i} i^{-2\alpha} \left(\sum_{i} i^{-\alpha} \right)^{-2}. \tag{5.43}$$

In Rouse model, C = 0.4 since $\sum_{1}^{\infty} i^{-2} = \frac{1}{6}\pi^2$ and $\sum_{1}^{\infty} i^{-4} = \frac{1}{90}\pi^4$, and in Zimm model (n = 3/2), C = 0.206.

In order to express J as a function of the concentration c, it is necessary to know how η depends on the concentration of the mixture. Since here we want to analyse generically the thermodynamic model for dilute solutions, we have preferred not to use a specific functional for $\eta(c)$ but we simply take the second-order expansion

$$\frac{\eta}{\eta_s} = 1 + [\eta]c + k_{\rm H}[\eta]^2 c^2,\tag{5.44}$$

where $k_{\rm H}$ is the so-called Huggins constant, which depends on the solution being analysed, and $[\eta]$ is the intrinsic viscosity defined as

$$[\eta] = \lim_{c \to 0} \frac{\eta - \eta_{\rm S}}{c \eta_{\rm S}},\tag{5.45}$$

where η is the viscosity of the solution, η_s the viscosity of the solvent, and c the mass of polymer per unit volume of solution.

Combining (5.42) and (5.45) we may write J as a function of the reduced concentration \tilde{c} , defined as $\tilde{c} = [\eta]c$, in the form

$$J = \frac{CM_2}{RT} [\eta] \Phi(\tilde{c}), \tag{5.46}$$

where $\Phi(\tilde{c})$ is a function defined as

$$\Phi(\tilde{c}) = \tilde{c} \left[\frac{1 + k_{\rm H} \tilde{c}}{1 + \tilde{c} + k_{\rm H} \tilde{c}^2} \right]^2. \tag{5.47}$$

Note that the simplest scaling law for J in terms of c mentioned at the end of Sect. 5.1.2 would yield $J \approx c^{-1}M$. This is true for relatively large concentrations, where the contribution of the polymer to the viscosity is much higher than that of the solvent, but not in the very dilute regime, where the viscosity of the solvent cannot be neglected (Holmes et al. 1966, 1968). The dependence of η on the concentration is crucial in the analysis of the shear-induced shift of the critical point, as will be discussed in the next chapter.

The experimental values for J are usually obtained by several methods, such as from creep recovery, by integration over the stress relaxation data following sudden start or sudden cessation of steady flows, or from normal stress measurements.

The transition from the behaviour described by Zimm to the behaviour described by Rouse with increasing polymer concentration is monotonous and reflects the fact

that with increasing concentration the hydrodynamic effects become less relevant. It may be qualitatively described by assuming that the parameter C in (5.46) depends on the composition of the system. To describe the gradual transition from the Zimm to the Rouse behaviour one may assume (Criado-Sancho et al. 1995)

$$C(\tilde{c}) = 0.206 + \frac{0.194\alpha \tilde{c}}{1 + \alpha \tilde{c}},$$
 (5.48)

where α is a parameter which indicates how steep the transition is. In Chap. 6 this expression will be used in an analysis of the influence of the hydrodynamic interactions on the shear-induced shift of the critical point.

5.3 Maximum-Entropy Approach

In Sect. 2.1 we have used the maximum-entropy approach to find the thermodynamic functions of ideal gases under shear flow. Here we again use this procedure to derive the steady-state configurational distribution function (5.35) for bead–spring chains, which was previously derived as a solution of the kinetic Eq. (5.30). In this way, we stress the parallelism in the study of two rather different physical systems, namely ideal gases and dilute polymer solutions, and we also underline two different methods for the analysis of dilute polymer solutions (Jou et al. 1999b).

We have seen in Sect. 2.2 that in a non-equilibrium steady state characterized by a non-vanishing viscous pressure tensor, the maximum-entropy distribution function is given by (2.29), which we rewrite here in the form

$$f \cong \exp\left[-\frac{\mathcal{H}}{k_{\rm B}T} - \Lambda : \hat{\mathbf{P}}^{\nu}\right],$$
 (5.49)

with \mathcal{H} the Hamiltonian, $\hat{\mathbf{p}}^{\nu}$ the microscopic operator for the viscous pressure tensor, and Λ a tensorial Lagrange multiplier which accounts for the restriction on the average value of the viscous pressure tensor. In (2.44) we have identified Λ as

$$\Lambda = -\frac{\tau}{2\eta k_{\rm B}T} \mathbf{P}^{\nu} = \frac{\tau}{k_{\rm B}T} (\nabla \nu)^{s}. \tag{5.50}$$

For a bead-spring chain, $\hat{\mathbf{P}}^{\nu}$ and \mathbf{P}^{ν} are sums of N independent contributions each with its own relaxation time τ_i and therefore (5.49) generalises to

$$f \propto \exp\left[-\frac{\mathcal{H}}{k_{\rm B}T} - \sum_{i} \frac{\tau_{i}}{k_{\rm B}T} (\nabla \mathbf{v})^{s} : \hat{\mathbf{P}}_{i}^{v}\right].$$
 (5.51)

The contribution of the *i*th normal mode of one single molecule to the viscous pressure \mathbf{P}^{ν} is, according to Kramers expression (5.23)

$$\mathbf{P}_{i}^{\nu} = \frac{1}{V} \left(k_{\mathrm{B}} T \mathbf{U} - H \mathbf{Q}_{i}^{\prime} \mathbf{Q}_{i}^{\prime} \right). \tag{5.52}$$

Introducing this expression into (5.51), and restricting our attention to the configurational part of the total distribution function it is found

$$\psi_i = \psi_{ieq} \exp \left[-\frac{\tau_i}{k_B T} (\nabla v)^s : (k_B T \mathbf{U} - H \mathbf{Q}_i' \mathbf{Q}_i') \right], \tag{5.53}$$

where ψ_{ieq} is the equilibrium part of ψ_i . Since $(\nabla v): \mathbf{U} = \nabla \cdot v$ and in view of the incompressibility condition $\nabla \cdot v = 0$, the contribution of the first term in the exponent of (5.53) vanishes. Finally, we recall that $\tau_i = \zeta/(2H\lambda_i)$. Thus, (5.53) may be finally rewritten as (5.31). In this situation, information theory and kinetic theory yield the same result for the distribution function, instead of coinciding only in the first-order non-equilibrium corrections.

5.4 Entangled Solutions. Reptation Model

When the concentration becomes sufficiently higher, the macromolecules begin to overlap with each other and can no longer be considered as independent: hydrodynamic interactions, excluded volume effects, and entanglement interactions must be considered, and the microscopic analysis becomes very complicated. A well known model for the analysis of concentrated solutions is the so-called reptation model (de Gennes 1971; Doi and Edwards 1978a, b, 1986; Doi 1996; Marrucci and Grizzutti 1983).

The reptation model, initially proposed by de Gennes in 1971, assumes that the average effect of the meshwork of macromolecules on a given macromolecule is to impede its transverse motions across the strands of the other macromolecules. Thus, the macromolecular chain must move inside an effective tube formed by the other chains, in such a way that the motion of the chain is that of reptation, namely, a diffusive wriggling of the molecular chain along the length of such a tube. If the system is deformed, the cages along which the chain moves are distorted and the chains are carried into new configurations, in such a way that stress relaxation proceeds first by a relatively rapid equilibration of chain configurations within the distorted cages (of the order of the Rouse relaxation times), and then by a relatively slow diffusion of chains out of the distorted cages (of the order of the so-called disengagement time).

The relation (5.16) for the free energy in terms of the distribution function may also be used in these models, but with a different meaning of the distribution function, by defining $\psi(u, s, t)$ as the probability that the unit tangent vector at a position s (a scalar which denotes the position along the chain) and time t is in the direction u(s, t). The connection of u with the viscous pressure tensor \mathbf{p}^v is given by

$$\mathbf{P}^{v} = -\frac{3nk_{\mathrm{B}}T}{Nb^{2}} \left\{ \int_{0}^{L(t)} \mathrm{d}s \left[\mathbf{u}(s,t)\mathbf{u}(s,t) - \frac{1}{3}\mathbf{U} \right] \right\}. \tag{5.54}$$

This formula, which generalises (5.8), shows that the viscous pressure tensor is determined by two quantities, the length of the tube L(t) and the orientation of u(s, t).

In the limit of small deformations of the polymer, one may consider that the length is the same as in equilibrium, and that the deformation only changes the local orientation in space. This is called the independent-alignment approximation, in which the primitive chain segments, i.e. the tube segments which connect two consecutive entanglements along a polymer chain, are taken to behave as rigid rods in such a way that their distribution function is completely specified in the space of unit vectors u. In this approximation, one has

$$\Delta f = nNk_{\rm B}T \int \psi \ln \left[\psi(\boldsymbol{u}, s, t)/\psi(\boldsymbol{u}_0, s, t)\right] d\boldsymbol{u}, \tag{5.55}$$

where n is the number of polymer chains per unit volume, N the number of monomers per polymer and $\psi(\boldsymbol{u}, s, t)$ the orientation distribution function in the deformed state for a primitive segment located a distance s along the primitive chain; $\psi(\boldsymbol{u}_0, s, t)$ is the corresponding distribution function in the undeformed fluid. This expression is analogous to (5.16).

The change in the orientational distribution function $\psi(u)$ due to the deformation of the fluid is obtained by requiring the continuity condition

$$\psi_0(\mathbf{u}_0)\mathrm{d}\Omega_0 = \psi(\mathbf{u})\mathrm{d}\Omega,\tag{5.56}$$

with \mathbf{u}_0 , \mathbf{u} , $\mathrm{d}\Omega_0$ and $\mathrm{d}\Omega$ corresponding to the unit vectors and solid angles before and after the deformation. On the other hand, since the continuum deforms at constant volume, one must have $r_0^3\mathrm{d}\Omega_0=r^3\mathrm{d}\Omega$, with r the magnitude of the position vector \mathbf{r} . Then, the ratio $\psi(\mathbf{u})/\psi_0(\mathbf{u}_0)$ can be written as r^3/r_0^3 and (5.55) becomes

$$\Delta f = nNk_{\rm B}T\langle\ln\left(r/r_0\right)^3\rangle,\tag{5.57}$$

with $\langle \cdots \rangle$ indicating the average value over the orientation distribution function. The ratio r^3/r_0^3 may also be written in terms of the deformation gradient tensor **E**, defined by means of the relation $\mathbf{r} = \mathbf{E} \cdot \mathbf{r}_0$, as $r^3/r_0^3 = \det(\mathbf{E})$, so that (5.57) becomes

$$\Delta f = nNk_{\rm B}T \left\langle \ln\left[\det\left(\mathbf{E}\right)\right]\right\rangle. \tag{5.58}$$

It is interesting to show some explicit results for the free energy in simple plane situations. In this case, one must take in (5.57) $\ln{(r^2/r_0^2)}$ rather than $\ln{(r^3/r_0^3)}$. For a plane shear deformation γ in the z direction, one has $x = z_0 \gamma + x_0$ and $z = z_0$, and then

$$r^2 = r_0^2 + \gamma^2 z_0^2 + 2\gamma x_0 z_0. {(5.59)}$$

If instead of a static shear deformation one has a steady shear flow, the simplest naive way to proceed would be to take x = 0 (i.e. to follow the motion of the fluid) and for the shear deformation the value $\gamma = \dot{\gamma}\tau$, with τ the relaxation time, which

in the reptation model may be identified with the disengagement time τ_d . For small values of the shear rate, writing $\ln{(r^2/r_0^2)} = \ln{(1 + \gamma^2 \cos^2{\theta})} \approx \gamma^2 \cos^2{\theta}$ with $\cos{\theta} = x_0/r_0$, and taking into account that the mean value of $\cos^2{\theta}$ is 1/2, we have

$$\Delta f = \frac{1}{2} n N k_{\rm B} T \dot{\gamma}^2 \tau^2, \tag{5.60}$$

which coincides with the usual expression of EIT for low values of $\dot{\gamma}$.

A more general approximation (Marrucci and Grizzutti 1983), valid for any arbitrary deformation, is given by

$$\Delta f = nNk_{\rm B}T \left\langle \int_{-\infty}^{t} \left[\partial \mu(t - t') / \partial t \right] \ln \left[\det \mathbf{E}(t') \right] dt' \right\rangle, \tag{5.61}$$

with $\mu(t-t')$ the relaxation function giving the fraction of segments which at time t are still trapped in the deformed tubes. In the reptation model this function has the form

$$\mu(t) = (8/\pi^2) \sum_{p,\text{odd}} p^{-2} \exp\left[-p^2 t/\tau_d\right].$$
 (5.62)

The disengagement time τ_d is (Doi and Edwards 1978b)

$$\tau_{\rm d} = \frac{b^2 \zeta M^3}{\pi^2 k_{\rm B} T M_{\rm e} M_0^2},\tag{5.63}$$

where M_0 is the mass of a monomer and $M_{\rm e}$ the average molecular mass between successive entanglement points. The main difference of the relaxation times $\tau_j = \tau_d/j^2$ and the relaxation times (5.37b) following from the Rouse theory with the expression (5.63) is the term $M/M_{\rm e}$, which becomes equal to 1 when there are no entanglements, because then $M_{\rm e}$ coincides with M. This term shifts the scaling law for τ in terms of M from $\tau \approx M^2$ to $\tau \approx M^3$. In fact, experimentally it is observed that $\tau \approx M^{3.4}$. It is thought that the scaling law with the exponent 3 is exact for very high molecular mass, whereas for lower molecular mass other mechanisms different from that of reptation may contribute to the relaxation, thus changing the scaling law.

The scaling laws for the shear viscosity and the steady state compliance are the following ones. In the reptation model, one has

$$\eta_i = \frac{24}{5\pi^2} \frac{ck_{\rm B}T}{M_{\rm e}} \frac{\tau_i}{i^2}.$$
 (5.64)

In (5.64), only odd values of i are admissible, and the relaxation times of the different modes have the form $\tau_i = \tau_d i^{-2}$ with τ_d the reptation or disengagement time given in (5.63). Then, the total contribution of the polymer to the viscosity is

$$\eta_{\rm p} = \frac{24}{5\pi^2} \frac{ck_{\rm B}T}{M_{\rm e}} \tau_{\rm d} \sum_{i,\rm odd} i^{-4}.$$
 (5.65)

Thus, the scaling laws for η_p in (5.65) is $\eta \approx M^3 c$, in the limit of high molecular masses, and $\eta \approx M^{3.4} c^b$, with b an exponent close to 1, in many experimental results.

Expression (5.40) for the steady-state compliance *J* may be written in this case as

$$J = \frac{24}{5\pi^2} \frac{ck_{\rm B}T}{M_{\rm e}} \frac{\tau_{\rm d}^2}{\eta^2} \sum_{i \text{ odd}} i^{-6}.$$
 (5.66)

Taking into account that for a concentrated solution the solvent viscosity is negligible as compared to the polymer viscosity, one has $\eta = \eta_s + \eta_p \approx \eta_p$, and using the ratio (5.65) one may write (5.66) as

$$J = \frac{CM_{\rm e}(c)}{ck_{\rm B}T},\tag{5.67}$$

with the constant C given by

$$C = \frac{5\pi^2}{24} \left(\sum_{i,\text{odd}} i^{-6} \right) \left(\sum_{i,\text{odd}} i^{-4} \right)^{-2} = 2.$$
 (5.68)

The appearance in (5.67) of $M_{\rm e}(c)$ instead of M modifies the scaling laws of J in terms of c, since $M_{\rm e}$ depends on the concentration: it becomes smaller when c increases because the average length between successive entanglements is shorter for higher concentrations. The dependence is of the order of c^{-2} ; more explicitly, it may be written as $M_{\rm e}(\phi) = M_{\rm e}^0(\rho(\phi_{\rm p})/\rho_{\rm p}^0)\phi_{\rm p}^{-2}$, where $\phi_{\rm p}$ is the volume fraction of the polymer, $M_{\rm e}^0$ the value of $M_{\rm e}$ for the melt of the pure polymer, $\rho_{\rm p}^0$ the mass density of the pure melt and $\rho(\phi_{\rm p})$ the density of the solution with polymer volume fraction $\phi_{\rm p}$.

5.5 Polymer Blends. Double Reptation Model

Besides dilute and entangled polymer solutions, shear-induced effects have also been studied in polymer blends. In this case, instead of having long macromolecules solved in a solvent of small molecules, one has a mixture of long macromolecules A and long macromolecules B. Often, these blends are formed by seeking for an optimal combina-tion of the physical properties of the separate components. Entropic considerations, always relevant in mixing processes, are especially important in the blending of polymers, where the length of the macromolecules and their high number of microscopic configurations make entropy a large quantity.

The memory function for the stress relaxation of the blend must take explicitly the relaxational properties of each component. Intuitively, one could expect that the stress relaxation function is the weighted sum of the corresponding functions for each component, but this is not realistic because of the mixing and topological interaction of chains of both kinds. Clarke and McLeish (1998) take the following expression

$$G(t - t') = \left\{ \phi_{A} \left(G_{A} \exp\left[-(t - t')/\tau_{A} \right] \right)^{1/2} + \phi_{B} \left(G_{B} \exp\left[-(t - t')/\tau_{B} \right] \right)^{1/2} \right\}^{2},$$
(5.69)

where ϕ_i , G_i and τ_i are respectively the volume fraction, plateau modulus and relaxation time of pure polymer i, G_i being, as in (1.21), $G_i = \eta_i/\tau_i$. This non-linear mixing rule follows from the model of double-reptation (des Cloizeaux 1988) which, in physical terms, accounts for the fact that polymers do not reptate in fixed tubes, but that the surrounding polymers which form the tube also relax with a characteristic time scale. Thus, stress relaxation depends not only on the dynamics of an individual polymer, but also on the dynamics of the surrounding ones, which are molecules of both kinds A and B. This is the simplest way to describe the details of stress relaxation in polymer blends, by taking into account that the relaxation of both components is coupled, with a degree of coupling depending on the relative concentrations. The relaxation times τ_i correspond to the tube survival time for chains of species i in an environment in which the chemical heterogeneity is that of the blend, but all chains have the same relaxation time.

Equation (5.69) yields for the steady viscous stresses the following expressions

$$\sigma_{xy} = \gamma \left[\phi_{A}^{2} G_{A} \tau_{A}^{2} + 8 \phi_{A} \phi_{B} (G_{A} G_{B})^{1/2} \left(\frac{\tau_{A} \tau_{B}}{\tau_{A} + \tau_{B}} \right) + \phi_{B}^{2} G_{B} \tau_{B}^{2} \right], \quad (5.70)$$

and for the first normal stress coefficient

$$N_{1} = \sigma_{xx} - \sigma_{yy} = 2\gamma^{2} \left[\phi_{A}^{2} G_{A} \tau_{A}^{2} + 8\phi_{A} \phi_{B} (G_{A} G_{B})^{1/2} \left(\frac{\tau_{A} \tau_{B}}{\tau_{A} + \tau_{B}} \right)^{2} + \phi_{B}^{2} G_{B} \tau_{B}^{2} \right],$$
(5.71)

whereas the second stress $N_2 = \sigma_{yy} - \sigma_{zz}$ is equal to zero in the Maxwell model. The terms in $\phi_A \phi_B$ describe the coupling between both kind of chains.

The diagonal components of the stress tensor are assumed to have the form

$$\sigma_{xx} = \frac{2}{3}N_1, \quad \sigma_{yy} = \sigma_{zz} = -\frac{1}{3}N_1,$$
 (5.72)

so that $\text{Tr } \sigma = 0$ Note that this assumption is different from the one from the Maxwell upper-convected model, where $\sigma_{xx} = N_1$ and $\sigma_{yy} = \sigma_{zz} = 0$.

The explicit form of the steady state compliance J for such polymer blends may be obtained from the general formula (5.40), namely,

$$J = \frac{\sum_{i} \tau_{i} \eta_{i}}{\left(\sum_{i} \eta_{i}\right)^{2}} = \frac{\sum_{i} \tau_{i}^{2} G_{i}}{\left(\sum_{i} G_{i} \tau_{i}\right)^{2}},\tag{5.40}$$

and from the fact that the memory function G(t) in (5.69) may be explicitly rewritten as

$$G(t) = \phi_{A}^{2} G_{A} \exp(-t/\tau_{A}) + \phi_{B}^{2} G_{B} \exp(-t/\tau_{B})$$

$$+ 2\phi_{A} \phi_{B} (G_{A} G_{B})^{1/2} \exp(-t/\tau_{C})$$

$$\equiv \sum_{i} G_{i}(t), \qquad (5.73)$$

where $\tau_C^{-1} = 2(\tau_A^{-1} + \tau_B^{-1})$. In (5.73), the functions $G_i(t)$ and τ_i do not correspond to the pure A and B fluids, but are formal expressions to be used in (5.40). By combining (5.40) and (5.73), it follows for the steady-state compliance

$$J = \frac{\phi_{\rm A}^2 \tau_{\rm A}^2 G_{\rm A} + \phi_{\rm B}^2 \tau_{\rm B}^2 G_{\rm B} + 2\phi_{\rm A}\phi_{\rm B} \tau_{\rm C}^2 (G_{\rm A} G_{\rm B})^{1/2}}{\left[\phi_{\rm A}^2 \tau_{\rm A} G_{\rm A} + \phi_{\rm B}^2 \tau_{\rm B} G_{\rm B} + 2\phi_{\rm A}\phi_{\rm B} \tau_{\rm C} (G_{\rm A} G_{\rm B})^{1/2}\right]^2}.$$
 (5.74)

For pure A (ϕ_A =1) or pure B (ϕ_B =1), this expression tends respectively to J=1/ G_A , J=1/ G_B , as it should be. The expressions (5.46–5.47), (5.67) and (5.74) for the steady-state compliance will be used in the Chap. 6 for analysing shear-induced effects.

Chapter 6 Non-equilibrium Chemical Potential and Shear-Induced Effects in Polymer Solutions and Blends

In equilibrium thermodynamics, the chemical potential plays one of the most important roles in the analysis of multicomponent systems and, in particular, it is the most useful tool to study the phase coexistence and the equilibrium and stability conditions in chemical reactions. In the previous chapters we have shown, from macroscopic and microscopic perspectives, that the free energy of flowing fluids and, consequently, the chemical potential may depend on the flow.

The definition of the chemical potential for non-equilibrium situations points out the possibility of generalising the classical equilibrium analysis of phase diagrams and of reacting systems to non-equilibrium steady states. Indeed, it is well known that shear flows modify the phase diagram of polymer solutions and blends, for which the application of a viscous stress may induce phase segregation or a modification of the molecular weight distribution of the polymer because of shear-induced degradation. Thus, it is worthwhile to study in detail the predictions of the non-equilibrium chemical potential to compare them with the experimental results.

Shear-induced effects have practical importance, because many industrial processing involving polymers are carried out in flowing systems, and temperature and flow are expected to control the microstructure and the mesoscopic morphology of materials. The use of equilibrium results in these situations may be misleading, predicting, for instance, a homogeneous mixture whereas in actual fact the system separates into two fluid phases as a consequence of flow-induced effects. If a fast solidification of the system is then produced, the mechanical and elastic properties of the final product may be influenced by the degree of local inhomogeneity of the corresponding fluid system from which it was originated.

However, an analysis of stability in flowing systems must not be based on an extrapolation of the equilibrium thermodynamic equations to non-equilibrium situations, by simply introducing into the stability conditions the non-equilibrium potential instead of the local-equilibrium one. Each proposition must be carefully and critically examined from a dynamical basis, as it will be done in Chap. 7, where it is seen that the relations between thermodynamic stability and dynamic stability become much more involved in non-equilibrium states. The present chapter is devoted to the discussion of the chemical potential and its application to the analysis of thermodynamic stability in shear flows of polymer solutions and blends.

6.1 Survey of Experimental Results

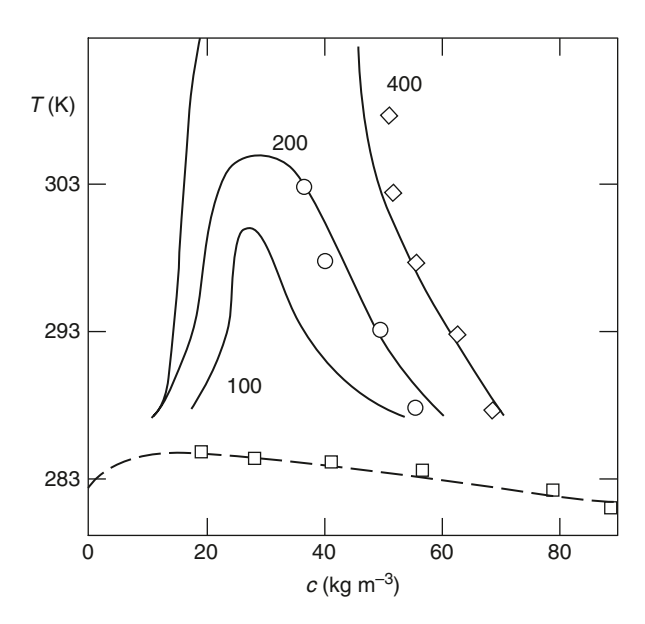
In this section, we give an overview of some shear-induced effects on the phase diagram of polymer solutions, as a physical motivation for the subsequent analysis. The influence of the shear flow on the phase separation in fluids has been analysed from different points of view, in particular the shear-induced shift of the critical point and the spinodal line. The observations are usually made on the basis of turbidity or of viscosity. In the first case, they are based on the direct observation of a change in the appearance of turbidity in the flowing solution as compared with the solution at rest. In other cases, the observation stems from changes in the viscosity. These results are interpreted in several different ways: some authors propose that the observed turbidity is due to dynamically enhanced concentration fluctuations in the presence of the flow, rather than to a true phase separation. Other authors have suggested that there is a true shift of the coexistence line and the spinodal line, implying an actual phase separation, leading to turbidity, which may be further enhanced by the dynamical effects of the flow on the concentration fluctuations. In principle, the shift due to purely thermodynamic effects should be manifested in other independent phenomena where the chemical potential plays a role, such as, for instance, in chemical equilibrium or on the intensity of fluctuations.

Changes in solubility of polymers due to the presence of a flow have been reported many times in the literature since the 1950s and have received attention from several points of view. We do not presume here to cover all the literature on this topic, which is very extensive. The papers by Rangel-Nafaile et al. (1984) and of Barham and Keller (1990), Hashimoto et al. (1993) and Wang and Chatterjee (2002) as well as the reviews (Jou et al. 1995, 2003; Onuki 1997, 2002) cover a wide bibliography on the subject, which is updated in this book.

To our knowledge, the first reports on the influence of flow on the polymer solubility are due to Silberberg and Kuhn (1952, 1954). These authors studied a solution of two different polymers (polystyrene and ethylcellulose) in a common solvent (benzene). In this system, the critical temperature (at the concentrations studied by the authors) below which phase separation occurs is $T_{\rm c}=31.7^{\circ}{\rm C}$. The presence of a flow with shear rate $\dot{\gamma}=200\,{\rm s}^{-1}$ was able to reverse the separation and to lower the critical temperature some 10°C, up to $T_{\rm c}=21.7^{\circ}{\rm C}$. In many other situations, however, the critical temperature is raised by the presence of the shear flow.

Inclusion of the effects of the flow into the free energy for the analysis of the phase separation problems was made for the first time by Ver Straate and Philipoff (1974), by using Marrucci's formula (5.1) for the free-energy excess. These authors observed that a clear polymer solution upon passing from a reservoir into a capillary, a region of high shear rate, became turbid in the capillary. After leaving it, the solution became clear again. This phenomenon was exhibited only above a certain shear rate depending on the polymer, solvent, concentration and temperature. The viscosity of the solution was seen to undergo unusual changes in this turbid state, also called a turbidity point or cloud point, passing through a minimum as the shear rate increased. The visual observation of the cloud points, always made in laminar flow, showed an increase in the cloud point temperature, instead of the decrease

Fig. 6.1 Shear-induced shift of the coexistence line of polymer solutions. Results reported by Rangel-Nafaile et al. (1984) where the *dashed line* corresponds to the equilibrium solution



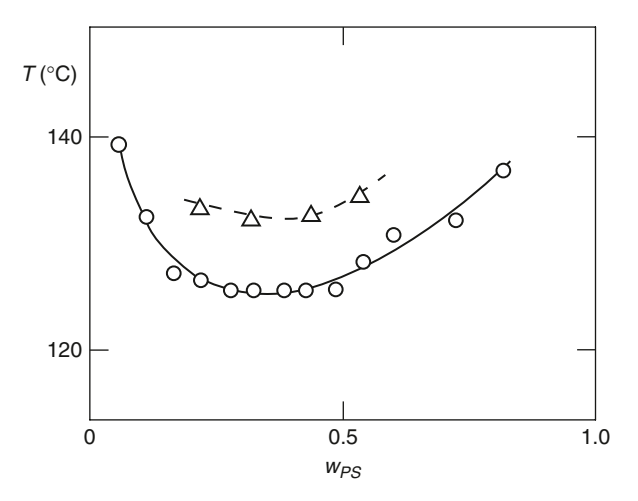
seen in the two-polymers-one-solvent system of Silberberg and Kuhn, i.e. the turbidity curves were shifted to higher temperatures.

In 1984, Rangel-Nafaile et al. (1984) studied solutions of polystyrene in dioctyl-phthalate and observed a shift of the cloud point curves towards higher temperatures (Fig. 6.1). The shift in the critical temperature could reach 24° C (at $P_{12}^{\nu} = 400 \text{ N/m}^2$). They also used a thermodynamic formalism based on Marrucci's formula (5.1) for the excess free energy. Also Wolf (1984) used a thermodynamic theory based on the Flory–Huggins equation for the mixing free energy and Marrucci's formula (5.1) for the change in the free energy due to the flow. By studying the phase separation of polystyrene solutions in transdecalin, he observed a decrease in the cloud point temperatures for relatively low-molecular-weight polystyrene and an increase for high-molecular-weight polystyrene, and attributed this behaviour to non-Newtonian effects arising in high-weight molecular solutions. Furthermore, Wolf found that the turbidity curves of the flowing solutions could exhibit two maxima instead of one. Spinodal curves with two maxima under flow have also been studied by Lyngaae-Jorgensen and Sondergaard (1987).

Non-equilibrium phase diagrams of PMMA in dimethyl-phthalate, depending on temperature, concentration and shear rate, for solutions in Couette cylindrical flow have also been studied by Barham and Keller (1990), who observed a shift of the coexistence lines towards higher temperatures, of the order of up to 30°C.

The detailed evolution of the separation process has been studied experimentally by Takebe et al. (1989, 1990); the time rate and the geometrical structures which appear in the intermediate stages of the separation exhibit a rich phenomenology, which is beyond the present thermodynamic approach. In Chap. 7 we will introduce the dynamical aspects needed to describe these time-varying phenomena.

Fig. 6.2 In solutions with a lower critical point, a shear-induced increase of the spinodal temperature enhances the solubility. The *continuous line* corresponds to the quiescent solution and the *dashed* one to the solution under shear. (From Mazich and Carr 1983)



Here we have referred to upper critical points, i.e. to the maximum temperature below which phase separation is found. Some mixtures present, in contrast, a lower critical point: the solution is miscible at low temperatures but it separates at high enough temperatures. The effect of shear on the lower critical temperature of a polystyrene solution under shear has been explored by Mazich and Carr (1983). Here, the flow raises the phase transition temperature of the polymer blend and favours solubility (see Fig. 6.2). An analogous situation is found in micellar solutions (Hamano et al. 1995, 1997).

Still another subject of study concerns the changes in the shear viscosity. Time-dependent changes of the viscosity under certain conditions were observed and attributed to a network formation induced by the flow. The entanglement and disentanglement dynamics would then produce time-dependent changes in the apparent viscosity. Temporary network formation in sheared polymer solutions was observed by Peterlin and Turner (1965), Peterlin et al. (1965) and by Matsuo et al. (1967).

Barham and Keller (1990) have scrutinized possible different explanations for the anomalous flow phenomena observed in solutions. Indeed, appearance of turbidity, or changes in flow rate at constant stress or of shear stress at constant shear rate, could be attributed either to some change of phase induced by the flow or to the formation of an adsorption entanglement layer. To discriminate both situations, one could perform experiments under an oscillatory flow, in which the adsorption layer effects could be much reduced with respect to a steady-state experiment, because only a small number of macromolecules could pass near the layer. In contrast, the shear stress in the bulk would be maintained at a relatively high value. In this way, bulk phenomena would not be much affected by rapid oscillations whereas surface phenomena would be much reduced. These authors presented a classification of the different oscillatory experiments according to the most plausible kind of explanation (phase separation, or adsorption-entanglement layers).

6.2 Equilibrium Chemical Potential and Stability Analysis

In this Section we briefly recall the essential ideas about thermodynamic stability applied to a quiescent polymer solution. The usual definition of the chemical potential μ_i of component i in equilibrium thermodynamics is

$$\mu_i = \left(\frac{\partial G}{\partial n_i}\right)_{T,p,n_i},\tag{6.1}$$

where G is the Gibbs free energy and n_i , the number of moles of the species i.

The equilibrium Gibbs function for a dilute polymer solution may be expressed according to the Flory–Huggins model, whose level of approximation is the same as that obtained by a random phase approximation developed in the context of a mean-field model applied to a polymer solution. Because a lattice model is inherent in the Flory–Huggins theory, the volume of the system is expressed in such a way that $V = v_1 \Omega$ where the parameter Ω is defined as

$$\Omega = n_1 + m n_p, \tag{6.2}$$

with n_1 the number of moles of the solvent, v_1 its molar volume, n_p the number of moles of the polymer and m a new parameter (characteristic of the lattice model on which the Flory–Huggins approximation is based), which allows one to express the volume fraction ϕ as

$$\phi = mn_{\rm p}/\Omega. \tag{6.3}$$

At first sight, *m* may be identified as the polymerization index and its value should coincide with the ratio of the molar volumes of the polymer and the solvent, but in practice there is not such a coincidence and this leaves open the way to several options to determine *m* (Rangel-Nafaile et al. 1984, Krämer-Lucas et al. 1988, Criado-Sancho et al. 1991, Onuki 1989). The total Gibbs function of the system is given by

$$\frac{G}{RT} = n_1 \ln(1 - \phi) + n_p \ln \phi + \chi (1 - \phi) \Omega \phi, \tag{6.4}$$

with χ the Flory–Huggins interaction parameter, which depends on the temperature as

$$\chi = \frac{1}{2} + \Psi(T^{-1}\Theta - 1), \tag{6.5}$$

where Θ is the theta temperature (the temperature at which the repulsive excluded volume effects balance the attractive forces between the segments, in such a way that the polymer has the behaviour of an ideal chain) and Ψ is a parameter which does not depend on T.

From Eqs. (6.1) and (6.4) we can derive the chemical potentials of the solvent, μ_1 , and of the polymer, μ_p , which are given, respectively, by

$$\frac{\mu_1}{RT} = \ln(1 - \phi) + \left(1 - \frac{1}{m}\right)\phi + \chi\phi^2,\tag{6.6}$$

$$\frac{\mu_p}{RT} = \ln\phi + (1 - m)(1 - \phi) + \chi m(1 - \phi)^2. \tag{6.7}$$

The limit of stability of the homogeneous solution corresponds to the spinodal line in the plane T- ϕ , built from the condition (see Sect. 4.1 for a discussion)

$$\left(\frac{\partial \mu_1}{\partial \phi}\right)_{T,p,n_j} = 0. \tag{6.8}$$

When $(\partial \mu_1/\partial \phi)$ is positive, the homogeneous solution is stable; otherwise, the solution splits into two phases with different polymer concentrations. The maximum of the spinodal line is the critical point, which is specified by the further condition

$$\left(\frac{\partial^2 \mu_1}{\partial \phi^2}\right)_{T,p,n_j} = 0. \tag{6.9}$$

From the expression (6.6) and the conditions (6.8), (6.9) one immediately obtains that the critical point is defined by the following system of equations

$$-(1-\phi)^{-1} + (1-m^{-1}) + 2\chi\phi = 0, (6.10a)$$

$$-(1-\phi)^{-2} + 2\chi = 0. \tag{6.10b}$$

The first equation describes the spinodal line in a diagram T- ϕ (recall that χ depends on T as (6.5)). The combination of (6.10a) and (6.10b) yields for the coordinates of the critical point

$$\phi_{\rm c} = \frac{1}{1 + m^{1/2}}, \quad \chi_{\rm c} = \frac{1}{2} + \Psi\left(\frac{\Theta}{T_{\rm c}} - 1\right) = \frac{1}{2}\left(1 + \frac{1}{m^{1/2}}\right)^2.$$
 (6.11)

Note that instead of writing directly $T_{\rm c}$ we have written $\chi_{\rm c}$, which is related to $T_{\rm c}$ by the definition (6.5), and which comes out in a more direct form from the equations. For high molecular mass polymers, m is very high and the critical temperature $T_{\rm c}$ tends towards the theta temperature and the critical volume fraction tends towards zero.

6.3 Non-equilibrium Chemical Potential and Stability Analysis

As it has been remarked in Chap. 5, the presence of a flow elongates and orients the macromolecules in the solution, thus modifying its internal energy and its entropy and, consequently its free energy. To incorporate these effects, the expression (6.1) can be generalised to non-equilibrium situations by including in G the contribution ΔG due to the flow. In accordance with this criterion, the chemical potential of component j for a flowing system is then defined as

$$\mu_{j} = \left(\frac{\partial G}{\partial N_{j}}\right)_{T,p,N_{i},P^{\nu}} = \left(\frac{\partial (G_{\text{eq}} + \Delta G)}{\partial N_{j}}\right)_{T,p,N_{i},P^{\nu}}.$$
(6.12)

Note that here we have favoured \mathbf{P}^{ν} as the variable to be kept fixed during the differentiation; since the pressure p is a natural variable of G in equilibrium, it seems tempting to take the total pressure tensor (i.e. both p and \mathbf{P}^{ν}) as a natural variable for G in non-equilibrium states. However, other independent variables could be used, as for instance the configuration tensor, which is especially appealing because of its relation with the microstructure of the solution and, therefore, for a microscopic understanding of the phenomena. In the next subsection we consider a Legendre transform allowing passing from viscous pressure to configuration tensor as independent variable.

6.3.1 The Choice of Non-equilibrium Variables: Viscous Pressure or Configuration Tensor

The choice of the non-equilibrium variable kept constant in (6.12) is not completely arbitrary. Indeed, recall that in equilibrium $\mu_i = (\partial G/\partial n_i)_{T,p}$, but $\mu_i \neq (\partial G/\partial n_i)_{T,V}$, i.e. given a thermodynamical potential, the quantities to be kept constant during differentiation for the definition of the chemical potential or other thermodynamic quantities are not arbitrary. However, this point is not yet clear out of equilibrium: for instance, Rangel-Nafaile et al. (1984) used (though not directly) a definition at constant P_{12}^{ν} , Wolf (1984) at constant $\dot{\gamma}$, and Onuki (1989) at constant configuration tensor **W**.

To clarify this point, we explore the form of the non-equilibrium free energy for a polymer solution, when one takes as a non-equilibrium variable the viscous pressure tensor P^{ν} or, alternatively, the macromolecular configuration tensor W, defined as

$$\mathbf{W} = \frac{H}{k_{\rm B}T} \langle \mathbf{Q} \mathbf{Q} \rangle - \frac{1}{3} \mathbf{U}, \tag{6.13}$$

where Q is the end-to-end vector of the macromolecule (for the sake of simplicity, we consider only one normal mode of the macromolecule and a dilute solution), H the elastic constant of the springs in the bead-and-spring model of macromolecules, U the unit tensor, and $\langle \cdots \rangle$ stands for an average over the macromolecules in the unit volume. This tensor, or the closely related tensor $\langle QQ \rangle$, may be measured through light-scattering techniques. Recall that \mathbf{P}^{ν} and \mathbf{W} are related, for a dilute polymer solution, through the Kramers relation (5.8) or (5.23), namely $\mathbf{P}^{\nu} = -J^{-1}\mathbf{W}$, where J is the steady-state compliance given by $J = \tau/\eta$, with τ and η the relaxation time and the viscosity corresponding to the macromolecule.

In equilibrium thermodynamics, several choices of variables may contain the whole information on the system, provided that one uses the suitable thermodynamic potential (Callen 1960): the internal energy U(S, V, N), when S, V and N are taken as variables; the Helmholtz free energy F(T, V, N) when T is used as variable instead of S; or the Gibbs free energy G(T, p, N), when S and V are replaced by T and P. These thermodynamic potentials are connected by Legendre transforms, which allow one to pass from one choice of variables to another without losing information. However, information is lost if thermodynamic functions are not expressed in terms of their natural variables, as for instance S(T, P, N), or F(T, P, N).

Here, we examine a Legendre transform connecting a non-equilibrium Gibbs free energy $G_1(T, p, N, VP^v)$ depending on P^v , and a non-equilibrium Gibbs free energy $G_2(T, p, N, W)$ depending on W (Casas-Vázquez et al. 2001, 2002). The viscous pressure tensor is more macroscopic than the configuration tensor, and is especially suited for the description of non-equilibrium steady states, as it directly accounts for the effects of the external forces acting on the system, whereas the second one is more useful for a microscopic understanding of the problem. According to EIT, the Gibbs equation in non-equilibrium has the form (1.31), which may be rewritten as

$$dU = TdS - pdV + \mu dN - \frac{1}{2}J\mathbf{W}:d(V\mathbf{P}^{\nu})$$
 (6.14)

where we have used the relation $\mathbf{P}^{\nu} = -J^{-1}\mathbf{W}$ to write explicitly the conjugate of $V\mathbf{P}^{\nu}$. Note that we are using $V\mathbf{P}^{\nu}$ rather than \mathbf{P}^{ν} as the variable of U, in order to use extensive quantities, as S, V and N. We can thus write for the Gibbs free energy G_1 the expression

$$G_1(T, p, N, V\mathbf{P}^{\nu}) \equiv U - \frac{\partial U}{\partial S}S - \frac{\partial U}{\partial V}V = U - TS + pV,$$
 (6.15)

in which S and V have been replaced by T and p as independent variables.

If, instead of $V\mathbf{P}^{\nu}$, **W** is preferred as independent variable, the corresponding Gibbs free energy G_2 should also incorporate the change of $V\mathbf{P}^{\nu}$ by **W**, analogously to the changes introduced in (6.15), namely

$$G_2(N, \mathbf{W}) \equiv G_1 - \frac{\partial U}{\partial (V \mathbf{P}^{\nu})} : V \mathbf{P}^{\nu} = G_1(N, \mathbf{W}) + \frac{1}{2} \mathbf{W} : V \mathbf{P}^{\nu}, \qquad (6.16)$$

where, for the sake of notation's simplicity, we do not write explicitly the dependence of G_1 nor G_2 on T and p. The use of the suitable expression for the Gibbs free energy is essential to obtain correct results for the chemical potential. Indeed, in equilibrium thermodynamics it is well known that $\mu = (\partial G/\partial N)_{T,p}$ but $\mu \neq (\partial F/\partial N)_{T,p}$. Similarly, in the presence of a viscous flow the chemical potential would be given by

$$\mu = \left(\frac{\partial G_1(N, V\mathbf{P}^{\nu})}{\partial N}\right)_{T, \nu, V\mathbf{P}^{\nu}} = \left(\frac{\partial G_2(N, \mathbf{W})}{\partial N}\right)_{T, \nu, \mathbf{W}},\tag{6.17}$$

but, in contrast,

$$\mu \neq \left(\frac{\partial G_1(N, \mathbf{W})}{\partial N}\right)_{T, p, \mathbf{W}}.$$
(6.18)

It follows that both $V\mathbf{P}^{\nu}$ and \mathbf{W} can legitimately play the role of independent variables in the definition of the chemical potential, provided one uses the respective correct expression for the free energy. Unfortunately, misunderstandings about the definition of μ in non-equilibrium situations have been influential in the literature, because of lack of due attention to the non-equilibrium variables, and constitute a serious difficulty to assess the validity of thermodynamics in non-equilibrium steady states.

To illustrate explicitly this discussion, consider, for instance,

$$G_1(N, V\mathbf{P}^{\nu}) = G_{\text{eq}}(N) + \frac{1}{4}JV\mathbf{P}^{\nu}: \mathbf{P}^{\nu}, \tag{6.19}$$

where $G_{\rm eq}(N)$ stands for the local-equilibrium free energy at given T and p. Taking into account (6.16), the corresponding expression for the free energy G_2 in terms of ${\bf W}$ is

$$G_2(N, \mathbf{W}) = G_{eq}(N) - \frac{1}{4}J^{-1}\mathbf{W}: V\mathbf{W}.$$
 (6.20)

In contrast, if one writes directly G_1 in terms of **W**, i.e. if one simply expresses $V\mathbf{P}^{\nu}$ in terms of **W** in (6.19), one gets

$$G_1(N, \mathbf{W}) = G_{eq}(N) + \frac{1}{4}J^{-1}V\mathbf{W} : \mathbf{W}.$$
 (6.21)

Note the different sign in the non-equilibrium term in (6.20) and (6.21), which yields therefore opposite predictions for the non-equilibrium contributions.

The corresponding expressions for the chemical potential derived from (6.19) and (6.20) will be

$$\mu = \left(\frac{\partial G_1}{\partial N}\right)_{T, n, V\mathbf{P}^v} = \mu_{\text{eq}} + \frac{1}{4} \left(\frac{\partial J}{\partial N}\right)_{T, n, V\mathbf{P}^v} V\mathbf{P}^v : \mathbf{P}^v, \tag{6.22}$$

and

$$\mu = \left(\frac{\partial G_2}{\partial N}\right)_{T,p,\mathbf{W}} = \mu_{eq} - \frac{1}{4} \left(\frac{\partial J^{-1}}{\partial N}\right)_{T,p,\mathbf{W}} V\mathbf{W} : \mathbf{W}.$$
(6.23)

By using the relation $\mathbf{P}^{\nu} = -J^{-1}\mathbf{W}$, it is easy to see that (6.22) and (6.23) coincide. In contrast, these results are different from that obtained by direct differentiation of (6.21), namely

$$\left(\frac{\partial G_1(N, \mathbf{W})}{\partial N}\right)_{T, p, \mathbf{W}} = \mu_{\text{eq}} + \frac{1}{4} \left(\frac{\partial J^{-1}}{\partial N}\right)_{T, p, \mathbf{W}} V \mathbf{W} : \mathbf{W}.$$
(6.24)

The chemical potential (6.24) is incorrect and the qualitative trends predicted by it on the shear-induced shift of the critical temperature are opposite to experimental observations.

6.3.2 Stability Analysis

The stability condition (6.8) is valid in equilibrium but it cannot be taken for granted in non-equilibrium steady states. For the latter, a general dynamical stability analysis must be undertaken, starting from the whole set of balance and constitutive equations for the concentration c, the average velocity u, the diffusion flux J, and the polymer viscous pressure tensor P^v , namely

$$\frac{\partial c}{\partial t} + \boldsymbol{u} \cdot \nabla c = -\nabla \cdot \boldsymbol{J},\tag{6.25}$$

$$\rho \frac{\partial \boldsymbol{u}}{\partial t} + \rho \boldsymbol{u} \cdot \nabla \boldsymbol{u} = -\nabla p + \eta_{s} \nabla^{2} \boldsymbol{u} - \nabla \cdot \mathbf{P}_{p}^{\nu}, \tag{6.26}$$

$$\tau_1 \left(\frac{\mathrm{d} \mathbf{J}}{\mathrm{d}t} \right) + \mathbf{J} = -D' \nabla \mu + D' T \nabla \cdot (\beta \mathbf{P}_{\mathrm{p}}^{\nu}), \tag{6.27}$$

$$\tau_2 \left(\frac{\mathrm{d} \mathbf{P}_{\mathrm{p}}^{\nu}}{\mathrm{d}t} \right) + \mathbf{P}_{\mathrm{p}}^{\nu} = -2\eta_{\mathrm{p}}(\nabla \mathbf{u}) + 2\eta_{\mathrm{p}} T \beta(\nabla \mathbf{J}). \tag{6.28}$$

Equations (6.25) and (6.26) are the mass and momentum balance equations, and Eqs. (6.27) and (6.28) have been discussed in Sect. 1.2 (see Eqs. (1.51) and (1.52)). In these equations η_s and η_p are the solvent and the polymer contributions to the viscosity, respectively, \mathbf{P}_p^{ν} is the polymer contribution to the pressure tensor, and D' is related to the diffusion coefficient D through $D' = D(\partial \mu_{\text{eq}}/\partial n_i)_{T,p}^{-1}$. Note that in (6.27) it appears the chemical potential, for which the non-equilibrium expression

(6.12) should be used instead of the local-equilibrium form because the macromolecules are stretched and oriented by the flow, and this effect is obviously lacking in equilibrium. The stability of (6.25-6.28) to perturbations of the concentration and the velocity must be studied in detail. This will be done in Chap. 7. Here, we restrict our attention to situations where the coupling between J and P^{ν} as expressed through the β in (6.27) and (6.28) are absent, in which case it will be shown in Chap. 7 that the dynamical stability criterion coincides with the thermodynamic criterion (6.8).

6.3.3 Two-Fluids Model

Another description which has been often used is a two-fluid description in which the solute and the solvent are considered as two independent fluids, each one with its mass density and velocity ρ_A , v_A , ρ_B , v_B , and whose relative velocity $v_A - v_B$ is related to the diffusion flux. This model is more transparent, from a microscopic perspective, than the one-fluid model analyzed above. Such a description has been used as the starting point of the analysis by Doi and Onuki (1992) (see Sect. 6.6 for more detailed discussion). The main result of this approach is the following expression for the evolution of the volume fraction ϕ_A of one of the fluids, say, polymer A,

$$\frac{\partial \phi_{A}}{\partial t} = -\nabla \cdot (\mathbf{v}\phi_{A}) + \nabla \cdot \left\{ \mathbf{M} \cdot \left[\nabla (\mu_{A} - \mu_{B}) + \alpha \nabla \cdot \mathbf{P}_{p}^{\nu} \right] \right\}, \tag{6.29}$$

where v is the volume average velocity, M the mobility tensor, and α a parameter coupling the viscous pressure to the diffusion flux, which is given by

$$\boldsymbol{J} = -\mathbf{M} \cdot \left[\nabla (\mu_{\mathbf{A}} - \mu_{\mathbf{B}}) + \alpha \nabla \cdot \mathbf{P}_{\mathbf{p}}^{\mathbf{v}} \right], \tag{6.30}$$

where the parameter α plays a role analogous to $-T\beta$ in Eq. (6.27).

Once the chemical potentials are known in terms of the volume fraction, Eqs. (6.29) and (6.30) may be used as a basis for the analysis of the stability of the system. In usual analyses, μ_A and μ_B are taken as the local-equilibrium chemical potentials of fluids A and B respectively, and the coupling of the diffusion with the viscous pressure comes only from the latter term in (6.30). Another possibility is to take into account non-equilibrium contributions to the chemical potentials μ_A and μ_B , as those analyzed in (6.22) and (6.23), which provide an additional coupling between diffusion and viscous pressure. As stressed above, it is logical to use the non-equilibrium form for the chemical potential to take into consideration the stretching and orientation of the macromolecules in flow. Though it is evident that this may play a crucial role in shear-induced phenomena, it could be argued whether these effects are sufficiently well represented by \mathbf{P}_p^{ν} , and their inclusion into the chemical potential is redundant. Two facts illustrate that incorporation of non-equilibrium effects in μ and \mathbf{P}_p^{ν} is not redundant: in μ , they are quadratic in \mathbf{P}_p^{ν} , whereas in \mathbf{P}_p^{ν} they are linear; second, $\nabla \mu$ and $\nabla \cdot \mathbf{P}^{\nu}$ have usually different directions.

6.4 Phase Diagram of Polymer Solutions Under Shear Flow

The inclusion of non-equilibrium contributions to the Gibbs free energy and the chemical potential leads to modifications in the phase diagram of flowing polymer solutions, whose essential phenomenology has been described in Sect. 6.1. Here, we address our attention to the shift of the critical point and the spinodal line corresponding to the separation of two phases in the polymer solution as described by the non-equilibrium chemical potential. In Sect. 6.6 the corresponding analysis will be carried out for polymer blends.

Let us now evaluate the flow contribution to the chemical potential. In accordance with (1.37) the flow contribution to the Gibbs function can be written as

$$\Delta G = VJ(P_{12}^{\nu})^2, \tag{6.31}$$

where V is the volume of the system and J the steady-state compliance. Thus, when a flowing system is considered, the Gibbs energy function is given by the equilibrium contribution (6.4) plus the flow contribution (6.31) as

$$\frac{G}{RT} = n_1 \ln(1 - \phi) + n_p \ln \phi + \chi (1 - \phi) \Omega \phi + \frac{v_1 (P_{12}^v)^2}{RT} \Omega J, \quad (6.32)$$

where $V = v_1 \Omega$ with Ω defined by (6.2). Differentiation of (6.32) allows us to write for the chemical potentials of the solvent and of the polymer the equations homologous to (6.6) and (6.7)

$$\frac{\mu_1}{RT} = \ln\left(1 - \phi\right) + \left(1 - \frac{1}{m}\right)\phi + \chi\phi^2 + \frac{v_1(P_{12}^v)^2}{RT} \left[\Omega\left(\frac{\partial J}{\partial \phi}\right)_{P_{12}^v} \frac{\partial \phi}{\partial n_1} + J\right],\tag{6.33}$$

$$\frac{\mu_{\rm p}}{RT} = \ln \phi + (1 - m)(1 - \phi) + \chi m(1 - \phi)^2
+ \frac{v_1 (P_{12}^{\nu})^2}{RT} \left[\Omega \left(\frac{\partial J}{\partial \phi} \right)_{P_{12}^{\nu}} \frac{\partial \phi}{\partial n_p} + mJ \right].$$
(6.34)

To have a more compact notation, it is useful to introduce a new variable F defined as

$$F = \left(\frac{\partial \ln J}{\partial \ln \phi}\right),\tag{6.35}$$

in terms of which the expressions for the chemical potential take, after consideration of (6.2) and (6.3), the following form

$$\frac{\mu_1}{RT} = \ln(1 - \phi) + \left(1 - \frac{1}{m}\right)\phi + \chi\phi^2 + \frac{v_1(P_{12}^v)^2}{RT}J(1 - F), \quad (6.36)$$

$$\frac{\mu_{\rm p}}{RT} = \ln\phi + (1 - m)(1 - \phi) + \chi m(1 - \phi)^2
+ \frac{v_1(P_{12}^{\nu})^2}{RT} J\left(\frac{1 - \phi}{\phi}F + 1\right).$$
(6.37)

From these expressions, we will obtain the flow-induced influence on the spinodal line and the critical point. As a generalization of the equilibrium results (6.8) and (6.9), and under the conditions mentioned in Sect. 6.3.2, namely coefficient $\beta = 0$ in (6.27) and (6.28), we assume that the spinodal line satisfies the equation

$$\left(\frac{\partial \mu_1}{\partial \phi}\right)_{T,p,n_i,Z} = 0,\tag{6.38}$$

and the critical temperature is determined from the additional condition

$$\left(\frac{\partial^2 \mu_1}{\partial \phi^2}\right)_{T,p,n_i,Z} = 0. \tag{6.39}$$

Here, Z is a non-equilibrium quantity which depends on the physical conditions to which the system is submitted, in contrast with the differentiation in (6.12) defining the chemical potential, where P_{12}^{ν} must be kept constant. We consider here two different situations, by keeping constant either $\dot{\gamma}$ or P_{12}^{ν} during the differentiation of the chemical potential in (6.38) and (6.39). These two situations are not mere formal choices, but they correspond to different physical situations; for instance, if the viscosity depends on the concentration, namely $P_{12}^{\nu} = -\eta(c)\dot{\gamma}$, to keep P_{12}^{ν} constant when the concentration fluctuates, $\dot{\gamma}$ must be changed accordingly and, reciprocally, P_{12}^{ν} must be changed if one wants to keep $\dot{\gamma}$ constant under fluctuations of the concentration. In a flow along a tube, these situations would be related to keep a constant pressure head or a constant flow rate, respectively.

Conditions (6.38), (6.39) are like (6.8) and (6.9), but with the non-equilibrium chemical potential instead of the local-equilibrium chemical potential. As we have emphasized above, the range of applicability of condition (6.38) will be justified by dynamical analysis in Sect. 7.1, where it is shown that (6.38) is valid in non-equilibrium states where $P_{yy}^{\nu} = 0$, as in upper-convected Maxwell fluids in Couette flow, but it must be generalised otherwise.

6.4.1 Dilute and Semidilute Polymer Solutions

The differences in the several kinds of materials are reflected in the different expressions for the steady-state compliance J(c) which have been analysed in Chap. 5. We begin our analysis with dilute and semidilute solutions as described respectively by the Rouse and Zimm models of Sects. 5.1 and 5.2. When we take into account

expression (5.46) for J(c) and (6.31) for ΔG we may write the non-equilibrium contribution to G as

$$\frac{\Delta G^{(s)}}{RT} = BC \frac{\left(P_{12}^{\nu}\right)^2}{T^2} \Omega \Phi(\tilde{c}), \tag{6.40}$$

where *C* is the Rouse–Zimm parameter introduced in (5.42), *B* a parameter defined as $B = v_1 M_2 [\eta]/R^2$, and $\Phi(\tilde{c})$ is a function of the reduced concentration given by (5.47). Furthermore, we take for $C(\tilde{c})$ the expression proposed in (5.48) to describe the transition from the Rouse to the Zimm model with increasing concentration.

The explicit expression for the non-equilibrium contribution to the chemical potential is

$$\frac{\Delta\mu_1}{RT} = -\frac{2B(P_{12}^{\nu})^2}{T^2}C\frac{P_5(\tilde{c})}{P_6(\tilde{c})} - \frac{B(P_{12}^{\nu})^2}{T^2}C'\tilde{c}\Phi(\tilde{c}),\tag{6.41}$$

where C' stands for the derivative of the Rouse–Zimm parameter in (5.48) with respect to \tilde{c} and where we have introduced the auxiliary functions

$$P_5(\tilde{c}) = (k_{\rm H} - 1)\tilde{c}^2 + (k_{\rm H}^2 - 3k_{\rm H})\tilde{c}^3 - 3k_{\rm H}^2\tilde{c}^4 - k_{\rm H}^3\tilde{c}^5, \tag{6.42a}$$

$$P_6(\tilde{c}) = (1 + \tilde{c} + k_{\rm H}\tilde{c}^2)^3,$$
 (6.42b)

with $k_{\rm H}$ the Huggins constant defined in (5.44).

The stability criterion (6.38) yields the following expression for the spinodal line

$$\frac{\partial}{\partial \tilde{c}} \left(\frac{\mu_1}{RT} \right)_s = \frac{\partial}{\partial \tilde{c}} \left(\frac{\mu_1^{(0)}}{RT} \right)_s + \frac{\partial}{\partial \tilde{c}} \left(\frac{\Delta \mu_1}{RT} \right)_s = 0 \qquad (s = P_{12}^{\nu}, \dot{\gamma}). \tag{6.43}$$

The explicit expression of the equilibrium term is given by

$$\frac{\partial}{\partial \tilde{c}} \left(\frac{\mu_1^{(0)}}{RT} \right) = -\frac{\varphi}{1 - \varphi \tilde{c}} + \left(1 - \frac{1}{m} \right) \varphi + 2\chi \varphi^2 \tilde{c}, \tag{6.44}$$

with φ a constant defined as $\varphi = v_2/M_2[\eta]$, being v_2 the polymer molar volume. For the corresponding derivatives of the non-equilibrium contribution to (6.43) at constant shear pressure and constant shear rate one obtains, respectively

$$\frac{\partial}{\partial \tilde{c}} \left(\frac{\mu_1}{RT} \right)_{p_{12}^{\nu}} = \frac{2B \left(P_{12}^{\nu} \right)^2}{T^2} \left[C \frac{P_6 P_5' - P_5 P_6'}{P_6^2} + C' \left(\frac{P_5}{P_6} = F \right) + C'' \tilde{c} \Phi \right], \tag{6.45a}$$

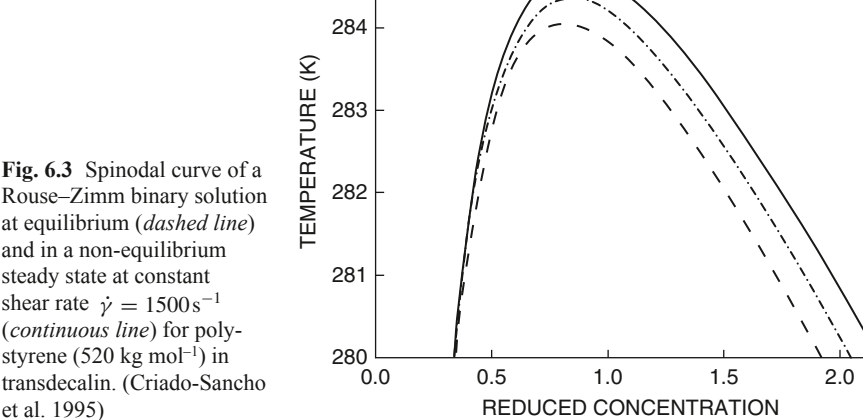
$$\begin{split} \frac{\partial}{\partial \tilde{c}} \left(\frac{\mu_1}{RT} \right)_{\dot{\gamma}} &= -\frac{2BC\eta_s^2 \dot{\gamma}^2}{T^2} (1 + \tilde{c} + k_{\rm H} \tilde{c}^2)^2 \\ &\times \left[2 \frac{(1 + 2k_{\rm H} \tilde{c})}{1 + \tilde{c} + k_{\rm H} \tilde{c}^2} \frac{P_5}{P_6} + \frac{P_6 P_5' - P_5 P_6'}{P_6^2} \right]. \end{split} \tag{6.45b}$$

In the latter expressions P_n' stand for the derivatives of P_n with respect to \tilde{c} , and C' and C'' the two first derivatives of the parameter C (5.48) with respect to \tilde{c} . We have written the cumbersome expressions (6.45a, b) only to show explicitly that the stability conditions at constant P_{12}^{ν} or constant $\dot{\gamma}$ will be in general different from each other.

The results for the spinodal line at constant $\dot{\gamma}$ for the Rouse–Zimm model are given in Fig. 6.3. The spinodal line is shifted again to higher temperatures but there is a difference between this behaviour and the shift at constant P_{12}^{ν} . In the latter, the shift is higher for lower values of concentration, whereas at constant shear rate the shift is higher at higher values of concentration. Accordingly, at constant P_{12}^{ν} the value of the critical concentration is lowered, but it shows an opposite trend at constant $\dot{\gamma}$. The role of the hydrodyamic interactions is more relevant in the shift of the critical temperature $T_{\rm c}$ than in the shift of the critical concentration.

The results at constant P_{12}^{ν} , in Fig. 6.4, show a shift of the spinodal line towards higher temperatures and, consequently, an increase in the critical temperature. This means that a shear flow will enhance demixing in systems which, at rest, would be totally mixed. An interesting point in the Fig. 6.4 is the role of hydrodynamic effects. It is seen that when these effects are neglected, as in the Rouse model, the shift in the critical point is maximum, and it is minimum in the Zimm model, where hydrodynamic interactions play a relevant role. Our model also shows that the role of hydrodynamic interactions is more relevant in the shift (increase) of the critical temperature T than in the shift (decrease) of the critical concentration.

285



Rouse-Zimm binary solution at equilibrium (dashed line) and in a non-equilibrium steady state at constant shear rate $\dot{v} = 1500 \,\mathrm{s}^{-1}$ (continuous line) for polystyrene (520 kg mol⁻¹) in transdecalin. (Criado-Sancho

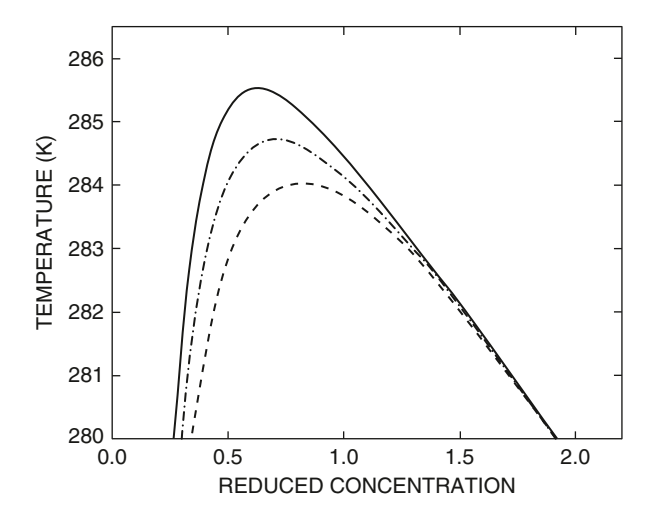


Fig. 6.4 Spinodal curve of the binary solution at equilibrium (the *dashed line* corresponds to Flory–Huggins) and in a non-equilibrium steady state at constant shear viscous pressure $P_{12}^{\nu} = 150 \,\mathrm{Nm^{-2}}$. In the figure are shown the *lines* corresponding to the Rouse model (without hydrodynamic interactions), the Zimm model (which takes into account hydrodynamic interactions) and two intermediate models for the values $\alpha = 0.5$ and $\alpha = 1.5$ in expression (5.48) for polystyrene (520 kg mol⁻¹) in transdecalin. (Criado-Sancho et al. 1995)

6.4.2 Entangled Solutions

To describe concentrated solutions where the different macromolecules become entangled with each other, we use the reptation model. The corresponding expression for the steady state compliance, as derived in (5.65), may be written as

$$J = \frac{2M^*}{RT} \left(\frac{M[\eta]}{mv_1}\right)^2 [\eta] \tilde{c}^{-3}, \tag{6.46}$$

with $M^* = M_{\rm e}^0[\rho(\phi)/\rho_{\rm p}^0]$ and v_1 the molar volume of the solvent. The appearance of $M_{\rm e}$ namely, the average molecular mass between neighbouring entanglement points, in (5.67) instead of M, the full molecular mass, modifies the scaling laws of J in terms of c with respect to that of dilute solutions, since $M_{\rm e}$ depends on the concentration: it becomes smaller when c increases because the average length between successive entanglements is shorter for higher concentrations; the dependence may be written as $M_{\rm e}(\phi) = M_{\rm e}^0[\rho(\phi)/\rho_p^0]\phi^{-2}$, where $M_{\rm e}^0$ is the value of $M_{\rm e}$ for the melt of the pure polymer, $\rho_{\rm p}^0$ the mass density of the pure melt and $\rho(\phi)$ the density of the solution with polymer volume fraction ϕ .

In the entangled regime, Eq. (6.40) together with (6.46) yields

$$\frac{\Delta G^{(s)}}{RT} = \frac{2B^*}{T^2} (P_{12}^{\nu})^2 \left(\frac{M[\eta]}{m\nu_1}\right) \Omega \tilde{c}^{-3}, \tag{6.47}$$

and the non-equilibrium contribution to chemical potential is given by

$$\frac{1}{RT}(\mu_1)_{\text{ent}} = \frac{8B^*}{T^2} (P_{12}^{\nu})^2 \left(\frac{M[\eta]}{m\nu_1}\right) \tilde{c}^{-3} \nu, \tag{6.48}$$

where the new parameter $B^* = v_1 M^* [\eta] / R^2$ is introduced.

As in the previous section, we study stability by keeping constant either $\dot{\gamma}$ or P_{12}^{ν} during the experiment. The thermodynamic criterion for the stability limit (6.38) yields the spinodal line. The explicit expression of the derivative of the equilibrium contribution is (6.44). The corresponding derivative of the non-equilibrium contribution (6.48) at constant viscous pressure is

$$\left[\frac{\partial}{\partial \tilde{c}} \left(\frac{(\mu_1)_{\text{ent}}}{RT}\right)\right]_{P_{12}^{\nu}} = -\frac{24B^*}{T^2} (P_{12}^{\nu})^2 \left(\frac{M[\eta]}{m\nu_1}\right)^2 \tilde{c}^{-4}.$$
 (6.49)

Since the non-equilibrium contribution (6.49) is negative, it favours stability of the solution and therefore the spinodal curve is shifted to lower values of the temperature in contrast with the behaviour obtained for dilute solutions in Fig. 6.4. The results are explicitly shown in Fig. 6.5. To obtain them, we consider a solution of polystyrene of molecular mass 520 kg mol⁻¹ in transdecalin taking for the parameters the same values used in Criado-Sancho et al. (1995), and we have taken for M^* the estimative values 2.6×10^{-3} kg mol⁻¹ and 5.2×10^{-3} kg mol⁻¹ (Criado-Sancho et al. 2002). The shift is higher for the higher value of M^* .

To study the situation at constant shear rate, we need to express the viscous pressure in (6.48) in terms of the shear rate. Considering the non-truncated Martin formula for the shear viscosity in terms of the reduced concentration \tilde{c} , defined as $\tilde{c} = [\eta] c$

$$\frac{\eta}{n_c} = 1 + \tilde{c} \exp(k_{\rm H} \tilde{c}),\tag{6.50}$$

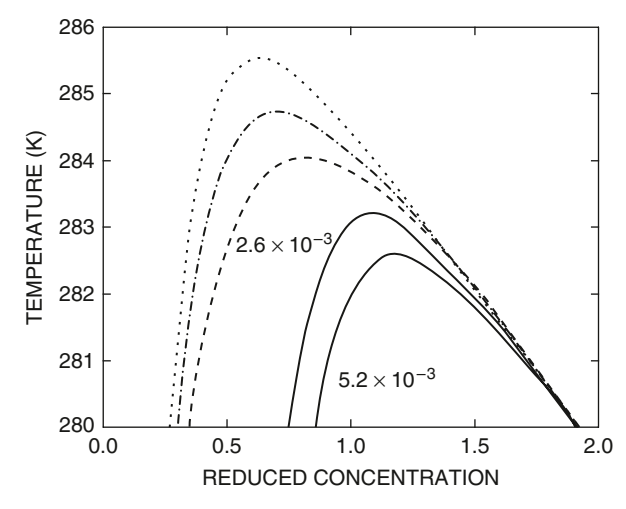


Fig. 6.5 Shear-induced shift of the spinodal line at constant P_{12}^{ν} for an entangled polymer solution of polystyrene (520 kg mol⁻¹) in transdecalin for two different values of the parameter M^* , indicated in this figure. The upper *dotted curve* corresponds to the equilibrium spinodal line. (Criado-Sancho et al. 2002)

Eq. (6.48) takes the form

$$\frac{1}{RT}\mu_{1,\text{ent}} = D\dot{\gamma}^2 [1 + \tilde{c}\exp(k_{\text{H}}\tilde{c})]^2 \tilde{c}^{-3}, \tag{6.51}$$

where the constant D is given by

$$D = \frac{4B^* C_{\text{rep}} \eta_0^2}{T^2} \left(\frac{M[\eta]}{m \nu_1} \right)^2.$$
 (6.52)

The derivative of (6.51) with respect to the concentration at constant shear rate yields

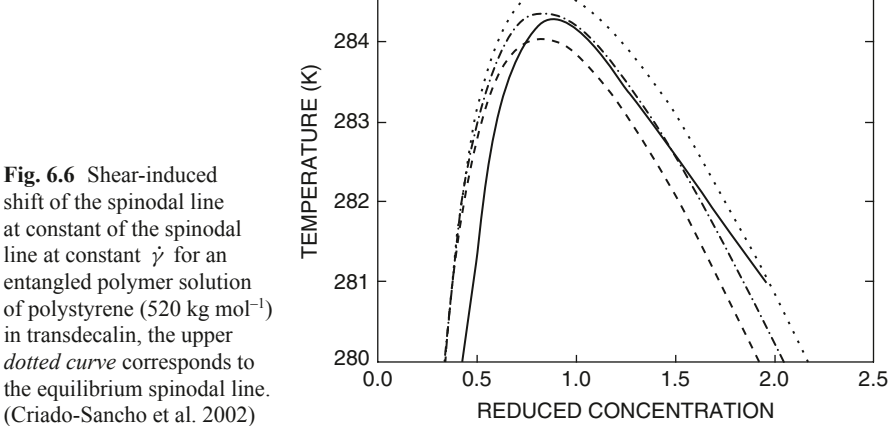
$$\left[\frac{\partial}{\partial \tilde{c}} \left(\frac{\mu_{1,\text{ent}}}{RT}\right)\right]_{\dot{\gamma}} = -D\dot{\gamma}^{2}$$

$$\times \left[3 + 2(2 - k_{\text{H}}\tilde{c})\tilde{c}\exp\left(k_{\text{H}}\tilde{c}\right) + (1 - 2k_{\text{H}}\tilde{c})\tilde{c}^{2}\exp\left(2k_{\text{H}}\tilde{c}\right)\right]\tilde{c}^{-4}.$$
(6.53)

In this case, the sign of (6.53), determining increase or decrease of the stability region, depends on the concentration. The value of the concentration at which there is a crossover from a shift to lower stability to a shift to higher stability depends only on the value of the Huggins constant $k_{\rm H}$. The modifications in spinodal line are plotted in Fig. 6.6 (Criado-Sancho et al. 2002).

For the reptation model at constant shear rate and for low concentrations, the spinodal line is shifted to lower temperature whereas for high concentrations (where the reptation model is more realistic and useful), the shift is towards higher temperature, i.e. it produces demixing. Thus, the different characteristics of dilute, semi-dilute or entangled polymer solutions are reflected, through the steady-state compliance and the viscous pressure, in different behaviours in shear flows; these behaviours depend, furthermore, on the physical constraints, namely fixed shear rate or fixed viscous pressure, acting on the system.

285



shift of the spinodal line at constant of the spinodal line at constant $\dot{\gamma}$ for an entangled polymer solution of polystyrene (520 kg mol⁻¹) in transdecalin, the upper dotted curve corresponds to the equilibrium spinodal line.

6.5 A Practical Illustration: Flow Effects in Polymer Extraction from a Porous Matrix

As a practical illustration of the former results, we consider polymer extraction from a porous matrix, which is a problem of much practical interest as, for instance, in oil extraction or pollutant extraction from a soil, or in chromatographic techniques, which have received a big impulse from microfluidics. The thermodynamic force driving the polymer from the porous medium to the fluid along a channel drilled in the matrix is the free energy difference between the polymer in the pores and in the fluid (the situation is sketched in Fig. 6.7).

The entropy of the polymer is much higher in the bulk fluid than in the channels of the porous medium, because a much higher number of microscopic configurations is accessible for it in the absence of walls. This will produce an entropic force tending to pull the macromolecule out of the pores towards the bulk fluid. Usually, it is assumed that the motion of the bulk fluid does not contribute to the free energy of the polymer, but in fact if the fluid is in motion, the polymer will be elongated and oriented by the flow, thus increasing its internal energy and reducing its entropy with respect to its corresponding value in the fluid at rest. In this way, the tendency of the polymer to go from the pores to the bulk fluid will be less than predicted by the local equilibrium theory. The flow contribution to the free energy of the polymer in the fluid and, consequently, on the thermodynamic force driving the transport of the polymer from the porous matrix to the fluid is given by (6.31) and it may be relevant in the practice, as it has been seen in the previous section.

Here, to be simple and specific, we consider a cylindrical channel of radius R_0 and length L along the z-axis inside a porous matrix of infinite extension in the x-y directions. We study the influence of the flow contribution to the chemical potential on the mass of polymer extracted from the matrix per unit time, which is given by

$$\frac{\mathrm{d}w}{\mathrm{d}t} \equiv \frac{\text{mass of polymer extracted}}{\text{time}} = c(L)Q, \tag{6.54}$$

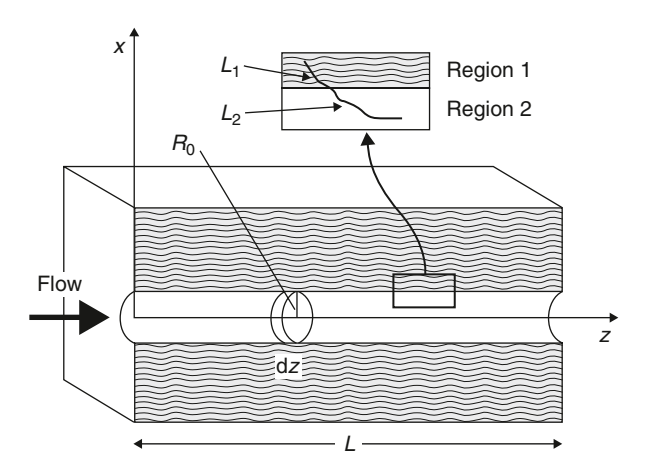


Fig. 6.7 Sketch of the situation considered in this section. Polymers embedded in the porous region are extracted by means of a suitable solvent flowing along a cylindrical tube drilled in it

where Q is the flow rate along the channel and c(L) the concentration of the polymer in the outgoing solution. To obtain c(L) one needs to know the profile c(z) of the average polymer concentration along the tube. The equation governing the longitudinal concentration profile is the mass conservation equation complemented with an equation for the rate J_p of polymer transfer per unit area between the porous medium and the flowing fluid, given by

$$J_{p} = \alpha \left[\mu_{1}(T, c_{1}) - \mu(T, c, P_{rz}^{\nu}) \right], \tag{6.55}$$

where $\mu_1(T, c_1)$ stands for the chemical potential of the polymer in the porous matrix, c_1 being an effective concentration of polymer in the porous matrix, and $\mu(T, c, P_{rz}^{\nu})$ the chemical potential of the polymer in the flowing fluid, P_{rz}^{ν} the viscous pressure acting on the fluid, and α a phenomenological coefficient related, for instance, to the size of pores arriving to the unit area of the walls of the channel.

We take into consideration the flow contribution to the chemical potential, as in Sect. 6.4. When (6.55) is combined with the mass conservation equation, one gets for the transfer of polymer per unit time and unit length of the channel

$$Q\frac{dc}{dz} = 2\pi R_0 \alpha \left\{ \mu_1(c_1) - \mu \left[c(z), P_{rz}^{\nu} \right] \right\}.$$
 (6.56)

To obtain this expression we have equated the polymer inflow across the lateral walls of the tube, $2\pi R_0 J_p dz$, to the increase in the axial flow of polymer along the tube between z and z + dz, namely $c(z + dz)Q - c(z)Q \approx (dc/dz)Qdz$. Using the auxiliary quantities $\tilde{z} = z/L$, $\tilde{c} = [\eta]c$, $Q_0 = Q/R_0^3$, $\tilde{w} = [\eta]w/R_0^3$ with $[\eta]$ the intrinsic viscosity (see (5.45)), Eq. (6.56) can be written in a compact form as

$$\frac{\mathrm{d}\tilde{c}}{\mathrm{d}\tilde{z}} = \frac{\lambda \alpha_0}{Q_0} \left[\frac{\mu_{\mathrm{FH}}(\tilde{c}_1, \chi_1)}{RT} - \frac{\mu_{\mathrm{FH}}(\tilde{c}, \chi)}{RT} - \frac{\mu_{\mathrm{flow}}(\tilde{c}, P_{rz}^{\nu})}{RT} \right], \tag{6.57}$$

being λ and α_0 the new coefficients $\lambda = L/R_0$, $\alpha_0 = (2\pi[\eta]RT\alpha)/R_0$, and R the gas constant. In this notation, Eq. (6.54) takes the form $d\tilde{w}/dt = \tilde{c}(1)Q_0$. As for the flow contribution to the chemical potential we use (6.39) with the transversal average $\langle \mathbf{P}^v : \mathbf{P}^v \rangle$ approximated by

$$\langle \mathbf{P}^{\nu} \colon \mathbf{P}^{\nu} \rangle = \frac{16Q_0^2}{\pi^2} \eta^2(\tilde{c}). \tag{6.58}$$

This average corresponds to the parabolic velocity profile in Poiseuille flow. Note however that we assume that the viscosity of the solution will be in principle a function of the polymer concentration $\eta(\tilde{c})$, which is a realistic assumption.

When P^{ν} does not influence the chemical potential, Eq. (6.57) simplifies to

$$\frac{\mathrm{d}\tilde{c}}{\mathrm{d}\tilde{z}} = \frac{\lambda \alpha_0^0}{Q_0} (\tilde{c}_1 - \tilde{c}),\tag{6.59}$$

where $\alpha_0^0 = (\alpha_0/RT)(\partial \mu_{\rm FH}/\partial \tilde{c})_{\tilde{c}_1}$. After integration of (6.59) one finds for the reduced concentration profile

$$\tilde{c} = \tilde{c}_1 \left[1 - \exp\left(-\frac{\lambda \alpha_0^0}{Q_0} \tilde{z} \right) \right]. \tag{6.60}$$

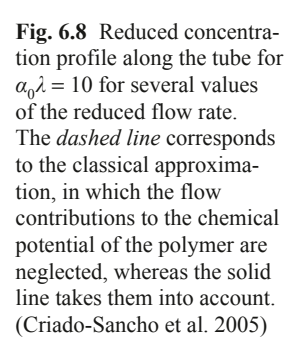
Introducing it into Eq. (6.54) for the rate of polymer extraction yields

$$\frac{\mathrm{d}\tilde{w}}{\mathrm{d}t} = Q_0 \tilde{c}_1 \left[1 - \exp\left(-\frac{\lambda \alpha_0^0}{Q_0}\right) \right]. \tag{6.61}$$

Thus, the extraction will be small either for very low or very high dimensionless flow rate Q_0 , and will be an intermediate optimum flow rate of the extracting solvent. This is to be expected, because for low flow rates the outgoing fluid has a relatively high polymer concentration, but only a small amount of fluid goes out per unit time. In contrast, at high values of the flow rate, the amount of outgoing fluid per unit time is high but the polymer concentration is very low, as the fluid has not been a long time enough inside the porous matrix to absorb the polymer. Furthermore, low λ (short channel) or low α_0 (low transport coefficient) will imply low extraction rates, as it is logical.

In Figs. 6.8 and 6.9 we compare the results obtained from the local-equilibrium Eq. (6.59) with those from (6.57), incorporating the flow contribution to the chemical potential, for polystyrene in transdecalin (Criado-Sancho et al. 2005). Of course, the analysis would be of higher practical interest if oil was considered, but we do not know, at present, the necessary parameters.

In Fig. 6.8 the longitudinal concentration profile along the tube is plotted. Solid lines refer to the results of the full Eq. (6.57), incorporating the effects of the non-equilibrium chemical potential as described by (6.31). Dashed lines correspond to the simple exponential profile (6.60), where such effects are ignored. The lines correspond to $\alpha_0\lambda=10$ (corresponding to a long tube or a high exchange coefficient). The gross features of the profiles, obtained for three different values of $Q_0\equiv Q/R^3$,



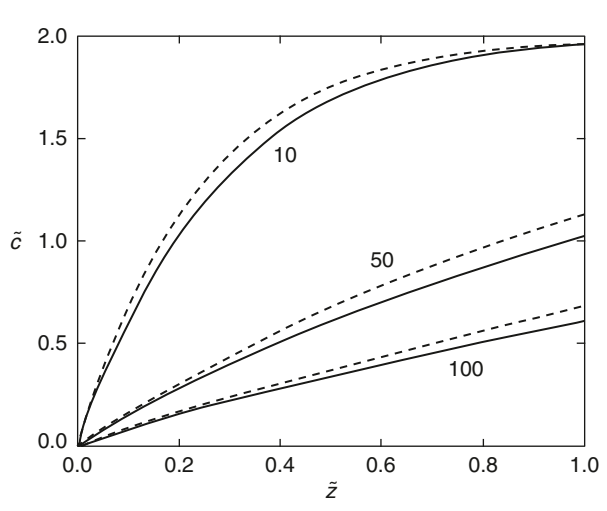
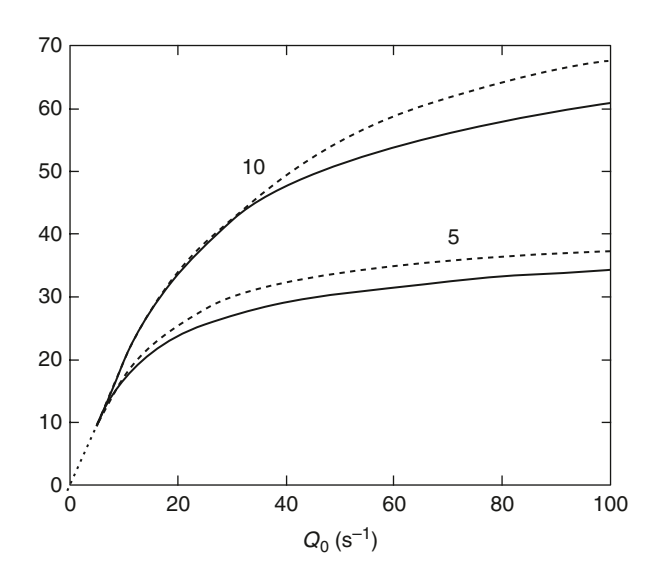


Fig. 6.9 Polymer extraction rate (in reduced units) as a function of the reduced flow rate of the fluid, for $\alpha_0 \lambda = 5$ and $\alpha_0 \lambda = 10$. The dashed line corresponds to the classical approximation whereas the solid line incorporates the flow contributions to the chemical potential (Criado-Sancho et al. 2005). The latter imply a considerable reduction of the polymer extraction



are as expected: of course, they increase with z and, for a given z, they decrease with the flow rate. The flow contribution to the chemical potential of the polymer is mainly reflected in the comparison of the full lines and dashed lines. It is seen that the concentration in the tube is lower when the flow contribution is included, because in this case the thermodynamic force driving the polymer from the soil to the tube, namely, the difference of the chemical potentials in the porous matrix and the flowing fluid will be less than in local-equilibrium model.

Concerning the rate of extraction $\mathrm{d} \tilde{w} / \mathrm{d} t$ as a function of the reduced flow rate Q_0 , it is plotted in Fig. 6.9 for different values of the coefficient $\alpha_0\lambda$. Solid lines refer to the full situation and dashed lines to the classical one. It is seen that the non-equilibrium effects lower the extraction rate, in 12 and 10% approximately for $\alpha_0\lambda=10$ (longer tubes) and $\alpha_0\lambda=5$ (shorter tubes) respectively. The fact that the flow effects are more important for high values of $\alpha_0\lambda$ is easy to understand from a qualitative point of view. Indeed, high values of λ , for given values of Q_0 and of the tube length L, correspond to narrow channels, where the velocity gradients will be higher for a given flow rate, and so will be non-equilibrium effects. This is also the case of parameter α_0 , which is inversely proportional to the radius of the channel. For more details, the reader is referred to Criado-Sancho et al. (2005).

6.6 Flow-Induced Effects in Polymer Blends: Two-Fluid Approach and Extended Approach

Shear-flow effects on phase separation of polymer blends where two kinds of macromolecules, A and B, are mixed and entangled with each other have some peculiar aspects which are not found in usual solutions discussed in Sect. 6.4. Whereas in a polymer solution in a small molecular solvent there is only one relevant relaxation time, corresponding to macromolecules, in polymer blends there are two different relevant relaxation times, with corresponding viscoelastic effects, and characteristic viscosities. Thus, some new effects not found in polymer solutions appear in blends; for instance, both shear-induced mixing and demixing may be found, depending on the relative relaxation times and viscosities of the two components.

6.6.1 Two-Fluid Approach

In this section we compare the two-fluid approach and the EIT approach to illustrate the main differences between both. Clarke and McLeish (1998) and Clarke (1999) used a two-fluid description of polymer blends proposed by Doi and Onuki (1992). This model, briefly introduced in Sect. 6.3.3, starts from the force balance equations for the two components A and B, which are

$$\varsigma(\nu_{A} - \nu_{B}) + \phi_{A} \nabla \mu_{A} + \phi_{A} \nabla p + \frac{\varsigma_{A}}{\varsigma_{A} + \varsigma_{B}} \nabla \cdot \mathbf{P}_{p}^{\nu} = 0, \tag{6.62a}$$

$$\varsigma(\nu_{\rm B} - \nu_{\rm A}) + \phi_{\rm B} \nabla \mu_{\rm B} + \phi_{\rm B} \nabla p + \frac{\varsigma_{\rm B}}{\varsigma_{\rm A} + \varsigma_{\rm B}} \nabla \cdot \mathbf{P}_{\rm p}^{\nu} = 0, \tag{6.62b}$$

where $\mathbf{v}_{\rm A}$ and $\mathbf{v}_{\rm B}$ are the velocities of both components, ς_i their respective friction coefficients, defined as $\varsigma_i = \phi_i(N_i/N_{ei})\varsigma_0$, with N_i the total number of monomers of chain i, N_{ei} the average number of monomers between successive entanglements, ϕ_i the volume fraction, and ς_0 the friction coefficient of a single monomer, which for the sake of simplicity is assumed to be equal for both species. The coefficient ς is defined by $\varsigma = \varsigma_{\rm A} \varsigma_{\rm B} (\varsigma_{\rm A} + \varsigma_{\rm B})^{-1}$. The first term in (6.62a, b) is the frictional force, which is balanced by the osmotic pressure term $\nabla \mu_{\rm A}$, the pressure gradient ∇p , and the viscous effect $\nabla \cdot \mathbf{P}_{\rm p}^{\rm v}$, with $\mathbf{P}_{\rm p}^{\rm v}$ the polymer contribution to the viscous pressure tensor. Note that inertial effects implying acceleration of the components have been neglected.

Eliminating ∇p from (6.62a) and (6.62b), expression (6.62a) can be written as

$$\varsigma(\nu_{A} - \nu_{B}) = \phi_{A}\phi_{B} \left[-\nabla(\mu_{A} - \mu_{B}) - \alpha\nabla \cdot \mathbf{P}_{p}^{\nu} \right], \tag{6.63}$$

where the coefficient α is given by

$$\alpha = \left(\frac{\varsigma_{A}}{\phi_{A}} - \frac{\varsigma_{B}}{\phi_{B}}\right) \frac{1}{\varsigma_{A} + \varsigma_{B}}.$$
(6.64)

The sign of α depends on $N_{\rm A}$ and $N_{\rm B}$; in particular, $\alpha > 0$ for $N'_{\rm A} \equiv N_{\rm A}/N_{\rm Ai} > N_{\rm B}/N_{\rm Bi} \equiv N'_{\rm B}$. This possible difference in the sign will be the key factor in the difference of behaviour in blends with $N'_{\rm A} > N'_{\rm B}$ or $N'_{\rm A} < N'_{\rm B}$. Instead, for a dilute solution, component B

could be identified as the Newtonian solvent, with $N'_{\rm B} = 1 \ll N'_{\rm A}$. Here, A is taken as the component with longest relaxation time.

Equation (6.63) may be combined with the continuity equation for constituent A

$$\frac{\partial \phi_{\mathbf{A}}}{\partial t} = -\nabla \cdot (\mathbf{v}_{\mathbf{A}}\phi_{\mathbf{A}}). \tag{6.65}$$

This leads finally to

$$\frac{\partial \phi_{A}}{\partial t} = -\nabla \cdot (\nu \phi_{A}) + \nabla \cdot \left\{ \mathbf{M} \cdot \left[\nabla (\mu_{A} - \mu_{B}) + \alpha \nabla \cdot \mathbf{P}_{p}^{\nu} \right] \right\}, \tag{6.66}$$

where ν is the volume average velocity defined as $\nu = \phi_A \nu_A + \phi_B \nu_B$ and the mobility tensor $\mathbf{M} = (\phi_A^2 \phi_B^2 / \varsigma) \mathbf{U}$. This is the equation introduced in (6.29). In the analysis by Clarke and McLeish (1998), the coupling term $\alpha \nabla \cdot \mathbf{P}_p^{\nu}$ plays an essential role in the shift of the spinodal line, whereas μ_A and μ_B are the local-equilibrium chemical potentials of polymers A and B respectively.

For the shear and normal viscous stresses of polymer blends, it is usual to take the "quadratic mixing rule" expressions (5.70) and (5.71), derived from the double reptation model, which exhibit the influence of two different relaxation times τ_A and τ_B , and two different plateau moduli G_A and G_B , namely

$$P_{12,p}^{\nu} = -\dot{\gamma} \left[\phi_{A}^{2} G_{A} \tau_{A} + 4\phi_{A} \phi_{B} (G_{A} G_{B})^{1/2} \frac{\tau_{A} \tau_{B}}{\tau_{A} + \tau_{B}} + \phi_{B}^{2} G_{B} \tau_{B} \right]$$

$$\equiv -G_{A} \tau_{A} \dot{\gamma} Y(\phi_{A}), \tag{6.67}$$

$$\begin{split} N_1 &= P_{12}^{\nu} - P_{22}^{\nu} = -2\dot{\gamma}^2 \left[\phi_{\rm A}^2 G_{\rm A} \tau_{\rm A}^2 + 8\phi_{\rm A} \phi_{\rm B} (G_{\rm A} G_{\rm B})^{1/2} \left(\frac{\tau_{\rm A} \tau_{\rm B}}{\tau_{\rm A} + \tau_{\rm B}} \right)^2 + \phi_{\rm B}^2 G_{\rm B} \tau_{\rm B}^2 \right] \\ &\equiv -2G_{\rm A} (\tau_{\rm A} \dot{\gamma})^2 X(\phi_{\rm A}), \end{split}$$

(6.68)

where $X(\phi_{\rm A})$ and $Y(\phi_{\rm A})$ are polynomials in $\phi_{\rm A}$ defined to have compact expressions in (6.67) and (6.68). The two relaxational features are mixed in a way depending on the respective volume fractions. Some alternative mixing rules have been proposed, but the quadratic mixing in (6.67) and (6.68) is up to now the one with a clearest theoretical background. For a polymer solution in a Newtonian solvent $\tau_{\rm B}=0$ and (6.67) and (6.68) reduce to $P_{12,\rm p}^{\nu}=-\dot{\gamma}G_{\rm A}\tau_{\rm A}=-\dot{\gamma}\eta_{\rm A}$, $N_1=-2\dot{\gamma}^2\eta_{\rm A}\tau_{\rm A}$, which are the expressions found in Chap. 5 for upper-convected Maxwell model. The diagonal components of the pressure tensor are assumed by Clarke and McLeish to be $P_{11,\rm p}^{\nu}=-\frac{2}{3}N_1$ and $P_{22,\rm p}^{\nu}=P_{33,\rm p}^{\nu}=\frac{1}{3}N_1$, so that ${\rm Tr} {\bf P}_{\rm p}^{\nu}=0$.

One may define an effective diffusion coefficient $D_{\rm eff}$ by rewriting the perturbed form of (6.66) as

$$\frac{\partial \delta \phi_{\mathcal{A}}}{\partial t} = -D_{\text{eff}} q^2 \delta \phi_{\mathcal{A}},\tag{6.69}$$

where q is the wavevector and $\delta \phi_A$ the perturbation in the volume fraction of polymer A. For wavevectors in the z direction (when the velocity is in the x direction and the velocity gradient in the y direction), the effective diffusion coefficient is

$$D_{\text{eff}} = 2M \left[\chi_{\text{c}} - \chi + \kappa q_z^2 + \Delta \chi_{\text{c}}(\dot{\gamma}, q_z) \right], \tag{6.70}$$

where χ is the Flory–Huggins interaction parameter given in Eq. (6.5), χ_c its value on the quiescent spinodal (6.11) and κ the interfacial energy between both phases, and $\Delta\chi_c(\dot{\gamma},q_z)$ describes the $\dot{\gamma}$ dependent shift in the spinodal line. The spinodal line indicating the onset of instability of the homogeneous phase is given by the condition $D_{\rm eff}=0$. Indeed, for positive values of the effective diffusion coefficient, inhomogeneities will tend to disappear according to (6.69), whereas a negative value of $D_{\rm eff}$ will enhance inhomogeneities. In Clarke and McLeish (1998), $\Delta\chi_c(\dot{\gamma},q_z)$, describing the shift in the spinodal line is found to be

$$\Delta \chi_{\rm c}(q_z) = \frac{2\alpha}{3k_{\rm B}T} (\dot{\gamma}\tau_{\rm A})^2 G_{\rm A}X'. \tag{6.71}$$

In the y direction, the shift of the spinodal line is given by

$$\Delta \chi_{\rm c}(\dot{\gamma}, q_{\rm y}) = \frac{2\alpha}{3k_{\rm B}T}(\dot{\gamma}\tau_{\rm A})^2 G_{\rm A}\left(\frac{1}{2}X' - \frac{XY'}{Y}\right),\tag{6.72}$$

X' and Y' being the derivatives of the functions $X(\phi_A)$ and $Y(\phi_A)$ defined in (6.67) and (6.68). When $\Delta\chi_c < 0$, there is shear-induced demixing, i.e. phase separation is enhanced by the flow, whereas $\Delta\chi_c > 0$ corresponds to shear-induced mixing, which contributes to the stability of the one-phase system. The sign of $\Delta\chi_c$ will depend on the sign of α , which depends on whether $N'_A > N'_B$ (with $\alpha > 0$) or $N'_A < N'_B$ (with $\alpha < 0$). Thus, when $N'_A > N'_B$ shear flow will contribute to stability, and $N'_A < N'_B$ to instability, leading to constituent separation. According to this model, for polymer solutions in a Newtonian solvent one has $\tau' = 0$ and $\Delta\chi_c > 0$, leading to increased stability, i.e. to a shift of the spinodal line towards lower temperatures.

6.6.2 Extended Approach

Note that in (6.71), (6.72) $\Delta\chi_c$ comes exclusively from the coupling between the viscous stress and the diffusion flux, namely, from the last term in (6.66), whereas the chemical potentials μ_A and μ_B are assumed to retain their local-equilibrium form. Another possibility is to consider that non-equilibrium chemical potentials include the flow contributions (6.31) and taking an upper-convected Maxwell model, for which $P_{11,p}^{\nu} = -N_1$, $P_{22,p}^{\nu} = P_{33,p}^{\nu} = 0$, in contrast with the model by Clarke and

McLeish. From (6.31), (6.67) and (6.68) one may derive the non-equilibrium contributions to the chemical potentials as

$$\Delta \mu_{A} = \nu_{0} N_{A} G_{A} (\tau_{A} \dot{\gamma})^{2} \frac{Z(\phi_{A}) + W(\phi_{A})}{Y(\phi_{A})}, \tag{6.73}$$

$$\Delta \mu_{\rm B} = \nu_0 N_{\rm A} G_{\rm A} (\tau_{\rm A} \dot{\gamma})^2 \frac{Z(\phi_{\rm A})}{Y(\phi_{\rm A})},\tag{6.74}$$

where $Z(\phi_A)$ and $W(\phi_A)$ are polynomials in ϕ_A similar to $X(\phi_A)$ and $Y(\phi_A)$ whose explicit cumbersome expressions is found in (Criado-Sancho et al. 2002a). According to the second term of expression (6.66), these non-equilibrium contributions to the μ_A and μ_B contribute to the effective diffusion coefficient as

$$(\Delta D_{\text{eff}})_{\text{this work}} = M \frac{\partial}{\partial \phi_{A}} \left[\frac{\partial (VJ)}{\partial N_{A}} - \frac{\partial (VJ)}{\partial N_{B}} \right] (P_{12}^{\nu})^{2}. \tag{6.75}$$

The explicit form of the steady state compliance J for polymer blends has been obtained in (5.74), and it may be introduced into (6.75).

The corresponding shift in the z and y directions are

$$\Delta \chi_{c}(\dot{\gamma}, q_{y}) = \frac{v_{0} N_{A}}{2k_{B}T} G_{A}(\tau_{A} \dot{\gamma})^{2} \times [-3WY' + YW' + (1 - \lambda)(-3ZY' + YZ')]Y^{-2}, \tag{6.76}$$

$$\Delta \chi_{c}(\dot{\gamma}, q_{z}) = \frac{v_{0} N_{A}}{2k_{B} T} G_{A}(\tau_{A} \dot{\gamma})^{2} \times [-WY' + YW' + (1 - \lambda)(-ZY' + YZ')]Y^{-2}, \tag{6.77}$$

with Z', W' and Y' standing for the derivatives of $Z(\phi_A)$, $W(\phi_A)$ and $Y(\phi_A)$ introduced in (6.72) and (6.73). As in the Clarke and McLeish model, one is led to the conclusion that in the presence of the flow one should consider an effective diffusion coefficient of the form $D_{\text{eff}} = D - a(\dot{\gamma}\tau_A)^2$, with a coefficient different in both models, but leading to similar qualitative results.

The results are plotted in Fig. 6.10. In the y direction (\mathbf{P}^{v} constant) both the Clarke and McLeish (CML) model and the EIT model predict an increase of the critical temperature of the same order, but opposite trends for the shift of the critical concentration, positive in the former model and negative in the latter one. In the z direction ($\dot{\gamma}$ constant), EIT predicts a shear-induced increase in the critical temperature whereas the CML predicts a decrease. Detailed experimental analyses are still lacking.

Furthermore, it is interesting to see that constant viscous pressure and constant shear rate conditions may coexist in the same problem. In the direction *y*, the direction of the velocity gradient, shear rate must be constant (in the plane Couette flow).

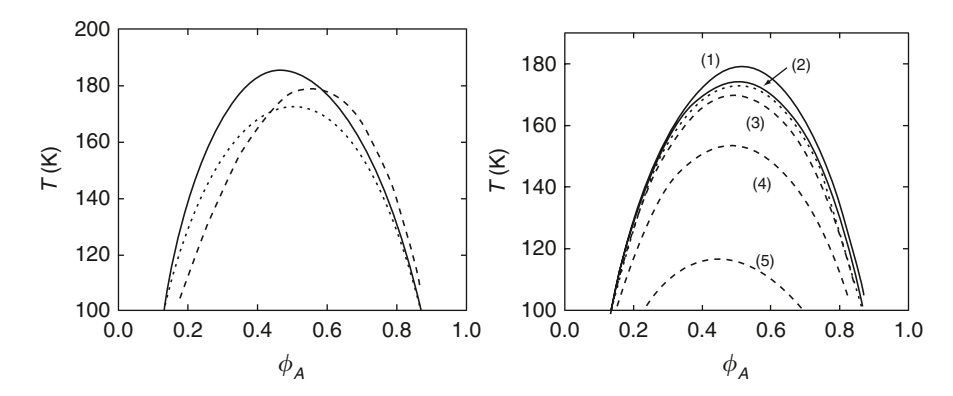


Fig. 6.10 Spinodal lines for polymer blends at constant P^{ν} (*left*). Spinodal lines for polymer blends at $\dot{\gamma}$ constant (*right*) (Criado-Sancho et al. (2002)). The *dotted line* corresponds to the equilibrium spinodal. The *continuous line* corresponds to the EIT model, and the dashed one to the Clarke-McLeish model

Instead, along the z direction, orthogonal to the velocity and the velocity gradient, the shear pressure is constant. Thus, the shear flow may induce separation in the y direction and suppress it in the z direction.

A two-fluid model analogous to (6.65), (6.66) has also been used by Yuan and Jupp (2002), Jupp et al. (2003), Jupp and Yuan (2004), Ouyang et al. (2004) to study the formation of concentration bands and mechanical shear bands in complex fluids, a topic which will be discussed in Chap. 8. In particular, they find that dynamic asymmetry between components A and B can have a strong influence in the dynamics of the phase transition and can produce a diversity of intermediate morphologies during the separation processes.

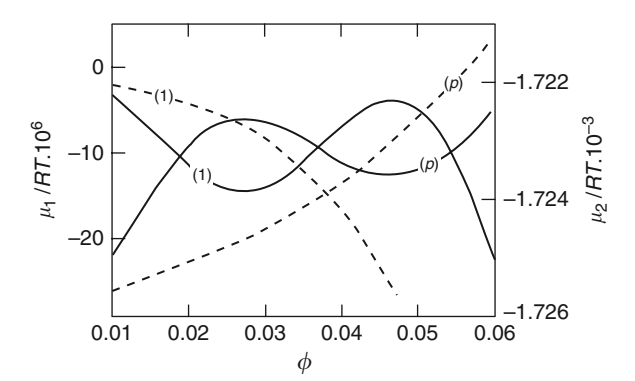
6.7 Non-Newtonian Effects in Phase Separation

In the Sects. 6.4–6.6, we have assumed that the steady-state compliance J is a function of the volume fraction ϕ (or the concentration c). Here, we briefly introduce the more general situation in which J depends also on P_{12}^{ν} as it may be expected in non-Newtonian fluids, where the viscosity depends on the shear rate. We suppose that the expression for the non-equilibrium entropy is still given by (6.31) but with $J(\phi, P_{12}^{\nu})$ instead of $J(\phi)$, and explore the phase diagram of dioctyl-phthalate and polystyrene by taking into account this dependence.

The spinodal curve is given by the condition (6.38), i.e.

$$\left(\frac{\partial(\mu_1/RT)}{\partial\phi}\right)_{P_{12}^{\nu}} = -\frac{1}{1-\phi} + \left(1 - \frac{1}{m}\right) + 2\chi\phi
+ \frac{\nu_1(P_{12}^{\nu})^2}{RT} J \left[\frac{F(1-F)}{\phi} - F'\right] = 0,$$
(6.78)

Fig. 6.11 Chemical potential of the solvent (subindex 1) and solute (subindex 2) for a solution of dioctyl-phthalate and polystyrene as a function of the volume fraction ϕ at $P_{12}^{\nu} = 200 \,\mathrm{Nm}^{-2}$ and $T = 286 \,\mathrm{K}$. The *dashed line* corresponds to the equilibrium situation. (Criado-Sancho et al. 1994)



where F' denotes the derivative of F with respect to ϕ defined in (6.35). On the other hand, the composition of the coexisting phases is given by the so-called coexistence line, given from the condition set by the equality of the chemical potentials, namely

$$\mu_1(\phi^{(\alpha)}) = \mu_1(\phi^{(\beta)}), \quad \mu_p(\phi^{(\alpha)}) = \mu_p(\phi^{(\beta)})$$
 (6.79)

where μ_1 and μ_p correspond to the expressions (6.24) and (6.25), respectively, and are represented in Fig. 6.11.

In Fig. 6.12, the coexistence and spinodal curves of polystyrene in dioctyl-phthalate are plotted for several values of the applied shear stress P_{12}^{ν} . Both curves have a common critical point. It is convenient to note that the composition of the phases coexisting in the steady state is simpler to obtain than that corresponding to the limits of stability indicated by the spinodal lines.

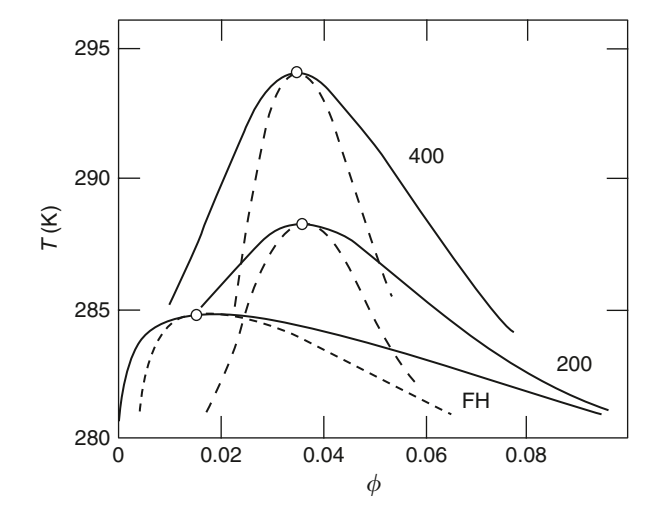


Fig. 6.12 The coexistence (continuous lines) and spinodal curves (dashed lines) in the diagram T- ϕ for polystyrene in dioctylphthalate calculated for the Flory–Huggins model (FH) and for several values of the applied shear stress p_{12}^v . (Criado-Sancho et al. 1998)

solution of polystyrene in dioctyl philiaduce, at different values of 1 ₁₂			
$P_{12}^{\nu} \text{ (N m}^{-2})$	100	200	400
Experimental	4	14	24
Criado-Sancho et al. (1991)	1.6	3.5	9.2

Table 6.1 Experimental and theoretical values of the shift in the critical temperature (K) for a solution of polystyrene in dioctyl-phthalate, at different values of P_{12}^{ν}

In Table 6.1 are listed the values of the shift of the critical temperature for three different values of the shear viscous pressure, and they are compared with the corresponding experimental results. It is seen that the predicted values are systematically lower than the observed ones. As will be discussed in Chap. 7, this difference is due to the effects of shear-enhanced density fluctuations, which contribute to the turbidity of the flowing mixtures in the experimental observations.

6.8 Other Approaches: Flexibility and Droplet Approaches

In this last section, we briefly describe two other thermodynamic approaches to shear-induced effects, one is based on a model of semi-flexible molecules and the other one emphasizes the role of the surface tension of the droplets in the phase separation process. In these models, a flow contribution to the free energy is also proposed, but interpreted in a different way than we have done in Chap. 5.

6.8.1 The Flexibility Approach

An alternative thermodynamic approach to the description of phase separation of polymer solutions under flow has been undertaken by Vrahopoulou-Gilbert and McHugh (1984). These authors start from the idea that, since the frictional forces due to the flow cause the macromolecules to uncoil from their quiescent conformation to a more extended state of lower conformational entropy, this is equivalent to introducing a variable degree of rigidity into the polymer coils, because more rigid coils have a longer average length than more flexible coils. In this way, the thermodynamic properties of the solution become those of a system of semi-flexible chains. This approach (modification of macromolecular rigidity), and the one discussed in this monograph (addition of stored free energy), are not completely equivalent and they may produce, according to the authors, different phase diagrams. Vrahopoulou-Gilbert and McHugh (1984) have criticized that the usual expressions for the stored free energy were based on solution properties rather than on individual polymer molecules, and that no distinction of the stored free energy in the different phases was made.

The effective flexibility parameter ϑ of a semi-flexible macromolecule stretched by a force F has been proposed to be (Vrahopoulou-Gilbert and McHugh 1984, 1986)

$$\vartheta = \frac{(z-2)\exp\left[-(E/k_{\rm B}T) - (Fl/k_{\rm B}T)\right]}{1 + (z-2)\exp\left[-(E/k_{\rm B}T) - (Fl/k_{\rm B}T)\right]},\tag{6.80}$$

with F the stretching force of the viscous flow applied to a segment of length I, and z and E are respectively the lattice coordination number and the intrinsic segment energy in the energetically favoured configuration in absence of the flow.

The relation between ϑ and the mean-square end-to-end separation of the macromolecule is

$$\langle r^2 \rangle = N\vartheta^{-1}l^2(2-\vartheta), \tag{6.81}$$

for a chain having N segments of length l. For complete flexibility (E = 0, F = 0), $\langle r^2 \rangle = Nzl^2/(z-2)$. For z = 3 this formula leads to $\langle r^2 \rangle = Nb^2$, with $b^2 = 3l^2$, which corresponds to the result (5.2) for Gaussian chains.

The Gibbs free energy change per mole associated with the flow is

$$\frac{\Delta G_s}{RT} = (N-2) \ln [(1-\vartheta)(z-1)]. \tag{6.82}$$

It is zero when $1-\vartheta=1/(z-1)$, which corresponds to (6.80) in the absence of flow (F=0). For the construction of thermodynamic diagrams it is important, according to this view, to make a distinction between the situation when the flexibility of the macromolecules is the same in both phases, or when they are different. In the first case, upon equating the chemical potentials in the two phases, the non-equilibrium contributions cancel out. When the flexibility ϑ'' of macromolecules in the concentrated phase differs from that in the dilute phase ϑ one obtains changes in the binodal curves provided that $\vartheta > \vartheta'$.

6.8.2 The Droplet Approach

Another description is based on the consideration of the role of the shear flow on the droplets constituting one phase inside the other one (Wolf 1980, 1984). The underlying idea is that, since near the critical point the surface tension is very low, the flow may be very effective in producing smaller and smaller droplets. Homogenization of the system in a single phase would be achieved when the dimension of the droplets is of the order of the macromolecular gyration radius (Wolf 1980).

Also in the droplet model, the non-equilibrium free energy is needed referred in this case to the droplets rather than to macromolecules. Vanoene (1972) takes for

the flow contribution to the free energy the expression proposed by Janeshitz-Kriegl (1969)

$$\Delta F = \frac{1}{2}(-\text{Tr}\mathbf{P} + 3P_z),\tag{6.83}$$

with $P_z = P_{rr} = -P_{\theta\theta}$ the corresponding components of the total pressure tensor **P**.

Besides this flow contribution, analogous to that considered in Sect. 6.4, where it was assumed that $P_{yy}^{\nu} = 0$, an additional contribution of the droplets interfacial tension under flow $\gamma_{\alpha\beta}$ of a droplet of fluid α in a matrix fluid β must be considered. This contribution, which has not been included in the previous sections, but which should be taken into account in the case that one phase is constituted of small droplets inside the other phase, is given by

$$\gamma_{\alpha\beta} = \gamma_{\alpha\beta}^{(0)} + \frac{1}{6} a_{\alpha} \left[(N_2)_{\alpha} - (N_2)_{\beta} \right],$$
(6.84)

with a_{α} the droplet radius and $\gamma_{\alpha\beta}^{(0)}$ the interfacial tension in the absence of flow, and N_2 the second normal stress coefficient of the corresponding phase.

Following Coleman and Markovitz (1964), Vanoene (1972) uses $N_2 = -JP_{rz}^2$ for relatively low shear stress, and takes for J, the steady state compliance,

$$J = \frac{0.4}{\rho RT} \frac{M_z M_{z+1}}{M_w^2} M_w, \tag{6.85}$$

with M_w the weight-average molecular weight and M_z and M_{z+1} the so-called z and z+1 averages (see Sect. 10.3 for a discussion of these averages in Eq. (10.30)). This is analogous to (5.42) for Rouse model, but with a different expression taking account that there is not a single macromolecular mass M but a whole distribution. If only a single macromolecular mass is present, one gets $J=0.4M/(\rho RT)$, which is the simple scaling law for J discussed in (5.40). As a final result, Vanoene obtains that the criterion for the formation of a droplet of phase α in phase β requires that

$$\frac{0.4}{RT} \left[\rho_{\alpha}^{-1} \left(\frac{M_z M_{z+1}}{M_{\rm w}^2} \right)_{\alpha} M_{\rm w\alpha} - \rho_{\beta}^{-1} \left(\frac{M_z M_{z+1}}{M_{\rm w}^2} \right)_{\beta} M_{\rm w\beta} \right] > 0.$$
 (6.86)

From here it follows that: (1) if phase β does not form droplets in phase α , then phase α will form droplets in phase β ; (2) since the shear rate does not appear explicitly in (6.86), it follows that if a particular morphology is observed, it should not be influenced by the magnitude of the shear rate except for effects which can be attributed to the hydrodynamic stability of a particular mode of dispersion; (3) the phase with the largest normal stress function will form droplets. The interfacial tension may also play a role in the dynamics and the geometrical features of the phase separation process, which are not studied in this chapter.

Chapter 7 Comparison of Thermodynamical and Dynamical Approaches

There are many reasons to study dynamical effects instead of limiting ourselves to a purely thermodynamic analysis. First, as we have repeatedly stressed, it is important to recall that thermodynamic arguments cannot be automatically extrapolated to non-equilibrium steady states. Indeed, it is not clear a priori whether the classical thermodynamic stability criteria, such as, for instance, those based on the derivatives of the chemical potential with respect to the concentration, may be used or not in non-equilibrium steady states. In Sect. 7.1 we provide a dynamical basis to the stability criteria (6.38) and (6.39) used in Chap. 6, and analyse their conditions of applicability. It turns out that, in some occasions, the stability criteria of classical thermodynamics must be modified in presence of the flow.

On the other hand, it has been argued by several authors that the turbidity observed in polymer solutions in some flow conditions may be attributed either to density fluctuations of thermodynamical origin or to a purely dynamical enhancement, due to the flow, of density fluctuations. It is not easy to establish how both contributions are related. Thus, in Sects. 7.2 and 7.3 a dynamical analysis is carried out to study how the enhanced density fluctuations due to the shear flow contribute to the dynamical structure factor. This factor is the Fourier transform of the density autocorrelation function, and it provides a very useful way to describe the response of the solution to the fluctuations, because it is a quantity directly measurable by means of light-scattering experiments. It is shown that both thermodynamical and purely dynamical effects contribute to the apparent shift of the critical point.

Finally, dynamical descriptions are necessary to study time-dependent features of the phase separation, as well as the modifications in transport properties and the different structures appearing in the flow during the separation. For instance, Tanaka (1996) observed, in deep-quench experiments of polymer solutions, that in addition to the usual initial diffusive and final hydrodynamic stages of the classical separation process, there is also an intermediate viscoelastic stage, where elastic forces have a predominating influence on the domain structure. Although there is much experimental and theoretical activity on these topics, they are beyond the reach of a strictly thermodynamical analysis and we will not deal with them in this monograph, but they may provide very fruitful challenges for future developments of the theory.

7.1 Dynamical Derivation and Generalization of Thermodynamical Stability Criteria

Some authors (Helfand and Fredrickson 1989; Onuki 1990, 1997; Milner 1991) have proposed purely dynamical approaches in which the phase separation under shear is examined as an instability of stationary solutions to some dynamical equations. A dynamical approach is not at all incompatible with the thermodynamical approach. In fact, the use of equations of state (such as, for instance, that for the chemical potential) is unavoidable in dynamical analyses but, in contrast to transport equations, these equations have received insufficient attention, because one usually takes for them their local-equilibrium form. Here we will carry out the dynamical analysis but with generalised equations of state incorporating the flow contribution.

To study in detail the thermodynamical and dynamical approaches we start from the Gibbs Eq. (1.42) that includes the effects of diffusion and of viscous pressure, and which we rewrite here as

$$ds = T^{-1}du + T^{-1}pdv - T^{-1}\tilde{\mu}dc_1 - v\alpha_1 \mathbf{J}_1 \cdot d\mathbf{J}_1 - v\alpha_2 \mathbf{P}^{\nu} : d\mathbf{P}^{\nu}.$$
 (7.1)

Recall that c_1 is the mass fraction of the solute, $\tilde{\mu} = \mu_1 - \mu_2$ the difference between the specific chemical potentials of the solute and the solvent, J_1 the diffusion flux of the solute, and \mathbf{P}^{ν} the viscous pressure tensor. According to (1.29) the parameter α_2 is equal to $\tau_2/(2\eta T)$ and α_1 turns out to be given by $\tau_1/(D'T)$. The coefficient D' is related to the diffusivity D through $D = D'(\partial \tilde{\mu}/\partial c_1)_{T,p}$, and τ_1 and τ_2 are the relaxation times of J_1 and \mathbf{P}^{ν} , respectively.

The corresponding generalised expression for the entropy flux given by (1.43) is rewritten as

$$\boldsymbol{J}^{s} = T^{-1}\boldsymbol{q} - T^{-1}\tilde{\mu}\boldsymbol{J}_{1} + \beta \mathbf{P}^{v} \cdot \boldsymbol{J}_{1}, \tag{7.2}$$

where β is a coupling coefficient which will appear in the dynamical equations. As shown in Sect. 1.2.2, the dynamical equations for the dissipative fluxes \mathbf{P}^{ν} and \mathbf{J}_1 are then

$$\tau_1 \boldsymbol{J}_1^* + \boldsymbol{J}_1 = -D\nabla \tilde{\mu} + D'T\nabla \cdot (\beta \mathbf{P}^{\nu}), \tag{7.3}$$

$$\tau_2(\mathbf{P}^{\nu})^* + \mathbf{P}^{\nu} = -2\eta(\nabla\nu)^s + 2\eta T\beta(\nabla \mathbf{J}_1)^s, \tag{7.4}$$

[see (1.56), (1.57)]. The upper star stands for an objective time derivative such as, for instance, the upper-convected time derivative used in (1.8a) or in (1.58), and the brackets with an upper s indicate the symmetric part of the corresponding tensor.

For situations where the diffusion effects in (7.1) may be neglected as compared with those of \mathbf{P}^{ν} (e.g. when the system is subjected to a relatively high shear stress

but when the diffusion flux is sufficiently low) one has for the non-equilibrium chemical potential including the flow contributions

$$\tilde{\mu}(T, p, c_1, \mathbf{P}^{\nu}) = \tilde{\mu}(T, p, c_1) + \frac{1}{2} T \left[\frac{\partial (\nu \alpha_2)}{\partial c_1} \right]_{T, p} \mathbf{P}^{\nu} : \mathbf{P}^{\nu}, \tag{7.5}$$

as it has been discussed in Sect. 6.3.

We will explore here under which conditions the usual thermodynamic stability criterion $(\partial \tilde{\mu}/\partial c_1) \geq 0$, which is valid in equilibrium (see Sect. 4.1), may be used with the generalised chemical potential (7.5) to obtain the spinodal line in the presence of a shear, as we have assumed in Sect. 6.3. Later, we will also include the contributions of the diffusion flux to the free energy.

7.1.1 Situations Without Coupling Between Diffusion and Shear

First, we will assume that $\beta = 0$ in (7.3, 4) i.e. absence of coupling between diffusion and viscous pressure. In this case, (7.3) reduces in the steady state to

$$\mathbf{J}_1 = -D'(c_1, \dot{\gamma}) \nabla \tilde{\mu}(c_1, \dot{\gamma}). \tag{7.6}$$

Note that both $\tilde{\mu}$ and D' may, in principle, depend on $\dot{\gamma}$. The dependence of the chemical potential on the shear rate may be obtained from thermodynamic arguments if the steady-state compliance τ/η appearing in α_2 of (7.5) is known as it has been discussed at length in Chap. 6. In contrast, the dependence of the transport coefficient D' on the shear rate depends entirely on kinetic microscopic arguments and the only thermodynamic restriction is that it must be positive to satisfy the second law.

If we focus our attention on a situation with homogeneous shear rate, i.e. with uniform $\dot{\gamma}$, (7.6) can be written as

$$\boldsymbol{J}_{1} = -D'(\phi, \dot{\gamma})(\partial \tilde{\mu}/\partial \phi)_{T, \dot{\gamma}} \nabla \phi, \tag{7.7}$$

where, in order to compare with previous chapters, we have replaced the solute mass fraction c_1 by the volume fraction ϕ . Thus, one may identify an effective diffusion coefficient $D_{\rm eff}$ as

$$D_{\text{eff}} = D'(\phi, \dot{\gamma})(\partial \tilde{\mu}/\partial \phi)_{T, \dot{\gamma}}. \tag{7.8}$$

When $D_{\rm eff}$ becomes negative, the homogeneous state becomes unstable and the system separates into two or more phases: the inhomogeneities in the solute concentration are amplified with time. In Chap. 8 we will deal at length with this point, with explicit illustrations and paying attention to applications. According to the positiveness of entropy production, $D'(\phi, \dot{\gamma})$ is always positive. Thus, for thermodynamically

stable states $(\partial \tilde{\mu}/\partial \phi)_{T,\dot{\gamma}} > 0$ and $D_{\text{eff}} > 0$, but when $(\partial \tilde{\mu}/\partial \phi)_{T,\dot{\gamma}}$ becomes negative, D_{eff} becomes negative. Then, the criterion $(\partial \tilde{\mu}/\partial \phi)_{T,\dot{\gamma}} = 0$ yields the separation between stable and unstable situations, both from the thermodynamical and the dynamical points of view.

An example of a generalised chemical potential dependent on the shear rate is provided by Nozières and Quemada (1986). They assumed that the diffusion flux is modified by the shear and described it as

$$\boldsymbol{J}_1 = \alpha(n_1)n_1\boldsymbol{F},\tag{7.9}$$

with $a(n_1)$ a friction coefficient, F a "thermodynamic force" which, for local-equilibrium systems, is given by $F = -\nabla \tilde{\mu}_{eq}$, and n_1 is the number density of the solute. They assumed that fluid flows along the x-direction, and that the velocity v_x changes along the y-axis, and they generalised F by including a hydrodynamic lift force F_{lift} as $F_{lift} = \frac{1}{2}\chi(\partial \dot{\gamma}^2/\partial y)$, with χ a constant coefficient (Nozières and Quemada 1986). Then, they write

$$F = -\frac{\partial \tilde{\mu}_{eq}}{\partial v} - \frac{1}{2} \chi \frac{\partial \dot{\gamma}^2}{\partial v}.$$
 (7.10)

If χ is a constant, one may introduce it into the derivative and write a generalised chemical potential of the form

$$\tilde{\mu}' = \tilde{\mu}_{eq} + \frac{1}{2}\chi\dot{\gamma}^2,\tag{7.11}$$

so that in this case, the non-equilibrium chemical potential $\tilde{\mu}'$ is related to the diffusion flux as

$$\boldsymbol{J}_1 = -\alpha(n_1)n_1 \frac{\partial \tilde{\mu}'}{\partial y}.\tag{7.12}$$

Introducing this flux in the evolution equations for the concentration n and the velocity v_{x} , it is found

$$\rho \frac{\partial v_x}{\partial t} = -\frac{\partial P_{xy}^{\nu}}{\partial y} = \eta \frac{\partial \dot{\gamma}}{\partial y} + \dot{\gamma} \frac{\partial \eta}{\partial n_1} \frac{\partial n_1}{\partial y}, \tag{7.13}$$

$$\rho \frac{\partial n_1}{\partial t} = -\frac{\partial J_{1y}}{\partial y} = \frac{\partial}{\partial y} \left[\alpha n_1 \left(\frac{\partial \mu_{eq}}{\partial n_1} \frac{\partial n_1}{\partial y} + \chi \dot{\gamma} \frac{\partial \dot{\gamma}}{\partial y} \right) \right]. \tag{7.14}$$

In (7.13) is has been assumed that $P_{xy}^{\nu} = -\eta(n_1)\dot{\gamma}$ and in (7.14) we have used (7.12). It follows from a linear stability analysis of (7.13), (7.14) that the homogeneous state is unstable when $\dot{\gamma}$ is higher than a critical value $\dot{\gamma}_{\rm c}$ given by

$$\dot{\gamma}_{\rm c}^2 = \eta \left(\frac{\partial \tilde{\mu}_{\rm eq}}{\partial n_1} \right) \left[\chi \left(\frac{\partial \eta}{\partial n_1} \right) \right]^{-1}. \tag{7.15}$$

This result coincides with the purely thermodynamical result based on the requirement $(\partial \tilde{\mu}/\partial n_1) = 0$ with $\tilde{\mu}'$ given by (7.11) and the derivative calculated at constant \mathbf{P}^{ν} . Thus, in this model the dynamical and thermodynamical criteria for the spinodal line lead to the same result for the limit of stability but on the condition to use a generalised non-equilibrium chemical potential dependent on the shear rate.

7.1.2 Situations with Coupling Between Diffusion and Shear

Assume now that the coefficient β in (7.3) is different from zero (Casas-Vázquez et al. 1993). The last term in (7.3) may be interpreted as the viscous reaction to the differential swelling produced by the change of composition of the mixture due to the diffusion. In a steady state and in a shear flow with a velocity distribution $v_x(y)$, (7.3) for the component of the diffusion flux along the shear direction, J_y , reduces to

$$J_{y} = -D'(n_{1}, \dot{\gamma}) \frac{\partial}{\partial y} \left[\tilde{\mu}(n_{1}, \dot{\gamma}) - T\beta P_{yy}^{v} \right], \tag{7.16}$$

where we have taken into account that the quantities appearing in (7.3) do not change along the direction of the flow, corresponding to the x axis.

This equation is at the basis of the Thomas–Windle model for case-II diffusion (Thomas and Windle 1982). These authors identify $-T\beta=\bar{\nu},\ \bar{\nu}$ being the partial molar volume of the solvent. In this way, one may identify a generalised chemical potential $\tilde{\mu}''$ as

$$\tilde{\mu}''(n_1, \dot{\gamma}) = \tilde{\mu}(n_1, \dot{\gamma}) + \bar{\nu} P_{yy}^{\nu}, \tag{7.17}$$

with $\tilde{\mu}(n_1, \dot{\gamma})$ the chemical potential of EIT used in (7.6) or (7.11). The basic idea below this interpretation of β (Thomas and Windle 1982; Jou et al. 1991) is that the normal pressure P_{yy}^{ν} may be interpreted as a supplementary osmotic pressure acting on the system. In terms of $\tilde{\mu}''$, (7.16) can be simply written as

$$J_{y} = -D'(n_{1}, \dot{\gamma}) \frac{\partial}{\partial y} \tilde{\mu}''(n_{1}, \dot{\gamma}). \tag{7.18}$$

In this case, the stability condition, i.e. the condition for a positive effective diffusion coefficient defined as $D'(\partial \tilde{\mu}''/\partial \phi)$ is

$$\frac{\partial \tilde{\mu}''}{\partial \phi} > 0 \tag{7.19}$$

instead of the condition $(\partial \tilde{\mu}/\partial \phi)_{T,\dot{\gamma}} > 0$ found in (6.8). In situations where the normal viscous pressure P_{yy}^{ν} along the direction of the shear is zero (such as, for instance, in Maxwell upper-convected derivative models, where the normal pressure

along the x-direction is different from zero but the normal pressures along the y and z directions are zero, as seen in (1.13)) $\tilde{\mu}''(n_1, \dot{\gamma})$ in (7.17) coincides with the chemical potential of EIT, namely $\tilde{\mu}(n_1, \dot{\gamma})$. Therefore, the results obtained in Chap. 6 about the stability and the shear-induced shift of the polymer solutions are valid as long as the upper-convected Maxwell model may be used.

To further illustrate this situation, we comment on the analysis of phase separation in polymer solutions under shear by Onuki (1990, 1997). This author examines the linear stability of a homogeneous shear flow of a semi-dilute polymer solution against perturbations of the volume fraction ϕ and the velocity v_x , under constant shear pressure. Onuki considers a non-equilibrium free energy which includes the effects of the flow by incorporating the configuration tensor as an independent non-equilibrium variable. However, he does not directly use the thermodynamic criterion $(\partial \tilde{\mu}/\partial \phi) \geq 0$ for the analysis of the stability but a dynamical analysis based on the stability of the evolution equations for v and ϕ which take the form (Onuki 1990)

$$\rho_0 \frac{\partial \mathbf{v}}{\partial t} = -\nabla \cdot (\mathbf{P}_p^v + \pi \mathbf{U}) - \nabla p - \eta_0 \nabla^2 \mathbf{v}, \tag{7.20}$$

$$\frac{\partial \phi}{\partial t} + \nabla \cdot (\phi \mathbf{v}) = -\nabla \cdot \mathbf{J}. \tag{7.21}$$

Here, \mathbf{P}_{p}^{v} is the polymer contribution to the viscous pressure, π the osmotic pressure, η_{0} the solvent shear viscosity and \mathbf{J} , the diffusion flux, is described under the form (Onuki 1990)

$$\boldsymbol{J} = -(\phi/\zeta) \left[\nabla (\pi_{\phi} + \pi_{\text{el}}) + \nabla \cdot \mathbf{P}_{p}^{\nu} \right], \tag{7.22}$$

where ζ is a friction coefficient, π_{ϕ} and $\pi_{\rm el}$ are the equilibrium and the non-equilibrium contributions to the osmotic pressure and stand, respectively, for $\pi_{\phi} = (\phi \partial/\partial \phi - 1) f_{\rm eq}$, $\pi_{\rm el} = (\phi \partial/\partial \phi - 1) f_{\rm el}$, with $f_{\rm el}$ being the elastic contribution of the flow to the Helmholtz free energy f. This equation, analogous to Eq. (6.30), yields for the component of the diffusion flux J_{ν} along the shear direction the result

$$J_{y} = -D_{T}(n, \dot{\gamma}) \frac{\partial \phi}{\partial y}, \tag{7.23}$$

with D_T an effective diffusion coefficient in the shear direction, given by

$$D_T = \zeta^{-1} \phi \frac{\partial}{\partial \phi} (\pi_\phi + \pi_{\rm el} + P_{yy}^{\nu}). \tag{7.24}$$

Notice that (7.22) may be obtained from (7.16), i.e. the normal viscous pressure P_{yy}^{v} is included into the osmotic pressure as an additional contribution. Onuki writes (7.22) following a model by Doi (1990) and uses as a stability criterion the positive character of D_T . It is interesting to note that this result is equivalent to the criterion (7.19), as one has that $\phi d\pi_{\rm eff} \propto d\tilde{\mu}''$, in which $\pi_{\rm eff} = \pi_{\phi} + \pi_{\rm el} + P_{yy}^{v}$, so that one may write $\partial \tilde{\mu}''/\partial \phi \propto \phi \partial \pi/\partial \phi$.

7.2 Structure Factor 161

Thus, we have seen in this section that the instability condition (6.38) defining the spinodal region is the same in the thermodynamic analysis as in the dynamical analysis when $P_{yy}^{\nu} = 0$, so that there is no contradiction between them as far as one limits oneself to a phase stability analysis. In contrast, a dynamical approach is necessary to describe the evolution of the phase separation process.

7.2 Structure Factor

Probably, one of the best perspectives to carry out a dynamical analysis is provided by the structure factor, i.e. by the Fourier transform of the correlation function of the density fluctuations, which is measurable through light scattering or neutron scattering experiments. This point of view has been followed, for instance, in (Helfand and Fredrickson 1989; Onuki 1990; Milner 1991; Criado-Sancho et al. 1997; Sun et al. 1997; Clarke and McLeish 1998; Ortiz de Zárate and Sengers 2006). In this section, it will be seen that non-equilibrium contributions both of thermodynamic and dynamic origin appear in the structure factor, the former stemming from the contribution of the viscous pressure tensor to the non-equilibrium equation of state for the chemical potential (namely (7.5)), and the second arising from the contribution of the velocity gradients to the dynamical balance equations. It has been a topic of intense debate whether the observed shift of the critical temperature in the presence of a shear flow is due to a modification of the equations of state or whether it is a purely hydrodynamical effect related to the enhancement of fluctuations in the presence of a velocity gradient. In fact, both points of view will be seen to be complementary, rather than mutually exclusive, as both effects contribute to a shift of the critical temperature.

In the usual literature concerning the structure factor under shear (Helfand and Fredrickson 1989; Onuki 1990; Milner 1991) it is considered that the effect of spatial inhomogeneities on the free energy and on the density fluctuations is of the so-called Ginzburg–Landau or Cahn–Hilliard form, in which the free energy per unit volume is expanded up to second order in the concentration gradient (Landau and Lifshitz 1969), namely

$$G(c, \nabla c) = G_0 + \frac{1}{2}a(c - c_0)^2 + \frac{1}{2}b(\nabla c) \cdot (\nabla c), \tag{7.25}$$

where the subscript 0 refers to a homogeneous reference equilibrium state $G_0 \equiv G(c_0)$, c is the concentration, and a and b are coefficients depending on the temperature T and the pressure p. In particular, a is given by $a = (\partial^2 G/\partial c^2)_{T,p}$, and $(1/2)a(c-c_0)^2$ corresponds to the second-order term in an expansion of G in powers of the concentration fluctuations. The ratio b/a has dimensions of the square of a length (we will denote b/a as l^2) which is the correlation length of the concentration fluctuations. The last term in (7.25) describes that the fluctuations with stronger inhomogeneities imply a higher increase in free energy and have less probability to appear.

The chemical potential corresponding to the free energy (7.25) is obtained from G by the functional derivative $\delta/\delta c$ defined as

$$\mu = \left(\frac{\delta G}{\delta c}\right)_{T,p,P_{xy}^{\nu}} = \left(\frac{\partial G}{\partial c}\right)_{T,p,P_{xy}^{\nu}} - \nabla \cdot \left(\frac{\partial G}{\partial (\nabla c)}\right)_{T,p,P_{xy}^{\nu}}.$$
 (7.26)

Therefore, for G given by (7.25) it has the form

$$\mu(c) = \mu_{\text{eq}} - b\nabla^2 c, \tag{7.27}$$

in which $\mu_{eq} = a(c - c_0)$.

The structure factor S(k) is the most important quantity in the analysis of the dynamics of concentration fluctuations, since it may be measured by light scattering experiments: it is defined as

$$S(\mathbf{k}) = \langle \phi(\mathbf{k})\phi(-\mathbf{k}) \rangle, \tag{7.28}$$

with k the wavevector and $\phi(k)$ the Fourier transform of the density fluctuations, and $\langle \cdots \rangle$ denotes an equilibrium ensemble average. The form of S(k) around equilibrium is usually obtained in a straightforward way by combining the well known expression for the probability of fluctuations (Callen 1960; Landau and Lifshitz 1969)

$$\Pr \propto \exp\left[-\frac{\delta^2 G}{k_{\rm B}T}\right],\tag{7.29}$$

where $\delta^2 G$ stands for the second variation of the Gibbs free energy, namely, $\delta^2 G = \frac{1}{2} (\partial^2 G/\partial \phi^2)(\delta \phi)^2$ or, in terms of μ , $\delta^2 G = \frac{1}{2} (\partial \mu/\partial \phi)(\delta \phi)^2$. The explicit expression for $\delta^2 G$ may be obtained from (7.25). This yields the so-called Ornstein–Zernike form for the structure factor (Landau and Lifshitz 1969), namely

$$S(k) = \frac{S(k=0)}{1 + (b/a)k^2},\tag{7.30}$$

where the Fourier transform of $\langle (\delta \phi)^2 \rangle$ has been used. This expression is a good approximation to S(k) for values of $(b/a)k^2 = l^2k^2 \ll 1$ around equilibrium, and must be modified near to critical points, where the exponent 2 of k in the denominator is changed to a different value.

7.2.1 Generalized Ginzburg–Landau Potential in Flowing Systems

Though the potential (7.25) is very well known in quiescent systems, in the presence of a velocity gradient one should consider the more general form (Criado-Sancho et al. 1999)

7.2 Structure Factor 163

$$G(c, \nabla c, \nabla \boldsymbol{u}) = G_0 + \frac{1}{2}a(c - c_0)^2 + \frac{1}{2}b(\nabla c) \cdot (\nabla c) + d(\nabla c)^T \cdot (\nabla \boldsymbol{u}) \cdot (\nabla c),$$
(7.31)

where u is the barycentric velocity of the fluid and d a new coefficient which may depend on T and p, and the upper-index T denoted the transposition. The new term in (7.31) implies that the concentration fluctuations whose gradient is perpendicular to the shear direction require a different energy from those whose gradient is parallel to the shear direction. Thus, the presence of the velocity gradient makes the basic state anisotropic, in contrast to the isotropic equilibrium state which refers to the concentration fluctuations appearing in the usual Ginzburg–Landau Eq. (7.25).

According to (7.26), the corresponding expression for the chemical potential derived from (7.31) would be

$$\mu = \mu_{\text{eq}} - b\nabla^2 c - 2d\nabla \cdot [(\nabla \boldsymbol{u}) \cdot (\nabla c)], \tag{7.32}$$

which reduces to (7.27) for a fluid at rest or in uniform velocity flows.

To estimate the value of the last term in (7.31) we write the Gibbs free energy of EIT in the presence of a diffusion flux J and of a viscous pressure tensor \mathbf{P}^{ν} , up to third-order approximation

$$G = G_{eq} + \frac{1}{2}\alpha_{(1)}\boldsymbol{J} \cdot \boldsymbol{J} + \frac{1}{2}\alpha_{(2)}\mathbf{P}^{\nu} : \mathbf{P}^{\nu} + \alpha_{(3)}\boldsymbol{J} \cdot \mathbf{P}^{\nu} \cdot \boldsymbol{J}.$$
 (7.33)

The terms in $J \cdot J$ and in $\mathbf{P}^{\nu} : \mathbf{P}^{\nu}$ are well known in the usual formulations of extended irreversible thermodynamics, where the coefficients $\alpha_{(1)}$ and $\alpha_{(2)}$ are given by $\alpha_{(1)} = \tau_1/D$ and $\alpha_{(2)} = \tau_2/2\eta$ [see Chap. 1, (1.42)]. The last term in (7.33), coupling J and \mathbf{P}^{ν} , has not been considered up to now, but it arises from simple tensorial arguments. An analogous contribution to the extended entropy of the form $\mathbf{q} \cdot \mathbf{P}^{\nu} \cdot \mathbf{q}$, with \mathbf{q} the heat flux, was considered in Jou and Casas-Vázquez (1983), where its coefficient was expressed in terms of the third moments of the equilibrium fluctuations of \mathbf{q} and \mathbf{P}^{ν} , was explicitly computed for ideal gases, and it was shown that the result is identical with that obtained from the kinetic theory of gases.

The coefficient $\alpha_{(3)}$ may be obtained from fluctuation theory. According to (Jou and Casas-Vázquez 1983), the coefficient $\alpha_{(3)}$ may be written as

$$\alpha_{(3)} = -\frac{2}{(k_{\rm B}T)^2} \alpha_{(1)}^2 \alpha_{(2)} \langle \delta J_x \delta P_{xy}^{\nu} \delta J_y \rangle, \qquad (7.34)$$

where δ stands for the fluctuation of the corresponding quantity. Using again fluctuation theory [see for instance Chap. 5 of (Jou et al. 2010)] according to which $\alpha_{(1)} = k_{\rm B}T \langle \delta J_x \delta J_x \rangle^{-1}$ and $\alpha_{(2)} = k_{\rm B}T \langle \delta P_{xy}^{\nu} \delta P_{xy}^{\nu} \rangle^{-1}$, (7.34) may also be written as

$$\alpha_{(3)} = -2k_{\rm B}T \frac{\left\langle \delta J_x \delta P_{xy}^{\nu} \delta J_y \right\rangle}{\left\langle \delta J_x \delta J_x \right\rangle^2 \left\langle \delta P_{xy}^{\nu} \delta P_{xy}^{\nu} \right\rangle}.$$
 (7.35)

The microscopic operator for J_x is given by $J_x = n\zeta_x$ with ζ_x the component along the x axis of the relative speed of the centre of mass of the macromolecules with respect to the barycentric velocity \boldsymbol{u} of the polymer solution. This leads to the result $\langle \delta J_x \delta J_x \rangle = n^2 \langle \xi_x^2 \rangle$. On the other hand, P_{xy}^v has a contribution of the form $m\xi_x\xi_y$ owing to the motion of the centre of mass plus another one due to the internal (configurational) degrees of freedom. Since the latter ones are uncorrelated with the motion of the centre of mass, the only contribution to $\langle \delta J_x \delta P_{xy}^v \delta J_y \rangle$ in (7.34) will be $n^2 \langle m\xi_x^2 \xi_y^2 \rangle$. This allows us to write $\alpha_{(3)} = -2\alpha_{(1)}\alpha_{(2)} = \alpha_{(1)}(\tau_2/\eta)$.

If the frequencies involved in the system are not too high, in order that the relaxation terms may be neglected, one may use the Fick's law $J = -D\nabla c$ and (7.33) becomes

$$G = G_{\text{eq}} + \frac{\alpha^2}{2} (\nabla c) \cdot (\nabla c) + \frac{\alpha_{(2)}}{2} \mathbf{P}^{\nu} : \mathbf{P}^{\nu} - \frac{\alpha^2 \tau_2}{\eta} (\nabla c)^T \cdot \mathbf{P}^{\nu} \cdot (\nabla c).$$
 (7.36)

The quantity α^2 stands for $\alpha_{(1)}D^2$ and may be written as $RT(l^2/c^2)$, l being a correlation length of the density fluctuations.

7.2.2 Dynamical Contributions to the Chemical Potential

Expression (7.36) contains quadratic terms in the concentration gradient and terms which couple the concentration gradient with the pressure tensor. The latter may be written in terms of the velocity gradient if one uses the Newton–Stokes law for the pressure tensor, i.e. $\mathbf{P}^{v} = -2\eta(\nabla \mathbf{u})^{s}$. In general, the chemical potential obtained from (7.36) through the functional differentiation (7.26) turns out to be

$$\mu = \mu_{eq} + \mu^{(P)} - \alpha^2 \nabla^2 c + 2\alpha^2 J_e \nabla \cdot (\mathbf{P}^{\nu} \cdot \nabla c), \tag{7.37}$$

where $\mu^{(P)}$ stands for the part coming from the third term in the right-hand side of (7.36), and $J_e = \tau_2/\eta$ is the steady-state compliance, where subscript e is used to avoid confusion with the symbol for the diffusion flux.

A rather general expression for the chemical potential (7.37) in terms of the velocity gradient may be obtained if instead of the simple Fick and Newton–Stokes equations for J and P^{ν} one takes

$$\mathbf{J} = -D'\nabla\mu - \beta\nabla\cdot\mathbf{P}^{\nu} \tag{7.38}$$

and

$$\tau_2 \left[\frac{\partial \mathbf{P}^{\nu}}{\partial t} + \mathbf{u} \cdot \nabla \mathbf{P}^{\nu} - (\nabla \mathbf{u})^T \cdot \mathbf{P}^{\nu} - \mathbf{P}^{\nu} \cdot (\nabla \mathbf{u}) \right] = -\mathbf{P}^{\nu} - 2\eta(\nabla \mathbf{u})^s, \quad (7.39)$$

where D' and β are transport coefficients. Note that (7.38) is a simplified version of (7.3). Equation (7.39) for the viscous pressure tensor corresponds to a generalised

upper-convected Maxwell model (1.8a) with τ_2 the relaxation time (which will be denoted simply as τ from now on).

If we expand (7.39) around the steady state for a simple shear flow, with a velocity profile $\mathbf{u} = (\dot{\gamma} y, 0, 0)$, with $\dot{\gamma}$ the shear rate, we find for the viscous pressure tensor the form given in (1.13). When this expression is introduced in (7.37), it yields for the chemical potential

$$\mu = \mu_{\text{eq}} + \mu^{(P)} - \alpha^2 \nabla^2 c$$

$$- 4\alpha^2 \dot{\gamma} J_e \left[\eta \nabla_x \nabla_y c + \tau \eta \dot{\gamma} \nabla_x \nabla_x c + \eta' \nabla_x \nabla_y c + (\tau \eta)' \dot{\gamma} \nabla_x \nabla_y c \right]. \quad (7.40)$$

The terms in the square bracket have an influence on the structure factor, which will be explicitly analysed in the next section.

7.3 Derivation of the Structure Factor

After having obtained a generalised expression for the contributions of the inhomogeneities to the chemical potential in the presence of a flow, we shall study its consequences on the structure factor for a polymer solution, generalising the previous analyses in (Helfand and Fredrickson 1989; Criado-Sancho et al. 1997).

7.3.1 Evolution Equations

To analyse the structure factor in the presence of a shear flow, one must solve the hydrodynamical equations describing the fluid. The mass balance law for the solute may be written in the form

$$\frac{\mathrm{d}c}{\mathrm{d}t} = -\nabla \cdot \boldsymbol{J},\tag{7.41}$$

with c the monomer concentration, related to the volume fraction ϕ by $\phi = v_{\rm m} c$, with $v_{\rm m}$ the molar volume of the monomer, and J the corresponding diffusion flux. As a constitutive equation for the diffusion flux we take (7.38), which when introduced into (7.41) yields

$$\frac{\partial c}{\partial t} + \boldsymbol{u} \cdot \nabla c = \frac{\lambda}{k_B T} \nabla \cdot (c \nabla \mu) + \frac{\lambda}{k_B T} \nabla \nabla : \mathbf{P}^{\nu} + \theta^{\nu}, \tag{7.42}$$

except for the hydrodynamic noise θ^{ν} , which has been included for the analysis of fluctuations. The relationship between λ (a parameter which we use for the sake of comparison with Helfand and Fredrickson 1989) and the transport coefficient D' is given by $D' = \lambda c/(k_B T)$, and we have taken $\beta T = -c^{-1}$, as in the above reference, and consistently with the proposal in (7.17).

The balance equation for the linear momentum is

$$\rho \frac{\partial \mathbf{u}}{\partial t} = T_{\perp} \left[-\rho \mathbf{u} \cdot \nabla \mathbf{u} + \eta_s \nabla^2 \mathbf{u} - \nabla \cdot \mathbf{P}^{\nu} + (\nabla c)\mu + \theta^{\mathbf{u}} \right], \tag{7.43}$$

where T_{\perp} is a transverse projection operator which projects the fluctuations on the plane perpendicular to the wavevector, because incompressibility $(\nabla \cdot \boldsymbol{u} = 0)$ requires that $\boldsymbol{k} \cdot \boldsymbol{n} = 0$. Equations (7.39), (7.42), (7.43) and the equation of state (7.40) for the chemical potential describe the evolution of the system. An alternative set of equations could be established from the two-fluid model discussed in Sect. 6.6.

7.3.2 Equations of State

In order to work out a specific situation we shall consider (7.40) for polymer solutions and we need expressions for $\mu^{(p)}$, α , J_e , and η . We use for the steady-state compliance J, the Rouse expression (5.42)

$$J_e = \frac{CM}{c'RT} \left(1 - \frac{\eta_s}{\eta} \right)^2, \tag{7.44}$$

where c' is the mass polymer per unit volume, C=0.4 (in the Rouse model) and M the polymer molecular mass. To obtain $\mu^{(p)}$ recall that for the system constituted by n_1 moles of solvent and n_2 moles of a polymer of degree of polymerization N, we have for G

$$G = G_{eq} + \nu_{m} (n_{1} + Nn_{2}) J_{e} (P_{xy}^{\nu})^{2} + \frac{1}{2} \alpha^{2} (\nabla c) \cdot (\nabla c), \qquad (7.45)$$

where $G_{\rm eq}$ is the local-equilibrium free energy, given by the classical Flory–Huggins expression (6.4); the second term is the non-equilibrium contribution due to the presence of the viscous pressure tensor (since we are considering a Couette flow, we only take the xy component), and is given by Eq. (6.17). For α we will take $\alpha^2 = RTv_{\rm m} \times (2\pi^{-2})R_{\rm g}^2\phi_0^{-1}N^{-1}$, $R_{\rm g}$ being the mean gyration radius of the macromolecules and ϕ_0 the mean-field value of the volume fraction.

The classical Flory–Huggins contribution $\mu_{\rm eq}$ obtained from (6.4) may be written as

$$\mu^{(\text{FH})} = \mu^{(\text{FH})}(\phi_0) + RTv_{\text{m}} \left[(1 - \phi_0)^{-1} + (N\phi_0)^{-1} - 2\chi \right] \delta c, \quad (7.46)$$

where χ is the Flory–Huggins interaction parameter defined in (6.5) and δc the perturbation in the concentration. Taking into account (7.44), the contribution of the shear viscous pressure to the Gibbs free energy is

$$G^{(P)} = \frac{CM\nu_m [\eta]}{RT} (P_{xy}^{\nu})^2 (n_1 + Nn_2) F(x), \tag{7.47}$$

with F(x) a function whose form comes from (5.42), namely

$$F(x) = x(1 + k_{\rm H}x)^2 (1 + x + k_{\rm H}x^2)^{-2}, \tag{7.48}$$

 $k_{\rm H}$ being the Huggins constant introduced in (5.44) and $x = [\eta] M_0 c$ where $[\eta]$ is the intrinsic viscosity (5.45) and M_0 the monomer molecular mass. The non-equilibrium contribution of the flow to the chemical potential of the solute may thus be written as

$$\mu^{(P)} = \frac{CM\nu_{\rm m}[\eta]}{RT} (P_{xy}^{\nu})^2 \left[\frac{F(x)}{1 - \nu_{\rm m}c} + \frac{[\eta]M_0F'(x)}{\nu_{\rm m}} \right],\tag{7.49}$$

and up to the first order in the fluctuation δ_c , it can be expressed as

$$\mu^{(P)} = \mu^{(P)}(x_0) + \frac{CN[\eta]^3 M_0^3}{RT} (P_{xy}^{\nu})^2 \left[\frac{1}{x_0^2} F(x_0) + \frac{1}{x_0} F'(x_0) + F''(x_0) \right] \delta c,$$
(7.50)

where $x_0 = [\eta] M_0 c_0$ and F' and F'' are the first and second derivatives of F with respect to x.

The dependence of the viscosity in terms of the concentration is given by (5.44), i.e.

$$\eta/\eta_{\rm S} = 1 + [\eta] M_0 c + k_{\rm H} [\eta]^2 M_0^2 c^2 \tag{7.51}$$

with the values of $\eta_{\rm s},\,k_{\rm H},\,[\eta]$ and M_0 for the system transdecalin-polystyrene given in Appendix A.

7.3.3 Flow Contribution to the Structure Factor

The flow contribution to the structure factor S(k) may be obtained by solving the equations of motion (7.39), (7.42), and (7.43), after introducing (7.40) into the two latter equations. We will restrict our analysis to first order in the amplitude of the fluctuations δc . This linear approach is suitable to describe the first stages of the spinodal decomposition but not the advanced stages where non-linear terms are essential. The viscosity η and the normal stress coefficient Ψ_1 are written in terms of the concentration perturbations $\delta c(\mathbf{r})$ around the average concentration c_0 as

$$\eta(c) = \eta(c_0) + \eta' \delta c, \tag{7.52a}$$

$$\Psi_1(c) = \Psi_1(c_0) + \Psi_1' \partial c. \tag{7.52b}$$

In the absence of concentration inhomogeneities, the velocity field is assumed to be the simple shear flow, i.e. $v_x = \dot{\gamma} y$. The dependence of η and Ψ_1 on the

concentration slightly modifies \mathbf{P}^{ν} and therefore the flow. By ignoring in (7.39), (7.42), and (7.43) the terms in $\partial/\partial t$ and $\mathbf{u} \cdot \nabla$, and introducing the expressions for \mathbf{P}^{ν} and μ (up to the first order in δc) in (7.42), one is led, after a Fourier transform, to the following closed equation for $S(\mathbf{k})$ (Helfand and Fredrickson 1989)

$$\left[2\overline{\lambda}\Omega(\overline{k}) - \overline{\dot{\gamma}}\,\overline{k}_x\frac{\partial}{\partial\overline{k}_y}\right]S(\overline{k}) = 2\overline{\lambda}\,\overline{k}^2,\tag{7.53}$$

where all the variables are reduced according to $\overline{\dot{\gamma}} = \dot{\gamma}\tau$, $\overline{k} = kR_{\rm g}$, and $\overline{\lambda} = \lambda T/(NR_{\rm g}^2)$.

The function Ω in (7.53) is given by

$$\Omega(k) = k^{2} \left[\varepsilon + \varepsilon^{(P)} - h(\beta) + \overline{\alpha}^{2} k^{2} - g(\beta) \right], \tag{7.54}$$

where the reduced variable $\overline{\alpha}^2 = (\alpha^2 N \phi_0)/(RT v_{\rm m} R_{\rm g}^2)$ has been introduced. In (7.54) it is manifest that $\Omega(k)$ also depends on the angle β that k makes with the x axis (i.e. with the velocity). The function $h(\beta)$ is given by (Helfand and Fredrickson 1989)

$$h(\beta) = 2l_x l_y \overline{\dot{\gamma}} \overline{\eta}' + l_x^2 \overline{\dot{\gamma}}^2 \overline{\Psi}'_1 - \left[\left(l_x^2 - l_y^2 \right) \overline{\dot{\gamma}} \overline{\eta}' - l_x l_y \overline{\dot{\gamma}}^2 \overline{\Psi}'_1 \right]$$

$$\times \frac{l_x^2 \overline{\dot{\gamma}}^2 \overline{\Psi}'_1}{\overline{\dot{\gamma}} (\overline{\eta} - \overline{\eta}_s) + l_x l_y \overline{\dot{\gamma}}^2 \overline{\Psi}'_1}, \tag{7.55}$$

where $l_x = \cos \beta$ and $l_x = \sin \beta$, whereas $g(\beta)$ is given by

$$g(\beta) = -4 \frac{\overline{k}^2 \overline{\alpha}^2}{RT \nu_m} \overline{\dot{\gamma}} \left(l_x l_y + \overline{\dot{\gamma}} l_x^2 \right). \tag{7.56}$$

The first normal stress coefficient is given by $\Psi_1 = 2\tau\eta$ in an upper-convected Maxwell fluid [see (1.15)], and the reduced quantities appearing in (7.55) and (7.56) have been defined as $\bar{\eta} = \eta N \phi_0 v_{\rm m}/(k_{\rm B} T \tau^2)$ and $\bar{\Psi}_1 = \Psi_1 N \phi_0 v_{\rm m}/(k_{\rm B} T \tau^2)$. The form of $h(\beta)$ and $g(\beta)$ in the range $0 \le \beta \le \pi/2$, are represented in Figs. 7.1 and 7.2 for polystyrene in transdecalin. Note that the values of $g(\beta)$ are one order of magnitude less than those of $h(\beta)$, and the form of the two functions is different and their sign opposite.

The symbol ε stands for the dimensionless expression of $\partial \mu / \partial c$ given by

$$\varepsilon = 1 + (1 - \phi_0)^{-1} N \phi_0 - 2N \chi \phi_0 + N \phi_0 (\partial \mu^{(P)} / \partial c), \qquad (7.57)$$

and, when $l\Omega(k) \ll \dot{\gamma}$, S is given by

$$S(k) \approx \frac{1}{\varepsilon + \varepsilon^{(P)} - h(\beta) + \overline{\alpha}^2 k^2 - g(\beta)}.$$
 (7.58)

Note that if $h(\beta) + g(\beta)$ is positive, the flow enhances the fluctuations.

Fig. 7.1 The function $h(\beta)$ appearing in (7.55) is plotted in terms of β for polystyrene in transdecalin for a given value of the shear rate and for different values of the volume fraction ϕ , which label the different curves. This function is maximum for β near 42°. (Criado-Sancho et al. 1997)

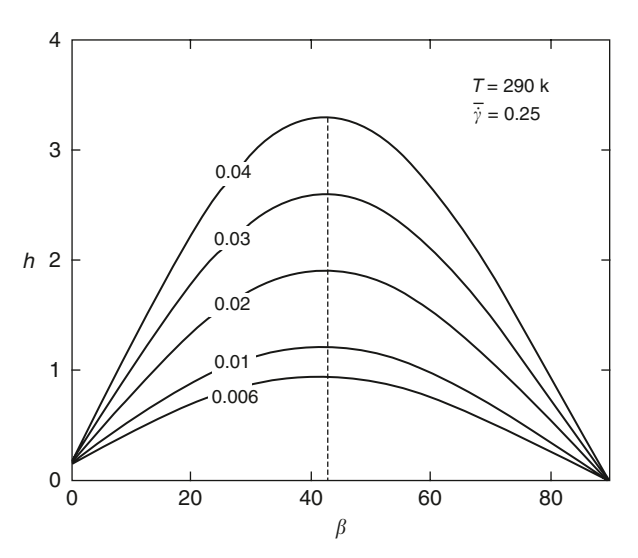
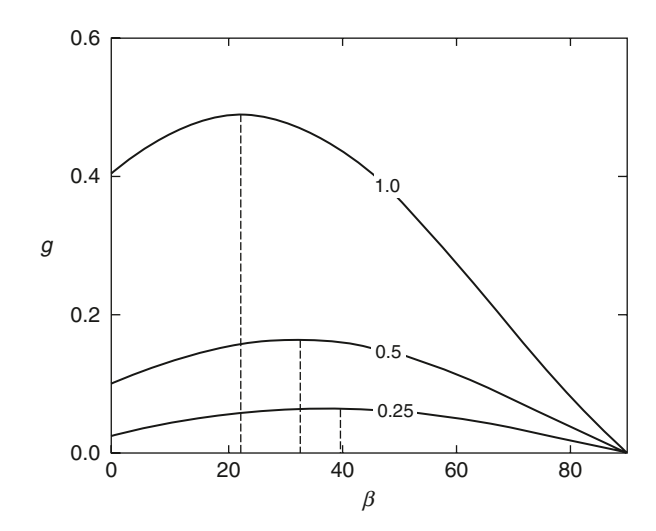
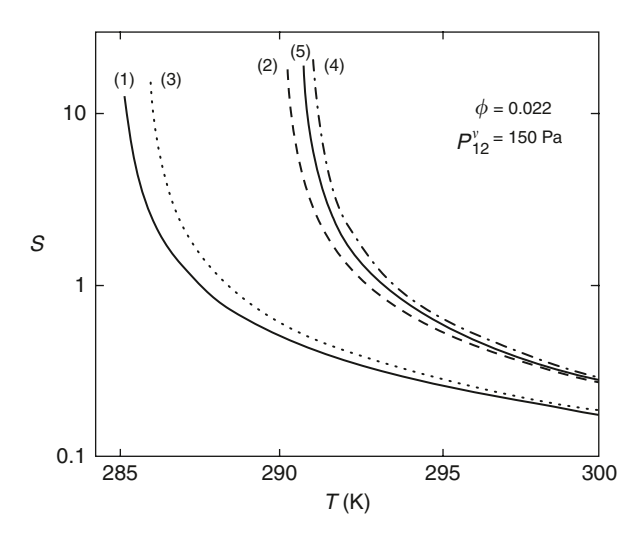


Fig. 7.2 The function $g(\beta)$ appearing in (7.56) for different values of the shear rate for polystyrene in transdecalin. This function does not depend on the volume fraction ϕ . (Criado-Sancho et al. 1997)



In Fig. 7.3 we represent the curves corresponding to S(k=1) at an angle $\beta=42^{\circ}$ (corresponding to the maximum of $h(\beta)$) which include, correspondingly: (1) the equilibrium structure factor; (2) the dynamical contribution $h(\beta)$; (3) the non-equilibrium thermodynamic contribution $\epsilon^{(P)}$; (4) both $\epsilon^{(P)}$ and $h(\beta)$; (5) $\epsilon^{(P)}$, $h(\beta)$ and $g(\beta)$. All the curves include the Ginzburg–Landau contribution $\ell^2 k^2$. It is seen that all the contributions modify the apparent critical point, which corresponds to the steep increase of S, i.e. of the fluctuations. Note that in Fig. 7.3 we have plotted the curves corresponding to $k=kR_{\rm g}=2\pi(R_{\rm g}/\lambda')=1$, with k=k the gyration radius of the chains and k=k the wavelength of the visible light (we are studying the onset of visible turbidity). Thus, k=k 1 corresponds

Fig. 7.3 Curves corresponding to s(k=1) at an angle $\beta=42^\circ$ including: (1) the equilibrium structure factor; (2) the dynamical contribution $h(\beta)$; (3) the nonequilibrium thermodynamic contribution ε^P ; (4) both ε^P and $h(\beta)$; (5) ε^P , $h(\beta)$ and $g(\beta)$. All the contributions modify the apparent critical point, which corresponds to the steep increase of S, i.e. of the fluctuations. (Criado-Sancho et al. 1997)



to $R_{\rm g}=9\times 10^{-8}$ m. Since the solution is under flow, the chains are stretched and it is not easy to specify exactly the value of $R_{\rm g}$ even when $R_{\rm g}$ in equilibrium is known. The dependence of $R_{\rm g}$ on N shows that for lower polymerization numbers one should consider $\bar{k}<1$ in the analysis of S(k).

It is seen that when one includes both hydrodynamic and thermodynamic effects, an increase in turbidity may appear for temperatures higher than the actual critical temperature. Thus, if one a priori identified this turbidity with the approach to the critical point, one would overestimate the value of the critical temperature under shear.

This does not mean that the critical temperature itself is not modified by the flow. Indeed, the results in Table 6.1 show that the thermodynamic contribution of the viscous pressure tensor in the equations of state yields values for the shift in the critical temperature which are lower than the experimental ones. Here, we see that a possible reason for this discrepancy is the effect of the dynamically enhanced fluctuations, whose contribution to the apparent shift in the critical point may be two or three times that due to purely thermodynamical effects.

The contribution of the last terms in (7.36) or (7.37), not found in the usual bibliography, to the apparent shift of the critical point is small, of the order of 5% of the total shift in the critical temperature. Nevertheless, since it depends on the shear viscosity and the normal shear coefficient, rather than on their derivatives, in situations where the shear viscosity does not depend on the concentration, and the first normal stress coefficient vanishes, $g(\beta)$ would be different from zero, whereas $h(\beta)$ would vanish.

In contrast to the dynamical contributions of $h(\beta)$, the non-equilibrium contribution $g(\beta)$ has a thermodynamical origin because it appears directly in the generalised entropy, as well as the contributions due to the viscous pressure tensor. Thus, the connections between thermodynamics and dynamics are multiple and subtle, not contradictory to each other, but complementary, as the generalized overview presented in this chapter has shown.

Chapter 8 Shear-Induced Migration and Flow Chromatography

The presence of inhomogeneities in the flow velocity is an ubiquitous feature in nature and laboratory, from flow in tubes to motion in rivers and oceans; in contrast with an uniform velocity profile, which simply adds a displacement to the usual Fickian diffusion, inhomogeneities in the velocity profile exert a deep influence on the behaviour of diffusion whose consequences have practical interest in many situations ranging from microfluidic chromatographic flows to pollutant transport in oceans and atmosphere. Some of these influences are purely dynamical; others, however, modify the equations of state and their analysis requires the use of non-equilibrium thermodynamics. In this chapter, we consider several examples of the modification of the usual diffusion behaviour in the presence of a velocity gradient.

In the situations considered here, the thermodynamic aspects of the coupling between flow and diffusion become especially relevant. For instance, we analyse how the non-equilibrium chemical potential depending on the shear rate, which has been used in Chaps. 6 and 7, contributes to shear-induced polymer migration. It is seen that its non-equilibrium contribution strongly enhances, above a threshold of polymer concentration and of shear rate, the migration of the polymer towards the regions with lower stress and accelerates the splitting of the initially homogeneous system into two different phases.

Since these migration effects are strongly dependent on the solute macromolecular mass, they may be used to separate macromolecules with different masses, which is a relevant operation in macromolecular biology and in chemical engineering. These separation techniques are known as flow chromatography, and offer an alternative to other well-known separation techniques as ultracentrifugation and electrophoresis, as for instance in protein purification.

8.1 Shear-Induced Migration of Polymers

The coupling between viscous effects and diffusion is a very active topic in rheological analyses (Highgate 1966; Agarwal et al. 1994; Olmsted 2008). In particular, shear-induced migration of polymers deserves attention for its practical aspects (chromatography, separation techniques, flow through porous media) and its theo-

retical implications in non-equilibrium thermodynamics and transport theory. Indeed, this topic implies the coupling between vectorial fluxes and tensorial forces, which is beyond the usual constitutive equations of classical irreversible thermodynamics, and it is a useful testing ground of non-equilibrium equations of state.

8.1.1 The Simplest Model for Shear-Induced Migration

The simplest constitutive equation coupling the diffusion flux J and the viscous pressure tensor \mathbf{P}^{ν} is

$$J = -D\nabla n - \frac{D}{RT}\nabla \cdot \mathbf{P}^{\nu},\tag{8.1}$$

where n is the polymer concentration, D the translational diffusivity, and \mathbf{P}^{ν} the symmetric second-order tensor representing the polymeric contribution to the viscous pressure. This constitutive equation has been examined from different macroscopic and microscopic points of view (Aubert and Tirrell 1980; Aubert et al. 1980; Lhuillier 1983; Bhave et al. 1991; Mavrantzas and Beris 1992; Öttinger 1992; Beris and Mavrantzas 1994; Zamankha et al. 1998; Curtiss and Bird 1999; Apostolakis et al. 2002). The coupling term may be interpreted in terms of the force acting on the macromolecules per unit volume $(-\nabla \cdot \mathbf{P}^{\nu})$ times the macromolecular mobility—or reciprocal of friction coefficient—which, according to Einstein's equation for the diffusion coefficient, is given by $D(k_{\rm B}T)^{-1}$ (per molecule) or $D(RT)^{-1}$ (per mol). In (1.51) and (7.38) we have presented a more general extension of the Fick equation which reduces to (8.1) when relaxation effects and the non-linear, non-equilibrium contributions to the chemical potential are ignored.

The physical meaning of the second term in (8.1) is clear: inhomogeneities in the viscous pressure will contribute to a migration of solute. For instance, consider a cone-and-plate configuration (see Fig. 8.1), where the only non-zero components of the viscous pressure tensor \mathbf{P}^{ν} are given by

$$P_{\phi\phi}^{\nu} = -2RTn(\tau\dot{\gamma})^2, \quad P_{\phi\theta}^{\nu} = -RTn\tau\dot{\gamma}. \tag{8.2}$$

Here r, ϕ and θ refer to the radial, axial and azimuthal directions, respectively, τ is the polymer relaxation time and $\dot{\gamma}$ the shear rate. Combination of (8.1) and (8.2) yields for the components of the diffusion flux the expressions

$$J_r = -D\frac{\partial n}{\partial r} - D\beta \frac{n}{r},\tag{8.3}$$

$$J_{\theta} = -D\frac{1}{r}\frac{\partial n}{\partial \theta} - D\beta\frac{n}{r}\cot\theta, \tag{8.4}$$

$$J_{\phi} = -D \frac{1}{r \sin \theta} \frac{\partial n}{\partial \phi} - D\beta \frac{n}{r} \cot \theta, \tag{8.5}$$

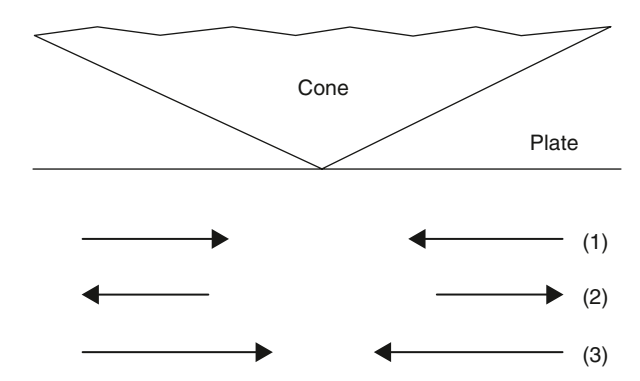


Fig. 8.1 The flows of matter are indicated in the cone-and-plate configuration. Arrow(I) shows the shear-induced flow described by the second term in the right-hand side of (8.1) and (8.9); arrows(2) and (3) indicate the diffusion flux corresponding to the first term in the right-hand side of (8.9) when the effective diffusion coefficient (8.13) is positive or negative. When it is positive, the diffusion flux (2) opposes to the shear-induced flow (I), whereas when it is negative, the diffusion flux (3) enhances the shear-induced effects

with the parameter β being defined as $\beta=2(\tau\dot{\gamma})^2$ and where the independence of n with respect to ϕ because of the rotational symmetry of the situation has been taken into account. The radial component (8.3) is especially relevant from the practical point of view. It is seen that the shear flow will produce a migration of macromolecules towards the apex of the cone (since r points towards the external region, a negative sign in J_r implies motion towards the centre of the device). Thus, if initially one has a homogeneous concentration profile $(\partial n/\partial r=0)$, the rotation will produce a migration of macromolecules towards the centre, until achieving a steady profile in which $J_r=0$. This allows to separate the solute from the solvent, because the internal part of the device will be richer in the solute.

Combination of (8.1-8.5) and the mass balance equation

$$\frac{\partial n}{\partial t} = -\nabla \cdot \boldsymbol{J} \tag{8.6}$$

vields

$$\frac{\partial n}{\partial t} = D\nabla^2 n + \frac{D}{RT} - \nabla \cdot (\nabla \cdot \mathbf{P}^{\nu}), \tag{8.7}$$

which leads to the closed evolution equation for the concentration

$$\frac{\partial n}{\partial t} = \frac{D}{r^2} \frac{\partial}{\partial r} \left(r^2 \frac{\partial n}{\partial r} + \beta r n \right) - D\beta \frac{n}{r^2}.$$
 (8.8)

To obtain (8.8) it has been assumed that the steady viscometric flow has only a non-zero component of the velocity (the r component), which depends on the r and θ coordinates and that the convection of molecules by migration contributes negligibly

to the stress. The term in β , arising from the second term in (8.2), induces a flux of solute towards the apex of the cone (shown as arrow 1 in Fig. 8.1) which is usually believed to produce the total induced migration.

However, as demonstrated by MacDonald and Muller (1996), this contribution cannot explain by itself the actual rate of migration; it falls short by two or three orders of magnitude in comparison with observations. These authors have obtained a short-time solution of (8.8) for n(r,t). In their analysis they miss the last term, which comes from the shear-induced flux in the θ direction, and which is negligible when the angle between the cone and the plate becomes small, as in the experiment they were analysing. They compared it with their experimental results for polystyrene macromolecules, nearly monodisperse, of different molecular weights $2.0 \times 10^6 \,\mathrm{g}\,\mathrm{mol}^{-1}$ and $4.0 \times 10^6 \,\mathrm{g}\,\mathrm{mol}^{-1}$ (denoted by 2M and 4M, respectively) in a solvent of oligomeric polystyrene molecules of 500 g mol⁻¹, when the cone is rotated producing a shear $\dot{\gamma} = 2 \,\mathrm{s}^{-1}$. The initial homogeneous concentration of the molecules of each solution was 0.20 and 0.12 wt% for the 2M and 4M solutions, respectively. According to an average value of τ obtained from the steady-state shear data, they obtained for the 2M and 4M solutions the values $\beta_2 = 240$ and $\beta_4 = 1500$, respectively.

Nevertheless, when they tried to fit the profile obtained from (8.8) with the observed concentration profiles, very severe discrepancies arose, as they found that the migration was much faster than predicted by (8.8). When they tried to fit the data by allowing β to be an adjustable parameter, they found that it is necessary that β_2 =200 000 and β_4 =1 100 000, instead of 240 and 1 500. Thus, the discrepancy between the observed and the measured β , which expresses the shear-induced flux in (8.8), is almost three orders of magnitude. It will be seen that this discrepancy may be overcome when the flow contributions to the chemical potential are considered.

8.1.2 Non-equilibrium Chemical Potential and Effective Diffusion Coefficient

According to thermodynamics, it is more fundamental to express the diffusion flux in terms of the gradient of the chemical potential as was done in (1.51) and (7.38) rather than in terms of the concentration gradient as in (8.1). Thus, we write instead of (8.1)

$$\boldsymbol{J} = -\tilde{D}\nabla\mu - \frac{D}{RT}\nabla\cdot\mathbf{P}^{\nu},\tag{8.9}$$

where μ is the chemical potential of the solute and \tilde{D} is related to the classical diffusion coefficient D by $D = \tilde{D}(\partial \mu_{\rm eq}/\partial n)$. Here, $\mu_{\rm eq}$ is the local-equilibrium chemical potential of the solute. The essential point is that in the presence of a non-vanishing ${\bf P}^{\nu}$, μ itself contains contributions of ${\bf P}^{\nu}$, thus providing an additional coupling between viscous effects and diffusion, besides the term in $\nabla \cdot {\bf P}^{\nu}$.

To be explicit, and as in the previous chapters, we use for the Gibbs free energy G in presence of a viscous stress \mathbf{P}^{ν} the expression

$$G(T, p, N_i, \mathbf{P}^{\nu}) = G_{eq}(T, p, N_i) + \frac{1}{4}JV\mathbf{P}^{\nu} : \mathbf{P}^{\nu},$$
(8.10)

where $G_{\rm eq}$ is the local-equilibrium value of the free energy at the corresponding values of T, p and N_i (we take N for the number of moles of the solute and N_0 the number of moles of the solvent) and J is the steady-state compliance.

The chemical potential of the solute is defined by $\mu = (\partial G/\partial N)_{T,p,\mathbf{p}^v}$. If we write N in terms of the solute concentration n (moles per unit volume) as N=nV, μ may be expressed as

$$\mu = \frac{1}{V} (1 - V'n) \left(\frac{\partial G}{\partial n} \right)_{T, p, \mathbf{P}'}, \tag{8.11}$$

where $V' = \partial V/\partial N$ is the partial molar volume of the solute. The term in parentheses in (8.11) takes into account the fact that a variation of N at constant p produces a change in the total volume V.

According to (8.10) and (8.11), the chemical potential of the solute is

$$\mu = \mu_{\text{eq}} + \frac{1}{4V} (1 - V'n) \frac{\partial}{\partial n} (VJ) \mathbf{P}^{\nu} : \mathbf{P}^{\nu}. \tag{8.12}$$

The use of the generalised chemical potential leads us to define an effective diffusion coefficient as $D_{\rm eff} = \tilde{D}(\partial \mu/\partial n)$ or, by writing \tilde{D} in terms of the classical diffusion coefficient D,

$$D_{\text{eff}} = D\Psi(n, \dot{\gamma}), \tag{8.13}$$

where the new function Ψ is defined as

$$\Psi(n,\dot{\gamma}) = \frac{(\partial \mu / \partial n)}{(\partial \mu_{\text{eq}} / \partial n)},\tag{8.14}$$

which, using (8.10), takes the explicit form

$$\Psi(n,\dot{\gamma}) = 1 + \frac{1}{(\partial \mu_{ea}/\partial n)} \frac{\partial}{\partial n} \left[\frac{(1 - V'n)}{4V} \frac{\partial}{\partial n} (VJ) \mathbf{P}^{\nu} : \mathbf{P}^{\nu} \right]. \tag{8.15}$$

If the contribution of the term in \mathbf{P}^{ν} : \mathbf{P}^{ν} were negative, it would induce a flow of solute towards higher solute concentrations, i.e. opposite to the usual Fickian diffusion. This would reinforce the contribution of the term in $\nabla \cdot \mathbf{P}^{\nu}$, which yields a migration of the molecules of the solute towards the centre, and would render the migration process much faster, as sketched in Fig. 8.1.

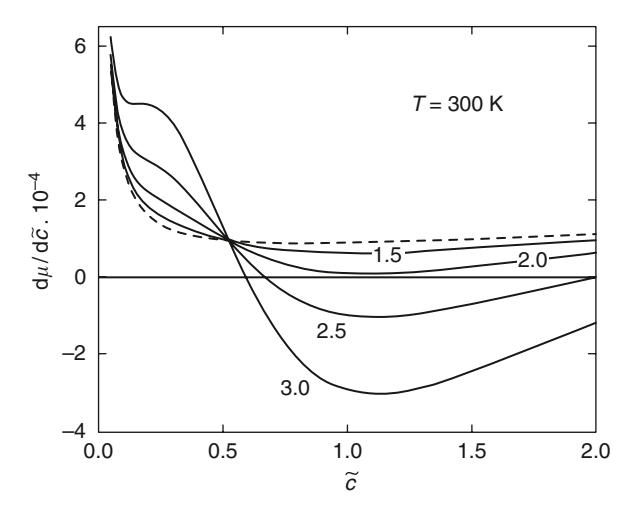


Fig. 8.2 For different Deborah numbers, the variation of $(\partial \mu/\partial \tilde{c})$, which is proportional to the polymer effective diffusivity, in terms of the reduced concentration \tilde{c} is presented, for polystyrene in transdecalin solution. The *discontinuous line* corresponds to the equilibrium Flory–Huggins contribution. It is seen that for \tilde{c} higher than a critical value approximately equal to 0.5, and for high enough values of the Deborah number, the effective diffusivity becomes negative. (del Castillo et al. 2000)

For this system, the derivative of chemical potential for different Deborah numbers $\tau\dot{\gamma}$ is plotted in Fig. 8.2. To obtain this figure we have used for the equilibrium chemical potential the expression from the classical Flory–Huggins model (6.4) and we have taken for J the formula (5.46) following from the Rouse–Zimm model combined with the Huggins expression (5.44) for $\eta(c)$. The expression for the non-equilibrium contribution to the chemical potential of the solute is thus

$$\frac{1}{RT}\mu_{\text{ne}} = \frac{CV_1M[\eta]}{4R^2T^2}\mathbf{P}^{\nu}:\mathbf{P}^{\nu}\left\{\frac{M[\eta]}{V_1}\frac{\Phi(\tilde{c})}{\tilde{c}} + 2\left[\frac{M_2[\eta]}{\tilde{c}V_1} - m\right]\frac{P_5(\tilde{c})}{P_6(\tilde{c})}\right\},\quad(8.16)$$

where m is the ratio between the molar volumes of the solute and the solvent, V_1 the molar volume of the solvent, \tilde{c} the reduced concentration defined by $\tilde{c} = [\eta]c$ (note that \tilde{c} is related to n by means of $\tilde{c} = [\eta]nM$) and $\Phi(\tilde{c})$, $P_5(\tilde{c})$ and $P_6(\tilde{c})$ the auxiliary functions defined in (6.42).

When a cone-and-plate experiment is considered, we can write the expressions

$$\mathbf{P}^{\nu}:\mathbf{P}^{\nu} = (P_{\phi\phi}^{\nu})^{2} + 2(P_{\phi\theta}^{\nu})^{2} = \Xi(\dot{\gamma})\tilde{c}^{2}, \tag{8.17}$$

$$\Xi(\dot{\gamma}) = \left(\frac{RT}{M[\eta]}\right)^{2} \left[4(\tau \dot{\gamma})^{4} + 2(\tau \dot{\gamma})^{2}\right]$$
(8.18)

and the derivative $(\partial \mu/\partial \tilde{c})$ is calculated from

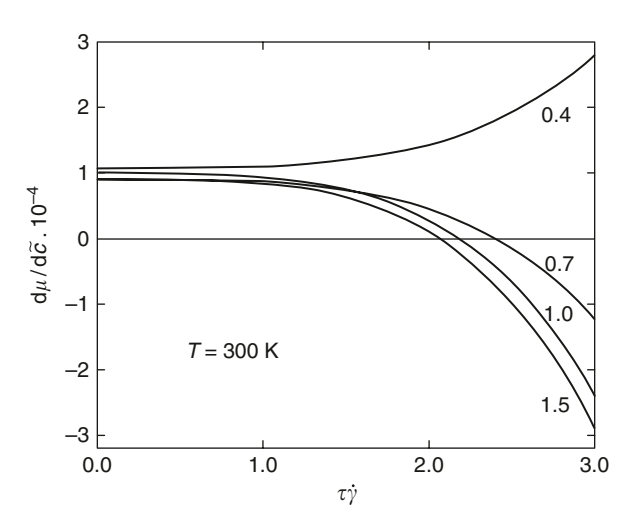
$$\frac{1}{RT} \frac{\partial \mu_{\text{neq}}}{\partial \tilde{c}} = \frac{C V_1 M[\eta]}{2RT} \Xi(\dot{\gamma}) \times \frac{M[\eta]}{V_1} \Phi(\tilde{c})
+ \left[\frac{M[\eta]}{V_1} - m\tilde{c} \right] \left[2 \frac{P_5(\tilde{c})}{P_6(\tilde{c})} + \tilde{c} \frac{d}{d\tilde{c}} \left(\frac{P_5(\tilde{c})}{P_6(\tilde{c})} \right) \right].$$
(8.19)

The numerical values of this derivative for the system PS/TD with a polymer molar mass of $520 \,\mathrm{kg} \,\mathrm{mol}^{-1}$, are plotted in Fig. 8.2, where the values k=1.40, $[\eta]=0.043 \,\mathrm{m}^3 \,\mathrm{kg}^{-1}$ and $\eta_e=0.0023 \,\mathrm{Pa}$ -s are used, as in Sect. 6.5.

It is seen in Fig. 8.2 that for low enough concentrations $(\partial \mu/\partial \tilde{c})$, and therefore $D_{\rm eff}$, is positive, whereas for higher concentrations $(\partial \mu/\partial \tilde{c})$, and consequently $D_{\rm eff}$ is negative. As can be appreciated in Fig. 8.2, the critical reduced concentration for this transition is near $\tilde{c}\approx 0.5\,\tilde{c}$. This value corresponds to a volume fraction ϕ (which in the system under consideration is given by $\phi=2.168\times 10^{-2}\,\tilde{c}$) of 0.01 and to a corresponding mass percentage of 1.2 wt%. We must insist, as we did in Sect. 6.5, that in the calculation leading to (8.16), use has been made of the Rouse expression (5.46) for the steady state compliance, instead of the simplest approximation $J=(nRT)^{-1}$, which would yield an opposite sign for the non-equilibrium contributions to the chemical potential. The need for the use of the rigorous expression for J is thus confirmed again.

Therefore, the effective polymer diffusivity depends on the shear rate, molecular weight (through the dependence of the relaxation time) and concentration. In Fig. 8.3, the corresponding effective polymer diffusivity versus the Deborah number $\tau \dot{\gamma}$ for the same system of Fig. 8.2 is presented, for several values of the reduced concentration. For low values of the latter, the effective diffusivity is always positive and increases with the shear rate and the molecular weight. In this range

Fig. 8.3 For different reduced concentrations \tilde{c} , $(\partial \mu/\partial \tilde{c})$, which is proportional to the polymer effective diffusivity, is shown as a function of the Deborah number $x = \tau \dot{\gamma}$, for polystyrene in transdecalin solution. For \tilde{c} lower than the critical value $\tilde{c} \approx 0.5$ the effective diffusivity is always positive, whereas for higher values of \tilde{c} , the effective diffusivity becomes negative for sufficiently high shear rates. (del Castillo et al. 2000)

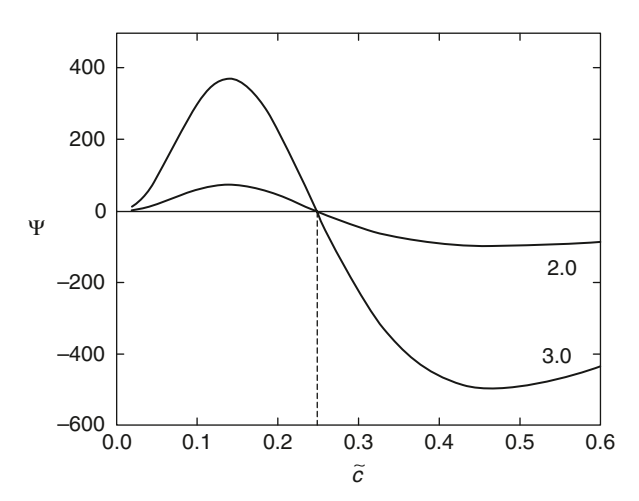


of concentrations the induced migration is expected to be very slow. However, for reduced concentrations higher than the critical one, the diffusivity becomes negative for sufficiently high values of the shear rate, the decrease being steeper for higher molecular weights.

Thus, it is seen that the stress contribution to the chemical potential of the polymer has important effects with respect to the formulation (8.1), where the gradient of n rather than the gradient of μ was considered. It is especially worth mentioning that for a given concentration (higher than a critical value), the effective diffusion coefficient is reduced when the shear stress increases, and it becomes negative. In this regime, the non-equilibrium contribution to the chemical potential considerably enhances the polymer migration. This may explain why the migration observed is much faster than that predicted by (8.1). Furthermore, it is seen in Fig. 8.3 that for a given value of the concentration, the effective diffusion coefficient is positive for values of the shear rate lower than some critical value. Thus, at low shear rates, the only thermodynamic force leading migration is the coupling of the second term in (8.9), and migration is very slow. For higher shear rates, the diffusion coefficient becomes negative and migration is much faster.

In the migration experiment in MacDonald and Muller (1996), the polymer solution confined in the cone-and-plate shear device has a homogeneous concentration \tilde{c}_0 before the system is sheared. During the shear, a dependence of concentration on time and radial position is observed, yielding a concentration profile $\tilde{c}(r,t)$. This radial migration can be explained by using the model we just have considered under the condition that $D_{\rm eff}$ takes negative values. Using (8.19) and the information about the system polystyrene dissolved in oligomeric polystyrene given in Appendix A, the numerical values of the derivative of chemical potential can be calculated and yield the results shown in Fig. 8.4 for the system called 2M by MacDonald and Muller (1996). In this figure a critical concentration \tilde{c}_c can be observed, for which the derivative of chemical potential is equal to zero for any shear rate considered.

Fig. 8.4 Numerical values of the function Ψ in (8.14) calculated from the Rouse–Zimm model using the information given in Appendix A for the system 2M of MacDonald and Muller (1996). The labels in the curves correspond to the values of the shear rate given in s⁻¹. (del Castillo et al. 2000)



When the calculations are carried out for several values of the polymer molecular mass M, it is possible to find that $\tilde{c}_c = 0.00545 M^{0.20}$.

In order to explain from a theoretical point of view the experimental results in (MacDonald and Muller 1996) we use (8.9) together with the mass balance equation (8.6) to obtain the differential equation which describes the shape of the concentration profile

$$\frac{\partial \tilde{c}}{\partial t} = D \left[\frac{\partial \Psi}{\partial \tilde{c}} \left(\frac{\partial \tilde{c}}{\partial r} \right)^2 + \Psi \frac{\partial^2 \tilde{c}}{\partial r^2} + (2\Psi + \beta) \frac{1}{r} \frac{\partial \tilde{c}}{\partial r} \right]. \tag{8.20}$$

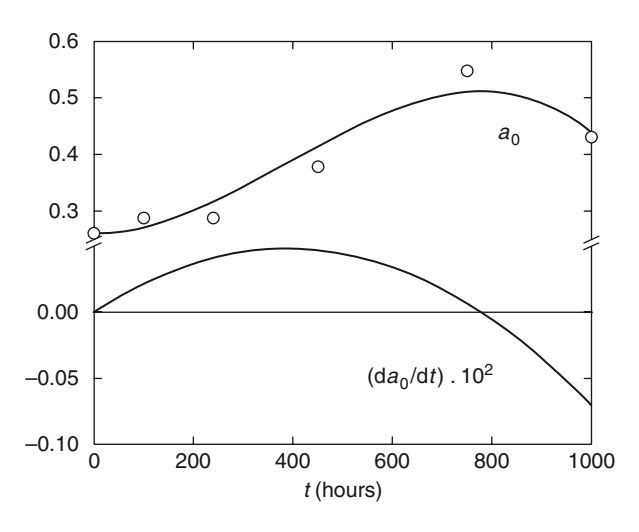
If a series expansion of the form

$$\tilde{c}(r,t) = \sum_{j=0} a_j(t)r^j \tag{8.21}$$

is assumed for the solution of the latter equation, we can conclude that in some particular conditions (homogeneous concentration at the beginning of the experiment) the following identifications can be established $a_0(0) = \tilde{c}_0$, $a_j(0) = 0$, $\tilde{c}(0,t) = a_0(t)$.

After the experimental results for system 2M it is possible to generate Fig. 8.5 where the numerical values of $a_0(t)$ and its derivative are plotted as functions of time. From this plot we verify the existence of two values of time for which the derivative is zero, one corresponds to the beginning of the experiment and the other is associated with a maximum for $a_0(0)$ at time t>0. The presence of this maximum prevents any monotone increase with the time of concentration in the cone apex. The reader interested in the details is referred to Criado-Sancho et al. (2000).

Fig. 8.5 The upper curve corresponds to the experimental and fitted values of reduced concentrations of system 2M of MacDonald and Muller (1996) at the apex cone at several times. In the lower curve the temporal derivative is plotted as a function of time. (del Castillo et al. 2000)



8.2 Shear-Induced Concentration Banding and Macromolecular Separation in Cone-and-Plate Flows

One of the consequences of shear-induced migration is the so-called shear-induced concentration banding, namely, the appearance of bands of different concentrations under the action of a viscous pressure in an initially homogeneous polymer solution (Goveas and Fredrickson 1999; Bautista et al. 2002, 2007). This phenomenon has practical outcomes in chromatography, i.e. for separation of macromolecules of different mass, as in other technical and biological situations, because the banding profile depends on the molecular mass. These procedures for separation are especially useful in biotechnology and pharmacology, as for instance for protein purification. Here we will deal with a simplified mathematical model. There are several configurations of interest: cone-and-plate, rotating concentric cylinders, flow along long tubes.

In Fig. 8.6 we plot the region of negative values of the effective diffusion coefficient $D_{\rm eff}$ for the system so called 2M in MacDonald and Muller (1996) for different values of the shear rate. It is seen that for $\dot{\gamma}$ higher than a threshold value, $D_{\rm eff}$ is negative for concentration values between \tilde{c}_1 and \tilde{c}_2 , which depend on $\dot{\gamma}$ (especially the upper value \tilde{c}_2 , whereas the lower one is relatively insensitive to $\dot{\gamma}$).

Figure 8.6 shows the domain of values of \tilde{c} and $\dot{\gamma}$ for which $D_{\rm eff}$ is negative (at given T and p): this corresponds to the region above the curve, which has a minimum for a given critical value $\dot{\gamma}_c$ of the shear rate. In fact, this curve is the spinodal line in the $\tilde{c}-\dot{\gamma}$ plane, as it corresponds to the limit of stability of the solution. For a fixed $\dot{\gamma}$, the values of \tilde{c}_1 and \tilde{c}_2 are given by the intersection of this curve with the corresponding horizontal line. Note the threshold $\tilde{c}_{\rm th}$, below which the effective diffusion coefficient is always positive: banding would not be present for concentrations lower than this value.

Figures 8.4 and 8.6 suggest directly a mechanism for shear banding. Assume one starts from an homogeneous solution with initial concentration \tilde{c}_0 and that one

Fig. 8.6 For values of shear rate and concentration in the region above the curve, the effective diffusion coefficient (8.13) is negative and therefore the system splits in two regions with different concentrations. For a given value of $\dot{\gamma}$ these concentrations are given by the intersection of the horizontal line corresponding to the value of $\dot{\gamma}$ with the curve plotted in the figure. The minimum of this curve corresponds to the threshold value of $\dot{\gamma}$ for shear banding. (Jou et al. 2001)

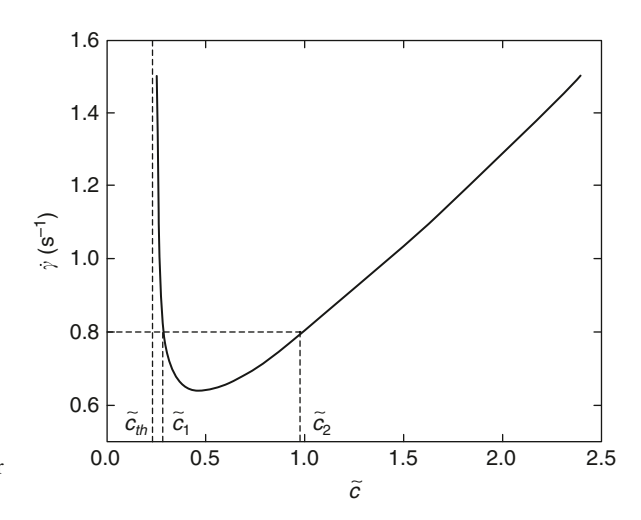
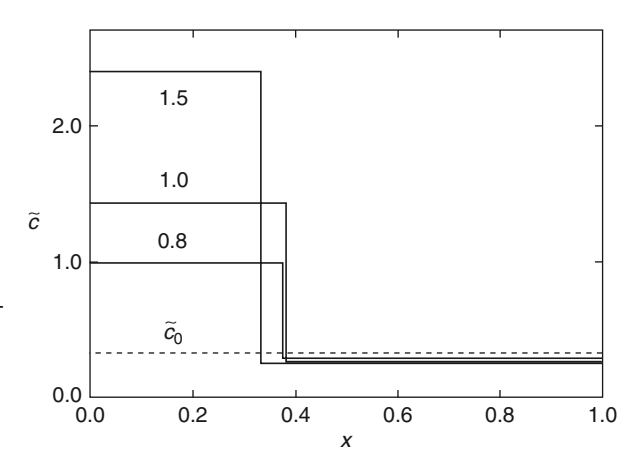


Fig. 8.7 Sketch of the steady-state concentration profile in a coneand-plate device for three different values of $\dot{\gamma}(1.5\,\mathrm{s}^{-1},1.0\,\mathrm{s}^{-1}$ and $0.8\,\mathrm{s}^{-1})$ as a function of the ratio $x\equiv r/R$ of the distance r to the apex of the cone and the outer radius R of the device. The initial homogeneous concentration value \tilde{c}_0 is higher than the value $\tilde{c}_{threshold}$. (Jou et al. 2001)



imposes on the system a constant shear rate by rotating the cone at suitable angular speed. The second term in Eq. (8.20) always produces a flux of solute towards the apex of the cone. When $D_{\rm eff}$ is positive, this flux will be opposed by the concentration-driven diffusion flux and an (usually smooth) inhomogeneous steady state will be reached eventually. If, in contrast, $D_{\rm eff}$ is negative, the inhomogeneization process will be much faster because the flux produced by $\nabla \cdot \mathbf{P}^{\nu}$ will be amplified.

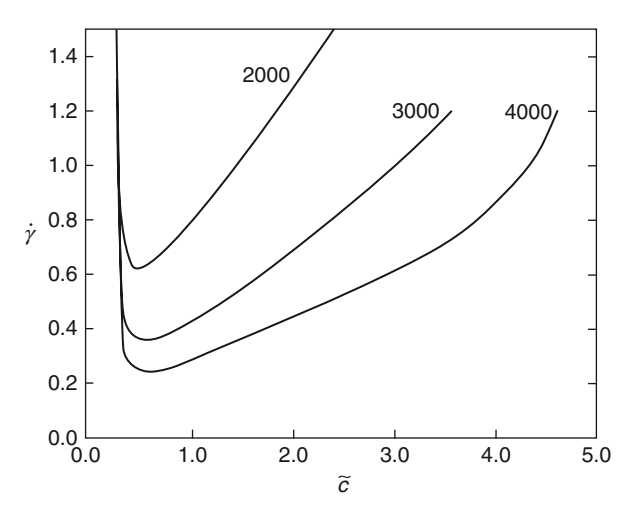
This migration will eventually lead to a steady state in which the system will be split in two different bands, as sketched in Fig. 8.7. The inner band will have a high solute concentration approximately equal to \tilde{c}_2 and the outer one a low solute concentration approximately equal to \tilde{c}_1 separated by a rather sharp region. The conditions imposed on the profile are $\tilde{c} = \tilde{c}_1$ for x=1 and $\tilde{c} = \tilde{c}_2$ for x=0, with x=r/R, being r the distance to the apex and R the outer radius of the device. In fact, this profile will be rounded-off as a compromise between the migration towards the centre due to the second term in (8.9) and the outgoing diffusion driven by the concentration gradient in the regions with positive $D_{\rm eff}$ but the detailed numerical analysis is far from trivial.

For initial inhomogeneous concentration higher than \tilde{c}_{th} (the lowest concentration for which D_{eff} may become negative for sufficiently high $\dot{\gamma}$, according to Fig. 8.6) banding will appear for values of the shear rate higher than the ones corresponding to the minimum of the curve in Fig. 8.6. Goveas and Fredrickson (1999) obtained a similar behaviour in their theoretical analysis of banding in a polymer solution in a wide-gap Couette flow between two coaxial cylinders; a steep part in the concentration profile appears for sufficiently high values of the shear rate.

Chromatographic techniques, i.e. the separation of different molecules initially mixed, have wide applications (Dill 1979; Dill and Zimm 1979; Schafer et al. 1974; Lou and Harinath 2004). To study it one needs to consider the effect of molecular mass on the banding.

In Fig. 8.8 we plot the boundary of the region where $D_{\rm eff}$ is negative in the plane of shear rate $\dot{\gamma}$ versus reduced concentration \tilde{c} for three different molecular masses (2 000, 3 000 and 4 000 kg/mol, respectively) of macromolecular polystyrene in

Fig. 8.8 The same as Fig. 8.6, but for different values of the polymer mass. The *curves* correspond to solutions of macromolecular polystyrene with $M=2\,000$, 3 000, 4 000 kg/mol, respectively, solved in oligomeric polystyrene of 0.5 kg/mol. (Jou et al. 2001)



oligomeric polystyrene. Figure 8.8 generalizes Fig. 8.6, in which the region of negative $D_{\rm eff}$ was plotted only for a single molecular mass (M=2 000 kg/mol). According to the experimental data, the critical value $\dot{\gamma}_c$ corresponding to the minimum of the curves is seen to depend on the macromolecular mass as $\dot{\gamma}_c(M) \propto M^{-1.35}$.

From this graph it is easy to find a semi-quantitative description of the mass separation process. Though the detailed analysis would be much cumbersome, a simplified semi-quantitative analysis is useful in understanding the role of $D_{\rm eff}$ in the separation process. Here, we will illustrate with two different situations the physical process. We consider a solution of three kinds of macromolecular polystyrene, of respective masses 2 000, 3 000 and 4 000 kg mol⁻¹ in oligomeric poslystyrene. We assume, for the sake of simplicity, that the reduced concentration of these three species is initially the same, namely $\tilde{c}_0 = 0.5$, in an homogeneous solution in the cone-and-plate device. As a further simplification, we assume that the concentration is low enough that the different macromolecular species behave independently of each other. We aim to describe the concentration profile of the three kinds of macromolecular species in the steady state reached after a sufficiently long time of rotation of the cone.

First, we consider a shear rate $\dot{\gamma}=0.35\,\mathrm{s}^{-1}$. The point corresponding to the initial conditions of the system is situated in the region where D_{eff} is negative for the macromolecules of $M=4\,000$, but it is positive for the two other molecular species. Thus, the concentration of the latter ones will vary slightly on the position, but, in contrast, since D_{eff} is negative for macromolecules of $M=4\,000$, the system will split into two different regions: one near the centre, with a high concentration of $M=4\,000$ macromolecules, and another with a low concentration near the wall. The values of these two concentrations are given approximately by the intersection of the horizontal line corresponding to $\dot{\gamma}=0.35\,\mathrm{s}^{-1}$ with the curve labelled 4 000 in Fig. 8.8. This situation is depicted schematically in Fig. 8.9 upper, where the almost-vertical part of the profile has been calculated from the mass conservation condition.

The second situation corresponds to a shear rate $\dot{\gamma}=1.0\,\mathrm{s}^{-1}$. For this value of $\dot{\gamma}$ and for $\tilde{c}_0=0.4$, D_{eff} is negative for the three macromolecular species. Now, the system will split into two regions for each species. The values of the concentration near the central region and in the external region are given approximately by the intersection of the horizontal line corresponding to $\dot{\gamma}=1.0\,\mathrm{s}^{-1}$ with the three corresponding curves plotted in Fig. 8.8. The situation is depicted in Fig. 8.9 lower when the same initial concentration is supposed for all the species. The change of effective viscosity related to phase separation is also a topic of interest (Criado-Sancho et al. 2003).

Of course, further analysis is necessary either to get higher precision and to apply it to other initial conditions, but we think that this short presentation may look sufficiently promising to encourage further development of this approach.

A related configuration with higher technological interest corresponds to the flow between two concentric cylinders rotating at different angular velocities, which is

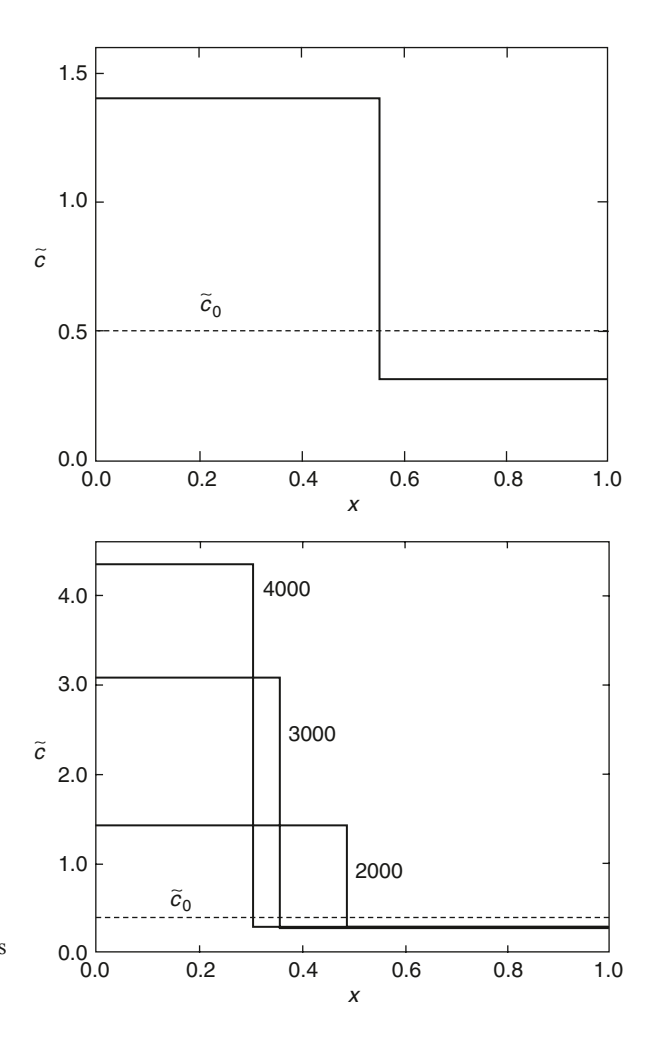


Fig. 8.9 Concentration profiles of polystyrene macromolecules of different molecular mass 2 000, 3 000, 4 000 kg/mol under shear viscous pressure. The two figures correspond to different initial homogeneous conditions, detailed in the text. (Jou et al. 2001)

the basis of the so-called radial flow chromatography (Gu et al. 1993; Lay et al. 2006). The central cylinder is porous and allows the transfer of macromolecules to the volume inside the smaller cylinder, from which the material is removed. This method has some advantages over the separation in flows along long tubes, because of a relatively large flow area with a short flow path. This has been the basis of new and more efficient methods for gluten separation in wheat flour (Peighambardoust et al. 2008, 2010) or in separation through hollow fiber membranes (Ren et al. 2002).

8.3 Shear-Induced Migration and Molecular Separation in Tubes

In Sects. 8.1 and 8.2 we have analyzed stress-induced migration in cone-and-plate experiments. A situation with even more practical interest is found in straight tubes (Tirrell and Malone 1977; Zhen and Yeung 2002). It was considered as a basis for flow-induced chromatography of long molecules of DNA—a difficult topic in usual electrically-driven chromatography because it becomes very inefficient in separating molecules of different high mass—and it is of interest for actual flows of polymer solutions in tubes. In straight tubes, the only non-vanishing components of the viscous pressure tensor are

$$P_{rz} = P_{zr} = -\eta \dot{\gamma}, \quad P_{zz} = (N_1 + N_2) \dot{\gamma}^2, \quad P_{rr} = N_2 \dot{\gamma}^2,$$
 (8.22)

where η is the shear viscosity and N_1 and N_2 the normal-stress coefficients. We will specialize our attention to upper-convected Maxwell fluids, for which $N_1 = 2\tau \eta$ and $N_2 = 0$. In this case, it turns out that the radial component of $\nabla \cdot \mathbf{P}^{\nu}$ is zero, because $P_{rr} = P_{\theta\theta} = P_{\theta r} = 0$ and P_{zr} does not depend on z. This is an important difference with respect to cone-and-plate flows, where the term $\nabla \cdot \mathbf{P}^{\nu}$ is different from zero and points towards the axis of the device, thus promoting a migration of the particles towards the centre. Thus, Eq. (8.9) reduces to $\mathbf{J} = -\tilde{D}\nabla\mu$. In the steady state, $\mathbf{J} = 0$ and therefore, according to (8.9), one must have

$$\nabla(\mu_{\rm eq} + \Delta\mu_{\rm flow}) = 0, \tag{8.23}$$

i.e.

$$\mu_{\text{eq}}(c) + \Delta \mu_{\text{flow}}(c, \mathbf{P}^{\nu}) = \text{const},$$
 (8.24)

where the constant does not depend on the radial position r. We assume Flory-Huggins expression for the equilibrium chemical potential, expression (8.16) for the flow contribution, and

$$\mathbf{P}^{\nu}:\mathbf{P}^{\nu}=2P_{rz}^{2}+P_{zz}^{2}=2\eta^{2}\dot{\gamma}^{2}+(2\tau\eta)^{2}\dot{\gamma}^{4}.$$
(8.25)

For Newtonian flow, with η independent of concentration and τ =0, one has a parabolic velocity profile (the Poiseuille profile) for which $\dot{\gamma}$ depends on the radial position as

$$\dot{\gamma}^2 = \frac{4v_{\rm m}^2}{R^4}r^2 = \beta r^2,\tag{8.26}$$

where $v_{\rm m}$ is the maximum velocity and R the radius of the tube. The parameter β can be also written as $\beta = 16Q^2/\pi^2R^8$ being Q the total flow rate. Here we assume that the velocity profile remains parabolic regardless of the concentration redistribution and non-Newtonian effects. Thus for consistency, we assume small values of $\dot{\gamma}$.

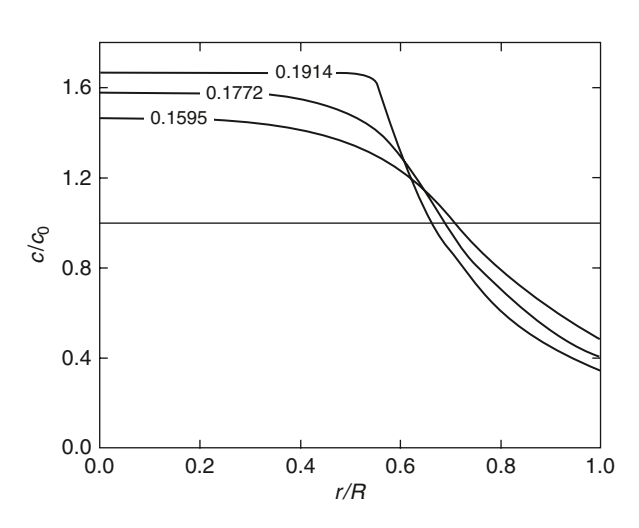
In order to determine the constant appearing in (8.24), for a given value of parameter Q/R^3 the concentration profile must satisfy the condition the mass conservation condition

$$\int_0^1 \frac{c(x)}{c_0} x \, \mathrm{d}x = \frac{1}{2} \tag{8.27}$$

being x=r/R. In Fig. 8.10 we show the steady-state concentration profile obtained for a solution of polystyrene of molecular mass 2 000 kg mol⁻¹ solved in an oligomeric polystyrene whose molecular mass is $0.5 \,\mathrm{kg}\,\mathrm{mol}^{-1}$ for several values of the flow rate Q.

Since $\Delta\mu_{\text{flow}}$ depends on the radius, through (8.25) and (8.26), the concentration profile determined from (8.24) will also depend on the radius in the steady state. Furthermore, since τ and η depend on the macromolecular mass, the profile will depend on molecular mass. In this way, an axial flow of the solution will induce a radial flow of the macromolecules.

Fig. 8.10 Concentration profiles of the solute (polystyrene of $M=2~000~\rm kg/mol$ solved in oligomeric polystyrene 0.5 kg/mol for several values of Q/R^3 (in s⁻¹). The horizontal line corresponds to the initial homogeneous profile, which would be stationary if the fluid were at rest (Q=0). (Jou et al. 2002a)



An important feature in the separation process is the separation rate. Indeed, if the separation is too slow, the length of the tubes needed to observe the steady concentration profile is very long, and the separation process is inefficient. Some of the existing evaluations predict in fact a slow separation. In the cone-and-plate device we found that for high enough shear rates, a shear-induced instability occurs which accelerates very much the separation with respect to the predictions based on the local-equilibrium chemical potential. In tubes a similar phenomenon may arise and may have interest in flow through porous systems or along arteries and veins.

Chapter 9 Taylor Dispersion and Anomalous Diffusion

Diffusion is a very rich phenomenon which goes beyond the classical simple description in quiescent systems. On the one side, inhomogeneities in the flow velocity exert a deep influence on the behaviour of diffusion and have enormous environmental and industrial importance, as for instance in the transport of pollutants or in the functioning of chemical reactors under continuous flow. Furthermore, the exponents characterizing the temporal behaviour of diffusion are drastically altered in the presence of velocity gradients. Indeed, the presence of a simple shear changes the usual behaviour $\langle x^2 \rangle \sim t$ to $\langle x^2 \rangle \sim t^3$, with x the displacement of the solute particles with respect to the moving solvent in the direction of the flow. This implies an enormous enhancement of diffusion along this direction. Note that an exponent 3 for time also appears in diffusion in turbulent situations (Isichenko 1992).

On the other side, in some systems the mentioned exponents also differ from those of classical Fickian ones even in quiescent states, in such a way that the average value of the square of the displacement of the particles is proportional to some fractional power of time, higher or lower than unity. These cases are known as anomalous diffusion, which can be sub-diffusive (slower than Fickian diffusion) or superdiffusive (faster than Fickian diffusion). This behaviour is found, for instance, in amorphous materials or, in general, in materials with a complex microstructure.

Both situations, Taylor dispersion and anomalous diffusion, whose purely dynamical features have been much studied, imply interesting thermodynamical challenges beyond the classical formalisms. The most well-known results for Taylor dispersion refer to asymptotically long times, and cannot be used for short times. Generalized transport equations for intermediate times are needed for practical purposes and extended irreversible thermodynamics has been used as a guide to obtain them. Finally, for the sake of completeness, we study Taylor dispersion in the context of anomalous diffusion.

Hydrodynamics and thermodynamics of flow have applications in domains that are not studied in the present book, but which have much practical and conceptual interest, as for instance the description of flow in porous media or the optimization of fluid transport systems. In porous media, the pores form a disordered tangle along which the fluid is transported. Thermodynamic principles have been used to restrict the possible forms of the constitutive equations describing the transport in

these systems (Sahimi 1995; Gray and Miller 2005, 2006; Miller and Gray 2008; Restuccia 2010), which are of obvious interest in hydrology or in oil extraction. The interplay between the viscosity of the fluid, the elasticity of the walls, erosion of the solid matrix, and other several factors make this topic a very rich one.

Still richer is the case of biological transport networks for blood in bodies, or sap in leaves, or air in lungs. In them, the ensemble of the vessels is organized in very subtle structures, in order to optimize some aspects of the transport (Bernot et al. 2009; Kizilova 2010). The configuration of such transport systems often corresponds to optimize the liquid delivering at the minimal costs on the liquid motion and on the vessel construction and maintenance. Bejan and Lorente (2006) have proposed the so-called constructal law, according to which for a finite-size flow system to persist in time, its configuration must evolve in such a way that it provides an easier access to the currents that flow through it. This principle describes not only natural systems, but is also applicable to the optimization of engineering problems.

9.1 Brownian Motion in Shear Flow

The drastic effect of a velocity gradient on diffusion may be directly described by the mathematical solution of the evolution equation for the concentration (in moles per unit volume) *n*, namely,

$$\frac{\partial n}{\partial t} + \mathbf{v} \cdot \nabla n = D \nabla^2 n, \tag{9.1}$$

with D the molecular diffusion coefficient. When one uses for the velocity \mathbf{v} appearing in the convective term, the expression for a simple shear flow, namely $\mathbf{v} = (\dot{\gamma} y, 0, 0)$ with $\dot{\gamma}$ the shear rate, the shear effects on diffusion may be found (see, for instance, Foister and van den Ven 1980).

The mentioned hydrodynamic result may also be obtained in a clear but rather lengthy way by analysing the behaviour of Brownian motion described by the Langevin equation for a particle under shear flow. We follow here the pedagogical approach by Katayama and Terauti (1996), which gives a deeper view of the microscopic process. The Langevin equation describing the motion of Brownian particles in the presence of the flow is

$$m\frac{\mathrm{d}\mathbf{u}}{\mathrm{d}t} = -\zeta(\mathbf{u} - \mathbf{v}) + \xi,\tag{9.2}$$

with m and u the mass and the velocity of the Brownian particle, v(r) the velocity of the fluid, ζ the friction coefficient of the particle, and ξ a random force due to the collisions with the particles in the fluid. As it is usual in the description of Brownian motion, this force is assumed to be Gaussian and to satisfy

$$\langle \xi_i(t) \rangle = 0, \quad \langle \xi_i(t_1)\xi_j(t_2) \rangle = 2k_{\rm B}T\zeta\delta_{ij}\delta(t_1 - t_2),$$
 (9.3)

where the subscripts i, j refer to the spatial components of the noise, δ_{ij} is Kronecker's delta and $\delta(t_1-t_2)$ is the Dirac delta expressing that the noise is purely Markovian, i.e. without memory. Conditions (9.3) state that the second moments of the noise are proportional to the friction coefficient and to the temperature.

From now on, we consider a plane Couette flow, with $v = (\dot{\gamma}y, 0, 0)$. Integration of (9.2) yields

$$u_x(t) = u_x(0)e^{-\alpha t} + \int_0^t e^{-\alpha(t-\tau)} \left[\alpha \dot{\gamma} y(\tau) + \xi_x'(\tau)\right] d\tau,$$
 (9.4)

where ξ' stands for ξ/m and $\alpha = \xi/m$. Analogously, the y component of (9.2) yields

$$u_y(t) = u_y(0)e^{-\alpha t} + \int_0^t e^{-\alpha(t-\tau)} \xi_y'(\tau) d\tau.$$
 (9.5)

By assuming x(0)=y(0)=(0), and integrating (9.5), it follows for the displacement y(t)

$$y(t) = \int_0^t u_y(\tau) d\tau = \frac{1}{\alpha} u_y(0)(1 - e^{-\alpha t}) + \frac{1}{\alpha} \int_0^t \left[1 - e^{-\alpha(t-\tau)} \right] \xi_y'(\tau) d\tau.$$
 (9.6)

When this expression is introduced into (9.4), one is led to

$$u_{x}(t) = u_{x}(0)e^{-\alpha t} + \frac{\dot{\gamma}}{\alpha}u_{y}(0)(1 - e^{-\alpha t}) - \dot{\gamma}u_{y}(0)e^{-\alpha t} + \frac{\dot{\gamma}}{\alpha}\int_{0}^{t} \left[1 - e^{-\alpha(t-\tau)}\right]\xi'_{y}(\tau)d\tau - \dot{\gamma}\int_{0}^{t} d\tau \int_{0}^{\tau} d\tau' e^{-\alpha(t-\tau')}\xi'_{y}(\tau') + \int_{0}^{\tau} e^{-\alpha(t-\tau)}\xi'_{y}(\tau)d\tau.$$
(9.7)

The expression for x(t) may now be obtained by introducing (9.7) into

$$x(t) = \int_0^t u_x(\tau) d\tau, \qquad (9.8)$$

and integrating it with respect to time. The reader is referred to Katayama and Terauti (1996) for the simple but cumbersome details.

By using (9.8) and (9.7), and taking into account only the dominant terms in the long-time behaviour, one obtains for the average value of the square of the displacement

$$\langle \langle x^2(t) \rangle \rangle = 2Dt \left(1 + 2\frac{\dot{\gamma}^2}{\alpha^2} - \frac{3}{2}\frac{\dot{\gamma}^2}{\alpha}t + \frac{1}{3}\dot{\gamma}^2t^2 \right), \tag{9.9}$$

$$\langle \langle y^2(t) \rangle \rangle = 2D \left(t - \frac{1}{\alpha} \right),$$
 (9.10)

where D is the diffusion coefficient which is identified as $D=k_{\rm B}T/\zeta$ in accordance with the Einstein formula and $\langle\langle\ldots\rangle\rangle$ stands for the double average over the initial velocity distribution and over the ensemble of the random force. Thus, the dominant terms when $t\gg 1/\alpha$ are

$$\langle \langle x^2(t) \rangle \rangle = 2Dt + \frac{2}{3}D\dot{\gamma}^2 t^3,$$
 (9.11a)

$$\langle \langle y^2(t) \rangle \rangle = 2Dt.$$
 (9.11b)

It is seen in (9.11) that in the absence of the shear i.e. $\dot{\gamma} = 0$, one recovers the classical result, whereas for $\dot{\gamma} \neq 0$, the new term coming from the flux becomes dominant and changes the temporal behaviour from t to t^3 , but this modification only appears on the longitudinal term.

Although the behaviour in t^3 may be obtained, as was noted, from a purely hydrodynamic analysis (Foister and van den Ven 1980), the terms in (9.9) including the parameter α (which is the inverse of a relaxation time) cannot be obtained from the hydrodynamic analysis, because (9.1) does not contain any microscopic relaxation time. For this reason, the analysis presented here is more detailed than the one based on the direct analytical solution of (9.1).

In this section, the coupling between diffusion and shear is purely dynamical, i.e. the constitutive equation for matter diffusion is the usual Fick's law, and no modification of the classical thermodynamics nor statistical framework is required.

9.2 Taylor Dispersion and Microfluidics

The coupling of an inhomogeneous convective flow and particle diffusion leads to dramatic effects on the dispersion of particles, which is much enhanced with respect to pure molecular diffusion. This situation is important in many circumstances, such as diffusion of pollutants in rivers and estuaries, or of medical products in arteries or veins. In this frame, Taylor (1953, 1954) showed that the combined action of a gradient in the velocity field and the transverse molecular diffusion leads after a relatively long time to a purely longitudinal diffusion, as shown in Fig. 9.1, with an effective diffusion coefficient given by

$$D_{\rm eff} = D_{\rm m} + D_{\rm T}, \tag{9.12}$$

 $D_{
m m}$ being the molecular diffusion coefficient in a fluid at rest and $D_{
m T}$ the Taylor correction, which is of the form

$$D_{\rm T} = AU^2 d^2 / D_{\rm m}, (9.13)$$

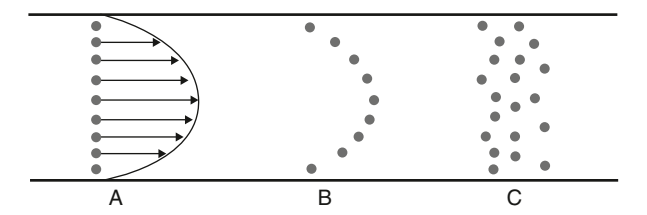


Fig. 9.1 Taylor's dispersion: in A the particles of the solvent are aligned perpendicular to the flow, whose parabolic velocity profile is shown; in B, the particles have moved with the fluid; in C, the combination of the velocity field and the transversal diffusion of the particles yields an enhanced longitudinal diffusion. This latter stage is known as Taylor's dispersion

with U the mean velocity, d the width of the duct and A a numerical coefficient which depends on the details of the flow (for a plane Couette flow between parallel plates separated by a distance d, A=1/210 and for a cylindrical Poiseuille flow in a duct of radius d, A=1/48). Note that $D_{\rm T}$ is much larger than $D_{\rm m}$, for instance, if $D_{\rm m} \sim 10^{-10}$ m²/s, $U=10^{-1}$ m/s, and $U=10^{-1}$ m, $U=10^{-1}$ m, $U=10^{-1}$ m, $U=10^{-1}$ m will be of the order of $U=10^{-1}$ m²/s. Thus, $U=10^{-1}$ m wide range of situations, and implies much faster diffusion than that in a quiescent fluid.

This feature may be qualitatively understood by considering an initially homogeneous band of solute perpendicular to the velocity direction and studying how it disperses under the combined action of the flow and the diffusion. If the diffusion did not play any role, the particles would be dragged by the flow and the initially flat band would be stretched into a paraboloidal band corresponding to the paraboloidal velocity profile of Poiseuille flow. However, diffusion induces a transversal flow of particles from the high to the low concentration regions, and it eventually produces a uniform plug with increasing width moving downstream. It may seem surprising that the Taylor dispersion coefficient (9.13) is higher for lower values of the molecular diffusion coefficient $D_{\rm m}$. However, the interpretation of this seemingly paradoxical feature is clear: the slower the transverse diffusion, the longer the fast particles remain in the fast layers and the slow particles in the slow layers, and, as a consequence, the rate at which they separate longitudinally from each other is faster.

The characteristic time that the particles take to cross the duct of width d is, according to (9.11b), of the order of $t_{\rm c} = d^2/2D_{\rm m}$. On the other hand, as it has seen in Sect. 9.1, the longitudinal diffusion along the flow, given by (9.11a), may be written in terms of an effective diffusion coefficient $D_{\rm eff}(t)$ depending on time as $\langle x^2 \rangle \equiv 2D_{\rm eff}(t)t$ with

$$D_{\text{eff}}(t) \equiv D_{\text{m}} \left(1 + \frac{1}{3} \dot{\gamma}^2 t^2 \right).$$
 (9.14)

If one introduces in (9.14) the time $t_{\rm c}$ characterizing the transversal diffusion and writes $\dot{\gamma}d=U$, one obtains $D_{\rm eff}(t)\equiv D_{\rm m}+AU^2d^2/D_{\rm m}$. Thus, the transversal diffusion modifies the effective longitudinal diffusion coefficient and enhances it dramatically. The original rigorous derivation for the expressions describing the shear-enhanced longitudinal diffusion may be found in Taylor (1953, 1954) and Aris (1956).

Another range of situations of potential interest is that arising in microfluidics and we will make an estimation in this regime. As an illustration in microfluidics, let us consider the longitudinal diffusion of glucose in water, for which $D_{\rm m} \simeq 5 \times 10^{-10} \ {\rm m^2 \ s^{-1}}$, in a cylindrical tube with radius $R=100 \ \mu{\rm m}$ with an average speed $v=10^{-3} \ {\rm m \ s^{-1}}$. In this case, the Taylor effective diffusion would be

$$D_{\rm T} = D \left[1 + \frac{1}{48} \left(\frac{vR}{D} \right)^2 \right] = 5 \times 10^{-10} \frac{\rm m^2}{\rm s} [1 + 800]. \tag{9.15}$$

To reach this effective value, one needs a time interval of the order of $t_{\rm eff} = R^2/2D = 10 \, \rm s$. Therefore, the minimum length of the tube is $l_{\rm eff} = v t_{\rm eff} = 10^{-2} \rm m = 10^4 \mu m$. If we have a tube of this length, the effective coefficient will change from the purely molecular value $D_{\rm m}$ to the effective value computed in this illustration. Thus, the short-time behaviour of $D_{\rm eff}(t)$ will be needed, unless the tube is much longer than this value.

Thus, Taylor's formula is only valid for asymptotic long times (i.e. $t \gg t_c$), and attempts have been made to obtain a description valid at any time (see Camacho 1993a, b, c; Smith 1981, 1987a, b for references) which are necessary for ducts shorter than Ut_c . A rough estimation of the actual value of the effective diffusion coefficient could be obtained, for instance, from expression (9.14) for times shorter than t_c . In this very simplified estimation, expression (9.15) would be modified as

$$D_{\rm T} = D_{\rm m} \left[1 + \frac{1}{48} \left(\frac{t}{t_{\rm c}} \right)^2 \left(\frac{vR}{D_{\rm m}} \right)^2 \right],$$
 (9.16)

for $t \le t_c$, and (9.15) for $t \ge t_c$.

This rough estimation may be improved by starting from the convection-diffusion hydrodynamic equations. However, the direct study of the intermediate time scales turns out to be very complicated and clever simplifications are useful for practical aims (Camacho 1993a, b, c; Berentsen et al. 2005; Berentsen and Kruijsdijk 2008; Hamdan et al. 2008). They will be considered in the next section.

9.3 Taylor Dispersion for Short and Intermediate Times

Camacho (1993a, b, c) proposed a simplified approach to the intermediate-time behaviour of Taylor dispersion based on a dynamical equation for the Taylor diffusion flux. The intuitive idea is that for very short times the longitudinal motion of the particles is determined by the drag of the flow, and therefore it could be reversed if the flow was reversed (this is the period during the transition from A to B in Fig. 9.1). In contrast, for longer times, the combination of the transversal spread and shear flow (transition from B to C in Fig. 9.1) would make the motion irreversible even if the flow was reversed. This generalization is especially useful in microfluidic flows, where the tubes must be very thin and very short (Tabeling 2005; Bruus 2008).

The advantage of such a model is that it allows elimination of one degree of freedom (the distribution of the particle in the y direction, perpendicular to the flow) yielding a description in terms of only one spatial component, namely x, the position along the flow. From the point of view of transport theory, this has the further interest of exhibiting a transition from a reversible behaviour at short times to an irreversible behaviour for times longer than τ .

9.3.1 Evolution Equation for the Flow of Matter

The generalized Maxwell–Cattaneo for the Taylor diffusion flux $J_{\rm T}$, proposed by Camacho (1993a) is

$$J_{\rm T} + \tau_{\rm T} \frac{\partial J_{\rm T}}{\partial t} + \tau_{\rm T} \beta \bar{u} \frac{\partial J_{\rm T}}{\partial x} = -D_{\rm T} \frac{\partial c}{\partial x} + l_{\rm T}^2 \frac{\partial^2 J_{\rm T}}{\partial x^2}, \tag{9.17}$$

where \bar{u} is the mean velocity in the direction of the flow, c the concentration, β a phenomenological coefficient, and $\tau_{\rm T}$ the characteristic relaxation time (of the order of t_c used in (9.14)). This relation contains relaxational and non-local terms—analogous to other generalized transport equations as the Guyer–Krumhansl equation for the heat flux—and includes, besides, a new term (the third term on the left-hand side) which describes a transient anisotropic dispersion due to the fact that the solute disperses differently down-flow and up-flow. For long times and relatively homogeneous situations, this equation reduces to $J_{\rm T} = -D_{\rm T}(\partial c/\partial x)$, i.e. the Fick's equation written in terms of Taylor's effective diffusion coefficient.

Substitution of (9.17) into the solute balance equation results in

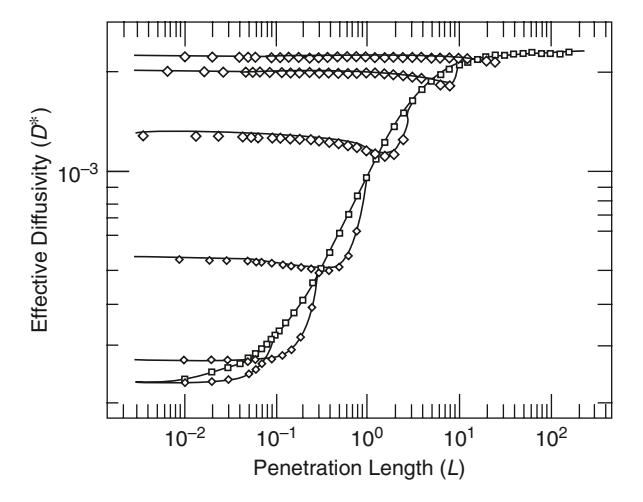
$$\tau_{\mathrm{T}} \frac{\partial^{2} c}{\partial t^{2}} + \frac{\partial c}{\partial t} + \tau_{\mathrm{T}} \beta \bar{u} \frac{\partial^{2} c}{\partial x \partial t} - (\tau_{\mathrm{T}} D_{\mathrm{m}} + l_{\mathrm{T}}^{2}) \frac{\partial^{3} c}{\partial x^{2} \partial t} \\
= D \frac{\partial^{2} c}{\partial x^{2}} + \tau_{\mathrm{T}} \beta \bar{u} D_{\mathrm{m}} \frac{\partial^{3} c}{\partial x^{3}} + l_{\mathrm{T}}^{2} D_{\mathrm{m}} \frac{\partial^{4} c}{\partial x^{4}}.$$
(9.18)

The results for the effective diffusion coefficient as a function of time, derived from this equation are plotted in Fig. 9.2. It is seen that it changes from the molecular diffusion coefficient at short times to the Taylor's diffusion coefficient at long times, and gives the value of the effective diffusion coefficient at all intermediate times.

9.3.2 Evolution of Effective Diffusion Coefficient: From Reversible to Irreversible Behaviours

Furthermore, the results from (9.18) are compared with a numerical simulation of a Taylor's dispersing flow between parallel plates (Camacho 1993b) (Fig. 9.2). In this simulated experiment (transmission dispersion simulation), one computes the

Fig. 9.2 Comparison between the theoretical predictions of reference by Camacho (1993b) according to (9.18) (solid lines) and the simulations. Squares and diamonds correspond to transmission and echo simulations, respectively. (Camacho 1993c)



average of the displacements of the particles with respect to the mean convective motion over the simulation distribution $\langle (\Delta x)^2(t) \rangle$ at different points as a function of time, and represents the ratio $\langle (\Delta x)^2(t) \rangle / 2t = D^*(t)$ versus the penetration length of the solute as a whole, given by $L = \langle \Delta x(t) \rangle$; D^* is called the effective dispersion coefficient, as it has the dimensions of a diffusion coefficient and tends asymptotically to D in the long-time limit and it provides a useful generalization of Taylor's results for all time regimes. Other simulations (echo dispersion simulations) consist of letting the system evolve during a time t and suddenly reversing the velocity field and representing again $D^*(t)$ as a function of L. As it could be expected, if the flow reversal is produced at very short times, most of the solute particles are still able to go back to their original position. The longer the time interval they have been carried out by the fluid, however, the more improbable will be that they recover their initial position. The results of the theoretical predictions based on (9.18) are compared with those of the simulations in Fig. 9.2. The agreement is very satisfactory for a wide range of velocities (always in the laminar regime) and therefore it provides an illustration of the transition from reversible short-time behaviour to an irreversible long-time behaviour, an interesting basic topic in generalized transport equations.

9.3.3 Entropy and Entropy Flux: From Exhaustive Information to the Relevant Information

Coefficients $\tau_{\rm T}$, $l_{\rm T}$ and $D_{\rm T}$ appearing in (9.17) are not arbitrary. They may be obtained from an analysis of the behaviour of the Fourier modes of the number particle density, $c_n(x,t)$, the velocity v_n and the fluxes $J_n=\frac{1}{2}c_n(x,t)v_n$, and by relating them to the Taylor flux as $J_{\rm T}=\sum_n J_n$. It was found (Camacho 1993b) that

$$\tau_{\rm T} = \frac{D_{\rm T}}{\langle v^2 \rangle}, \quad l_{\rm T}^2 = \tau_{\rm T} D_{\rm m}, \quad D_{\rm T} = \sum_{n=0}^{\infty} \frac{1}{2} v_n^2 \tau_n,$$
(9.19)

where the time spectrum τ_n (τ_n is the relaxation time of the *n*th mode J_n of the diffusion flux) is given by $\tau_n = (n^2 \pi^2 D/l^2)^{-1}$ and depends on the kind of hydrodynamic flow. The reader interested in further details is referred to Camacho (1993b).

For the sake of illustration, and for the interest from a thermodynamic perspective, we show that the non-equilibrium entropy incorporating the contribution of the fluxes and its relation with the evolution equation for the diffusion flux are in total agreement with extended irreversible thermodynamics and how they summarize the essentially relevant physical information coming from the elimination of irrelevant degrees of freedom. Indeed, according to EIT, the entropy is given by

$$s = s_{\text{eq}} - \sum_{n=1}^{\infty} \frac{1}{2} \alpha_n J_n \cdot J_n,$$
 (9.20)

and the entropy flux is given by

$$J^{s} = -\frac{\mu}{T}J - \frac{1}{2}\sum_{n,m=1}^{\infty} \alpha_{mn}J_{m} \cdot J_{n} - \sum_{n=1}^{\infty} \delta_{n}P_{n} \cdot J_{n}, \tag{9.21}$$

where J is the total particle flux, namely $J = J_m + J_T$, and P_n denotes the flux of J_n , whereas α_{mn} and δ_n are coefficients independent of the fluxes.

In order to corroborate expressions (9.20) and (9.21) from a more detailed point of view, Camacho started from the relation between entropy and concentration at a given point x, y, at time t,

$$s(x, y, t) = -kC(x, y, t)[\ln C(x, y, t) - 1]. \tag{9.22}$$

Here C(x, y, t) is the concentration at point x, y at time t. We are not interested in such a detailed description, but only in the behaviour of the concentration c(x, t) averaged over y. Therefore we are faced with the problem of the reduction of variables without losing the essential observable information. It is useful to express C(x, y, t) in terms of its Fourier components over the transverse direction as C(x, y, t) = c(x, t) $(1+\phi)$, with ϕ given by

$$\phi(x, y, t) = \frac{1}{c(x, t)} \sum_{n=1}^{\infty} c_n(x, t) \cos \frac{n\pi y}{d},$$
(9.23)

with d the width of the duct and c_n the corresponding Fourier component. After introducing (9.23) into (9.22) one obtains

$$s(x,t) = -kc(x,t)[\ln c(x,t) - 1] - kc(x,t) \int_0^d \frac{\mathrm{d}y}{d} (1+\phi) \ln(1+\phi). \tag{9.24}$$

The first term is the local-equilibrium entropy corresponding to the averaged concentration. When ϕ is small, i.e. when the transverse inhomogeneities are

small compared to the average value, the second-order expansion of the logarithm yields

$$s(x,t) - s_{eq}(x,t) = -\frac{1}{2}kc(x,t) \int_0^d \frac{dy}{d} \phi^2.$$
 (9.25)

Finally, substituting (9.22) into (9.24) and using $J_n = c_n v_n$, with J_n and v_n the corresponding Fourier components of J and v, one obtains

$$s - s_{\text{eq}} = -\frac{1}{4} \frac{k}{c(x,t)} \sum_{n=1}^{\infty} c_n^2 = -\frac{k}{c(x,t)} \sum_{n=1}^{\infty} \frac{1}{v_n^2} J_n^2.$$
 (9.26)

Therefore, we may identify

$$\alpha_n = \frac{k}{c(x,t)} \frac{2}{v_n^2}.\tag{9.27}$$

This approach confirms that the elimination of the transverse degrees of freedom gives a contribution to the entropy which is related to the fluxes. The situation has some similarity with that found in Chap. 3 in the kinetic theory of gases, where the elimination of the fast degrees of freedom in non-equilibrium contributes as a term additional to the local-equilibrium entropy.

Analogously, the non-equilibrium contributions to the entropy flux may be obtained by following a similar path by starting from the expression for the entropy flux in the bidimensional space, where

$$J_{x}^{s}(x, y, t) = s(x, y, t)v(x, y, t) - \mu(x, y, t)T^{-1}J_{\text{mol},x}.$$
 (9.28)

By expanding s, v, and J in terms of the Fourier components, one obtains expression (9.21) with

$$\alpha_{mn} = \frac{k}{c(x,t)} \frac{v_{m+n} + v_{m-n}}{v_m v_n}, \quad \delta_n = \frac{k}{c(x,t)} \frac{2}{v_4^2}.$$
 (9.29)

Thus, in this section the thermodynamic framework of EIT has been used to formulate a generalised hydrodynamics describing the relevant one-dimensional features of the matter transport along the flow, by capturing the relevant aspects of the transversal transport. Interesting generalizations of this procedure may be found in Berentsen and Kruijsdijk (2008) and Hamdan et al. (2008). This is of much practical interest because there are many situations where the length of the duct (tubes, arteries, veins) is not enough to reach the dispersion regime, and therefore a description for short and intermediate times is extremely useful.

9.4 Anomalous Diffusion and Non-equilibrium Thermodynamics

Anomalous diffusion is an interesting stochastic transport phenomenon in which the root-mean-square characteristic value of the displacement of the particles, which in classical diffusion grows proportionally to *t* in the long-time limit, behaves as

$$\langle (\Delta x)^2 \rangle \propto t^{\sigma},$$
 (9.30)

with $\sigma \neq 1$. If $\sigma = 1$ one recovers the usual diffusion and the behaviour for $\sigma < 1$ or $\sigma > 1$ is called subdiffusive or superdiffusive, respectively. This kind of behaviour is found, for instance, in diffusion in fractal spaces, transport in chaotic dynamics, flow in porous media, solid-on-solid surface growth, spreading of thin liquid films, particle diffusion in fluctuating magnetic fields, and, in general, in systems with a complex underlying microstructure (Bouchaud and Georges 1990; Schlesinger et al. 1993, 1995; Klages et al. 2008).

From a microscopic perspective, anomalous diffusion does not correspond to a classical Brownian motion but to Lévy flights, for superdiffusive systems. There are two main ways to derive dynamical behaviours leading to anomalous diffusion: one of them is to use the formalism of fractional derivatives, either temporal or spatial; the other one is to resort to a nonconventional statistical description, which takes into account our limited knowledge of the complexities of the microscopic structure. The dynamic aspects of diffusion leading to (9.30) have received much interest but, in contrast, the analysis of its thermodynamics aspects has been very scarce (Alemany and Zanette 1994; Zanette and Alemany 1995; Compte and Jou 1996; Frank 2002). We have proposed a thermodynamic model for anomalous diffusion which uses nonstandard nonadditive entropies, as the so-called Tsallis entropy, Renyi entropy, or the Sharma–Mittal entropy, which extend the classical thermodynamic formalism.

9.4.1 Classical Irreversible Thermodynamics and Diffusion

First, we recall the classical formalism of diffusion in the framework of non-equilibrium thermodynamics, in which one starts from the usual definition for entropy as applied to a continuous distribution function P(x, t):

$$S(t) = -k_{\rm B} \int P(x,t) \ln P(x,t) \mathrm{d}^{N} x, \qquad (9.31)$$

where x is the position in an N-dimensional space (for instance, the phase space, or the actual space). By taking the continuity equation $\partial P/\partial t = -\nabla \cdot J$ and

assuming, as is usual in classical irreversible thermodynamics, a linear relation between the diffusion flux J and the thermodynamic force $\nabla(\partial S/\partial P)$ in the form

$$J = L\nabla \frac{\partial S}{\partial P},\tag{9.32}$$

with L a transport coefficient, the following diffusion equation follows

$$\frac{\partial P}{\partial t} = k_{\rm B} \nabla (L \nabla \ln P). \tag{9.33}$$

Note that if an external force $F_{\rm ext}$ was acting on the system, a convective contribution of the form $\tilde{\mu}F_{\rm ext}P$ should be added to (9.32), with $\tilde{\mu}$ being the mobility, i.e. with $\tilde{\mu}F_{\rm ext}$ giving the drift velocity produced by the external force. In this case, (9.33) would have the corresponding additional term and would become the Fokker–Planck equation. Coming again to the purely diffusive situation, it is usually assumed that the transport coefficient L in (9.32) is a constant times the distribution function P, namely, $L = (D/k_{\rm B})P$. By using this relation one may finally cast (9.33) in the more familiar form of a diffusion equation

$$\frac{\partial P}{\partial t} = D\nabla^2 P,\tag{9.34}$$

with D the corresponding diffusion coefficient. More general equations could be obtained with other choices.

9.4.2 Non-conventional Statistical Mechanics

Anomalous diffusion is usually found, as it has already been mentioned, in systems with complex microstructures, such as fractal and porous media, polymer networks, micelles, and so on. It has been proposed that a convenient way to deal with systems with some hidden structure, implying that the researcher is unable to satisfy Fisher's criteria for efficiency and sufficiency in statistics, is to resort to non-conventional statistical mechanics which, among other features, are not additive and contain an adjustable power index, which must be obtained experimentally, and which depends on the dynamics, fractality, geometry, dimensions, thermodynamic state and the experimental protocols (Luzzi et al. 2002). This choice modifies the relative statistical weight of the different microscopic states with respect to their weight in conventional statistical physics. For instance, in a fractal underlying structure there will be an accumulation of microscopic states at small length scales: if a cut-off length scale is used, the number of "hidden" states below such a scale will be relevant, but it will not be directly described by a conventional statistical description in the space of states truncated by the limitations of the experimental accessibility. There is a

large family of such non-conventional statistics: one of the first ones to be proposed was Renyi's entropy, defined as

$$S_q^{\rm R} \equiv \frac{k_{\rm B}}{1 - q} \ln \left[\int P^q(x, t) \mathrm{d}^N x \right],\tag{9.35}$$

where q is a constant parameter; this entropy reduces to the Boltzmann one for $q \to 1$.

Another current non-standard thermodynamic formalism uses the Tsallis entropy, defined as

$$S_q(t) = -\frac{k_{\rm B}}{1 - q} \int P(x, t) l \left[1 - P^{q-1}(x, t) \right] d^N x, \tag{9.36}$$

where q is a constant parameter. For a system with a discrete set of possible states, the Tsallis entropy is written as

$$S_q = -\frac{k_{\rm B}}{1 - q} \left(1 - \sum_i p_i^q \right) = -\frac{k_{\rm B}}{1 - q} \sum_i p_i \left(1 - p_i^{q - 1} \right). \tag{9.37}$$

This generalised entropy, proposed by Tsallis (1995, 1999) and Tsallis et al. (1995) on the basis of multifractal analysis, reduces to Boltzmann's one in the limit when q tends to 1, as it may be easily seen by applying the L'Hôpital rule to (9.37). In this case, (9.37) tends to

$$S = -k_{\rm B} \sum_{i} p_i \ln p_i \tag{9.38}$$

or, in continuous terms, (9.36) tends to (9.31).

In contrast with the Boltzmann entropy, generalized entropies are not extensive. Indeed, if one has two independent systems (1) and (2) described, respectively, by the set of probabilities $p_i^{(1)}$ and $p_i^{(2)}$ it is easy to check that the total entropy of the system (1)+(2) is not the sum of the entropies of systems (1) and (2). In particular, and for the sake of illustration, in the Tsallis entropy (9.37), assuming that the value of the parameter q is the same for both systems, its value for the total system composed of subsystems (1) and (2) is

$$S_{\text{tot}} = S_q^{(1)} + S_q^{(2)} + \frac{1 - q}{k_{\text{B}}} S_q^{(1)} S_q^{(2)}. \tag{9.39}$$

Thus, 1-q is a measure of the lack of extensivity. It has been shown that the generalised thermodynamic formalism based on the Tsallis entropy is consistent with positivity, concavity (if q > 0), or convexity (if q < 0), irreversibility (*H*-theorem), and the Legendre-transformation framework of standard thermodynamics. Furthermore,

it is also consistent with the fluctuation-dissipation theorem, the Onsager reciprocity relations, and other relevant properties linking thermodynamics and statistical physics in non-equilibrium situations (Tsallis 1995, 1999; Tsallis et al. 1995).

Since one of the essential differences between unconventional entropies and Boltzmann entropy is the non-extensive (or non-additive) character of the former, it may be expected that it will play a relevant role in situations where non-additivity should be expected, i.e. when some long-range interactions are essential, as in self-gravitating systems and in systems with long correlations. Indeed, it has been shown that Tsallis entropy, by means of an adequate variational principle, makes it possible to find sensible distribution functions for stellar polytropes or to reproduce the distribution of the velocities of galaxies in clusters of galaxies, while the use of Boltzmann entropy yields unphysical distributions.

A different situation exhibiting long-range correlations arises in anomalous diffusion. Indeed, from a microscopic point of view, anomalous diffusion may be described, for instance, by random walks exhibiting either a long-tailed waiting time distribution or a long-tailed distribution of jump lengths, the paradigmatic situation in discrete time being the so-called Lévy flights, which are random motions without any defined spatial scale (Schlesinger et al. 1995; Metzler and Klafter 2000; Klages et al. 2008). Indeed, it turns out that the set of points visited by the random walker is self-similar, i.e. fractal. Thus, from this perspective, it is logical to seek a relation between unconventional entropies and anomalous diffusion.

9.4.3 Generalized Thermodynamics and Anomalous Diffusion

Here, we propose a thermodynamic model for anomalous diffusion based on Tsallis entropy (Compte and Jou 1996). There are some parallels between this idea and extended irreversible thermodynamics. In the latter, the introduction of memory and non-local effects in the transport equations implies non-equilibrium contributions to the entropy. Here, we inquire whether anomalous diffusion, which modifies the usual transport equation for diffusion, may also be related to some modifications of the entropy.

By analogy with the classical formalism presented in Sect. 9.4.1, we write the flux of probability in this generalised Tsallis thermodynamic formalism as

$$J = L\nabla \frac{\partial S_q}{\partial P} = \frac{k_{\rm B}q}{1 - q} L\nabla P^{q-1}.$$
 (9.40)

Introduction of (9.40) into the conservation equation for the probability yields

$$\frac{\partial P}{\partial t} = \frac{k_{\rm B}q}{1-q} \nabla (L \nabla P^{q-1}). \tag{9.41}$$

The corresponding entropy production may be found by evaluating the time derivative of the generalised entropy, namely

$$\frac{\mathrm{d}S_q}{\mathrm{d}t} = \frac{k_{\mathrm{B}}q}{1-q} \int P^{q-1}(x,t) \frac{\partial P}{\partial t} \mathrm{d}^N x. \tag{9.42}$$

By introducing (9.41), integrating by parts, and assuming that the surface term vanishes, one obtains

$$\frac{\mathrm{d}S_q}{\mathrm{d}t} = \left(\frac{k_{\mathrm{B}}q}{1-q}\right)^2 \int L(\nabla P^{q-1})^2 \mathrm{d}^N x. \tag{9.43}$$

Therefore, the entropy production in this formalism is positive definite, as it should be.

We note that, since in classical irreversible thermodynamics L depends on P as $L=DP/k_{\rm B}$, with D a constant, we are led to the possibility of a dependence for L on P as $L=DP^{\alpha}/k_{\rm B}$. For $\alpha=1$ one recovers the classical situation and for $\alpha\neq 1$ anomalous effects are introduced. A concentration-dependent diffusivity of this form has been proposed, for instance, for fractal diffusion, particle diffusion across magnetic fields and for the motion of a polytropic gas in porous media. Thus, anomalous diffusion may have thermodynamic contributions (due to $q\neq 1$) and dynamical contributions ($\alpha\neq 1$).

Introducing this expression for L into (9.41) we obtain the following diffusion equation which generalizes the classical one (9.34)

$$\frac{\partial P}{\partial t} = D \frac{q}{\alpha + q - 1} \nabla^2 P^{\alpha + q - 1}.$$
 (9.44)

This non-linear equation, which is sometimes referred to as the "porous media equation" (Vázquez 2007), as it was proposed in 1937 to describe the flow of water or oil in porous media, has been thoroughly studied in several mathematical publications. In N dimensions, the solutions are of the form

$$P(x,t) = t^{-\mu} f(xt^{-\mu/N}), \tag{9.45}$$

$$\mu = \frac{N}{N(q + \alpha - 2) + 2}. (9.46)$$

Thus, their characteristic scaling is easily seen to correspond to anomalous diffusive behaviour. To check that (9.45) leads to behaviour (9.30) we examine it with more detail. First of all, it must be commented that, since in some cases the second moments of (9.45) are divergent, we focus our attention on the measure of the radius

r(t) of the sphere which contains a given fraction β <1 of the total probability, defined as

$$\int_{0}^{r(t_0)} P(|x|, t_0) \,\Omega_N |x|^{N-1} \mathrm{d}|x| = \beta, \tag{9.47}$$

where Ω_N is the surface of N-dimensional sphere of unitary radius. Then, we consider the variation of (9.47) with time, for the change of variable

$$x' = \left(\frac{t}{t_0}\right)^{-\mu/N} |x|. \tag{9.48}$$

This leads to

$$\int_{0}^{(t/t_0)^{-\mu/N} r(t)} P(x', t_0) \Omega_N x'^{N-1} dx' = \beta.$$
 (9.49)

Comparison of (9.47) and (9.49) leads to the conclusion that

$$r(t) = \left(\frac{t}{t_0}\right)^{\mu/N} r(t_0),\tag{9.50}$$

independently of β . Thus, it is recognized the anomalous diffusive scaling

$$r \sim t^{\sigma/2},\tag{9.51}$$

with

$$\frac{\sigma}{2} = \frac{\mu}{N} = \frac{1}{N(q + \alpha - 2) + 2}. (9.52)$$

Then, $\sigma > 1$ (superdiffusion) if $q + \alpha < 2$, and $\sigma < 1$ (subdiffusion) for $q + \alpha > 2$. This expression shows that indeed both thermodynamic factors (q) and dynamic effects (α) may contribute to the anomalous diffusion, and that it reduces to the classical situation for $q = \alpha = 1$, in which case the classical Boltzmann entropy is recovered.

It is interesting to see that anomalous diffusion seems to require a modification of the classical entropy, in analogous way as memory and non-local effects require to modify the classical entropy in extended irreversible thermodynamics. Of course, in the present example it is not clear whether one is forced to modify the entropy $(q \neq 1)$ or if it is sufficient to assume a non-linear dynamical law without modifying the entropy $(q = 0 \text{ but } \alpha \neq 1)$. Frank (2002) has studied with more generality the relation between anomalous diffusion and several forms of generalized entropies in the framework of a generalized Fokker–Planck equation. It is interesting to note that the stationary solution of (9.44) maximize some unconventional entropies, as Tsallis' or Renyi's ones, thus adding a further relationship between thermodynamics and diffusion.

For an initial delta distribution, the solution of (9.44) is

$$P(x,t) = bt^{-\mu} (a^2 - x^2 t^{-2\mu/N})^{1/(q+\alpha-2)}$$
 for $q + \alpha > 2$, (9.53a)

$$P(x,t) = bt^{-\mu} \left(\frac{1}{a^2 + x^2 t^{-2\mu/N}} \right)^{1/(2-q-\alpha)} \quad \text{for} \quad 2\frac{N-1}{N} < q + \alpha < 2, \quad (9.53b)$$

where

$$b = \left\{ \frac{|q + \alpha - 2|}{2Dq[N(q + \alpha - 2) + 2]} \right\}^{1/(q + \alpha - 2)}, \tag{9.54}$$

with μ given by (9.46) and a a constant (depending on q and α) to be determined by normalization. These solutions correspond respectively to the subdiffusion and super-diffusion. These solutions generalise the standard Gaussian profile of classical diffusion for an initial delta profile.

9.5 Anomalous Diffusion in Flowing Systems

In this chapter we have been paying a special attention to the influence of inhomogeneous flows on diffusion (Compte et al. 1997a). In this section, we will generalize the previous analysis to anomalous diffusion. In the presence of a velocity distribution, we would have, instead of (9.44),

$$\frac{\partial P}{\partial t} + \nabla \cdot (P\mathbf{v}) = \frac{Dq}{\alpha + q - 1} \nabla^2 P^{\alpha + q - 1} = D' \nabla^2 n^{\gamma}. \tag{9.55}$$

In the last equality we have used $D' \equiv Dq(\alpha + q - 1)^{-1}$ and $\gamma \equiv \alpha + q - 1$, to have a more compact notation. To solve (9.55), we assume that the physical solution for an initial delta distribution has the form

$$P(x,t) = B(t) \left[1 + \frac{1 - \gamma}{2} (x - \bar{x}) \cdot \zeta^{-1}(t) \cdot (x - \bar{x}) \right]. \tag{9.56}$$

The functions B(t) and $\zeta(t)$ must be determined by substituting (9.56) into (9.55), which yields the following differential equations

$$\frac{\mathrm{d}B}{\mathrm{d}t} = -\gamma D' B^{\gamma} \mathrm{Tr} \boldsymbol{\zeta}^{-1} - B \mathrm{Tr}(\mathbf{A}), \tag{9.57}$$

$$\frac{\mathrm{d}\boldsymbol{\zeta}}{\mathrm{d}t} = 2\gamma D' B^{\gamma - 1} \mathbf{U} + \mathbf{A} \cdot \boldsymbol{\zeta} + [\mathbf{A} \cdot \boldsymbol{\zeta}]^{T}, \tag{9.58}$$

with **A** describing the velocity profile as $v = A \cdot x$. Furthermore, we will demand P(x, t) to be normalized throughout the evolution. This yields the condition

$$\frac{2\pi^{N/2}}{\Gamma(N/2)}\sqrt{\det \boldsymbol{\sigma}}B\left[\frac{1}{2}(1-\gamma)\right]^{-N/2}\int_0^\infty r^{N-1}(1+r^2)^{1/(q-1)}\mathrm{d}r = 1. \quad (9.59)$$

This gives an additional relation between the functions B(t) and $\zeta(t)$. A direct computation leads for the second moments of the displacements to the relation

$$\langle xx \rangle = \left[1 + \frac{1}{2}(N+2)(\gamma-1) \right]^{-1} \zeta.$$
 (9.60)

Thus, by solving $\zeta(t)$ from (9.57), (9.58), and (9.59) we directly obtain $\langle x^2 \rangle$ as a function of time. In particular, for N=2, (9.59) yields $B(t) = (\gamma/2\pi)(\det \zeta^{-1})^{1/2}$, which, when introduced into (9.56), allows us to obtain $\zeta(t)$. When one takes for the velocity distribution a pure shear, as in bidimensional Couette flow, namely

$$\mathbf{A} = \begin{pmatrix} 0 & 0 \\ \dot{\gamma} & 0 \end{pmatrix}, \tag{9.61}$$

one is led, after rather cumbersome calculations, to the asymptotic behaviour (Compte et al. 1997)

$$\langle x^2 \rangle \propto t^{2\sigma+1}, \quad \langle y^2 \rangle \propto t^{2\sigma-1}, \quad \langle xy \rangle \propto t^{2\sigma},$$
 (9.62)

with

$$\sigma = \frac{1}{\gamma} = \frac{1}{\alpha + q - 1}.\tag{9.63}$$

In the classical situation ($\sigma = 1$) one recovers the classical results for diffusion under shear flow mentioned in the introduction, namely, that $\langle x^2 \rangle \sim t^3$ whereas $\langle y^2 \rangle \sim t$.

An alternative way to describe anomalous diffusion instead of the non-linear Eq. (9.44) is to use fractional derivatives for time or space, such as

$$\frac{\partial^{\alpha} u}{\partial t^{\alpha}} = D\nabla^2 u,\tag{9.64}$$

$$\frac{\partial u}{\partial t} = D\nabla^{2\mu}u,\tag{9.65}$$

where $\partial^{\alpha}/\partial t^{\alpha}$ stands for the Riemann–Liouville fractional derivative of order α , and $\nabla^{2\mu}$ is defined as the inverse Fourier transformation of $-k^{2\mu}$. Equation (9.65) leads to a solution of the form $x^2 \sim t^{1/\mu}$.

The modifications of the exponents due to the shear flow would be different if, instead of starting from (9.44)—namely using (9.55)—, models based on fractional

time or space derivatives were used. For instance, when a plane shear flow is added to (9.65), namely, when one writes

$$\frac{\partial u}{\partial t} + \dot{\gamma} y \frac{\partial u}{\partial x} = D \nabla^{2\mu} u, \tag{9.66}$$

the solution becomes

$$\langle x^2 \rangle \sim t^{(1+2\mu)/\mu}.$$
 (9.67)

Thus, the influence of a shear leads to different modifications for $\langle x^2 \rangle$ in the descriptions (9.44) or (9.65). If in quiescent systems one has $\langle x^2 \rangle \sim t^{\nu}$, in shear flows (9.44) leads to $\langle x^2 \rangle \sim t^{2\nu+1}$, whereas (9.65) leads to $\langle x^2 \rangle \sim t^{\nu+2}$. For classical formalism, with $\nu=1$ both equations result $\langle x^2 \rangle \sim t^3$, as found in Sect. 9.1. However, the presence of the flow does not allow us to discriminate between thermodynamic and dynamic effects, as q and α always appear in the combination $q+\alpha$.

9.6 Taylor Dispersion and Anomalous Diffusion

In an analogous way that a velocity gradient modifies classical diffusion into Taylor dispersion, as it has been seen in Sect. 9.2, we ask for such a coupling in anomalous diffusion. This problem was dealt with by Compte and Camacho (1997) from Levy flight formalism. They start from the fractional diffusion equation of the form

$$\frac{\partial}{\partial t}P(y) = D_{\gamma} \frac{\partial^{1-\gamma}}{\partial t^{1-\gamma}} \frac{\partial^2}{\partial x^2} P(y), \tag{9.68}$$

with $\partial^{1-\gamma}/\partial t^{1-\gamma}$ stands for the Riemann–Liouville fractional derivative of order $1-\gamma$, and D_{γ} is a constant coefficient which generalizes the role of the usual diffusion coefficient to situations with $\gamma \neq 1$.

Their final result is

$$\langle (\Delta x(t))^2 \rangle = \frac{2D_{\gamma}t^{\gamma}}{\Gamma(1+\gamma)} + \frac{2D_{\mathrm{T}}(\gamma)t^{2-\gamma}}{\Gamma(3+\gamma)},\tag{9.69}$$

with

$$D_{\rm T}(\gamma) \equiv \frac{1}{2} \sum_{n=1}^{n} v_n^2 \tau_n, \tag{9.70}$$

a generalized Taylor dispersion coefficient, with v_n the *n*-th Fourier coefficient of $v_n(y)$ and τ_n the decay time of v_n , given by

$$\tau_n = \left(\frac{n^2 \pi^2}{l^2} D_{\gamma}\right)^{-1/\gamma},\tag{9.71}$$

This coefficient involves information on the velocity of the flow and the diffusion constant, and therefore represents a Taylor-like dispersion, because it corresponds to a coupling between advection and transversal diffusion. It is worthy to note that the anomalous Taylor dispersion contribution, i.e. the second term in (9.69), is not diffusive, but it grows as $\langle x^2 \rangle \sim t^{2-\gamma}$.

When $\gamma = 1$ both terms of the right-hand side in (9.69) have the same time dependence and the usual Taylor dispersion behaviour is recovered. When γ tends to zero, the tracer particles essentially follow the velocity profile and the anomalous Taylor dispersion behaves as $\langle v_x^2 \rangle t^2$, i.e. as a ballistic limit. For $\gamma < 1$, i.e. when the behaviour in quiescent systems would be sub-diffusive, the anomalous Taylor dispersion in (9.69) gives a super-diffusive contribution, because the exponent $2-\gamma$ is higher than 1. Analogously, when $\gamma > 1$ (super-diffusive behaviour in quiescent fluids), the anomalous Taylor dispersion would be sub-diffusive. It is surprising to find that for smaller γ , i.e. slower transverse diffusion, the faster is the longitudinal dispersion, but this is not inconsistent, but analogous to the inverse proportionality of the Taylor dispersion coefficient D_T of (9.14).

In (9.69), the dispersion coefficient $D_{\rm T}(\gamma)$ given in (9.70) is basically the same as in standard Taylor dispersion, but with the generalized coefficient D_{γ} replacing the usual diffusion coefficient D. Thus (9.69) may be rewritten in a form closer to (9.12) as

$$\langle x^2 \rangle = \frac{2D_{\gamma}}{\Gamma(1+\gamma)} t^{\gamma} + \frac{2\alpha_{\gamma}}{\Gamma(3-\gamma)} \frac{\langle v_x^2 \rangle d^2}{D_{\gamma}} t^{2-\gamma}, \tag{9.72}$$

with a_{γ} a constant depending on the velocity distribution characterizing the flow, $\langle v_x^2 \rangle$ the mean square velocity and d the width of the channel.

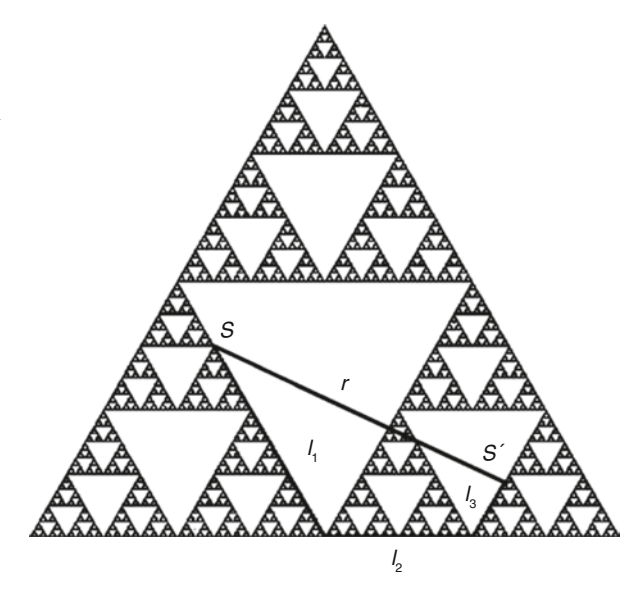
9.7 Diffusion on Fractals

In this last section, we complement the overview on non-Fickian diffusion by describing some recent approaches to diffusion in fractals; these approaches illustrate in an explicit way the relation between the fractal geometry of the space and the dynamics of diffusion. Fractals are geometric structures whose main characteristic is self-similarity in space. Mathematically, this easily connects with the idea of scale-invariance and power law scaling. From a formal point of view, one can define a fractal as a structure with a non-integer Hausdorff dimension. If M denotes the mass of the fractal (provided that the density is constant) then it is proportional to $L^{d_{\rm f}}$, where L is the characteristic fractal length and $d_{\rm f}$ is the Hausdorff (or fractal) dimension.

For random-walks on fractals one empirically finds that the mean square displacement follows asymptotically a scaling $\langle r^2 \rangle \sim t^{2/d_{\rm w}}$, where r is the distance from the origin of the walk and $d_{\rm w}$ is known as the random walk fractal dimension. This clearly departs from the scaling expected from Fickian diffusion, i.e. diffusion

9.7 Diffusion on Fractals 207

Fig. 9.3 Comparison between the chemical distance $l=l_1+l_2+l_3$ and the Euclidean distance r between two points a and a' of the Sierpinski gasket



on fractals is found to be anomalous. Also, several authors have pointed out the relevant role that the chemical distance l plays in diffusive transport. The chemical distance is defined as the distance of the shortest path within the fractal connecting two given points (see Fig. 9.3). The chemical and Euclidean distances are related by the fractal dimension of the minimum path d_{\min} , which is defined through the scaling $l \sim r^{d_{\min}}$.

So, $d_{\rm P}$ $d_{\rm w}$ and $d_{\rm min}$ are the main parameters necessary to understand random-walks on fractals. Of course, it would be desirable to have general relations between them in order to obtain the random-walk exponent $d_{\rm w}$ as a function of the geometrical dimensions $d_{\rm f}$ and $d_{\rm min}$. However, such relations are only known for very specific kinds of fractals (for example, for 1D topological fractals one has $d_{\rm f} = d_{\rm min} = \frac{1}{2} d_{\rm w}$ (Bunde and Havlin 1991), so at practice all the three parameters must be considered independently in order to formulate a model for transport in fractals.

For many years, the form of the probability distribution function (empirically obtained from random-walk simulations and from scaling arguments) was accepted to follow the scaling relation

$$P(r,t) \sim t^{-d_{\rm f}/d_{\rm w}} \exp\left[-c\left(\frac{r}{t^{1/d_{\rm w}}}\right)^{\frac{d_{\rm w}}{d_{\rm w}-1}}\right],\tag{9.73}$$

where c is a positive constant. Mosco (1997) considered an alternative approach and introduced an intrinsic metric for fractals, defined by

$$s \equiv r^{d_{\rm w}/2},\tag{9.74}$$

where *s* is the intrinsic distance (O'Shaugnessy and Procaccia 1995). Using scaling arguments in the intrinsic metrics he found

$$P(r,t) \sim t^{-d_{\rm f}/d_{\rm w}} \exp \left[-c \left(\frac{r}{t^{1/d_{\rm w}}} \right)^{\frac{d_{\rm w}d_{\rm min}}{d_{\rm w}-d_{\rm min}}} \right], \tag{9.75}$$

which can be viewed as a generalization of (9.73). Note that the parameter d_{\min} was not taken into account in the result (9.73). It must be stressed that for most fractal structures d_{\min} takes values equal or very close to 1, so in those cases the relation (9.73) is recovered from (9.75).

Now, the question remains of how to build a diffusion model able to account for the characteristics above for diffusion on fractals. One of the first attempts to solve this problem was given by O'Shaugnessy and Procaccia (1995), even before the results (9.73) or (9.75) had been derived (Mosco 1997). They proposed a generalized diffusion equation in a $d_{\rm F}$ -dimensional space which reads

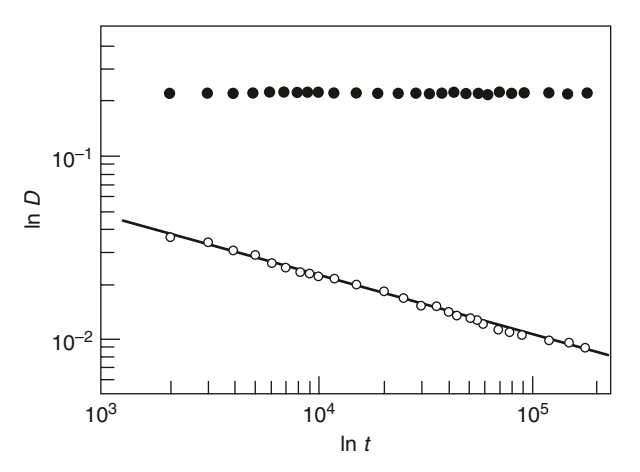
$$\frac{\partial P}{\partial t} = \frac{1}{r^{d_{\rm f}-1}} \frac{\partial}{\partial r} \left[D(r) r^{d_{\rm f}-1} \frac{\partial P}{\partial r} \right]. \tag{9.76}$$

D(r) here represents a generalized diffusion coefficient, and the scaling $D(r) \sim r^{2-d_w}$ was considered in order to recover the asymptotic behaviour $\langle r^2 \rangle \sim t^{2/d_w}$. Equation (9.76), however, cannot reproduce the probability density (9.75). Hence, several generalizations and approaches were conducted in the following years. In most cases, partial differential equations based on fractional derivatives were proposed in order to fit the behaviour required. However, there has been increasing evidence that equations based on fractional calculus are not appropriate to describe anomalous transport due to an underlying self-similar structure. Specifically, many diffusion equations with fractional derivatives are known to arise from models based on Continuous-Time Random Walks (Metzler and Klafter 2000). In this case, particles performing a random walk in a homogenous media experience very long waiting times (distributed according to a power-law decay) between consecutive jumps, leading to ergodicity breaking in the system. On the contrary, anomalous diffusion arising from heterogeneous or fractal media is known to be ergodic, which makes a clear difference between both situations. A way to reconcile the result (9.75) with the original approach by O'Shaugnessy and Procaccia (1995), without the need of fractional calculus, has been found by Campos, Méndez and Fort (2004). Using the idea of the intrinsic metrics proposed by Mosco, they assumed that the Eq. (9.76) should be correct if written in terms of the intrinsic distance s instead of r. When transformed to the Euclidean metrics r, their approach leads then to the diffusion equation

$$\frac{\partial P}{\partial t} = \frac{4D_0}{dw^2 r^{d_f - 1}} \frac{\partial}{\partial r} \left[\left(\frac{r}{t^{1/d_w}} \right)^{\frac{d_w^2 - 2d_w d_{\min}}{dw - d_{\min}}} r^{d_f - d_w + 1} \frac{\partial P}{\partial r} \right], \tag{9.77}$$

9.7 Diffusion on Fractals

Fig. 9.4 Time dependence of the diffusion coefficient for a percolation cluster in a 2D square lattice (open circles) in comparison with the results obtained for a homogeneous lattice (full circles). The solid line represents the theoretical scaling predicted by (9.78). (Campos et al. 2004)



whose exact point-source solution coincides with the result (9.73), and D_0 is a constant. Note that the main ingredient introduced in this approach is a space and time-dependent diffusion coefficient. This is made evident from the constitutive relation

$$J(r,t) = D(r,t)\frac{\partial P}{\partial r} = \frac{4D_0}{d_w^2} \left(\frac{r}{t^{1/d_w}}\right)^{\frac{d_w^2 - 2d_w d_{\min}}{d_w - d_{\min}}} r^{d_f - d_w + 1} \frac{\partial P}{\partial r}.$$
 (9.78)

To validate the model, they verified through random-walk simulations that Eq. (9.78) was fulfilled for several fractals. In Fig. 9.4 it is shown that the generalized diffusion coefficient for a random-walk on a 2D percolation cluster follows a power-law decay, with an exponent very close to the value $(2d_{\rm min}-d_{\rm w})/(d_{\rm w}-d_{\rm min})=-0.35$ predicted by (9.78).

Subsequently, Eq. (9.77) has been also used to explain satisfactorily propagation (front-like) processes on fractals (Méndez et al. 2004) with applications, for example, in the field of human migrations (Hamilton and Buchanan 2007), or in ecological and biomedical applications, and in reaction-transport systems (Méndez et al. 2010).

Chapter 10 Chemical Reactions and Polymer Degradation Under Flow

In Chaps. 6 and 8 we analysed some of the consequences of the non-equilibrium modifications of the chemical potential on the phase diagram of dilute polymer solutions and in shear-induced diffusion. It is logical to ask what are the consequences of such modifications in another situation where the chemical potential plays a crucial role, namely, chemical reactions. This is the aim of this chapter, where we deal with a thermodynamic description of polymer degradation under shear. This macroscopic study is complemented with a microscopic analysis of the modifications of the chemical equilibrium constant for reactions of dilute gases under shear on the basis of the kinetic theory.

In this analysis, a situation is found which is analogous to that studied in Chap. 7 in reference to the relation between dynamic and thermodynamic points of view. Here, we derive from the thermodynamic basis the equilibrium constant in the presence of a shear flow, without reference to the kinetic mechanisms. A more detailed point of view would take into account how the kinetic constants characterizing the direct and reverse elementary reactions are modified by the shear rate. This would allow one to obtain as a particular case the equilibrium constant under shear and, furthermore, it would describe how the kinetic details are modified.

Thus, it is clear that the kinetic approach is wider in scope than the thermodynamic one but, on the other hand, it requires more effort and its results are less general, i.e. they depend in a more crucial way on the particular microscopic model, than the thermodynamic approach. This is not surprising, as the same situation is found in equilibrium, where kinetic analyses are more detailed but less general than thermodynamic results. To compare both approaches, we have used here the thermodynamics in the analysis of shear-induced polymer degradation, whereas we have outlined the kinetic approach for reactions in ideal gases under shear flow.

10.1 Thermodynamic Formulation

Let us consider a chemical reaction described by

$$\sum_{k=1}^{r} \nu_k X_k = 0, \tag{10.1}$$

where the X_k denote the different chemical components participating in the reaction and v_k the respective stoichiometric coefficients (which are taken to be positive for the products of the reaction and negative for the reactans). Here, we will consider chemical equilibrium not in a quiescent fluid, as is the usual situation, but in a fluid submitted to an inhomogeneous but steady motion in the presence of a non-vanishing viscous pressure tensor \mathbf{P}^v . To find the condition of chemical equilibrium at constant temperature T, pressure p and viscous pressure \mathbf{P}^v we start from the Gibbs equation (1.29) which yields, for the differential of the Gibbs free energy, the following expression

$$dG = -SdT + Vdp + \sum_{k} \mu_k dN_k + \frac{1}{2} VJ \mathbf{P}^{\nu} : d\mathbf{P}^{\nu}, \qquad (10.2)$$

with J the steady state compliance, as used in (1.32) and in Chaps. 6 and 7. Here, μ_k is the generalised chemical potential of component k, which has been discussed in detail in Sect. 6.2, and which has the form

$$\mu_k(T, p, N_j, \mathbf{P}^{\nu}) = \mu_{k,eq}(T, p, N_j) + \frac{1}{4} \frac{\partial}{\partial N_k} (VJ) \mathbf{P}^{\nu} : \mathbf{P}^{\nu}, \tag{10.3}$$

where $\mu_{k,eq}$ is the usual local-equilibrium chemical potential. We have used this expression at length in Chaps. 6 and 8. The non-equilibrium chemical potential may be written also as

$$\mu_k(T, p, N_j, \mathbf{P}^{\nu}) = \mu_{k,eq}(T, p, N_j) + \mu_k^{(s)}(T, p, N_j, \mathbf{P}^{\nu}),$$
 (10.4)

where the term $\mu_k^{(s)}$ contains the flow contributions of \mathbf{P}^{ν} to the chemical potential. At constant T, p and \mathbf{P}^{ν} , the rate of variation of the generalised Gibbs free energy is

$$\frac{\mathrm{d}G}{\mathrm{d}t} = \sum_{k=1}^{r} \mu_k \frac{\mathrm{d}N_k}{\mathrm{d}t}.$$
 (10.5)

The variations of the different components are not arbitrary, but they are related by the stoichiometry of (10.1). We may express dN_k in terms of the degree of advancement of the reaction ξ (Callen 1960; Kondepudi and Prigogine 1998; Lebon et al. 2008) in the form

$$dN_k = \nu_k d\xi \tag{10.6}$$

and therefore (10.5) may be rewritten as

$$\frac{\mathrm{d}G}{\mathrm{d}t} = \sum_{k=1}^{r} \mu_k \nu_k \frac{\mathrm{d}\xi}{\mathrm{d}t}.$$
 (10.7)

In analogy with the classical theory of non-equilibrium thermodynamics (De Groot and Mazur 1962; Lebon et al. 2008), we define the affinity \mathcal{A} as

$$\mathcal{A} = -\sum_{k} v_k \mu_k. \tag{10.8}$$

Note that in (10.8) the generalised chemical potentials appear instead of the usual local-equilibrium chemical potentials.

According to the second law, the rate of variation of the Gibbs free energy at constant T and p must be definite negative (this is, in fact, equivalent to requiring that the entropy production is definite positive, because the production of free energy is given by minus the product of absolute temperature times the entropy production). This implies restrictions on the possible dependence of the reaction rate $d\xi/dt$ with the affinity \mathcal{A} . In the simplest linear approximation one may write this relation as

$$\frac{\mathrm{d}\xi}{\mathrm{d}t} = -L\mathcal{A},\tag{10.9}$$

with L a kinetic parameter, which must be positive. Since $\mathrm{d}\xi/\mathrm{d}t=0$ when equilibrium is reached, the condition of equilibrium is obtained by setting the affinity $\mathcal A$ equal to zero

$$\mathcal{A} = -\sum_{k} v_k \mu_k = 0. \tag{10.10}$$

When A > 0, the reaction will proceed in the direct direction (from reactants to products) and for A < 0 in the reverse direction. For vanishing \mathbf{P}^{v} , the generalised chemical potentials defined by (10.3) reduce to the local-equilibrium chemical potentials and Eq. (10.10) reduces to the well known condition for chemical equilibrium (Callen 1960; Prigogine 1961; de Groot and Mazur 1962; Kondepudi and Prigogine 1998; Gyarmati 1970). For non-vanishing \mathbf{P}^{v} , both the affinity A and the kinetic coefficient L may depend on \mathbf{P}^{v} (Tirrell 1986; Onuki 1997). The dependence of L on \mathbf{P}^{v} is a complicated kinetic problem, and therefore we will restrict our attention to the dependence of the affinity A, which is sufficient to study the equilibrium conditions.

From the expression for the non-equilibrium chemical potential, it is seen that the affinity is affected by the viscous pressure tensor. By imposing the equilibrium condition (10.10) one obtains the relation

$$\prod_{k} a^{\nu_k} = K(T, p)\lambda(T, p, N_j, \mathbf{P}^{\nu}), \tag{10.11}$$

where a_k is the activity, defined in the usual form

$$\mu_{k,\text{eq}} = \mu_{k,\text{eq}}^0(T, p) + RT \ln a_k,$$
(10.12)

with $\mu_{k,eq}^0(T,p)$ the chemical potential corresponding to pure component k at the corresponding standard reference at given T and p. Furthermore, K is the classical equilibrium constant given by

$$\ln K = -\frac{1}{RT} \sum_{k} \nu_k \mu_{k,\text{eq}}^0.$$
 (10.13)

The function λ in (10.11) contains the flow contributions to the chemical potentials, and is given by

$$\lambda = \exp\left\{-\frac{1}{RT} \sum_{j} \nu_{j} \left[\frac{1}{4} \partial(VJ) / \partial N_{j}\right] \mathbf{P}^{\nu} : \mathbf{P}^{\nu}\right\}.$$
 (10.14)

It will act as a correction to the effective equilibrium constant $K_{\rm eff} = \lambda K$ which takes into account the effects of the viscous shear pressure over the fluid and therefore will change the composition of the system at chemical equilibrium.

10.2 Shear-Induced Polymer Degradation: Kinetic Analysis

The flow contributions to the chemical potential are conceptually rather general. However, from the practical point of view, they are usually much higher in polymer solutions than in solutions of small molecules, due to the longer relaxation times for polymers. Therefore, we will concentrate our attention to polymer solutions and, as a concrete example, we will study the shear-induced degradation of polymers, i.e. the increase in the proportion of low-weight macromolecules as a consequence of the shear-induced breaking of the high-weight macromolecules. In order to underline the unity of the thermodynamic description we will take for the chemical potentials the expressions we have used in Chaps. 6–8.

The verification that mechanical stresses may produce the degradation of polymers and the first attempts to explain this phenomenon are due to Staudinger (1932). Since then, the phenomenon of degradation under flow has been studied by assuming that only the bonds between monomeric units are broken, and one of the problems has concerned the position of the breaking point along the macromolecule. Some authors in the 1930s considered that bond reactivity cannot be treated as a random process, because each bond in a macromolecule depends on its particular chemical environment. Some experimental results seem to indicate that in some degradation processes all bonds have a similar breaking behaviour, whereas in some other studies the breaking of macromolecules is produced preferentially in a central position along the chain.

The analysis of polymer degradation is usually undertaken through techniques which are typical of chemical kinetics, which is a methodology which implies some specific reaction mechanism as the basis to set the equations which describe the evolution of the system composition with time (Basedow and Ebert 1975; Basedow et al. 1978; Mark and Simha 1940; Montroll and Simha 1940; Simha 1941; Montroll 1941; Glynn et al. 1972).

A kinetic model has also been the basis of the studies carried out by Nguyen and Kausch (1992) on the mechanical degradation of polymers in transient elongational flows, where degradation is more efficient than in simple shear flows, because in the latter the particle rotates with the flow field and only spends, at each turn, a limited amount of time in high strain-rate regions, whereas in elongational flows the fluid element is in a continued state of dilatation. These authors have studied the evolution of the molecular size distribution during the degradation process starting from the expression of the kinetics describing the rate of bond scission, and have incorporated the spatial distribution and the time dependence of strain-rate in transient flow; their results, as well as a detailed comparison with experimental data, have been reviewed in (Nguyen and Kausch 1992).

The basic hypothesis underlying any kinetic mechanism for polymer degradation is to assume that each chain is broken only at one point (i.e. only two fragments are produced per broken macromolecule). The second hypothesis assumes that each elementary reaction

$$P_j \to P_i + P_{j-i} \tag{10.15}$$

follows a first-order kinetics, i.e.

$$\frac{\mathrm{d}n_i}{\mathrm{d}t} = k_{ji}n_j,\tag{10.16}$$

where n_i and n_j stand for the number of macromolecules with i and j degrees of polymerization, respectively, and k_{ji} is the kinetic constant describing the breaking of a macromolecule with j monomers to give a macromolecule with i monomers and another one with j-i monomers. Finally, the kinetic models assume that k_{ji} depend on the shear rate.

The kinetic model described here has been widely used since the work by Basedow et al. (1978). These authors consider a polydisperse macromolecular system, with r the maximum degree of polymerization, in such a way that the coupling of the degradation reactions is given by the following set of linear differential equations

$$\begin{pmatrix} dn_1/dt \\ \vdots \\ dn_r/dt \end{pmatrix} = \mathbf{A} \cdot \begin{pmatrix} n_1 \\ \vdots \\ n_r \end{pmatrix}, \tag{10.17}$$

where the matrix A of the coefficients has the form

$$\mathbf{A} = \begin{pmatrix} 0 & 2k_1 & k_{31} + k_{32} & \cdot & k_{r1}k_{r,r-1} \\ 0 & -k_{21} & k_{32} + k_{31} & \cdot & k_{r2}k_{r,r-2} \\ 0 & 0 & -\sum_{j=1}^{2} k_{3j} & \cdot & k_{r3}k_{r,r-3} \\ \cdot & \cdot & \cdot & \cdot & \cdot \\ 0 & 0 & 0 & 0 & -\sum_{j=1}^{r-1} k_{rj} \end{pmatrix}, \tag{10.18}$$

according to the reaction mechanism proposed by Simha (1941).

Besides numerical complexities, the solution of the above system is only possible through the classical techniques used in the analysis of differential equations, so that the only (and very non-trivial) problem is to determine the values of the kinetic constants k_{ii} . In the paper by Basedow et al. (1978), three situations are analysed: (1) the simplest one is to assume that all bonds have the same breaking probability, so that the value of k_{ii} is independent of i and j and the macromolecular fragmentation is a random process; (2) a slightly more complicated situation assumes that the kinetic constant depends on the length of the chain which is broken, but not on the length of the ensuing fragments, i.e. the value of k_{ii} depends on i but not on j; (3) the most complicated situation arises when k_{ij} depends on the position of the breaking point; this situation is usually dealt with by assuming that the value of the kinetic constant varies along the chain according to a parabola whose minimum is at the central point of the macromolecule, i.e. one assumes that the bonds near the ends of the chain are more easily broken than those in the central region. A different point of view is to assume that the central bonds are those preferentially broken (Basedow et al. 1978), and to suppose, for instance, that the breaking probability distribution of monomer-monomer bonds is a Gaussian function which has the maximum at the centre of the macromolecule. These conclusions have been experimentally verified on several occasions (Bueche 1960).

Thus, one could make the hypothesis that the kinetic constant for the breaking of any chain is given by a Gaussian function in such a way that k_{ij} is given by

$$k_{ij} = k(i-1)^X \left[\sigma_i (2\pi)^{1/2}\right]^{-1} \exp\left[-1/(2\sigma_1^2)(j-i/2)^2\right],$$
 (10.19)

where the standard deviation σ_i is supposed to be proportional to the length of the chain

$$\sigma_i = R(i-1). \tag{10.20}$$

The parameters R and X appearing in (10.19–10.20) are not known a priori and k is a global kinetic constant describing the breaking of bonds in a global analysis of all the macromolecules in the system, and which may be experimentally determined.

A polymer in solution is usually a polydisperse system, and the number of macromolecules of a given length is commonly given by the molecular weight distribution (MWD), from which one may obtain the set of values n_i . Such values are the solution of the differential equations (10.17–10.18) and, by fitting the subsequent curve with the experimental data, one may obtain the values of R and X.

However, the kinetic mechanism by Simha (1941) and Basedow et al. (1978) does not include the recombination of macromolecules. Therefore, in order that the experimental data are consistent with the results derived from the theoretical model it is necessary to carry out the measurements under conditions where the recombination of the fragments produced in the breaking of other macromolecules is inhibited. A usual technique to achieve this situation is to introduce some scavenger radicals in the system (Henglein 1956), which neutralize the fragments produced in the breaking of the chains. When such recombination inhibitors are not present, the MWD of a sample of polystyrene with a narrow distribution is practically not modified during the degradation, whereas such modification is more conspicuous for wide distributions of the kind of the most probable distribution (Ballauff and Wolf 1984, 1988). We will see below that these conclusions are also found by using a purely thermodynamic model (Criado-Sancho et al. 1994, 1998; Jou et al. 1995).

Therefore, the kinetic mechanism proposed in (10.15) is not the most general one, and we propose to consider it as a particular case of a degradation-combination scheme of the form

$$P_i \rightleftharpoons P_i + P_{i-1}. \tag{10.21}$$

When one considers the equilibrium in the scheme (10.21), one must include the new kinetic constant K_{ji} which corresponds to the recombination of the chains P_i and P_{i-1} and which is related to the chemical equilibrium constant K_{ij} in the usual form

$$K_{ij} = \frac{k_{ji}}{\kappa_{ji}}. (10.22)$$

Furthermore, the kinetic equations in the degradation-combination mechanism are now the non-linear set of differential equations

$$\frac{\mathrm{d}\boldsymbol{n}}{\mathrm{d}t} = [\mathbf{A} - \mathbf{B}(n_1, ..., n_r)] \cdot \boldsymbol{n},\tag{10.23}$$

where n is the column vector appearing on the right-hand-side member of (10.17), **A** is the matrix of coefficients defined in (10.18) and where one has introduced the new matrix

$$\mathbf{B} = \begin{pmatrix} \kappa_{21}n_1 & \kappa_{31}n_1 & \cdot & \kappa_{r1}n_1 & 0 \\ \kappa_{32}n_2 & \kappa_{42}n_2 & \cdot & 0 & 0 \\ \cdot & \cdot & \cdot & \cdot & \cdot \\ \kappa_{r,r-1}n_{r-1} & 0 & \cdot & 0 & 0 \\ 0 & 0 & 0 & 0 & 0 \end{pmatrix}.$$
 (10.24)

Although in the bibliography the effect of the shear rate on the degradation process is considered (Bestul 1956; Ballauff and Wolf 1981, 1984, 1988; Wolf 1987), it is easy to see in the previous expressions that $\dot{\gamma}$ does not appear explicitly in the formalism. One way to include the effects of the shear in the above reaction mechanisms would be to assume that the kinetic constants depend on the shear rate or on the shear viscous pressure. This would yield, as a consequence, a modification of the equilibrium constant defined in (10.22). Our aim in the next section is to study directly the modifications of the equilibrium constant from thermodynamic arguments without going through the process, more detailed but much more complicated, of studying the modifications of the kinetic constants.

10.3 Shear-Induced Polymer Degradation: Thermodynamic Analysis

Here we will use a purely thermodynamical approach to describe the change produced by the shear flow on the polymer weight distribution. We consider the system as a multicomponent mixture, constituted by the solvent (component 1) and a set of polymeric species P_i (with i the degree of polymerization, i.e. the number of monomeric units in the chain). In this way, the polydispersivity plays a fundamental role in the theoretical treatment, because the degradation is attributed to the change in the equilibrium constant of the breaking-recombination reactions of polymeric chains expressed in (10.21) due to the contribution of the viscous pressure to the chemical potentials.

The consideration of the solute as a mixture of the chemical species P_i leads to a change with respect to the formalism used in the analysis of the phase diagram in Chap. 6. There, polydispersivity did not appear explicitly in the formalism, but now it is crucial, of course, to take into account its effects by including the chemical potentials for macromolecules with different lengths

$$\mu_j = \mu_{j,\text{eq}} + \left(\frac{\partial \Delta G_s}{\partial n_j}\right)_{n_k, \dot{\gamma}},\tag{10.25}$$

where ΔG_s is the non-equilibrium contribution to the Gibbs free energy as explained in Chap. 6.

Furthermore, the average character of the polymeric molecular mass in the solution leads to consideration of M_2 as a function of n_i , i.e. each molecule with degree of polymerization i has a mass given by i times M_0 , M_0 being the mass of one monomer. Now, instead of a binary mixture, we have a system with \tilde{n}_1 moles of solvent and n_i moles of macromolecules for each degree of polymerization i. As a consequence, the total number of moles of solute is given by

$$\tilde{n}_2 = \sum_i n_i,\tag{10.26}$$

and one may define the global molar fraction of the solute as

$$x_2 = \tilde{n}_2 / \tilde{n}_0 \tag{10.27}$$

by introducing the new quantity $\tilde{n}_0 = \tilde{n}_1 + \tilde{n}_2$ which accounts for the total number of moles in the system.

The chemical potential of species j is given by the generalization of expression (6.23) and reads as

$$\frac{\mu_j}{RT} = \frac{\mu_{j,eq}}{RT} + \Xi(\phi, P_{12}^{\nu}) j N_j, \tag{10.28}$$

where we recall that the non-equilibrium contribution has the form

$$\Xi(\phi, P_{12}^{\nu}) = \frac{\nu(P_{12}^{\nu})^2}{RT} J\left(\frac{1-\phi}{\phi}F + 1\right)$$
 (10.29)

with ϕ the volume fraction, J the steady-state compliance and F a function of the concentration defined in (6.35).

For the mean molecular mass M_2 a generalised expression is used of the kind

$$M_2 = \sum_{i} n_i M_i^q / \sum_{i} n_i M_i^{q-1}, \tag{10.30}$$

where M_i is the molecular mass of macromolecules with degree of polymerization i and q is a parameter which depends on the kind of average carried out (q = 1, number average, q = 2, weight average, and q = 3, z average, are the most usual ones).

If one applies (10.11) to the equilibrium (10.21) and one assumes for simplicity an ideal mixture, for which $a_k = N_k/N_{\text{tot}}$, with N_k the number of chains with k units, one may write

$$\frac{N_j}{N_i N_{j-1}} = \frac{N_j^{(0)}}{N_i^{(0)} N_{j-i}^{(0)}} \lambda(i, j)^{-1}.$$
 (10.31)

The superscript (0) refers to values with $\dot{\gamma}=0$, for which the flow contribution λ introduced in (10.11) is equal to unity (the exponent of λ in (10.31) is -1 because the equilibrium constant of (10.21) would be given by $N_i N_{j-i} / N_j$ instead of $N_j / (N_i N_{j-i})$ we are writing in (10.31)).

To determine the explicit form of $\lambda(i, j)$ it is necessary to define the chemical potential for macromolecules with a given degree of polymerization N_i . Thus, the function $\lambda(i, j)$ is obtained by comparison with (10.11) and is given by

$$\lambda(j,i) = \exp\left\{-\Xi[(j-i)N_{j-1} + iN_i - jN_j]\right\}.$$
 (10.32)

To be specific, we will explicitly evaluate the shear-induced modification of the polymer weight distribution. To do this, we will use an explicit mathematical

expression for the polymer weight distribution. In particular, it is rather common to use the Schulz distribution (Kurata 1982)

$$W(i) = \frac{(yM_0)^n}{\Gamma(h)} i^{h-1} \exp(-yM_0i), \qquad (10.33)$$

where W(i) is the polymeric mass with a degree of polymerization between i and i + di (i is considered as a continuous parameter in this model), Γ is the gamma function and h and y are parameters which characterize the solution, and satisfy the relations

$$y = \frac{h+1}{M_m}, \quad h = \frac{1}{r-1},$$
 (10.34)

with M_w the average weight of the macromolecules and r the so-called polydispersivity index, defined as $r = M_w/M_n$, with M_n the number average as defined in (10.30) (with q = 1).

The presence of the flow will modify the values of h and y. Let $h^{(0)}$ and $y^{(0)}$ be the parameters of the distribution in the absence of shear. When one combines (10.28), (10.32) and (10.33) one arrives at the following results

$$\frac{N_j}{N_i N_{j-1}} = \frac{\Gamma(h^{(0)})}{(y^{(0)} M_0)^{h^{(0)}}} \left[\frac{j}{i(j-i)} \right]^{h^{(0)}-1} \lambda(i,j)^{-1}$$
 (10.35)

and

$$\lambda(i,j) = \exp\left[-\Xi(yM_0)^h [\Gamma(h)]^{-1} \left\{ (j-i)^h \exp\left[-yM_0(j-i)\right] + i^h \exp\left[-yM_0i\right] - j^h \exp\left[-yM_0j\right] \right\} \right].$$
(10.36)

Equations (10.35) and (10.36) allow one to determine how the parameters of the Schulz distribution are varied under the presence of P_{12}^{ν} . To do this, one may use the algorithm described in Sect. 10.5.

Another common expression for the polymer weight distribution is, instead of the Schulz one, the so-called most probable distribution, which has the form

$$W(i) = \alpha^2 i (1 - \alpha)^{i-1}, \tag{10.37}$$

where α is a parameter which characterizes the distribution. The parameters of the equilibrium distributions without shear, α_0 and with shear, α are related as

$$\alpha_0^2 (1 - \alpha_0)^{-1} = \alpha_2 (1 - \alpha)^{-1} \lambda^{-1}(\alpha)$$
 (10.38)

in the particular case when q = 1.

From (10.31) one may draw several conclusions about the degradation mechanism. In the case when one considers the molecular mass averaged over the number

(q=1) it is obvious that λ does not depend on i nor on j: this implies that the modification of the equilibrium constant does not depend on the length of the original chain nor on the length of the resulting fragments after the chain is broken. This result is not very satisfactory from the physical point of view and it corroborates the empirical equations by Graessley (1974) where other kind of averages appear, as the weight average (q=2) or even the z average (q=3) in the expressions for J. In contrast, when one adopts for M_2 a weight average (q=2) it follows that λ has a minimum when the chain is broken at the centre and, therefore, the modification of the MWD is maximum under these conditions, in agreement with the experimental results.

On the other hand, the molecular mass before the degradation and after the degradation due to the shear may be related through the following approximation

$$\frac{M_w}{M_w^{(0)}} = \lambda(i,j)^{-1/h},\tag{10.39}$$

where, in practice, λ is almost independent of *i* and *j*.

When this model is applied to the analysis of a solution of polystyrene of molecular mass 1 770 kg/mol in transdecalin, it is observed that in the degradation process the parameter q has only a very slight influence, whereas the changes in the polydispersivity index, $M_{\rm w}/M_{\rm n}$ influence the results much more strongly (Fig. 10.1) in agreement with the experimental observations (Ballauff and Wolf 1981).

Figure 10.2 shows the equilibrium distribution of segments and the difference between the probability N_i of finding a segment of length j for a solution of polystyrene in dioctyl-phtalate submitted to a shear flow. For $P_{12}^{\nu} = 400 \, \mathrm{Nm}^{-2}$, the modification of the probability weight distribution is of the order of 1%. A comparison of both curves yields the conclusion that the application of a shear implies a reduction in the number of long chains (negative values of the continuous curve), the chains with a length of the order of 20 000 segments being those which are most affected

Fig. 10.1 Differential mass fraction of the system polystyrene-transdecalin for a molecular weight of 1 170 kg/mol under several shear rates assuming a Schulz distribution with polydispersivity index 1.14 (experimental value). *Dashed line* corresponds to a equilibrium situation. (Criado-Sancho et al. 1994)

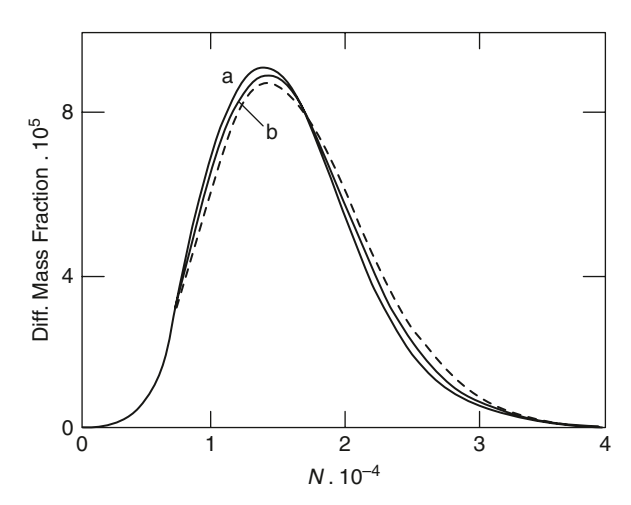
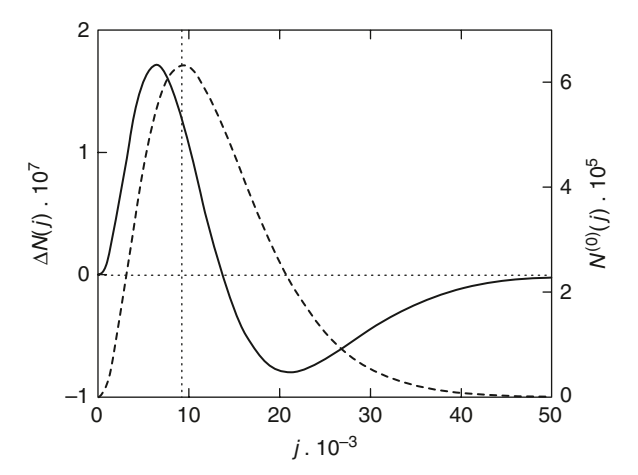


Fig. 10.2 Continuous curve representing the difference between the probability N_j of finding a segment of length j when the system (polystyrene in dioctyl-phthalate) is subjected to p_{12}^v and the value of such a probability in a rest state $N_j^{(0)}$ (dashed line). (Criado-Sancho et al. 1994)



by the degradation. In contrast, the positive values of $N_i - N_i^{(0)}$ for lengths below 15 000 segments shows the increase in the number of short chains. This increase is maximum for macromolecules of the order of 7 000 segments whereas the macromolecules of the order of 15 000 segments are almost unaffected by the degradation.

10.4 Kinetic Theory of Chemical Reactions

Chemical reactions in ideal gases should also show, in principle, non-equilibrium modifications such as those mentioned in the previous section. Although usually the corrections will be much smaller than those arising in polymer solutions, because of the much shorter relaxation times of the viscous pressure, we may use ideal gases to understand from a kinetic point of view the origin of the modification of the chemical constant in the presence of a viscous flow or a thermal flux. Analyses by these means were undertaken by Eu and Li (1977), Cukrowski and Popielawski (1986) and Fort et al. (1999).

Indeed, we consider a dilute gas A undergoing a simple bimolecular reaction

$$A + A \rightarrow B + C. \tag{10.40}$$

To simplify the calculations, we neglect the products B and C in the kinetic analyses, i.e. we assume that they are removed very efficiently from the system.

In the presence of the chemical reaction, the Boltzmann equation describing the evolution of the distribution function of particles A must take into account the different contributions of elastic and of reactive collisions; so, it takes the form

$$\frac{\partial f}{\partial t} + \mathbf{c} \cdot \frac{\partial f}{\partial \mathbf{r}} = \left(\frac{\partial f}{\partial t}\right)_{\text{el}} + \left(\frac{\partial f}{\partial t}\right)_{\text{ch}},\tag{10.41}$$

where f denotes the molecular velocity distribution function for component A and c the molecular velocity. The first term in the right-hand side of (10.41) indicates the change in f due to elastic collisions, the only ones which were considered in the kinetic theory analysis of Sect. 3.1, whereas the second term indicates the effects of the reactive collisions.

In Sect. 3.1 we gave the expression for $(\partial f/\partial t)_{el}$. The corresponding expression for the contribution of the reactive collisions is

$$\left(\frac{\partial f}{\partial t}\right)_{\rm ch} = -\iint f f_1 \alpha_{\rm ch}(\mathbf{g}) k_1 \mathrm{d}\mathbf{k} \mathrm{d}\mathbf{c}_1, \tag{10.42}$$

where f and f_1 stand for f = f(c) and $f_1 = f(c_1)$ and $g = c_1 - c$ is the relative velocity before collision, and k is a parameter of the binary encounter; and $\alpha_{ch}(g)$ is the probability that a collision with relative velocity g is reactive. Note that in (10.42) there are no inverse collisions, because the products are assumed to be removed efficiently, as has been already stated.

The rate of the chemical reaction in these conditions is then given by (10.42), i.e.

$$J_{\rm ch} = -\iint f f_1 \alpha_{\rm ch}(\boldsymbol{g}) k_1 d\boldsymbol{k} d\boldsymbol{c}_1 d\boldsymbol{c}. \tag{10.43}$$

The rate constant k for the forward chemical reaction is defined as

$$J_{\rm ch} = -k[A]^2, (10.44)$$

where [A] is the concentration of component A. We will denote $\varepsilon = \frac{1}{4}mg^2$ as the energy of the collision in the frame of centre of mass, and ε^* as the activation energy of the chemical reaction. We will assume, for simplicity, the following form for $\alpha(g)$

$$\alpha_{\rm ch}(g) = 0$$
 for $\varepsilon < \varepsilon^*$, $\alpha_{\rm ch}(g) = 1 - (\varepsilon/\varepsilon^*)$ for $\varepsilon > \varepsilon^*$. (10.45)

For hard spheres of diameter σ , k_1 is given by $k_1 = \sigma^2 \mathbf{g} \cdot \mathbf{k}$.

In thermal equilibrium, the reaction rate may be obtained by introducing the Maxwell–Boltzmann distribution function (3.7) in (10.39), and yields

$$J_{\rm ch}^{(0)} = -4n^2\sigma^2 \left(\frac{\pi k_{\rm B}T}{m}\right)^{1/2} \exp\left(-\frac{\varepsilon^*}{k_{\rm B}T}\right),$$
 (10.46)

which corresponds to the usual result of chemical kinetics, the so-called Arrhenius form.

In the presence of a velocity gradient or a temperature gradient, one should use in (10.43) the expression for the non-equilibrium distribution function. One could use either Grad's expression (3.15) or, in the Chapman–Enskog model, the form

$$f^{(1)} = f_{\text{eq}} \left[1 - \frac{mb}{2k_{\text{B}}Tn} CC : (\nabla v) \right], \qquad (10.47)$$

with $b = 2\eta_1(k_BT)^{-1}$, η_1 being the first-order approximation to the value of the viscosity. When (10.47) is introduced into (10.43) one obtains

$$J_{\rm ch} = J_{\rm ch}^{(0)} + J_{\rm ch}^{(\nu)},\tag{10.48}$$

in which the non-equilibrium contribution of the viscous flow is given by

$$J_{\rm ch}^{(\nu)} = -\frac{2}{15}\sigma^2 \left(\frac{\pi k_{\rm B}T}{m}\right)^{1/2} \exp\left(-\frac{\varepsilon^*}{k_{\rm B}T}\right) \left[\left(\frac{\varepsilon^*}{k_{\rm B}T}\right)^2 - \frac{\varepsilon^*}{k_{\rm B}T} - \frac{1}{4}\right] b^2(\nabla \nu) : (\nabla \nu).$$

$$(10.49)$$

This expression shows that the kinetic constants are modified in the presence of the viscous flow. Thus, it is logical to expect a change in the chemical equilibrium. Of course, in the simple situation where the products are immediately removed from the system, equilibrium cannot be reached. To study the modification of the equilibrium constant one should study both the direct and the reverse elementary equations. Thus, one would have for the complete reaction

$$A + A \rightleftharpoons B + C. \tag{10.50}$$

The equilibrium constant is then

$$K = \frac{[B]_{eq}[C]_{eq}}{[A]_{eo}^2} = \frac{k_{dir}}{k_{rev}},$$
(10.51)

with $k_{\rm dir}$ and $k_{\rm rev}$ the kinetic constants of the direct and reverse reactions. In (10.48) and (10.45) it has been seen that

$$k_{\text{dir}}(\dot{\gamma}) = k_{\text{dir}}(0) \left[1 + \chi_{\text{dir}}(T) \dot{\gamma}^2 \right], \tag{10.52}$$

with $\chi(T)$ a function of temperature which may be identified from (10.49). Assuming for the reverse reaction an analogous dependence, but with a different function

$$k_{\text{rev}}(\dot{\gamma}) = k_{\text{rev}}(0) \left[1 + \chi_{\text{rev}}(T) \dot{\gamma}^2 \right],$$
 (10.53)

one would obtain

$$K(\dot{\gamma}) = K(0) \frac{1 + \chi_{\text{dir}} \dot{\gamma}^2}{1 + \chi_{\text{rev}} \dot{\gamma}^2}.$$
 (10.54)

The thermodynamic analysis gives directly the modification of the equilibrium constant in terms of the shear rate, without the need to study the detailed microscopic mechanisms leading to the kinetic reaction constants.

Cuckrowski and Popielaski (1986) have evaluated the order of magnitude of these corrections in several situations. In particular, they have considered a shock wave where $\partial v_z/\partial z$ is the only non-vanishing component of ∇v . They obtain

$$\frac{J_{\rm ch}^{(\nu)}}{J_{\rm ch}^{(0)}} = \frac{25\pi}{1152} \left[\left(\frac{\varepsilon^*}{k_{\rm B}T} \right)^2 - \frac{\varepsilon^*}{k_{\rm B}T} - \frac{1}{4} \right] \left(\frac{\ell}{a'} \frac{\partial v_z}{\partial z} \right)^2, \tag{10.55}$$

with $a'=(5k_{\rm B}T/3m)^{1/2}$ and ℓ the mean free path of the molecules. For the values $m=10^{-23}$ g, $\sigma=10^{-8}$ cm, $n=2.69\times 10^{19}$ cm⁻³, and $\partial v_z/\partial z=4.3\times 10^8 {\rm s}^{-1}$, they obtain $J_{\rm ch}^{(\nu)}\approx 0.49J_{\rm ch}^{(0)}$. In less extreme situations and for monatomic gases, the non-equilibrium corrections are very small.

Viscous pressure is not the only dissipative flux that may change the reaction rates. A similar analysis in the framework of Grad's approach in the presence of a heat flux has been performed by Eu and Li (1977), and in terms of the information theory by Fort and Cuckrowski (1997, 1998), Nettleton (1996a, b) and by Nettleton and Torrisi (1991).

We will finally note, for the sake of completeness, that in the presence of a heat flux, the non-equilibrium distribution function is

$$f^{(1)} = f_{\text{eq}} \left[1 + \frac{1}{n} \sqrt{\frac{2k_{\text{B}}}{mT}} a \left(C^2 - \frac{5}{2} \right) C \cdot \nabla T \right],$$
 (10.56)

with $a = -3\eta_1(2k_BT)^{-1}$. The result for the chemical reaction rate is (Cuckrowski and Popielaski 1986)

$$J_{\text{ch}}^{q} = -\frac{1}{3}\sigma^{2} \left(\frac{\pi k_{\text{B}}T}{m}\right)^{1/2}$$

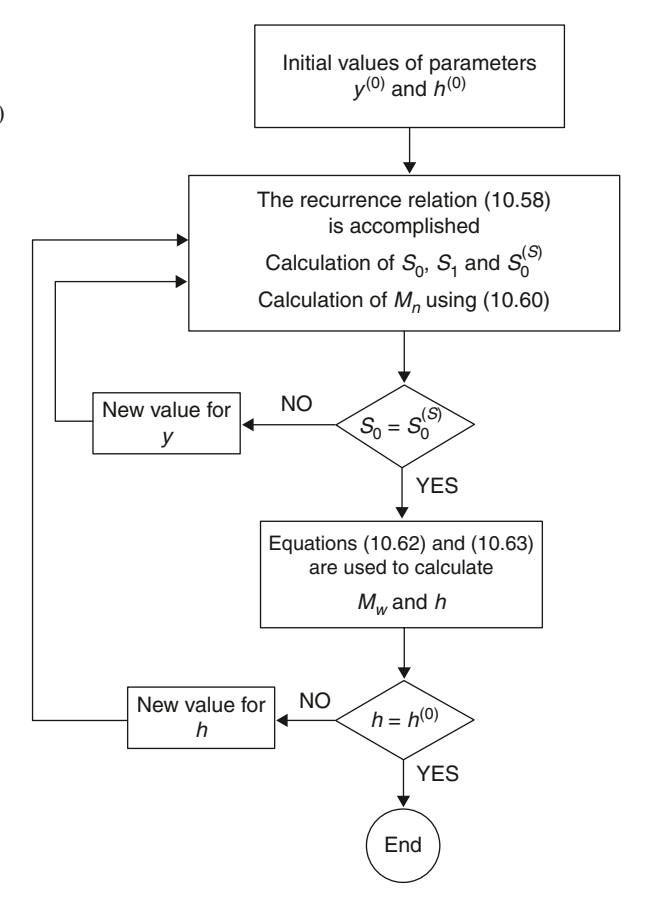
$$\times \exp\left(-\frac{\varepsilon^{*}}{k_{\text{B}}T}\right) \left[-\left(\frac{\varepsilon^{*}}{k_{\text{B}}T}\right)^{3} + \frac{17}{2}\left(\frac{\varepsilon^{*}}{k_{\text{B}}T}\right)^{2} + \frac{15}{4}\left(\frac{\varepsilon^{*}}{k_{\text{B}}T}\right) + \frac{29}{8}\right] \frac{k_{\text{B}}a^{2}}{mT} \nabla T \cdot \nabla T. \quad (10.57)$$

Thus, in general, it is expected that the reaction rate may depend on viscous pressure or temperature gradients. A possible domain of interest for this influence could be the prebiotic reactions taking place on a thin hot layer, carried by a heat flux or, in general, other kinds of reactions between antigens and antibodies in the blood flow, in the presence of a shear flow.

10.5 Recurrence Method for Probability Weight Distribution Under Viscous Pressure

Here we show a recurrence method to obtain the probability distribution function in the presence of a non-vanishing shear viscous pressure by iteratively solving (10.35) and (10.36). The general method is shown in Fig. 10.3.

Fig. 10.3 Diagram showing how the probability weight distribution out of equilibrium is obtained from (10.35) and (10.36). (Criado-Sancho et al. 1994)



We adopt as the starting point the recurrence relation

$$N_{j} = \frac{1}{L} \sum_{i=1}^{L} \lambda(i, j) N_{i} N_{j-1}, \qquad (10.58)$$

where L = E(j/2) is the integer part of j/2 and the explicit expression for $\lambda(i, j)$ is derived from (10.36). In this way, a discrete distribution N_i is generated for which the sums

$$S_n = \sum_j j^n N_j \quad (n = 0, 1, ...)$$
 (10.59)

allow one to determine the normalization constant and the number average molecular weight

$$M_n = \frac{S_1}{S_0} M_0. {(10.60)}$$

The former distribution does not necessarily coincide with Schulz's distribution given in (10.32), which will now be denoted as $N_j^{(S)}$, and for which are defined the sums analogous to (10.59)

$$S_n^{(S)} = \sum_j j^n N_j^{(S)} \quad (n = 0, 1, ...).$$
 (10.61)

Furthermore, recalling (10.34) and the definition of polydispersivity index ($r = M_w/M_n$) it is concluded that the weight-averaged molecular mass satisfies the following relations

$$M_w = \frac{h+1}{h} M_n, \tag{10.62}$$

$$h = yM_w - 1. (10.63)$$

If one formulates the hypothesis that for the considered values of P_{12}^{ν} the probability weight distribution is still of the Schulz's form and only its parameters are modified, the new parameters h and y are obtained by means of the algorithm sketched in Fig. 10.3.

Chapter 11 Non-equilibrium Thermodynamics of Laminar and Turbulent Superfluids

In this chapter we present an overview of some applications of non-equilibrium thermodynamics to flowing superfluids, both in the laminar as in the turbulent regimes. Since the flowing behaviour of superfluids is especially surprising and challenging, and as it crucially depends on thermodynamical parameters, it is logical to include this topic in a book devoted to the special thermodynamic features of flowing fluids.

As a basic theoretical framework for the description of superfluids one could choose the classical and well-known two-fluid model, proposed by Tisza (1938) and by Landau (1941), or a one-fluid model with a vectorial internal degree of freedom, which may be identified, for instance, as the heat flux, or the relative velocity between normal and superfluid components of the two-fluid model. Since in this book we use extended irreversible thermodynamics as a unifying framework, which finds in superfluids an especially suitable field of application, because of the very long relaxation time of the heat flux, we will use and compare both models. The translation from one model to the other in linear situations is easy, as the heat flux q is closely related to the relative velocity $V = v_n - v_s$ between normal and superfluid components of the two-fluid model.

Phenomena in the laminar regime have been studied for decades and are well understood. However, at high enough values of the relative velocity or the heat flux, a turbulent regime appears which exhibit peculiar quantum feature. Quantum turbulence has the special feature that vorticity is quantized, and the flow is characterized by an irregular tangle of quantized vortex filaments, whose total length per unit volume depends on the heat flow. Thus, in turbulent states the fluid is populated by a mesh of lines which in turn, influence the dynamics of the fluid. The dynamics of quantized vortices is a topic of much current interest not only in usual superfluids, but also in rotating Bose–Einstein condensates and in superconductors submitted to external magnetic fields.

11.1 Essential Concepts and Phenomena of Superfluids

Helium was the last gas to be liquefied. This achievement was due to Kammerling Onnes in 1908, at 4.2 K and a pressure of 25 atm. However, the superfluid properties of liquid helium were not discovered until much later, from 1937, by Mendelsohn, Kapitza, Allen, Misener and other scientists. Helium II, namely, superfluid liquid ⁴He below the so-called lambda point, at approximately 2.2 K, at which there is a sharp and narrow peak in the specific heat due to the phase transition between normal fluid and superfluid, exhibits a number of exceptional features which make it a physically outstanding system. Its most well-known peculiarities are its ability to flow along narrow capillaries or porous media without viscous resistance, which has given it its characteristic name; however, when a rotating disk is introduced in it and allowed to oscillate as a torsion pendulum, such rotating oscillations are damped as in a usual fluid. The contrast between these so different behaviours, one of them compatible with a total lack of viscosity and the other exhibiting a considerable viscosity, is very challenging and it was one of the intuitive motivations for the two-fluid model.

The propagation of two kinds of longitudinal waves, namely first sound (a density or pressure wave identical to usual sound) and an exceptional second sound (a temperature wave), and the so-called fountain effect and thermomechanic effect, which are related to crossed effects between heat transport and mass transport, are other peculiar effects of superfluids, as well as the ability to creep along surfaces and to escape by climbing up the walls of the containers. Helium II has a practically infinite thermal conductivity, the heat flux has a practically infinite relaxation time, and its viscosity at low temperature is vanishingly small. It could flow during years along a closed circuit without decaying to rest (Wilks 1967).

The research on these phenomena has been a very active frontier of knowledge for many years. These frontiers were much enlarged when in 1970, it was found that ³He also present superfluid phases. But ³He has spin 1/2 and is therefore a fermion, in contrast with ⁴He, which is a boson; thus ³He cannot directly have a Bose–Einstein transition. A necessary requirement to have it is to form pairs—analogous to the Cooper pairs in superconductors—which have total spin 1 and are bosons. Superfluidity appears in ³He at much lower temperatures than in ⁴He, namely, at the scale of millikelvin. Furthermore, since the ³He pairs have a vectorial degree of freedom, as they have spin 1, which is lacking in ⁴He, which has spin 0, superfluidity in ³He is richer and far more complex than in ⁴He.

Superfluids have practical use in cryogenics, to keep at very low temperatures superconducting magnets or smaller devices, as they flow very efficiently and have a high thermal conductivity. Futhermore, they are thought to play a role in neutron stars, after pair formation of neutrons.

When the flow reaches a critical velocity, however, some resistance to the flow suddenly appears, and the attenuation of second sound correspondingly increases. These effects can be explained by the formation of quantized vortex filaments in Helium II, and their friction with the flow of helium giving rise to a very rich phenomenology, which will be discussed in Sect. 11.4–11.7.

11.2 The Two-Fluid Model and Second Sound

The classical and most widely known model of superfluids is the two-fluid model, which assumes that Helium II is a mixture of two components: a superfluid one and a normal one. The superfluid component has zero viscosity (vanishing resistance) and zero entropy, and its flow is irrotational; the normal component exhibits some resistance (normal viscosity) and has non-vanishing entropy. Each component is characterized by a density and a velocity, namely, ρ_s , ν_s , ρ_n and ν_n , respectively, in such a way that the total density ρ is $\rho = \rho_s + \rho_n$ and the bulk velocity of the liquid ν is defined as $\rho \nu = \rho_s \nu_s + \rho_n \nu_n$. The densities ρ_n and ρ_s strongly depend on temperature. At the lambda temperature $T = T_\lambda$, and above it, $\rho_s = 0$ and all the fluid is found in the normal phase; at decreasing T, below T_λ , $\rho_s(T)$ increases and $\rho_n(T)$ decreases until the limit of T = 0, in which the normal component has completely disappeared and the liquid is entirely in the pure superfluid state. The proportion of the normal component may be measured, for instance, with a rotating disk experiment, whose attenuation shows the viscous effects characterizing the normal component.

The microscopic idea behind the two-fluid model is the so-called Bose–Einstein condensation, a typical quantum effect, predicted by Einstein in 1925, in which a macroscopic fraction of the total number of particles condensates into the fundamental state of the system and exhibits a coherent global behaviour of the collective quantum wave function of the system, which strongly reduces its viscosity. In 1938, Laszlo Tisza and Fritz London independently suggested that the condensed phase would correspond to the superfluid component and the remaining part would be the normal component, which may be considered as a sum of elementary excitations, or quasiparticles, of two kinds: phonons and rotons, as proposed by Landau in 1949; phonons predominate below 0.8 K, and rotons are the main contributors above 0.8 K. This quantum feature of the reduction of viscosity is analogous to the drastic reduction of electrical resistivity in superconductors, where pairs of electrons—Cooper pairs—constitute a kind of superfluid which is able to flow within the material without resistance due to the coherence of the collective wavefunction describing the condensed phase. In most of the superfluids, the interaction amongst the particles makes the phenomenon a little bit different than the true Bose-Einstein condensation, but since 1995 it has been possible to achieve a true Bose-Einstein condensation in dilute monatomic gases with negligible interatomic interactions, which exhibit, in some domains, superfluid behaviour, especially related to the quantization of vortices.

The two-fluid model explains in an intuitive and efficient way the several observations: the flow without resistance along narrow capillaries corresponds to the flow of the superfluid component; the thermomechanical effect—which is the fact that the flow of heat is accompanied by a flow of momentum—is also explained by the fact that the superfluid carries both momentum and heat; the first sound corresponds to a wave where both normal and superfluid components oscillate in phase with each other, and the total density changes; in the second sound, the normal and superfluid components have opposite oscillations, in such a way that density does not change but temperature does; in the fountain effect, giving heat to the fluid communicates also momentum and sets it in motion, and so on (Putterman 1974).

11.2.1 Evolution Equations and Wave Propagation

As an illustration of the behaviour of superfluids, and for the sake of further comparison, we present the description of longitudinal wave perturbations, which lead to first and second sounds. It is usual to take as variables the total mass density ρ , the total momentum density $\mathbf{j} \equiv \rho \mathbf{v} = \rho_{\rm s} \mathbf{v}_{\rm s} + \rho_{\rm n} \mathbf{v}_{\rm n}$, the entropy density ρs , and the velocity $\mathbf{v}_{\rm s}$ of the superfluid component. In the absence of viscous effects and neglecting non-linear terms the evolution equations are

$$\frac{\partial \rho}{\partial t} + \nabla \cdot \mathbf{j} = 0, \tag{11.1}$$

$$\frac{\partial(\rho s)}{\partial t} + \rho s \nabla \cdot \mathbf{v}_{n} = 0, \tag{11.2}$$

$$\frac{\partial \mathbf{j}}{\partial t} + \nabla p = 0, \tag{11.3}$$

$$\frac{\partial \mathbf{v}_{\mathbf{s}}}{\partial t} + \nabla \mu = 0. \tag{11.4}$$

Equation (11.1) is the mass conservation equation, (11.2) is the entropy balance equation, with $\rho s v_n$ the entropy flux and where entropy production, being nonlinear, has been neglected, and (11.4) is the equation of motion of the superfluid component, with μ the superfluid chemical potential. This equation may understood from (11.6), and taking into account that for the superfluid s = 0. In these expressions, viscous effects due to the normal component have been neglected in (11.3) for the sake of simplicity; they will be introduced in the last section. Obtaining the derivative of (11.1) with respect to time and using (11.3) we have

$$\frac{\partial^2 \rho}{\partial t^2} = \nabla^2 p. \tag{11.5}$$

Because of the Gibbs-Duhem thermodynamic relation, we may write

$$\nabla p = \rho s \nabla T + \rho \nabla \mu, \tag{11.6}$$

and using this expression in (11.3) and (11.4) it is found

$$\rho_{\rm n} \frac{\partial}{\partial t} (\mathbf{v}_{\rm n} - \mathbf{v}_{\rm s}) + \rho s \nabla T = 0. \tag{11.7}$$

Futhermore, note that

$$\nabla \cdot (\mathbf{v}_{s} - \mathbf{v}_{n}) = \frac{\rho}{\rho_{s} s} \frac{\partial s}{\partial t}.$$
 (11.8)

This result comes from the equality

$$\frac{\partial s}{\partial t} = \frac{1}{\rho} \frac{\partial (\rho s)}{\partial t} - \frac{s}{\rho} \frac{\partial \rho}{\partial t} = -s \nabla \cdot \boldsymbol{v}_{n} + \frac{s}{\rho} \nabla \cdot \boldsymbol{j} = \frac{s \rho_{s}}{\rho} \nabla \cdot (\boldsymbol{v}_{s} - \boldsymbol{v}_{n}). \tag{11.9}$$

If we combine now (11.7) and (11.8) we obtain

$$\frac{\partial^2 s}{\partial t^2} = \frac{\rho_{\rm s} s^2}{\rho_{\rm n}} \nabla^2 T. \tag{11.10}$$

Equations (11.5) and (11.10) determine the propagation of density and entropy perturbations in superfluids. Writing the perturbations as s', p', T' and ρ' , and expanding ρ' and s' in terms of p' and T' one has

$$\rho' = \left(\frac{\partial \rho}{\partial p}\right)_T p' + \left(\frac{\partial \rho}{\partial T}\right)_p T',\tag{11.11a}$$

$$s' = \left(\frac{\partial s}{\partial p}\right)_T p' + \left(\frac{\partial s}{\partial T}\right)_p T'. \tag{11.11b}$$

Introduction of these expressions into (11.5) and (11.10) yields

$$\frac{\partial p}{\partial \rho} \frac{\partial^2 p'}{\partial t^2} - \nabla^2 p' + \frac{\partial \rho}{\partial T} \frac{\partial^2 T'}{\partial t^2} = 0, \tag{11.12}$$

$$\frac{\partial s}{\partial \rho} \frac{\partial^2 p'}{\partial t^2} + \frac{\partial s}{\partial T} \frac{\partial^2 T'}{\partial t^2} - \frac{\rho_s s^2}{\rho_n} \nabla^2 T' = 0.$$
 (11.13)

Looking for plane wave solutions for p' and T' of the form

$$p' = \tilde{p}' \exp\left[i(\omega t - kx)\right],\tag{11.14a}$$

$$T' = \tilde{T}' \exp\left[i(\omega t - kx)\right],\tag{11.14b}$$

with \tilde{p}' and \tilde{T}' the amplitude, ω and k the angular frequency and wavevector, Eqs. (11.12) and (11.13) yield

$$\omega^2 \left(\frac{\partial p}{\partial \rho}\right) \tilde{p}' - k^2 \tilde{p}' + \left(\frac{\partial p}{\partial T}\right) \omega^2 \tilde{T}' = 0, \tag{11.15a}$$

$$\omega^2 \left(\frac{\partial s}{\partial \rho} \right) \tilde{p}' + \omega^2 \left(\frac{\partial s}{\partial T} \right) \tilde{T}' - \frac{\rho_s}{\rho_n} s^2 k^2 \tilde{T}' = 0.$$
 (11.15b)

The compatibility condition of these set of equations, namely, the condition that the associated determinant is null, is

$$u^{4} - u^{2} \left[\left(\frac{\partial p}{\partial \rho} \right)_{s} + \frac{\rho_{s} T s^{2}}{\rho_{n} c_{v}} \right] + \frac{\rho_{s} T s^{2}}{\rho_{n} c_{v}} \left(\frac{\partial p}{\partial \rho} \right)_{T} = 0, \tag{11.16}$$

where $u=\omega/k$ is the propagation speed and $c_v=T(\partial s/\partial T)_v$ the heat capacity per unit volume. Equation (11.16) determines two values for the wave propagation speed u. Note that if $\rho_s=0$, i.e. in the absence of the superfluid component, (11.16) simplifies in such a way that one of these velocities is zero and the other one is the usual sound velocity $u_{10}^2=(\partial p/\partial \rho)_s$. In the presence of the superfluid component $(\rho_s\neq 0)$, a new wave appears. Since the thermal expansion coefficient is very small in helium, the adiabatic and isothermal compressibility coefficients $(\partial p/\partial \rho)_s$ and $(\partial p/\partial \rho)_T$ are very similar to each other, as well as c_p and c_v . With this simplification, the solutions of (11.16) are

$$u_{10}^2 = \left(\frac{\partial p}{\partial \rho}\right)_T,\tag{11.17a}$$

$$u_{20}^2 = \frac{\rho_s T s^2}{\rho_n c_v}.$$
 (11.17b)

The first wave is the first sound, and its velocity does not change much with temperature. This wave is a pressure and velocity wave. The second wave, a purely temperature wave, is called second sound and is a temperature (and heat) wave characteristic of superfluids, as it vanishes for $\rho_s = 0$, and it was experimentally observed by the first time in 1944, 6 years after the theoretical prediction, by Peskov. The velocity u_{20} is very sensitive to temperature, as $\rho_s(T)$ and $\rho_n(T)$ are strongly temperature dependent. If the entropy of the superfluid component was not strictly zero, but s' per unit volume, the term s^2 in (11.17b) should be replaced by $(s - s')^2$, and would reduce the speed (and increase the attenuation).

As it has been said before, in the first sound, normal and superfluid components oscillate in phase, as a whole, i.e. as if there was a single fluid. Instead, in the second sound they oscillate out of phase, with the relation $\rho \mathbf{v} = \rho_s \mathbf{v}_s + \rho_n \mathbf{v}_n = 0$. In this case, there is no mass flow, but the internal oscillations of the normal component imply an oscillation in entropy and temperature, leading to propagating temperature waves, which are completely different from the damped temperature waves produced in usual media by periodic variation of temperature on the boundaries of the system. Non-linear aspects of these waves were studied for the first time by Khalatnikov.

The interesting property of liquid helium II of flowing along very narrow channels without any resistance, for sufficiently small velocities, leads also to two new kinds of waves, predicted by Atkin in 1959, and called third sound and fourth sound,

which have special interest in helium flow through porous media. Fourth sound is a pressure wave that travels only in the superfluid, when the normal fluid is immobilized by, for instance, a very fine powder. The analysis of this flow requires a detailed attention to the boundary conditions of the fields, especially for higher-order fields. Indeed, these boundaries establish a connection between the variations of the average speed and of the heat flux. As a consequence, in this wave all the fields vibrate, as it was discussed in Sect. 11.1.1. The results of the fourth sound establish an upper experimental bound on the entropy carried by the superfluid component, which turns out to be less than 1% of the total entropy (Mongiovì 2001). Third sound is a surface wave on thin films of liquid helium and also requires a careful specification of boundary conditions on the wall.

11.2.2 Thermodynamics of Superfluid Helium

From the thermodynamic point of view, the Gibbs equation for the superfluid does not depend only on the classical variables (entropy and volume, for instance) but also on the momentum density j, and is given, in the superfluid rest frame and referred to unit volume, by (Landau and Lifshitz 1970)

$$d(\rho u) = \mu d\rho + T d(\rho s) + (v_n - v_s) \cdot dj. \tag{11.18}$$

The two first terms are the standard ones in usual fluids; the last one expresses the fact that the derivative of the energy with respect to momentum is the velocity, which in the superfluid rest frame corresponds to the relative velocity of the normal component minus the velocity of the superfluid component.

On the other hand, the chemical potential may be expressed in terms of p, T and $v_n - v_s$ as (Landau and Lifshitz 1970)

$$d\mu = -sdT + \frac{1}{\rho}dp - \frac{\rho_n}{\rho}(\nu_n - \nu_s) \cdot d(\nu_n - \nu_s). \tag{11.19}$$

Expanding the expressions for s and ρ , attained from Eq. (11.17), i.e. from $s = -(\partial \mu/\partial T)_{p,\nu_n-\nu_s}$ and $\rho^{-1} = -(\partial \mu/\partial p)_{T,\nu_n-\nu_s}$, we obtain

$$s(p, T, \nu_{\rm n} - \nu_{\rm s}) \simeq s(p, T) + \frac{1}{2}(\nu_{\rm n} - \nu_{\rm s})^2 \frac{\partial}{\partial T} \left(\frac{\rho_{\rm n}}{\rho}\right),$$
 (11.20a)

$$\rho(p, T, \mathbf{v}_{n} - \mathbf{v}_{s}) \simeq \rho(p, T) + \frac{1}{2} \rho^{2} (\mathbf{v}_{n} - \mathbf{v}_{s})^{2} \frac{\partial}{\partial p} \left(\frac{\rho_{n}}{\rho}\right). \tag{11.20b}$$

These expressions are valid up to the second order in $(v_n - v_s)$, and explicitly show the influence of the dynamical variable $v_n - v_s$ on the thermodynamic

quantities. Also, from the Euler form for the entropy it follows that the pressure p is given by

$$p = -\rho u + \rho T s + \rho \mu + \rho_{\rm n} (v_{\rm n} - v_{\rm s})^2,$$
 (11.20c)

thus exhibiting the contribution of the relative motion between normal and superfluid components.

11.3 The Extended One-Fluid Model of Liquid Helium II

An alternative way to describe most of the properties mentioned above without using the two-fluid model is to assume a one-fluid model with a vector internal degree of freedom which, in extended thermodynamics, may be identified as the heat flux q. It may be shown that in terms of the two-fluid model, q may be identified as

$$q = \rho_{\rm s} T s(\mathbf{v}_{\rm n} - \mathbf{v}_{\rm s}). \tag{11.21}$$

Indeed, the non-convective part of the entropy flux is $J_{\text{non-convective}}^s = \rho s(\mathbf{v}_n - \mathbf{v}) = \rho_s s(\mathbf{v}_n - \mathbf{v}_s)$, where the second equality arises by writing $\mathbf{v} = (\rho_n \mathbf{v}_n + \rho_s \mathbf{v}_s)/\rho$. Identifying this non-convective entropy flux as $T^{-1}\mathbf{q}$ leads to (11.21). Thus, \mathbf{q} describes the energy transport associated to the relative motion between normal and superfluid components. Furthermore, the heat flow turns out in this case to be related to a flow of momentum, this setting a basis for thermomechanic and fountain effects.

The idea of a one-fluid model with an internal degree of freedom is less intuitive than the two-fluid model, but it has also some physical appeal because, in actual fact, the two fluids cannot be directly separated and observed as such, because they do not correspond to individually different particles (Atkin and Fox 1975, 1984; Greco and Müller 1984; Lebon and Jou 1979; Mongiovì 1991, 1992, 1993a, b, 2000, 2001). In fact, in expressions (11.18–11.20) it is seen that $\nu_n - \nu_s$ does indeed play a role in the thermodynamic functions of the superfluid component. Furthermore, superfluid helium is not strictly a Bose–Einstein condensate, but the strong interactions amongst atoms make it to deviate from this ideal model, which was one of the original motivations of the two-fluid model.

In the one-fluid model of helium II, the basic variables are the total density ρ , barycentric velocity ν , absolute temperature T, and the heat flux q. Thus, a difference with the two-fluid model is that the former one uses $j \equiv \rho \nu$, and ν_s as variables, whereas here, instead of ν_s , the heat flux (related to $\nu_n - \nu_s$) is used. The generalized Gibbs equation would be

$$d(\rho s) = T^{-1}d(\rho u) - T^{-1}\mu d\rho - \left[\tau_1/(\lambda T^2)\right] \boldsymbol{q} \cdot d\boldsymbol{q}, \qquad (11.22)$$

with τ_1 the relaxation time of the heat flux. A Gibbs equation of this form is typical of extended thermodynamics, and it should be compared to the Gibbs equation of

the two-fluid model (11.18), but formulated in the centre of mass frame of reference, which is

$$d(\rho u) = T d(\rho s) + \mu' d\rho + \frac{\rho_s}{\rho} (v_n - v_s) \cdot d \left[\rho_n (v_n - v_s) \right], \qquad (11.23)$$

where the chemical potential μ' is related to the chemical potential μ in the superfluid rest frame appearing in (11.18) as

$$\mu' = \mu + \frac{1}{2} \left[\frac{\rho_{\rm n}}{\rho} \left(\nu_{\rm n} - \nu_{\rm s} \right) \right]^2. \tag{11.24}$$

Introducing the relation (11.21) into (11.23) one obtains that the term in $\mathbf{q} \cdot d\mathbf{q}$ in $d(\rho u)$ has the form $\rho_n(\rho_s T^2 s^2)^{-1} \mathbf{q} \cdot d\mathbf{q}$. Comparing with the last term in $\mathbf{q} \cdot d\mathbf{q}$ in $d(\rho u)$ as obtained from (11.22) one finds that

$$\frac{\tau_1}{\lambda} = \frac{\rho_n}{\rho_s s^2 T},\tag{11.25}$$

a result which will be used below.

The linearized set of evolution equations, neglecting viscous phenomena due to the normal component and written in an inertial frame, is

$$\frac{\mathrm{d}\rho}{\mathrm{d}t} + \rho \nabla \cdot \mathbf{v} = 0,\tag{11.26}$$

$$\rho \frac{\mathrm{d}\mathbf{v}}{\mathrm{d}t} + \nabla p = 0, \tag{11.27}$$

$$\rho \frac{\mathrm{d}u}{\mathrm{d}t} + \nabla \cdot \boldsymbol{q} + p \nabla \cdot \boldsymbol{v} = 0, \tag{11.28}$$

$$\tau_1 \frac{\mathrm{d}\mathbf{q}}{\mathrm{d}t} + \mathbf{q} + \lambda \nabla T = 0, \tag{11.29}$$

where u is the internal energy per unit mass, p the thermodynamic pressure, τ_1 the relaxation time of the heat flux, and λ the thermal conductivity. Viscous effects will be taken into consideration in the last section of the chapter. Equation (11.29) is the relaxational extension of Fourier's law, the so-called Maxwell–Cattaneo equation; in superfluids, τ_1 and λ are very long, in contrast with what happens in ordinary fluids.

We will study here the longitudinal waves, corresponding, as it has been said, to the first and second sounds. To do so, we consider the propagation of harmonic plane waves of the form

$$\rho = \rho_0 + \tilde{\rho} \exp\left[i(k\mathbf{n} \cdot \mathbf{x} - \omega t)\right],\tag{11.30a}$$

$$v = \tilde{v} \exp\left[i(k\boldsymbol{n} \cdot \boldsymbol{x} - \omega t)\right],\tag{11.30b}$$

$$T = T_0 + \tilde{T} \exp\left[i(k\mathbf{n} \cdot \mathbf{x} - \omega t)\right],\tag{11.30c}$$

$$q = \tilde{q} \exp\left[i(k\mathbf{n} \cdot \mathbf{x} - \omega t)\right],\tag{11.30d}$$

where $k = k_r + \mathrm{i} k_i$ is the complex wave number, ω the real frequency, n the unit vector in the direction of wave propagation, the subscript 0 refers to the equilibrium reference state and the oversigned quantities denote small amplitudes of the perturbations, whose product may be neglected in a linear approximation. The real part k_r is related to the propagation speed u as $u = \omega/k_r$, whereas the imaginary part k_i is proportional to the reciprocal of the characteristic attenuation length of the waves.

We introduce (11.30a, b, c, d) into (11.26–11.29) and keep terms linear in the amplitudes. One obtains

$$-\omega\tilde{\rho} + k\rho_0\tilde{\mathbf{v}} \cdot \mathbf{n} = 0, \tag{11.31a}$$

$$-\omega \tilde{\mathbf{v}} + k\rho_0^{-1} (\partial p/\partial \rho)_0 \tilde{\rho} \mathbf{n} = 0, \tag{11.31b}$$

$$-\omega \tilde{T} + k\rho_0^{-1} c_{v0}^{-1} \tilde{\boldsymbol{q}} \cdot \boldsymbol{n} + k \frac{T_0}{c_{v0}} \left(\frac{\partial p}{\partial T} \right)_{\rho} \tilde{\boldsymbol{v}} \cdot \boldsymbol{n} = 0, \tag{11.31c}$$

$$-\omega \tilde{\boldsymbol{q}} + k(\lambda/\tau_1)_0 \tilde{T} \boldsymbol{n} = 0. \tag{11.31d}$$

This leads, for longitudinal waves and neglecting thermal dilation, i.e. assuming $(\partial p/\partial T)_{\rho} \approx 0$, to the following dispersion relation

$$(\omega^2 - k^2 u_1^2)(\omega^2 - k^2 u_2^2) = 0, (11.32)$$

where u_1 and u_2 are the phase speeds of the longitudinal waves, given by

$$u_{10}^2 = \left(\frac{\partial p}{\partial \rho}\right)_T, \quad u_{20}^2 = \frac{\lambda}{c_v \tau_1},$$
 (11.33)

where the subscripts 10 and 20 refer to waves 1 and 2 in the absence of thermal dilation. The first one corresponds to the normal sound wave, where only pressure and velocity vibrate, and it is called first sound, and the second one is the temperature wave, or second sound in which only temperature and heat flux vibrate. Introducing the relation (11.25) in (11.33) it is found that the result for the second sound speed becomes identical to that found in (11.17), as it is the case of the first sound speed.

When thermal dilation is taken into account, more complicated dispersion relations follows, which leads to the conditions

$$u_1^2 u_2^2 = u_{10}^2 u_{20}^2, (11.34a)$$

$$u_1^2 + u_2^2 = u_{10}^2 + u_{20}^2 + w_1 w_2,$$
 (11.34b)

with $w_1 = \rho_0^{-1} (\partial p/\partial T)_\rho$ and $w_2 = (T/\rho c_v)_0 (\partial p/\partial T)_\rho$. In this case first and second sounds become coupled with each other.

11.4 Quantized Vortices in Rotation and Counterflow

From the historical point of view, the first surprises concerning vorticity in superfluids were experiments carried out in the 1950s in rotating cylindrical containers filled with helium II (Osborne 1950). Vorticity is defined as the curl of the fluid, i.e. the circulation per unit area. In principle, the superfluid, due to its non-viscous and irrotational character, should not participate in the rotation. However, it was realized that the free surface of the liquid in the rotating cylinder assumed a paraboloidal shape exactly of the same form that would result from the rigid rotation of both normal and superfluid constituents, thus meaning that the superfluid was dragged by the normal component, but this seemed in contrast with its irrotational character. It was predicted that the superfluid, in fact, could develop vorticity singularities corresponding to very thin vortices, whose core would have a radius of the order of the atomic radius, with quantized vorticity, the quantum of vorticity being $\kappa = h/m$, with h Planck's constant and m the mass of the helium atom ($\kappa = 9.97 \times 10^{-4} \text{ cm}^2 \text{s}^{-1}$).

The quantized character of vorticity in superfluid helium had been predicted by Onsager in 1949, and further elaborated by Feynman in 1950, from a more microscopic perspective (Donnelly 1991; Barenghi et al. 2001). This quantization is analogous to Bohr quantization condition for electronic orbits in the atoms, namely, $2\pi mvr = nh$ with n an integer. Since the vorticity (defined as the integral of the velocity along a closed line) is $2\pi vr$ for a circular line of radius r and velocity v, one has $2\pi vr = n(h/m) = nk$. However, in the superfluid it is much more costly, from an energetic perspective, the formation of vortices with n=2 than elongating a vortex with n=1, for a given total value of the vorticity; thus stronger vorticity extends the existent vortex lines and loops rather than keeping constant the length and increasing the rotational velocity.

In rotating cylinders, it was observed an array of straight quantized vortices parallel to the rotation axis, whose density per unit of transverse area (or the corresponding vortex line density per unit volume of the system, L) is

$$L = \frac{2\Omega}{\kappa}.\tag{11.35}$$

The interpretation of this equation is very simple, since for straight parallel vortex lines the vortex line density is equal to the number of vortex lines per unit transversal area. The total vorticity of the fluid will be $2\pi Rv = 2\pi R^2\Omega$ with R the external radius of the cylinder, but this vorticity is equal to the total number of vortices $L\pi R^2$ multiplied by the vorticity quantum κ . By equating both expressions, (11.35) is immediately obtained. This array of parallel quantum vortices has strong analogies with electrical vortex lines in superconductors submitted to intense magnetic fields. Thus, an understanding of vortices in superfluids may be also useful in superconductors.

Furthermore, Hall and Vinen (1956) studied the second-sound propagation in rotating superfluids and realized that when its direction of propagation is perpendicular to the rotation axis it suffers an extra attenuation compared to the non-rotating container, proportional to the angular velocity. In contrast, there was no extra attenuation when the second sound propagated along the rotation axis. It was then suggested that the extra attenuation should be due to a friction force between the normal fluid and the quantized vortices. Such a force was seen to have the form

$$\boldsymbol{F} = B(T)\frac{\Omega}{\Omega} \times \Omega \times \boldsymbol{V} + B'(T)\Omega \times \boldsymbol{V}, \tag{11.36}$$

where B(T) and B'(T) are two frictional coefficients which depend on the temperature and which express the longitudinal and transversal components of the friction force between the normal component of the superfluid and the vortices. Here, V is the relative velocity of the normal component with respect to the superfluid component, namely $V = \nu_n - \nu_s$. From a microscopic perspective, the longitudinal and transversal friction forces arise from the collisions of the quasi-particles of the normal component with the vortex line, thus leading to a difference between longitudinal and transversal forces. The collision cross section of the vortex line is a function of the direction of the excitations relative to the vortex line.

A further observation was carried out in the early 1960s in the presence of a heat flux across the system. In particular, the heat transport was carried out without net transport of mass, in a closed container, i.e. the flow of mass of superfluid component in one direction was compensated by an opposite flow of normal fluid, namely $\rho_n v_n + \rho_s v_s = 0$. The heat applied to an end of the system excites the fluid and produces a normal component with velocity v_n leaving from it. This fluid is replaced by the superfluid component arriving with velocity $v_s = -(\rho_n/\rho_s)v_n$. When the value of the heat flow is higher than some characteristic value, it was found a transition to a turbulent state, characterized by a non-vanishing value of the vortex line density L. In this case, the vortex lines form a disordered tangle, whose total length density increases with increasing heat flow (Donnelly 1991; Nemirovskii and Fiszdom 1995; Barenghi et al. 2001; Mongiovi and Jou 2006). In fact, if the heat flow is further increased, another transition arises from the first turbulent state with a low value of L (TI turbulence) to a second turbulent state with a high value of L (TII turbulence). Again in this case, the attenuation of second sound was increased with respect to its attenuation in the fluid in the absence of heat flux as a consequence of its interaction with the vortex lines of the tangle; the corresponding increase in attenuation allows one to measure the vortex line density L.

In the presence of the turbulent vortex tangle, the superfluid does no longer flow without resistance, as it experiences a friction with the vortex lines. This is the reason that for a velocity sufficiently high, the superfluid flow along a capillary presents a non-vanishing resistance. An alternative way to produce turbulence in superfluid helium explored since the 1990s, is by towing thin grids through the superfluid, which is able to create very intense turbulence, spanning five orders of

magnitude in the vortex density. To achieve comparable results in classical wind tunnel in usual fluids it would need a length of a thousand kilometres as compared with the half meter length in superfluid helium (Donnelly 1991); this shows clearly the interest of turbulence in superfluid helium as a benchwork to deepen into the subtleties of turbulence at very high Reynolds numbers.

11.4.1 Macroscopic Description of Vortex Friction

It is possible to describe these two seemingly very different situations (rotating fluid, counterflow) by introducing in the evolution equations the frictional effects of the vortex array or the vortex tangle—i.e. their contribution to viscous dissipation in the superfluid by means of a tensor $\mathbf{P}_{\omega}^{\nu}$. As it has been said above, this friction results from the collisions of the excitations constituting the normal fluid—mainly the rotons—with the core of the vortex lines. The collision cross section is a maximum when the roton travels perpendicular to this line, and it is a minimum—in fact, zero—when it moves parallel to it. The microscopic mechanisms are the same in rotating helium II and in counterflow turbulence. It is logical to ask for a tensor incorporating the local direction of the vortex lines through their local tangent unit vector \mathbf{s}' , and the vortex line density. We are therefore led to take

$$\mathbf{P}_{\omega}^{v} = \tilde{\lambda} \kappa L \langle \mathbf{U} - \mathbf{s}' \mathbf{s}' + \mathbf{W} \cdot \mathbf{s}' \rangle, \tag{11.37}$$

where L is the vortex line density, s' the unit vector tangent to the vortices at a given point—the vortices may be represented parametrically by a vectorial function $s(\xi,t)$, ξ being the arc-length along the line, so that the derivative of s with respect to ξ , denoted as s', is the unit tangent vector—the angular brackets denote an average over the different orientations of the vortices in a given volume, \mathbf{U} is the unit tensor, and \mathbf{W} a third-order completely antisymmetric tensor, i.e. the term in $\mathbf{W} \cdot \mathbf{q}$ is an antisymmetric second-order tensor. Finally, $\tilde{\lambda}(T,\rho)$ is a coefficient related to the energy of the vortices and describing the probability of interaction between the elementary excitations and the vortex unit length.

We assume that the interaction between the vortices and the heat flux may be described by adding to the evolution equation (11.29) for the heat flux a source term proportional to $-\mathbf{P}_{\omega}^{\nu} \cdot \mathbf{q}$, because the heat flux \mathbf{q} is related to a flow of excitations and $\mathbf{P}_{\omega}^{\nu}$ describes the force produced by the vortices on the excitations. To be specific, we generalize the evolution equations (11.2–11.5) to a rotating framework with angular speed Ω in the presence of vortices. We have

$$\frac{\mathrm{d}\rho}{\mathrm{d}t} + \rho \nabla \cdot \mathbf{v} = 0,\tag{11.38}$$

$$\rho \frac{\mathrm{d}\mathbf{v}}{\mathrm{d}t} + \nabla p - \mathbf{i}^0 + 2\rho \mathbf{\Omega} \times \mathbf{v} = 0, \tag{11.39}$$

$$\rho \frac{\mathrm{d}u}{\mathrm{d}t} + \nabla \cdot \boldsymbol{q} + p\nabla \cdot \boldsymbol{v} = 0, \tag{11.40}$$

$$\frac{\mathrm{d}\boldsymbol{q}}{\mathrm{d}t} + \frac{1}{\tau}\boldsymbol{q} + \frac{\lambda}{\tau}\nabla T + 2\boldsymbol{\Omega} \times \boldsymbol{q} = -\alpha \mathbf{P}_{\omega}^{\nu} \cdot \boldsymbol{q}, \tag{11.41}$$

where α is a phenomenological coefficient, and $i^0 - 2\rho\Omega \times v$ denotes the inertial force. The term $2 \times q$ in (11.41) accounts for the time variation of the vector q due to the rotation. Below we show that the source term on the right-hand side of (11.41) is able to describe in an unified way the effect of the vortices on the dynamics of the heat flux, both in the rotating system as in the counterflow situation, provided the coefficients α and $\tilde{\lambda}$ are suitably identified in terms of the frictional coefficients B(T) and B'(T) of (11.36) (Jou et al. 2002b; Mongiovì et al. 2004).

11.4.2 Rotating Frame

In the rotating frame, the vortices are parallel to the angular velocity vector Ω and $L = a_1 |\Omega|$, which in virtue of (11.35) it turns out that $a_1 = 2/\kappa$; then, the unit tangent vectors s' are parallel to Ω , i.e. $s' = \Omega/|\Omega|$, and the production term on the right-hand side of (11.41) becomes

$$-\mathbf{P}_{\omega}^{\nu} \cdot \mathbf{q} = -a_{1}\kappa\lambda\frac{\mathbf{\Omega}}{|\mathbf{\Omega}|} \times \mathbf{\Omega} \times \mathbf{q} - a_{2}\kappa\lambda\mathbf{\Omega} \times \mathbf{q}, \qquad (11.42)$$

where a_2 is a coefficient linked to the antisymmetric tensor **W** as $W_{ijk} = -a_2 \varepsilon_{ijk}$, being the Ricci third-order tensor, i.e. the complete antisymmetric tensor whose coefficients are 0, 1 or -1. The first term on the right hand side of (11.42) comes from the relation $(\mathbf{U} - s's') \cdot \mathbf{q} = -s' \times (s' \times \mathbf{q})$, and the second one from the relation $\boldsymbol{\varepsilon} \cdot s' \cdot \mathbf{q} = -s' \times \mathbf{q}$. Then, we may write (11.41) as

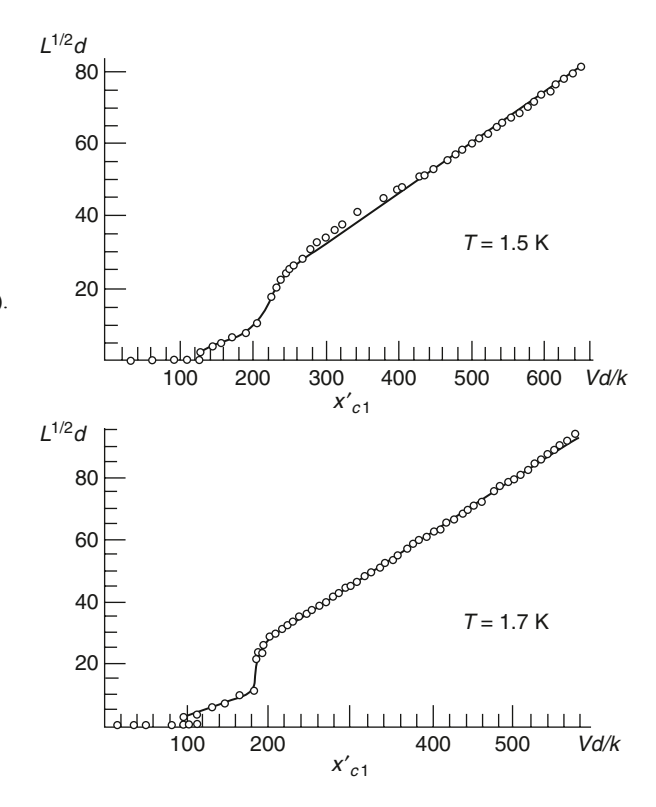
$$\frac{\mathrm{d}\boldsymbol{q}}{\mathrm{d}t} + \frac{1}{\tau}\boldsymbol{q} + \frac{\lambda}{\tau}\nabla T + 2\boldsymbol{\Omega} \times \boldsymbol{q} = -B\frac{\boldsymbol{\Omega}}{|\boldsymbol{\Omega}|} \times \boldsymbol{\Omega} \times \boldsymbol{q} - B'\boldsymbol{\Omega} \times \boldsymbol{q}, \quad (11.43)$$

where B and B' are the friction coefficients appearing in (11.36) and are related to the coefficients in (11.42) as $B = a_1 \kappa \tilde{\lambda}$ and $B' = a_2 \kappa \tilde{\lambda}$. The rotation has therefore an important influence on the dynamics of the heat flux.

11.4.3 Counterflow Turbulence

Now that we have identified the coefficient α appearing in (11.41) in terms of the friction coefficients, we may use (11.41) to describe counterflow turbulence in a

Fig. 11.1 The vortex line density as a function of the relative velocity $v_n - v_s \equiv V$. The figure is the plot of $y \equiv L^{1/2}d$ versus $x \equiv Vd/\kappa$ for T = 1.5 K and T = 1.7 K. The circles correspond to experimental data from Martin and Tough (1983), and the lines are determined from Eq. (11.57). (Mongiovì and Jou 2005c)



non-rotating tube with diameter d, submitted to a longitudinal heat flow q. The experiments indicate that when the counterflow velocity increases beyond a first critical value $V_{c1} = c_1 \kappa/d$, with c_1 a numerical constant, there suddenly appears a contribution to dissipation, and when it reaches a second critical value $V_{c2} = c_2 \kappa/d$, with $c_2 > c_1$ the dissipation has a second sudden increase (Fig. 11.1). For higher values of V, the flow resistance associated with dissipation increases continuously as V^2 . The values of c_1 and c_2 depend on the temperature; for Helium II at 1.5 K, c_1 = 127 and c_2 = 129; at 1.7 K, c_1 = 98 and c_2 = 186 (Martin and Tough 1983).

It is generally accepted that this dissipation is the result of the interaction between the normal fluid and a disordered tangle of quantized vortex filaments. In the first transition, the vortex tangle appears, but with a relatively low value of the vortex line density. The discontinuity from L=0 (laminar regime) to this first turbulent regime TI at $V=V_{c1}$ is of the order of $L_1d^2\approx 2.5$. Afterwards, L increases as $L_1^{1/2}=\gamma_1V-(b_1/d), \gamma_1$ and b_1 being numerical parameters. At the second critical counterflow velocity V_{c2} , there is a sudden change in the slope of L as a function of V^2 , and for higher V a regime $L_2^{1/2}=\gamma_2V-(b_2/d)$ is reached, of fully developed turbulence with high values of L_2 . Below, we will briefly discuss the relation between L and V. Now, our aim is to describe dissipation in counterflow turbulence in general terms.

To do that, we will use again (11.41). The essential difference with rotation comes from the geometry of the vortices, which form a tangle where the vortex segments are distributed in a (quasi)isotropic way instead of being a regular array of parallel vortices. Then,

$$\langle \mathbf{U} - \mathbf{s}' \mathbf{s}' \rangle = \frac{2}{3} \mathbf{U},\tag{11.44}$$

where it has been taken into account that s' is a unit vector and that $\langle s's' \rangle = \mathbf{U}$. As a consequence, the production term in (11.41) takes the form

$$-\mathbf{P}_{\omega}^{v}\cdot\boldsymbol{q}=-\frac{2}{3}\kappa\tilde{\lambda}L\boldsymbol{q}.\tag{11.45}$$

Often this expression is written by assuming that $L \approx \gamma q^2$, a result which will be further commented since it is a good approximation for high values of q, and one writes (11.44) as

$$-\mathbf{P}_{\omega}^{\nu} \cdot \mathbf{q} = -B''q^2\mathbf{q}, \tag{11.46}$$

with $B'' = \frac{2}{3}\kappa\tilde{\lambda}\gamma$. This describes a friction force proportional to the third power of the heat flux, known as Görter–Mellink force. Thus, the use of the production term $-\mathbf{P}^{\nu}_{\omega} \cdot \mathbf{q}$ in the evolution equation (11.41) for the heat flux is able to summarize in a single compact expression the vortex contribution to dissipation, both in rotating cylinders as in counterflow turbulence, the difference between both cases being the geometrical distribution of vortex orientation, whereas the microscopic interaction between rotons and vortices has the same form in both cases.

11.5 Second Sound Propagation in the Presence of Ouantized Vortices

Propagation of the low amplitude second sound, which does not appreciably perturb the vortex lines but experiences their frictional effects, is a very useful experimental tool to obtain information about the density and the distribution of vortex lines. Because of this practical interest, we will study it starting from Eqs. (11.38–11.41) with the suitable expressions for the dissipation term $-\mathbf{P}_{\omega}^{w} \cdot \mathbf{q}$, (11.43) for rotating cylinders and (11.46) for thermal counterflow.

11.5.1 Rotating Cylinders

We assume again the set of plane harmonic waves specified in (11.30) and introduce them into (11.38–11.41). The linearized set of equations is now

$$-\omega\tilde{\rho} + k\rho_0\tilde{\mathbf{v}} \cdot \mathbf{n} = 0, \tag{11.47a}$$

$$-\omega \tilde{\mathbf{v}} + k\rho_0^{-1} (\partial p/\partial \rho)_0 \tilde{\rho} \mathbf{n} - 2i\mathbf{\Omega} \times \mathbf{v} = 0, \tag{11.47b}$$

$$-\omega \tilde{T} + k\rho_0^{-1} (\partial u/\partial T)_0^{-1} \tilde{\mathbf{q}} \cdot \mathbf{n} = 0, \tag{11.47c}$$

$$-\omega \tilde{\boldsymbol{q}} + k(\lambda/\tau)_0 \tilde{T} \boldsymbol{n} - i(2 - B') \boldsymbol{\Omega} \times \tilde{\boldsymbol{q}} + iB \frac{\boldsymbol{\Omega}}{|\boldsymbol{\Omega}|} \times \boldsymbol{\Omega} \times \tilde{\boldsymbol{q}} = 0. \quad (11.47d)$$

For the waves parallel to the rotation axis, one has $\Omega \times \tilde{q} = 0$ and $\Omega \times \nu = 0$, and the dispersion relation is the same as (11.32), and thus, neither the first nor the second sound are influenced by the rotation.

In contrast, when the direction of propagation of the waves is orthogonal to the rotation axis, one obtains, up to first order terms in $|\Omega|$,

$$(\omega^2 - k^2 u_1^2)(\omega^2 + iB\omega |\Omega| - k^2 u_2^2) = 0.$$
 (11.48)

The first sound is not influenced, whereas the second sound or temperature wave is attenuated. Explicitly, it is found for the phase speed u'_2 and attenuation coefficient $k_{s,2}$ of the second sound

$$u_2' = u_2 \left(1 - k_{s,2}^2 \frac{u_2^2}{2\omega^2} \right), \quad k_s^{(2)} = \frac{B}{2u_2} |\mathbf{\Omega}| + \mathcal{O}(\Omega^2).$$
 (11.49)

Thus, measurement of the attenuation coefficient of these waves allows us to obtain the friction coefficient *B*.

11.5.2 Second Sound and Counterflow Turbulence

In this case, (11.47a) and (11.47c) remain as before, whereas in absence of rotation, and taking into account the expression (11.46) for the source term, (11.47b) and (11.47d) are changed into

$$-\omega \tilde{\mathbf{v}} + k\rho_0^{-1} (\partial p/\partial p)_0 \tilde{\rho} \mathbf{n} = 0, \tag{11.50a}$$

$$-(\omega + iB''L_0/\gamma)\tilde{\mathbf{q}} + k(\lambda/\tau)_0\tilde{T}\mathbf{n} = 0.$$
 (11.50b)

From here, it follows the dispersion relation, independently of the propagation direction.

$$(\omega^2 - k^2 u_1^2) \left(\omega^2 + iB'' \omega \frac{L_0}{\gamma} - k^2 u_2^2 \right) = 0.$$
 (11.51)

As in the previous situation, the sound wave is not influenced by the vortex tangle, whereas the second sound experiences changes in phase speed and attenuation given by

$$u_2' = u_2 \left(1 - \frac{u_2^2}{2\omega^2} k_{s,2}^2 \right), \quad k_{s,2}^{(2)} = \frac{B''}{2\nu_2} \frac{L_0}{\gamma^2}.$$
 (11.52)

The measurements of k_s and v_2 allow us to obtain the vortex line density L_0 . This makes second sound a very valuable tool for the measurement of L_0 in superfluid turbulence.

11.6 Evolution Equation for the Vortex Line Density

The most relevant quantity for the description of turbulent vortex tangles in counterflow experiments is the vortex line density L, i.e. the total length of quantized vortices per unit volume of the fluid, which becomes a new independent variable characterizing the turbulent state. Then, an evolution equation is needed for it. We consider here a well-known equation derived by Vinen (1957a, b). He assumed that

$$\frac{\mathrm{d}L}{\mathrm{d}t} = \left(\frac{\mathrm{d}L}{\mathrm{d}t}\right)_f - \left(\frac{\mathrm{d}L}{\mathrm{d}t}\right)_d,\tag{11.53}$$

where the subscripts f and d stand for formation and destruction, respectively. He then considered dimensional arguments, by combining L (length⁻²), the vorticity quantum κ (length²/time), and $V = \nu_{\rm n} - \nu_{\rm s}$, the relative velocity between normal and superfluid components (length/time) to explore the form of the formation and destruction terms. Note that with these quantities one can construct three combinations having the dimensions of reciprocal of time, namely

$$\frac{1}{t_1} \propto V L^{1/2}, \quad \frac{1}{t_2} \propto V^2 \kappa^{-1}, \quad \frac{1}{t_3} \propto \kappa L.$$
 (11.54)

Vinen used only t_1 and t_3 , but for the moment we will keep the three times; t_1 and t_2 are usually associated to the formation terms, because the velocity V is necessary to

form vortices, and t_3 to the destruction term, because the vortices will decay when V is equated to zero. Thus, one may write

$$\frac{dL}{dt} = \frac{L}{t_1} + \frac{L}{t_2} - \frac{L}{t_3} = \alpha V L^{3/2} + \alpha' \frac{V^2}{\kappa} L - \beta \kappa L^2,$$
(11.55)

where α , α' and β are dimensionless constants which depend on temperature. In Vinen's approach, $\alpha'=0$. The L^2 dependence of the destruction term may be understood intuitively from the idea that two vortices rotating in opposite way may anihilate each other, or may cross and break each other, in such a way that this term should depend on the pairs of vortices per unit volume. These equations have been given a microscopic ground on the dynamics of vortices by Schwarz (1985, 1988) and have been derived on thermodynamic grounds by Geurst (1989) from the energy and impulse balance equations of the vortex tangle. In the steady state, Vinen's equation (11.55) with $\alpha'=0$ leads to

$$L = \left(\frac{\alpha}{\beta}\right)^2 \frac{1}{\kappa^2} V^2. \tag{11.56}$$

The same dependence $L \sim V^2$ in the steady state is obtained with the full equation (11.55) in such a way that it cannot provide arguments in favour or against the possible vanishing of coefficient α' . The solution L=0 corresponds to the laminar regime. In fact, (11.55) is too simplistic, because it leads to turbulence as soon as $V \neq 0$, instead of having a threshold value of V.

11.6.1 Transition from the Laminar to the Turbulent Regime

Equation (11.55) does not describe the transition from the laminar to the turbulent regime, as it yields $L \neq 0$ for any value of V, even for low values of V. A description of this transition may be achieved when the influence of the walls, as described by the diameter d of the tube, is taken into account. This leads to the following generalization of (11.55) (Mongiovì and Jou 2005a, 2006)

$$\frac{\mathrm{d}L}{\mathrm{d}t} = \alpha V L^{3/2} \left(1 - \tilde{\omega} \frac{L^{-1/2}}{d} \right) + \alpha' \frac{V^2}{\kappa} L - \beta \kappa L^2. \tag{11.57}$$

In the ratio $L^{-1/2}/d$, the numerator $L^{-1/2}$ indicates the average separation between vortex lines. When L is low, the separation becomes comparable to the diameter d of the cylinder, and the effects of the walls become dominant because the vortex lines have a higher probability of hitting the walls than other vortices. The new term (the term in $\tilde{\omega}$, which is a constant coefficient that must not be confused with the angular frequency) describes a reduction of the vortex production when the vortex density is

low, because there are less crossings. In contrast, for dense tangles with high values of L, the separation between vortex lines becomes very small and Vinen's equation (Eq. (11.55) with $\alpha' = 0$) is recovered.

The steady state solutions of (11.57) are

$$L_1^{1/2} = 0, \quad L_{2,3}^{1/2} = \frac{\alpha V}{2\beta\kappa} \left[1 \pm \sqrt{1 + \frac{4\beta\kappa}{\alpha V} \left(\frac{\alpha'}{\alpha} \frac{V}{\kappa} - \frac{\tilde{\omega}}{d} \right)} \right]. \tag{11.58}$$

The solutions $L_{2,3}$ correspond to the + and – signs, respectively. These solutions are real only for values of V higher than

$$V_{c1} = \frac{4\beta\alpha\tilde{\omega}}{\alpha^2 + 4\beta\alpha'} \frac{\kappa}{d}.$$
 (11.59)

Note in (11.59) that the dimensionless quantity Vd/κ plays in counterflow turbulence a role analogous to the Reynolds number (Vd/ν , with ν the kinematical viscosity) in the turbulence of classical viscous fluids. Instead of the kinematical viscosity, which appears in the denominator of the Reynolds number but which is zero in the superfluid component, this combination has in the denominator the quantum of vorticity, which has the same dimensions as a kinematical viscosity. For low values of Vd/κ , the flow is laminar whereas beyond a critical value of Vd/κ , the flow becomes turbulent. A Reynolds number could also be defined for the normal component, which has a finite kinematic viscosity ν_n . When this Reynolds number is sufficiently high, the normal component may also become turbulent.

At the transition, when $V = V_{c1}$, there is a discontinuity in L from L = 0, corresponding to the laminar regime, to a vortex tangle with length density given by

$$L_{c1}^{1/2} = \frac{2\alpha^2 \omega}{\alpha^2 + 4\alpha\beta} \frac{1}{d}.$$
 (11.60)

The discontinuity in L is higher for thinner cylinders, as seen in (11.60) and as it is observed in experiments (Martin and Tough 1983).

The stability of the solutions (11.58) may be studied from the equation for a perturbation δL of L, obtained from (11.57), and which is given by

$$\frac{\mathrm{d}\delta L}{\mathrm{d}t} = -\left(2\beta\kappa L - \frac{3}{2}\alpha V L^{1/2} - \alpha' \frac{V^2}{\kappa} + \alpha\omega \frac{V}{d}\right)\delta L. \tag{11.61}$$

From this equation follows that $L_1=0$ is stable up to a value V'_{c1} given by $V'_{c1}=(\alpha_1\omega/\alpha')(\kappa/d)$. The solution L_2 is stable where it exists, i.e. for $V>V'_{c1}$ and L_3 is unstable. Furthermore, according to (11.59) the critical velocity V_{c1} for the appearance of turbulence is lower than the maximum speed V'_{c1} where the laminar solution becomes necessarily unstable. In the range between V_{c1} and V'_{c1} , the solution $L_1=0$, corresponding to the laminar regime, is metastable. These results are in qualitative agreement with experiments: one recovers the dependence $V\propto \kappa/d$

and $L_{c1}^{1/2} \propto d^{-1}$, the discontinuity in the transition from laminar to turbulent flow, and the existence of a metastable region of the laminar state. However, this equation does not describe the transition from TI to TII regimes. This topic is too specialized to be dealt here. It is discussed at length in Mongiovì and Jou (2005a, b).

11.6.2 Simultaneous Rotation and Counterflow

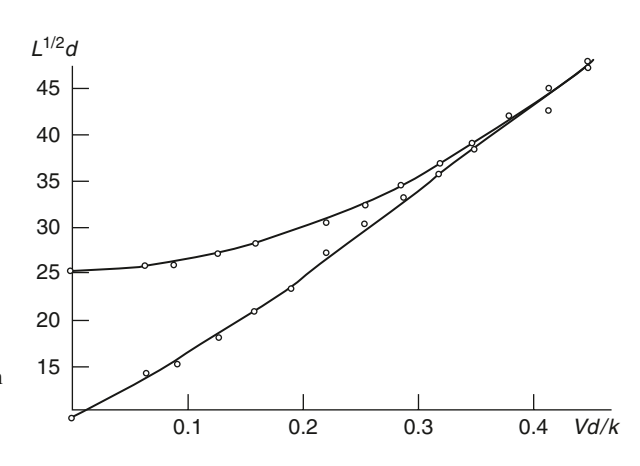
Rotation and counterflow, which have been dealt with separately in the previous sections, may be simultaneously combined, by allowing heat to flow parallel to the rotation axis of a rotating container. It is experimentally found (Swanson et al. 1983) that the effects of rotation and counterflow are not additive, i.e. the total vortex length density in the combined situation is not the sum of the vortex length densities corresponding to pure rotation and pure counterflow, and the ordered array of vortices is deformed and mixed by the counterflow tangle, thus leading to an anisotropic tangle (Jou and Mongiovì 2004, 2005, 2006).

When the container is rotating at a given angular speed Ω and an increasing heat flow parallel to Ω is imposed, the laminar regime disappears and two critical counterflow velocities V_{c1}^{HR} and V_{c2}^{HR} are found, scaling as $\Omega^{1/2}$. For $V < V_{c1}^{HR}$ the length density L is independent of V and proportional to Ω , namely, $L = 2\Omega/\kappa$, as in absence of counterflow. For $V_{c1}^{HR} < V < V_{c2}^{HR}$ the situation is analogous, but the proportionality constant between L and Ω is slightly increased. For $V_{c2}^{HR} < V$, L becomes dependent on V and increases with it, becoming proportional to V^2 at high values of V, with a proportionality constant independent on Ω , as in the situation of pure counterflow (see Fig. 11.2).

These features may be described by means of a generalized Vinen's equation of the form (Mongiovì and Jou 2005c)

$$\frac{\mathrm{d}L}{\mathrm{d}t} = -\beta\kappa L^2 + \left(\alpha V + \alpha_2 \sqrt{\kappa \Omega}\right) L^{3/2} - \left(\beta_1 \Omega + \beta_2 \frac{V\sqrt{\Omega}}{\sqrt{\kappa}}\right) L. \quad (11.62)$$

Fig. 11.2 Values of $L^{1/2}d$ as a function of Vd/κ in rotating containers for a rotation frequency of 0.0073 Hz (lower line) and 0.05 Hz (upper line). The dots correspond to experimental data from Swanson et al. (1983) and the lines are determined from Eq. (11.62). (Mongiovì and Jou 2005b)



The new terms are the simplest dimensional combinations of V, Ω , κ and L describing a rate of change of L. When $\Omega = 0$, the classical Vinen's equation (11.55), with $\alpha' = 0$, is recovered. Though there are three new terms related to Ω , it may be shown that relatively general arguments about the form of the observed solutions yield two independent relations between their coefficients, namely,

$$\beta_2 = \sqrt{2}\alpha, \quad \beta_1 = \sqrt{2}\alpha_2 - 2\beta. \tag{11.63}$$

Thus, in fact there is only one independent coefficient, α_2 , which may be obtained by fitting the experimental data. The signs of the different terms are given by comparison with the experimental data. The term in $V\sqrt{\Omega}$ deserves special attention, as it establishes the non-additive coupling between rotation and counterflow. An interesting topic arising in this domain is the degree of anisotropy of the tangle. The effects of rotation tend to orient the vortex lines along the rotation axis, whereas the counterflow tends to randomize their directions. Thus, Ω and V play, respectively, analogous roles to a magnetic field and temperature on magnetic systems: the magnetic field tends to orient the magnetic dipoles along its direction, whereas the disordered thermal energy tends to randomize them. This magnetic analogy has been a basis for several heuristic analyses of the anisotropy of the vortex tangle in terms of Ω and V (Tsubota et al. 2003; Mongiovì and Jou 2005c).

11.6.3 Non-equilibrium Thermodynamics of Vortex Tangles

Up to now we have assumed that the vortex array or the vortex tangle is essentially homogeneous, and that the temperature wave of the second sound does not modify the vortices. This is reasonable if the amplitude of the wave is small, since it will not be able to produce nor destroy vortex tangles. However, the wave may displace or deform a little bit the vortices, thus producing a wave in the vortex length density L itself. Thus, a more complete analysis of the turbulent tangle would be achieved if L itself is added to the set of independent space-dependent fields. In other words, we will generalize (11.57) as

$$\frac{\mathrm{d}L}{\mathrm{d}t} = -\nabla \cdot \boldsymbol{J}_L + \sigma_{\mathbf{L}},\tag{11.64}$$

where σ_L is the net production term as given, for instance, by the right-hand side of (11.57), and J_L a vortex diffusion flux. The addition of this new flux will also produce a coupling with the heat flux.

We thus write the Gibbs equation incorporating L as

$$ds = T^{-1}du - T^{-1}\mu_L dL - \alpha_q \rho^{-1} T^{-1} \mathbf{q} \cdot d\mathbf{q},$$
 (11.65)

where μ_L is the chemical potential corresponding to variations of L. If only the energetic contribution to μ_L is taken into account—and not the entropic one—it turns out that, according to vortex theory,

$$\mu_L = \frac{\rho_s \kappa^2}{4\pi} \ln \left(\frac{1}{a_0 L^{1/2}} \right), \tag{11.66}$$

where a_0 is a length of the order of the radius of the core of the vortices. The entropy production and entropy flux obtained from (11.65)—disregarding the contribution of the production terms in the evolution equations for q and L, for simplicity—is

$$\sigma_{\mathbf{s}} = -\boldsymbol{J}_L \cdot \nabla (T^{-1}\mu_L) + T^{-1}\boldsymbol{q} \cdot (\nabla T^{-1} - \alpha_q \dot{\boldsymbol{q}}). \tag{11.67}$$

From here, we may write the following equations for J_I and q

$$\nabla T^{-1} - \alpha_q \dot{\boldsymbol{q}} = \mathcal{L}_{qq} \boldsymbol{q} + \mathcal{L}_{qL} \boldsymbol{J}_L, \tag{11.68}$$

$$-\nabla (T^{-1}\mu_L) = \mathcal{L}_{Lq}\boldsymbol{q} + \mathcal{L}_{LL}\boldsymbol{J}_L, \qquad (11.69)$$

or, equivalently,

$$\tau \dot{\boldsymbol{q}} + \boldsymbol{q} = -\lambda \nabla T + \mathcal{L}'_{qL} \boldsymbol{J}_L, \tag{11.70}$$

$$\boldsymbol{J}_{L} = -D\nabla L + \mathcal{L}'_{Lq}\boldsymbol{q}, \qquad (11.71)$$

where D denotes the diffusion coefficient of vortex lines. Indeed, in inhomogeneous vortex tangles the vortices tend to distribute homogeneously and go from high L to low L regions, as it is typical in diffusive processes. If we replace J_L on the right-hand side of (11.70) by (11.71) we get

$$\tau \dot{q} + q = -\lambda' \nabla T + \chi_0 \nabla L, \qquad (11.72)$$

with $\lambda' = \lambda + \mathcal{L}'_{qL}\mathcal{L}'_{Lq}$, i.e. the coupling between J_L and q produces a modification in the thermal conductivity, which instead of being simply λ becomes increased in the coupling quantity. Introducing (11.72) into (11.64) and taking into account the production terms in the evolution equation for q, we obtain for the joint evolution of q and L the following equations

$$\frac{\partial \mathbf{q}}{\partial t} + \frac{1}{\tau} \mathbf{q} + \varsigma \nabla T + \chi \nabla L = -KL\mathbf{q}, \tag{11.73a}$$

$$\frac{\partial L}{\partial t} = D\nabla^2 L + \mathcal{L}'_{qL} \nabla \cdot \boldsymbol{q} + \sigma_L, \tag{11.73b}$$

where $\varsigma = \lambda/\tau$ and $\chi = D'_{qL}/\tau$, and K a friction coefficient between the vortex lines and the normal fluid, as expressed in (11.45), i.e. $K = \frac{2}{3}\alpha\kappa$.

Note that if $\mathcal{L}'_{qL}=0$, we obtain from (11.64) a reaction-diffusion equation for L, with the reaction term given by the right-hand side of (11.57) or some analogous expression. Second, there is the possibility of coupled heat and vortex waves, implying local changes in T and L simultaneously. The simplest expression for them is obtained by ignoring the production terms and the coefficient D, and assuming that the relaxation time is long. The behaviour of vortex density waves and high-frequency second sound and their mutual interplay has been studied by Sciacca et al. (2007). In fact, to Eqs. (11.73a, 11.7b) one should add an equation for the velocity of the superfluid. This topic is dealt with from a thermodynamic perspective in Nemirovskii and Fiszdom (1995) and in Jou and Mongiovì (2005) and Mongiovi et al. (2007). Further details are given in Sect. 11.7.

Let us finally mention that in (11.65) we have assumed that the entropy of the vortex tangle depends only on L. However, it has also a configurational entropy, related to the length distribution function of the vortex loops constituting the tangle and to the orientation distribution of the vortex lines. From the point of view of the length distribution of the vortex lines, it must be noted that the vortex lines are either closed vortex loops or lines which have their ends pinned on the walls. For fully developed turbulence, closed vortex loops are dominating. The vortex length distribution function has a potential form (Nemirovskii and Fiszdom 1995)

$$\Pr(\ell)d\ell = C \frac{\ell^{-a}d\ell}{(\ell_{\min})^b},$$
(11.74a)

where a and C are positive constants, b = 4-a and ℓ_{\min} is the minimum vortex loop length. Nemirovski obtained a = 5/2. From here follows that the contribution to the entropy has the form (Jou and Mongiovì 2009)

$$S_1(L) = C'L^{3/2}V,$$
 (11.74b)

with C' a positive constant. Since L is roughly proportional to the internal energy density, (11.74b) may be written as

$$S_1(U, V) = C''U^{3/2}V^{-1/2}.$$
 (11.74c)

Jou and Mongiovì (2009) have studied in detail the thermodynamic consequences of (11.74). In particular, it follows from $T^{-1} = (\partial S/\partial U)_V$ and $pT^{-1} = (\partial S/\partial V)_U$ that

$$\frac{U}{V} = \frac{2}{3C''}T^{-2}; \quad p = -\frac{1}{3}\frac{U}{V}.$$
 (11.74d)

The first of these expressions implies a negative heat capacity, analogously to black holes, and the second one indicates a negative contribution to the pressure, in a form which could be of interest for the analysis of dark energy in cosmology, assuming that it is constituted by cosmic string loops, because dark energy needs a negative enough pressure to accelerate the cosmic expansion. Analogies between vortex loops and topological cosmic defects are an interesting topic (Volovik 2005), but we cannot deal with them here.

To estimate the configurational entropy of the tangle related to the orientation, we make an analogy with polymer physics. In the latter, the configuration tensor C is defined as (see Eq. (1.110))

$$\mathbf{C} = \langle \mathbf{R}\mathbf{R} \rangle \,, \tag{11.75}$$

with R the end-to-end vector—or simply the orientation vector, if the molecule is rigid, as in rigid dumbbells or liquid crystals, and $\langle \cdots \rangle$ standing for average. Analogously, the geometry of the tangle may be described by the tensor $\langle s's' \rangle$, or by U - s's', as it has been said in (11.37). Then, as well as in polymer physics, one may define the orientational contribution to the configurational entropy of the tangle as

$$S = k_{\rm B} L \left[\frac{1}{2} \text{Tr} \langle \mathbf{U} - \mathbf{s}' \mathbf{s}' \rangle + \ln \left| \det \langle \mathbf{s}' \mathbf{s}' \rangle \right| \right]. \tag{11.76}$$

(see Eqs. (1.111) and (5.22)). In this way, the detailed study of the thermodynamics of vortex tangles should in fact incorporate not only the vortex line density L but also the configuration entropy, being still this an open topic.

11.7 Hydrodynamics of Turbulent Superfluids

In Sect. 11.1.1 we have presented a hydrodynamic approach for superfluid flows by using as dynamical variables ρ , s, $j = \rho v$ and v_s . There we did not consider the viscous contribution of the normal component nor the presence of vortices which arise in turbulent flows and contribute to internal dissipation. In Sect. 11.6 we have paid a detailed attention to the vortices in rotating cylinders and in counterflow situations, but we have considered that v_s and $v_n - v_s$ were fixed, and we concentrated our study on the vortex array or the vortex tangle.

To end this chapter we take a more general perspective and consider that ν_s and ν_n themselves are varying with time and space, and discuss the so-called Hall–Vinen–Bekarevich–Khalatnikov hydrodynamical model for the description of the evolution of the system (Donnelly 1991; Mongiovì and Jou 2007).

The evolution equations for v_n and v_s in HVBK framework are (Donnelly 1991)

$$\rho_{n} \frac{\partial \mathbf{v}_{n}}{\partial t} + \rho_{n} \mathbf{v}_{n} \cdot \nabla \mathbf{v}_{n} = -\frac{\rho_{n}}{\rho} \nabla p_{n} - \rho_{s} s \nabla T + \mathbf{F}_{ns} + \eta_{n} \nabla^{2} \mathbf{v}_{n}, \quad (11.77)$$

$$\rho_{\rm s} \frac{\partial \mathbf{v}_{\rm s}}{\partial t} + \rho_{\rm s} \mathbf{v}_{\rm s} \cdot \nabla \mathbf{v}_{\rm s} = -\frac{\rho_{\rm s}}{\rho} \nabla p_{\rm s} + \rho_{\rm s} s \nabla T - F_{\rm ns} + \rho_{\rm s} T, \qquad (11.78)$$

where η_n is the dynamic viscosity of the normal component. The effects of the vortices on the motion of the components of the superfluid are described by F_{ns} , the friction force of the superfluid component on the normal fluid, which bears an opposite sign in the Eq. (11.78), as it is consistent with its character of an internal force, and by $\rho_s T$, the vortex tension force, related to the average curvature of the vortices. The quantities p_n and p_s , the effective pressures acting on the normal and the superfluid components, respectively, are defined as

$$\nabla p_{\rm n} = \nabla p + \frac{1}{2} \rho_{\rm s} \nabla (\mathbf{v}_{\rm n} - \mathbf{v}_{\rm s})^2, \tag{11.79a}$$

$$\nabla p_{\rm s} = \nabla p - \frac{1}{2} \rho_{\rm n} \nabla (\mathbf{v}_{\rm n} - \mathbf{v}_{\rm s})^2, \tag{11.79b}$$

with *p* being the total hydrodynamic pressure.

The expressions for F_{ns} and T describing the effect of the vortices on the evolution of the velocities v_n and v_s in the HVBK model, in terms of the vortex lines, are (Donnelly 1991)

$$\boldsymbol{F}_{\rm ns} = \rho_{\rm s}\alpha\hat{\boldsymbol{\omega}} \times \left[\boldsymbol{\omega} \times (\boldsymbol{v}_{\rm ns} - \tilde{\boldsymbol{\beta}}\nabla \times \hat{\boldsymbol{\omega}})\right] + \rho_{\rm s}\alpha'\boldsymbol{\omega} \times (\boldsymbol{v}_{\rm ns} - \tilde{\boldsymbol{\beta}}\nabla \times \hat{\boldsymbol{\omega}}), \quad (11.80)$$

$$T = (\tilde{\beta} \nabla \times \hat{\boldsymbol{\omega}}) \times \boldsymbol{\omega} = \tilde{\beta} \boldsymbol{\omega} \cdot \nabla \hat{\boldsymbol{\omega}}, \tag{11.81}$$

where ν_{ns} is used for the difference $\nu_n - \nu_s$, $\omega = \nabla \times \nu_s$ is the rotational of the superfluid vorticity, $\hat{\omega} \equiv \omega/|\omega|$ is the unit vector along ω , and $\tilde{\beta}$ is the vortex tension parameter defined as

$$\tilde{\beta} = \frac{\kappa}{4\pi} \ln \left(\frac{c}{a_0 L^{1/2}} \right),\tag{11.82}$$

c being a constant of the order of unity, a_0 the radius of the vortex core, and α and α' the friction coefficients appearing in (11.41). Note that in Sect. 11.6 we have used the symbol V for the average of $v_n - v_s$ on the whole system, whereas in (11.80), (11.81) we are considering the local values of v_n and v_s in the inhomogeneous situation, and v_{ns} for their difference.

In the case of isotropic vortex tangles, the tension T appearing in (11.78) is T = 0, because the averaged curvature is zero, and the friction force F_{ns} in (11.77–11.78) reduces to

$$\boldsymbol{F}_{\rm ns} = -\frac{2}{3}\rho_{\rm s}\kappa\alpha L \boldsymbol{v}_{\rm ns}.\tag{11.83}$$

Thus, the description of F_{ns} requires the knowledge of the vortex line density L, whose evolution equation in inhomogeneous situations may be taken as (11.60), with σ_L given by (11.55) or some of its generalizations.

The set of Eqs. (11.77), (11.78) and (11.80), (11.81) describes the evolution of v_n , v_s and L in superfluid helium flows, and is able to cover a wide range of physical situations, although a generalization may be required in some circumstances. We will not go further in this direction because it would take us to specialized problems as Taylor–Couette flow and Poiseuille flow (Jou et al. 2008). These are interesting physical situations, of practical interest in cryogenic flows of liquid helium.

Furthermore, it is thought that internal parts of neutrons stars, submitted to high pressures, may be in superfluid state. Since many of these stars have a very fast rotation, it is expected that a dense array of quantized vortices will be present in them. In some circumstances, there may be sudden transitions from ordered parallel vortices to a disordered vortex tangle (Peralta et al. 2006). This implies changes in the inertia of the rotating fluid and, therefore, changes in the angular speed of the stars. Finally, turbulent superfluids provide models of topological defects—vortex lines—which may be of interest for the analysis of topological defects in other systems, as in cosmic strings (Volovik 2005; Jou and Mongiovì 2009), or in superconducting materials.

Appendix A

Experimental Data on Polymer Solutions

The experimental information about the different polymer solutions studied in this monograph is collected in this Appendix. These data, taken from the bibliography, have been used in Chaps. 5–10 to verify the capacity of prediction of the proposed theoretical models.

A.1 Polystyrene in Dioctyl-Phthalate (PS/DOP)

The experimental information for the analysis of this system is taken from Rangel-Nafaile et al. (1984), where a solution of polystyrene of molecular weight $M_{\rm w}=1.8\times10^3$ kg mol⁻¹ and polydispersivity index ($r=M_{\rm w}/M_{\rm n}=1.3$) in dioctylphthalate (solvent density 900 kg m⁻³) is considered. For this solution, the parameters of the Flory–Huggins model (Jou et al. 1991; Casas-Vázquez et al. 1993) are $\Theta=288$ K and $\Psi=1.48$ and the critical temperature at rest is 285 K. The parameter m is estimated by fitting the critical point predicted by the Flory–Huggins model and the experimental one with the result m=3516.

When the system is under shear stress at P_{12}^{ν} constant, the following functional relation for the steady state compliance J can be obtained by fitting the experimental data of Rangel-Nafaile et al. (1984),

$$J = \frac{b_3 \phi_0^{-b_0}}{2} (P_{12}^{\nu})^{-2} \phi^{b_0} \exp \left[b_4 (P_{12}^{\nu})^{1/2} + \frac{b_0}{b_1} (P_{12}^{\nu})^{b_2} - \frac{b_0}{p \phi_0^p} \phi^p \right], \quad (A.1)$$

where the values of the corresponding parameters are $b_0 = 4$, $b_1 = 7.85$, $b_2 = 0.319$, $b_3 = 14.7$, $b_4 = 0.164$, and $\phi_0 = 0.042$, and where we have introduced the function

$$p = b_1 (P_{12}^{\nu})^{-b_2}. (A.2)$$

In order to obtain explicit expressions for the non-equilibrium chemical potential, defined in Chap. 6 and its derivatives, the functional dependence on ϕ and P_{12}^{ν} of

the auxiliary functions (6.35) and (6.78) must be known. Using (A.1) and (A.2) the following results are obtained

$$\left(\frac{\partial F}{\partial \phi}\right)_{w_{12}} = -b_0 p \Xi,\tag{A.3}$$

$$Y = \left(\frac{\partial \ln J}{\partial \ln P_{12}^{\nu}}\right)_{\phi} = -2 + \frac{b_4}{2} (P_{12}^{\nu})^{1/2} + \frac{b_0 b_2}{b_1} (P_{12}^{\nu})^{b_2} - \frac{b_0 b_2}{p} \left(\frac{\phi}{\phi_0}\right)^p \left[1 - \ln\left(\frac{\phi}{\phi_0}\right)^p\right] \frac{\partial^2 \Omega}{\partial \nu^2}.$$
 (A.4)

When the empirical fit (A.1) is used for J, (A.2)–(A.4) lead, straightforwardly, to

$$\left(\frac{\partial F}{\partial \phi}\right)_{w_{12}} = -b_0 p \Xi,\tag{A.5}$$

$$\left(\frac{\partial F}{\partial \phi}\right)_{w_{12}} = \left[\frac{b_4}{2} \left(b_2 - \frac{1}{2}\right) (P_{12}^{\nu})^{1/2} - b_2 (Y+2)\right] \frac{F}{Y+1} \phi^{-1} + b_0 b_2 \Xi \ln\left(\frac{\phi}{\phi_0}\right)^p, \tag{A.6}$$

where Ξ is the auxiliary function defined as

$$\Xi = \phi^{-1} \left(\frac{\phi}{\phi_0} \right)^p \left[1 + b_2 \frac{F}{Y+1} \ln \left(\frac{\phi}{\phi_0} \right) \right]. \tag{A.7}$$

A.2 Polystyrene in Transdecalin (PS/TD)

According to the experimental results of Nakata et al. (1976) it is possible to determine the critical temperature of this system and the parameters of the Flory–Huggins model. When the molecular mass of the PS is 520 kg mol⁻¹ ($M_0 = 0.104$ kg mol⁻¹, N = 5 000), the values $\Theta = 294.4$ K and $\Psi = 0.50$ are obtained. Furthermore, starting from the values for the molar volumes given by Wolf (1984), namely, 1.586×10^{-4} m³ mol⁻¹ for the solvent (transdecalin, molar mass $M_1 = 0.138$ kg mol⁻¹) and 0.486×10^{-4} m³ mol⁻¹ for the polystyrene, one obtains m = 3 064, in agreement with the result obtained by interpolating the values calculated from the data of the critical concentration f_c proposed by Nakata et al. (1976) for several molecular masses of PS. When one uses the latter values of m, Θ , and Ψ , one obtains, from the Flory–Huggins theory, $T_c = 284.1$ K for the equilibrium critical temperature.

To describe how the viscosity of the system depends on the polymer concentration we use the Martin equation (Bird et al. 1987a)

$$\frac{\eta}{\eta_s} = 1 + \tilde{c} \exp(k_{\rm H}\tilde{c}) \tag{A.8}$$

where η_s is the viscosity of the pure solvent, k_H the Huggins constant, $[\eta]$ the intrinsic viscosity, and $\tilde{c} = [\eta]c$ the reduced concentration.

It is an easy exercise to yield (5.44) as a power expansion of the Martin equation. In (Wolf 1984) the values of the parameters appearing in (A.8), and consequently in (5.45), are reported for the system PS/TD with the molecular mass previously quoted. Those values are 1.40 for the Huggins constant $k_{\rm H}$, 0.0023 Pa s for the solvent viscosity and 0.043 m³ kg⁻¹ for the intrinsic viscosity.

However, in (Wolf 1984) a different model for the equilibrium contribution to the chemical potential was used. This model is in agreement with further results proposed by Flory et al. (1964a, b) and Flory (1965) and its main difference with the previous model is the dependence on composition of the interaction parameter χ through the expression

$$\chi = (A_0 - A_1) + 2(A_1 - A_2)\phi + 3A_2\phi^2, \tag{A.9}$$

where ϕ is the volume fraction and A_i are functions of the temperature defined as

$$A_i = (g_{i0}/T) + g_{i1}T, (A.10)$$

 g_{ij} being parameters whose values have been determined in (Wolf 1984) from measurements of the chemical potential of the solvent in different conditions of temperature and composition.

For polymers with high molecular mass, the behaviour is far from Newtonian, and expressions (5.26) and (5.44) are no longer a good approximation. This is the case for the system PS/TD described by Kramer and Wolf (1985) and Krämer-Lucas et al. (1988) where the molecular mass of the polymer is 1770 kg mol⁻¹. These authors propose for the non-equilibrium contribution to the Gibbs function a modification of the one proposed by Vinogradov and Malkin (1980)

$$\Delta G = VJ[\eta(\dot{\gamma})\dot{\gamma}]^{2(1+B)},\tag{A.11}$$

where *B* is the slope of the curve $\eta(\dot{\gamma})$.

For the explicit form of J we take that proposed by Graessley (1974)

$$J = 0.7[\eta(0) - \eta_s] [\eta(0)^2 \dot{\gamma}_{0.8}]^{-1}, \tag{A.12}$$

where $\dot{\gamma}_{0.8}$ is defined as the value of the shear rate for which $\eta(\dot{\gamma})$ is the 80% of $\eta(0)$.

In dealing with the dependence of non-Newtonian viscosity with respect to shear rate, we have proposed (Criado-Sancho et al. 1992) the following modelization

$$\eta = \begin{cases} \eta_0 (\dot{\gamma} / \dot{\gamma}_0)^B & \dot{\gamma} > \dot{\gamma}_0 \\ \eta_0 & \dot{\gamma} < \dot{\gamma}_0, \end{cases}$$
(A.13)

where to a first approximation the parameter B is directly proportional to the molar fraction of the polymer and $\dot{\gamma}_0$ is inversely proportional to this quantity. Prior to assuming this dependence on composition of parameters $\dot{\gamma}_0$ and B, use has been made of the fact that $B \approx -0.5$ and that in the whole expression for ΔG the factor $(\dot{\gamma}/\dot{\gamma}_0)^{2B+1}$ appears.

A.3 Polystyrene Dissolved in Oligomeric Polystyrene

In this section we consider some solutions of polystyrene of high molecular mass dissolved in an oligomeric polystyrene of molecular mass 0.5 kg mol⁻¹ and viscosity 80 Pa s. Using the density of a polystyrene chain with 5 000 segments reported by Wolf (1984), the molar volume of a monomer unit can be estimated as 9.7×10^{-5} m³ mol⁻¹, in such a way that the molar volume of the oligomeric solvent is $v_1 = 4.66 \times 10^{-4}$ m³ mol⁻¹.

Experimental information for three solutions with different values of the solute molecular mass M_2 can be found in MacDonald and Muller (1996), where relaxation times calculated from the Rouse model are also reported. Using these times, the intrinsic viscosity for the systems considered may be calculated, yielding the values collected in Table A.1.

Whereas in MacDonald and Muller (1996) concentration is given by the weight fraction, in Table A.1 the concentration is expressed by the mass of solute by unit volume c To relate c to the weight fraction defined in the usual form

$$w_2 = \frac{n_2 M_2}{n_1 M_1 + n_2 M_2},\tag{A.14}$$

with n_i the number of moles of the component i and M_i its molecular mass, we used the expression

$$c = \frac{M_1}{v_1} w_2 \cong \frac{M_0}{v_0} w_2,\tag{A.15}$$

Table A.1

M_2 (kg mol ⁻¹)		Viscosity of the solution (Pa s)	Intrinsic viscosity (m³ kg ⁻¹)
2 000	2.14	165	0.122
4 000	1.28	136	0.171
6 850	0.963	120	0.233

with M_0 and v_0 the molecular mass and molar volume of a segment of polystyrene and where it was assumed that $M_2 = mM_1$ and $v_2 = mv_1$, where m may be calculated from the polymerization index of the solute.

Using the values of the intrinsic viscosity collected in Table A.1 we obtain the following dependence on the molecular mass of the solute

$$[\eta] = 2.25 \times 10^{-3} M_2^{0.524}. \tag{A.16}$$

Concerning the Huggins constant $k_{\rm H}$ to be used in (5.44), the best value is obtained by fitting of experimental dates of Table A.1 and yields the result

$$k_{\rm H} = 497.9 M_2^{-0.49}$$
. (A.17)

These results will be used in Chaps. 5–10 to illustrate the predictions on shear induced phase transitions, shear-induced polymer diffusion and molecular separation, and shear-induced degradation. In the future, it would be of interest to have these data for a wider variety of systems.

Appendix B Liquid Crystals

In liquid crystals, there is a marked coupling between flow and orientation and therefore the presence of velocity gradients does affect the phase transitions such as, for instance, the first-order nematic-isotropic transition. This topic has some differences from the problems studied throughout this monograph: orientation, rather than the concentration, is the main relevant variable. Therefore, the application of the non-equilibrium chemical potential which has been used as the unifying basis of Chaps. 6–9 is not directly applicable to this situation, but one should work with a chemical potential referred to the orientation of the particles. We have already remarked in Chap. 5 that, since shear flow is rotational, an orientational steady state is not strictly reached because the molecules rotate. When concentration is the relevant variable, as in the previous chapters, this is not important, because one may average over the period of rotation. In contrast, when orientation is the essential variable, there arise new challenges to the applicability of thermodynamic potentials to determine the steady state, and a wider use of dynamic concepts is needed.

Despite this, we devote an appendix to this important problem for the sake of completeness, because there is an increasing bibliography on it, and because it indicates a line of progress for future extensions of the thermodynamic perspective.

B.1 Equilibrium Thermodynamics and the Isotropic-Nematic Phase Transition

Liquid crystals are composed of long rigid molecules. In the isotropic phase, the orientation of the molecules is random. In the nematic phase, the long axis of the molecules, denoted by the vector \mathbf{n} , is oriented, on average, along a particular direction characterised by a unit vector \mathbf{n}' called the director. The simplest models suppose that all the molecules are aligned along the director, whereas more detailed models assume that the direction of the axis is described by an orientational distribution function designated as $\Psi(\mathbf{n})$. The system may undergo a phase transition from isotropic to nematic phase due to density effects or to temperature effects: higher density implies more interactions amongst the molecules, which will be ordered by purely steric effects; lower temperatures imply less ability to rotate. Here, we will

give a simple discussion of the isotropic-nematic phase transition in equilibrium (the fluid at rest) due to temperature effects. For a detailed introduction to the physics of liquid crystals see (de Gennes and Prost 1990; Chandrasekhar 1992; Chaikin and Lubenski 1995).

Assume a rigid rod-like polymer characterized by a direction n. The order parameter tensor or orientation tensor is defined as

$$S_{\alpha\beta} = \int (n_{\alpha}n_{\beta} - \frac{1}{3}\boldsymbol{n} \cdot \boldsymbol{n}\delta_{\alpha\beta})\Psi(\boldsymbol{n})d\boldsymbol{n}, \tag{B.1}$$

where n (which is often taken to be a unit vector with $n \cdot n = 1$) indicates the axis of the molecules and $\Psi(n)$ is the orientational distribution function. The tensor S may be measured experimentally through shear-induced birefringence.

For uniaxial nematic liquid crystals, $S_{\alpha\beta}$ takes the simpler form

$$S = S\left(\mathbf{n}'\mathbf{n}' - \frac{1}{3}\mathbf{U}\right),\tag{B.2}$$

where the scalar parameter S is given by

$$S = \frac{1}{2} \int (3\cos^2\theta - 1)\Psi(\theta)d\theta,$$
 (B.3)

 θ being the angle between the molecular axis and the director n', which expresses the average orientation of the molecules.

The free energy F in equilibrium depends on the temperature, pressure and also on the scalar invariants of the tensor **S** (Hess 1975, 1976, 1977; de Gennes and Prost 1990; Blenk et al. 1991). F is usually assumed to have the Landau–de Gennes form, namely

$$F = a_2 \text{Tr}(\mathbf{S} \cdot \mathbf{S}) + a_3 \text{Tr}(\mathbf{S} \cdot \mathbf{S} \cdot \mathbf{S}) + a_4 \text{Tr}(\mathbf{S} \cdot \mathbf{S} \cdot \mathbf{S} \cdot \mathbf{S}) + a_4' \text{Tr}(\mathbf{S} \cdot \mathbf{S}) \text{Tr}(\mathbf{S} \cdot \mathbf{S}) + a_5 \text{Tr}(\mathbf{S} \cdot \mathbf{S}) \text{Tr}\mathbf{S},$$
(B.4)

with the parameters a_i being functions of the temperature and the density. In fact, for 3×3 symmetric traceless tensors the term in $\text{Tr}(\mathbf{S} \cdot \mathbf{S} \cdot \mathbf{S})$ is proportional to $\text{Tr}(\mathbf{S} \cdot \mathbf{S}) \times \text{Tr}(\mathbf{S} \cdot \mathbf{S})$, but these terms may be different in more general situations. Note, furthermore, that since $\text{Tr}\mathbf{S} = 0$ the last term is rather formal and it is written here for purposes which will be described below. To this expression one often adds the so-called Frank's terms, which account for the contributions due to the inhomogeneities in \mathbf{S} , and which depend therefore on the gradients of \mathbf{S} .

B.1.1 Phase Transition Induced by Temperature Changes

In terms of the parameter S introduced in (B.2), the free energy (B.4) may be written as

$$F = \frac{1}{2}rS^2 - wS^3 + uS^4, (B.5)$$

with r, w, and u suitable combinations of the coefficients a_i . The transition from the isotropic (S = 0) to the nematic $(S \neq 0)$ phases under the effect of a temperature change is described in a simple way by assuming that $r = a'(T - T^*)$ whereas w and u are independent of temperature. The presence of the cubic term makes that transition discontinuous in S, i.e. a first-order transition.

The transition temperature $T_{\rm c}$ and the value $S_{\rm c}$ of S at $T=T_{\rm c}$ are calculated by requiring that F is an extremum with respect to S in equilibrium, and that the free energies of both phases are equal at equilibrium. The first condition yields

$$\frac{\partial F}{\partial S} = (r - 3wS + 4uS^2)S = 0. \tag{B.6}$$

Since $\Delta F = 0$ for the isotropic phase, the second condition states

$$\Delta F = \left(\frac{1}{2}r - wS + uS^2\right)S^2 = 0.$$
 (B.7)

Thus, by solving the set of Eqs. (B.6) and (B.7) one obtains

$$S_{\rm c} = \frac{w}{2u}; \quad r_{\rm c} = a'(T_{\rm c} - T^*) = \frac{w^2}{2u}.$$
 (B.8)

The latent heat may be obtained by comparing the entropy per unit volume of the isotropic phase, which is taken to be zero, and that of the nematic phase, which is lower than that of the isotropic phase, as it is a more ordered phase. The latter entropy may be obtained from the free energy (B.5) as

$$S = -\frac{\partial F}{\partial T} = -\frac{1}{2}a'S_{c}^{2} = -\frac{1}{2}a'\left(\frac{w}{2u}\right)^{2},\tag{B.9}$$

and therefore the latent heat Q is $Q = T_c S = -(1/2)a' T_c (w/2u)^2$. Note indeed that if w = 0, i.e. if the cubic term was absent in (B.5), the transition would be of second order, i.e. continuous in the order parameter S and with a vanishing latent heat.

B.1.2 Phase Transition Induced by Density Changes

Another important situation arises when the phase transition is induced by density changes. In fact, the first statistical mechanical theory of a phase transition for a fluid consisting of rigid long molecules which interact through an infinite repulsion was developed by Onsager (see Onsager 1942), by considering changes in the density. In this case, one writes (B.4) as

$$F = \frac{1}{2} (U - 3) \operatorname{Tr}(\mathbf{S} \cdot \mathbf{S}) - \frac{U}{3} \operatorname{Tr}(\mathbf{S} \cdot \mathbf{S} \cdot \mathbf{S}) + \frac{U}{4} \operatorname{Tr}(\mathbf{S} \cdot \mathbf{S}) \operatorname{Tr}(\mathbf{S} \cdot \mathbf{S}), \quad (B.10)$$

where U is a parameter proportional to nbL^2 , with n the number density of the rod-like polymers in solution, b their thickness and L their length. This form

of *F* corresponds to the following identification of the coefficients in (B.4) $a_2 = \frac{1}{2}[1 - (U/3)], a_3 = -(U/3), a_4 = 0, a_4' = U/4, a_5 = (U/3)$. It follows that

$$\frac{\partial F}{\partial \mathbf{S}} = (3 - U)\mathbf{S} - 3U\mathbf{S} \cdot \mathbf{S} + U\operatorname{Tr}(\mathbf{S} \cdot \mathbf{S})\mathbf{U} + U\operatorname{Tr}(\mathbf{S} \cdot \mathbf{S})\mathbf{S}.$$
 (B.11)

Equating this expression to zero, and taking into account the form (B.2), yields for the parameter S the equation

$$6S - 2US(2S+1)(1-S) = 0.$$
 (B.12)

This is a cubic equation, analogous to the van der Waals equation, which may have one (stable) solution for S, or three solutions (two stable and one unstable), depending on the value of the parameter U, i.e. on the density. It turns out that for U < 3, i.e. for a number density lower than $bL^2/3$, the only solution is S = 0, which corresponds to the isotropic case, whereas for U > 3, correspondingly $n > bL^2/3$, the stable solutions correspond to $S \neq 0$, i.e. to the nematic situation. It is logical to expect that an increase in the number density may produce a phase change, because the molecules will be close enough to each other to make rotations of their orientation vector very unlikely. Another more microscopic formulation, closely related to the original formulation by Onsager, is based on the orientational distribution function $f(\Omega)$ (Thirumalai 1986; Lee 1987).

B.2 Dynamic Equations in the Presence of a Flow

In Sect. B.1 we considered the fluid at rest. Now, we will show how the presence of a flow changes the phase transition. Indeed, since the flow is an ordering factor, it is to be expected that the transition will be changed (see Olmsted and Goldbard 1990; Wang et al. 1993; Berret et al. 1994 for bibliography on this rich subject). We start from the dynamical equations coupling **S** with the flow, which will be obtained here microscopically. For a thermodynamic derivation of evolution equations of **S** see (Blenk et al. 1991a, b; Hess 1975, 1976, 1977).

The evolution equations for the order parameter tensor around equilibrium may be obtained from the generalised kinetic equation for the orientational distribution function $\Psi(\mathbf{n}, t)$, which has the form (Marrucci and Ciferri 1977; Doi and Edwards 1986)]

$$\frac{\partial \Psi}{\partial t} = D\nabla_n \cdot (\nabla_n \Psi + \Psi \nabla_n \mathcal{U}) - \nabla_n \cdot (\Psi \mathbf{n}), \tag{B.13}$$

where D is the rotational diffusion coefficient of the rods, \mathcal{U} the effective potential due to the interparticle (excluded volume) interactions, and ∇_n stands for the gradient with respect to \mathbf{n} . By multiplying this equation by $\mathbf{n}\mathbf{n} - (1/3)\mathbf{U}$, which is the

microscopic expression for the order parameter, and integrating with respect to n, one obtains

$$\frac{\partial S_{\alpha\beta}}{\partial t} = -D \frac{\partial F}{\partial S_{\alpha\beta}},\tag{B.14}$$

with F given by (B.10). Then, it turns out that the stable solutions of this equation correspond to the thermodynamically stable solutions obtained above.

When a homogeneous flow field v of the form $v = \kappa \cdot r$, with κ the velocity gradient and r the position vector, is imposed on the system, the evolution equation for the tensor S becomes (Doi and Edwards 1986; See et al. 1990)

$$\frac{\partial S_{\alpha\beta}}{\partial t} = -D \frac{\partial F}{\partial S_{\alpha\beta}} + G_{\alpha\beta}(\mathbf{S}), \tag{B.15}$$

with

$$G_{\alpha\beta} = \frac{1}{3} \left(\kappa_{\alpha\beta} + \kappa_{\beta\alpha} \right) + \kappa_{\alpha\mu} S_{\mu\beta} + \kappa_{\beta\mu} S_{\mu\alpha}$$
$$- \frac{2}{3} \delta_{\alpha\beta} \kappa_{\mu\nu} S_{\nu\mu} - 2\kappa_{\mu\nu} S_{\mu\nu} S_{\alpha\beta}.$$
(B.16)

See et al. (1990) have studied the effect of steady flow fields on such a phase transition of rigid rod-like polymers starting from this set of equations and analysing the stability of their solutions for several flows. For a shear flow, the only non-zero components of S are S_{xx} , S_{yy} , and S_{xy} . The corresponding evolution equations for these components are

$$\frac{1}{D}\frac{\partial S_{xx}}{\partial t} = -(3 - U)S_{xx} + US_{xx}^2 - 2US_{yy}^2 + S_{xy}^2 - 2S_{xx}S_{yy},$$
 (B.17a)

$$\frac{1}{D}\frac{\partial S_{yy}}{\partial t} = -(3 - U)S_{yy} - 2US_{xx}^2 + US_{yy}^2 + S_{xy}^2 - 2S_{xx}S_{yy},$$
 (B.17b)

$$\frac{1}{D}\frac{\partial S_{xy}}{\partial t} = -(3 - U)S_{xy} + 3US_{xx}S_{xy} + 3US_{yy}S_{xy} + \frac{1}{2}\frac{\dot{\gamma}}{D}.$$
 (B.17c)

The final solutions are

$$S_{xx} = S_{yy} = \frac{1}{6(1+\sqrt{3})}(U^* - U) \cong 0.061(U^* - U),$$
 (B.18a)

$$S_{xy} = \frac{(2\sqrt{3}+3)^{1/2}}{2(\sqrt{3}+3)}(U^*-U) \cong 0.027(U^*-U),$$
 (B.18b)

$$\left|\frac{\dot{\gamma}}{D}\right| = \frac{(2\sqrt{3}+3)}{2\sqrt{3}+4}^{1/2} (U^*-U)^2 \cong 0.341(U^*-U)^2,$$
 (B.18c)

with $U^* = 3$, i.e. the critical value of U (or, equivalently, of the number density of rods, since $U = nbL^2$, as noted in the previous section) corresponding to a vanishing shear rate, i.e. $\dot{\gamma} = 0$. The equality (B.18c) may be rewritten as

$$U_{\rm c}(\dot{\gamma}) = U_{\rm c}(0) - 1.712 \left(\left| \frac{\dot{\gamma}}{D} \right| \right)^{1/2}.$$
 (B.19)

Thus, as a consequence of the ordering effect of the flow, the value of the density required to produce the phase transition is lowered with respect to the value without flow.

See et al. (1990) have also studied with special emphasis the situation of extensional flow defined by $v_z = \xi z$; $v_x = -\frac{1}{2}\xi x$; $v_x = -\frac{1}{2}\xi y$, where ξ is a constant parameter, with dimensions of inverse of time. In this case, the only non-vanishing components of **S** are $S_{zz} = 2S$ and $S_{xx} = S_{yy} = -S$. The completely isotropic situation corresponds to S = 0 and the completely nematic one to S = 1. The kinetic equation for S is

$$\frac{\partial S}{\partial t} = -6DS + 2UDS(2S+1) + \xi + 2\xi S - S(2S+1)(2UDS+\xi).$$
 (B.20)

In the steady state $(\partial S/\partial t = 0)$, this equation may be rewritten as

$$\frac{\xi}{D} = \frac{6S}{(2S+1)(1-S)} - 2US. \tag{B.21}$$

Analogously to the van der Waals equation of state, depending on the values of U and ξ there can be only one stable solution for S or three solutions (two stable and one unstable). The boundary between the stable and unstable regions is described by $(\partial \xi/\partial S)_U = 0$. For small values of ξ , and neglecting higher-order corrections in S and in S and in S one obtains for the critical value of S in the presence of the flow

$$U_{\rm c}(\xi) = -6(\xi/D)^{1/2}.$$
 (B.22)

The elongational flow plays an important role in the comparison between dynamical and thermodynamical approaches in non-equilibrium states, as will be mentioned below. For values of U between $U_c(\xi)$ and $U_c(0)$ the fluid would be isotropic in the absence of flow, but it is nematic in the presence of the flow.

See et al. (1990) showed that for irrotational flows (i.e. for flows where the velocity field may be derived from a potential), the results derived from a dynamical method based on the evolution equations for the order parameter tensor and on a thermodynamical method based on a free energy depending on the flow are equiva-

lent, whereas they stated that a thermodynamic approach based on a thermodynamic potential is not possible in the case of shear flow.

Several authors have generalised the thermodynamic description to situations corresponding to an extensional flow (Peterlin 1966; Auvray 1981; Thirumalai 1986; Lee 1987). Since extensional flows are irrotational, the velocity derives from a potential. Furthermore, since in a low-Reynolds number the hydrodynamic forces are proportional to the velocity of the particles with respect to the flow, it follows that the hydrodynamic forces in this case derive from a potential. Thus, this potential may be included in the energy, and one may define a generalised free energy, as suggested by Kramers (1946). This line of analysis has been followed by Thirumalai (1986), whose analysis was refined by Lee (1987). Olmsted and Goldbart (1990) and Olmsted and Yu (1997) have studied the effects of the shear on a thermotropic nematic liquid crystal and have provided a phase diagram in terms of T and $\dot{\gamma}$. The basis for their analysis was a set of evolution equations for the order parameter S obtained from linear irreversible thermodynamics.

B.3 Thermodynamic Formulation

In Sect. B.2 we studied the effect of the flow on the isotropic-nematic transition from a purely dynamical point of view. Since in this monograph we are especially interested in the thermodynamical approach, we will discuss here the possibility of a pure thermodynamic description of the transition, i.e. a description based on the equations of state rather than on the evolution equations. One possible interpretation of non-equilibrium thermodynanics would be to find a potential related to the dynamics, as in (B.12), i.e. in such a way that the time derivative of the thermodynamic variables is proportional to the functional derivative of the free energy. From this point of view, one could ask under which conditions one may write the dynamical Eq. (B.13) as the derivative of the equilibrium free energy plus a contribution of the flow to the free energy, namely

$$\frac{\partial S_{\alpha\beta}}{\partial t} = -L \frac{\partial (A + A_{\text{flow}})}{\partial S_{\alpha\beta}},\tag{B.23}$$

with A_{flow} being given by

$$A_{\text{flow}} = b_2 \text{Tr}(\kappa \cdot \mathbf{S}) + b_3 \text{Tr}(\mathbf{S} \cdot \kappa \cdot \mathbf{S}) + b'_4 \text{Tr}(\mathbf{S} \cdot \mathbf{S}) \text{Tr}(\mathbf{S} \cdot \kappa) + b'_4 \text{Tr}(\mathbf{S} \cdot \mathbf{S} \cdot \kappa \cdot \mathbf{S}) + b_5 \text{Tr}(\mathbf{S} \cdot \kappa) \text{Tr}\mathbf{S},$$
(B.24)

where b_i are coefficients which should be identified by comparison of the derivative of (B.24) with (B.13). It turns out that this is possible only in the linear regime, where only the first term in (B.13) and in (B.24) play a role, provided one identifies $b_2 = -(1/3)L$.

In general terms, (B.16) may be obtained from (B.24) only when the following conditions are satisfied: (1) κ is symmetric; (2) S is proportional to κ . Indeed, since S is symmetric, the antisymmetric part of the velocity gradient disappears in $Tr(S \cdot \kappa)$. As a consequence, the derivative of the second term in expression (B.24) leads to $(\kappa_{\alpha\mu})^s S_{\mu\beta} + (\kappa_{\beta\mu})^s S_{\mu\alpha}$ instead of the second and third terms of (B.16), where $\kappa_{\alpha\beta}$ rather than its symmetric part appears. Furthermore, the derivative of the third term in (B.24) yields $Tr(S \cdot S)\kappa + 2Tr(S \cdot \kappa)S$. The first of these two terms may be related to the last term in (B.14) but the second has no corresponding term in (B.16). Thus, only when S is proportional to κ may both terms be superposed into the last one of (B.16). These conditions are satisfied in the extensional flows but not in shear flows, provided we identify $b_3 = -2/L$, $b_5 = -2/3L$. Thus, apparently, for shear flows it is possible to use a non-equilibrium thermodynamic potential only when the first term in (B.24) is considered, i.e. when non-linear terms may be neglected in the non-equilibrium dynamical contribution. Although this is rather restrictive, it is precisely this situation which has been studied in (See et al. 1990). In Chap. 5 we found an analogous situation, where the dynamical Eq. (5.30) for the distribution function has a steady-state solution only for irrotational flows, because the polymers rotate with the fluid. However, to build the thermodynamic function, as well as to evaluate the shear viscosity, it is sufficient to consider the average of the distribution function over a period of rotation.

B.4 Maximum-Entropy Approach

In Chap. 2 we used the maximum-entropy approach to find the thermodynamic functions of ideal gases under shear flow. Here we will again use this procedure for rigid dumbbells, which are considered here as a simple microscopic model for liquid crystals (Camacho and Jou 1990). First, recall that the canonical distribution function in equilibrium reads as

$$f \cong \exp\left[-\frac{\mathcal{H}}{k_{\rm B}T}\right],$$
 (B.25)

with \mathcal{H} the unperturbed equilibrium Hamiltonian and T the absolute temperature. We have commented in Sects. 2.2 and 4.1.4 that in a non-equilibrium steady state characterized by a non-vanishing viscous pressure tensor, one should use instead of (B.25) the more general expression (4.51), namely

$$f \cong \exp\left[-\frac{\mathcal{H}}{k_{\rm B}T} - \Lambda : \hat{\mathbf{P}}^{\nu}\right],$$
 (B.26)

with $\hat{\mathbf{p}}^{\nu}$ the microscopic operator for the viscous pressure tensor and Λ a matrix of Lagrange multipliers (Jou et al. 1999a, b), which we have identified in (4.52). We will show that the thermodynamic analyses using the classical expression (B.25)

with a suitable "potential energy" for the flow is indeed a particular situation of (B.27), provided the identification (B.27) is made. This reinforces such identification. We consider a solution of rigid dumbbells for which the microscopic operator for the viscous pressure tensor is (Bird et al. 1987b, p. 135)

$$\hat{\mathbf{P}}^{v} = \sum_{i} \hat{\mathbf{P}}_{i}^{v(1)} + \sum_{i} \hat{\mathbf{P}}_{i}^{v(2)}, \tag{B.27}$$

where the subindex i indicates a sum over the dumbbells, with (Bird et al. 1987b)

$$\hat{\mathbf{P}}_{i}^{\nu(1)} = k_{\mathrm{B}}T\mathbf{U} - 3k_{\mathrm{B}}T\mathbf{n}_{i}\mathbf{n}_{i}, \tag{B.28}$$

$$\mathbf{P}_{i}^{\nu(2)} = -6k_{\mathrm{B}}T\lambda_{2}(\nabla\nu)^{T} : \mathbf{n}_{i}\mathbf{n}_{i}\mathbf{n}_{i}, \tag{B.29}$$

with n_i the vector indicating the orientation of the *i*th dumbbell and λ_2 a time constant which depends on the hydrodynamic interactions among the particles.

According to (B.26), the distribution function should have the form

$$f \propto \exp\left[-\frac{H}{k_{\rm B}T} - \frac{\tau_1}{k_{\rm B}T} \left(\nabla \nu\right) : \sum_i \mathbf{P}_i^{\nu(1)} - \frac{\tau_2}{k_{\rm B}T} \left(\nabla \nu\right) : \sum_i \mathbf{P}_i^{\nu(2)}\right], \quad (B.30)$$

where we have taken into account the identification of the Lagrange multipliers discussed in Chap. 2. The respective values of τ_1 and τ_2 are (Bird et al. 1987b)

$$\tau_1 = \frac{\varsigma L^2}{12k_{\rm B}T}; \quad \tau_2 = 0.$$
(B.31)

Therefore, (B.30) reduces to

$$f \propto f_{\text{eq}} \exp \left[\tau_1 (\nabla \mathbf{v})^T : \sum_i (k_B T \mathbf{U}_i - 3\mathbf{n}_i \mathbf{n}_i) \right].$$
 (B.32)

The expression for ∇v for the extensional flow is

$$\nabla \mathbf{v} = \begin{pmatrix} -\frac{1}{2}\Gamma & 0 & 0\\ 0 & -\frac{1}{2}\Gamma & 0\\ 0 & 0 & \Gamma \end{pmatrix}. \tag{B.33}$$

Now, if one denotes $n_x = \cos\theta \sin\phi$, $n_y = \cos\theta \cos\phi$, $n_z = \sin\theta$, (B.32) and (B.33) yield

$$f \propto f_{\rm eq} \exp \left[-\frac{9}{2} \tau_1 \Gamma \sin^2 \theta \right] \propto f_{\rm eq} \exp \left[-\frac{\varsigma L^2 \Gamma}{8 k_{\rm B} T} \sin^2 \theta \right].$$
 (B.34)

This expression coincides with that obtained in (Bird et al. 1987b) as the solution of the dynamical equations.

Thus, the idea that a thermodynamic formalism is only possible when the flow is irrotational (potential) is too restrictive. In the presence of a non-vanishing viscous pressure, the classical equilibrium form (B.25) should be generalised to (B.26), which is, in fact, the direct non-equilibrium steady-state extension of the canonical distribution function. In turn, (B.26) yields, for extensional flows (and also for other potential flows), the results obtained from (B.25) by adding to it the corresponding non-equilibrium potential. Thus, (B.25) indeed represents a valid extension of the equilibrium distribution function to potential situations, but it is too restrictive to deal with non-potential situations, as simple shear flow, which may be studied through (B.26). It must be noted, however, that whereas (B.26) yields a result coincident with that obtained from dynamical arguments in the extensional situation, in the shear flow the form (B.26) only coincides with the dynamical solution up to the first order in the viscous pressure, which is of the form

$$f \propto f_{\text{eq}} \left[1 - \tau(\nabla v) : (3nn - \mathbf{U}) \right].$$
 (B.35)

The situation is, in fact, analogous to that found in ideal gases, where the results for the distribution function obtained by maximum-entropy arguments coincide with the results of the Boltzmann equation up to first order in the shear rate. This is an illustration of the fact that the maximum-entropy distribution function is not the exact distribution function, but it is sufficient to describe the thermodynamics in the chosen space of states.

Appendix C

Summary of Vector and Tensor Notation

In general, we have used tensorial notation throughout the book. Tensors of rank 0 (scalars) are denoted by means of italic type letters a; tensors of order 1 (vectors) by means of boldface italic letters a and tensors of rank two and higher orders by capital boldface letters a. In some special circumstances, three-dimensional Cartesian coordinates are used:

 $a(a_i)$ vector,

 $\mathbf{A}(A_{ii})$ tensor of rank 2,

 $\mathbf{U}(\delta_{ij})$ unit tensor (δ_{ij} is Kronecker's symbol),

 $J(J_{iik})$ tensor of rank 3.

C.1 Symmetric and Antisymmetric Tensors

Denoting by superscript T the transpose, the symmetric and antisymmetric tensors are respectively defined as

symmetric
$$\mathbf{A} = \mathbf{A}^T (A_{ij} = A_{ji})$$
, antisymmetric $\mathbf{A} = -\mathbf{A}^T (A_{ij} = A_{ji})$. (C.1)

The trace of a tensor is defined as the sum of its diagonal components, namely

trace of a tensor Tr
$$\mathbf{A} = \sum_{i} A_{ii}$$
. (C.2)

C.2 Decomposition of a Tensor

It is customary to decompose second-order tensors into a scalar (invariant) part A, a symmetric traceless part \mathbf{A} , and an antisymmetric part \mathbf{A}^a as follows

$$\mathbf{A} = \frac{1}{3} (\text{Tr} \mathbf{A}) \mathbf{U} + \mathbf{A}^{0} + \mathbf{A}^{a} = \frac{1}{3} A \delta_{ij} + A_{ij}^{0} + A_{ij}^{a}.$$
 (C.3)

Note that this decomposition implies $\operatorname{Tr} \overset{0}{\mathbf{A}} = 0 \left(\sum_{i} \overset{0}{A}_{ii} = 0 \right)$.

The antisymmetric part of the tensor is often written in terms of an axial vector a^a whose components are defined as

$$a_i^a = \sum_{j,k} \varepsilon_{ijk} A_{jk}^a, \tag{C.4}$$

where the permutation symbol ε_{iik} has the values

$$\varepsilon_{ijk} = \begin{cases} +1 & \text{for even permutations of indices (i.e. 123, 231, 312)} \\ -1 & \text{for odd permutations of indices (i.e. 321, 132, 213)} \\ 0 & \text{for repeated indices.} \end{cases}$$
 (C.5)

C.3 Scalar (or Dot) and Tensorial (Inner) Products

We have used for the more common products the following notation: Dot product between

two vectors
$$\mathbf{a} \cdot \mathbf{b} = \sum_{i} a_{i} b_{i}$$
 (scalar),
a vector and a tensor $\mathbf{A} \cdot \mathbf{b} = \sum_{j} a_{ij} b_{i}$ (vector),
a tensor and a vector $\mathbf{b} \cdot \mathbf{A} = \sum_{j} b_{j} a_{jk}$ (vector),
two tensors $\mathbf{A} \cdot \mathbf{B} = \sum_{k} a_{ik} b_{kj}$ (tensor).

Double scalar product between tensors

$$\mathbf{A}:\mathbf{B} = \sum_{i,k} a_{ik} b_{kj} \quad \text{(scalar)}. \tag{C.7}$$

The trace of a tensor may also be written in terms of its double scalar product with the unit matrix as TrA = A : U.

C.4 (Inner) Tensorial Product (Also Named Dyadic Product)

between two vectors
$$(ab)_{ij} = a_ib_j$$
 (tensor of rank 2),
a vector and a tensor $(aB)_{ijk} = a_iB_{jk}$ (tensor of rank 3),
a tensor and a vector $(Ba)_{ijk} = B_{ij}a_k$ (tensor of rank 3),
two tensors $(AB)_{ijkl} = A_{ij}B_{kl}$ (tensor of rank 4).

C.6 Differentiation 275

C.5 Cross Multiplication Between Two Vectors and Between a Tensor and a Vector

$$(\boldsymbol{a} \times \boldsymbol{b})_k = \varepsilon_{ijk} a_i b_j$$
 (vector),
 $(\mathbf{B} \times \boldsymbol{a})_{ik} = \sum_{j,l} \varepsilon_{jkl} B_{ij} b_l$ (tensor). (C.9)

C.6 Differentiation

The most usual differential operators acting on tensorial fields may be expressed in terms of the so-called nabla operator, defined in Cartesian coordinates as

$$\nabla = \left(\frac{\partial}{\partial x_1}, \frac{\partial}{\partial x_2}, \frac{\partial}{\partial x_3}\right). \tag{C.10}$$

Gradient (defined as dyadic product)

$$(\nabla a)_i = \frac{\partial a}{\partial x_i} \quad \text{(vector)},$$

$$(\nabla a)_{ij} = \frac{\partial a_j}{\partial x_i} \quad \text{(tensor of rank 2)},$$

$$(\nabla \mathbf{A})_{jki} = \frac{\partial A_{jk}}{\partial x_i} \quad \text{(tensor of rank 3)}.$$

Divergence (defined as the scalar product)

$$\nabla \cdot \boldsymbol{a} = \sum_{i} \frac{\partial a_{i}}{\partial x_{i}} \quad \text{(scalar)}, \qquad (\nabla \cdot \mathbf{A})_{i} = \sum_{j} \frac{\partial A_{ji}}{\partial x_{j}} \quad \text{(vector)}. \quad (C.11)$$

Rotational or curl (defined as the cross product)

$$(\nabla \times \boldsymbol{a})_i = \sum_{j,k} \varepsilon_{ijk} \frac{\partial a_k}{\partial x_j} \text{ (vector)}, \qquad (\nabla \times \mathbf{A})_{ik} = \sum_{j,l} \varepsilon_{ijk} \frac{\partial A_{ij}}{\partial x_l} \text{ (tensor of rank 2)}.$$

The most usual second-order differential operator in tensorial analysis is the Laplacian, defined as

$$\nabla \cdot \nabla = \sum_{i} \frac{\partial^{2}}{\partial x_{i} \partial x_{i}}.$$
 (C.12)

C.7 Tensor Invariants

Some combinations of the elements of a tensor remain invariant under changes of coordinates. Such invariant combinations are

$$I_{1} = \operatorname{Tr} \mathbf{A} = \mathbf{A} : \mathbf{U} = \sum_{i} A_{ii},$$

$$I_{2} = \operatorname{Tr} \mathbf{A} \cdot \mathbf{A} = \mathbf{A} : \mathbf{A} = \sum_{i,j} A_{ij} A_{ji},$$

$$I_{3} = \operatorname{Tr} \mathbf{A} \cdot \mathbf{A} \cdot \mathbf{A} = \sum_{i,j,k} A_{ij} A_{jk} A_{ki}.$$
(C.13)

Other invariant combinations may also be formed, but they are combinations of I_1 , I_2 , and I_3 ; for instance, one often finds the invariants I, II, and III defined as

$$I = I_1, \quad II = \frac{1}{2}(I_1^2 - I_2), \quad III = \frac{1}{6}(I_1^3 - 3I_1I_2 + 2I_3) = \det \mathbf{A}.$$
 (C.14)

The invariants I, II, and III appear as coefficients in the "characteristic equation"

$$\det(\lambda \mathbf{U} - \mathbf{A}) = 0.$$

It is also possible to form joint invariants of two tensors A and B as

$$I_{11} = \text{Tr} \mathbf{A} \cdot \mathbf{B},$$

$$I_{21} = \text{Tr} \mathbf{A} \cdot \mathbf{A} \cdot \mathbf{B},$$

$$I_{12} = \text{Tr} \mathbf{A} \cdot \mathbf{B} \cdot \mathbf{B},$$

$$I_{22} = \text{Tr} \mathbf{A} \cdot \mathbf{A} \cdot \mathbf{B} \cdot \mathbf{B}.$$
(C.15)

Appendix D

Useful Integrals in the Kinetic Theory of Gases

We present here some useful integrals appearing in several calculations based on the kinetic theory of gases. Let F(C) be any scalar function of the peculiar velocity C such that the integrals appearing below converge, and let C_x and C_y be two components of C. Then

$$\int F(C)C_x^2 dC = \frac{1}{3} \int F(C)C^2 dC,$$
 (D.1)

$$\int F(C)C_x^4 dC = \frac{1}{5} \int F(C)C^4 dC,$$
 (D.2)

$$\int F(C)C_x^2C_y^2 dC = \frac{1}{15} \int F(C)C^4 dC.$$
 (D.3)

The following definite integrals are also useful

$$\int_0^\infty \exp(-\alpha C^2) \, C^r dC = \frac{\sqrt{\pi}}{2} \frac{1}{2} \frac{3}{2} \frac{5}{2} \cdots \frac{r-1}{2} \alpha^{-(r+1)/2} \quad (r \text{ even}), \tag{D.4}$$

$$\int_0^\infty \exp(-\alpha C^2) C^r dC = \frac{1}{2} [(r-1)/2]! \alpha^{-(r+1)/2} \quad (r \text{ odd}).$$
 (D.5)

Appendix E Some Physical Constants

k_{B}	$1.38 \times 10^{-23} \text{ J K}^{-1} = 8.62 \times 10^{-5} \text{ eV K}^{-1}$
$\sigma_0^{}$	$5.67 \times 10^{-8} \text{ W m}^{-2} \text{ K}^{-4}$
$\alpha = 4\sigma_0/c$	$7.56 \times 10^{-16} \text{ J m}^{-3} \text{ K}^{-4}$
amu	$1.66 \times 10^{-27} \text{ kg}$
e	$1.60 \times 10^{-19} \text{ C}$
m_e	$9.11 \times 10^{-31} \text{ kg}$
m_{p}	$1.673 \times 10^{-27} \text{ kg}$
h^{r}	$6.63 \times 10^{-34} \text{ J s} = 4.14 \times 10^{-15} \text{ eV s}$
	σ_0 $\alpha = 4\sigma_0/c$ amu e m_e m_p

References

- Agarwal US, Dutta A, Mashelkar RA (1994) Migration of macromolecules under flow: the physical origin and engineering implications. Chem Eng Sci 49:1693–1717
- Alemany PA, Zanette DH (1994) Fractal random walks from a variational formalism for Tsallis entropies. Phys Rev E 49:R956–R958
- Alvarez FX, Jou D (2007) Memory and nonlocal effects in heat transport: from diffusive to ballistic regimes. Appl Phys Lett 90:083109 (3 p)
- Alvarez FX, Jou D (2008) Size and frequency dependence of effective thermal conductivity in nanosystems. J Appl Phys 103:094321 (8 p)
- Alvarez FX, Jou D, Sellitto A (2009) Phonon hydrodynamics and phonon-boundary scattering in nanosystems. J Appl Phys 105:014317 (6 p)
- Alvarez FX, Jou D, Sellitto A (2010) Pore-size dependence of the thermal conductivity of porous silicon: a phonon-hydrodynamic approach. Appl Phys Lett 97:033103
- Apostolakis MV, Mavrantzas VG, Beris AN (2002) Stress gradient-induced migration effects in the Taylor–Couette flow of a dilute polymer solution. J Non-Newtonian Fluid Mech 102:409–445
- Aris R (1956) On the dispersion of a solute in a fluid flowing through a tube. Proc R Soc London Ser A 235:67–78 (Reprinted in Process Systems Eng, 1999, 1:109–120)
- Atkin RJ. Fox N (1975) A multipolar approach to liquid He II. Acta Mech 21:221–239
- Atkin RJ, Fox N (1984) On the foundation of Landau's theory of superfluid helium. Arch Rat Mech Anal 87:1–9
- Aubert JH, Tirrell M (1980) Macromolecules in non-homogeneous velocity gradient field. Part I. J Chem Phys 72:2694–2701
- Aubert JH, Prager S, Tirrell M (1980) Macromolecules in non-homogeneous velocity gradient field. Part II. J Chem Phys 73:4103–4112
- Auvray L (1981) Solutions de macromolecules rigides: effets de paroi, de confinement et d'orientation par un écoulement. J Phys (Paris) 42:79–95
- Ballauff M, Wolf WA (1981) Degradation of chain molecules. 1. Exact solution of the kinetic equations. Macromolecules 14:654–658
- Ballauff M, Wolf WA (1984) Degradation of chain molecules. 2. Thermodynamically induced shear degradation of dissolved polystyrene. Macromolecules 17:209–216
- Ballauff M, Wolf WA (1988) Thermodynamically induced shear degradation. Adv Polym Sci 85:1-31
- Baranyai A (2000a) On the configurational temperature of simple fluids. J Chem Phys 112: 3964–3966
- Baranyai A (2000b) Numerical temperature measurement in far from equilibrium model systems. Phys Rev E 61:R3306–R3309
- Baranyai A, Evans DJ (1989) Direct entropy calculation from computer simulation of liquids. Phys Rev A 40:3817–3822
- Baranyai A, Evans DJ (1991) Comments on thermodynamic integration methods for the determination of nonequilibrium entropy. Mol Phys 74:353–365

Baranyai A, Evans DJ, Daivis PJ (1992) Isothermal shear-induced heat flow. Phys Rev A 46: 7593–7600

- Barenghi CF, Donnelly RJ, Vinen WF (eds) (2001) Quantized vortex dynamics and superfluid turbulence. Springer, Berlin
- Barham PJ, Keller A (1990) Flow-induced liquid-liquid phase separation and adsorption entanglement layer formation in high-molecular-weight polymer solutions. Macromolecules 23: 303–309
- Barrat J-L, Berthier L (2000) Fluctuation-dissipation relation in a sheared fluid. Phys Rev E 63:012503 (4 p)
- Basedow AM, Ebert KH (1975) Zum Mechanismus des Abbaus von Polymeren in Lösung durch Ultraschall. Makromol Chem 176:745–757
- Basedow AM, Ebert KH, Ederer HJ (1978) Kinetic studies on the acid hydrolysis of dextran. Macromolecules 11:774–781
- Bautista F, Soltero JFA, Macias ER, Puig JE, Manero O (2002) Irreversible thermodynamics approach and modelling of shear-banding flow of wormlike micelles. J Phys Chem B 106: 13018–13026
- Bautista F, Perez-López JH, Garcia JP, Puig JE, Manero O (2007) Stability analysis of shear banding flow with the BMP model. J Non-Newtonian Fluid Mech 144:160–169
- Bejan A, Lorente S (2006) Constructal theory of generation of configuration in nature and engineering. J Appl Phys 100:041301 (27 p)
- Benedetto G, Boarino L, Spagnolo R (1997) Evaluation of thermal conductivity of porous silicon layers by a photoacoustic method. Appl Phys A 64:155–159
- Berentsen CWJ, van Kruijsdijk CPJW (2008) Relaxation and reversibility of extended Taylor dispersion from Markovian–Lagrangian point of view. Adv Water Res 31:609–629
- Berentsen CWJ, Verlaan ML, van Kruijsdijk CPJW (2005) Upscaling and reversibility of Taylor dispersion in heterogeneous porous media. Phys Rev E 71:046308 (16 p)
- Beris AN, Edwards SJ (1994) Thermodynamics of flowing fluids with internal microstructure. Oxford University Press, New York
- Beris AN, Mavrantzas VG (1994) On the compatibility between various macroscopic formalisms for the concentration and flow of dilute polymer solutions. J Rheol 38:1235–1250
- Bernot M, Caselles V, Morel J-M (2009) Optimal transportation networks: models and theory. Springer, Berlin
- Berret J-F, Roux DC, Porte G, Lindner P (1994) Shear-induced isotropic-to-nematic phase transition in equilibrium polymers. Europhys Lett 25:521–526
- Berthier L, Barrat J-L (2002) Nonequilibrium dynamics and fluctuation-dissipation relation in a sheared fluid. J Chem Phys 116:6228–6242
- Bestul AB (1956) Kinetics of capillary shear degradation in concentrated polymer solutions. J Chem Phys 24:1196–1201
- Beysens D, Gbadamassi M (1979) Shear-induced transition to mean-field critical behaviour. J Phys (Paris) Lett 40:L565–L567
- Beysens D, Gbadamassi M, Boyer L (1979) Light-scattering study of a critical mixture with shear flow. Phys Rev Lett 43:1253–1256
- Bhave AV, Armstrong RC, Brown RA (1991) Kinetic theory and rheology of dilute, non-homogeneous polymer solutions. J Chem Phys 95:2988–3000
- Bidar H (1997) Non-equilibrium free energy under shear flow. J Non Equilib Thermodyn 22: 156–161
- Bidar H, Jou D (1998) A generalized Gibbs equation for nuclear matter out of equilibrium. Phys Rev C 57:2068–2070
- Bidar H, Jou D, Criado-Sancho M (1996) Thermodynamics of ideal gases under shear: a maximum-entropy approach. Physica A 233:163–174
- Bird RB, Armstrong RC, Hassager O (1987a) Dynamics of polymeric liquids, vol 1: Fluid mechanics, 2nd edn. Wiley, New York
- Bird RB, Curtiss CF, Armstrong RC, Hassager O (1987b) Dynamics of polymeric liquids, vol 2: Kinetic theory, 2nd edn. Wiley, New York

References 283

Blenk S, Ehrentraut H, Muschik W (1991a) Orientation-balances for liquid crystals and their representation by alignment tensors. Mol Cryst Liq Cryst 204:133–141

Blenk S, Ehrentraut H, Muschik W (1991b) Statistical foundation of macroscopic balances for liquid crystals in alignment tensor formulation. Physica A 174:119–138

Booij HC (1984) The energy storage in the Rouse model in a arbitrary flow field. J Chem Phys 80:4571-4572

Bouchaud JP, Georges A (1990) Anomalous diffusion in disordered media: statistical mechanisms, models and physical applications. Phys Rep 195:127–293

Brey JJ, Santos A (1992) Nonequilibrium entropy of a gas. Phys Rev A 45:8566-8572

Bruus H (2008) Theoretical microfluidics. Oxford University Press, Oxford

Bueche F (1960) Mechanical degradation of high polymers. J Appl Polym Sci 4:101–106

Bunde A, Havlin S (eds) (1991) Fractals and disordered systems. Springer, Berlin

Cahill DC, Ford WK, Goodson KE, Mahan GD, Majumdar A, Maris HJ, Merlin R, Phillpot SR (2003) Nanoscale thermal transport. J Appl Phys 93:793–818

Callen HB (1960) Thermodynamics. Wiley, New York

Camacho J (1993a) Thermodynamics of Taylor dispersion: constitutive equations. Phys Rev E 47:1049–1053

Camacho J (1993b) Purely global model for Taylor dispersion. Phys Rev E 48:310–321

Camacho J (1993c) Thermodynamic functions for Taylor dispersion. Phys Rev E 48:1844–1849

Camacho J, Jou D (1990) On the thermodynamics of dilute dumbbell solutions under shear. J Chem Phys 92:1339–1344

Camacho J, Jou D (1995) Equations of state of a dilute gas under a heat flux. Phys Rev E 52: 3490-3494

Campos D, Méndez V, Fort J (2004) Description of diffusive and propagative behaviour on fractals. Phys Rev E 69:031115 (5 p)

Casas-Vázquez J, Jou D (1994) Nonequilibrium temperature versus local equilibrium temperature. Phys Rev E 49:1040–1048

Casas-Vázquez J, Jou D (2003) Temperature in non-equilibrium states: a review of open problems and current proposals. Rep Prog Phys 66:1937–2023

Casas-Vázquez J, Criado-Sancho M, Jou D (1993) Dynamical and thermodynamical approaches to phase separation in polymer solutions under flow. Europhys Lett 23:469–474

Casas-Vázquez J, del Castillo LF, Jou D, Criado-Sancho M (2001) Legendre transform in the thermodynamics of flowing polymer solutions. Phys Rev E 63:057101 (3 p)

Casas-Vázquez J, Criado-Sancho M, Jou D (2002) Comparison of three thermodynamic descriptions of nonlocal effects in viscoelasticity. Physica A 311:353–360

del Castillo LF, Criado-Sancho M, Jou D (2000) Nonequilibrium chemical potencial and shear-induced migration of polymers in dilute solution. Polymer 41:2633–2638

Cercignani C (2000) Rarefied gas dynamics: from basic concepts to actual calculations. Cambridge University Press, Cambridge

Chaikin PM, Lubenski TC (1995) Principles of condensed matter physics. Cambridge University Press, Cambridge

Chandrasekhar S (1992), Liquid Crystals, 2nd edn. Cambridge University Press, Cambridge

Chapman S, Cowling TG (1970) The mathematical theory of non-uniform gases. Cambridge University Press, Cambridge

Chen G (2005) Nanoscale energy transport and conversion. Oxford University Press, Oxford

Ciancio V, Verhas J (1991) A thermodynamic theory for heat radiation through the atmosphere. J Non Equilib Thermodyn 16:57–65

Ciancio V, Restuccia L, Kluitenberg GA (1990) A thermodynamic derivation of equations for dielectric relaxation phenomena in anisotropic polarisable media. J Non Equilib Thermodyn 15:157–171

Cimmelli VA (2007) An extension of the Liu procedure in weakly nonlocal thermodynamics. J Math Phys 48:113510 (13 p)

Cimmelli VA (2009) Different thermodynamic theories and different heat conduction laws. J Non Equilib Thermodyn 34:299–333

Clarke N (1999) The effect of shear flow on phase separation in entangled polymer blends. Faraday Disscuss 112:249–265

- Clarke N, McLeish TCB (1998) Shear flow on phase separation of entangled polymer blends. Phys Rev 57:R3731–R3734
- des Cloizeaux J (1988) Double reptation vs simple reptation in polymer melts. Europhys Lett 5:437–443
- Coleman BD, Markovitz H (1964) Normal stress effects in second-order fluids. J Appl Phys 35:1–9 Coleman BD, Markovitz H, Noll W (1966) Viscometric flows of non-Newtonian fluids. Springer, New York
- Compte A, Camacho J (1997) Lévy statistics in Taylor dispersion. Phys Rev E 56:5445–5449
- Compte A, Jou D (1996) Nonequilibrium thermodynamics and anomalous diffusion. J Phys A Math Gen 29:4321–4329
- Compte A, Jou D, Katayama Y (1997a) Anomalous diffusion in shear flows. J Phys A Math Gen 30:1023-1030
- Compte A, Metzler R, Camacho J (1997b) Biased continuous time random walks between parallel plates. Phys Rev E 56:1445–1454
- Criado-Sancho M, Jou D, Casas-Vázquez J (1991) Definition of non-equilibrium chemical potential: phase separation of polymers in shear flow. Macromolecules 24:2834–2840
- Criado-Sancho M, Jou D, Casas-Vázquez J (1992) On the spinodal line of polymer solutions under shear. J Non-Equilib Thermodyn 18:103–120
- Criado-Sancho M, Jou D, Casas-Vázquez J (1994) Nonequilibrium thermodynamics and degradation of polymers under shear flow. J Non Equilib Thermodyn 19:137–152
- Criado-Sancho M, Casas-Vázquez J, Jou D (1995) Hydrodynamic interactions and the shear-induced shift of the critical point in polymer solutions. Polymer 36:4107–4112
- Criado-Sancho M, Casas-Vázquez J, Jou D (1997) Hydrodynamic fluctuations, nonequilibrium equations of state, and the shift of the spinodal line in polymer solutions under flow. Phys Rev E 56:1887–1890
- Criado-Sancho M, Jou D, Casas-Vázquez J (1998) Nonequilibrium generalization of chemical potential of flowing fluids. J Phys Chem B 102:5335–5340
- Criado-Sancho M, Jou D, Casas-Vázquez J (1999) On the Ginzburg–Landau expression for the free energy of solutions under flow. Physica A 274:466–475
- Criado-Sancho M, Jou D, del Castillo LF, Casas-Vázquez J (2000) Shear induced polymer migration: analysis of the evolution of concentration profiles. Polymer 41:8425–8432
- Criado-Sancho M, Jou D, Casas-Vázquez J, del Castillo LF (2002) Shear-induced shift of spinodal line in entangled polymer blends. Phys Rev E 66:061803 (6 p)
- Criado-Sancho M, Jou D, Casas-Vázquez J (2003) Viscous pressure behaviour in shear-induced concentration banding. Polymer 44:6965–6971
- Criado-Sancho M, Jou D, Casas-Vázquez J (2005) Non-equilibrium chemical potential and polymer extraction from a porous matrix. Polymer 46:10372–10377
- Criado-Sancho M, Jou D, Casas-Vázquez J (2006) Nonequilibrium kinetic temperatures in flowing gases. Phys Lett A 350:339–341
- Criado-Sancho M, Jou D, Casas-Vázquez J (2008) Temperature in ideal gas mixtures in Couette flow: a maximum-entropy approach. Phys Lett A 372:2172–2175
- Crisanti A, Ritort F (2003) Violation of the fluctuation-dissipation theorem in glassy systems: basic notions and the numerical evidence. J Phys A Math Gen 36:R181–R290
- Cukrowski AS, Popielawski J (1986) The effect of viscous flow and thermal flux on the rate of chemical reaction in dilute gases. Chem Phys 109:215–226
- Curtiss CF, Bird RB (1999) Diffusion-stress relations in polymer mixtures. J Chem Phys 111:10362-10370
- Daivis PJ (2008) Thermodynamic relationships for shearing linear viscoelastic fluids. J Non-Newtonian Fluid Mech 152:120–128
- Danielewicz P (1984) Transport properties of excited nuclear matter and the shock-wave profile. Phys Lett B 146:168–175
- Denicol GS, Kodama T, Koide T, Mota PH (2007a) Causal theory of relativistic dissipative hydrodynamics. Braz J Phys 37:1047–1054

References 285

Denicol GS, Kodama T, Koide T, Mota PH (2007b) Effects of finite size and viscosity in relativistic hydrodynamics. Nucl Phys A 787:60c–67c

- Denicol GS, Mota Ph, Kodama T, Koide T (2007c) Causal structure of relativistic dissipative hydrodynamics. Braz J Phys 37:102–105
- Denicol GS, Kodama T, Koide T, Mota Ph (2008) Shock propagation and stability in causal dissipative hydrodynamics. Phys Rev C 78:034901 (12 p)
- Denicol GS, Kodama T, Koide T, Mota PH (2009) Extensivity of irreversible current and stability in causal dissipative hydrodynamics. J Phys G Nucl Part Phys 36:035103 (22 p)
- Dill KA (1979) Theory of separation of very large DNA molecules by radial migration. Biophys Chem 10:327–334
- Dill KA, Zimm BH (1979) A rheological separator for very large DNA molecules. Nucleic Acids Res 7:735–749
- Doi M (1990) Dynamics and pattern in complex fluids: new aspects of physics and chemistry interfaces. In: Onuki A, Kawasaki K (eds) Springer, Berlin
- Doi M (1996) Introduction to polymer physics. Clarendon press, Oxford
- Doi M, Edwards SF (1978a) Dynamics of concentrated polymer systems. Part 1. Brownian motion in the equilibrium state. J Chem Soc Faraday Trans II 74:1789–1801
- Doi M, Edwards SF (1978b) Dynamics of concentrated polymer systems. Part 2. Molecular motion under flow. J Chem Soc Faraday Trans II 74:1802–1817
- Doi M, Edwards SF (1986) The theory of polymer dynamics. Clarendon Press, Oxford
- Doi M, Onuki A (1992) Dynamic coupling between stress and composition in polymer solutions and blends. J Phys II France 2:1631–1656
- Domínguez R, Jou D (1995) Thermodynamic pressure in nonequilibrium gases. Phys Rev E 51:158–163
- Donnelly RJ (1991) Quantized vortices in helium II. Cambridge University Press, Cambridge
- Dressler M, Edwards BJ, Öttinger HC (1999) Macroscopic thermodynamics of flowing polymeric liquids. Rheol Acta 38:117–136
- Dreyer W, Struchtrup H (1993) Heat pulse experiments revisited. Continuum Mech Thermodyn 5:3–50
- Dreyer W, Herrmann M, Kunik M (2004) Kinetic solutions of the Boltzmann-Peierls equation and its moment system. Continuum Mech Thermodyn 16:453–469
- Drost A, Steiner P, Moser H, Lang W (1995) Thermal conductivity of porous silicon. Sens Mater 7:111-120
- Edwards BJ, Öttinger HC, Jongschaap RJJ (1997) On the relationships between thermodynamic formalisms for complex fluids. J Non Equilib Thermodyn 22:356–373
- Eu BC (1992) Kinetic theory and irreversible thermodynamics. Wiley, New York
- Eu BC (1998) Nonequilibrium statistical mechanics: ensemble method. Kluwer, Dordrecht
- Eu BC (2002) Generalized thermodynamics: the thermodynamics of irreversible processes and generalized hydrodynamics. Kluwer, Dordrecht
- Eu BC, Li KW (1977) Kinetic theory of reacting systems. Physica A 88:135-157
- Evans DJ (1981) Rheological properties of simple fluids by computer simulation. Phys Rev A 23:1988–1997
- Evans DJ (1989) The entropy of nonequilibrium states. J Stat Phys 57:745–758
- Evans DJ, Hanley HJM (1981) Thermodynamic fluctuation theory for shear flow. Physica A 108:567–574
- Evans DJ, Morriss G (1990) Statistical mechanics of nonequilibrium liquids. Academic Press, London (Electronic version in Australian National University E Press 2007)
- Fai G, Danielewicz P (1996) Non-equilibrium modifications of the nuclear equation of state. Phys Lett B 373:5–8
- Farhat H, Eu BC (1998) Nonequilibrium statistical thermodynamics: Nonequilibrium grand ensemble method for sheared dilute gases. J Chem Phys 109:10169–10179
- Ferry JD (1980) Viscoelastic properties of polymers, 3rd edn. Wiley, New York
- Flory PJ (1965) Statistical thermodynamics of liquid mixtures. J Am Chem Soc 87:1833–1838
- Flory PJ, Orwoll RA, Vrij A (1964a) Statistical thermodynamics of chain molecule liquids. I. An equation of state for normal paraffin hydrocarbons. J Am Chem Soc 86:3507–3514

Flory PJ, Orwoll RA, Vrij A (1964b) Statistical thermodynamics of chain molecule liquids. II. Liquid mixtures of normal paraffin hydrocarbons. J Am Chem Soc 86:3515–3520

- Foister RT, Van De Ven TGM (1980) Diffusion of Brownian particles in shear flows. J Fluid Mech 96(1):105–132
- Fort J, Cukrowski AS (1997) The effect of heat conduction on the rate of chemical reaction in dilute gases. Chem Phys 222:59–69
- Fort J, Cukrowski AS (1998) Applications of information statistical theory to the description of the effect of heat conduction on the chemical reaction rate in gases. Acta Phys Pol B 29:1633–1646
- Fort J, Casas-Vázquez J, Méndez V (1999) Extended irreversible thermodynamics of chemically reacting systems. J Phys Chem B 103:860–867
- Frank TD (2002) Generalized Fokker-Planck equations derived from generalized linear nonequilibrium thermodynamics. Physica A 310:397–412
- Galenko P (2007) Solute trapping and diffusionless solidification in a binary system. Physical Review E 76:031606 (9 p)
- Galvão Ramos J, Vasconcellos AR, Luzzi R (1995) A classical approach in predictive statistical mechanics: a generalized Boltzmann formalism. Fortschritte der Physik/Prog Phys 43:265–300
- Gariel J, Le Denmat G (1994) Relationship between two theories of dissipative relativistic hydrodynamics applied to cosmology. Phys Rev D 50:2560–2566
- Garzó V, Santos A (2003) Kinetic theory of gases in shear flow. Kluwer, Dordrecht
- de Gennes PG (1971) Reptation of a polymer chain in the presence of fixed obstacles. J Chem Phys 55:572–579
- de Gennes PG, Prost J (1990) The physics of liquid crystals, 2nd edn. Clarendon Press, Oxford
- Gesele G, Linsmeier J, Drach V, Arens-Fischer R (1997) Temperature-dependent thermal conductivity of porous silicon. J Phys D Appl Phys 30:2911–2916
- Geurst JA (1989) Hydrodynamics of quantum turbulence in HeII: Vinen's equation derived from energy and impulse of vortex tangle. Physica B 154:327–343
- Glynn PAR, Van Der Hoof BME, Reilly PM (1972) A general model for prediction of molecular weight distribution of degraded polymers. Development and comparison with ultrasonic degradation experiment. J Macromol Sci Part A 6:1653–1664
- Goldstein P, García-Colín LS (1993) A thermodynamic basis for transport phenomena in viscoelastic fluids. J Chem Phys 99:3913–3918
- Goldstein P, García-Colín LS (1994) Transport processes in a viscoelastic binary mixture. J Non Equilib Thermodyn 19:170–183
- Gorban AN, Karlin IV (2005) Invariant manifold for physical and chemical kinetics, Lectures Notes in Physics. Springer, Berlin
- Goveas JL, Fredrickson GH (1999) Curvature-driven shear banding in polymer melts. J Rheol 43:1261–1277
- Grad H (1958) Principles of the kinetic theory of gases. In: Flugge S (ed) Handbuch der Physik XII. Springer, Berlin
- Graessley WW (1974) The entanglement concept in polymer rheology. Adv Polym Sci 16:1–179 Grandy WT Jr (1987–1988) Foundations of statistical mechanics, vol 2. D. Reidel, Dordrecht
- Gray WG, Miller CT (2005) Thermodynamically constrained averaging theory approach for modelling flow and transport phenomena in porous medium systems: 1. Motivation and overview. Adv Water Res 28:161–180
- Gray WG, Miller CT (2006) Thermodynamically constrained averaging theory approach for modelling flow and transport phenomena in porous medium systems: 3. Single-fluid-phase flow. Adv Water Res 29:1745–1765
- Greco A, Müller I (1984) Extended thermodynamics and superfluidity. Arch Rat Mech Anal 85:279-294
- Grmela M (1987) Thermodynamics of a generalized gas under shear. Phys Lett A 120:276-280
- Grmela M, Öttinger HC (1997) Dynamics and thermodynamics of complex fluids. I. Development of a general formalism. Phys Rev E 56:6620–6632
- de Groot SR, Mazur P (1962) Non-equilibrium thermodynamics. North-Holland, Amsterdam (Republication by Dover in 1984)

Gu T, Tsai G-J, Tsao GT (1993) Multicomponent radial flow chromatography. Adv Biochem Eng Biotechnol 49:76–95

- Gulminelli F (2004) Phase coexistence in nuclei. Ann Phys 29:1-121
- Gulminelli F, Chomaz P (2004) Equilibrium under flow. Nucl Phys A 734:581-588
- Guyer RA, Krumhansl JA (1966a) Solution of the linearized phonon Boltzmann equation. Phys Rev 148:766–778
- Guyer RA, Krumhansl JA (1966b) Thermal conductivity, second sound, and phonon hydrodynamic phenomena in non-metallic crystals. Phys Rev 148:778–788
- Gyarmati I (1970) Non-equilibrium thermodynamics. Springer, Berlin
- Hall HE, Vinen WF (1956) The rotation of liquid helium II. The theory of mutual friction in uniformly rotating helium II. Proc R Soc A 238:204–214
- Hamano K, Senger JV, Krall AH (1995) Critical dynamics of a sheared micellar solution. Int J Thermophys 16:355–361
- Hamano K, Ushiki H, Tsunomori F, Senger JV (1997) Shear effects in a micellar solution near the critical point. Int J Thermophys 18:379–386
- Hamdan E, Milthorpe JF, Lai JCS (2008) An extended macroscopic model for solute dispersion in confined porous media. Chem Eng J 137:614–635
- Hamilton MJ, Buchanan B (2007) Spatial gradients in Clovis-age radiocarbon dates across North America suggest rapid colonization from the north. PNAS 104:15625–15630
- Hanley HJM, Evans DJ (1982) A thermodynamics for a system under shear. J Chem Phys 76:3225-3232
- Hashimoto T, Takebe T, Asakawa K (1993) Phase transition of polymer mixtures under simple shear flow. Physica A 194:338–351
- Helfand E, Fredrickson GH (1989) Large fluctuations in polymer solutions under shear. Phys Rev Lett 62:2468–2471
- Henglein A (1956) The combination of the free macro-radicals, which are formed in the ultrasonic degradation of polymethylmethacrylate and polystyrene (in German). Makromol Chem 18/19:37–47
- Hess S (1975) Irreversible thermodynamics of nonequilibrium alignment phenomena in molecular liquids and in liquid crystals. Z Naturforsch 30a:728–733, 1224–1232
- Hess S (1976) Pre- and post-transitional behaviour of the flow alignment and flow-induced phase transition in liquid crystals. Z Naturforsch 31a:1507–1513
- Hess S (1977) Non-Newtonian viscosity and normal pressure associated with the flow alignment in macromolecular liquids. Physica A 86:383–399
- Highgate D (1966) Particle migration in cone-and-plate viscometry of suspensions. Nature 211:1390–1391
- Hochbaum AI, Chen R, Delgado RD, Liang W, Garnett EC, Najarian M, Majumdar A, Yang P (2008) Enhanced thermoelectric performance of rough silicon nanowires. Nature 451: 163–167
- Holmes LA, Ferry JD (1968) Dependence of the steady-state compliance on concentration and molecular weight in polymer solutions. J Polym Sci Part C 23:291–299
- Holmes LA, Ninomiya K, Ferry JD (1966) The steady-state compliance of dilute polymer solutions. J Phys Chem 70:2714–2719
- Hoover WG (1985) Canonical dynamics: equilibrium phase-space distributions. Phys Rev A 31:1695–1697
- Isichenko MB (1992) Percolation, statistical topography, and transport in random media. Rev Mod Phys 64:961–1043
- Ichiyanagi M (1997) The second law and Boltzmann's H-theorem. J Phys Soc Japan 66:589–597 Ikenberry E, Truesdell C (1956) On the pressures and the flux of energy in a gas according to Maxwell's kinetic theory I. J Rat Mech Anal 5:1–54
- Janeschitz-Kriegl H (1969) Flow birefringence of elastico-viscous polymer systems. Adv Polym Sci 6:170–318
- Jongschaap RJJ (1990) Microscopic modelling of the flow properties of polymers. Rep Prog Phys 53:1–55

Jongschaap RJJ, de Haas KH, Damen CAJ (1994) A generic matrix representation of configuration tensor rheological models. J Rheol 38:769–796

- Jou D, Casas-Vázquez J (1983) Equilibrium third moments and non-equilibrium second moments of fluctuations of hydrodynamic dissipative fluxes. J Non Equilib Thermodyn 8:127–142
- Jou D, Casas-Vázquez J (1990) Nonequilibrium absolute temperature, thermal waves and phonon hydrodynamics. Physica A 163:47–58
- Jou D, Casas-Vázquez J (2001) Extended irreversible thermodynamics and its relation with other continuum approaches. J Non-Newtonian Fluid Mech 96:77–104
- Jou D, Criado-Sancho M (2001) Thermodynamics of dilute gases in shear flow. Physica A 292: 75–86
- Jou D, Mongiovì MS (2004) Phenomenological description of counterflow superfluid turbulence in rotating containers. Phys Rev B 69:094513 (7 p)
- Jou D, Mongiovì MS (2005) Nonequilibrium thermodynamics of unsteady superfluid turbulence in counterflow and rotating situations. Phys Rev B 72:144517 (11 p)
- Jou D, Mongiovì MS (2006) Description and evolution of anisotropy in superfluid vortex tangles with counterflow and rotation. Phys Rev B 74:054509 (11 p)
- Jou D, Mongiovì MS (2009) Non-equilibrium temperature of well-defined quantum turbulence. Phys Lett A 373:2306–2310
- Jou D, Pérez-García C (1983) Generalized van der Waals equation for nonequilibrium fluids. Phys Rev A 28:2541–2543
- Jou D, Casas-Vázquez J, Lebon G (1988) Extended irreversible thermodynamics. Rep Prog Phys 51:1105–1179
- Jou D, Camacho J, Grmela M (1991) On the nonequilibrium thermodynamics of non-Fickian diffusion. Macromolecules 24:3597–3602
- Jou D, Casas-Vázquez J, Lebon G (1992) Extended irreversible thermodynamics: an overview of recent bibliography. J Non-Equilib Thermodyn 17:383–396
- Jou D, Casas-Vázquez J, Criado-Sancho M (1995) Thermodynamics of polymer solutions under flow: phase separation and polymer degradation. Adv Polym Sci 120:207–266
- Jou D, Casas-Vázquez J, Lebon G (1996) Recent bibliography on extended irreversible thermodynamics and related topics (1992–1995). J Non Equilib Thermodyn 21:103–121
- Jou D, Casas-Vázquez J, Lebon G (1998) Recent bibliography on extended irreversible thermodynamics and related topics (1995–1998). J Non Equilib Thermodyn 23:277–297
- Jou D, Casas-Vázquez J, Lebon G (1999a) Extended irreversible thermodynamics revisited. Rep Prog Phys 62:1035–1142
- Jou D, Casas-Vázquez J, Criado-Sancho M (1999b) Information theory and thermodynamics of polymer solutions under flow. Physica A 262:69–75
- Jou D, Criado-Sancho M, del Castillo LF, Casas-Vázquez J (2001) A thermodynamic model for shear-induced concentration banding and macromolecular separation. Polymer 42:6239–6245
- Jou D, Criado-Sancho M, Casas-Vázquez J (2002a) Non-equilibrium chemical potential and stress-induced migration of polymer in tubes. Polymer 43:1599–1605
- Jou D, Lebon G, Mongiovi MS (2002b) Second sound, superfluid turbulence and intermittent effects in liquid helium II. Phys Rev B 66:224509 (9 p)
- Jou D, Casas-Vázquez J, Criado-Sancho M (2003) Thermodynamics and dynamics of flowing polymer solutions and blends. Contrib Sci 2:315–332
- Jou D, Criado-Sancho M, Casas-Vázquez J (2005) Nonequilibrium temperature and fluctuationdissipation temperature in flowing gases. Physica A 358:49–57
- Jou D, Sciacca M, Mongiovi MS (2008) Vortex dynamics in rotating counterflow and plane Couette and Poiseuille turbulence in superfluid helium. Phys Rev E 78:024524 (7 p)
- Jou D, Casas-Vázquez J, Lebon G (2010) Extended irreversible thermodynamics, 4th edn. Springer, Heidelberg
- Jupp L, Yuan XF (2004) Dynamic phase separation of a binary polymer liquid with asymmetric composition under rheometric flow. J Non-Newtonian Fluid Mech 124:93–101 (Special issue)
- Jupp L, Kawakatsu T, Yuan XF (2003) Modeling shear-induced phase transitions of binary polymer mixtures. J Chem Phys 119:6361–6372

Katayama K, Terauti R (1996) Brownian motion of a single particle under shear flow. Eur J Phys 17:136–140

- Kestin J (1990) A note on the relation between the hypothesis of local equilibrium and the Clausius–Duhem inequality. J Non Equilib Thermodyn 15:193–212
- Kestin J (1993) Internal variables in the local-equilibrium approximation. J Non Equilib Thermodyn 18:360–379
- Kizilova N (2010) Optimal transport networks in nature. World Scientific, Singapore
- Klages R, Radons G, Sokolov IM (eds) (2008) Anomalous transport. Foundations and applications. Wiley VCH, Weinheim
- Kodama T, Koide T, Denicol GS, Mota Ph (2007) Open problems in the hydrodynamical approach to relativistic heavy ion collisions. Int J Mod Phys E 16:763–775
- Koide T (2007) Microscopic formula for transport coefficients of causal hydrodynamics. Phys Rev E 75:060103
- Koide T, Kodama T (2008) Transport coefficients of non-Newtonian fluid and causal dissipative hydrodynamics. Phys Rev E 78:051107 (11 p)
- Koide T, Krein G, Ramos RO (2007a) Memory effect and fast spinodal decomposition. Braz J Phys 37:601–604
- Koide T, Denicol GS, Mota PH, Kodama T (2007b) Relativistic dissipative hydrodynamics: a minimal causal theory. Phys Rev C 75:034909 (10 p)
- Kondepudi D, Prigogine I (1998) Modern thermodynamics: from heat engines to dissipative structures. Wiley, New York
- Kramer H, Wolf BA (1985) On the occurrence of shear-induced dissolution and shear-induced demixing within one and the same polymer/solvent system. Makromol Chem Rapid Commun 6:21–27
- Krämer-Lucas H, Schenck H, Wolf BA (1988a) Influence of shear on the demixing of polymer solutions. I. Apparatus and experimental results. Makromol Chem 189:1613–1625
- Krämer-Lucas H, Schenck H, Wolf BA (1988b) Influence of shear on the demixing of polymer solutions. II. Stored energy and theoretical calculations. Makromol Chem 189:1627–1634
- Kramers HA (1946) The behaviour of macromolecules in inhomogeneous flow. J Chem Phys 14:415–424
- Kurata M (1982) Thermodynamics of polymer solutions. Harwood Academic, Chur
- Landau LD (1941) The theory of superfluidity of He II. J Phys (USSR) 5:71–90
- Landau LD, Lifshitz EM (1969) Statistical physics. Pergamon, London
- Landau LD, Lifshitz EM (1970) Fluid mechanics. Pergamon, London
- Lay MC, Fee CJ, Swan JE (2006) Continuous radial flow chromatography of proteins. Food Bioprod Process 84:78–83
- Lebon G, Jou D (1979) A continuum theory of liquid helium II based on the classical theory of irreversible processes. J Non Equilib Thermodyn 4:259–275
- Lebon G, Pérez-García C, Casas-Vázquez J (1986) On a new thermodynamic description of viscoelastic materials. Physica A 137:531–545
- Lebon G, Pérez-García C, Casas-Vázquez J (1988) On the thermodynamic foundations of viscoelasticity. J Chem Phys 88:5068–5075
- Lebon G, Jou D, Casas-Vázquez J (2008) Understanding non-equilibrium thermodynamics, foundations, applications, frontiers. Springer, Berlin
- Lecoq N, Zapolsky H, Galenko P (2009) Evolution of the structure factor in a hyperbolic model of spinodal decomposition. Eur Phys J Spec Top 177:165–175
- Lee J-H, Grossman JC, Reed J, Galli G (2007) Lattice thermal conductivity of nanoporous Si: molecular dynamics study. Appl Phys Lett 91:223110 (p 3)
- Lee S-D (1987) Comment on effects of elongational flow on the isotropic-nematic phase transition in rod-like systems. J Chem Phys 86:6567–6568
- Levine RD, Tribus M (eds) (1979) The maximum entropy formalism. MIT Press, Cambridge, MA Lhuillier D (1983) Phenomenology of polymer migration. J Phys France 44:303–309
- Lhuillier D, Ouibrahim A (1980) A thermodynamic model for solutions of deformable molecules. J Mécanique 19:725–741

Li D, Wu Y, Kim P, Shi L, Yang P, Majumdar A (2003) Thermal conductivity of individual silicon nanowire. Appl Phys Lett 83:2934–2936

- Lockerby DA, Reese JM, Emerson DR, Barber RW (2004) Velocity boundary condition at solid walls in rarefied gas calculations. Phys Rev E 70:017303
- Loose W, Hess S (1987) Velocity distribution function of a streaming gas via non-equilibrium molecular dynamics. Phys Rev Lett 58:2443–2445
- Loose W, Hess S (1991) Anisotropy in velocity space induced by transport processes. Physica A 174:47–59
- Lou JZ, Harinath V (2004) Effects of molecular weight and flow rate on stress-induced migration of polystyrene. J Liq Chromatogr Relat Technol 27:2819–2835
- Luzzi R, Vasconcellos AR (1990) On the nonequilibrium statistical operator method. Fortschr Phys/Progr Phys 38:887–922
- Luzzi R, Vasconcellos AR, Casas-Vázquez J, Jou D (1997) Characterization and measurement of a nonequilibrium temperature-like variable in irreversible thermodynamics. Physica A 234: 699–714
- Luzzi R, Vasconcellos AR, Galvao-Ramos J (2001) On the statistical foundations of irreversible thermodynamics. Teubner Verlag, Berlin
- Luzzi R, Vasconcellos AR, Ramos JS (2002) Predictive statistical mechanics: a non-equilibrium ensemble formalism. Kluwer, Dordrecht
- Lyngaae-Jorgensen J, Sondergaard K (1987) Phase transitions during shear flow of two phase polymer blends. II Styrene-acrylonitrile/poly(methylmethacrylate) transition to "homogeneous" melt states. Polym Eng Sci 27:351–358
- Lysenko V, Gliba V, Strikha V, Dittmar VA, Delhomme G, Roussel PH, Barbier D, Jaffrezic-Renault DN, Martelet C (1998) Nanoscale nature and low thermal conductivity of porous silicon layers. Appl Surf Sci 123/124:458–461
- Lysenko V, Roussel PH, Remaki B, Delhomme G, Dittmar A, Barbier D, Strikha V, Martelet C (2000) Study of nano-porous silicon with low thermal conductivity as thermal insulating material. J Porous Media 7:177–182
- MacDonald MJ, Muller SJ (1996) Experimental study of shear-induced migration of polymers in dilute solutions. J Rheol 40:259–283
- Manero O, Pérez-López JH, Escalante JI, Puig JE, Bautista F (2007) A thermodynamic approach to rheology of complex fluids: the generalized BMP model. J Non-Newtonian Fluid Mech 146:22–29
- Mark H, Simha R (1940) Degradation of long chain molecules. Trans Faraday Soc 35:611–618 Marrucci G (1972) The free energy constitutive equation for polymer solutions from the dumbbell model. Trans Soc Rheol 16:321–330
- Marrucci G, Ciferri A (1977) Phase equilibria of rod-like molecules in a extensional flow field. J Polym Sci Polym Lett Ed 15:643–648
- Marrucci G, Grizzutti N (1983) The free energy function of the Doi–Edward theory: analysis of the instabilities in stress relaxation. J Rheol 27:433–450
- Martin KP, Tough JT (1983) Evolution of superfluid turbulence in thermal counterflow. Phys Rev B 27:2788–2799
- Matsuo T, Pavan A, Peterlin A, Turner DT (1967) Time-dependent changes of viscosity in dilute polymer solutions. J Colloid Interface Sci 24:241–248
- Maugin GA (1999) The thermomechanics of nonlinear irreversible behaviors. An introduction. World Scientific, Singapore
- Maugin GA, Drouot R (1983) Internal variables and the thermodynamics of macromolecule solutions. Int J Eng Sci 21:705–724
- Maugin GA, Muschik W (1994a) Thermodynamics with internal variables. Part I. General concepts. J Non Equilib Thermodyn 19:217–249
- Maugin GA, Muschik W (1994b) Thermodynamics with internal variables. Part II. Applications. J Non Equilib Thermodyn 19:250–289
- Mavrantzas VG, Beris AN (1992) Modelling the rheology and flow-induced concentration changes in polymer solutions. Phys Rev Lett 69:273–276

Mazich KA, Carr SH (1983) The effect of flow on the miscibility of a polymer blend. J Appl Phys 54:5511-5114

- Meixner J (1949) Thermodynamik und relaxationserscheinungen. Z Naturforschung 4a:594a
- Meixner J (1954) Thermodynamische theorie der elastischen relaxation. Z Naturforschung 9a:654b
- Méndez V, Campos D, Fort J (2004) Dynamical features of reaction-diffusion fronts on fractals. Phys Rev E 69:016613 (7 p)
- Méndez V, Fedotov S, Horsthemke W (2010) Reaction-transport systems. Mesoscopic foundations, fronts, and spatial instabilities. Springer, Berlin
- Metzler R, Klafter J (2000) The random walk's guide to anomalous diffusion: a fractional dynamics approach. Phys Rep 339:1–77
- Miller CT, Gray WG (2008) Thermodynamically constrained averaging theory approach for modelling flow and transport phenomena in porous medium systems: 4. Species transport fundamentals. Adv Water Res 31:577–597
- Millikan RA (1923) The general law of fall of a small spherical body through a gas and its bearing upon the nature of the molecular reflection from surface. Phys Rev 22:1–23
- Milner ST (1991) Hydrodynamics of semidilute polymer solutions. Phys Rev Lett 66:1477–1480 Mongiovì MS (1991) Superfluidity and entropy conservation in extended thermodynamics. J Non Equilib Thermodyn 16:225–239
- Mongiovì MS (1992) Thermomechanical phenomena in extended thermodynamics of an ideal monatomic superfluid. J Non Equilib Thermodyn 17:183–189
- Mongiovì MS (1993a) The link between heat flux and stress deviator in extended thermodynamics of an ideal monatomic superfluid. J Non Equilib Thermodyn 18:147–156
- Mongiovì MS (1993b) Extended irreversible thermodynamics of liquid helium II. Phys Rev B 48:6276-6283
- Mongiovì MS (2000) Non-linear extended thermodynamics of a non-viscous fluid in the presence of heat flux. J Non Equilib Thermodyn 25:31–47
- Mongiovì MS (2001) Proposed measurements of the small entropy carried by the superfluid component of liquid helium II. Phys Rev B 63:012501 (4 p)
- Mongiovì MS, Jou D (2005a) Nonlocal effects in superfluid turbulence. Application to TI-TII transition and to vortex decay. Phys Rev B 71:094507 (7 p)
- Mongiovì MS, Jou D (2005b) Superfluid turbulence in rotating containers: phenomenological description of the influence of the wall. Phys Rev B 72:104515 (8 p)
- Mongiovì MS, Jou D (2005c) Generalization of Vinen's equation including transition to superfluid turbulence. J Phys Condens Matter 17:4423–4440
- Mongiovì MS, Jou D (2006) Evolution equations in superfluid turbulence. In: Das MP (ed) Condensed matter: new research. Nova Publishers, Hauppauge, New York, pp 1–53
- Mongiovì MS, Jou D (2007) A thermodynamical derivation of a hydrodynamical model of inhomogeneous superfluid turbulence. Phys Rev B 75:024507 (14 p)
- Mongiovì MS, Peruzza RA, Jou D (2004) Extended thermodynamics of liquid helium II: laminar and turbulent flows. Recent Res Dev Phys 5:1033–1056
- Mongiovì MS, Jou D, Sciacca M (2007) Energy and temperature of superfluid turbulent vortex tangles. Phys Rev B 75:214514 (10 p)
- Montanero JM, Santos A (1996) Nonequilibrium entropy of a sheared gas. Physica A 225:7-18
- Montroll E (1941) Molecular size distributions and depolymerization reactions in polydisperse systems. J Am Chem Soc 63:1215–1220
- Montroll EW, Simha R (1940) Theory of depolymerisation of long chain molecules. J Chem Phys 8:721–727
- More AL, Saha SK, Prasher RS, Shi L (2008) Phonon backscattering and thermal conductivity suppression in sawtooth nanowires. Appl Phys Lett 93:083112 (3 p)
- Mornas K, Ornik U (1995) On the role of dissipation in the early stages of relativistic heavy ion collisions. Nucl Phys A 587:828–852
- Mosco U (1997) Invariant field metrics and dynamical scaling on fractals. Phys Rev Lett 79:4067–4070

- Müller I, Ruggeri T (1998) Rational extended thermodynamics. Springer, Berlin
- Muschik W (1990) Internal variables in non-equilibrium thermodynamics. J Non Equilib Thermodyn 15:127–137
- Muschik W (1993) Comment to J. Kestin: internal variables in the local-equilibrium approximation. J Non Equilib Thermodyn 18:380–388
- Nakata M, Higashida S, Kuwahara N, Saeki S, Kaneko M (1976) Thermodynamic properties of the system polystyrene-*trans*-decalin. J Chem Phys 64:1022–1027
- Nemirovskii SK, Fiszdom W (1995) Chaotic quantized vortices and hydrodynamic processes in superfluid helium. Rev Mod Phys 67:37–84
- Nettleton RE (1987) Shear rate nonanalyticity in simple liquids. J Non Equilib Thermodyn 12:273–290
- Nettleton RE (1988) Non-linear isotopic diffusion in dense fluids. J Phys A Math Gen 21: 1079–1090
- Nettleton RE (1993) Statistical basis for extended thermodynamics of diffusion in dense fluids. J Chem Phys 99:3059–3066
- Nettleton RE (1996a) Non-equilibrium corrections to chemical rate constants in gases under flows of heat and diffusion. Z Phys Chem 196:177–185
- Nettleton RE (1996b) Nonequilibrium flow-dependent corrections to chemical rate constants in gases. J Chem Phys 100:11005–11008
- NetTleton RE, Torrisi M (1991) Extended thermodynamics of heat flow coupled to a unimolecular reaction. Nuovo Cimento B 106:525–535
- Nettleton RE, Sobolev SL (1995a) Applications of extended thermodynamics to chemical, rheological, and transport processes: a special survey. Part I. Approaches and scalar rate processes. J Non Equilib Thermodyn 20:205–229
- Nettleton RE, Sobolev SL (1995b) Applications of extended thermodynamics to chemical, rheological, and transport processes: a special survey. Part II. Vector transport processes, shear relaxation and rheology. J Non Equilib Thermodyn 20:297–331
- Nettleton RE, Sobolev SL (1996) Applications of extended thermodynamics to chemical, rheological, and transport processes: a special survey. Part III. Wave phenomena. J Non Equilib Thermodyn 21:1–16
- Nguyen TQ, Kausch HH (1992) Mechanochemical degradation in transient elongational flow. Adv Polym Sci 100:73–182
- Nosé S (1984) A unified formulation of the constant temperature molecular dynamics methods. J Chem Phys 81:511–519
- Nozières P, Quemada D (1986) A possible instability mechanism for plug formation in a sheared suspension flow. Europhys Lett 2:129–135
- Olmsted PD (2008) Perspectives on shear banding in complex fluids. Rheol Acta 47:283–300
- Olmsted PD, Goldbart PM (1990) Theory of the nonequilibrium phase transition for nematic liquid crystal under shear flow. Phys Rev A 41:4578–4581
- Olmsted PD, Lu C-YD (1997) Coexistence and phase separation in sheared complex fluids. Phys Rev E 56:R55–R58
- Olson TS, Hiscock WA (1989) Relativistic dissipative hydrodynamics and the nuclear equation of state. Phys Rev C 39:1818–1826
- Onsager L (1942) Anisotropic solution of colloids. Phys Rev 62:558-559
- Onuki A (1980a) Steady states with heat flow near critical points. Local equilibrium theory. Prog Theor Phys 63:1854–1864
- Onuki A (1980b) Steady states with Helium near the superfluid transition under heat flow. Prog Theor Phys 64:1902–1917
- Onuki A (1989) Elastic effects in the phase transition of polymer solutions under shear flow. Phys Rev Lett 62:2472–2475
- Onuki A (1990) Dynamic equations of polymers with deformations in semidilute regions. J Phys Soc Jpn 59:3423–3426
- Onuki A (1997) Phase transitions of fluids in shear flow. J Phys Condens Matter 9:6119–6157
- Onuki A (2002) Phase transition dynamics. Cambridge University Press, Cambridge

Onuki A, Yamazaki K, Kawasaki K (1981) Light scattering by critical fluids under shear flow. Ann Phys (NY) 131:217–242

- Ortiz de Zárate JM, Senger JV (2006) Hydrodynamic fluctuations in fluids and fluid mixtures. Elsevier, Amsterdam
- Osborne DV (1950) The rotation of liquid helium II. Proc Phys Soc A 63:909-912
- O'Shaugnessy B, Procaccia I (1995) Analytical solutions for diffusion on fractal objects. Phys Rev Lett 54:455–458
- Öttinger HC (1992) Incorporation of polymer diffusivity and migration into constitutive equations. Rheol Acta 31:14–21
- Öttinger HC (2005) Beyond equilibrium. Thermodynamics. Wiley, Hoboken
- Öttinger HC, Grmela M (1997) Dynamics and thermodynamics of complex fluids. II. Illustrations of a general formalism. Phys Rev E 56:6633–6655
- Ouyang WB, Li GX, Yang Q (2004) Shear-induced apparent shift of phase boundary of binary polymer blends. Macromol Theory Simul 13:178–188
- Pavón D (1992) Astrophysical and cosmological applications of extended relativistic thermodynamics. In: Sieniutycz S, Salamon P (eds) Extended thermodynamic systems. Taylor and Francis, New York
- Peighambardoust SH, Van Der Goot AJ (2010) Migration of gluten under shear flow: influence of process parameters on separation behaviour. Food Chem 118:712–718
- Peighambardoust SH, Hamer RJ, Boom RM, Van Der Goot AJ (2008) Migration of gluten under shear flow as a novel mechanism for separating wheat flour into gluten and starch. J Cereal Sci 48:327–338
- Peralta C, Melatos A, Giacobello M, Ooi A (2006) Transitions between turbulent and laminar superfluid vorticity states in the outer core of a neutron star. Astrophys J 651:1079–1091
- Pérez-Guerrero AN (1997) Wave equations for heat flux and the pressure tensor in nonequilibrium thermodynamics. J Non Equilib Thermodyn 22:20–23
- Pérez-Guerrero AN, García-Colín LS (1991) Anomalous difusión in polymers: a generalized thermodynamic approach. J Non Equilib Thermodyn 16:201–215
- Pérez-García C, Casas-Vázquez J, Lebon G (1989) A nonequilibrium thermodynamic description of dilute polymer solutions. J Polym Sci B Polym Phys 27:1807–1821
- Peterlin A (1966) Hydrodynamics of linear macromolecules. Pure Appl Chem 12:563-586
- Peterlin A, Turner DT (1965) Temporary network formation in shearing solutions of poly(methyl methacrylate) in aroclor. J Polym Sci Part B Polym Lett 3:517–520
- Peterlin A, Quan C, Turner DT (1965) Role of molecular aggregates in the flow properties of poly(methyl methacrylate) in aroclor. J Polym Sci Part B Polym Lett 3:521–524
- Pratt S (2008) Formulating viscous hydrodynamics for large velocity gradients. Phys Rev C 77:024910
- Pratt S, Vredevoogd J (2008) Femtoscopy in relativistic heavy ion collisions and its relation to bulk properties of QCD matter. Phys Rev C 78:054906
- Prigogine I (1961) Introduction to thermodynamics of irreversible processes. Interscience, New York Putterman SJ (1974) Superfluid hydrodynamics. North Holland, Amsterdam
- Rangel-Nafaile C, Metzner AB, Wissbrun KF (1984) Analysis of stress-induced phase separations in polymer solutions. Macromolecules 17:1187–1195
- Ren JZ, Chung TS, Li DF, Wang R, Liu Y (2002) Development of asymmetric 6FDA-2,6 DAT hollow fiber membranes for CO2/CH4 separation: 1. The influence of dope composition and rheology on membrane morphology and separation performance. J Membr Sci 207:227–240
- Restuccia L (2010) Thermomechanics of porous solids filled by fluid flow in applied and industrial mathematics in Italy II. In: de Bernardis E, Spigler R, Valente V (eds) World Scientific, Singapore, pp 485–495
- Roldughin VY (1996) Nonequilibrium thermodynamics of boundary conditions for rarefied gases and related phenomena. Adv Colloid Interface Sci 65:1–35
- Rouse PE (1953) A theory of linear viscoelastic properties of dilute solutions of coiling polymers. J Chem Phys 21:1272–1280
- Sahimi M (1995) Flow and transport in porous media and fractured rock. VCH, Weinheim

Santos A, Garzó V (1995) Exact moment solution of the Boltzmann equation for uniform shear flow. Physica A 213:409–425

- Sarti GC, Marrucci G (1973) Thermomechanics of dilute polymer solutions: multiple bead-spring model. Chem Eng Sci 28:1053–1059
- Schukraft J (1993) Ultra-relativistic heavy-ion collisions: searching for the quark-gluon plasma. Nucl Phys A 553:31–44
- Schwarz KW (1985) Three-dimensional vortex dynamics in superfluid ⁴He: line-line and line-boundary interactions. Phys Rev B 31:5782–5804
- Schwarz KW (1988) Three dimensional vortex dynamics in superfluid ⁴He: homogeneous superfluid turbulence. Phys Rev B 38:2398–2417
- Schafer DA, Wudl F, Thomas GA, Ferraris JP, Cowan DO (1974) Apparent giant conductivity peaks in an anisotropic medium: TTF-TCNO. Solid State Commun 14:347–351
- Sciacca M, Mongiovi MS, Jou D (2007) A mathematical model of counterflow superfluid turbulence describing heat waves and vortex-density waves. Mathemat Comput Model 48:206–221
- See H, Doi M, Larson R (1990) The effect of steady flow fields on the isotropic-nematic phase-transition of rigid rod-like polymers. J Chem Phys 92:792 (9 p)
- Sellitto A, Alvarez FX, Jou D (2010a) Second law of thermodynamics and phonon-boundary conditions in nanowires. J Appl Phys 107:064302 (7 p)
- Sellitto A, Alvarez FX, Jou D (2010b) Temperature dependence of boundary conditions in phonon hydrodynamics of smooth and rough nanowires. J Appl Phys 107:114312 (7 p)
- Schlesinger MF, Zavlavsky GM, Klafter J (1993) Strange kinetics. Nature 363:31–37
- Schlesinger MF, Zaslavsy GM, Frisch U (eds) (1995) Lévy flights and related topics in physics. Springer, Berlin
- Sharipov F (2004) Heat transfer in the Knudsen layer. Phys Rev E 69:061201 (4 p)
- Sieniutycz S (1994) Conservation laws in variational thermohydrodynamics. Kluwer, Dordrecht
- Sieniutycz S, Salamon P (eds) (1992) Extended thermodynamic systems. Advances in Thermodynamics, vol 7. Taylor and Francis, New York
- Silberberg A, Kuhn W (1952) Miscibility of liquids influenced by rate of shear. Nature 170: 450-451
- Silberberg A, Kuhn W (1954) Size and shape of droplets of demixing polymer solutions in a field flow. J Polym Sci Polym Phys 13:21–42
- Silhavy M (1997) The mechanics and thermodynamics of continuous media. Springer, Berlin
- Simha R (1941) Kinetics of degradation and size distribution of long chain polymers. J Appl Phys 12:569–577
- Smith R (1981) A delay-diffusion description for contaminant dispersion. J Fluid Mech 105: 469–486
- Smith R (1987a) Diffusion in shear flows made easy: the Taylor limit. J Fluid Mech 175:201–214 Smith R (1987b) Shear dispersion looked at from a new angle. J Fluid Mech 182:447–466
- Song D, Chen G (2004) Thermal conductivity of periodic microporous silicon films. Appl Phys Lett 84:687–689
- Staudinger H (1932) Die hochmolekularen organischen Verbindungen. Springer, Berlin
- Struchtrup H (2005) Macroscopic transport equations for rarefied gas flows: approximation methods in kinetic theory. Springer, Heidelberg
- Sun T, Balazs AC, Jasnow D (1997) Dynamics of phase separation in polymer solutions under shear flow. Phys Rev E 55:R6344–R6347
- Sun Z-S, Denn MM (1972) Stability of rotational Couette flow of polymer solutions. AIChE J 18:1010-1015
- Swanson CE, Barenghi CF, Donnelly RJ (1983) Rotation of a tangle of quantized vortex lins in HeII. Phys Rev Lett 50:190–193
- Tabeling P (2005) Introduction to microfluidics. Oxford University Press, Oxford
- Takebe T, Sawaoka R, Hashimoto T (1989) Shear-induced homogenization of semidilute solution of polymer mixture and unmixing after cessation of the shear. J Chem Phys 91: 4369–4379

Takebe T, Fujioka K, Sawaoka R, Hashimoto T (1990) Self-assembled structure of a semidilute solution of polymer mixtures under shear flow. J Chem Phys 93:5271–5280

Tanaka H (1996) Universality of viscoelastic phase separation in dynamically asymmetrical fluid mixtures. Phys Rev Lett 76:787–790

Tanner RI (1988) Engineering rheology. Clarendon Press, Oxford

Taylor G (1953) Dispersion of soluble matter in solvent flowing slowly along a tube. Proc R Soc Ser A 219:186–203

Taylor G (1954) Conditions under which dispersion of a solute in a stream of solvent can be used to measure molecular diffusion. Proc R Soc Ser A 255:473–477

Thirumalai D (1986) Effect of elongational flow on the isotropic-nematic phase transition in rod-like systems. J Chem Phys 84:5869 (5 p)

Thomas NL, Windle AH (1982) A theory of case II diffusion. Polymer 23:529-542

Tirrell M (1986) Phase behaviour of flowing polymer mixtures. Fluid Phase Equilib 30:367–380

Tirrell M, Malone MF (1977) Stress-induced diffusion of macromolecules. J Polym Sci Polym Phys 15:1569–1583

Tisza L (1938) Transport phenomena in He II. Nature 141:913

Todd BD, Evans DJ (1995) The heat flux vector for highly inhomogeneous non-equilibrium fluids in narrow pores. J Chem Phys 103:9804–9809

Todd BD, Evans DJ (1997) Temperature profile for poiseuille flow. Phys Rev E 55:2800-2807

Truesdell C (1971) Rational thermodynamics. McGraw-Hill, New York (2nd enlarged edition 1984)

Tsallis C (1995) Non-extensive thermostatistics: brief review and comments. Physica A 221: 277–290

Tsallis C (1999) Nonextensive statistics: theoretical, experimental and computational evidences and connections. Braz J Phys 29:1–35

Tsallis C, Levy SVF, Souza AMC, Maynard R (1995) Statistical-mechanical foundation of the ubiquity of Lévy distributions in nature. Phys Rev Lett 75:3589–3593

Tsubota M, Araki T, Barenghi CF (2003) Rotating superfluid turbulence. Phys Rev Lett 90:205301 (4 p)

Tzou DY (1997) Macro-to-microscale heat transfer. The lagging behavior. Taylor & Francis, New York

Vanoene H (1972) Modes of dispersion of viscoelastic fluids in flow. J Colloid Interface Sci 40:448–467

Vázquez JL (2007) The porous medium equation. Mathematical Theory. Oxford mathematical monographs. Oxford University Press, Oxford

Ver Straate G, Philipoff W (1974) Phase separation in flowing polymer solutions. J Polym Sci Polym Lett 12:267–275

Verhas J (1997) Thermodynamics and rheology. Kluwer, Dordrecht

Vinen WF (1957a) Mutual friction in a heat current in liquid helium II, I. Experiments on steady heat current. Proc R Soc London Ser A 240:114–127

Vinen WF (1957b) Mutual friction in a heat current in liquid helium II, II. Experiments on transient effects. Proc R Soc London Ser A 242:128–143

Vinogradov GA, Malkin AY (1980) Rheology of polymers: viscoelasticity and flow of polymers. Springer, Berlin

Volovik GE (2005) The universe in a helium droplet. Oxford University Press, Oxford

Vrahopoulou-Gilbert E, McHugh AJ (1984) Thermodynamics of flux-induced phase separation in polymers. Macromolecules 17:2657–2663

Wang C, Vugmeister BE, Ou-Yang HD (1993) Pretransitional orientational ordering of rigid-rod polymers in shear flow. Phys Rev E 48:4455–4457

Wang XL, Chatterjee AP (2002) Shear-induced effects on miscibility in polymer solutions. Mol Phys 100:2587–2595

Wilks J (1967) The Properties of Liquid and Solid Helium. Clarendon Press. Oxford

Wilmanski K (1998) Thermomechanics of continua. Springer, Berlin

Wolf BA (1980) Theoretical description of phase separation in flowing polymer solutions. Makromol Chem Rapid Commun 1:231–234

- Wolf BA (1984) Thermodynamic theory of flowing polymer solutions and its application to phase separation. Macromolecules 17:615–618
- Wolf BA (1987) On the mechanisms of polymer degradation by laminar shear. Makromol Chem Rapid Commun 8:461–466
- Woods LC (1993) An introduction to the kinetic theory of gases and magneto-plasmas. Oxford University Press, Oxford
- Yuan XF, Jupp L (2002) Interplay of flow-induced phase separations and rheological behaviour of complex fluids in shear-banding flows. Europhys Lett 60:691–697
- Zamankha P, Polashenski W Jr, Tafreshi HV, Manesh AS, Sarkomaa PJ (1998) Shear-induced particle diffusion in inelastic hard sphere fluids. Phys Rev E 58:R5237–R5240
- Zanette DH, Alemany PA (1995) Thermodynamics of anomalous diffusion. Phys Rev Lett 75:366–369
- Zhang ZM (2007) Nano/Microscale heat transfer. McGraw-Hill, New York
- Zheng J, Yeung ES (2002) Anomalous radial migration of single DNA molecules in capillary electrophoresis. Anal Chem 74:4536–4547
- Zheng J, Yeung ES (2003) Mechanism for the separation of large molecules based on radial migration in capillary electrophoresis. Anal Chem 75:3675–3680
- Zimm BH (1956) Dynamics of polymer molecules in dilute solutions: viscoelasticity, flow refringence and dielectric loss. J Chem Phys 24:269–278
- Zubarev DN, Morozov V, Röpke G (1997) Statistical mechanics of nonequilibrium processes, vol 2. Akademie Verlag, Berlin

A Absolute temperature, 2, 11, 17, 38, 53, 54, 213, 236, 270 Affinity, 213 Angular velocity, 240, 242 Anomalous diffusion, 187, 188, 190, 192, 194, 196–206, 208	109, 144, 147, 151, 163, 187, 195, 200, 202, 229, 236, 237 Chemical reactions, 123, 211, 212, 214, 216, 218, 220, 222–224, 226 Coexistence line, 82, 99, 124, 125, 150 Collision frequency, 52 Computer simulations, 35, 90, 91, 93, 95 Cone-and-plate experiments, 184
B Bead-and-spring model, 130 Boltzmann equation, 52, 57–65, 68, 77, 88, 97, 222, 272 Boltzmann entropy, 87, 199, 200, 202 ideal gases, 87 non-ideal gases, 85, 86 polymer solutions, 109 Bose-Einstein transition, 230 Boundary conditions, 57, 58, 70–73, 76, 235 Brownian motion, 188, 189, 197 Bulk viscous pressure, 14, 60, 87, 100	Configuration tensor, 14, 23, 24, 29, 129, 130, 160, 253 Configurational distribution function, 23, 28, 106, 108, 111, 115 Constitutive equations, 1, 8, 10, 11, 17, 19, 24, 60, 100, 132, 172, 187 Continued-fraction expansion, 76 Co-rotational time derivative, 5 Co-rotational Maxwell model, 6 Cosmic string loops, 253 Counterflow experiments, 246 Couette flow, 3, 44, 45, 47, 50, 81, 92, 96, 102, 135, 148, 166, 181, 189, 191, 204, 255 Critical point, 79–81, 83, 84, 114, 115, 124, 126, 128, 134, 135, 137, 150, 152, 155,
C Causal hydrodynamics, 99, 100 Chemical potential, 2, 10, 14, 33, 38, 41, 42, 44, 48, 49, 66, 83, 84, 99, 123, 124, 126–136, 138–144, 146–148, 150, 152, 155–167, 171, 172, 174–178, 184, 186, 211–214, 218, 219, 232, 235, 237, 251, 257, 259, 263 classical, 1, 2, 10, 11, 15, 17–20, 23, 27, 34, 49, 57, 59, 60, 70, 74, 76, 80, 85, 100, 103, 104, 123, 144, 155, 166, 172, 174–176, 187, 190, 197, 198, 200–205, 213, 214, 216, 229, 231, 235, 241, 248, 250, 270, 272 extended, 1, 10, 11, 13–21, 37, 38, 49, 52, 57, 74, 77, 85, 86, 95, 99, 102, 105,	D Dark energy, 252, 253 Deborah number, 176, 177 Density autocorrelation function, 155 Diffusion, 2, 10, 11, 14–16, 31, 103, 116, 132, 133, 146–148, 156–160, 163–165, 171, 172, 174, 175, 178, 180, 181, 187, 188, 190–209, 211, 250–252, 261, 266 classical, 174, 175, 187, 197, 198, 201, 202, 204, 205 in shear flow, 211, 260–262 shear-induced, 211, 261

Diffusion flux, 2, 10, 11, 14, 15, 31, 132, 133, 147, 156–160, 163–165, 172, 174, 181, 102, 103, 105, 108, 250	Flow chromatography, 171, 172, 174, 176, 178, 180, 182, 184, 186
192, 193, 195, 198, 250	Fokker-Planck equation
Double-reptation model, 101	Fourth cound, 234, 235
Droplet approach, 151–153	Fourth sound, 234, 235 Fractal dimension, 206, 207
	Fractal media, 208
E	Fractional derivatives, 197, 204, 208
Echo simulations, 194	Frame-indifference, 17
Effective diffusion coefficient, 146–148, 157,	Free energy, see Helmholtz free energy, or
159, 160, 174, 175, 178, 180, 190–193	Gibbs free energy
Effective thermal conductivity, 70–74, 76, 77	Freely jointed chain, 101, 102, 104
End-to-end vector, 23, 28, 102–105, 130, 253	11001) Jonitou enum, 101, 102, 101
Energy balance equation, 24	G
Entangled polymer solutions, 119, 140	Generalized Maxwell model, 8
Energy-momentum tensor, 99	GENERIC formalism, 28–30
Entropy, 1, 2, 10–19, 22–24, 26, 28–30,	Gibbs equation, 10, 11, 14, 21, 22, 24, 37, 38,
33–46, 48–50, 52, 54, 57, 59–62, 64,	43, 96, 97, 130, 212, 235, 236, 250
65, 68, 69, 73, 86, 87, 89–95, 97,	classical, 10, 11, 235
100–102, 104, 106, 107, 111, 115, 119,	extended, 10, 14, 38, 236
129, 141, 149, 151, 156, 157, 163, 170,	Gibbs free energy, 14, 83, 127, 130, 131,
194–197, 199–202, 213, 231–236, 251–253, 265, 270–272	134, 152, 162, 163, 166, 175, 212,
classical, 1, 10, 11, 49, 57, 59, 197, 202,	213, 218
235	Ginzburg-Landau free energy, 161-164
extended, 10, 86, 102, 151, 163, 200, 202	Görter–Mellink force, 244
kinetic, 65, 92, 107, 111	Grad's approach, 61, 66, 225
informational, 37, 38, 43	Guyer–Krumhansl equation, 68
superfluids, 233	
Entropy flux, 10, 15, 19, 22, 24, 57, 59, 61,	H
62, 68, 156, 194–196, 232, 236, 251	H theorem, 58, 59
classical, 57	HVBK model, 254
extended, 15, 20, 21, 69	Hamiltonian formulations, 26, 27, 29, 31
kinetic, 57	Heat flux, 1, 2, 10, 15, 18, 19, 22, 34, 39,
Entropy production, 2, 10, 15, 18, 19, 24, 60,	51, 57, 61, 62, 66, 67, 72–74, 85, 86,
65, 69, 73, 157, 201, 213, 232, 251	91, 97, 100, 163, 193, 225, 229, 230, 235–238, 240–242, 244, 250
Equations of state, 1, 2, 17, 31, 35, 37, 46,	Helium (superfluid), 230–253
79–81, 83, 95, 98, 100, 101, 156, 161,	Helmholtz free energy, 12, 13, 94, 104, 107,
166, 170–172, 269	109, 130, 160
Equipartition, 50, 52–54, 105	Higher-order moments, 60, 61, 64, 67
Evolution equations of the fluxes, 16, 68	Hooke's law, 104
Extended irreversible thermodynamics, 1, 10, 11, 13, 15, 17, 37, 49, 57, 77, 99, 109,	Huggins constant, 114, 136, 140, 167, 259, 261
163, 187, 195, 200, 202, 229	Hydrodynamic noise, 165
Extensional flow, 7, 110, 268–272	
Extensional now, 7, 110, 200-272	I
	Ideal gases, 23, 33–36, 38, 40, 42, 44, 46, 48,
<u>F</u>	50, 52, 54, 59, 65–67, 79–81, 85–89,
First sound, 230, 231, 234, 238, 245	96, 107, 109, 115, 163, 211, 222, 270,
Flexibility approach, 151	272
Flory–Huggins model, 127, 128	Information theory, 33, 35, 37, 42, 57, 94–96,
Fluctuations, 38, 47, 51, 91, 124, 135, 151,	116, 225
155, 161–170 Fluctuation-dissipation theorem, 47, 51, 91,	Internal energy, 2, 10–13, 18, 28, 34–40, 52,
200	54, 93, 101, 102, 105, 107, 109, 111, 129, 130, 141, 237, 252
	147. 130. 141. 437. 434

Internal variables, 1, 23, 25, 26, 30 Intrinsic viscosity, 114, 142, 167, 259–261 Isothermal shear-induced heat flow, 93 Isotropic-nematic phase transition, 263–265	N Nanowires, 57, 69–73, 76, 77 Navier–Stokes equations, 16 Newtonian fluids, 3, 149 Non equilibrium statistical energator, 25, 46
J Jacobi identity, 31 Jeffreys model, 9	Non-equilibrium statistical operator, 35, 46 Non-conventional statistical mechanics, 198 Non-extensive entropy, 199 Non-linear viscoelastic models, 8
K Kinetic temperature, 13, 50–53, 92–94 Kinetic theory, 20, 26, 30, 33, 35, 42, 46, 52, 53, 57–60, 62–68, 70–72, 74, 76, 79, 81, 85–87, 89, 91, 97, 102, 103, 105, 107, 109, 111, 116, 163, 196, 211, 222, 223, 277 gases, 20, 33, 35, 57, 63, 65, 67, 79, 85, 86, 91, 163, 196, 211, 277 phonons, 57, 65, 74 polymer solutions, 211	Non-Newtonian effects, 125, 149, 185 Normal stress coefficients, 3, 40 Normal component, 231, 232, 234, 235, 237, 239, 240, 248, 253, 254 Nosé-Hoover thermostat, 91 Nuclear collisions, 54, 79, 80, 82, 84, 86, 88, 90, 92, 94–100 Nuclear matter, 79, 95–100 transport coefficients, 97 compressibility, 98
Knudsen number, 70, 71, 73, 76, 77 Knudsen layer, 70 Kramer's expression for viscous pressure, 104, 109, 111, 115, 127 L	Oldroyd model, 9, 10 One-fluid model of liquid helium, 236, 238 Onsager–Casimir relations, 10, 24, 200 Orientational distribution function, 117, 263, 264, 266
Lagrange multipliers, 18, 19, 36–43, 45, 47, 52, 55, 96, 270, 271	Ornstein-Zernike expression, 162 Osmotic pressure, 145, 159, 160
Lambda temperature, 231 Langevin equation, 105, 188 Legendre transform, 13, 14, 129, 130 Lévy flights, 197 Light scattering, 161, 162 Liquid crystals, 101, 253, 263, 264, 266, 268, 270, 272	P Pair correlation function, 81, 86 Partition function, 37, 41, 43, 47, 54, 55 Phase diagram, 80, 123–125, 134, 135, 137, 139, 149, 151, 211, 218, 269 Phonon hydrodynamics, 57, 58, 60, 62, 64–68,
M	70–77
Macromolecular separation, 180, 181, 183 Marrucci's expression for free energy, 124, 125 Mass balance equation, 15, 173, 179 Matrix model, 2, 31 Maximum-entropy approach, 33, 65, 115, 270,	Planck distribution, 66 Poiseuille flow, 39, 69, 70, 142, 191, 255 Poisson brackets, 27, 31 Polydispersivity, 218, 220, 221, 227, 257 Polymer blends, 101, 119–121, 134, 144–148
271 Maxwell–Boltzmann distribution, 59 Maxwell–Cattaneo equation, 237 Maxwell relations, 13, 93, 94 Maxwell viscoelastic model, 5, 7 Mean free path, 60, 68–71, 73, 74, 92, 225	Polymer solutions, 23, 28, 31, 33, 80, 84, 87, 99, 101, 102, 115, 119, 123, 124, 126, 134, 135, 137, 139, 140, 145, 147, 151, 155, 160, 166, 184, 211, 214, 222, 257, 258, 260
Memory functions, 1 Micellar solutions, 126, 285 Microfluidics, 76, 141, 190–192 Mixtures, 50–53, 126, 151 Molecular dynamics simulations, 2, 13, 77, 93 Molecular weight distribution, 123, 217 Momentum balance equation, 18, 132	Polymer degradation, 211, 212, 214–222, 224, 226 Polymer extraction, 141, 143 Polystyrene in dioctyl-phthalate, 125, 150, 257 Polystyrene in transdecalin, 143, 168, 258, 259 Polystyrene in oligomeric polystyrene, 174, 260, 261

Porous media, 171, 187, 197, 198, 201, 230, 235 Porous silicon, 74, 75, 77 Pressure, 1–8, 10–14, 16, 18, 23–25, 29–31, 33, 34, 37, 39–47, 49–55, 60, 61, 63, 64, 69, 75, 79–83, 85–87, 92–100, 104, 105, 107, 109–111, 113, 115–117, 129, 130, 132, 133, 135, 136, 139, 140, 142, 145, 146, 148, 149, 151, 153, 156, 157, 159–161, 163–166, 170, 172, 180, 184, 212–214, 218, 222, 225, 227, 230, 234–238, 252–255, 264, 270–272	Shear rate, 3, 4, 6, 8, 10, 13, 42, 46, 52–54, 63, 64, 81, 85, 86, 88, 91–95, 118, 124–126, 136, 137, 139, 140, 148, 149, 153, 157–159, 165, 171, 172, 177, 178, 180–183, 186, 188, 211, 215, 218, 224, 259, 260, 268, 272 Shear-induced degradation, 123, 214, 261 Shear-induced migration, 171–180, 182, 184–186 Shear-induced shift of critical point, 85, 114, 115 Shear thinning, 8, 46 Slip heat flow, 57, 69
Q Quantum turbulence, 229 Quark–gluon plasma, 79 Quantum vortices, 239	SLLOD equations, 92 Spinodal line, 80, 83, 84, 124, 128, 134–137, 139, 140, 146, 147, 150, 157, 159, 180 Stability condition, 83, 100, 123, 132, 137, 159, 161 Structure factor, 155, 161–163, 165, 167, 169 Steady-state compliance, 8, 11, 101, 112, 113,
R Random walk, 103, 200, 206, 208 Rational thermodynamics, 1, 2, 17, 19, 23 Rational extended thermodynamics, 17, 19, 21 Reduced concentration, 114, 136, 139, 142, 176–178, 181, 182, 259 Regular binary solutions, 79, 83 Relativistic ideal gas, 54, 55	119, 121, 130, 134, 135, 140, 149, 157, 164, 166, 175, 219 definition, 8 Stokes law, 11, 74, 75, 164 Superfluids, 229–234, 236–240, 242, 244, 246, 248, 250, 252–255 Subdiffusion, 202, 203 Superdiffusion, 202
Relaxation time, 3, 5, 7, 8, 11, 14, 16, 25, 42, 51, 60, 62, 65, 68, 80, 87, 89, 90, 94, 97, 100, 101, 106, 108, 111–113, 115–118, 120, 130, 145, 146, 156, 165, 172, 177, 190, 193, 195, 214, 222, 229, 230, 236, 237, 252, 260 Renyi entropy, 197 Reptation model, 101, 102, 116–119, 121, 138, 140, 146 Reversible-to-irreversible transition, 193	T Taylor dispersion, 187, 188, 190–196, 198, 200, 202, 204–206, 208 Temperature, 1, 2, 10–14, 17, 19, 33–36, 38, 40–42, 44, 46, 48, 50–54, 63, 65, 70, 71, 75, 82–85, 91–94, 96–98, 104, 112, 123–128, 132, 135, 137, 139, 140, 147, 148, 151, 161, 170, 189, 212, 213,
Reynolds number, 241, 248, 269 Rheological models, 3–5 Rotating superfluids, 240 Rotons, 96, 231, 241, 244 Rouse–Zimm model, 105–115	223–225, 230, 231, 234, 236, 238, 240, 243, 245, 247, 250, 257–259, 263–265, 270 Thermal conductivity, 21, 68, 70–77, 97, 230, 237, 251 Theta temperature, 127, 128 Thirteen-moments approximation, 61–63
S Second sound, 230–235, 237–240, 244–246, 250, 252 Second law, 17–19, 27, 59, 69, 73, 157, 213 Shear flow, 6, 9, 12, 33, 40, 53, 57, 63, 79, 82, 86, 91, 98, 101, 109, 111, 115, 117, 123, 124, 134, 135, 137, 139, 140, 147, 149, 152, 155, 159–161, 165, 167, 173, 188, 189, 192, 204, 205, 211, 215, 218, 221, 225, 263, 267, 269, 270, 272	Transport equations, 1, 2, 39, 57, 100, 156, 187, 193, 194, 200 Transport networks, 188 Tsallis entropy, 197, 199, 200 Two-fluids model, 133 in polymers, 145–147 in superfluids, 231–236 Turbidity point, 124 Turbulence, see quantum turbulence

U Upper-convected Maxwell model, 6, 147, 160, 165

V
van der Waals fluid, 80
Variational principle, 200
Velocity distribution function, 34, 52, 60, 61, 64, 81, 223
Vinen equation, 246–248
Viscoelasticity, 8, 106
Viscosity coefficient, 42
Viscous pressure tensor, 1–8, 10–12, 14, 18, 23–25, 30, 31, 33, 37, 39, 41, 43,

61, 63, 80, 85, 87, 97, 100, 104, 107, 109–111, 115–117, 129, 130, 132, 145, 156, 161, 163–166, 170, 172, 184, 212, 213, 270, 271 general, 2, 7, 14, 39, 42–47, 132, 270 ideal gases, 23, 33, 85, 87, 107 real gases, 33 polymer solutions, 31, 33, 80, 87, 145, 184 Vortex length distribution, 252 Vortex line density, 239–241, 243, 246, 247, 249, 251, 253, 254 Vortex loops, 252, 253 Vorticity quantum, 239, 246